

THE FRONTIERS COLLECTION

Jack A. Tuszynski (Ed.)

THE EMERGING PHYSICS OF CONSCIOUSNESS



 Springer

THE FRONTIERS COLLECTION

THE FRONTIERS COLLECTION

Series Editors:

A.C. Elitzur M.P. Silverman J. Tuszynski R. Vaas H.D. Zeh

The books in this collection are devoted to challenging and open problems at the forefront of modern science, including related philosophical debates. In contrast to typical research monographs, however, they strive to present their topics in a manner accessible also to scientifically literate non-specialists wishing to gain insight into the deeper implications and fascinating questions involved. Taken as a whole, the series reflects the need for a fundamental and interdisciplinary approach to modern science. Furthermore, it is intended to encourage active scientists in all areas to ponder over important and perhaps controversial issues beyond their own speciality. Extending from quantum physics and relativity to entropy, consciousness and complex systems – the Frontiers Collection will inspire readers to push back the frontiers of their own knowledge.

Information and Its Role in Nature

By J. G. Roederer

Relativity and the Nature of Spacetime

By V. Petkov

Quo Vadis Quantum Mechanics?

Edited by A. C. Elitzur, S. Dolev,
N. Kolenda

Life – As a Matter of Fat

The Emerging Science of Lipidomics
By O. G. Mouritsen

Quantum-Classical Analogies

By D. Dragoman and M. Dragoman

Knowledge and the World

Challenges Beyond the Science Wars
Edited by M. Carrier, J. Roggenhofer,
G. Küppers, P. Blanchard

Quantum-Classical Correspondence

By A. O. Bolivar

Mind, Matter and Quantum Mechanics

By H. Stapp

Quantum Mechanics and Gravity

By M. Sachs

Extreme Events in Nature and Society

Edited by S. Albeverio, V. Jentsch,
H. Kantz

The Thermodynamic

Machinery of Life

By M. Kurzynski

The Emerging Physics

of Consciousness

Edited by J. A. Tuszynski

Weak Links

Stabilizers of Complex Systems
from Proteins to Social Networks

By P. Csermely

Jack A. Tuszynski (Ed.)

**THE EMERGING
PHYSICS OF
CONSCIOUSNESS**

With 135 Figures and 10 Tables



Springer

Prof. Jack A. Tuszynski

University of Alberta

Department of Physics

T6G 2J1 Edmonton, AB

Canada

e-mail: jtus@phys.ualberta.ca

Series Editors:

Avshalom C. Elitzur

Bar-Ilan University, Unit of Interdisciplinary Studies,
52900 Ramat-Gan, Israel email: avshalom.elitzur@weizmann.ac.il

Mark P. Silverman

Department of Physics, Trinity College,
Hartford, CT 06106, USA email: mark.silverman@trincoll.edu

Jack Tuszynski

University of Alberta, Department of Physics, Edmonton, AB,
T6G 2J1, Canada email: jtus@phys.ualberta.ca

Rüdiger Vaas

University of Gießen, Center for Philosophy and Foundation of Science
35394 Gießen, Germany email: Ruediger.Vaas@t-online.de

H. Dieter Zeh

University of Heidelberg, Institute of Theoretical Physics, Philosophenweg 19,
69120 Heidelberg, Germany email: zeh@urz.uni-heidelberg.de

Cover figure:

The cover image shows a detail from ‘Molecular Dynamics Simulation of Crack Propagation Visualization’. Courtesy of the Scientific Computing and Imaging Institute, University of Utah (www.sci.utah.edu).

Library of Congress Control Number: 2005937896

ISSN 1612-3018

ISBN-10 3-540-23890-5 Springer Berlin Heidelberg New York

ISBN-13 978-3-540-23890-4 Springer Berlin Heidelberg New York

This work is subject to copyright. All rights are reserved, whether the whole or part of the material is concerned, specifically the rights of translation, reprinting, reuse of illustrations, recitation, broadcasting, reproduction on microfilm or in any other way, and storage in data banks. Duplication of this publication or parts thereof is permitted only under the provisions of the German Copyright Law of September 9, 1965, in its current version, and permission for use must always be obtained from Springer. Violations are liable to prosecution under the German Copyright Law.

Springer is a part of Springer Science+Business Media
springer.com

© Springer-Verlag Berlin Heidelberg 2006
Printed in Germany

The use of general descriptive names, registered names, trademarks, etc. in this publication does not imply, even in the absence of a specific statement, that such names are exempt from the relevant protective laws and regulations and therefore free for general use.

Typesetting by LE-T_EX Jelonek, Schmidt & Vöckler GbR, Leipzig
Cover design by KünkelLopka, Werbeagentur GmbH, Heidelberg

Printed on acid-free paper SPIN: 10991992 57/3100/YL - 5 4 3 2 1 0

Contents

1 The Path Ahead

<i>Jack A. Tuszynski, Nancy Woolf</i>	1
1.1 Definition and Fundamentals	1
1.1.1 Definition of Consciousness and the Classical Approach	2
1.1.2 Quantum Theories	4
1.1.3 Quantum Processing by Microtubules and Neurocognition	8
1.2 Overview of the Contributions	11
1.3 New and Notable Developments	17
1.3.1 An Electromagnetic Fingerprint of Transport Along Microtubules	17
1.3.2 Extrapolations to Mesoscopic and Macroscopic Levels	22
1.4 Conclusions	23
References	24

2 Consciousness and Quantum Physics: Empirical Research on the Subjective Reduction of the Statevector

<i>Dick J. Bierman, Stephen Whitmarsh</i>	27
2.1 Introduction	27
2.1.1 The Measurement Problem	27
2.1.2 Objective Reduction and Consciousness	29
2.1.3 Previous Empirical Work on Subjective Reduction	30
2.1.4 Current Investigation	33
2.2 Experimental Design	33
2.3 Experimental Procedure	36
2.3.1 Subjects	36
2.3.2 Physiological Measurement	36
2.3.3 Further Procedure	36
2.4 Data Analysis	37
2.5 Results	38
2.6 Conclusions	40
2.7 Further Research	45
Appendix	47
References	47

3 Microtubules in the Cerebral Cortex: Role in Memory and Consciousness

<i>Nancy J. Woolf</i>	49
3.1 Introduction	49
3.1.1 General Features of the Brain	49
3.1.2 Neuronal Assemblies: Patterns of Connection	51
3.1.3 Neurons, Synapses and Neurotransmitter Molecules.....	52
3.2 Functions of Microtubules and MAPs	56
3.2.1 Transport along Microtubules	57
3.2.2 Signal Transduction and Anchoring of Signal-Transduction Molecules	57
3.3 Learning and Memory: Neuroplasticity vs. Stability	65
3.3.1 Synaptic Change: Hebb's Rule Revisited	66
3.3.2 Microtubules and MAPs in Dendrites Play a Critical Role in Memory	70
3.3.3 Microtubules Influence Synaptic Efficacy	77
3.4 Consciousness	77
3.4.1 Attention: The Spotlight of Consciousness	78
3.4.2 Waking, Sleeping and Dreaming: Different Levels of Consciousness	80
3.4.3 Mental Force to Think and Act	81
3.4.4 Consciousness, Memory and Microtubules	83
3.5 Microtubules and Quantum Entanglement: A Possible Basis for Memory and Consciousness	85
3.6 Conclusion	89
References	90

4 Towards Experimental Tests of Quantum Effects in Cytoskeletal Proteins

<i>Andreas Mershin, Hugo Sanabria, John H. Miller, Dharmakeerthna Nawarathna, Efthimios M.C. Skoulakis, Nikolaos E. Mavromatos, Alexadre A. Kolomenskii, Hans A. Schuessler, Richard F. Luduena, Dimitri V. Nanopoulos</i>	95
4.1 Introduction	96
4.1.1 Overview	96
4.1.2 Tubulin and Microtubules	97
4.1.3 Motivation	101
4.2 QED Model of Tubulin and its Implications.....	102
4.2.1 Introduction	102
4.2.2 Quantum Coherence in Biological Matter?	105
4.2.3 Implications for Cell Function.....	115
4.2.4 Conclusions	120
4.3 Tau Accumulation in Drosophila Mushroom Body Neurons Results in Memory Impairment	120
4.3.1 Introduction	120

4.3.2	Drosophila	121
4.3.3	Genetic Engineering	123
4.3.4	Conditioning	126
4.3.5	Controls	128
4.3.6	Results	132
4.3.7	Conclusions	134
4.3.8	Discussion	134
4.4	Refractometry, Surface Plasmon Resonance, and Dielectric Spectroscopy of Tubulin and Microtubules	136
4.4.1	Theory of Dielectrics	136
4.4.2	Optics	141
4.4.3	Surface Plasmon Resonance (SPR)	145
4.4.4	Dielectric Spectroscopy	153
4.5	Emerging Directions of Experimental Tests of the Quantum Consciousness Idea	159
4.5.1	Entanglement	159
4.5.2	Molecular Electronics	160
4.5.3	Proposed Further Research	160
4.6	Unification of Concepts and Conclusions	163
4.6.1	Putting It All Together	163
4.6.2	Conclusions	164
	References	165

5 Physicalism, Chaos and Reductionism

<i>Alwyn Scott</i>	171	
5.1	Introduction	171
5.2	Quantum and Classical Dynamics	172
5.3	What Are Classical Nonlinear Phenomena?	173
5.4	The Biological and Cognitive Hierarchies	174
5.5	Reductionism	177
5.6	Objections to Reductionism	179
5.6.1	Constructionism versus Reductionism	179
5.6.2	Immense Numbers of Possibilities	180
5.6.3	Sensitive Dependence on Initial Conditions	181
5.6.4	The Nature of Causality	181
5.6.5	Nonlinear Causality	183
5.6.6	The Nature of Time	184
5.6.7	Downward Causation	184
5.6.8	Open Systems	185
5.6.9	Closed Causal Loops	186
5.7	Concluding Comments	188
	References	190

**6 Consciousness, Neurobiology and Quantum Mechanics:
The Case for a Connection**

<i>Stuart Hameroff</i>	193
6.1 Introduction: The Problems of Consciousness	193
6.2 Time and Consciousness	197
6.2.1 Is Consciousness Continuous or a Sequence of Discrete Events?	197
6.2.2 The Timing of Conscious Experience	198
6.2.3 Taking Backward Time Referral Seriously	202
6.3 The Neural Correlate of Consciousness	206
6.3.1 Functional Organization of the Brain	206
6.3.2 Cerebral Cortex and Neuronal Assemblies	208
6.3.3 Axons and Dendrites	208
6.3.4 Neural Synchrony	212
6.3.5 Gap-Junction Assemblies – “Hyperneurons”	215
6.3.6 The Next NCC Frontier – Neuronal Interiors and the Cytoskeleton	216
6.4 The Neuronal Cytoskeleton	217
6.4.1 Microtubules and Networks inside Neurons	217
6.4.2 Microtubule Automata	220
6.4.3 Protein Conformational Dynamics – Nature’s Bits and Qubits	224
6.4.4 Anesthesia	225
6.5 Quantum Information Processing	226
6.5.1 Quantum Mechanics	226
6.5.2 Quantum Computation	228
6.5.3 Quantum Computing with Penrose OR	229
6.6 The Quantum Unconscious	230
6.7 Quantum Computation in Microtubules – The Orch OR Model ..	232
6.7.1 Specifics of Orch OR	232
6.7.2 Decoherence	235
6.7.3 Testability and Falsifiability	236
6.8 Applications of Orch OR to Consciousness and Cognition	236
6.8.1 Visual Consciousness	236
6.8.2 Volition and Free-Will	238
6.8.3 Quantum Associative Memory	239
6.8.4 The Hard Problem of Conscious Experience	239
6.8.5 What is Consciousness?	240
6.8.6 Consciousness and Evolution	241
6.9 Conclusion	242
Appendix	242
References	244

7 Life, Catalysis and Excitable Media:	
A Dynamic Systems Approach to Metabolism and Cognition	
<i>Christopher James Davia</i>	255
7.1 Life and Robustness	255
7.2 Life and Catalysis	260
7.3 Catalysis, Traveling Waves and Excitable Media	271
7.4 The Brain as an Excitable Medium	274
7.5 Conclusion	288
References	289
8 The Dendritic Cytoskeleton as a Computational Device:	
An Hypothesis	
<i>Avner Priel, Jack A. Tuszyński, Horacion F. Cantiello</i>	293
8.1 Introduction	293
8.1.1 Neurobiological Introduction	293
8.1.2 Neuro computational Introduction	297
8.1.3 Dendritic Channel Function	299
8.1.4 Actin–Microtubule Cytoskeletal Connections	299
8.2 C-Termini in Microtubules	301
8.2.1 Potential Configurations of Microtubular C-Termini	303
8.2.2 Dynamic Model of the C-Termini	305
8.2.3 Ionic Wave Propagation along MAP2	306
8.3 Ion Waves along Actin Filaments	308
8.3.1 Ionic Condensation along the Actin Filament	308
8.3.2 Electrical Modeling of Actin	309
8.3.3 Implications of Actin Filament’s Electrical Activity	312
8.4 Dendritic Cytoskeleton Computation – Vision of Integration	313
8.4.1 MTN Control of Synaptic Plasticity, Modulation, and Integration	318
8.5 Final Statement	320
References	320
9 Recurrent Quantum Neural Network and its Applications	
<i>Laxmidhar Behera, Indrani Kar, Avshalom C. Elitzur</i>	327
9.1 Intelligence – Still Ill-Understood	327
9.2 Intelligent Filtering – Denoising of Complex Signals	328
9.2.1 RQNN Architecture used for Stochastic-Filtering	329
9.2.2 Integration of the Schrödinger Wave Equation	331
9.2.3 Simulation Results I	333
9.3 A Comprehensive Quantum Model of Intelligent Behavior	337
9.4 RQNN-based Eye-Tracking Model	338
9.4.1 A Theoretical Quantum Brain Model	338
9.4.2 An Eye–Tracking Model using RQNN with Nonlinear Modulation of Potential Field	339
9.4.3 Simulation Results II	342

9.5 Concluding Remarks	347
References	348
10 Microtubules as a Quantum Hopfield Network	
<i>Elizabeth C. Behrman, K. Gaddam, J.E. Steck, S.R. Skinner</i>	351
10.1 Introduction	351
10.2 Microtubulin Model	352
10.3 Hopfield Model.....	354
10.4 Quantum Model.....	355
10.5 Quantum Hopfield Network	358
10.6 QHN as Information Propagator for a Microtubules Architecture	360
10.7 Conclusions and Future Work	367
References	369
11 Consciousness and Quantum Brain Dynamics	
<i>Gordon Globus</i>	371
11.1 Deconstruction	371
11.2 Quantum Brain Dynamics	373
11.3 Hermitean Dual-Mode Quantum Brain Dynamics.....	375
11.4 Non-Hermitean Dual-Mode Quantum Brain Dynamics	376
11.5 Application to Mathematics: The Riemann Hypothesis	377
11.6 Monadological Implications of Non-Hermitean Dual-Mode QBD .	381
11.7 Comment	383
References	384
12 The CEMI Field Theory: Seven Clues to the Nature of Consciousness	
<i>Johnjoe McFadden</i>	387
12.1 Why Do we Need a Theory of Consciousness?.....	387
12.2 Field Theories of Consciousness	393
12.3 The Brain's Electromagnetic Field	394
12.4 The Influence of the Brain's Electromagnetic Field on Neural Firing	395
12.5 The CEMI Field Theory	396
12.6 Why don't External Fields Influence our Minds?	397
12.7 Does the CEMI Field Theory Account for the Seven Clues to the Nature of Consciousness?	398
12.8 A Last Word, Concerning Quantum Theories of Consciousness ..	401
12.9 Conclusions and the Way Forward	404
References	404
13 Quantum Cosmology and the Hard Problem of the Conscious Brain	
<i>Chris King</i>	407
13.1 Subject–Object Complementarity and the Hard Problem	407

13.2	Wave–Particle Complementarity, Uncertainty and Quantum Prediction	410
13.3	Two-Timing Nature of Special Relativity	415
13.4	Reality and Virtuality: Quantum Fields and Seething Uncertainty	416
13.5	The Spooky Nature of Quantum Entanglement.....	417
13.6	Quantum Match-Making: Transactional Supercausality and Reality	420
13.7	Exploring the “Three Pound Universe”	423
13.8	Chaos and Fractal Dynamics as a Source of Sensitivity, Unpredictability and Uncertainty	428
13.9	Classical and Quantum Computation, Anticipation and Survival.	430
13.10	The Cosmic Primality of Membrane Excitation	433
13.11	Chaotic Excitability and Quantum Sensitivity as a Founding Eucaryote Characteristic	437
13.12	Models of the Global-Molecular-Quantum Interface	440
13.13	Quantum Mind and Transactional Supercausality	442
13.14	Complementarity and the Sexuality of Quantum Entanglement ..	448
13.15	The Hard Problem: Subjective Experience, Intentional Will and Quantum Mind Theories	449
13.16	Consciousness and Neurocosmology	451
	References	454

14 Consciousness and Logic in a Quantum Computing Universe

<i>Paola Zizzi</i>	457	
14.1	Introduction	458
14.2	The “Big Wow”	459
14.3	How the “Big Wow” Drove Human Minds	461
14.3.1	Entanglement with the Environment	463
14.3.2	Holography and Cellular Automata	463
14.4	Consciousness and Tubulins/Qubits	464
14.5	Consciousness Arises in the “Bits Era”	465
14.5.1	The Boolean Observer	465
14.5.2	The Analogy	466
14.6	The Double Logic of the Observer Inside a Quantum Universe ..	467
14.7	IT from Qubit: The Whole Universe as a Quantum Computer ..	468
14.8	Quantum Minds and Black – Hole Quantum Computers in a Quantum Game	469
14.9	Qualia and Quantum Space-Time	470
14.10	Mathematical Intuition and the Logic of the Internal Observer ..	473
14.11	The Self	475
14.11.1	14.11.1 The Self and the Mirror Measurement	475
14.11.2	14.11.2 Nonself	476

XII Contents

14.11.3 The Universal Self: The Universe and the Mirror	476
14.11.4 The Universal Self: The Mathematical Truth.....	477
14.12 Conclusion	477
References	479
Index	483

List of Contributors

Laxmidhar Behera

Department of Electrical
Engineering
Indian Institute of Technology
Kanpur, 208016, UP, INDIA

E.C. Behrman

Department of Physics
Wichita State University
Wichita, KS 67260-0032, USA
elizabeth.behrman@wichita.edu

Dick J. Bierman

Department of Psychology
University of Amsterdam
The Netherlands

Horacio F. Cantiello

Massachusetts General Hospital
and Harvard Medical School
Charlestown, Massachusetts, USA

Christopher James Davia

Department of Psychology
Carnegie Mellon University
Pittsburgh, PA 15213, USA
phone: 412-268-2792
c.j.davia@sussex.ac.uk

Avshalom C. Elitzur

Unit of Interdisciplinary Studies
Bar-Ilan University
52900 Ramat-Gan, Israel

K. Gaddam

Department of Mechanical
Engineering
Wichita State University
Wichita, KS 67260-0032, USA

Gordon Globus, M.D.

Professor Emeritus
of Psychiatry and Philosophy
University of California Irvine
phone: 949 759 9515
fax: 949 760 3671
2990 Zurich Ct. Laguna Beach,
CA 92651 USA
ggllobus@aol.com

Stuart Hameroff

Departments of Anesthesiology
and Psychology
Center for Consciousness Studies
The University of Arizona
Tucson, Arizona, USA
www.consciousness.arizona.edu/
hameroff

Indrani Kar

Unit of Interdisciplinary Studies
Bar-Ilan University
52900 Ramat-Gan, Israel

Chris King

Department of Mathematics
University of Auckland
Private Bag 92019, Auckland,
New Zealand

Alexandre A. Kolomenskii

Texas A&M University
Department of Physics
College Station
TX 77843-4242, USA

Richard F. Luduena

Department of Biochemistry
University of Texas Health Science
Center at San Antonio
San Antonio, TX 78229-3900, USA

Nikolaos E. Mavromatos

Department of Physics
Theoretical Physics Group
University of London
King's College
Strand, London WC2R 2LS, U.K.

Johnjoe McFadden

School of Biomedical
and Molecular Sciences
University of Surrey
Guildford, Surrey, GU2 5XH, UK
Tel: +44-1483-686494
Fax: +44-1483-686401
j.mcfadden@surrey.ac.uk

Andreas Mershin

Massachusetts Institute
of Technology
Center for Biomedical Engineering
77 Massachusetts Ave.
Rm. NE47-376 Cambridge
MA 02139-4307, USA
and
Texas A&M University
Department of Physics
College Station
TX 77843-4242, USA
mershin@mit.edu

John H. Miller

Dept. of Physics and
Texas Center for Superconductivity
University of Houston
Houston, TX 77204-5005, USA

Dimitri V. Nanopoulos

Texas A&M University
Department of Physics
College Station
TX 77843-4242, USA
and

Academy of Athens
Natural Science Division
Athens, 10679, Greece

Dharmakeerthna Nawarathna

Dept. of Physics and
Texas Center for Superconductivity
University of Houston
Houston, TX 77204-5005, USA

Avner Priel

Department of Physics,
University of Alberta
Edmonton, AB, T6G 2J1, Canada

Hugo Sanabria

Dept. of Physics and
Texas Center for Superconductivity
University of Houston
Houston, TX 77204-5005, USA

Hans A. Schuessler

Texas A&M University
Department of Physics
College Station
TX 77843-4242, USA

Alwyn C. Scott

Emeritus Professor
Department of Mathematics
University of Arizona
Tuscon, Arizona 85721, USA

S.R. Skinner

Department of Electrical
and Computer Engineering
Wichita State University
Wichita, KS 67260-0032, USA

Efthimios M.C. Skoulakis
Texas A&M University
Department of Physics
College Station
TX 77843-4242, USA
and
Institute of Molecular Biology
and Genetics Biomedical Sciences
Research Centre
“Alexander Fleming”
34 Fleming St., Vari 16672, Greece

J.E. Steck
Department of Aerospace
Engineering
Wichita State University
Wichita, KS 67260-0032, USA

Jack A. Tuszyński
Department of Physics

University of Alberta
Edmonton, AB, T6G 2J1, Canada

Stephen Whitmarsh
Department of Psychology
University of Amsterdam
The Netherlands

Nancy J. Woolf
Behavioral Neuroscience
Department of Psychology
University of California
Los Angeles, CA 90095-1563, USA

Paola Zizzi
Dipartimento di Matematica
Pura ed Applicata
Via Belzoni, 7
35131 Padova, Italy
zizzi@math.unipd.it

1 The Path Ahead

Jack A. Tuszynski and Nancy Woolf

Summary. This chapter provides an introduction to the rest of the book, which has a multidisciplinary approach to the physics of consciousness. We summarize the various contributions and present our own point of view, which is that there are some deficiencies in defining higher-order consciousness in strict terms of classic physics. We favor a proposal that considers some aspects of quantum-mechanical operations among molecules involved with neurotransmission and mechanical transport of synaptic proteins. In our view, the wiring of the brain is not as complex, and certainly not as integrated, as commonly assumed. Instead, the wiring pattern redundantly obeys a few general principles focused on high resolution rather than crossmodal integration. Basing cognitive functions, such as higher-order consciousness, solely on electrophysiological responses in neural networks thus wired may not suffice. On the other hand, coherent quantum computing, executed by tubulins, the protein subunits of microtubules, may exert en masse influences over the transport of many receptor and scaffolding proteins to various activated synapses, thereby accounting for the unity of conscious experience. We discuss the potential problems of quantum computing, such as decoherence, and also present counterarguments, as well as recent empirical results consistent with the notion that quantum computing in the interiors of neurons, in particular, within the interiors of dendrites may indeed be possible.

1.1 Definition and Fundamentals

Consciousness is one of the major unsolved and poorly understood problems in biology. How do the elemental feelings and sensations making up conscious experience arise from the concerted actions of nerve cells and their associated subcellular, synaptic and molecular processes? Can such feelings be explained by modern molecular science, or is there an entirely different kind of explanation needed? How can this seemingly intractable problem possibly be investigated experimentally and what kind of theory is appropriate? How do the operations of the conscious mind emerge out of the specific interactions involving billions of neurons connected with thousands of neurons each? This multiauthor book seeks answers to these questions within a range of physically based frameworks. In other words, the underlying assumption is that consciousness should be understood using the combined intellectual potential of modern physics and the life sciences. We have gathered contributions from a number of scientists representing a spectrum of disciplines taking

a biophysics-based approach to consciousness. Thus, we have attempted to provide the reader with a broad range of vantage points to choose from.

There are a number of theories of consciousness in existence, some of which are based on classical physics while others require the use of quantum concepts. Although quantum mechanics lie at the heart of the material realm, it remains to be determined if these seemingly peculiar phenomena contribute significantly to human cognition and consciousness. Quantum theory has invoked new perspectives of consciousness almost since its inception. Neuroscientists widely accept that cognition, and possibly consciousness, are correlated with the physiological behavior of the material brain (for example, membrane depolarizations and action potentials). Quantum theory is the most fundamental theory of matter known thus far; as such, it appears likely that quantum theory can help us to unravel the mysteries of consciousness. We will try to present the reader with a spectrum of opinions from both sides of this scientific divide letting him/her decide which of these approaches are most likely to succeed. While classical physics is easily grasped by our intuition, quantum theory often defies the common sense developed through everyday experiences. Therefore, a general introduction into quantum phenomena needs to be presented in this context to better understand detailed discussions presented in the chapters that follow.

1.1.1 Definition of Consciousness and the Classical Approach

There are several possible definitions of consciousness, but the general consensus is that the state of being conscious is a condition of being aware of one's surroundings and one's own existence or self-awareness. The status quo or the currently accepted view is that the substrate of consciousness emerges as a property of an ever-increasing computational complexity among neurons. This framework envisions neurons and synapses as the fundamental units of information processing hardware in the brain, acting much like chips manipulating information bits in a computer. It is often argued that although individual neurons are assumed to have only two different states, on when the neuron is firing and off when it is not, there is a critical level of complexity required such that when it is reached, many neurons interact with each other to form a conscious experience. While this appears to be the currently accepted approach to explaining consciousness, it may fall short, especially in cases where the apparent randomness of neural processing is represented simply as white noise.

Moreover, the fact that neuronal assemblies can be fully described by classical physics does not rule out significant quantum effects, especially at the level of subneuronal components such as individual proteins, or strands of DNA or RNA. The brain contains both electrical and chemical synapses, named according to the type of signal they transmit [30]. Although relatively sparse in the brain, electrical synapses, which are also called gap junctions, literally connect the cytoplasm of the presynaptic neuron with that of the

postsynaptic cell. Although gap junctions conduct electrical impulses according to the laws of classical physics, these structures may be important for transmitting quantum states from neuron to neuron [73].

Chemical transmission is the much more prevalent type in the mammalian brain, but also operates much more slowly than electrical transmission. In chemical transmission there is release of a chemical neurotransmitter, such as glutamate or acetylcholine. Neurotransmitters are sequestered in presynaptic vesicles, which bind docking proteins that cause the vesicles to fuse with the presynaptic membrane and then release their contents. The neurotransmitter molecules then cross the synaptic cleft to bind with the exposed surface of specific receptor subtypes in the postsynaptic membrane. This results in the opening or closing of ion channels or in the initiation of signal-transduction cascade, some of which act on the cytoskeleton. Although these steps operate according to classical physics, quantum processes can come into play. As will be detailed later, a physical model developed by Beck and Eccles [6] proposes that quantum tunneling among vesicles occurs, which in turn regulates quantal neurotransmitter release and subsequently determines the state of consciousness.

In an approach based solely on classical physics, Flohr [14, 15] suggests chemical synapses using NMDA receptors are critical to perception and consciousness because NMDA receptors are involved in developmental plasticity and learning. That anesthetic agents block NMDA receptors and consequently lead to a loss of consciousness supports his theory to some extent. Nonetheless, not all synapses possess NMDA receptors. In contrast, the neuronal cytoskeleton is the most ubiquitous and basic cellular protein thus far proposed for quantum processes in consciousness. The cytoskeleton consists of three types of protein networks: microfilaments, intermediate filaments and microtubules. Microtubules are essential for axoplasmic transport, signaling and neuronal plasticity, among other key cellular processes within neurons. A growing number of researchers are focusing their attention on the biophysics of the cytoskeleton in order to better understand its role in neurophysiology and consciousness.

Another reason to look beyond classical models is that currently accepted models for consciousness are unable to properly explain the rather primitive consciousness in single-celled organisms. Single-celled organisms, such as the paramecium, have no neurons or synapses, but still exhibit protoconsciousness, an apparent awareness of and responsiveness to their environment [22]. One can conclude from this that the rudiments of consciousness lie someplace other than the complex interactions between neurons and synapses, although the latter are certain to contribute to the richness of sensory experience and the resulting behavioral repertoire. In many respects, the cytoskeleton can be viewed as the control center of the cell. Microtubules control cell division and cell migration (i.e. replication and motility). Microtubules also provide an ideal bridge between classical and quantum processing; moreover, these

structures literally fill the interiors of neurons. They are composed of tubulin dimers arranged into longitudinal protofilaments. The interior milieu of tubulin can be likened to a caged qubit, capable of quantum computation, linked into a long polymer chain responsible for transmitting classical information. Substantial efforts have been made to fuse quantum theory with microtubules and consciousness, the result being one unified theory that still awaits experimental verification. This effort is considerably advanced from a mathematical point of view. According to this model, preconscious thought and experience exists in terms of multiple quantum states, and the conscious experience is realized when one of the many possible states prevails.

1.1.2 Quantum Theories

The physical term quantum means the smallest unit of a physical quantity the system is able to possess. The quantum world is the microworld of elementary particles, which are the fundamental building blocks of matter. The brain is made up of physical matter like all other living and nonliving systems. The ultimate pursuit for brain science is to give an explanation of how matter that comprises the physical structure of the brain gives rise to its functions, in particular higher cognition and consciousness. That the brain does give rise to consciousness is a key assumption of modern neuroscience and we will take it as a given, otherwise we would be compelled to seek these answers in the realm of religion or metaphysics. A search for that link has occupied numerous philosophers and scientists for at least two millennia [29]. In recent years some scientists have begun to probe the brain at the quantum level of physical description, facing considerable opposition from the traditionally inclined academics in both physics and neuroscience.

Perhaps the most bizarre quantum feature is the effect called superposition that implies that quantum particles can exist in multiple spatial locations or states being described by a mathematical superposition of pure state wave functions simultaneously. Such quantum superposition states can end when out of each multiplicity of the possible states the system selects one definite state or spatial location. Because quantum systems are described mathematically by a quantum wave function, and because quantum systems switch states they occupy very rapidly, the transition from quantum to classical states is often termed wave-function collapse (or sometimes state reduction). A number of experiments in the early 20th century demonstrated that quantum superpositions persisted until they were observed or measured by an experimentalist (observer). If a machine measured a quantum system, the results appeared to remain in superposition within the machine until actually viewed by experimenters. Therefore, the prevalent view in physics at that time (expressed within the famous Copenhagen interpretation) was that conscious observation led to a collapse of the wave function. To illustrate this paradox and the apparent absurdity of the notion, Erwin Schrödinger in 1935 described his celebrated thought experiment known as Schrödinger's cat. In

this example, a cat is placed in a box with a vial of poison. Outside the box, a quantum event (e. g., passage/not passage of a single photon through a half-silvered mirror) is causally connected to the release of the poison inside the box. Since the photon is a quantum object in a superposition state, it both passes and does not pass through the mirror. Hence the poison is both triggered and not triggered. Therefore, by quantum logic, the cat must be both dead and alive until the box is opened and the cat observed. (Analogous to quantum logic, superposition of mental events is commonplace, further suggesting that the mind is a quantum system. Cognitively, we are simultaneously prepared for the cat being alive and prepared for the cat being dead until we open the box.) At the moment the box is opened, the system chooses either to reveal a dead cat or a live cat. Therefore, consciousness essentially selects reality. The precise choice in any given quantum collapse experiment was believed to be probabilistic, an idea Einstein found unsettling by proclaiming in a famous statement that: “God does not play dice with the universe.”

Today the generally accepted view is that any interaction of a quantum superposition state with the classical environment causes decoherence. Due to these difficulties many physicists maintain that quantum theory is incomplete and that other approaches to the problem of collapse of the quantum wave function need to be found. One suggestion, called the multiple-worlds hypothesis, was put forward by Hugh Everett [13] and it holds that each collapse event is a branching of reality into parallel manifolds, so for example, a dead cat in this universe corresponds to a live cat in a newly formed parallel universe. If so, there must exist an infinity of parallel worlds, a bizarre notion to many. David Bohm’s theory of quantum reality [8] avoids collapse altogether, while still other views hold out for an objective factor causing wave-function collapse. These latter ones are called objective reduction (OR) theories. For example, Ghirardi et al. [18] predicted that OR would occur at a critical number (on the order of 10^{17}) of superpositioned particles.

Complementarity and entanglement are quantum-level concepts with potential explanatory power with regard to some properties of consciousness [5]. A number of prominent figures in quantum physics, including Planck, Bohr, Schrödinger, and Pauli, argued for the irreconcilability of physical determinism and conscious free-will (for reviews see [4, 31, 60]). These early physicists sometimes used terms such as entanglement, superposition, collapse, and complementarity metaphorically without defining precisely how they should be applied to specific situations in cognition. Later, approaches were proposed that described neurophysiological and/or neuropsychological processes in some detail (e. g., [54, 62, 70, 72]). In his 1999 paper, Stapp addresses potential causal interactions, raising possibility that: “conscious intentions of a human being can influence the activities of his brain”. Stapp further argues that the probabilities for eigenstates after collapse can be mentally influenced and that conscious mental events are assumed to correspond to

quantum collapses of superposition states at the level of macroscopic brain activity.

Quantum field theory has been used in a preliminary way to describe memory. Ricciardi and Umezawa [49] emphasized many-particle systems and vacuum states of quantum fields as potential memory storage devices (see also [27, 63]). This type of memory would not be accessible to consciousness without external stimuli activating a neuronal assembly, however. The activation of coherent neuronal assemblies enables a conscious recollection of the content encoded in the vacuum state. Pessa and Vitiello [47] speculate that dissipation, chaos and quantum noise generate an arrow of time for the system. This would not be a plausible mechanism for long-term memory, however, because the model gives rise to a temporally limited memory [3].

Up until John Eccles' death in 1997, Beck and Eccles applied the principles of quantum mechanics to vesicular release at the synaptic cleft, hypothesizing that quantum indeterminacy was a factor in the all-or-none quantal release of neurotransmitter (see posthumous account in Beck and Eccles [6]). Chemical synapses depend upon vesicular release of transmitters from the presynaptic terminal, and this is triggered by a nerve impulse reaching the axon terminal. Although the biochemistry of vesicular docking and exocytosis is reasonably well understood, the trigger mechanism can also be viewed in a statistical way. In the latter case, either stochastic, thermodynamics or quantum mechanics should apply. Due to the nanometer size range of most proteins or macromolecules in the presynaptic terminal, quantum processes would be expected to prevail over thermal processes and purely stochastic release is less attractive as a correlate of consciousness. Beck and Eccles built their quantum concept of a release trigger on quasiparticle tunneling, which results in a probability of exocytosis in the range between 0 and 0.7, comparable to experimental observations. Beck and Eccles relied on theory worked out by Marcus [38] and Jortner [28], who similarly modeled quantum-based electron transfer between biomolecules.

More recently, Penrose [43, 44, 45] has claimed that the underlying reality itself, namely the fundamental space-time geometry, actually bifurcates during the superposition process. This is similar to the multiple-worlds view except the separations are unstable and hence they rapidly reduce to a single, undivided reality. Classical noncomputability is a key feature of conscious processes, which may also elevate our mental processes above that of mechanistic determinism that appears grossly inadequate. In Penrose's books "The Emperor's New Mind" and "Shadows of the Mind", he claims that the phenomenon of quantum collapse can explain the features of consciousness since the spontaneous wave function collapse is what distinguishes our thought processes from the behavior of completely deterministic classical computers (for a review, see [34]). According to Penrose, consciousness involves a time-ordered series of quantum-state reductions corresponding to individual thoughts. Although such ideas are controversial, the fact

that quantum theory is being applied successfully to a new kind of computing (called quantum computing) where the collapse of multiple quantum possibilities to definite classical states is the key element lends credence to quantum approaches to consciousness. Applications of quantum physics to new modes of computation are currently being hotly pursued in the hope of finding a more powerful technology where the possibility of manipulating quantum states gives rise to the ultimate miniaturization of computer chips that would ultimately represent individual atoms or particles. While in classical computation, elementary units of information are the discrete bits (1 or 0), the basic units of quantum computation are quantum superposition states called qubits, where both 1 and 0 are represented simultaneously with arbitrary relative amplitudes. While qubits interact (or compute) with each other, they then reduce or collapse to a particular set of measurable states. Quantum computers would offer enormous potential advantages for certain applications, and prototype devices have already been constructed. Hence, comparisons involving the brain, mind, and quantum computers are logically linked and worth further investigation.

Other quantum properties of microscopic physical systems offer possible explanations of various aspects of consciousness. Because of a physical property called quantum coherence, individual particles lose their separate identity and become part of a common unit described by one wave function, as is the case with lasers where they produce optical coherence. Hameroff [24], Vitiello [69], Jibu and Yasui [27] and others have suggested this type of quantum coherence as an explanation for the unitary nature of self and the binding property in conscious experience. In nonlocal quantum entanglement, particles once unified in a common quantum state remain physically connected at a distance [17]. When one particle is measured, its quantum entangled partner particle reacts instantaneously, regardless of its location. This quantum interaction-over-distance has been proposed to provide a basis for associative memory, as well as an explanation of emotional connections between conscious individuals [73].

If validated, these speculations would indicate that biological evolution has taken advantage of quantum processes, one use being quantum computation in the brain. Indeed, modern biochemistry can easily identify molecules in the brain that operate at least partially in a quantum manner at the sub-neuronal level. Examples include various receptor proteins, enzymes, membrane lipids, presynaptic vesicle structures, gap junctions, neurotransmitter molecules, calcium ions, DNA, RNA, and microtubules and other protein filaments. The key question still remains: At what level of organization do quantum effects cease to exist, or become thermalized in a noisy system like the brain? In other words, where can we place the quantum/classical boundary? Conservative scientists argue that quantum effects are destroyed already at the level of individual molecules and ions in a thermal environment. On the other hand, advocates of quantum consciousness theories see

more highly organized and spatially extended quantum states, for example, involving a number of different microtubules in the same neuron or even in several neurons forming a coherent cluster. Penrose and Hameroff [46] have put forth a highly original model of consciousness based on quantum computation in microtubules within the brain's neurons. This and other quantum models elucidate a number of enigmatic features of consciousness; however, a few hurdles remain in establishing their likelihood. Some of these difficulties are identified when designing prototype quantum computers. One such obstacle is that quantum computers will require a high degree of isolation from decoherence effects of the local environment, or alternatively some kind of fault-tolerant architecture that permits delicate quantum computing in the presence of realistic levels of decoherence [36]. The brain operates at body temperature, its mass comprises 60 percent water, and is electromagnetically, chemically and mechanically noisy, all of which would seem to severely shorten the time allowed for quantum computation. Long-lasting, large-scale quantum states are deemed to be impossible in the brain because a single ion, photon, or thermal vibration can cause decoherence and hence random reduction to classical states. On the other hand, proponents of a quantum approach to consciousness point to a number of physical mechanisms in the brain that may lengthen the time of quantum coherence and provide necessary quantum isolation. Firstly, microtubules may be able to perform quantum computations at room temperature because basic maintenance of microtubules is energy dependent, resulting in energy being continuously pumped in and out. This situation is analogous to that of lasers, which work according to quantum optical principles at room temperature [21, 39]. Secondly, the water of hydration surrounding microtubules appears to be in an ordered state, which decreases noise [21]. Thirdly, topological error correction (in a manner similar to that of the fault-tolerant architecture described above) may protect delicate quantum states [21].

1.1.3 Quantum Processing by Microtubules and Neurocognition

It is tantalizing to pursue the idea of subneuronal information processing since information processing at the level of microtubules within each neuron would provide an enormous increase in the brain's computing power. The currently accepted scientific model suggests that consciousness arises as a result of computational complexity among the approximately 10^{11} neurons in the brain. There are on the order of 10^4 synapses per large neuron, which switch their states at a rate of some 10^3 switches per second, so that we arrive at a number of 10^{18} operations per second in the brain on average. While this is a truly huge number, it may pale by comparison with the yield given by the brain if neuronal microtubules were actively involved in computational processes. Consider that at the cytoskeletal level there are roughly 10^7 microtubule–tubulin dimers in each neuron that can switch their conformational states on the order of nanoseconds resulting in on the order of 10^{16}

operations per second per neuron or 10^{27} operations per second in an entire brain instead of 10^{18} operations per second estimated for the coarse-grained approach where neurons are taken as the smallest computational units. Moreover, if each tubulin dimer does function as a qubit and not a classical bit processor, then the computational power becomes almost unimaginably vast. It has been claimed that as few as 300 qubits have the same computational power as a hypothetical classical computer comprised of as many processing units as there are particles in the universe.

Classical flow of information along the microtubule length putatively links tubulin qubits together. Indeed, some experimental evidence shows that microtubules do propagate signals in cells, as will be discussed in this book. Moreover, several types of interactions between microtubules and membrane activities are clearly recognized. That computations are carried out by microtubule subunits may imply that one of the brain's fundamental units of information is tubulin's protein conformational state. Other processes involved in the functioning of the brain, such as ion channels opening and closing, enzymes catalyzing, motor proteins moving cargo inside cells, and the propagation of ionic waves along filaments, may be inextricably linked to, or even determined by, tubulin's conformational changes, as will be detailed later in this chapter and in various other chapters of this volume. Tubulin consumes a large amount of chemical and thermal energy in the process of microtubule assembly, and is only marginally stable. Consequently, tubulin's conformation must strike a balance in response to delicate countervailing forces. The nature of tubulin and of these complex and opposing forces may confer a functional advantage and lie at the core of microtubules being able to carry out computations by component units.

There is accumulated evidence that microtubules are computationally relevant to neurocognition. Early work by Cronly-Dillon and Perry [10] showed that neurons in the visual cortex produce massive amounts of tubulin during the critical period (from the day the eyes open to postnatal day 35). The critical period is the time during which synaptogenesis and visual learning occur at highest rates. Thus, tubulin is implicated in these developmental cognitive processes. Aging is often viewed as the counterpart of postnatal development. In this regard, Alzheimer's disease, which is accompanied by deficits in intellect, memory and consciousness, has been linked to microtubule degradation [20]. Paired helical filaments are aberrant formations resulting from hyperphosphorylated microtubule-associated protein (MAP), tau. Axonal transport is compromised in Alzheimer's disease, not unexpectedly, given that microtubules are responsible for the transport of nutrients and other important substances from the cell body to the axon terminal [57]. Microtubules have been directly linked to consciousness because they provide a nonselective mechanism for general anesthesia. Anesthetics inhibit a number of neurotransmitter receptors, but differ from receptor inhibitors by having effects on the cytoskeleton, especially actin [7, 32]. Hameroff proposes

that the most likely mechanism for general anesthetics acting upon microtubules is inhibition of electron movement within the hydrophobic pockets of tubulin dimers [23]. These oil-based hydrophobic pockets occupy approximately 1/30th to 1/250th the total volume of the protein, which works out to be less than one half of a cubic nanometer; nonetheless, these pockets control the overall protein conformation of tubulin. Moreover, the properties of these hydrophobic pockets create a suitable environment to support electron delocalization [26]. Electron motion or motility may well be the critical site of action for anesthetic gases. In the presence of an anesthetic gas, electron mobility that is required for protein conformation and quantum superposition is inhibited. Hence we should expect to see a loss of consciousness. Conversely, instead of inhibiting electron movement, hallucinogenic drugs such as LSD appear to be potent electron donors [59]. Thus, actions of both anesthetics and hallucinogens may involve alterations in electron states within hydrophobic pockets, which in turn affect the state of human consciousness.

Hameroff further proposes that microtubules are the place where reductions of quantum states can take place in an effective way [25]. Microtubules are, in theory, capable of extending coherent superposition states to adjacent microtubules by way of MAP bridges and to neighboring neurons by way of gap junctions or electromagnetic fields. The question has been raised whether quantum states can survive long enough in the thermal environment of the brain to affect neurocognition [64]. Tegmark estimated that decoherence caused by the noisy environment typical of the brain is likely to disrupt tubulin superpositions in under 10^{-12} s. Microtubule protein functions take on the order of nanoseconds; moreover, neurophysiological events range in the order of milliseconds. Hence, it was Tegmark's contention that tubulin superpositions are much too short to significantly contribute to neurophysiological processes in the brain. Hagan et al. [21] argue that Tegmark's criticism is misplaced and that the calculations he did were on a reformulation of the Hameroff–Penrose model of his own making. After adjusting to account for that error made by Tegmark, revised calculations produce decoherence times between 10 and 100 μ s, which can be extended up to the neurophysiologically relevant range of 10 to 100 ms given that the particular physical mechanisms discussed earlier come into play.

In addition to exploring the potential for quantum approaches to consciousness (including quantum field theories), this multiauthor collection of chapters will discuss alternative theories that are based on physical and mathematical principles. In particular, an entirely classical formulation of the evolution of living systems culminating in the development of awareness and self-awareness is based on the idea of emergence. Emergent phenomena abound in the natural sciences and they are characterized by a higher level of complexity resulting from an aggregation of units whose individual properties differ from those of the aggregate. It is argued that while an individual neuron may only participate in information transfer, their clusters may col-

lectively process information and clusters of neuronal clusters may achieve a yet higher level of complex behavior giving rise to the emergence of awareness eventually leading to consciousness. Indeed most accepted views within neuroscience see the brain as a nested hierarchy of information-processing subsystems. The firings of nerve cells and the transmissions between them via action potential propagation are at the bottom rung of the hierarchy – the fundamental units of information, analogous to bits in a digital computer. Unfortunately, these classical, deterministic activities, while explaining a number of neurophysiological phenomena, are unable to account for a number of key properties of conscious experience, most notably free-will, the unitary sense of self and many other enigmatic features of consciousness. Hence we may be again driven to delve more deeply inside the neuron, searching for a way to connect with the quantum level. However, most physicists would also argue that the rule of quantum effects ceases to exist in warm biological systems. Presumably that would make them unavailable to influence activities on the level of the neuron.

The challenge is to show how brain-cell firings and communication between cells may be influenced by weak and delicate, very small-scale quantum processes. To put it another way, we need to answer: At what level of organization are quantum effects required in order to explain biological phenomena? Can that level, in turn, influence activities at the neural level? The search for answers to these questions is, in a nutshell, the objective of this book. We have solicited contributions from a number of eminent scientists in the field, some very original thinkers, and several well-known science writers. We are hoping that this book will set the tone for future explorations in this field by new generations of scientists. It would be gratifying if this volume made many of its readers think about the concept of consciousness as a journey of scientific discovery.

1.2 Overview of the Contributions

We begin this volume with several experimental chapters. In the first chapter, Dick Bierman and Stephen Whitmarsh describe several recent experiments testing the subjective reduction interpretation of the measurement problem in quantum physics. These experiments investigate the proposition that consciousness acts as the ultimate measurement device, where a measurement is defined as the collapse of the statevector describing the external physical system, due to interaction with a conscious observer. To briefly summarize earlier work, auditory evoked potentials (AEPs) of subjects observing (previously unobserved) radioactive decay were recorded. The timing and peak amplitudes of these AEPs were compared with AEPs from events that were already observed and thus supposedly already collapsed into a singular state. In these earlier studies, significant differences in brain signals of the observer were found. In this chapter the authors report a further replication, which is

improved upon the previous experiments by adding a nonquantum event as a control. Unfortunately, only marginal differences were found between the quantum and classical conditions. Possible explanations for the inability to replicate the previous findings are given in this chapter as well as suggestions for further research.

Nancy Woolf discusses the role that microtubules may play in neurocognition, in particular, how neurotransmitter receptors influence microtubules and how restructured microtubule/MAP networks could provide permanent memory storage in the subsynaptic zone underlying the synapse. She reviews her experimental work demonstrating that microtubules and microtubule-associated protein-2 (MAP2) are proteolyzed with learning, as exemplified in hippocampal neurons of rats with contextual fear conditioning. Corroborating data are discussed, including results indicating the critical involvement of MAP2 in contextual fear conditioning with knockout mice deficient for the N-terminus of MAP2 [33] and results that overexpression of the MAP, tau, disrupts memory in *Drosophila* ([40]; also see Mershin et al., this volume). The role of MAP2 and microtubules in kinesin-mediated transport is also reviewed and the participation of this motility in cognition is noted. Related to the issue of transport, local storage of mRNA within neuronal dendrites raises the possibility of rapid dispatch to synapses. Microtubules and actin filaments provide the needed tracks for protein cargo to reach synapses in response to increased synaptic activation. A number of researchers have proposed that the parameters of this transport result from microtubule-based computations, as opposed to the cytoskeleton acting as a system of passive cables. A model is presented in which microtubules compute on the basis of their protein conformational states determined by the binding of MAPs and motor proteins, such as kinesin. These computations are responsible for the mobilization of specific receptors to specific sites. Rather than synapses or spines being the locus of permanent memory storage, the microtubules that carry cargo to the synapse or spine are proposed as the storage site. The overall pattern is stored at multiple neural locations, such that it can be reconstructed as the proteins involved turnover. Finally, it is argued that microtubules possess the capability of self-organization, and that through this capacity; microtubules initiate mobilization of receptors and postsynaptic density proteins to synapses on spine heads. Thus, the model is able to account for the fact that ideas can occur spontaneously and can exist independently from sensory inputs. Other chapters in this volume elaborate on the key physical properties of microtubules mentioned above; in particular, the chapter by Priel et al. is devoted to microtubule computations.

Andreas Mershin et al. in their chapter entitled “Towards Experimental Tests of Quantum Effects in Cytoskeletal Proteins” emphasize the absolute need for properly controlled and replicable experimental work if one is to take seriously any proposed quantum phenomena in biological matter, let alone consciousness. These authors detail the critical kinds of experiments that one

must devise to test hypotheses that quantum effects have a fundamental place in the phenomenon of consciousness. These authors astutely identify that the three different scale ranges to address are: (1) tissue-to-cell, (2) cell-to-protein and (3) protein-to-atom. The authors exclude experiments that aim to detect quantum effects at larger levels arguing negative results and inconsistencies. Mershin and coauthors pay particular attention to those consciousness experiments belonging to the tissue-to-cell scale frequently utilizing techniques such as electroencephalography (EEG) or magnetic resonance imaging (MRI) to track the activity of living, conscious human brains. They point to experiments by Christoff Koch's group, for example, designed to elucidate the multi- and single-cellular substrate of visual consciousness and likely to lead to profound insights into the working human brain. Nonetheless, because of the large spatial and long temporal resolution of these methods, Mershin et al. argue it is unclear whether they can reveal possible underlying quantum behavior (unless of course classical physics is obviously violated in some manner such as with nonlocality of neural firing). Mershin and co-authors argue that the second size scale that is explored for evidence of quantum behavior related to aspects of consciousness (memory in particular) is that between a single cell and a protein. They point to experimental work done by Nancy Woolf on dendritic expression of MAP2 in rats followed by significant experiments from their own laboratory on MAP-tau overexpression on the learning and memory of transgenic *Drosophila*. They argue the merits of such approaches, while specifying that it is still hard to see how experiments involving tracking the memory phenotypes and intracellular redistribution of proteins can show a direct quantum connection. These authors conclude that experimentation at the cell-to-protein size scale can at best provide evidence that is consistent with quantum consciousness. Lastly, these authors spend a great deal of time discussing the protein-to-atom scale, where quantum effects are likely to play a significant role in whole-protein function. It is at this level that the authors give an overview of their theoretical quantum electrodynamics (QED) model of microtubules and the extensive experimental work undertaken.

Alwyn Scott in his chapter entitled: "Physicalism, Chaos and Reductionism" strongly argues against the need for quantum basis of consciousness using a number of examples such as the decoherence issue. Instead, he puts forward an argument that the concept of emergence is sufficient to explain the onset of consciousness as an evolutionary development.

Stuart Hameroff, on the other hand, equally vigorously stresses the presence of connections between consciousness, neurobiology and quantum mechanics. This chapter enumerates and discusses the crucial unresolved problems in consciousness research ranging from those related to the neural correlates of conscious perception to the binding problem, to the electrophysiological correlates and their properties to the distinction between conscious and unconscious behavior and finally, to the hard problem. The author then states that prevalent approaches assume that consciousness arises from in-

formation processing in the brain, with the level of relevant detail varying among philosophical stances. Hameroff strongly disagrees that all-or-none firings of axonal action potentials (spikes) could alone account for higher brain functions. Moreover, these simple binary states are comparable to unitary information states and switches in classical computers, which may not suffice in recapitulating consciousness given that consciousness presumably emerges from nonlinear dynamics of neuronal networks. Hameroff further argues that conscious states are sculpted by the modulation of electrochemical synapses and form metastable patterns identified with conscious experience (e.g. [16, 55]). Hameroff applies his analogy to a nonliving robot, and argues that if a robot were precisely constructed to mimic the brain activities, which modern neuroscience assumes to be relevant to consciousness, then the robot would be conscious regardless of its material basis. Lastly, Hameroff presents an overview of the elegant Orch OR model he and coauthor Roger Penrose have been working on over the last decade. Hameroff provides support for his own model, which has had a major impact on current thinking in consciousness studies, and goes on to further define the need for quantum approaches to consciousness studies.

Christopher Davia in his chapter entitled: “Life, Catalysis and Excitable Media: A Dynamic Systems Approach to Metabolism and Cognition” examines how life maintains its organization and describes an entirely novel principle that unites all living processes, from protein folding to macroprocesses. Davia’s hypothesis is that the same excitable media principle applies at every scale: living processes involve catalysis, biological processes mediate transitions in their environments, and enzymatic reactions act accordingly. By pinpointing enzyme catalysis as a prototypical process, Davia identifies energy dissipation as playing a major role in biology. Possible mechanisms contributing to excitable media are identified, including solitons and traveling waves, nondissipative and robust waves, all of which maintain their energy and structure in their biologically relevant environments. Particular emphasis is placed upon the relationship between microscopic instances of catalysis and traveling waves in excitable media. Pertinently to the topic of this volume, it is suggested that the brain is an excitable medium, and that cognition and possibly consciousness correlate with the spatiotemporal pattern of traveling waves in the brain. Davia offers this theory as an alternative to the functionalist perspective that underlies much of current theoretical biology. A key strength of his theory is that the same principle applies at multiple scales, potentially explaining how many biological processes that comprise an organism work and cooperate.

Avner Priel, Jack Tuszyński and Horacio Cantiello, discuss the biophysical model representing the dendritic cytoskeleton as a computational device. This chapter presents a molecular dynamical description of the functional role of cytoskeletal elements within the dendrites of a neuron. These authors present the working hypothesis that the dendritic cytoskeleton, which

includes both microtubules and actin filaments, plays an active role in computations affecting neuronal function. Critical to their model is the assumption that cytoskeletal elements are affected by, and in turn regulate, a number of processes inside the neuron. Ion channel activity, MAPs and other cytoskeletal motors such as kinesin, for example, are viewed in terms of their interface with microtubules. Priel and coauthors go on to advance the novel and specific hypothesis that it is the C-termini protruding from the surface of a microtubule, existing in several conformational states, which lead to collective dynamical properties of the neuronal cytoskeleton. From a physics point of view, these collective states of the C-termini on microtubules have a significant effect on the ionic condensation and ion-cloud propagation. This is similar to what has been found recently for actin filaments. The authors provide an integrated view of their model using a bottom-up scheme. They marshal considerable evidence to support their model of ionic wave propagation along cytoskeletal structures impacting on channel function and computational capabilities of whole dendrites and entire neurons. The theoretical approach advanced in this chapter is conceptually consistent with the experimental evidence put forth by Nancy Woolf in her chapter.

Laxmidhar Behera and colleagues develop a theoretical brain model using a nonlinear Schrödinger equation. In the general scope, their model proposes the existence of a quantum process that mediates the collective response of a neural lattice representing the classical brain. The specific example used in their model is eye movements when tracking moving targets. By using a recurrent quantum neural network while simulating the quantum brain model, the authors find two novel phenomena. The first is that eyesensor data are processed in the classical brain, while a wave packet is triggered in the quantum brain. The second is that when the eye tracks a fixed target, the wave packet moves in a discrete mode, with jumps and rest periods reproducing experimental observations very accurately. These authors have accomplished a great deal and offer a very interesting theoretical development that combines the robustness of classical approaches with the quirkiness of quantum theories.

Elizabeth Behrman and her collaborators present a mathematical model of microtubules as a quantum Hopfield neural network. The motivation behind this work is the suggested existence of quantum computation in microtubule protein assemblies inside living cells as proposed by Hameroff and Penrose. The authors set up their equations within the constraints of a quantum Hopfield network with qubits representing tubulins interacting electrostatically by Coulomb forces. Simulations presented in this work focus on the existence of stable states, such as local minima, of the network. The authors report quantum information processing in microtubules is feasible, though at temperatures much lower than physiological temperatures. They conclude that microtubules can be used as information storage devices but not as quantum information devices at physiological temperatures.

Gordon Globus, in his chapter entitled “Consciousness and Quantum Brain Dynamics” argues that the opposition to quantum brain theory is deconstructed. The author refers back to quantum brain theory originated by Umezawa and coworkers, reiterating the differences between unimode quantum brain dynamics (QBD), a Hermitean-dual mode QBD and a non-Hermitean dual-mode QBD. Globus argues that unlike the non-Hermitean version, the Riemann hypothesis offers a unique approach. This chapter is rich in philosophical discussion and traces interesting connections to advanced mathematics.

Johnjoe McFadden outlines conscious electromagnetic field theory (CEMI) revealing seven clues to the nature of consciousness. The author argues that if consciousness is an epiphenomenon then, as scientists, we must turn aside and leave the topic to the philosophers and theologians to make sense of. However, consciousness does generate observable phenomena and thus belongs to the realm of empirical science. One undeniable example is that consciousness has had a major impact on the lives of philosophers, scientists and theologians who have studied the subject. In his chapter, McFadden examines the seven clues to the nature of consciousness and discusses how the conscious electromagnetic field theory (CEMI field theory) makes sense of them. As McFadden cogently argues, any successful theory of consciousness needs to include a physical mechanism enabling our conscious mind to interact with the matter of our brain.

Chris King, through the use of quantum cosmology addresses the hard problem of the conscious brain. The author explores a model resolving many aspects of the hard problem in consciousness research through cosmic subject-object complementarity. King’s model combines a number of mathematical topics, including: transactional quantum theory, chaos, and fractal dynamics. These serve as a basis for a direct relationship between phase coherence in global brain states and anticipatory boundary conditions in quantum systems, which complement conscious perception and intentional will. King’s aim is to describe unusual physical properties of excitable cells, which may form a basis for the evolutionary selection of subjective consciousness.

Paola Zizzi ambitiously deals with the issue of consciousness and logic in a model of a quantum-computing universe. The universe is described at various stages. The early inflationary universe is seen as a superposed state of quantum registers. In the end, at the close of the inflationary period, one universe is selected out of a superposition of many by a self-reduction mechanism. This kind of reduction is similar to Penrose’s objective reduction (OR) model; moreover, it depends on gravity and can be numerically specified in terms of quantum registers (10^9 quantum registers). Zizzi then draws an analogy between the very early quantum-computing universe and our mind. Zizzi argues that events at the end of inflation of the universe (the so-called “Big Wow”) acted to indelibly imprint on future minds to come, dictating future modes of computation, consciousness and logic. From this point on, the uni-

verse organized itself according to two computational modes: quantum and classical, like the two conformations assumed by the cellular automaton of tubulins in our brain, as in Hameroff's model. Zizzi speculates that the universe uses, as subroutines, black holes – quantum computers and quantum minds, which operate in parallel. He further suggests that the outcomes of the overall quantum computation are universal attributes endowed with subjective meaning. In other words, qualia are related to Planckian black holes. The author then considers two aspects of the quantum mind that are not algorithmic in the usual sense: the self and mathematical intuition. Zizzi argues the self corresponds to a self-measurement of a quantum state of superposed tubulins and that mathematical intuition is due to the consistent pattern of logic of the internal observer in a quantum-computing universe.

1.3 New and Notable Developments

In accordance with suggestions made in this book, it is imperative first to unequivocally demonstrate both theoretically and experimentally that quantum interactions exist at the atomic/molecular level. Only then is it possible to credibly build up to mesoscopic and macroscopic dimensions. One need not look to phenomena that are exceedingly difficult or impossible to measure to assess possible quantum level involvement. Electromagnetic and electrochemical energies are known to exist in neurons. Increased transport of proteins and receptors is likely to have an electromagnetic basis to the extent that this function is a result of microtubule computations. Electromagnetic events in the form of individual photons obey the principles of quantum mechanics and thus potentially bring with them intriguing phenomena such as wave propagation, wave interference, quantum entanglement, and collapse of the wave function.

1.3.1 An Electromagnetic Fingerprint of Transport Along Microtubules

Each chapter in this volume presents a viewpoint or model that provides a unique window into how a biophysical state might correlate with higher cognition. The perspective advanced in this introductory chapter is that a specific fingerprint defined by a particular electromagnetic state of a microtubular array potentially corresponds to a unique unit of cognition (e.g., a basic visual parameter, a sound, an irreducible idea, a morpheme, etc.). Recently, it has been shown that visual components can be represented musically [11]; hence the idea that there is one common type of energy underlying divergent percepts or qualia appears likely. Activation of one electromagnetic fingerprint could, in turn, activate another electromagnetic fingerprint, irrespective of sensory input. Thus, the model is able to account for the stream of consciousness and the fact that ideas self-perpetuate with their existence

becoming increasingly abstract and independent from sensory inputs over time. Lastly, the subjective feels of this widespread pattern of electromagnetic energy can be specified according to those key physical properties of microtubules that influence the transport of proteins to synapses. Factors influencing kinesin-mediated transport include the protein conformation of tubulin and the nature of the C-termini (see [58]; Priel et al., this volume).

Not only is the protein conformation of tubulin critical to effective transport, motor proteins appear to alter the conformation of tubulin. Kinesin binding and that of the low molecular weight MAP, tau, significantly alter the direction of the protruding protofilament ridges along microtubules, which in turn influences their further binding abilities [52]. More than mere local adaptation to binding, microtubules may alter their conformation ahead of kinesin processivity [35], supporting the notion of long-range cooperative effects between tubulin dimers located along longitudinal protofilaments of microtubules. These biochemical relationships have consequences for electromagnetic fields. The dipole moment of tubulin depends on its configuration in the microtubule [21, 39, 40]. Thus, electromagnetic fields (and possibly quantum coherence) among microtubules could, in theory, be induced or inhibited by synaptic inputs that affect the protein conformation of tubulin directly or through alterations in kinesin or MAP binding. Synaptic effects upon microtubules could be mediated through ionic currents, by propagation via actin filaments [68], or by signal transduction cascades resulting in the phosphorylation of MAPs [51].

Due to lengthwise electric dipoles of tubulin dimers, information in the form of traveling waves propagated along microtubular tracks can, in principle, be transmitted between synapses with high fidelity [67]. MAP2 bridges keep microtubular arrays within the dendritic core parallel and antiparallel by aligning portions of polarized microtubules. The antiparallel alignment of microtubules, which specifically occurs in dendrites, would severely attenuate any electromagnetic field generated by microtubules, at least under baseline conditions. However, during enhanced kinesin-mediated transport, as is likely to occur with heightened synaptic activity, MAP2 bound to the microtubule would be perturbed and may even temporarily detach from the microtubule. A similar phenomenon might also occur due to dynein-mediated transport, which occurs largely in the opposite direction to that of kinesin-mediated transport. Assuming that at least some MAP2 stays attached to the antiparallel microtubules, keeping the dendritic array intact, any net unidirectional transport along the microtubule array (via oppositely directed kinesin and dynein motors traveling on oppositely directed tracks) should increase the strength of the electromagnetic field associated with the fingerprint and should further result in the spread of that electromagnetic field to adjacent microtubules. Once a sufficient number of microtubules were engaged in dynamically sending and receiving complementary electromagnetic energies, whole neuronal compartments (e.g., dendrites) might be expected

to interact. Due to the parallel/antiparallel arrangement of microtubules in cortical dendrites and the ability of electromagnetic fields to pass from one dendrite to adjacent dendrites, information could, in principle, pass between neurons when such electromagnetic fields were sufficiently amplified as a result of changes in the binding of MAPs or kinesin. Quantum effects at the level of electron movement across an energy barrier in a hydrophobic pocket of tubulin can be related to electromagnetic waves traveling down microtubules because the hydrophobic pocket determines the overall conformation of tubulin and the overall conformation of tubulin regulates its binding to kinesin and MAPs and thus its ability to transport.

Due to their topographical arrangement, one can build the argument that electrochemical synapses are unlikely candidates for permanent storage of information. The electrochemical synaptic wiring of the brain is an enormously complex network, or is it? Viewed another way, the system is massive, but nonetheless built upon a simple principle that is redundantly executed. Each cortical area provides a highly organized representation of each part of a sensory field (e.g., visuotopic, tonotopic, somatotopic, etc.). This topographic representation is carried over to the next higher sensory field (e.g., from V1 to V2; from A1 to A2). One might imagine a cartoon of the entire cerebral cortex as multiple video monitors, each of which faithfully represents the sensory field from which all information supplying that area ultimately derives. While it is true that there are some 20 billion neurons and some 100 trillion synapses in the human cerebral cortex, so too does each sensory field afford the luxury of extremely high resolution. The fovea of the retina, for example, contains roughly 1 million receptor cells that relay information to the cerebral cortex, diverging to eventually drive the synaptic activity of at least 1 billion cortical cells. So the mammalian cortex has many neurons, and even more synapses; nonetheless, its connectivity can be readily grasped by one recurrent theme, repetitive high-resolution topographic representation. Despite this simple organizational plan, cells in cortical areas, in particular cells in higher sensory or association areas, inexplicably show correlated responses during cognitive tasks. Does this mean that activity at electrochemical synapses is the sole basis? Not necessarily so. An idea that has been around a long time, and has not been ruled out, is that electromagnetic events in neurons contribute in an important way. Our best imaging techniques to date do not distinguish electrochemical from electromagnetic activities in neurons. Both types of events require metabolic energy. Moreover, the two types of activities are likely to induce each other, although these interactions may be highly filtered.

One can also construct the argument that synaptic activity is less likely to be available to perceptual awareness than are quantum-level intracellular events in brain microtubules. Experience alters the basic structure of dendrites, and as a consequence, would also alter any electromagnetic fields generated by microtubules as a result of transport proteins moving along them. As described in the beginning of this chapter, a rearrangement of the

cytoskeleton occurs during early development, with learning, and with neurodegeneration underlying dementia. Listed below are five arguments against changes in efficacy for electrochemical synapses, alone, being responsible for permanent memory.

1. The topographic organization of virtually all cortical circuits, exemplified by the visual cortex, is largely one of point-to-point representation of labeled line sensory fields, with only a very small percentage of divergently projecting neurons [56]. This organization scheme is predominantly vertical; information from a specific part of a sensory MAP projects to a vertical minicolumn of cortex and then to a higher vertical minicolumn of cortex, and so on [41]. With the possible exception of local pericolumnar inhibition, cortical spread of information along the horizontal axis may not be as widespread as would be needed to account for widely interconnected neural network models. Strictly synaptic models (electrochemical) suggest complex neural networks increase synaptic weights (i. e. neurons that fire together wire together). Nonetheless, visual cortical regions do not have massively random interconnections among all parts of the visuotopic map, thereby making many of the changes in synaptic efficacy necessary for encoding complex perceptual features impossible.
2. Probabilistically speaking, no stimulus is ever going to activate the same set of electrochemical synapses twice. Visual stimuli, for example, are never exactly the same distance away, presented at exactly the same angle, or strike exactly the same part of the retina. Nonetheless, to activate a memory, as in perceptual recognition, one needs to have a critical degree of matching between the stimulus input and the pattern of change in synaptic efficacy. It is unlikely that the critical degree of matching would be met in the vast majority of cases. In the case of storage by a fingerprint electromagnetic wave, however, future inputs need not directly activate circuits responsible for storage. There is more flexibility in finding a match to new inputs, because electromagnetic waves can, in principle, pass from microtubule to microtubule and from dendrite to dendrite.
3. We perceive the world differently from the actual inputs. There are countless examples: fill-in phenomena, attentional distortion and masking. As we view any stationary scene, our eyes quickly make saccadic movements. Yet we perceive the scene as stationary, and not darting about [50]. Current neural networks rely on top-down information to account for this; yet it is not clear how a network of cells connected according to a strict topography would be able to generate a concept such as stationarity.
4. Although models of changes in synaptic efficacy, e. g., long-term potentiation or depression (LTP or LTD), offer great potential as memory mechanisms [37], one often overlooked problem is that large numbers of synapses are affected in concert. If only a few synapses exhibited LTP or LTD with each learning experience, then the entire cortical system

might have a near unlimited capacity, but since many synapses are affected by LTP, there appears to be a serious ceiling effect. Explanations such as, a large number of synapses are potentiated initially but only a few synapses remain permanently altered, still fail to account for the fact that we are able to process new stimuli immediately after learning. This means that potentiated synapses most likely participate in unrelated perceptual tasks.

5. Changes in the size and shape of synaptic spines following learning appear to be temporary, according to experimental observations [42]. This perhaps leaves us without much in the way of a biological correlate for permanent memory storage. The model presented here suggests that temporary changes in synaptic efficacy, which occur with learning or LTP, immediately induce permanent electromagnetic storage in the neuronal cytoskeleton, although that is fine tuned or expanded during memory consolidation. If, as predicted, the classical electromagnetic waves transmitted by microtubules, furthermore, bear a relationship to electron movements in the hydrophobic pockets of tubulin, then quantum entanglement provides a nearly unlimited storage capacity for associations.

The biophysical properties of microtubules are just beginning to be understood at the molecular and atomic levels and recent empirical evidence suggests quantum-based interactions occur between microtubules, at least under certain experimentally induced conditions. Two groups, one led by Watt Webb at Cornell and another led by Paul Campagnola and William Mohler at the University of Connecticut, observed that microtubules give rise to intense second-harmonic generation, a frequency doubling upon exposure to a sapphire laser in the 880 nm range. (Other frequencies were partially effective.) Microtubules were one of the few biological materials having electric dipoles that constructively interfered with the dipoles of neighboring microtubules [9, 12]. This occurred for parallel microtubules in axons, but not for antiparallel microtubules in dendrites. This could be interpreted as a rudimentary kind of experimental evidence for quantum coherence among adjacent microtubules, because second-harmonic generation is a nonlinear quantum optics phenomenon. Webb noted that: “In sound waves, we can hear the second harmonic of a vibrating guitar string when the guitar body resonates and produces a tone twice as high in pitch as the original tone. The same thing happens with light waves, although no one knew it until lasers were invented, when a laser beam hits certain kinds of materials in our bodies.”

Could such a phenomenon be expected to occur with natural learning or upon exposure to oscillatory input, an LTP-inducing tetanus or various pharmacological agents? To the extent that these induce electromagnetic energy, it is conceivable. In addition to being sensitive to electromagnetic radiation, microtubules may themselves produce this kind of energy. Second-harmonic generation by microtubules is consistent with their ferroelectric properties.

Materials with ferroelectric properties, i. e. exhibiting spontaneous symmetry breaking with respect to electrical polarization, are perhaps ideal for quantum computing and consciousness. Microtubules are implicated as generators of quantum electromagnetic radiation for the following reasons:

1. Materials that are nonlinear optically exhibit second-harmonic generation: microtubules are a salient example.
2. In second-harmonic generation, the most strongly enhanced wavelength is 880 nm, supporting the frequently overlooked reports of electromagnetic signaling by cells. Guenther Albrecht-Buehler [1] observed electromagnetic energy in the near-infrared region overlapping the 880 nm value that was generated by centrioles for the purpose of cell-to-cell communication, leading him to suggest that: “... one of the functions of microtubules may be to play the role of cellular ‘nerves’”. Infrared light in this range of wavelengths also induces cell aggregation [2]. Since frequency (and hence wavelength) determines the long-range effect of dielectric polarization of a given microtubule, one would expect this effect to be length dependent just as the length of the guitar string determines the values of the harmonics. The distance between microtubules was shown to be critical in second-harmonic generation by microtubules.
3. Parallel orientations of microtubules in axons support frequency doubling, yet antiparallel orientations in dendrites do not. This may make sense in view of axial orientation of the net polarization vector. Whether this supports quantum coherence is not entirely clear. In principle it may, because this may be an example of a quantum of electromagnetic radiation propagating in a nonlinear medium. However, the medium (i. e. the microtubule) is not itself in a coherent state. That state is created by external means (i. e. by sending infrared radiation) and maintained as a coherent state. In other words, it is an induced coherent state. Moreover, it remains to be shown what holds true for living neurons that communicate with other neurons, with respect to the language of coherent states.
4. The role of motor proteins in this phenomenon may be crucial. The nonlinear polarized state of the microtubule depends on the conformations of tubulins, which depend on the interactions with kinesins, dyneins, and other motors. Microtubules may support a coherent state induced in them by external means depending on the conformational states. This may, in turn, regulate consciousness states.

1.3.2 Extrapolations to Mesoscopic and Macroscopic Levels

If quantum-mechanical properties of atoms can affect the behavior of whole proteins through the influence of electromagnetic waves, wave interference, and quantum entanglement, does this introduce the possibility of quantum nonlocal relationships at larger scales? There is some empirical evidence suggesting this may be possible.

A number of studies have been done using Faraday cages. These cages effectively block electromagnetic radiation. Hence correlations between electrophysiological activity in cells or in human subjects in different Faraday cages might be attributable to manifestations of quantum coupling or entanglement, bearing in mind that alternative explanations are possible.

Cultures of dopamine-containing ventral tegmental area cells derived from human stem cells and grown on circuit boards demonstrate an unusual non-local phenomenon that is not accounted for by classical physics [48]. Stimulating one culture with a 630 nm laser results in maximal levels of cross-correlational activity between the stimulated culture and another culture kept separate and shielded. Both cultures share the same nonlinear response properties. This effect is only seen in cells that derive from the same source. Thaheld [65] has proposed additional experiments to determine if there are Einstein–Podolsky–Rosen (EPR) nonlocal correlations between two neuron transistors. These experiments, which allude to quantum interactions in the whole brain, have the potential to explain a number of neural phenomena, including the binding problem, massively parallel searches, and associative memory.

It was during the mid-1990s that the first experiment was conducted indicating that a quantum nonlocal relationship might exist between the brains of different individuals [19]. Photostimulation causing a visual evoked potential (VEP) in one subject shielded in a Faraday cage, corresponded with a potential possessing a similar brain wave morphology in the brain of the nonstimulated subject located several meters away in another Faraday cage. This so-named transferred potential has been variously supported in some, but not all, subject pairs reported in the literature [61, 71]. Thaheld [66] has recently reviewed the earlier literature.

1.4 Conclusions

A number of authors in this book propose that quantum computing plays a role in human consciousness, although the counterview is also represented. A large number of contributors provide various arguments for microtubules being pivotal to consciousness, in particular, because they may well form the central nervous system of the cell. Quantum computations in microtubules, or in other brain proteins, may be a viable tenet, but how does the scientific community proceed to prove or disprove such an idea? Secondly, how does one extrapolate from essentially biophysical studies on brain proteins to assessments of higher cognitive functions in individuals alone or in groups? Within a single brain or mind, one might imagine that nonlocal quantum interactions occur in relation to neural connections or electromagnetic waves linking different neurons or brain areas. Considering small groups of individuals or large societies, we again have classical communication of information between individuals and the genetically determined similarity of neural tissue

within the species. The resulting nonlocal phenomena may provide the basis for social psychological effects, such as emotional connection and empathy, as well as for group dynamics, such as polarization and unanimity. Both the nonlocal quantum effects and psychological effects described here are subtle, yet very real effects.

We hope that in assimilating these chapters we have posed some relevant questions and begun to address them.

Acknowledgement. The authors wish to thank the following individuals: Angela Lahee for encouragement, Adele Behar and Mike Weiner for constant support, Stuart Hameroff and Al Scott for inspiration and friendship, and Fred Thaheld for suggestions.

References

1. Albrecht-Buehler, G. (1998). *Cell Motil Cytoskeleton* **40**:183–192.
2. Albrecht-Buehler, G. (2005). *Proc Natl Acad Sci USA* **102**:5050–5055.
3. Alfinito, E., and Vitiello, G. (2000). *International Journal of Modern Physics B* **14**:853–868.
4. Atmanspacher, H. (2004). *The Stanford Encyclopedia of Philosophy* (Winter 2004 Edition), Edward, N. Zalta (ed.) <http://plato.stanford.edu/archives/win2004/entries/qt-consciousness/>.
5. Atmanspacher, H., Römer, H., and Walach, H. (2002). *Foundations of Physics* **32**:379–406.
6. Beck, F. and Eccles, J.C (2003). In: *Neural Basis of Consciousness*, N. Osaka (ed.), Benjamins, Amsterdam:141–165.
7. Bjornstrom, K., Eintrei, C. (2003). *Acta Anaesthesiol Scand.* **47**:157–164.
8. Bohm, D. (1990). *Philosophical Psychology* **3**:271–286.
9. Campagnola, P.J., Millard, A.C., Terasaki, M., Hoppe, P.E., Malone, C.J., Mohler, W.A. (2002). *Biophys. J.* **82**:493–508.
10. Cronly-Dillon, J. and Perry, G.W. (1979). *Journal of Physiology* **293**:469–84.
11. Cronly-Dillon, J., Persaud, K., Gregory, R.P. (1999). *Proc Biol Sci* **266** (1436):2427–33.
12. Dombeck, D.A., Kasischke, K.A., Vishwasrao, H.D., Ingesson, M., Hyman, B.T., Webb, W.W. (2003). *Proc Natl Acad Sci USA* **100**:7081–7086.
13. Everett, H. (1957). *Reviews of Modern Physics*:29.
14. Flohr, H. (1995). *Behav Brain Res.* **71**:157–61.
15. Flohr, H. (2000). In *Neural Correlates of Consciousness. Empirical and Conceptual Questions*, T. Metzinger (ed.), MIT Press, Cambridge:245–258.
16. Freeman, W.J., Kozma, R., Werbos, P.J. (2001). *Biosystems* **59**:109–123.
17. Fröhlich, H. (1968). *International Journal of Quantum Chemistry* **2**:641–649.
18. Ghirardi, G.C., Rimini, A., Weber, T. (1986). *Physical Reviews D* **34**:470–491.
19. Grinberg-Zylberbaum, Delaflor, M., Attie, L., Goswami, A., (1994). *Phys. Essays* **7**:422–428.
20. Gundersen, G. (1997). *Biomed. Front.* **4**, Special Section.

21. Hagan, S., Hameroff, S.R., and Tuszynski, J.A. (2002). *Phys. Rev. E* **65**:061901–1 to -11.
22. Hameroff, S. (1998a). In: *Toward a Science of Consciousness II: The Second Tucson Discussions and Debates* (eds.) Hameroff, S.R., Kaszniak, A.W. and Scott, A.C., Cambridge, MA: MIT Press:421–437.
23. Hameroff, S. (1998b). *Toxicol Lett.* **23**:31–9.
24. Hameroff, S. (2001). *Ann. N Y Acad Sci.* **929**:74–104.
25. Hameroff, S.R., and Penrose, R. (1996). *Journal of Consciousness Studies* **3**:36–53.
26. Hameroff, S. and Tuszynski, J. (2002). *Biosystems* **64**:149–168.
27. Jibu, M., and Yasue, K. (1995) *Quantum Brain Dynamics and Consciousness*. Benjamins, Amsterdam.
28. Jortner, J. (1976). *Journal of Chemical Physics* **64**:4860–4867.
29. Jung, C.G., and Pauli, W. (1955) *The Interpretation of Nature and the Psyche*. Pantheon, New York. Translated by P. Silz. German original *Naturerklärung und Psyche*. Rascher, Zürich, 1952.
30. Kandel, E.R., Schwartz, J.H., and Jessell, T.M. (2000). *Principles of Neural Science*. McGraw-Hill, New York.
31. Kane, R. (1996) *The Significance of Free Will*. Oxford University Press, Oxford.
32. Kaech, S., Brinkhaus, H., Matus, A. (1999). *Proc Natl Acad Sci USA* **96**:10433–10437.
33. Khuchua, Z., Wozniak, D.F., Bardgett, M.E., Yue, Z., McDonald, M., Boero, J., Hartman, R.E., Sims, H., Strauss, A.W. (2003). *Neuroscience* **119**:101–111.
34. Klein, S. (1995). *Psyche* **2** <http://psyche.cs.monash.edu.au/v2/psyche-2-03-klein.html>.
35. Krebs, A., Goldie, K.N., Hoenger, A. (2004). *J Mol Biol.* **335**(1):139–53.
36. Knill, E. (2005). *Nature* **434**:39–44.
37. Malenka, R.C., Bear, M.F. (2004). *Neuron* **44**:5–21.
38. Marcus, R.A. (1956). *Journal of Chemical Physics* **24**:966–978.
39. Mershin, A., Kolomenski, A.A., Schuessler, H.A., Nanopoulos, D.V. (2004a). *Biosystems* **77**:73–85.
40. Mershin, A., Pavlopoulos, E., Fitch, O., Braden, B.C., Nanopoulos, D.V., Skoulakis, E.M. (2004b). *Learning and Memory* **11**:277–287.
41. Mountcastle, VB. (2003). *Cereb Cortex* **13**:2–4.
42. Murphy, K.J., Regan, CM. (1998). *Neurobiol Learn Mem* **70**:73–81.
43. Penrose, R. (1989). *The Emperor's New Mind*. Oxford University Press, Oxford.
44. Penrose, R. (1994). *Shadows of the Mind*. Oxford University Press, Oxford.
45. Penrose, R. (2001). *Ann. N Y Acad Sci.* **929**:105–110.
46. Penrose, P. and Hameroff, S. (1996). *Math Comp. Sim.* **40**:453–480.
47. Pessa, E. and Vitiello, G. (2003). *Mind and Matter* **1**:59–79.
48. Pizzi, R., Fantasia, A., Gelain, F., Rosetti, D., Vescovi, A. (2004). In: *Quantum Information and Computation II. Proceedings of SPIE 5436*, (eds.) Donkor, E., Pirick, A., Brandt, H.:107–117.
49. Ricciardi, L.M., and Umezawa, H. (1967). *Kybernetik* **4**:44–48.

50. Ross, J., Morrone, M.C., Goldberg, M.E., Burr, D.C. (2001). *Trends Neurosci.* **24**(2):113–21.
51. Sanchez, C., Diaz-Nido, J., Avila, J. (2000). *Prog Neurobiol.* **61**(2):133–68.
52. Santarella, R.A., Skiniotis, G., Goldie, K.N., Tittmann, P., Gross, H., Mandelkow, E.M., Mandelkow, E., & Hoenger, A. (2004). *Journal of Molecular Biology* **339**:539–553.
53. Schrödinger, E. (1935) *Naturwiss.* **23**:807, translated to English in: Quantum Theory and Measurement, (eds.) J.A. Wheeler and W.H. Zurek, Princeton Univ Press (1983).
54. Schwartz, J.M., Stapp, H.P. and Beauregard, M. (2005). To appear in *Phil. Trans. Royal Society, Biol.*
55. Scott, A.C. (1995). *Stairway to the Mind*. Springer-Verlag, New York.
56. Sincich, LC, Horton, JC. (2003). *J Neurosci.* **23**:5684–5692.
57. Sisodia, S.S. (2002). *Science* **295**:805–807.
58. Skiniotis, G., Cochran, J.C., Muller, J., Mandelkow, E., Gilbert, S.P., Hoenger, A. (2004). *EMBO J.* **23**:989–999.
59. Snyder, S.H., Merril, C.R. (1965). *Proc Natl Acad Sci USA* **54**:258–266.
60. Squires, E. (1990). *Conscious Mind in the Physical World*. Adam Hilger, Bristol.
61. Standish, L.J., Kozak, L., Johnson, L.C., Richards, T., (2004). *J. Alter. Compl. Med.* **10**(2):307–314.
62. Stapp, H.P. (1999). *Journal of Consciousness Studies* **6**:143–164.
63. Stuart, C.I.J., Takahashi, Y., and Umezawa, H. (1978). *Journal of Theoretical Biology* **71**:605–618.
64. Tegmark, M. (2000). *Physical Review E* **61**:4194–4206.
65. Thaheld, F.H. (2000). *Apeiron* **7**:202–205.
66. Thaheld, F.H. (2004). *Neuroscience Lett.* **360**:178.
67. Tuszyński, J.A., Brown, J.A., Hawrylak, P. (1998). *Philos. Trans. R. Soc. London Ser. A* **356**:1897.
68. Tuszyński, J.A., Portet, S., Dixon, J.M., Luxford, C., Cantiello, H.F. (2004). *Biophys J.* **86**:1890.
69. Vitiello, G. (2002). In *No Matter, Never Mind*, (eds.) K. Yasue, M. Jibu, and T. Della Senta, Benjamins, Amsterdam:43–61.
70. von Neumann, J. (1932) *Mathematischen Grundlagen der Quantenmechanik*. Springer, Berlin. English translation (1955) Mathematical Foundations of Quantum Mechanics. Princeton University Press, Princeton.
71. Wackermann, J., Seiter, C., Keibel, H., Walach, H., (2004). *Neurosci. Lett.* **336**:60–64.
72. Wigner, E.P. (1977). *Hellenike Anthropostike Heaireia*, Athens, pp. 283–294. Reprinted in Wigner's Collected Works Vol. VI, J. Mehra (ed.), Springer, Berlin, 1995:584–593.
73. Woolf, NJ, Hameroff, S.R. (2001). *Trends Cogn Sci.* **5**:472–478.

2 Consciousness and Quantum Physics: Empirical Research on the Subjective Reduction of the Statevector

Dick J. Bierman and Stephen Whitmarsh

Summary. There are two major theoretical perspectives on the relation between quantum physics and consciousness. The first one is the proposal by Hameroff and Penrose [16] that consciousness arises from the collapse of the statevector describing nonconscious brainstates. The second perspective is the proposition that consciousness acts as the ultimate measurement device, i.e. a measurement is defined as the collapse of the statevector describing the external physical system, due to interaction with a conscious observer. The latter (dualistic) proposition has resulted in the thought experiment with Schrödinger's cat and is generally considered as extremely unlikely. However, that proposition is, under certain assumptions, open to empirical verification. This was originally done by Hall et al. [15]. A refined experiment to test the "subjective" reduction interpretation of the measurement problem in quantum physics was reported by Bierman [3]. In the latter experiment, auditory evoked potentials (AEPs) of subjects observing (previously unobserved) radioactive decay were recorded. These were compared with AEPs from events that were already observed and thus supposedly already collapsed into a singular state. Significant differences in brain signals of the observer were found. In this chapter we report a further replication that is improved upon the previous experiments by adding a nonquantum event as control. Differential effects of preobservation were expected not to appear in this classical condition since the quantum character of the event is presumed crucial. No differential effects were found in either condition, however. Marginal differences were found between the quantum and classical conditions. Possible explanations for the inability to replicate the previous findings are given as well as suggestions for further research.

2.1 Introduction

2.1.1 The Measurement Problem

In the quantum-mechanical theory of (e.g. radioactive) emission from a single atom, a nucleus (or equally true, a collection of nuclei) is regarded as being in a superposition of an "undecayed" state and a "decayed" state. The Schrödinger evolution of quantum states does not place hard restrictions on ascribing this superpositioned state to the entire composite system of nuclei and their measuring apparatus. This gives rise to the "Schrödinger's cat" thought experiment:

"A cat is penned up in a steel chamber, along with the following device (which must be secured against direct interference by the cat): in a Geiger counter there is a tiny bit of radioactive substance, so small, that perhaps in the course of the hour one of the atoms decays, but also, with equal probability, perhaps none; if it happens, the counter tube discharges and through a relay releases a hammer which shatters a small flask of hydrocyanic acid. If one has left this entire system to itself for an hour, one would say that the cat still lives if meanwhile no atom has decayed. The psi-function [the wave packet] of the entire system would express this by having in it the living and dead cat (pardon the expression) mixed or smeared out in equal parts." [26]

Of course we don't perceive the world as composed of superpositioned states; so although the theory of quantum mechanics lets us predict the indeterminate behavior of (superpositioned) particles on the microscopic scale with remarkable accuracy, the same theory cannot account for the fact that we do get definite determinate results when a measurement is undertaken. An additional projection postulate has to be introduced. Schrödinger continues:

"It is typical of these cases that an indeterminacy originally restricted to the atomic domain becomes transformed into macroscopic indeterminacy, which can then be resolved by direct observation."

When, for instance, we observe a Geiger counter (or when we open Schrödinger's box and take a look) the superpositioned states seem to have been collapsed into a singular state (the cat is either dead or alive). The Schrödinger evolution does not account for this transition, leaving the different quantum states evolving in a superpositioned state described by a statevector. However, when the possible states of a physical system are known, these can be described as a wave packet¹, making possible the calculations of encountering the quantum system in a certain state (using Born rules). Measuring a property (e.g. magnetic momentum or "spin") of this quantum system, will lead to the discovery of a certain value of this property (e.g. "spin up") corresponding to one of the superpositioned quantum states. The value is then ascribed to the system – the projection postulate –, which somehow seems to have been transitioned into a singular state. This transition from a quantum to a singular state, has been termed the "collapse of the wave packet" and it has been a problem ever since. This problem that for some time could be hidden by assuming that the statevector represented our "lack of knowledge" rather than an actual and real state of affairs became explicit after Bell showed that not only our knowledge but also the physical situation of a system actually changed upon measurement. What constitutes a measurement thus has become an extremely important question. Many attempts have been made to

¹ We use the terms "wave packet" and "statevector" both as referring to the superposition of potential outcomes.

remove the measurement problem, like the relative-state interpretation [11], leading to exotic proposals as the bare theory [1, 2], the many-worlds interpretation [9], the many-minds theory [1] and the many-histories theory [13]. Hidden variables are introduced in bohmian mechanics [6, 4] giving a deterministic character to quantum physics, while substituting the measurement problem with a preparation problem. None of these attempts including the many attempts to introduce nonlinearity in the quantum formalism [14], with an automatic collapse as a consequence have received universal acceptation. This failure to clearly resolve the problem has left the physics community polarized with some contending the problem remains a fundamental shortcoming in the quantum formalism and others holding that there is no reduction of the wave packet at all [5, 8]. Costa de Beauregard [7], Walker [28–30] and later Stapp [24] have argued, using arguments provided by, among others, von Neumann [27] and Wigner [31], that none of these solutions are acceptable and that subjective reduction is still a possible and even preferred alternative.

2.1.2 Objective Reduction and Consciousness

Most mainstream physicists assume that relating consciousness to quantum physics is an example of supposing a relation between two not well understood phenomena just because both are not well understood. Although this might often be the case in the popular literature there are two noteworthy exceptions. They are noteworthy because both proposals do result in testable predictions. And interestingly both are related to the measurement problem.

Penrose [20, 21] proposed an objective reduction, in which the difference between the superpositioned states, expressed in space-time gravity, determines the moment of wave-packet reduction. He even goes as far as proposing that our minds are capable of sustaining and selectively collapsing superpositioned states – coined orchestrated objective reduction (Orch OR) – giving rise to, among others, noncomputable properties of conscious experience. In other words the conscious experience is a consequence of the “collapse” of the statevector describing the nonconscious brain states preceding a conscious moment. The idea here is that nonconscious processing utilizes quantum computing and is highly parallel in nature, while the conscious moments are like the outcomes of the preceding quantum computing. This model has been attacked on several grounds. First, it seems not to fit well with the traditional chemical models of brain functioning that until now seem to describe processes underlying mental events rather satisfactorily. Secondly, the proposal that coherent quantum events do play a fundamental role in the warm and wet environment of the brain has met a lot of opposition. However, ultimately any theory should be tested against empirical findings and the Orch OR model makes several testable predictions (see other chapters in this volume).

In the same vein the second “subjective reduction” proposition that consciousness is “external” to physics and plays the crucial causal role in the

collapse of the statevector can be tested empirically. Like Hall et al. [15], we do not wish to quarrel theoretically about positions with regard to the proper interpretation of the quantum formalism and the role of measurement therein, but instead we would like to investigate the issue experimentally.

2.1.3 Previous Empirical Work on Subjective Reduction

In 1977, Hall, Kim, McElroy and Shimony addressed the measurement problem of quantum physics in an experimental way, investigating the rather radical proposal of subjective reduction. Stating

“that the reduction of the wave packet is a physical event which occurs only when there is an interaction between the physical measuring apparatus and the psyche of some observer”

they proposed a dualistic ontology in which mental entities interact with the physical world, leaving both changed and consequently subjectable to scientific scrutiny. In the Hall experiment, particles of a gamma emitter were detected and fed into two scalars, A and B, the latter getting a slightly delayed signal with respect to the first (see Fig. 2.1). The observation of a radioactive decay by a subject on one of the scales will supposedly collapse the wave packet into the “decayed” state. When the decay has first been observed on scalar A and subsequently, after a short delay, by a different subject on scalar B, the latter is supposed to observe a then already singular state. Hall designed his experiment so that sometimes scalar A is observed before scalar B, and sometimes scalar A is not observed at all, leaving the

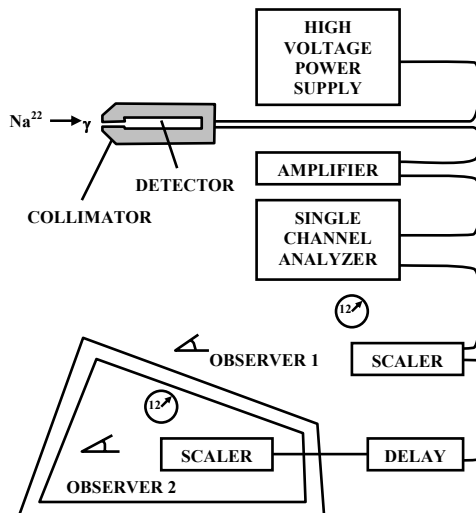


Fig. 2.1. Hall's experiment

superpositioned state to be collapsed only by observing scalar B. The subject at scalar A was asked to sometimes look at the scalar, and sometimes look the other way. Of the subject at scalar B (the final observer) he asked to report if he/she thought that he/she was observing a quantum or a singular state. The comparison between both subjects revealed a 50% (chance) agreement. It was concluded that the experiment did not provide support for the hypotheses that it is the interaction with consciousness that causes the wave packet to collapse.

However, the authors did not only assume that (i) the interaction of the psyche of an observer with the physical apparatus is responsible for the reduction of the wave packet, but also assumed (ii) that there is a phenomenological difference between making an observation that is responsible for the reduction of a wave packet and making one that is not. The second assumption led the authors to an implicit third assumption, namely (iii) that this difference can be communicated consciously.

In 2003, Bierman further tested the hypothesis of subjective reduction. He noted that if consciousness is expected to collapse the wave packet (i), a conscious report will be based on the physical state of the wave packet after consciousness has developed. At that time, he presumed, the wave packet will already be collapsed even if no preobservation has taken place at all.

In Hall's arrangement, the delay between the first and the second observer was a very short one ($1\mu\text{s}$). Hall himself noted in the discussion of his article that it might be argued

“that the $1\mu\text{s}$ delay of the pulse to B's scalar does not suffice for A to be unequivocally responsible for the reduction of the wave packet in case both of them make observations.”

Stated otherwise, the short time delay between the pre- and second observer may not give the preobserver enough time to experience the quantum event consciously, not leading to the collapse of the wave function, before the second observation occurs. Bierman noted that according to Libet [18] it takes far more time for an observation to be experienced consciously (300–500 ms), and designed his experiment accordingly. In this experiment, instead of asking the second observer for a consciously given report of the state of the observed event, his/her EEG was measured. This measurement made it possible to tap into the preconscious experience of the subject, yielding objective measures of the (possibly but not necessarily phenomenological) experience (ii) of the quantum event before consciousness develops. This bypasses the inherent weakness of Hall's design (iii). Also, the time delay between the two observers was increased, far beyond Libet's interval, to 1000 ms (1 second), giving the preobserver ample time for conscious experience before the second observer comes into play. See Fig. 2.2 for a conceptual presentation of both experiments.

The results of Bierman's [3] experiment were very promising. The differences in the ERP traces of the two preobserver conditions reached statistical

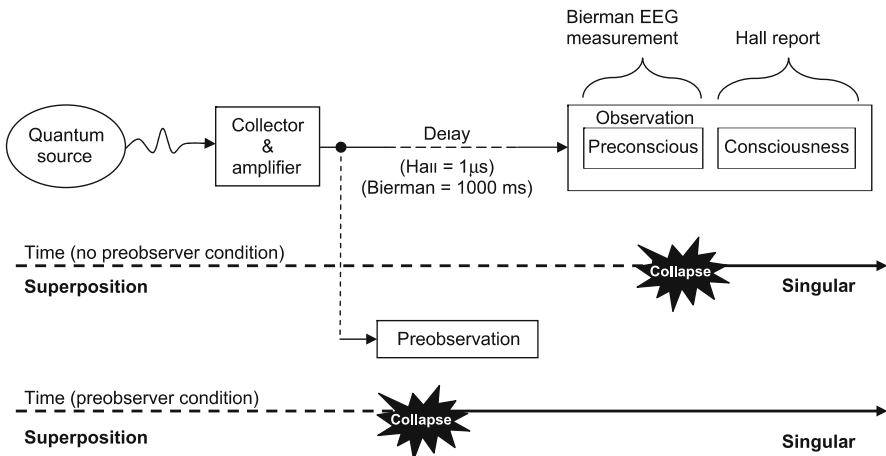


Fig. 2.2. Design and timeline of the Hall experiment in which conscious report always occurs at the already singular state, and the Bierman experiment with a preconscious measurement in superposition time

significance on three of the ten analyzed peaks. Namely, the N20 ($p = 0.043$), P40 ($p = 0.013$) and N200 ($p = 0.0005$), at exactly 17, 41 and 212 ms after the onset of the stimulus. The author permitted himself to draw the following two preliminary conclusions:

“(1) With regard to the signal from frontal and central leads there is a significant difference between the conditions in the very early peaks. This difference is gone after about 100 milliseconds. (2) On the parietal leads the difference is into the other direction and arises later with a clear maximum at 200 milliseconds. The results seem to support a solution of the measurement problem that gives a special status for conscious observation in the measurement process. Furthermore, the absence of significant differences in the late evoked potentials appears to be in line with the fact that in the original Hall experiment no differences were found when one asked the second observer to consciously express his feeling if the observed quantum event had already been observed. This finding should, however, be treated cautiously because of the lack of statistical power in the later phases of the response. This lack of power is caused by the increased variance with increasing latency times...” (pp. 53–54).

The possibility of sensory cueing of the second observer should be considered. This was the reason behind Bierman’s use of different modalities for presenting the quantum event. While the first observer was observing a visual representation, the second observer was hearing an *audio* beep through a headphone. Although both observers were in different rooms, these were adjacent and not auditorily or electromagnetically shielded. Ultrasonic or elec-

tromagnetic signatures from the monitor displaying the signal to the first observer might still have presented sensory cues to the final observer.

Although Bierman's results look pretty robust, they are not extremely improbable in terms of statistics. As the author himself noted, one may argue that the reported p values might be inflated due to the analysis of 10 peaks without applying a Bonferroni correction for multiple analyses. Although peak N200 will easily survive this correction, as the author duly remarks: "*strong claims need strong evidence*".

2.1.4 Current Investigation

The current experiment will further investigate the possibility of subjective reduction. We will compare events originating from a pseudorandom classical source with quantum events. *We expect to have the differential EEG effect found in Bierman's [3] experiment to appear in the latter but to disappear in the former condition as the quantum character of the event is presumed crucial.*

In Bierman's experiment [3], the analysis was cautiously restricted only to peak amplitudes. Of these peaks, the effect was strongest in the first 200 ms after stimulus presentation, specifically at N20, P40 and the N200. Our primary analysis will be focused on these peaks. More explicitly, only in the quantum condition do we expect the peak amplitudes of N20 and P40 to be increased and the N200 to be decreased in the non-preobserver condition with respect to the preobserver condition. We expect no significant differences in (any) peak amplitudes for the classic event trials. In our investigation of the *role of consciousness in the collapse of the wave function*, our independent variables will thus be the classical/quantum source, and the preobserver condition. Our dependent variable will be the final observer's auditive evoked potential (AEP) as measured by EEG on the scalp (see Fig. 2.3). We expect to find a difference between the preobserver conditions only for the quantum trails (AEP III minus AEP IV).

	No preobserver	Preobserver
Classical event	<i>Final observer AEP I</i>	<i>Final observer AEP II</i>
Quantum event	<i>Final observer AEP III</i>	<i>Final observer AEP IV</i>

Fig. 2.3. Dependent (italic) and independent (bold) variables

2.2 Experimental Design

The current design is schematically depicted in Fig. 2.4. Quantum events will be generated by an alpha particle source (as used in smoke detectors; 2P40-76-18), mounted on a slider that allows the source to be moved with

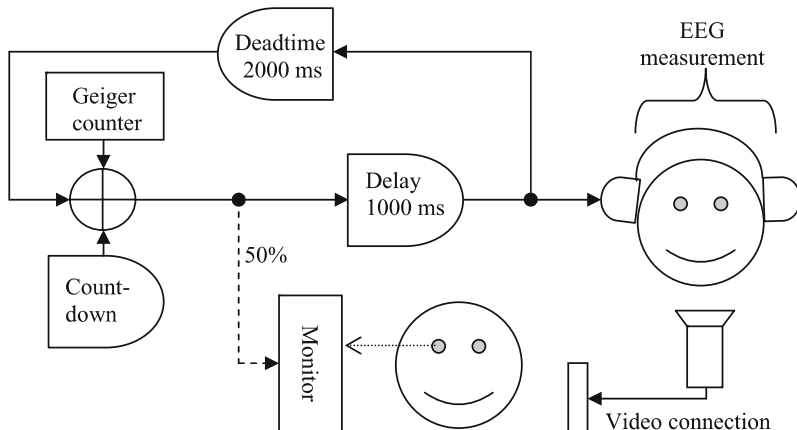


Fig. 2.4. Experimental design. Note that the separated locations of the subjects are not shown. The crosshair depicts the alternating choice of quantum/classical event (absent in [3])

respect to a Geiger–Muller counter (Automess 6150-100). The distance is set so that on the average 1 particle about every 1.2 s will be detected. The counter pulse is then amplified and fed to the trigger channel of an EEG data acquisition system (*Biosemi Active-2*, 2003). *National Instruments LabView* software (NI, 2003) is used to detect this trigger and to transform it, after a delay of 1000 ms, into a 1500-Hz audio beep of 50 ms duration. It is followed by a subsequent delay (dead time) of 2000 ms. The software will randomly, on 50% of the trials, generate a visual stimulus of 65 ms duration *directly* upon the trigger. The visual stimulus therefore precedes the audio beep by a time (1000 ms) sufficient for the first observer for consciously experiencing the quantum event *before* the second observer. Both subjects will be asked to count the number of observed (quantum and classical) events.

For simulating the radioactive decay in a classical way we reasoned that computer processes could also be affected by quantum-mechanical principles. This will make the classical attribution of the processor's internal randomizer questionable. So instead of simulating radioactive decay by using the internal randomizer, we recorded the radioactive decay, in milliseconds, continuously for some time using the exact same experimental constellation as would be used in the actual experiment. Forty time-till-next-decay's were thus measured and put into a table (see Table 2.1).

The random decision to show the visual stimulus to the first observer, before submitting the beep to the second observer or not, is pseudorandom with the seed determined by the computer clock. The argument of a possible quantum character of the randomizer does not apply here as it is a condition *within* a quantum/classical condition, not between. Following from our postulate, (pre-)observing will always collapse the wave function, also when

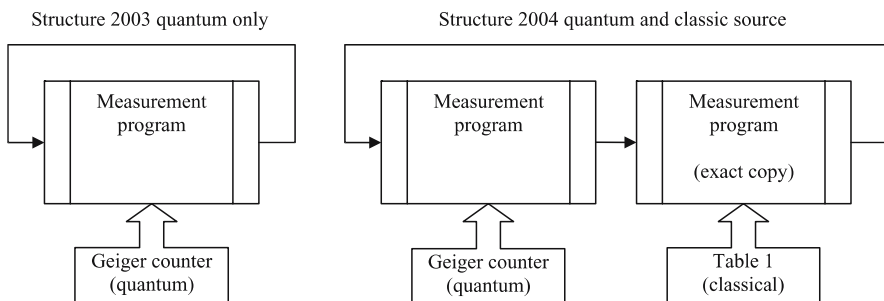
Table 2.1. Decay times in milliseconds

21	825	860	829
836	62	534	4564
1005	252	1161	2323
1703	1806	403	920
2096	1207	1824	1614
18	5302	1394	958
644	569	87	673
3477	535	305	171
421	163	264	2455
181	912	4809	1485

it is prior decided to occur by quantum probabilities. Should the randomizing create a quantum superposition of prepresentation/no prepresentation (of the quantum or classical event to the preobserver), this will occur in both classical and quantum condition and will not explain a resistant *differential AEP effect*.

After each quantum event measured there is a dead time of 2000 ms during which the input of the Geiger–Muller counter will be discarded and after which a countdown starts with the time delay as indicated by Table 2.1. Upon the generation of this singular event, *exactly the same procedure as for the quantum event* will be followed. The sequence of quantum/classical event is thus alternating in which the table is read successively. Randomizing the occurrence of these conditions was considered. We wanted, however, to replicate the previous [3] experiment as accurately as possible. By using this setup, the classical condition could be an almost exact copy of the quantum condition. The Geiger–Muller input had only to be replaced by the table of decay times. See Fig. 2.5 for a conceptual visualization. We think this setup approaches a more formal replication.

The video connection (see Fig. 2.4), as was already implemented in Bierman's experiment, will again be used in the current experiment. Were this

**Fig. 2.5.** Illustration of internal program structure

visual connection not made, a transfer of information (e.g. by selectively collapsing the wave function by the preobserver resulting in a difference in brain potentials of the second observer – an instant Morse code) could transgress the light cone, violating the relativity theory.

2.3 Experimental Procedure

2.3.1 Subjects

Volunteer subjects were invited in pairs. They were generally freshman psychology students who participated for course credit. In total, 10 males and 53 females participated in the experiment providing useful data. One subject was removed from the analysis due to improper recording of the brain signals. The roles of observers 1 and 2 were played by both subjects in two separate runs.

2.3.2 Physiological Measurement

Thirty-four sintered AgCl EEG electrodes (consisting of 32 leads and 2 reference electrodes) with active preamplifiers (*Biosemi Active 2*) are connected to the head of observer II using the standardized 10/20 system (Electrocap, see Appendix 1) for placement details. EEG recordings (2048 Hz sample rate) are made using *National Instruments LabView* software (NI, 2003). The subject is then seated into a relaxing chair and given pneumatic earphones (Earlink; Aearo Company Auditory Systems). The experimenter and the other subject then leave the room.

2.3.3 Further Procedure

First, a short “calibration” experiment is run consisting of an oddball task in which observer II is presented with an audio beep of 30 ms duration for every 3 s (with one second random jitter). One hundred beeps with either a frequency of 1200 Hz or a frequency of 2000 Hz will be presented. The choice of frequency is randomly determined with the probability for the higher frequency being 20%. The subject will be asked to count these higher-frequency beeps. When the task is finished the experimenter asked for the number of beeps counted.

The “Schrödinger” run will be started with observer I sitting in front of a computer screen in the experimenter’s room, observing the visual stimulus. The experimenter refrains from looking at the screen. The total run consists of 65 radioactive decay events and an equal amount of computer-generated events. This takes about 12 min. Afterwards both subjects will be asked about the number of events they witnessed. After a short break the roles will be switched and the procedure repeated. The total experiment takes less than 1.5 h, including the preparation of the subjects.

2.4 Data Analysis

First, a 50-Hz notch filter is applied. Then the data are filtered through a bandpass filter between 1 and 45 Hz (slopes = 24 Db/Oct). The data are then downsampled to 256 Hz (as the original 2048 Hz will only slow down computing). The data are then manually inspected for noneye artifacts after which the data are separated into segments ranging from 2000 ms before until 1000 ms after stimulus presentation. Those segments that contained manually selected artifacts are ignored and excluded from further analysis. This segmentation retains the maximum of valid EEG data (see Fig. 2.2) for the subsequent ICA algorithm.

The ICA algorithm² is thus run over as much data as possible. In our case this is the segmented data in which only noneye artifacts were removed. No separation into conditions is yet made. The ICA algorithm then starts “learning” in the sense of *unsupervised competitive learning*, eventually coming up with the best solution for explaining the signal in independent components. This results in a component-electrode weight matrix. It is then up to the experimenter to determine which components originate from eye blinks or eye movements. This is quite easily done after some practice, by comparing the components with the actual EEG trace and by mapping the components onto a head model. However, when the EEG trace is only minimally disrupted by eye artifacts, the algorithm will not always return suitable components as the variance, that will be explained by such components, will be small compared to more dominant sources. This is also the reason that large noneye artifacts must first be (manually) removed as they can take on a large part of the total variance. The more eye artifact, then, the better the ICA algorithm will be able to identify their source. To finally clean up the signal, the weights of these components on the electrodes are made zero and the EEG trace is

² Independent component analysis in the experiment. No electrodes for recording eye blinks or eye movements (saccades) are used. Instead, ICA, a recently developed technique for performing blind-source separation, will be applied. The ICA algorithm is highly effective at performing source separation in domains where (1) the mixing medium is linear and propagation delays are negligible, (2) the time courses of the sources are independent, and (3) the number of sources is the same as the number of sensors; that is, if there are N sensors, the ICA algorithm can separate N sources [19]. In our case, we assume that the recorded signals are mixtures of brain signals and artifact signals from eye blinks and eye movements. Since volume conduction is thought to be linear and instantaneous, assumption (1) is satisfied. Assumption (2) is also reasonable because the sources of eye activity are not generally time locked to the sources of EEG activity. Assumption (3) could be somewhat questionable when ICA is used for identifying an unknown number of sources. In our case, however, ICA is only used to extract known sources of interference from eye blinks and eye movements. For this purpose ICA has been shown to preserve and recover more brain activity than regression and principal component analysis (PCA) [17].

then again composed by linear derivation of the remaining components and the ICA matrix.

To remove those subjects that contributed most to noise in the total average, crosscorrelations between the individual average AEP and the total average AEP signal (of all subjects) will be computed. Subjects that correlate low ($r < 0.80$) will be excluded from further analysis. The data are then segmented and averaged per condition, after which a baseline correction (250 ms till 0 ms before stimulus) is applied over all segments. In Bierman [3] the electrodes were combined in a *frontocentral* (C3, C4, Cz, F3, F4, F7, F8, Fp1, Fp2, Fz) and a *parietal* (P3, P4) pool. As our data acquisition was done with a different number of electrodes (32 instead of 16), a different pooling will be used. Combinations will be formed on the basis of correlations between electrode signals in the oddball task. Per pooling, the peak latencies of the average of all conditions are determined. These latencies are used to measure and compare the peak amplitudes of the different conditions.

2.5 Results

We calculated the correlations between all electrodes and decided to create four pools, namely a *frontal* (AF3, AF4, F7, F8, Fp1, Fp2), *frontocentral* (F3, F4, FC1, FC2, Fz), *parietal* (C3, C4, CP5, CP6, FC5, FC6, T7, T8) and *occipital* pool (CP1, CP2, O1, O2, Oz, P3, P4, P7, P8, PO3, PO4, Pz). All electrodes within one pool correlated at least 0.90. The crosscorrelation indexes between the individual average AEP signals and the total average AEP signal (of all subjects) are plotted in Fig. 2.6. All those subjects with a correlation index r smaller than 0.80 were removed from further analysis. This resulted in the removal of 15 subjects in the oddball task (leading to an average $r = 0.90$ with 48 subjects instead of $r = 0.85$ with 63 subjects) and 15 subjects in the Schrödinger task (leading to an average $r = 0.90$ with 49 subjects instead $r = 0.86$ with 64 subjects). All subjects reported a close approximation of the number of beeps (give or take 5). The ICA algorithm

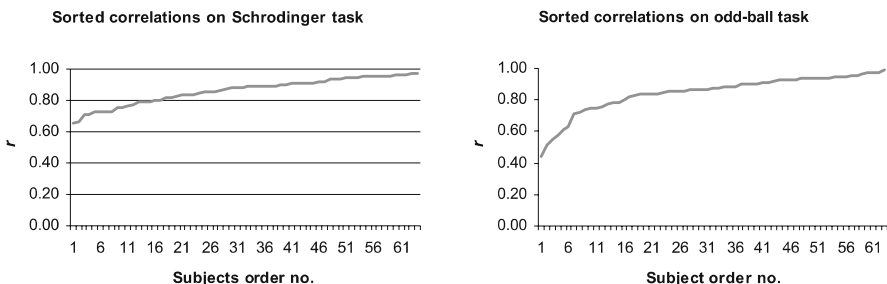


Fig. 2.6. Correlation of subject's AEP trace with average AEP over all subjects. Note that the subjects are sorted by ascending correlation index r

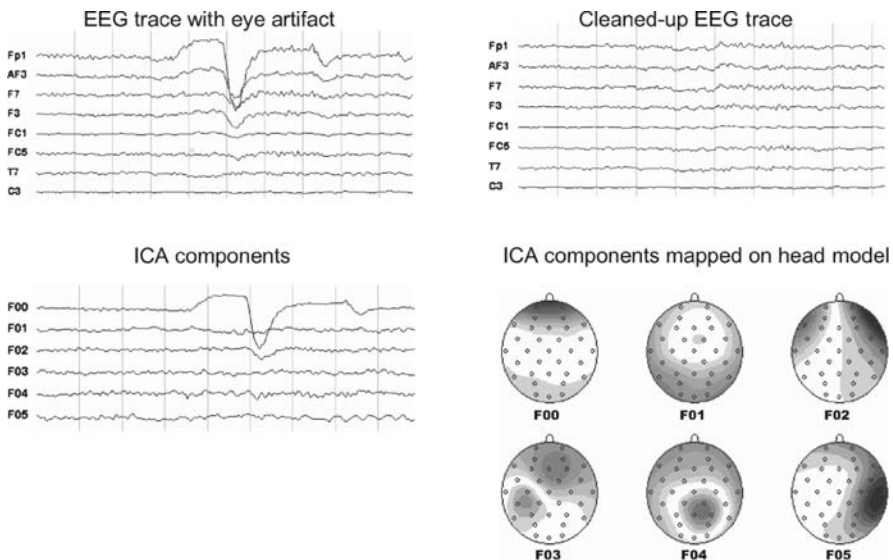


Fig. 2.7. An example of removing eye artifact with ICA

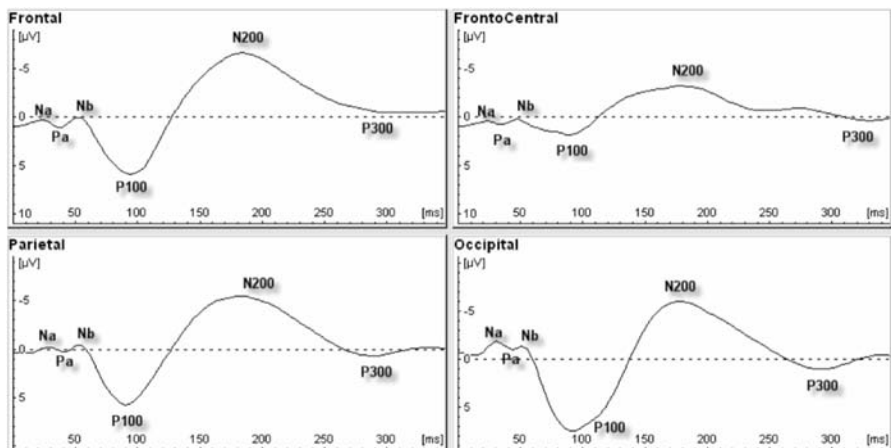


Fig. 2.8. Peaks of the average of all conditions

resulted in nicely cleaned-up signals. See Fig. 2.7 for an example from the data (pp16, segment 25).

The peak latencies of the AEP trace, as measured from the average of all conditions, are shown in Fig. 2.8 and Table 2.2. In Table 2.2, the amplitudes on those latencies of the quantum and classical preobserve conditions are also compared.

The amplitudes of the AEP traces on these latencies were determined per condition. All four conditions are overlaid in Fig. 2.9.

Table 2.2. Peak latencies (in milliseconds), amplitudes and differences (both in μV) of all conditions per pooling

	Peaks	Latency	I	II	I-II	III	IV	III-IV
<i>Frontal</i>	Na	23	-0.181	-0.169	-0.012	-0.175	-0.395	0.220
	Pa	39	0.536	0.757	-0.221	0.426	0.545	-0.119
	Nb	51	-0.502	-0.321	-0.181	-0.681	-0.44	-0.241
	P100	94	4.901	5.281	-0.380	5.800	5.65	0.150
	N200	184	-7.266	-7.335	0.069	-7.137	-6.748	-0.389
	P300	301	-1.131	-1.036	-0.095	-0.679	-0.933	0.254
<i>FrontoCentral</i>	Na	23	-0.134	-0.021	-0.113	-0.088	0.031	-0.119
	Pa	35	0.522	0.402	0.120	0.149	0.183	-0.034
	Nb	47	-0.300	-0.198	-0.102	-0.450	-0.175	-0.275
	P100	90	1.064	1.195	-0.131	1.565	1.445	0.120
	N200	180	-3.819	-3.646	-0.173	-3.841	-3.542	-0.299
	P300	332	0.000	-0.056	0.056	-0.294	-0.119	-0.175
<i>Parietal</i>	Na	27	-0.396	-0.434	0.038	-0.475	-0.515	0.040
	Pa	39	0.005	0.137	-0.132	-0.013	0.056	-0.069
	Nb	55	-0.802	-0.601	-0.201	-0.747	-0.549	-0.198
	P100	90	5.208	5.415	-0.207	5.584	5.632	-0.048
	N200	184	-5.957	-6.019	0.062	-5.468	-5.528	0.060
	P300	289	0.309	0.189	0.120	0.596	0.737	-0.141
<i>Occipital</i>	Na	31	-1.444	-1.534	0.090	-1.599	-1.384	-0.215
	Pa	43	-0.829	-0.639	-0.190	-0.666	-0.467	-0.199
	Nb	51	-1.146	-0.894	-0.252	-0.943	-0.795	-0.148
	P100	90	7.543	7.990	-0.447	7.425	7.81	-0.385
	N200	180	-5.707	-5.362	-0.345	-5.908	-5.373	-0.535
	P300	293	1.173	1.249	-0.076	1.322	1.833	-0.511

Differences of amplitude on the peaks between the preobserve conditions were tested for statistical significance using a standard t-test. The results are shown in Table 2.3.

We also did an explorative analysis of the differences between the AEP from the quantum source and the classic source. No differentiation was made between the (pre-) observed states. The results are shown in Fig. 2.10, Fig. 2.11 and Table 2.4.

2.6 Conclusions

No significant differences were found between peak amplitudes of the auditory evoked brain potentials when a quantum event was first observed and when it was observed for the second time. A difference of the N20, P40 (frontal leads) and N200 (parietal leads) was expected on the basis of Bierman's [3] results. To replicate these results, care was taken to minimize differences in experimental setting and data analysis. Some technical differences were made, though, so one could question if they could account for our inability to replicate the previous findings.

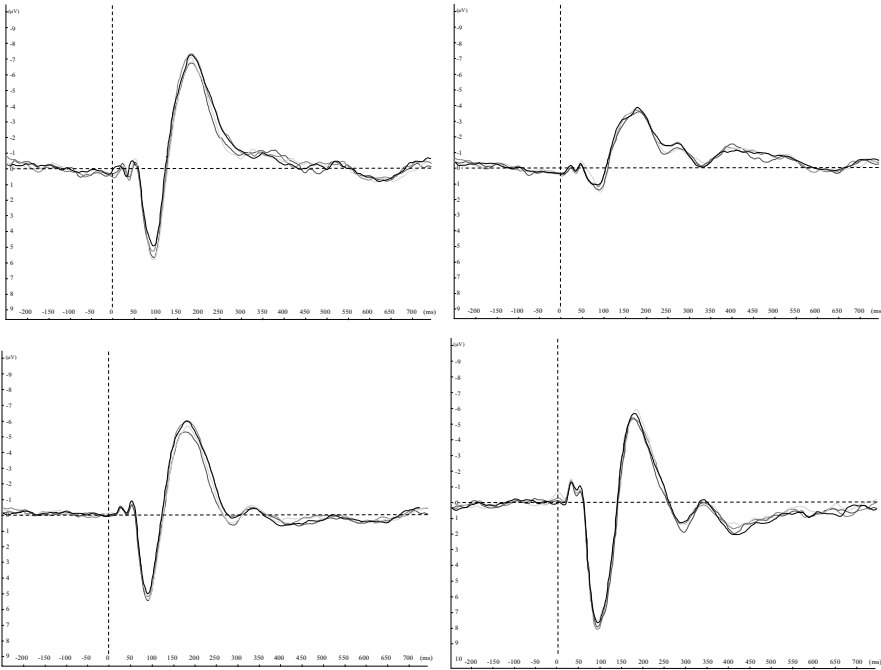


Fig. 2.9. The individual curves shown represent: classic, classic preobserved, quantum and quantum preobserved cases, respectively

First, in order to reduce the total variance, quite a few subjects were removed from the analysis by comparing individual traces with the total average of all subjects. Subjects that correlated low were supposed to be noisy. One could argue, however, that the sought-for effect is only manifest in a minority of subjects who would therefore differ from the total average and be erroneously removed from analysis. We regard this as improbable because the difference would more likely consist of noise from bad recordings rather than of real signal. To be sure, however, we applied the same analysis on the 15 rejected subjects. We found no significant brain signal differences between the preobserved and non-preobserved conditions.

Secondly, instead of removing all data that was confounded by eye artifacts, we used the ICA algorithm to subtract the artifact from the EEG trace and therefore retained almost all of the recorded data. It remains difficult to assess which of the two procedures removes most of the error variance. A smaller error variance would of course result in larger p values. However, if we focus on effect size rather than p value we observe that the amplitude differences in the current study are about 40% of the values obtained earlier [3]. It is unlikely that amplitudes are systematically affected differently

Table 2.3. T-tests of differences of AEP peak amplitudes for pre- and non-pre-observed conditions

		I-II (Classic)			III-IV (Quantum)		
	Peaks	t	df	p 2-tailed	t	df	p 2-tailed
<i>Frontal</i>	Na	-0.060	49	0.952	0.736	49	0.465
	Pa	-0.892	49	0.377	-0.435	49	0.665
	Nb	-0.674	49	0.503	-0.961	49	0.341
	P100	-1.284	49	0.205	0.386	49	0.701
	N200	0.145	49	0.885	-1.364	49	0.179
	P300	-0.255	49	0.800	0.778	49	0.440
<i>FrontoCentral</i>	Na	-0.816	49	0.418	-0.589	49	0.559
	Pa	-0.798	49	0.429	-0.218	49	0.828
	Nb	-0.482	49	0.632	-1.264	49	0.212
	P100	-0.531	49	0.598	0.417	49	0.678
	N200	-0.742	49	0.462	-1.519	49	0.135
	P300	0.198	49	0.844	-0.799	49	0.428
<i>Parietal</i>	Na	0.101	49	0.920	0.296	49	0.768
	Pa	-0.485	49	0.630	-0.178	49	0.859
	Nb	-0.862	49	0.393	-0.636	49	0.528
	P100	-0.886	49	0.380	-0.212	49	0.833
	N200	0.246	49	0.807	-1.451	49	0.153
	P300	0.385	49	0.702	-0.537	49	0.594
<i>Occipital</i>	Na	0.261	49	0.795	-0.712	49	0.480
	Pa	-0.616	49	0.541	-0.68	49	0.500
	Nb	-0.890	49	0.378	-0.503	49	0.617
	P100	-1.474	49	0.147	-1.021	49	0.312
	N200	-1.052	49	0.298	-1.598	49	0.116
	P300	-0.417	49	0.678	-1.419	49	0.162

by the two procedures. However, we cannot exclude the possibility that the “collapse” effect is in some way included in the eye-artifact components and thus (erroneously) removed.

There were also three differences that might have had a conceptual consequence.

- Firstly, the presentation of the beeps by loudspeakers was replaced by air-pressure headphones. In our view it is not likely that this could account for a different response from the (post-) observer. It should be noted though, that the preobserver in the previous experiment [3] could remotely hear these beeps and thus the formal description in terms of observation was different.
- Secondly, in Bierman’s [3] experiment the subjects were made fully aware of the video connection between the two rooms. Therein care was taken that the preobserver made some glances at the video monitor to ensure

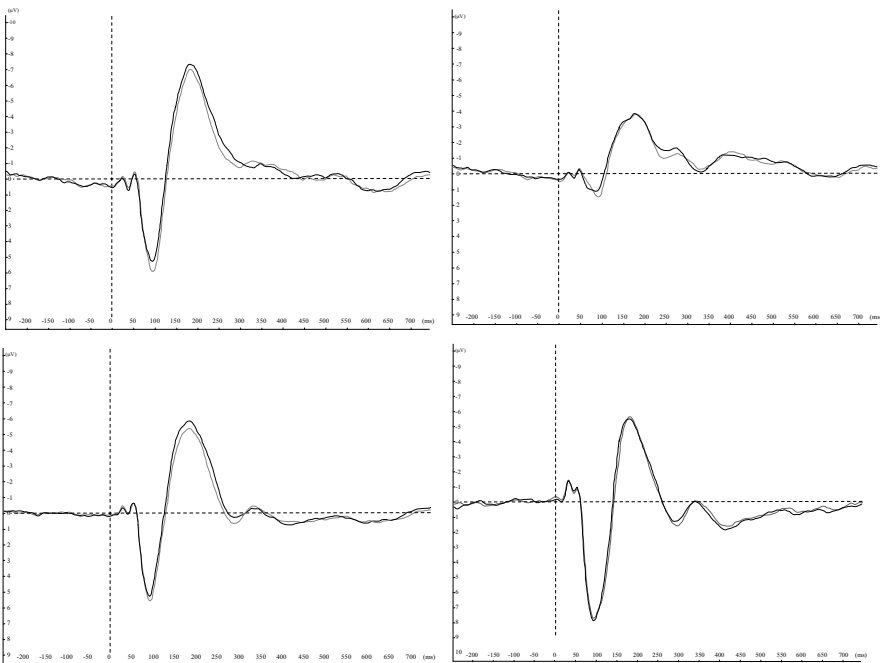


Fig. 2.10. The two curves shown represent classic and quantum cases, respectively



Fig. 2.11. Difference wave of AEP of quantum (pre- and not preobserved) and classic (pre- and non-preobserved) origin with t values overlaid shown in the curve that has a greater amplitude

Table 2.4. Differences of AEP peak amplitudes from the quantum and classic sources

	Peaks	II+IV	I+III	(II+IV)-(I+II)	t	df	p 2-sided
<i>Frontal</i>	Na	-0.287	-0.182	-0.105	-0.503	49	0.617
	Pa	0.485	0.642	-0.157	-0.808	49	0.423
	Nb	-0.554	-0.416	-0.138	-0.683	49	0.498
	P100	5.725	5.074	0.651	2.697	49	0.010
	N200	-6.956	-7.279	0.323	1.200	49	0.236
	P300	-0.834	-1.090	0.256	1.096	49	0.278
<i>FrontoCentral</i>	Na	-0.033	-0.066	0.033	0.230	49	0.819
	Pa	0.165	0.322	-0.157	-1.052	49	0.298
	Nb	-0.307	-0.258	-0.049	-0.447	49	0.657
	P100	1.503	1.126	0.377	2.457	49	0.018
	N200	-3.700	-3.718	0.018	-0.068	49	0.946
	P300	-0.237	-0.047	-0.190	-1.311	49	0.196
<i>Parietal</i>	Na	-0.508	-0.413	-0.095	-0.515	49	0.609
	Pa	0.006	0.070	-0.064	-0.352	49	0.726
	Nb	-0.659	-0.695	0.036	0.178	49	0.859
	P100	5.612	5.309	0.303	1.242	49	0.220
	N200	-5.477	-5.979	0.502	2.301	49	0.026
	P300	0.633	0.238	0.395	1.984	49	0.053
<i>Occipital</i>	Na	-1.513	-1.488	-0.025	-0.143	49	0.887
	Pa	-0.587	-0.742	0.155	0.687	49	0.495
	Nb	-0.888	-1.028	0.140	0.640	49	0.525
	P100	7.633	7.765	-0.132	-0.774	49	0.443
	N200	-5.652	-5.538	-0.114	-0.454	49	0.652
	P300	1.536	1.204	0.332	1.508	49	0.138

an interaction of “states” of both observers enters the state description of the experiment. An instruction for this purpose or a thorough explanation about its implications was absent in our experiment.

- Finally, and possibly most importantly, there is a possible conceptual difference between the two experiments. The observation by the preobserver in the second experiment was incomplete in the sense that this observer was unaware if (s)he observed a quantum event or a classical event. One could argue qualitatively that this lack of knowledge corresponds to only a partial collapse and hence a situation where preobservation does not really make a difference or makes a smaller difference for the final observer. Interestingly, under this assumption one would expect a smaller or no difference between the preobserved and non-preobserved condition but one still would expect a difference between the classical and the quantum events. This is exactly what was found. Some consistent differences were found when comparing the AEP of quantum events with those of classic events (see Fig. 2.11 and Table 2.4).

No differences were expected on the basis of identical beep frequency, duration or simulated decay times between events. Only the latter could possibly differ between the two conditions. The table of classical latencies was generated by recording the radioactive decay in the same experiment. Radioactive decay, however, has such a large variance that it is difficult to ensure a perfect simulation. When we later compared the average of the table with the average of radioactive events that occurred during the recording of the subjects, we noticed considerable differences. The real quantum events had average latencies that sometimes fell below a tenth of those of the table. The selection was therefore unlucky. It is not, however, straightforward to attribute the differences to this difference in latency. When one expects a stimulus at a certain time, a contingent negative variation (CNV) will precede the moment of stimulation after which the AEP will start at a more negative baseline. In the AEP of the frontal and frontocentral pooling this CNV is clearly seen (Figs. 2.9 and 2.10 between 250 ms and 0 ms before stimulus), in which there does not seem to be a differential effect between conditions. A CNV will only have an effect on the amplitude, not on the latency of early endogenous components. Also, the difference wave (Fig. 2.11) shows a consistent difference in the positive direction. This cannot be explained by a difference of latency for that would result in a difference wave that crosses the baseline. It must be explained in terms of a difference in surface. Interpreting this difference, however, is inappropriate at this stage of investigation and needs further investigation.

2.7 Further Research

Further investigation is needed to determine the conditions under which subjective reduction can take place. We differed in our experiment with Bierman's [3] in the emphasis we placed on the video connection. Making hereby sure the "states" of both observers are included in the state description of the experiment could very well be crucial, as was already remarked, and should be included as a variable in further investigations.

A question already posed by Bierman [3] remains unanswered:

"So far the concept of a conscious observation has not been worked out in detail. In Libet's work, which we used to estimate the delay between perceptual input and the conscious experience thereof, the conscious observation is by definition an observation which is stored in memory. However there is suggestive evidence, for instance from 'change blindness' experiments, that there is another form of 'faster' conscious experience directly related to perceptual input (Landman et al., 2003). This experience is not stored in memory. In further work it might be necessary to discriminate between these and possibly other forms of conscious experience." (pp. 55).

To ensure a conscious memory of the observed events, several suggestions can be made. The observed events can be remembered by introducing differing stimuli. In other words; the stimuli can be made more complex so that they can be remembered at a later time. This could be accomplished by presenting words or pictures to both observers. Afterwards, conscious memory of these observed events can be tested with a recollection task. Another aspect of conscious experience apart from memory is meaning. The meaning of the preobservation was vague in the second experiment because the preobserver was unable to discriminate between classical and quantum events. Thus in a follow up study these two conditions should result in a different feedback for the preobserver.

To get more control over the quantum events, especially regarding the moment of the event, a different quantum source can be used. For instance, using a Stern–Gerlach apparatus for measuring the magnetic moment (spin) of elemental particles, more clearly dichotomous (“spin-up” or “spin-down”) observations can be made instead of our “decayed” or “nondecayed” states. Seven decades since Schrödinger’s “cat paradox” [22], the problem of the collapse of the statevector is still a major unresolved issue of modern physics. With the advance of scientific methods, however, we can be hopeful that future scientists can account for these issues that today seem paradoxal. Even now, John Archibald Wheeler, one of the founders of quantum physics, poses the question:

“(. . .) whether the universe really existed before you start looking at it.” [12].

Along with a scientific community that is no longer afraid of these “ideas for ideas” as he himself puts it, we, in line with previous experiments [15, 3] show that among these questions, the role of consciousness on the reduction of the wave function can indeed be scientifically investigated.

Appendix

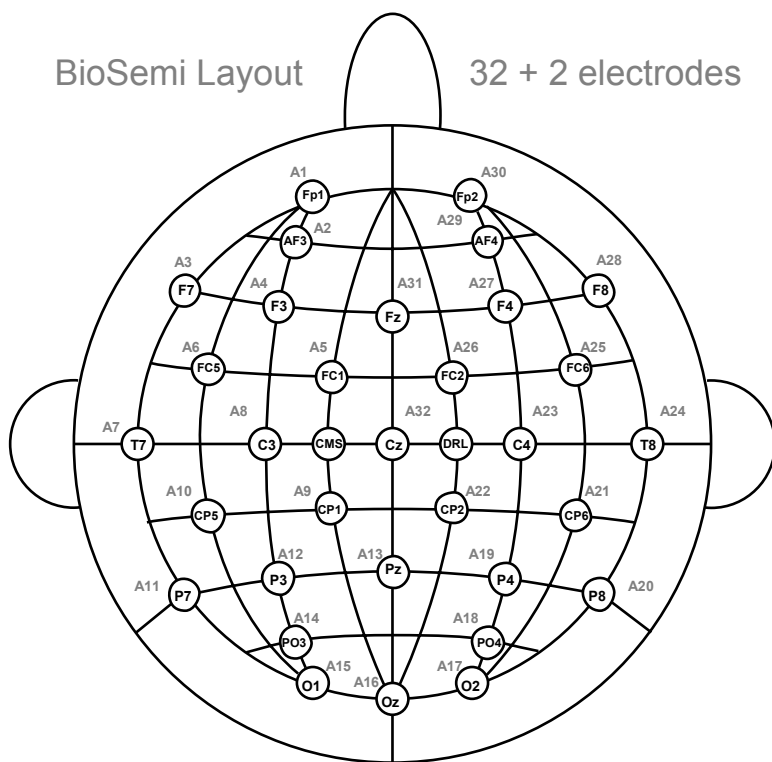


Fig. 2.12. Placement of electrodes

References

1. Albert, D. Z. and Loewer, B. (1988). *Synthese* **77**:195–213.
 2. Albert, D. Z., (1992), *Quantum Mechanics and Experience*, Harvard University Press, Cambridge, MA.
 3. Bierman, D.J., (2003). *Mind and Matter* **1**:1.
 4. Bohm, D. (1952). *Physical Review* **85**:166–193.
 5. Bohm, D. and Hiley, B. (1997). *The Undivided Universe*.
 6. de Broglie, L. (1928). In *Solvay* (1928).
 7. Costa de Beauregard, O. (1976). *Foundations of Physics*, **6**:539.
 8. Dieks, D. and Vermaas, P.E. (eds.), (1998). *The University of Western Ontario Series in Philosophy of Science*, **Vol. 60** (Dordrecht: Kluwer).

9. DeWitt, B.S. (1971). *Foundations of Quantum Mechanics* (Academic Press, NY). Reprinted in DeWitt and Graham (1973):167–218.
10. DeWitt, B.S. and Graham, N. (1973), *The Many-Worlds Interpretation of Quantum Mechanics* (Princeton University Press, Princeton).
11. Everett, H. (1957). *Reviews of Modern Physics* **29**:454–462.
12. Folger, T. (2002). Discover.com: <http://www.discover.com/issues/jun-02/features/featuriverse/>.
13. Gell-Mann, M. and Hartle, J.B. (1990). In *Complexity, Entropy, and the Physics of Information, Proceedings of the Santa Fe Institute Studies in the Sciences of Complexity*, vol. **VIII**, Zurek, W.H. (ed.), (Addison-Wesley, Redwood City, CA):425–458.
14. Ghiradi, G., Rimini, A., and Weber, T. (1986). *Physical Review* **D34**:470–491.
15. Hall, J., Kim, C., McElroy, and Shimoni, A. (1977).
16. Hameroff, S.R. and Penrose, R. (1996). In: *Toward a Science of Consciousness – The First Tucson Discussions and Debates*. (eds.) Hameroff, S.R., Kasznia, A.W., and Scott, A.C., Cambridge, MA, MIT Press:507–540.
17. Jung, T.-P., Makeig, S., Humphries, C., Wong Lee, T.-W., McKeown, M.J., Iragui, V., and Sejnowski, T.J. (2000). *Psychophysiology*, **37**:163–178 (Cambridge University Press).
18. Libet, B. (1991). *Nature*, **352**:27.
19. Makeig, S., Jung, T.-P., Ghahremani, D., and Sejnowski, T.J. (1996). *Tech. Rep. INC* (Institute for Neural Computation, University of California San Diego), No. **9606**.
20. Penrose, R. (1989), *The Emperor's New Mind*, American Philological Association.
21. Penrose, R. (1996), *Shadows of the Mind*, Oxford University Press, Oxford.
22. Schrödinger, E. (1935) Naturwiss. 23, 807, translated into English in: *Quantum Theory and Measurement*, (eds.) J.A. Wheeler and W.H. Zurek, Princeton Univ Press (1983).
23. Solvay Congress (1927), 1928, *Electrons et Photons: Rapports et Discussions du Cinquième Conseil de Physique tenu à Bruxelles du 24 au 29 Octobre 1927 sous les Auspices de l'Institut International de Physics Solvay*, Paris: Gauthier-Villars.
24. Stapp, H.P. (1993). *Mind, Matter, and Quantum Mechanics*. N.Y.
25. Stapp, H.P. (2001). *Foundations of Physics*, **31**:1465–1499.
26. Trimmer, J.D. (1983). *Proceedings of the American Philosophical Society* **124**, 323–38. [Schrödinger, E. (1935) “Die gegenwärtige Situation in der Quantenmechanik”, *Naturwissenschaften* **23**:807–812, 823–828, 844–849.]
27. von Neumann, J. (1932) Mathematischen Grundlagen der Quantenmechanik. Springer, Berlin. English translation (1955) Mathematical Foundations of Quantum Mechanics. Princeton University Press, Princeton.
28. Walker, E.H. (1971). *Physics Today* **24**:39.
29. Walker, E.H. (1988). *Physica B* **151**:332–338.
30. Walker, E.H. (2000). In *The Physical Nature of Consciousness*, (ed.) Philip Van Loocke, John Benjamins, Amsterdam/Philadelphia:63–82.
31. Wigner, E.P., (1967). In: *Symmetries and Reflections* (Indiana University Press, Bloomington)

3 Microtubules in the Cerebral Cortex: Role in Memory and Consciousness

Nancy J. Woolf

Summary. This chapter raises the question whether synaptic connections in the cerebral cortex are adequate in accounting for higher cognition, especially cognition involving multimodal processing. A recent and novel approach to brain mechanics is outlined, one that involves microtubules and microtubule-associated protein-2 (MAP2). In addition to effects on the neuronal membrane, neurotransmitters exert actions on microtubules. These neurotransmitter effects alter the MAP2 phosphorylation state and rates of microtubule polymerization and transport. It is argued that these processes are important to the physical basis of memory and consciousness. In support of this argument, MAP2 is degraded with learning in discrete cortical modules. How this relates to synaptic change related to learning is unknown. The specific proposal is advanced that learning alters microtubules in the *subsynaptic zone* lying beneath the synapse, and that this forms the physical basis of long-term memory storage because microtubule networks determine the synapse strength by directing contacts with actin filaments and transport of synaptic proteins. It is argued that this is more probable than memory-related physical storage in the synapse itself. Comparisons to consciousness are made and it is concluded that there is a link between microtubules, memory and consciousness.

3.1 Introduction

The human brain is a complex mass of tissue endowed with extraordinary capabilities. Two such phenomena are memory and consciousness. In the following chapter, I present an overview of the brain and those intrinsic molecules key to cognitive function. Microtubules turn out to be a common target of neurotransmitter action and play a significant role in learning and memory. Microtubules may also play a role in consciousness. Memory and consciousness are interrelated; thus, microtubules could be the link between these two phenomena. These are the main points covered in subsequent sections.

3.1.1 General Features of the Brain

The human brain is larger than brains of most other species, particularly animals of similar or smaller size. Recent studies using magnetic resonance imaging (MRI) verify earlier research that the typical human brain is approximately 1100 cm^3 in volume and has a surface area averaging 1700 cm^2 [67].

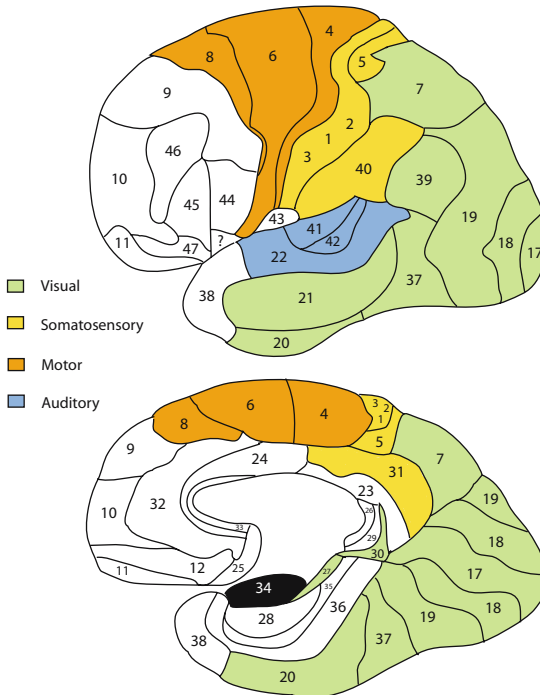


Fig. 3.1. Areas of the human brain drawn according to the scheme of Brodmann [10]. The colors refer to areas of the same (visual, somatosensory, auditory or motor) modality. Prefrontal and limbic (cingulate and parahippocampal) areas are shown in white. Olfactory area is shown in black

Similar measurements made from MRI scans show that the average cortical thickness ranges from 2.5 to 3.5 mm [29]. Given that the cerebral hemispheres are imperfect spheres with many convolutions, the cortical thickness multiplied by cortical surface area equals about half the cortical volume. Slabs of cortex are functionally divided into vertical minicolumns measuring 40–50 μm in diameter that are further linked by short-range horizontal connections into modules measuring approximately 300–600 μm^2 in diameter, and finally, modules are linked into areas by long-range horizontal connections¹. In his seminal 1909 publication, Brodmann described 47 cortical areas (Fig. 3.1).

¹ Each minicolumn contains approximately 100 neurons arranged in a vertical column, an exception being that approximately 250 cells are localized to vertical columns in the primary visual area [88, 87].

The Brodmann classification system is still used today, even though some of his original cortical areas have been further subdivided.

The brain is protected in a bath of cerebral spinal fluid (CSF). Circulating CSF is especially important for the birth of new neurons and cushioning the brain. The skull confines the brain in a restricted space and the volume is kept constant. The intracranial space has a conserved mass equalizing inflow and outflow [73]. Blood flow to particular brain regions increases during specific cognitive tasks. By increasing oxygen and glucose delivery to neurons, higher levels of activity can be maintained. Methods such as positron emission tomography (PET) and functional magnetic resonance imaging (fMRI) take advantage of these changes in local energy metabolism and hemodynamics to pinpoint increases in correlated neural activity.

Two features of the human brain are believed to account for its elevated cognitive capabilities: increased number of modules in association areas and more convolutions compared to lower animals. The cerebral cortex is hierarchical in nature. Higher association areas receive projections from lower levels of sensory cortex, as well as from thalamic regions specifically supplying those regions. These higher association areas are affiliated with the most complex cognitive abilities. The prefrontal association cortex and olfactory-emotional brain circuitry occupy some of the highest tiers among cortical areas (see white areas in Fig. 3.1). Buried in the temporal lobe lies the hippocampus, a critical part of olfactory-emotional brain circuitry. Functions of the hippocampus include contextual learning², which may be similarly expressed in laboratory animals and humans. Studies on contextual fear conditioning and correlative biochemical and cellular changes in rodents will be discussed in this chapter because, for obvious reasons, it is not possible to analyze the chemical properties of cells in the human brain after learning a task.

3.1.2 Neuronal Assemblies: Patterns of Connection

The basic patterns of connection are similar across mammals: this includes rodents, nonhuman primates and humans. There is a general misconception that the mammalian cortex is completely interconnected by classical synapses³, when in fact, most cortical connections are segregated with other regions devoted to the same sensory modality (i. e. sight, hearing, touch, taste or smell). Hilgetag et al. [51] analyzed known cortical connections and found several discrete cortical clusters that are strongly interconnected. These clusters include cortical regions of the same modality; crossmodality interconnections range from sparse to absent⁴.

² Contextual learning is when an animal forms a memory of the surroundings in which an aversive or appetitive event occurs.

³ The most common synapses are between axon terminals and dendrites or cell bodies.

⁴ Some absent connections may be false negatives that could be revealed in future studies.

There are a few cortical regions where multisensory convergence has been demonstrated anatomically⁵. These multisensory areas include the posterior auditory association cortex, the superior temporal polysensory area and the intraparietal sulcus [76, 110]. It is possible that more multisensory areas will be discovered in the future.

3.1.3 Neurons, Synapses and Neurotransmitter Molecules

By definition, neurons are brain cells that are involved in communication of information. There are an estimated 100 billion neurons in the human brain at the time of birth [72]. The actual number could vary by an order of magnitude or more. Using unbiased stereology, a rigorous sampling method, 13–23 billion neurons are estimated in the human neocortex [9, 97]. Sex and age appear to be factors affecting cell number.

The neocortex has 6 layers arranged parallel to the surface of the brain, each of which contains different cell types that play different roles. Pyramidal cells populate layers III and V. Layer III pyramidal cells project to other cortical regions (corticocortical connections), whereas layer V pyramidal cells project to subcortical structures. Layer V pyramidal cells are the largest with cell diameters averaging 50 micrometer. Layer III pyramidal cells are generally smaller. Nonpyramidal local circuit cells, which do not project out of the immediate cortical area, are smaller and more numerous than pyramidal cells. These local circuit cells can be of many shapes; some are excitatory local relays and some mediate local inhibition. One type of local circuit cell, the horizontal cell, interconnects cells across the module and is generally inhibitory. Minicolumns and modules are organized around the large pyramidal cells. Sensory inputs are relayed from the thalamus to layer IV of the corresponding cortical area. The many excitatory local circuit cells relay information up and down the vertical column. In this manner, the large dendrite tree of the pyramidal cell receives many inputs via local circuit cells.

There are at least 1.25 trillion synapses in the human cerebral cortex⁶. Synapses are the tight spaces between two neurons that provide a conduit for chemical communication, but they also include the membranes on both sides of the space. Pyramidal cells receive many of their inputs onto dendrite spines, appendages that increase the surface area of dendrites and compartmentalize the molecular machinery relevant to receiving inputs. As the cortical hierarchy increases, pyramidal cells receive more inputs. As an example, pyramidal

⁵ Some demonstrated anatomical connections might be false positives due to the leakage of track tracer into neighboring regions and uptake by underlying fibers-of-passage.

⁶ Mouton et al. [89] estimated the neocortex contains only 1 billion neurons, an order of magnitude less than other reports; thus, the actual number of synapses may be higher than reported in this study.

cells in the prefrontal cortex have 23 times more spines (and inputs) than pyramidal cells in the primary visual cortex [26].

Synaptic Proteins

Synapses convey chemical messengers that alter the membrane potential of the receiving neuron. If strong enough, or if accompanied by sufficient additional input, the receiving neuron will generate an action potential that will reach another neuron. Thus, the sequence of events repeats itself. The traditional view is that the synapse is the only computationally relevant apparatus in the neuron. Hence molecules related to synaptic transmission have been studied exhaustively. Neurons generally communicate with each other using small molecule neurotransmitters released into the synapse. Many neurotransmitters are amino acids or slight modifications thereof. Major neurotransmitters in the cerebral cortex include: glutamate, GABA, acetylcholine, dopamine, norepinephrine and serotonin⁷.

Synaptic proteins relevant to receiving inputs include: (1) receptors that bind to neurotransmitters, (2) ion channels, (3) signal-transduction molecules that are activated when neurotransmitters bind to the receptor and (4) anchoring proteins that hold signal transduction molecules in place. These proteins work together to generate a local response when a neurotransmitter is released and then binds the receptor. Receptors can be ionotropic, meaning the receptor is also an ion channel. Conversely, metabotropic receptors do not have an ion channel as an integral part of the molecule. Instead, metabotropic receptors have integral G-proteins that trigger intracellular signal transduction. These intracellular signals can affect ion channels and the neuronal cytoskeleton.

Table 3.1 lists the signal transduction molecules activated by a number of metabotropic receptors.

Each cell type of the cerebral cortex uses a particular neurotransmitter for sending chemical messages. The pyramidal cells and most excitatory local circuit cells release glutamate, but these cells respond to multiple neurotransmitters. Synapses on spines usually receive glutamate inputs. Glutamate is responsible for relaying sensory information throughout the entire central nervous system. Receptors that bind glutamate are both ionotropic (AMPA, kainate and NMDA receptors) and metabotropic (mGluR). Some interneurons in the cerebral cortex use GABA, which is an inhibitory neurotransmitter. GABA_A receptors are ionotropic and GABA_B receptors are metabotropic. Acetylcholine, norepinephrine, dopamine and serotonin are considered neuromodulators because their actions are often best understood in terms of how they modify the effects of glutamate neurotransmission. Acetylcholine interacts predominantly with muscarinic receptors in

⁷ There are also a large number of neuropeptides that play specialized roles in the cerebral cortex. Due to their diversity, these will not be discussed further.

Table 3.1. Major neurotransmitters, receptors and signal transduction molecules

Neurotransmitter	Receptors	Second messengers	Protein kinases/phosphatases	Phosphorylation of MAP2
Glutamate	AMPA/kainate NMDA mGlu1, mGlu5 mGlu2, mGlu3	K ⁺ Ca ²⁺ PI-PLC ↓AC	calcineurin PKC, CaCMK II ↓PKA, presynaptic	decreased (slow) ^a increased (rapid) ^a —
Acetylcholine	M1, M3, M5 M2, M4	PI-PLC ↓AC	PKC, CaCMK II ↓PKA, presynaptic	increased ^b —
Norepinephrine	α-1 α-2 β-1	PI-PLC AC ↓AC	PKC, CaCMK II PKA ↓PKA, presynaptic	increased ^b increased ^b —
Serotonin	5-HT2 5-HT4, 5-HT7	PI-PLC AC	PKC, CaCMK II PKA	increased ^b increased ^b
Dopamine	D1, D5 D2, D3, D4	AC ↓AC	PKA ↓PKA, presynaptic	increased ^b —

^a Measured effects [104].

^b Predicted effects based on known neurotransmitter actions upon second messengers and protein kinases [108].

the cerebral cortex; however, nicotinic acetylcholine receptors are also present at low levels in the cerebral cortex. Except for nicotinic receptors, which are ionotropic, all the receptors for the neuromodulators named above are metabotropic. These receptors are linked to G-proteins that trigger an intracellular cascade of chemical responses, many of which involve the phosphorylation of key signal transduction molecules (see Table 3.1). Protein kinases responsible for phosphorylation include protein kinase C (PKC), cAMP-dependent kinase (PKA), calcium/calmodulin-dependent kinase II (CaCMK II) and mitogen-activated protein kinase (MAP kinase). Phosphatases are responsible for dephosphorylating signal-transduction molecules. One such example is calcineurin. Usually, phosphorylation activates and dephosphorylation inactivates a signal-transduction molecule; however, the phosphorylation of some proteins can interfere with polymerization of other multimolecular complexes⁸.

Neurons also contain proteins related to synthesizing, packaging and releasing neurotransmitters. Finally, there are proteins that traverse the synapse linking the presynaptic membrane with the postsynaptic membrane. Neural cell adhesion molecules (nCAMs) traverse the synapse linking the presynaptic element with the postsynaptic element. In the case of gap junctions (also known as electrical synapses) there is cytoplasmic continuity between neurons. There exists a family of connecting proteins called connexins⁹. Pannexins form another class of gap junction proteins that are found in cerebral cortex, including pyramidal cells [13].

⁸ An example is the polymerization of microtubules being decreased by the phosphorylation of microtubule-associated proteins [108].

⁹ In the early postnatal period, connexin-36 has been found in murine cortical and thalamic cells [78].

Microtubules, Microtubule-Associated Protein-2 (MAP2) and Actin Filaments

Microtubules are a class of cytoskeletal protein found in all living cells. Neurons are generously filled with microtubules, along with actin filaments and neurofilaments, two other major cytoskeletal components. Microtubules are composed of $\alpha - \beta$ tubulin dimers longitudinally arranged in protofilaments having plus and minus ends. Plus ends of microtubules undergo polymerization/depolymerization cycles to a much greater extent than do minus ends. Tubulin, the building block of microtubules, accounts for as much as 12–26% of the total soluble protein in the brain [18, 52].

Microtubule-associated proteins (MAPs) are also found in high concentrations in neurons. MAP2 is particularly abundant in dendrites where the polarities of microtubules are mixed¹⁰. Closer inspection reveals that a population consisting of many pyramidal cells and a few local circuit cells are enriched with MAP2, suggesting this cytoskeletal protein plays a prominent role in those select cortical cells involved with higher cognition¹¹. Approximately 15% of the total cortical cell population is MAP2 rich. The expression of MAP2, its phosphorylation and degradative state, varies from module to module (see Fig. 3.2)¹².

A role in cognition is further indicated by the pattern of MAP2 expression being altered by recent experience or learning; thus, the MAP2 pattern is not a permanent feature of any cortical module¹³.

The abundances of microtubules and MAP2 in dendrites, as well as MAP2 plasticity with learning, provides sound reasons to suspect a role for these molecules in information processing. For microtubules to participate in information processing, however, they must interact with synapses. The connection from synapse to microtubule is not direct. Microtubules are located in the cell body, the axon and deeper in the dendrite shaft, in a region termed the *subsynaptic zone* (the region beneath the spine neck, for spinous synapses). Typically, polymerized microtubules are absent from dendrite spines, a major postsynaptic site on neurons. The localization of actin filaments complements the localization of microtubules, however, with actin filaments filling dendrite spines. Actin filaments thus connect the synapses to the microtubules in the subsynaptic zone.

¹⁰ Plus-end directed microtubules alternate with minus-end directed microtubules in dendrites, whereas in the axon, all microtubule are aligned with the plus-end directed towards the axon terminal.

¹¹ MAP1, MAP5, Neurofilament proteins and muscarinic acetylcholine receptor also enrich in this cortical population [147].

¹² MAP2 is in a state of continuous flux with respect to its phosphorylation and degradation.

¹³ Different kinds of training alter MAP2 immunostaining in cortical modules [144, 145, 130].

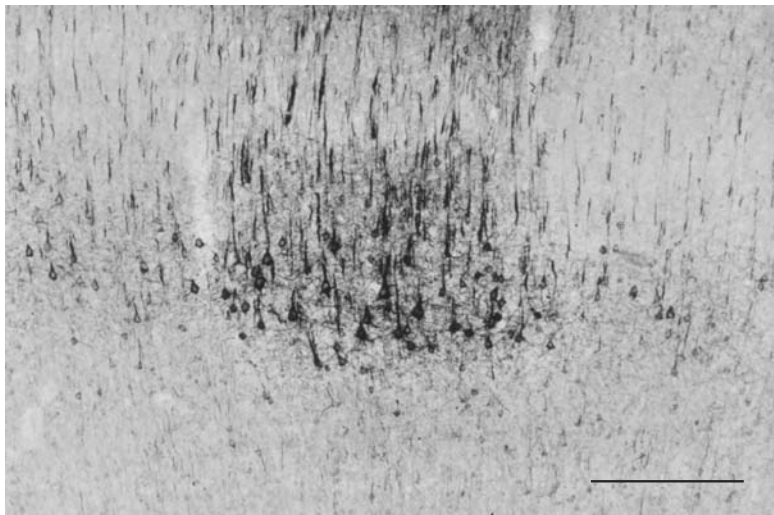


Fig. 3.2. Module of neocortex in rat brain having elevated immunohistochemical reaction for MAP2. Mainly the large layer V pyramidal cells and their thick apical dendrites extending towards the surface of the brain are intensely stained, especially in the middle module. This intensely stained module is flanked by other cortical regions that are less intensely stained for MAP2. Scale bar equals 200 μm . Adapted from [148].

MAP2 and MAP1B have been shown to provide a link between microtubules and actin filaments [21]. This bridging mechanism is a dynamic one. MAP2 alternately binds microtubules or actin filaments, often sequentially. Also, it is a dynamic pool of actin filaments that attaches to the postsynaptic density [45]. For MAP2 to bind microtubules efficiently, it must be partially dephosphorylated. Protein kinases regulate phosphorylation and the binding process. PKA, for example, favors MAP2 dissociation from microtubules and association with actin [96]. In this manner, signal-transduction molecules regulate the switching of MAP2 from microtubules to actin filaments.

3.2 Functions of Microtubules and MAPs

Microtubules were first described as providing structure to the cell. This basic function can be related to information processing, insofar as modifications to dendrite structure and branch geometry will alter the topography of inputs and thereby influence neuronal computation. Today, however, we know much more about the biochemistry and biophysics of microtubules. Our increased understanding of the molecular underpinnings of basic microtubule function is beginning to elucidate precisely how microtubules can participate in information processing.

3.2.1 Transport along Microtubules

Transport occurs along microtubules in dendrites and axons in both anterograde and retrograde directions via distinct motor proteins. Transported cargos include receptors, signal-transduction molecules, cytoskeletal proteins and mRNA. Brain-specific motor proteins include examples from the superfamily of kinesin proteins (KIFs), each of which binds to a specific cargo determined by specific amino acid sequences in the tail region and usually transports cargo towards the plus end of the microtubule [90]. Dynein is a microtubule motor that transports neurofilaments to the minus ends of microtubules [112]. Myosin-V, yet another motor protein, may facilitate the transfer of cargo from microtubules to actin filaments [12].

Kinesin-mediated transport along microtubules is affected by the biophysical state of the microtubule, as determined by posttranslational modifications and binding to MAP2 and neurofilaments. Kinesin binding to microtubules is enhanced by polyglutamylation of tubulin when up to three glutamate residues are added [137]. Adding more than three glutamate residues interferes with kinesin binding. Kinesin binding to microtubules is hindered by MAP2 also being bound due to steric interferences caused by both molecules binding near the C-termini of tubulin [2]. Once bound to the microtubule, kinesin processivity along a microtubule protofilament is unaffected by MAP2, the interpretation being that MAP2 lays down as kinesin walks over it [111]. Individual strands of MAP2, not reinforced by pairing with another MAP2, are flexible enough to be capable of lying down on the microtubule as suggested. Highly stabilized microtubules, for example, those connected to phosphorylated neurofilaments, have decreased transport rates among kinesins¹⁴. Kinesin also exerts biophysical effects on the microtubule. This motor contributes to the instability of microtubules as it interferes with tubulin polymerization [56]. Although the situation is far from being simple, an inverse relationship often exists between transport and microtubule stability.

3.2.2 Signal Transduction and Anchoring of Signal-Transduction Molecules

In addition to being a structural protein, MAP2 has been identified as a signal-transduction molecule. MAP2 can be activated through phosphorylation and inactivated through dephosphorylation. MAP2 is also an anchoring protein, meaning that it tethers, or fastens, other signal-transduction molecules together. MAP2 has also been identified as a gelation factor, rigidifying actin filaments and microtubules into a gel [68, 40].

There are over 40 sites that can be phosphorylated or dephosphorylated on MAP2. MAP2 is phosphorylated by multiple protein kinases: being an excellent substrate for CaCMK II, PKC, PKA and MAP kinase, among others [108]. CaCMK II mediates phosphorylation at as many as 18 binding

¹⁴ This is the case in axons (see Shea [114]) and remains to be studied in dendrites.

sites on the MAP2 protein, and PKC mediates phosphorylation at as many as 15 sites [133]. PKC is responsible for phosphorylation at binding sites Ser-1703, Ser-1711 and Ser-1728, which dramatically inhibits MAP2 binding with microtubules [1]. The N-terminus of MAP2 is an anchoring site for the regulatory subunit II of PKA [48]. In this manner, MAP2 is able to trap and disable PKA, and then release and enable PKA when it is necessary to phosphorylate microtubule proteins. The phosphorylation state of MAP2 regulates the polymerization and depolymerization of microtubules [108]. Phosphorylated MAP2 is much less efficient at stimulating the polymerization of microtubules; however, even in the absence of MAP2, tubulin can polymerize into microtubules at a slow rate. Calcineurin dephosphorylates MAP2.

In the brain, these signal-transduction pathways, of which MAP2 is an integral part, are triggered by neurotransmitter actions arising from synaptic inputs. These neurotransmitter inputs utilize a number of receptors triggering specific signal-transduction cascades (see Table 3.1). These actions will be elaborated on in the next section.

Glutamate Effects on Microtubules Mediated by AMPA, Kainate, mGlu and NMDA Receptors

Glutamate mediates sensory input to the cerebral cortex, where many of these excitatory presynaptic terminals contact spines. AMPA and kainate glutamate receptors respond quickly, within a few ms, altering ion conductances across the membrane (Na^+ influx $\gg \text{Ca}^{2+}$ influx). Under physiological conditions, there are a few ways that AMPA receptors (and similarly kainate receptors) can influence microtubules (see Fig. 3.3).

AMPA receptor activation can affect microtubules directly through ionic currents that passively diffuse along the membrane and penetrate the subsynaptic zone. The outermost microtubules are roughly a hundred nanometers below the membrane surface, such that these microtubules will be most readily affected by ion influxes. Possible consequences of AMPA receptor activation (and subsequent increased Na^+ influx) are initial increases, and eventual decreases, in microtubule polymerization expected to occur as the Na^+ concentration in the cell adds to the already high K^+ concentration inside the neuron (see Fig. 3.3).

Sodium or potassium ion concentrations of 150–160 mM increase microtubule polymerization, whereas Na^+ or K^+ concentrations over 250 mM decrease microtubule polymerization [92, 141]. Thus, ionic strength exerts tight bidirectional control over microtubule polymerization and thereby stands to affect other biophysical aspects of microtubules. MAP2, which crosslinks microtubules and actin, is also sensitive to pH shifts¹⁵.

¹⁵ An ATP and Mg-dependent, serine/threonine-specific MAP2 kinase can be converted to a phosphatase with certain pH changes [150].

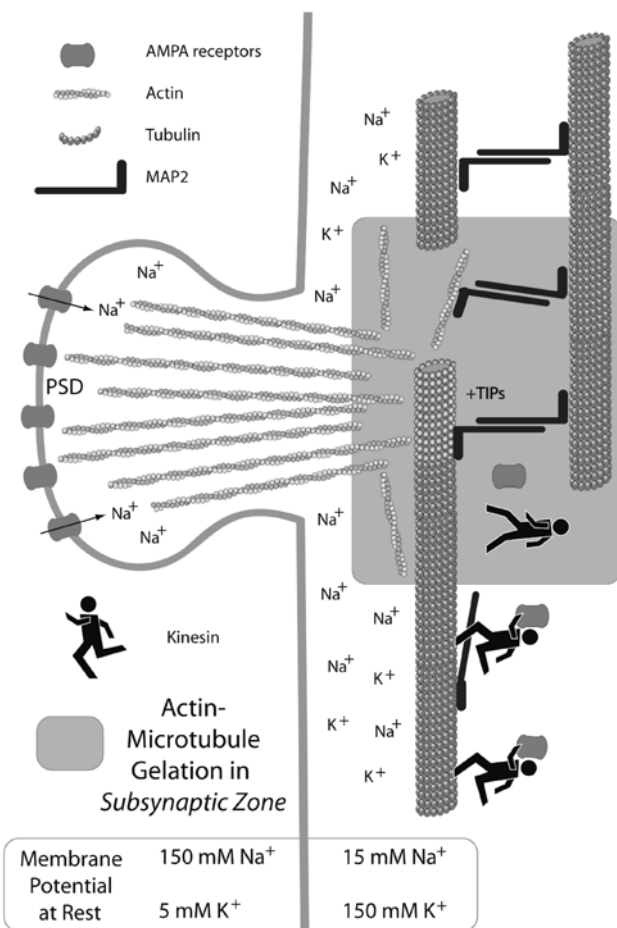


Fig. 3.3. AMPA receptor activation: effects on microtubules. A population of AMPA receptors located on a dendrite spine is shown. Microtubules are diagrammed as orange polymers composed of tubulin. Pairs of MAP2 molecules link microtubules, whereas single MAP2 molecules are flexible enough to allow kinesin to walk over. The following responses are illustrated: AMPA receptor activation opens sodium (Na^+) channels and sodium ion influx increases the sodium ion concentration inside the neuron, adding to the potassium ion (K^+) concentration (insert lists sodium and potassium concentrations at rest). This is likely to initially increase polymerization (indicated by green tubulins) of the nearest microtubules located approximately 100 nm beneath the spine or neuronal membrane. Plus-end binding proteins (+TIPs) will stabilize newly polymerized microtubule ends. If the sodium concentration becomes too high, however, microtubule depolymerization will occur. Actin filaments connect the postsynaptic density (PSD) to microtubules. AMPA receptor activation is likely to increase actin-filament interaction with microtubules (actin-microtubule gelation) in the subsynaptic zone, and this is likely to slow transport along microtubules. Decreased transport near the spine may facilitate unloading cargo, conceivably providing more AMPA receptor to the spine

The second way in which activating AMPA receptors could affect microtubules is indirectly, through actin filaments. Large spines that are enriched with AMPA receptors contain many actin filaments. Multidomain scaffolding proteins link actin filaments with the postsynaptic density [103], and actin links to microtubules. The interaction between microtubules and actin is likely to involve many proteins, including MAPs and motor proteins¹⁶. A functional relationship between AMPA receptors and MAP2 exists. AMPA administered at cytotoxic levels exerts long-term effects, maximally increasing MAP2 at 5 days [71].

The third way that AMPA receptor activation might influence microtubules is through actin filament–microtubule gelation. Actin filament–microtubule gelation is mediated by MAP2, among other molecules [40]. When MAP2 complexes to actin filaments and microtubules, the viscosity of the complex increases by one hundred-fold or more. Glutamate, acting through ionotropic receptors, inhibits actin dynamics and decreases filopodia motility in dendrites and axons [19], an effect that appears to reflect increased viscosity. Increased polymerization of microtubules in the subsynaptic zone would also increase interaction between actin filaments and microtubules and thereby further favor the formation of highly viscous MAP2–actin–MAP2–microtubule complexes (see Fig. 3.3).

Increased viscosity is known to slow the transport of kinesin [33]. An AMPA-enriched spine cannot operate at full capacity without replenishing AMPA receptors. The transport of AMPA receptors depends on both actin motors and microtubule motors,¹⁷ indicating that coordination between these cytoskeletal components is necessary for proper function. Increased viscosity would impede this process. To summarize, the net result of AMPA (and kainate) receptor activation is likely to increase polymerization of microtubules, perturb actin dynamics and slow transport along microtubules. Decreased transport near the spine may facilitate unloading cargo, such as the AMPA receptor (see Fig. 3.3).

Upon release of glutamate at the spinous synapse, mGluRs are also activated. At least eight mGlu subtypes have been identified, many with further subdivisions within subtypes. A certain class of mGlu receptors mediates rapid phosphorylation of MAP2 via CaCMK II and PKC [104]. These kinases are triggered by the PI-PLC signal-transduction pathway and mGlu1 and mGlu5 receptors. As shown in Fig. 3.4, mGlu activation would be expected to phosphorylate MAP2, which in turn would interfere with the polymerization of microtubules in the subsynaptic zone. Consistent with this, mGlu1 α has been shown to inhibit microtubule formation by a mechanism that depends on the PI-PLC pathway [57]. Since metabotropic receptors can

¹⁶ Microtubule–actin interactions studied during neurite formation implicate MAPs [21].

¹⁷ Kim and Lisman [66] were able to interfere with AMPA receptor transport by inhibiting dynein, an actin motor, and kinesin, a microtubule motor.

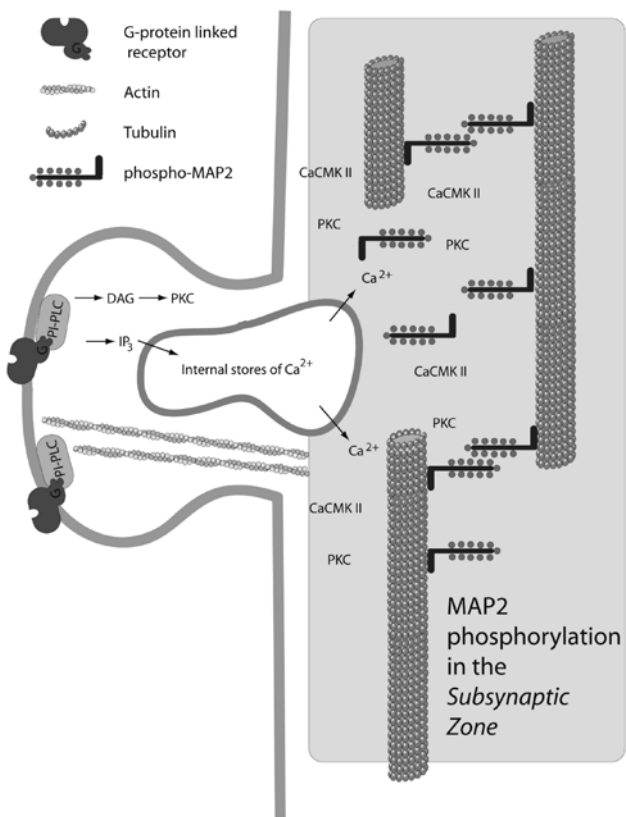


Fig. 3.4. Metabotropic glutamate (mGlu) receptors activate PI-PLC; this in turn activates diacylglycerol (DAG) and inositol triphosphate (IP₃), which in turn activate PKC and release endogenous Ca²⁺. Upon its release, endogenous Ca²⁺ activates CaCMK II. Both PKC and CaCMK II phosphorylate MAP2, and this interferes with microtubule polymerization in the subsynaptic zone beneath the dendrite spine. Microtubules repel one another when MAP2 is highly phosphorylated

activate many second messengers, widespread inhibition of microtubule polymerization would be expected.

Released glutamate will also bind NMDA receptors. The NMDA receptor acts as a calcium channel and its activation results primarily in the influx of calcium (see Fig. 3.5). Calcium ionic fluxes caused by NMDA receptor activation have penetrating effects that reach the mitochondria, which can be located deep beneath the membrane [134], so NMDA effects on microtubules via increased calcium ion concentration are likely. The activation of the NMDA receptor stimulates a number of calcium-activated proteins. These include: calmodulin (a ubiquitous Ca²⁺-sensing protein), calpain (a protease), CaCMK II and calcineurin. NMDA receptor activation causes a persistent

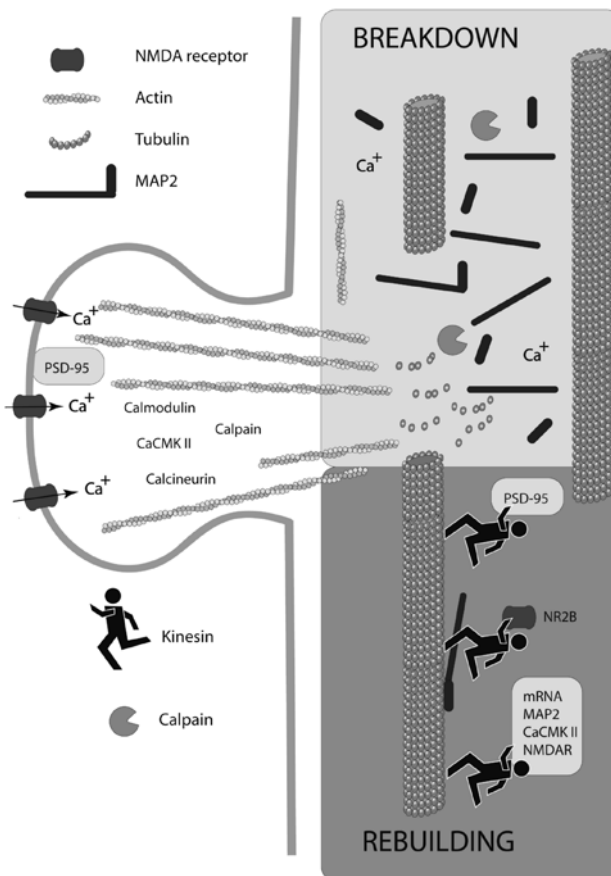


Fig. 3.5. NMDA receptors act as calcium (Ca^{2+}) channels. Calcium enters the neuron and activates calmodulin, calcium/calmodulin kinase II (CaCMK II), calcineurin and calpain. Calpain is responsible for the proteolytic breakdown of MAP2 and may also lead to the breakdown of tubulin. Calcineurin causes a long-lasting increase in MAP2 dephosphorylation (not illustrated), which may enhance microtubule polymerization during rebuilding. Other events occurring during rebuilding include increased transport of postsynaptic density protein, PSD-95, and NMDA receptor subunits, e.g., NMDA receptor subunit 2B (NR2B). Rebuilding also includes increased transport of mRNA for MAP2, CaCMK II and NMDA receptor (NMDAR), essential elements of the overall complex

dephosphorylation of MAP2 mediated through calcineurin [104]. Calcineurin activation by NMDA receptors would favor enhanced polymerization of microtubules. However, the proteolytic effects of calpain degrading both MAP2 and tubulin counterbalance this effect. Thus, NMDA receptors appear capable of exerting opposing effects on microtubule polymerization.

Additional evidence supports NMDA receptors mediating breakdown and then rebuilding of glutamate synaptic sites on spines. Hence, this receptor is key to neuroplasticity. Fundamental to this role, NMDA receptors form complexes with the postsynaptic density protein, PSD-95 [85], with F-actin via the actinbinding protein, α -actinin [149], and with MAP2 [14]. Activation of NMDA receptor is critical in triggering the transport of MAP2 mRNA to dendrites [58]. Kinesin-mediated transport along microtubules occurs for the NMDA receptor subunit NR2B [42] and for PSD-95 [85]. As illustrated in Fig. 3.5, direct and indirect interactions between NMDA receptors and the cytoskeleton are key in the breakdown and rebuilding of the subsynaptic zone.

Acetylcholine, Dopamine, Norepinephrine and Serotonin Trigger G-Protein Cascades that Phosphorylate MAPs

The neuromodulators – acetylcholine, dopamine, norepinephrine and serotonin – are often released onto dendrite shafts rather than onto spines. Their actions are slower than the actions of glutamate, but by no means less influential. Glutamate provokes a large membrane potential change, but this decays as it passively diffuses along the dendrite. Acetylcholine, on the other hand, produces modest membrane potentials, but these are nondecremental, indicating that a self-propagating intradendritic mechanism is involved¹⁸. This intradendritic mechanism relies, in part, upon G-protein receptor signal-transduction cascades. Because of G-protein cascades, acetylcholine and monoamines could, in principle, alter MAP2 phosphorylation all along the dendrite, thereby affecting widespread microtubule stability. Not all parts of the microtubules are equally unstable, however. Stable linkages at minus ends of microtubules are less susceptible to MAP2 binding alterations influencing microtubule stability (see Fig. 3.6).

Unstable MAP2 linkages, however, would be affected as far as signal-transduction molecules and protein kinases were able to passively diffuse. Since the concentration of these would decline with distance, other mechanisms may be involved. To the extent that MAP2-tubulin binding affects the biophysical state of tubulin¹⁹, that biophysical state of tubulin could, in principle, be propagated to other tubulins down the microtubule. Deformations in dimer–dimer interactions are suggested, which begin at minus ends, travel the length of the microtubule and promote destabilization or depolymerization at the plus ends [109]. These kinds of biophysical effects could conceivably account for the fact that acetylcholine produces effects that extend a long distance along the dendrite shaft.

¹⁸ Acetylcholine iontophoresed onto pyramidal cell dendrites produced effects that remained equal in amplitude along the entire dendrite, in contrast to effects of glutamate, which decayed dramatically at increased distance from the infusion site [83].

¹⁹ Biophysical states of tubulin include parameters such as dipole moments, conformational states, and surface electrostatic charge.

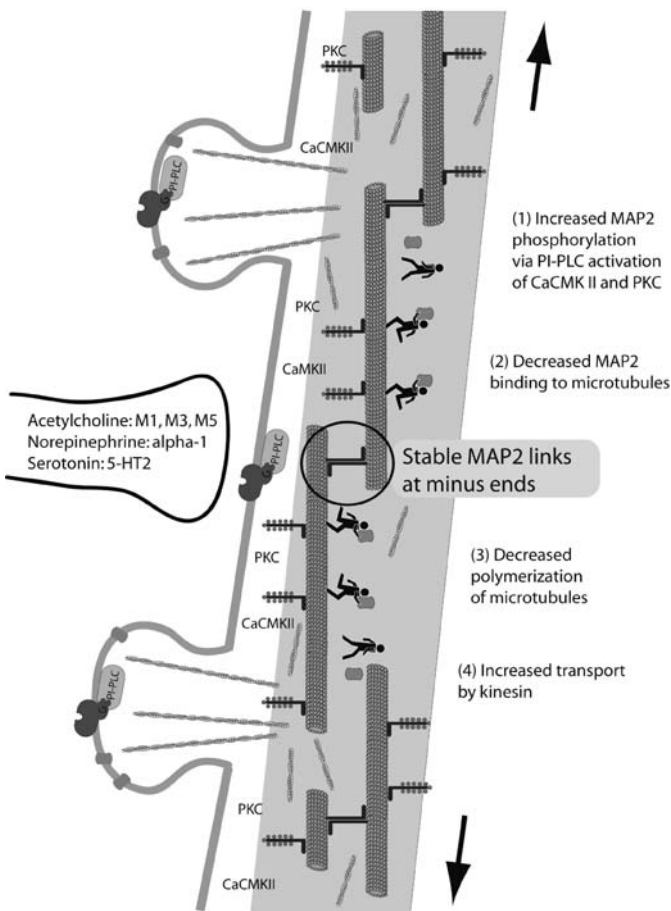


Fig. 3.6. Terminals releasing acetylcholine, norepinephrine and serotonin generally contact the dendrite shaft. Illustrated receptor actions include acetylcholine-M1, M3 and M5; α 1-adrenergic and serotonergic-5-HT2, all of which activate PI-PLC, which in turn activates CaCMK II and PKC. The subsynaptic zone that is affected is much more extensive for these nonspiny inputs; these action may extend the entire length of the dendrite. Phosphorylation of MAP2 will decrease polymerization of microtubules and cause microtubules to repel one another. This would be expected to increase the rate of transport by kinesin. Periodic MAP2 links would be expected to remain intact, and the highly stable MAP2 links between minus ends of microtubules may remain intact even near the release sites of acetylcholine, norepinephrine or serotonin. See Figs. 3.3–3.5 for definition of symbols

Acetylcholine muscarinic receptors are colocalized within the same neurons as MAP2 and PKC, and these proteins appear to form multimolecular complexes [129, 147]. Acetylcholine muscarinic receptors M1, M3 and M5, serotonin 5-HT2 receptors, and α 1-adrenergic receptors activate the PI-

PLC pathway (similarly to mGlu1 and mGlu5). The PI-PLC pathway then activates diacylglycerol (DAG) and inositol triphosphate (IP₃), which, respectively, activate PKC and release endogenous Ca²⁺. Upon its release, endogenous Ca²⁺ activates CaCMK II. Both PKC and CaCMK II phosphorylate MAP2 [108]. Thus, the PI-PLC pathway, which is strongly activated by acetylcholine (and to a lesser extent by serotonin and norepinephrine), is capable of exerting powerful effects on microtubule polymerization via phosphorylative effects on MAP2. Alterations of microtubule polymerization will influence microtubule transport. These molecular dynamics effects may underlie the strong involvement of acetylcholine in memory, attention and dream sleep.

A number of additional receptors activate PKA. These include: dopamine D1 /D5, β 1-adrenergic, and serotonin 5-HT3, 5-HT4, 5-HT6 and 5-HT7 receptors, all of which increase levels of cAMP, and this in turn activates PKA. PKA is known to phosphorylate MAP2 [108], and PKA also stimulates the binding of MAP2 to actin and its dissociation from microtubules [96]. MAP2 alternating between the binding to microtubules and the binding to actin filaments might be important for keeping the microtubule network linked with synaptic activity. This would be consistent with the role of norepinephrine (and other monoamines) in vigilance, a heightened state of awareness of environmental stimuli. Receptors that decrease cAMP, due to the fact that they are negatively coupled to adenylyl cyclase, are frequently located on presynaptic terminals, in which case they do not come into contact with dendritic microtubules or MAP2. Thus, one would only expect these receptors to be involved in dendritic information processing to the extent that they are present on dendrites or to the extent that they regulate presynaptic neurotransmitter release and this release, in turn, has affects on the postsynaptic cell.

Those multiple presynaptic sites releasing acetylcholine or monoamines emerge from single axonal fibers often following the entire dendrite length, which enables these inputs to modulate long stretches of microtubules. This anatomical match to the intradendritic network of microtubules may make these synapses anatomically well suited to convey the global states involved with learning, memory, attention and consciousness. These global states will be discussed in the subsequent sections.

3.3 Learning and Memory: Neuroplasticity vs. Stability

The brain changes whenever an animal learns an association or when an operant behavior is strengthened because of a reinforcer²⁰. More than mere accompaniment, it is assumed that the change in the brain is responsible for the change in behavior. Many kinds of neuroplasticity are found during early

²⁰ During operant conditioning, positive reinforcers increase “reward-producing” behaviors and negative reinforcers increase behaviors such as escape and avoidance.

development and with learning that could account for the behavioral changes observed. The expectation of neural plasticity is fulfilled by supportive experimental data.

Once a change has occurred, however, then it becomes important to stabilize the neural substrate that is responsible for the recently acquired, adaptive behavior. Thus, the same neuronal compartments must be involved in both change and stability or the two compartments must interact. Experimental data do not consistently indicate that changes in synapses are stable. Thus, a new paradigm may be needed to replace the long-held notion of information storage in synapses. The new learning and memory model advanced here is that information storage occurs in the subsynaptic zone, wherein microtubules determine synaptic properties based on previous synaptic activity.

3.3.1 Synaptic Change: Hebb's Rule Revisited

Since Donald Hebb [50] first proposed that synaptic knobs might reorganize with learning, there have been hundreds of studies examining brain tissue for synaptic reorganization following learning or following comparable physiological stimulation that might resemble learning-related events²¹. I will preferentially address those studies that assessed synapse and spine changes accompanying learning in behaving animals.

Temporary Nature of Synaptic Change

Researchers have studied synaptic change with learning using either the electron microscope to visualize synapses or light microscopy to visualize spines. Numerous studies have found evidence for change in spine morphology with learning or enriched experiences (for a review, see Yuste and Bonhoeffer [151]). Regarding the more specific issue of synaptogenesis²², recent studies have shown that synapse and spine densities are altered following learning. In a recent study of associative learning, adult male rats trained on a trace eye-blink conditioning task showed increased the density of spines on basilar dendrites of pyramidal neurons in CA1 of hippocampus [75]. Apical and basilar dendrite lengths were not altered by the training, indicating that the increased spine densities represented increases in total numbers of spines and were not secondary to shrinkage of dendrites. NMDA antagonists blocked both acquisition of the conditioned response and the spine density changes, further indicating that the spine alterations were correlated with learning and not due to some other variable affiliated with the task. Synapse

²¹ Long-term potentiation (LTP), triggered by a strong repetitive stimulus or tetanus, is a physiological change in response thought to reproduce learning-related changes in synaptic efficacy.

²² Synaptogenesis, the formation of new contact between neurons, has been more difficult to demonstrate than has change in synapse and spine morphology.

and spine density changes are not limited to associative learning. In a study of operant conditioning, chicks showed increased spine densities in the dorsal hippocampus at 24 h and 48 h after avoidance conditioning [128]. Synaptic change clearly occurs with learning.

A number of studies have further addressed whether these kinds of learning-related plastic changes are permanent, and the consensus is that they are not. O’Malley and colleagues [93, 94] have shown that increases in spine density in the dentate gyrus of hippocampus following both avoidance training and spatial learning on a water maze task are transient. By 72 h after training, spine densities revert to control levels. Transient changes in spine densities were also found in the chick brain following a passive avoidance task. Different brain regions showed increases in spine density at different time points. Olfactory areas in the chick brain showed significantly heightened spine densities at 24 h after training, but not at 48 h [59]. On the other hand, the hyperstriatum of the chick brain showed increased spine densities at 1 h, but not at 24 h, following training [24]. If there is no net change in synapse or spine density that endures well after learning occurred, how is learning-related information permanently stored? Several ideas have emerged that will be discussed next.

Are there Plastic Versus Stable Spines?

In order to deal with the dilemma of permanent memory storage, several researchers have hypothesized that some spines are temporary and some permanent [63, 82, 115]. According to one view (see Kasai et al., [63]), spines with large heads and possessing many AMPA receptors are stable and represent permanent memory storage, while learning is represented in small mobile spines that continuously form and retract. These smaller spines may be “silent” under physiological conditions, but nonetheless represent a “reserve” of spines, which can change into large spines if sufficient conditions are met.

Although stable populations of large spines have been demonstrated in mouse neocortex,²³ spines are generally thought to be in a constant state of flux and this is regulated by the various neurotransmitter receptors. Glutamate receptors play a prominent role. AMPA receptor activation is important in spine stability, and constant levels of activation within the physiological range must be maintained [29]. The range of optimal activity is tightly regulated, since too high concentrations of glutamate produce a near complete retraction of dendrite spines and a significant reduction of F-actin in a process mediated by calcineurin, NMDA receptor and AMPA receptor [44]. Excessive AMPA receptor activation in developing neurons has also been shown to induce neurite retraction [101]. Similarly, kainate applied to neurites in cell culture produces a retraction of spines [49].

²³ Layer V pyramidal cells in visual cortex were tracked for 10 months and spines were found to be remarkably stable [41].

Although spines retract, they also reappear, often in their original locations. Curiously, actin-depolymerizing agents do not prevent the reappearance of spines in their original locations [49]. That spines are capable of reappearing in their original position without the aid of actin argues strongly against information (i.e. memory) being permanently stored within those actin-rich spines. Another piece of contradictory evidence to the hypothesis that memory is stored in stable actin filaments is that 85% of actin in spines is dynamic, not stable [118]. These findings suggest that the physical basis of memory must be stored elsewhere, perhaps in the subsynaptic zone that gives rise to the spine. Microtubules in the subsynaptic space are capable of storing important information concerning where spines were originally located, and to use that information to determine which synapses will persist or reappear in the event of dynamic retraction. Hence microtubules are satisfactory sites to store memory.

Transmembrane proteins may also play a role, along with microtubules. Neural cell adhesion molecules (nCAMs) are transmembrane glycoproteins that link the presynaptic and postsynaptic membranes. Both nCAM-140 and nCAM-180 bind α -tubulin, β -tubulin and α -actinin 1 [15]. Microtubules, in receiving neurons, may connect to microtubules in the axon terminals providing them inputs via a contact matrix composed of nCAMs and other proteins that traverse the synapse. This microtubule-nCAM-microtubule linkage may help guide new spines to form again in their original positions.

Another way to identify the site of memory storage is to pinpoint sites of high metabolic activity. The process of memory consolidation requires high metabolic activity, although once material is learned, the brain expends much less metabolic energy when using that information. In this regard, ATPase is sequestered in high concentrations in the subsynaptic space, not in the synapse [20]. At this location, ATPase is able to tightly regulate ATP levels, which are known to affect the viscosity and polymerization of the cytoskeleton [132].

A critical part of a microtubule mechanism of learning is that the microtubule assumes the role of an “active” participant, transiently crosslinking with actin filaments to selectively join subsynaptic zones together into a neuron-wide network. Self-organizing microtubules inside dendrites are able to polymerize and depolymerize and thereby search for subsynaptic sites with which they can connect to actin filaments²⁴. During learning, glutamate, acetylcholine and monoamines are likely to initiate microtubule polymerization or depolymerization²⁵. However, when there is no stimulus, such as

²⁴ By comparison, microtubules orchestrate mitosis by a search-and-contact strategy involving polymerization/depolymerization cycles, and by a third step that does not involve physical contact [121].

²⁵ These neurotransmitters affect microtubule polymerization through postsynaptic receptors that activate PI-PLC, and subsequently PKC and CaCMK II, which in turn phosphorylate MAP2.

during spontaneous recall of a memory, a biophysical state of the microtubule must self-induce a polymerization/depolymerization cycle. Microtubules have long been recognized as self-initiating mechanical operators in the cell²⁶. Given the complexity of microtubule networks, a single neuron gains the computing capability of a large neuronal ensemble. As will be discussed towards the end of this chapter, microtubules may use various strategies when participating in brain-wide networks.

Dendrites are Comparatively More Stable than Spines: Microtubules Maintain Dendrite Integrity

Microtubules show greater stability than actin spines [62]. Although microtubules continuously lengthen and shorten *in vitro* and *in vivo*, they can also be very stable, even when the neuronal membrane is removed [123]. Several conditions contribute to the stability of microtubules. For one, crosslinking with MAP2 or tau markedly increases the structural stability of microtubules in dendrites [22, 48, 81]. Secondly, posttranslational modifications, such as de-tirosination, polyglutamylation or acetylation, have the potential to enhance microtubule stability, not directly, but through increased binding to MAPs or neurofilaments [137]. Detyrosinated microtubules become associated with neurofilaments possibly via kinesin interactions [69]. Detyrosinated microtubules are exceptionally resistant to polymerization; tubulin dimers must first be fragmented in the presence of calcium before significant polymerization will occur [60]. Acetylation has been shown to stabilize microtubules in the subsynaptic region of the neuromuscular junction, which in turn, stabilizes acetylcholine receptors [61]. Posttranslational modifications of microtubules also perform a unique role in living cells. There is an abrupt change in tyrosinated tubulins and acetylated tubulins such that the composition of a microtubule gives a “snapshot” of its growth history [11]. This poses an exciting means to store information about when microtubule networks were reorganized.

Thirdly, attachment of the microtubule, especially at its ends, contributes to microtubule stability. There are a number of plus-end binding proteins (+TIPs) that stabilize the plus ends of microtubules in dendrites [119]. These +TIPs move bidirectionally along microtubules in the initial segment of dendrites, while movement is mostly outward in distal dendrites and axons. The initial segments of neurites are exceptionally stable [114]. The various means by which microtubules can be stabilized make these polymers good candidates for permanently encoding memory. These mechanisms of stabilization would favor the preservation of the overall structure during ongoing protein turnover.

²⁶ Microtubules self-assemble during cell mitosis.

3.3.2 Microtubules and MAPs in Dendrites Play a Critical Role in Memory

Microtubules and MAPs have a clear involvement in learning and memory. We showed MAP2 proteolytic breakdown occurs with memory consolidation [144–146]. We demonstrated MAP2 breakdown in two ways. First, we found increases in immunocytochemical staining in repeated experiments, using a panel of specific monoclonal antibodies. Increases in antibody binding are known to occur following proteolytic breakdown of cytoskeletal proteins because the breakdown exposes more antibody binding sites. The immunohistochemical method is superior at showing where breakdown occurs at the cellular level, but is not definitive at proving proteolysis. For this reason we also ran immunoblots. In these immunoblot experiments, we found an increased presence of breakdown products; results that proved proteolysis occurred.

The extent of MAP2 proteolysis spanned the entire cell body and main dendrites of the MAP-rich cells of those cortical area involved in the learning task. For the hippocampus-dependent task (learning an association between context and shock), MAP2 changes were found in CA1 and CA2 of the hippocampus. For the hippocampus-independent task (learning an association between tone and shock), MAP2 changes occurred in areas of the auditory cortex. In both these experiments, learning correlated with a simultaneous breakdown of MAP2 throughout an entire functional unit of the cerebral cortex (Fig. 3.7).

In our experiments, individual areas of cortex in each animal studied showed a different intensity of MAP2 staining. This, along with the learning-related changes, indicated that the modular variability of MAP2 staining reflects the recent experiences of the animal. Another group found a similar kind of modular variability for MAP2 and PKC immunostaining following passive avoidance training [130].

What induces this pattern of MAP2 proteolysis? Since MAP2 bound to microtubules is more susceptible to proteolysis [38], it is likely that the staining patterns we observed largely reflected the proteolysis of intact microtubules²⁷. Proteolysis is triggered by increased levels of Ca^{2+} , which activate calpain, which in turn degrade MAP2. Buddle and colleagues [14] have shown that calpain-induced MAP2 proteolysis during oxygen-glucose deprivation is triggered by NMDA-receptor activation. Acetylcholine M1, M3 and M5; serotonin 5-HT2; α 1-adrenergic and mGlu1 and mGlu5 receptors are also candidates for activating calpain through PI-PLC-stimulated release of endogenous Ca^{2+} . Destruction of cholinergic fibers innervating the cerebral cortex results in decreased MAP2 staining, indicating that a hypocholinergic state may reduce intact MAP2, reduce the proteolytic breakdown of MAP2 or both [147].

²⁷ We also observed a small, but significant breakdown of tubulin [145]. This probably reflected the breakdown of unbound tubulin; however, it could have been tubulin that dissociated from intact microtubules.

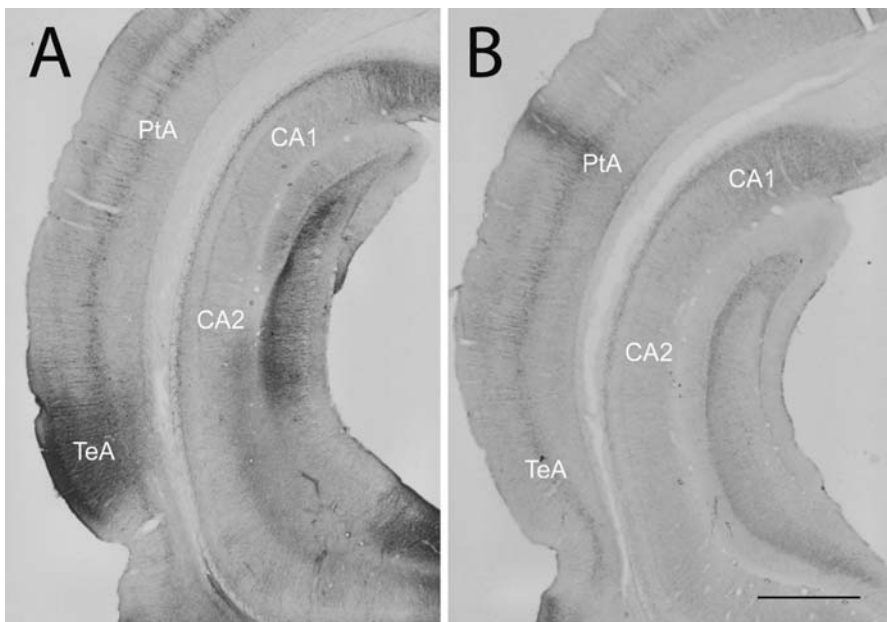


Fig. 3.7. Photomicrographs showing the distribution of intensified immunostaining for MAP2 in a module of temporal association cortex (TeA) of an animal trained on a fear-conditioning task (frame A) compared to that of a naive animal (frame B). Conversely, a more slender module in the parietal association cortex (PtA) is more intensely stained in the naive control animal than in the fear-conditioned animal. Sectors CA1 and CA2 of the hippocampus are lightly stained in both animals. Scale bar equals 1 mm

Cholinergic fibers arising from the basal forebrain have terminal fields that are approximately the same size as cortical areas or modules in the rat²⁸, further implicating acetylcholine as playing a role in the MAP2 response with learning. If our results had revealed MAP2 breakdown mainly in the fine distal dendrites, then a change in dendrite branch geometry would be the logical interpretation²⁹. In our observations, however, a significant amount of MAP2 degradation occurred in the cell body and in the proximal dendrites. This implies that a reconstruction of intradendritic microtubule networks occurred, since new branches are rarely added to the thick proximal dendrites or to the cell body. Hypothetically, updated microtubule networks could serve many

²⁸ Cholinergic fibers terminate in fields of 1–2 mm², whereas glutamate fibers terminate in vertical columns of 50 µm, and noradrenergic, dopaminergic, and serotonergic fibers diffusely innervate widespread expanses of cerebral cortex [148].

²⁹ Breakdown of MAP2 and subsequent phosphorylation may increase branching, since increases in the MAP2 phosphorylation state correlate with increases in dendrite branching [6]. Increased dendrite branching has been observed with certain types of learning (e.g., Withers and Greenough [140]; Greenough et al. [39]).

purposes. Newly formed intradendritic networks could connect different subsynaptic zones together, thereby storing information about the spatial and temporal relationships of activity at those synapses.

Plus ends of microtubules are primary sites of polymerization, and these sites are distributed throughout the neuron. Local polymerization/depolymerization is instrumental to updating the microtubule network in all parts of the neuron³⁰. When plus ends of microtubules near subsynaptic zones are affected by synaptic activation via glutamate neurotransmission, this triggers a localized response. The additional presence of a neuromodulator, such as acetylcholine, will promote widespread effects along the dendrite shaft. Thus, the coactivation of glutamate, along with acetylcholine or another neuromodulator, is likely to produce the greatest change to the intradendritic network of microtubules, in terms of both localized and widespread effects.

Relatively stable MAP2 bridges near the minus ends of microtubules may be most critical for linking together different coactivated subsynaptic zones and providing a possible means for long-term storage by microtubules (refer back to Fig. 3.6). Accordingly, the microtubule network, with its various MAP2 linkages, could serve as a coincidence detector for multiple synapses within the same neuron. More than merely linking two coactivated subsynaptic zones, layers of microtubules could build complex parallel networks representing coactivation patterns, using a reasonably small number of relatively stable MAP2 bridges³¹. Microtubules could, furthermore, weight synaptic inputs equally or unequally depending on their lengths, or series of microtubules of different lengths could store temporal sequences of activation. The possibilities are almost endless.

The various modes by which microtubules may store information could account for how microtubules might determine where spines are formed (and where they would reappear following retraction). There is preliminary experimental evidence that spine motility may depend on microtubules. The vinca alkaloid, vinpocetine, increases spine motility, apparently because of its effects on microtubules [74].

Reorganization of microtubule networks and their interactions with actin filaments could also increase (or decrease) the efficiency of transporting intact synaptic protein and mRNA to certain synapses and spines. In this manner, microtubule–actin networks could initiate or maintain potentiated or depotentiated synaptic activity. Evidence in support of this is found in long-term potentiation (LTP) relying upon the transport of AMPA receptors along microtubules and actin filaments [65, 66]. Also, LTP increases a number of presynaptic and postsynaptic proteins, including F-actin [5]. Maintenance of

³⁰ Stepanova et al. [119] used end-binding protein 3 (EB3) to show local microtubule polymerization.

³¹ Stable MAP2 bridges would be expected to turn over at slower rate, allowing for replacement with new MAP2 bridges that preserved the intradendritic pattern of connectivity.

the late phase of LTP depends upon F-actin [31]. Involvement of microtubules is also implicated during particular phases of LTP. The mRNAs for CaCMK II and MAP2 are increased during the induction of LTP [105]. During the intermediate phase of LTP, expression of CaCMK II and MAP2 is increased by calcium and PKA, respectively [3].

Microtubule networks also have a means to “date” when groups of new synapses are formed or changed. Posttranslational modifications such as de-tirosination reflect the age of microtubules. Synapses that are formed or modified at the same time will be associated with subsynaptic microtubules having the same “age”.

An Anchoring Site for PKA on the N-Terminus of MAP2 is Necessary for Learning

As emphasized earlier, MAP2 is not merely a structural protein. MAP2 also serves as a PKA-anchoring protein and it binds regulatory subunits RII α and RII β of PKA. This aspect of MAP2 has been studied in knockout mice. Mice bred homozygous for a genetic knockout of MAP2 (MAP2 $-/-$) show a reduction of microtubule density and dendritic length, as well as decreased PKA expression [48]. The RII α , RII β and catalytic subunits of PKA are decreased in MAP2 $-/-$ mice as compared to wild-type mice, whereas CaCMK II expression in MAP2 $-/-$ mice is about the same as in control mice. Thus, it appears that MAP2 tethers PKA to the microtubule, until PKA release into the cytoplasm is stimulated by cAMP.

The regulatory subunit RII β of PKA is located on the N-terminus of MAP2. Deletions of the N-terminal region of MAP2 were made in another set of transgenic mice, and then these mice were studied for effects on behavior [64]. These transgenics were impaired on a fear-conditioning task to context, but not with fear conditioning to tone³². Moreover, cAMP-dependent phosphorylation of MAP2 was significantly diminished in these transgenics. In heterozygous mice, cAMP-dependent phosphorylation was decreased by 90% and 80%, respectively, for truncated and full-length MAP2. Decreased phosphorylation for full-length microtubules was unexpected. The explanation given by these authors is that MAP2 forms multimolecular complexes and then transphosphorylates tubulin binding domains on neighboring MAP2 molecules. This transphosphorylation could lead to the dissociation of MAP2 and those microtubules. This result also indicates bridges linking microtubules in dendrites are likely to be composed of two overlapping MAP2 sidearms³³.

The conclusion of these studies is that MAP2 acting as an anchoring protein plays an essential role in learning. Additionally, MAP2 is part of

³² Conditioning to tone served as a control.

³³ Such an explanation would reconcile the impression in electron micrographs that MAP2 seamlessly links neighboring microtubules, yet only the C-terminal region of MAP2 has a binding site for tubulin.

a multimeric complex that regulates its own phosphorylation state and that of neighboring components of the cytoskeleton. The end result can affect the MAP2–microtubule linkages, the density of microtubules and microtubule length.

Microtubule Transport by Kinesin Participates in Learning

There are many kinesins. KIF17 belongs to the kinesin superfamily and it specializes in transporting NMDA receptor subunit NR2B in neurons. Guillard et al. [42] performed double-immunohistochemical analyses to determine the fate of NR2B subunits in hippocampal neurons. From their colocalization studies, they determined that KIF17 was responsible for transporting NR2B to synaptic sites labeled by PSD-95 or synaptophysin. Near to the synaptic site, NR2B detached from kinesin and colocalized with PSD-95 or synaptophysin. A separate study from the same laboratory showed that transgenic mice overexpressing KIF17 had improved working and spatial memory [142]. These authors propose a repeating cycle based on their results. The cycle starts with increased transport of NR2B in dendrites, which increases Ca^{2+} ion flux, and then increases in PKA and CaCMK II. Next, the transcription factor CREB is activated, which increases mRNA of NR2B, and then the cycle repeats.

Polyribosomes and mRNAs for signal-transduction molecules critically involved in learning and memory have been found in dendrites [120]. These include mRNA for NMDA receptor, CaCMK II, and MAP2. Local translation of these proteins within the spine is made possible by shifts of polyribosomes from dendrite shafts to spines following tetanic stimulation producing LTP [95]. These shifts among ribosomes further implicate transport as critical to learning. Other evidence suggests that kinesin plays a role in learning and plasticity. We have studied KIF17, NR2B and PSD-95 in rats for one week following training on the contextual fear task. In hippocampus CA1, contextual fear training decreased the binding of NR2 to kinesin and increased NR2 binding to PSD-95 (see Fig. 3.8).

Our results are consistent with the notion that brain reorganization following learning stabilizes increased levels of receptors bound to the postsynaptic density and decreases further transport. Since there is generally an inverse relationship between microtubule stability and transport, this would be consistent with increased microtubule stability at one week after training. Experiments done on MAP2, kinesin and learning can be summarized into an overall scheme that places microtubules in a central position during learning and memory (see Fig. 3.9).

Step 1. There is coactivation of acetylcholine and glutamate, as one would expect when a stimulus was receiving attention. Metabotropic receptors (e.g., muscarinic) increase phosphorylation of MAP2 and decrease its binding to microtubules.

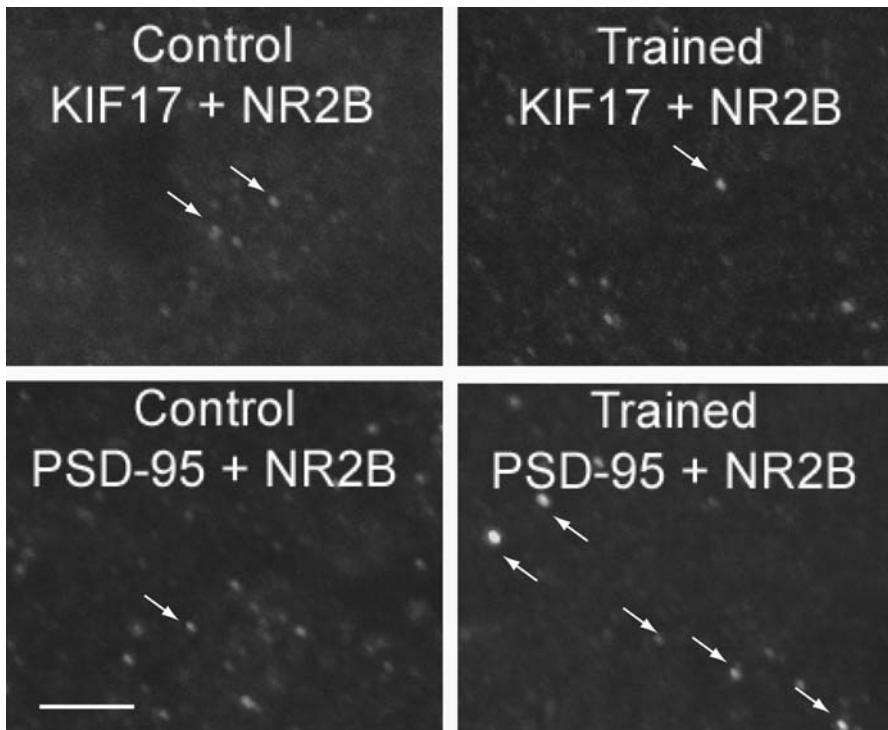


Fig. 3.8. Photomicrographs of hippocampal tissue from animals trained on a fear-conditioning task or naïve controls. *Top panels:* Kinesin, KIF17, is immunostained with fluorescein (illustrated as green puncta) and NR2B is immunostained with Texas red (illustrated in red). White arrows point to overlap between KIF17 and NR2B shown as yellow. *Bottom panels:* Postsynaptic density protein, PSD-95, is immunostained with Texas red (illustrated as red puncta) and NR2B is immunostained with fluorescein (illustrated as green puncta). White arrows point to overlap between PSD-95 and NR2B shown as yellow. Scale bar equals 10 µm

Step 2. Increased transport of protein, for example, NMDA receptor, would be expected as a result of decreased MAP2 binding, which would free up binding sites for kinesin. This is expected because MAP2 and kinesin bind to the same general vicinity on the microtubule.

Step 3. Upregulation of NMDA receptors would be expected as a result of increased transport of NMDA receptor subunits. This would also increase the influx of calcium ions, which would increase calpain.

Step 4. Proteolysis of MAP2 and tubulin leading to a dissociation of microtubule bridges and microtubules would be expected as a result of increased calpain.

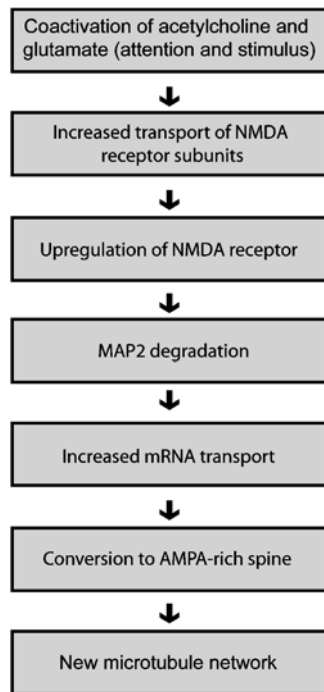


Fig. 3.9. The seven steps outlining the role of microtubules in memory. See text for elaboration

Step 5. Following MAP2 proteolysis, rebuilding would include increased transport of mRNA for NMDA, CaCMK II and MAP2, followed by local translation of these proteins essential to learning.

Step 6. More rebuilding would include the conversion of small spines into larger, AMPA-rich spines. These large AMPA-rich spines would be maintained at their increased size by regulating transport rates of AMPA receptors. Microtubule networks would be responsible for determining spine size and receptor content.

Step 7. A new microtubule network would be formed as a result of extensive reorganization. Consequently, microtubules would direct kinesin-mediated transport to the various subsynaptic zones throughout the neuron.

Spatial relationships between synapses could be represented by MAP2 bridges between the minus ends of two or more microtubules having plus ends reaching the subsynaptic zones of those synapses to be linked. MAP2 bridges near the minus ends are emphasized here because these linkages are relatively stable³⁴. Temporal relationships could be similarly represented, but

³⁴ Microtubule polymerization and binding to MAP2 are stable near the minus ends due to posttranslational modifications, such as detyrosination, and linkages to neurofilaments.

with different lengths of microtubules linking subsynaptic zones such that activity could be reproduced in particular sequences. Memories formed at the same time could be marked by similar “dates” indicated by similar posttranslational modification patterns. These types of modifications, among others, would represent long-term memory storage.

3.3.3 Microtubules Influence Synaptic Efficacy

Once memory is stored in newly stabilized microtubules, how is that stored information able to affect neural processing? There are a number of ways microtubules could affect electrophysiological events, such as membrane potentials and action potentials. For one, by determining the placement of synapses and their size, synaptic activity will be altered in the long term. Secondly, by altering transport rates of proteins and mRNA to synapses, microtubules will affect membrane potentials within minutes to hours. Thirdly, the biophysical state of the microtubule has the potential to actively control the synapse and the neuronal membrane directly, acting within milliseconds.

Although the integrity of ion channels does not appear to depend on the cytoskeleton [86], microtubules directly regulate or modulate some gated ion channels. For example, cytoskeletal proteins regulate the GABA_A-gated channel [138]. Stabilization of microtubules appears to directly block muscarinic acetylcholine receptors from inactivating the L-type calcium current [79]³⁵. Polymerization state of microtubules affects the function of glycine receptors [23]. Microtubules have also been shown to abruptly shift the properties of sodium channels [113] and are necessary for proper functioning of sodium channels in squid axon [80].

The ability of microtubules to commence electrophysiological activity is an entirely feasible proposal. Microtubules self-induce polymerization/depolymerization cycles during cell mitosis, and may do the same in order to initiate electrophysiological responses. Self-initiated changes in biophysical properties affecting the binding and unbinding between microtubules and MAPs may also influence local ion-channel activity. Any model of memory must address the issue of how synapses are activated in the absence of direct sensory activation. Models such as potentiation and depotentiation describe the nature of electrophysiological responses *elicited by stimuli* following conditioning, but not how such cellular responses are initiated in the *absence of stimuli*.

3.4 Consciousness

Consciousness, memory and attention are interrelated psychological phenomena, although key differences are found between them. Surface recordings

³⁵ This was found in guinea-pig myocytes.

from human subjects show synchronous oscillations of different frequencies typify memory in contrast with attention, and that consciousness is correlated with widespread synchronous oscillations³⁶. Nonetheless, it is difficult, if not impossible, to attempt to explain consciousness without addressing the psychological phenomena that it makes possible. An important concept often neglected is that conscious activity is action. Consciousness is covert behavior, the internalized brain function that is the counterpart of overt, observable behavior.

In order to make pragmatic use of information stored in some types of memory³⁷, that information must be brought to consciousness. Psychologists refer to this process as memory retrieval. A possible brain mechanism for memory outlined in the previous section of this chapter assigns an “actor” role to microtubules in the brain. This mechanism is also able to account for the action component of consciousness.

3.4.1 Attention: The Spotlight of Consciousness

Attention is a deliberate action whereby one directs conscious operations to a particular sensory stimulus, to a memory, or to a complex amalgam of both stimulus and memory. Sensation, attention and arousal are mediated through different neurotransmitter pathways, each of which will affect brain microtubules in different ways.

Glutamate neurotransmission transmits sensory data all along the sensory pathways. A sensory pathway begins in a sensory organ (i. e. the retina, cochlea, vestibular organ, skin, taste buds or nasal epithelium), usually makes synaptic contact in the thalamus, then relays to a primary sensory cortex, and then through a series of corticocortical circuits reaches higher association cortex. The glutamate system is topographically organized (e. g., visuotopic, tonotopic or somatotopic) such that the location of the visual field, the cochlea, or the body onto which stimuli are mapped is preserved at each relay. The sensory systems organize information from external sources in a point-to-point scheme. By analogy, it is like every person living in New York City being in phone or email contact with one person in Los Angeles who lives at the same north-south and east-west placement in the corresponding city. This system is “online”; new information is continually coming in.

Global systems of neurons utilize the neurotransmitters acetylcholine and monoamines: norepinephrine, serotonin and dopamine³⁸. These cellular aggregates receive sensory collateral branches from axons en route to the cere-

³⁶ Memory is related to oscillations in the theta and gamma range, whereas attention is related to alpha and gamma [135].

³⁷ Memory that reaches consciousness is called explicit or declarative.

³⁸ These groups of neurons form interconnected cellular aggregates throughout the hindbrain and basal forebrain enabling a high degree of crosstalk between constituent neurons [148].

bral cortex. In this manner, these neurons obtain a general idea of the overall pattern of incoming inputs and then base their outputs on those assessments. Cholinergic systems contribute to selective attention, whereas norepinephrine, serotonin and dopamine systems contribute to general arousal or vigilance. Cholinergic neurons from the basal forebrain are able to contribute to selective attention because they innervate discrete areas of cortex of a single modality measuring 1–2 mm². Noradrenergic, serotonergic and dopamine neurons in the brainstem innervate the cortex less restrictively. A single noradrenergic fiber, for example, may provide inputs to many different types of cortex, as these fibers are long and have many release sites along their paths.

Taking into consideration that attention is a deliberate act, what neurochemical component of the neural circuit could be responsible for it? The glutamatergic synapse *per se* cannot be the source of attention. Sensory inputs in some cases do reach consciousness, but often they do *not* reach consciousness. What part of the glutamate synapse would decide, and on what basis? These synapses are passive, responding to inputs. Even in the presence of enhanced synaptic efficacy (e.g., LTP), how would such potentiation lead to attention and consciousness? Going back to the analogy of one person in New York City being in direct contact with one similarly placed person in Los Angeles, we might view increased synaptic efficacy as an increase in information flow between selected persons in this one-to-one connected network. Would selectively increasing information flow attain an increased level of attention or reach consciousness? No, not in this one-to-one connected network, which is not too far from the way cortical systems are organized. A mechanism is needed that accesses the overall pattern of inputs and compares these patterns to input patterns occurring in the remembered past and input patterns anticipated in the future.

Cholinergic and monoaminergic inputs seem closer candidates for this role of accessing the overall pattern of inputs, insofar as these systems sample sensory activity en route to the cerebral cortex. On the other hand, the information these systems relay cannot be precise enough, since their terminal fields are diffusely distributed to cortical modules or to the entire cortex. These inputs are necessary, but not sufficient for attention and arousal. Activation by glutamate, acetylcholine and norepinephrine are obligatory steps for a stimulus to receive attention. But all these synapses are passive; none has the “actor” status needed to decide whether to deliberately arouse consciousness or to select content.

Self-organizing microtubule networks inside dendrites do have the “actor” status needed to deliberately direct attention and consciousness. Because microtubules can polymerize and depolymerize, they can search for and activate particular subsynaptic sites. Although release of glutamate, acetylcholine and monoamines is obligatory for full conscious awareness, this behavioral state must also rely on the biophysical state of the microtubule network. Just as phosphorylation of MAP2 and its subsequent binding can affect the biophys-

ical state of the microtubule, the biophysical state of the microtubule can affect the binding of MAP2. As a specific example, the biophysical state of the microtubule can induce the release PKA through effects on the regulatory subunit RII β of PKA. Bidirectional effects on PKA-mediated transphosphorylation of neighboring MAP2 causes the “zipping” and “unzipping” between neighboring microtubules, leading to subsequent increases and decreases in the rate of kinesin-mediated transport along microtubules³⁹. Regulation of transport is necessary to maintain large spines, which are laden with many AMPA receptors.

These, among other effects, would enable the microtubule network to direct attention and consciousness. Accordingly, the psychical sensation of attention could not possibly be associated with synaptic activity per se, since those activities occur both in the presence and in the absence of attention. Instead, the psychical sensation of directed attention and consciousness could well be associated with the biophysical state of microtubules that regulates (1) polymerization and depolymerization cycles linking synapses and (2) transport to active synapses.

3.4.2 Waking, Sleeping and Dreaming: Different Levels of Consciousness

Another way to look at consciousness is to see it as part of the sleep–wakefulness continuum. When a subject is awake, the electroencephalogram (EEG) is a complex mixture of fast waves (i.e. beta, alpha, gamma waves). When a subject falls into dreamless sleep (non-REM⁴⁰), the EEG pattern slows down markedly, each deeper step containing fewer theta waves and more delta waves. When a subject experiences REM or dream sleep, the EEG looks more like that of an awake person than that of a person during non-REM sleep. It is not known what provides the basis for the content of dreams.

Neurotransmitter levels change over the sleep–wakefulness cycle and bilateral damage to brainstem areas containing cholinergic, noradrenergic and serotonergic neurons results in coma [99]. Acetylcholine, norepinephrine and serotonin levels are high during wakefulness, low during non-REM sleep; and during REM sleep, acetylcholine is very high and norepinephrine and serotonin levels are very low [53, 55]. This pattern suggests norepinephrine

³⁹ When adjacent microtubules are linked by antiparallel MAP2s, transphosphorylation might be expected to repel these MAP2s leading to the “unzipping” of the two microtubules and thereby removing any physical block impeding kinesin binding. Although kinesin binding is not directly affected by MAP2s as it can travel on protofilaments not bound to MAP2s, attached cargo and other complexed proteins will affect the processivity of kinesin in a limited space.

⁴⁰ Sleep is characterized by periods of rapid eye movements (REM) and periods without rapid eye movements (non-REM). REM sleep corresponds to dream sleep most of the time.

and serotonin are critical in linking consciousness to incoming stimuli. These monoamine neurotransmitters often bind to receptors activating the second messenger PKA, suggesting that high levels of cAMP and PKA are important to wakeful consciousness. But during dream sleep, norepinephrine and serotonin levels sink very low. Since dreaming is a kind of conscious activity – consisting of visual imagery, thinking and emotion – acetylcholine might be particularly responsible for those aspects of consciousness reflecting inner experience. As mentioned earlier, however, cholinergic terminals are too diffusely organized to account for the specific content of inner experience, and the same argument would hold for the specific content of dreams. Perhaps effects of the combined release of acetylcholine and glutamate could account for the content of dreams. But during dreaming, activation of glutamate synapses must be entirely random. Also, combining neurotransmitters does not solve the problem concerning self-organization.

One is left with the only possible conclusion being that neurotransmitter release per se cannot be responsible for consciousness. Since a tenable scenario is that a biophysical state in the microtubule network is responsible, corelease of glutamate and acetylcholine could facilitate dream-state consciousness through enabling effects on microtubules. In this case, the psychological sensation of consciousness would be related to the biophysical state of the microtubule network, as described earlier.

The basis of anesthetic action demonstrates that a relationship between the cytoskeleton and consciousness does exist. Many of the cytoskeletal actions thought to be critical to memory are also blocked by anesthetics. Specific examples include: local anesthetics inhibiting kinesin motility [84], volatile anesthetics interfering with actin-based motility in dendritic spines [62] and volatile anesthetics interfering with MAP2 degradation in frontoparietal cortex and hippocampus [122]. These studies support a link between the cytoskeleton, memory and consciousness.

3.4.3 Mental Force to Think and Act

As a general rule, the more involved that analyses of cortical responses get, the more it becomes clear that to understand the simplest of cellular responses, one needs to simultaneously understand brain-wide activity. Consider a simple perceptual act, that of seeing a simple contour. Complex cells in the primary visual cortex respond to salient contours embedded in complex backgrounds [77]. Long-range horizontal connections provide a rudimentary basis for contour saliency; however, top-down influences and learning effects are needed to explain how this, one of the simplest percept, comes to be realized.

So what does one attempt to understand first: the complex multisensory processes or the simple early sensory responses? As stated earlier, there are a few known multisensory regions. These brain regions having multisensory

connections appear to use those connections for multisensory tasks. A recent fMRI study, for example, found a small region in the posterior intraparietal sulcus was activated specifically for the crossmodality component of a combined visual-auditory task [107]. One might not expect crossmodality responses during early processing in primary and secondary sensory cortices, yet many examples of these kinds of responses appear in the literature. Neurons in secondary auditory cortex tuned to precise frequencies of sound also respond weakly to somatosensory input [30]. Eye position affects processing in primary auditory cortex [136]. Visual stimuli enhance tactile acuity through modulation of responses in the primary and secondary somatosensory cortex [124]. There are crossmodal links in selective attention directed toward visual, auditory, somatosensory and olfactory stimuli [116]. One study found elevated activity on fMRI scans in primary, secondary and association visual areas when congenitally blind subjects read Braille, but not when their fingers were merely touched [35]. This last study proves that crossmodality responses are not driven through the growth of plastic connections between somatosensory and visual areas. Cortical plasticity, in terms on new axon growth, cannot account for how these effects rapidly appear under certain conditions and then disappear under other conditions instantly.

Crossmodal influences may occur through feedback connections from multisensory cortex. Sparse anatomical links from multisensory association cortex have been traced to primary and secondary visual cortex [27, 106]. Critical questions remain unanswered, however: Are the sparse connections currently known sufficient for the multitude of crossmodal tasks? How do these areas decide when to transmit information backward, and to where? Since most cognitive tasks we perform have multisensory components, it appears that: (1) the same few multisensory regions are involved in many tasks, (2) many anatomical connections remain undiscovered or (3) some kind of brain interactions other than corticocortical connections are additionally at play⁴¹.

Some researchers have acknowledged the lack of critical corticocortical connections implied by certain visuomotor tasks and have looked to subcortical connections [36]. Many, if not most, subcortical sites are also segregated according to sensory modality⁴². How is it then that we can guide complex voluntary motor acts for the first time? Human subjects are known to impart their own personal handwriting style when using their toe to write a message

⁴¹ Corticocortical connections link different cortical areas preserving much of the original sensory topography; thus, the anatomical scheme continues to be a point-to-point mapping with limited opportunity to synthesize and integrate data. Modulatory brain regions (e.g., the basal forebrain and locus ceruleus) are anatomically better suited to integrate and synthesize multisensory responses in crossmodal selective attention because their projections onto cortex are more diffuse. Projections from the locus ceruleus are more diffuse than those from the basal forebrain.

⁴² Edge et al. [25] found evidence for somatosensory and visual convergence in parts of the cerebellum.

in the sand⁴³. How much plasticity is needed to produce connections that are largely or completely absent before attempting such a behavior for the first time?

Perhaps a well-developed sensorimotor imagination is enough. Motor imagery is essential for simple movements. Recently, it has been shown that the motor cortex is activated as if sensory input had occurred in anticipation of a motor activity [91]. This shows that we experience sensory feedback before it occurs. Nonhuman primates have similar sensorimotor skills to ours. Monkeys can learn to produce coordinated activity in large ensembles of frontoparietal cortex in order to control robotic arms through implanted arrays of microwires [17]. Monkeys learn this task without any somatosensory feedback⁴⁴; it is as if these animals can imagine that feedback. This “imagined” somatosensory feedback and the enigmatic “will to move” are mainly driving the neural activity that moves the robotic arm.

What provides the “mental force” needed to begin a movement or to drive thought? Microtubule networks and motor proteins fit the bill because of their mechanical nature and their interactions with actin filaments in linking synapses. Through self-induced polymerization/depolymerization cycles, binding and unbinding to MAP2 and kinesin, microtubules are capable of influencing membrane potential differences, in both the short-term and long-term ranges.

3.4.4 Consciousness, Memory and Microtubules

If memory is stored in microtubules, and if microtubules are the site of consciousness in the brain⁴⁵, then it is a simple case to relate memory and consciousness. Instead of using one hypothesis upon which to base another, however, I will argue that we can eliminate certain possible bases of consciousness if those are not suitable bases for memory storage.

Changes in synaptic strength undoubtedly play a role in encoding memory, but is this also the mode of long-term storage? The contemporary view is that long-term memory storage is the change within the synapse, for example, a thickening of the postsynaptic membrane, a change in spine shape or receptor density. The view I propose in this chapter is that the site of memory storage is not within the synapse, but in the subsynaptic zone, in the microtubules of the dendrite shaft. In addition to the data presented earlier, the logic to this proposal is that the synapse is a channel transmitting information, much like a radio receiver. To record information transmitted on a channel, a separate recording material, such as magnetic tape, is needed. If

⁴³ Based on studies of motor equivalence in handwriting [139].

⁴⁴ Monkeys keep their own arms still in this task and receive no direct feedback from the implanted device.

⁴⁵ See supporting arguments and outline of potential falsifying experiments in Hameroff [46] and Hameroff and Penrose [47].

one permanently altered the receiving channels, the device would not maintain fidelity; it would not be able to faithfully transmit audio information in the future. It would be analogous to having Beethoven played on the radio today sounding exactly like Bach, which was played yesterday. That is not the way memory systems work, nor could they. It would serve no adaptive function to perpetually alter our sensory input channels; it would prevent any real comparisons and any degree of perceptual constancy.

In this analogy, the receiving channel is the synapse or spine. Although change in select populations of synapses or spines is part of memory encoding, altered synapses and spines soon revert back to baseline. Thus, there appears to be a homeostatic mechanism keeping the parameters of synapses and spines within certain boundaries. On the other hand, memory consolidation involves massive reorganization of microtubule networks⁴⁶. Reorganization this extensive is unlikely to revert back to baseline. Permanence of long-lasting change in microtubule networks is also revealed by changes to overall dendrite structure and dendrite-branching patterns long known to occur with learning. The arbitrator of dendrite morphology is the microtubule.

Most contemporary models of consciousness posit synaptic activity as the primary basis of consciousness. Since low levels of synaptic firing occur even when a subject is unconscious, it is clear that consciousness cannot be synaptic activity per se. Synchronous activity has been suggested as the neural correlate of consciousness; however, this concept has its counterexamples. Slow-wave sleep, for example, is the stage when neuronal synchrony is highest. Thus, it has been proposed that synchrony in certain frequency ranges, for example, in the gamma frequency range, constitutes consciousness. Here we have the problem that temporal information would not be preserved in such a scheme. How would one be conscious of a particular pattern of auditory clicks, for example, if that temporal pattern of input was obscured by a different consciousness-related frequency? Another notion put forward is that consciousness emerges as a function of complexity as groups of neurons fire together in various patterns. This idea is laudable, but arguably incomplete: a necessary element is missing.

A microtubule basis of memory and consciousness is a departure from current doctrine in neuroscience, but it may have fewer conceptual flaws than widely perceived. It is not a great leap in intellect to suggest that the subsynaptic zone, rather than the synapse, stores memory in the form of microtubule networks capable of self-organized polymerization/depolymerization cycles and transport, which in turn regulates synaptic activity. It is, furthermore, no monumental stretch of logic to postulate that the psychical sensation of consciousness is affiliated with the most directly relevant physical process, that being the biophysical state of the microtubule network.

⁴⁶ MAP2 degradation indicates widespread reorganization of microtubules with fear conditioning [144, 145].

3.5 Microtubules and Quantum Entanglement: A Possible Basis for Memory and Consciousness

Since the brain is not as widely interconnected as might be generally assumed, how is it that the brain acts as an integrated holistic system? How can activity at synapses on the same neuron or on different neurons become perfectly unified in order to represent a single idea or act? First, it is important to point out that being unified is not the same thing as being connected. During many perceptual tasks different parts of a whole are experienced as unified, but the parts do not necessarily *communicate* with one another. The left part of the visual field does not need to commutate with the right part of the visual field; nonetheless, they must be coexperienced. The same is arguably true for sensorimotor tasks. Given this perspective, it becomes clear that unified experience has more to do with coactivation of synapses rather than connections between neurons. But if mere coactivation of synapses fully accounted for the experience of mental events, then this would greatly reduce the need for learning-related change in the nervous system. The first instance of coactivation would suffice. All one would need is to re-experience that initial unified activation pattern again⁴⁷. This illustrates a possible fundamental error in the current viewpoint that neural-network-type learning is responsible for cognition, since, after periods of enhanced synaptic efficacy, the theory still relies on coactivation of synapses for the representation of ideas. One is left no closer to understanding the physical basis of the mental representation itself. If, on the other hand, the subsynaptic zones of highlighted synapses are connected by systems of microtubules, then quantum entanglement among those microtubules *is* a possible solution to unification, a solution with a real physical basis. This physical representation can then, in turn, be unified by quantum entanglement with other unified ideas represented by the coactivation of other subsynaptic zones.

Since the brain is so complex, I suggest the following scheme of quantum entanglement occurring at five levels of neural interaction based on the proximity of tubulin or microtubules to one another. These levels of neural interaction have nothing to do with the physics of entanglement per se, but rather with how one might expect brain tissue to be differently affected by this physical phenomenon at each level of neural interaction. A key point is that a small amount of entanglement is predicted to link the minimum number of subsynaptic zones required at each level. Accordingly, neural events will be tightly or loosely coupled depending on their degree of physical interaction.

The first level of neural interaction would include quantum entanglement among tubulins of the same microtubule. As is the case for all molecules in

⁴⁷ A possible counterargument is that learning is needed to reduce synaptic activity since experience leads to less, not more, cortical activation. Nonetheless, this is a quantitative issue and has little to do with the qualitative nature of the physical basis of mentation.

neurons, tubulins exist in a crowded molecular environment and perturb other molecules as they undergo chemical and physical changes. Under appropriate circumstances, these effects are likely to cascade. This is especially true since tubulin molecules are linked into long microtubule polymers; a biophysical change, such as deformations in dimer–dimer interactions, may perturb tubulins for several millimeters along the microtubule [109]. Since this level of neural interaction is between closely interacting particles, the degree or density of entanglement is likely to be high. Thus, the subsynaptic zones beneath adjacent synapses could, in principle, exhibit strong entanglement. Entanglement of this type is possible in brain tissue, according to recent calculations⁴⁸.

The second level of neural interaction would involve entanglement between microtubules in the same neuron. MAP2, for example, does link neighboring microtubules together (or to actin filaments) and these linkages dynamically associate and dissociate. Each MAP2 has one microtubule-binding site; however, it is likely that pairs of MAP2-microtubule complexes interact physically or via transphosphorylation, a process that promotes the exchange of phosphoryl groups between the two antiparallel MAP2-microtubule complexes. Microtubules connected (or having been connected) through MAP2 linkages or having exchanged phosphoryl groups would appear capable of entanglement due to present (or previous) interactions among particles. This would be especially true at the minus ends of microtubules, which tend to be stably linked to neighboring microtubules by MAPs and neurofilaments. This degree of entanglement would be somewhat less than that of tubulins in the same microtubule, meaning there might be more quantum discord. This would enable each neuron to assume many different states, linking different subsynaptic zones in a variety of ways.

The third degree of neural interaction would involve entanglement between neurons in modules. Our data showing uniform MAP2 proteolysis within neurons throughout cortical modules could be interpreted to reflect simultaneous degradation occurring in coherent quantum systems of microtubules within cortical modules. Horizontal gap junctions link microtubules from separate neurons together, physically connecting the cytoplasm of pyramidal neurons, horizontal interneurons and glial cells. Connexin-43, a widely expressed gap-junction protein, also binds to tubulin [34]. We have previously proposed that these gap junctions could underlie microtubule-based quantum entanglements spanning across neurons [143]. Again, this degree of entanglement would be expected to be less than that of tubulin in the same microtubule.

The fourth degree of neural interaction would involve entanglement within highly interconnected cortical areas (e.g., cortical areas of the same sen-

⁴⁸ Calculations that include brain temperature and decoherence issues indicate that quantum coherence is possible in brain (see Hagan et al., [43]) in spite of claims to the contrary [125].

sory modality). Entanglement can occur over long distances when there is a classical channel of information and a pre-existing entanglement. Qubits performing local operations can even send information to entangled qubits via classical channels⁴⁹. This kind of long-range quantum entanglement relies on a physical connection between the brain regions, for example, axonal connectivity between cortical areas or electromagnetic energy flow from one brain region to another. Microtubules binding to nCAMs that traverse the synapse may provide a physical link between the cytoskeleton in sending and receiving neurons.⁵⁰ This degree of entanglement might be expected to be medium to strong because of possible nCAM linkages between microtubules, but also limited to couplings between small groups of subsynaptic zones in widely different brain regions because of the limited nature of point-to-point connections.

The fifth level of neural interaction would involve entanglement among cortical areas having few or no axonal connections. Brain-wide entanglement might occur in a manner predicted by Bell's theorem stating that whenever a quantum measurement is made on one part of a holistic quantum system, this will produce an effect on other parts of the system [7]. This degree of entanglement would be weakest, thereby allowing for the great flexibility in brain response. The overall picture envisioned here is that there are weak, but widespread, couplings between microtubules in unrelated brain regions, with these microtubules, in turn, being strongly coupled to other microtubules in the same and in neighboring neurons and on the basis of specific long-distance connections. The grand total of microtubules involved at any instance may be quite large, but the grand scheme has an essential, self-defining architecture.

Regarding the basis of brain-wide entanglements, the brain arguably *is* a holistic system of directly and indirectly interacting parts, capable of entanglement⁵¹. Many anatomical and physiological factors, other than electrophysiology, contribute to the entire brain behaving as a holistic system. The skull rigidly encases the brain and limits hemodynamics; this in turn affects metabolic processes in an interactive manner. Since tissue mass and fluid volume needs to be kept constant, increased blood flow to one brain region must, of necessity, result in decreased blood flow to another brain region.

The skull protects the brain from some outside forces, albeit imperfectly, leaving neurons sensitive to external magnetic and gravitational fields, both of which can affect the biophysical state of microtubules [98, 102, 127]. While strong magnetic fields are safe for humans, transmagnetic stimulation (TMS)

⁴⁹ Although comparisons to neurons have not been made, entangled pairs can effectively communicate by sending 2 bits of information through a classical channel [16]

⁵⁰ Specific nCAMs bind actin, tubulin and actinin [15].

⁵¹ Although entanglements are generally limited to physically interacting systems, it is relevant to note here that entanglement can also be induced between non-interacting particles (e.g., Fattal et al., [28]).

increases neuronal excitability and can sometimes disrupt human cognitive processing [100]. Repetitive TMS, which has a more robust effect than single pulse TMS, has been shown to affect learning [37] and visual cognition [4]. Microgravity has negative effects on cognition and performance [8], but these skills quickly return in a normal gravity environment [126].

Neurons, especially the large pyramidal neurons, also generate electromagnetic activity due to their membrane potentials [70]. Thus, microtubules can, in principle, be affected by electromagnetic activity generated by nearby neurons. The geometry of cortical pyramidal cells may be significant in both the role of sender and receiver. Apical dendrites of large pyramidal cells radiate towards the surface in parallel with those from neighboring pyramidal cells. Basilar dendrites from pyramidal cells form a network parallel to the cortical surface. The convolutions of the cerebral cortex enable the spread of electromagnetic activity to skip over buried areas of cortex. It is not known how far weak electromagnetic activity can spread, but synchronous electromagnetic activity appears capable of having long-distance effects. It is indeed synchronous neuromagnetic activity in distant brain regions that accompanies consciousness [117].

In summary, the human brain defines a volume of space (on average 1100 cm^3) in which many types of interaction are possible. Space has a minimum nonzero volume of approximately 10^{-99} cubic centimeters (one cubic Planck length); this translates into 10^{102} cubic Planck lengths in the human brain. Since quantum states of entanglement in the human brain would be influenced by *all* possible factors – including electrophysiological (membrane potentials, action potentials), mechanical (transport along microtubules), biochemical (phosphorylation of MAP2; detyrosination, acetylation and polyglutamylation of microtubules), biophysical (microtubule polymerization), metabolic (energy utilization), electromagnetic and gravitational – one can argue that it can only be the state of brain-wide quantum coherence that corresponds with the cognitive state. Since tubulin and MAP2 compose a sizable percentage of brain protein, microtubules would be expected to contribute greatly to the equation. The presence of microtubules in the subsynaptic space and their ability to control synapse parameters only increases their importance.

The notion of brain-wide quantum entanglement depends on quantum entanglements scaling up to mesoscopic and macroscopic ranges. Ghosh et al. [32] provide data that quantum entanglement can scale up for a lithium magnetic salt compound. In a review of the Ghosh paper, Veral [131] notes with great enthusiasm: “a very small amount of entanglement can produce significant effects in the macroscopic world”. If this principle holds in brain, then quantum entanglement may prove highly successful at unraveling some of the greatest mysteries of the human mind.

For one, nonlocal quantum entanglement could explain how biophysical states among widespread microtubules can be unified into memory. Entan-

glement could be responsible for microtubules in different subsynaptic zones undergoing coherent polymerization/depolymerization cycles and for transport of synaptic proteins, such that a select composite of synapses are coherently activated. By controlling inputs, the output of the neuron is also under the control of its coherent microtubule network. If microtubules are particularly predisposed to quantum coherence during higher cognition, then all the information about a synapse's history stored in the subsynaptic microtubules could be shared by quantum coherence with other microtubules storing histories for other synapses.

Quantum entanglements also provide explanations for mental imagery that arises in the absence of sensory inputs, such as in dreams. One of the most widely accepted theory of dreams, the *activation-synthesis hypothesis* of Hobson and McCarley [54], does not fully explain the content of dreams beyond random neuronal firing that triggers the brain to generate stories. Quantum-entanglement theories of the mind get to the issue of how the brain generates those stories, as well as explaining the more enigmatic elements of perception (see Woolf and Hameroff, [143]). The prediction is that dream content is produced by sequences of quantum coherence among microtubules in various subsynaptic zones, linking sets of synapses that have previously shared histories. Furthermore, each component element of the temporal pattern (i.e. the dream plot) would be stored as a separate history, and presumably this would involve quantum entanglement among relevant subsynaptic zones over segments of time.

3.6 Conclusion

This chapter proposes that there is a novel way in which the brain may be unified, apart from traditional synaptic connections. It has long been known that the brain is highly interconnected through axons; nonetheless, these connections are most often confined to a single modality and connect brain areas in a restricted point-to-point fashion. Unified activity among brain microtubules is presently suggested to fill the void. The brain contains many neurotransmitters that affect the neuronal membrane potential; however, it is also true that these neurotransmitters affect the biophysical state of microtubules through ionic fluxes, actions on actin filaments and the phosphorylation of MAP2. Physical responses of microtubules include increased and decreased polymerization, transport and the regulation of receptor proteins inserted into the membrane. Microtubules in the subsynaptic space have properties making them more capable of storing information about synaptic activity than the constituents of the synapses themselves. Microtubules may also play a role in consciousness, thereby enabling attention, perception and dreams. The ubiquitous microtubule arguably sits at the interface between memory and consciousness.

Acknowledgement. I wish to thank my current collaborators: Stuart Hameroff, Jack Tuszynski and Avner Priel for intellectual discussions. Special thanks are due Adele Behar for supporting some of this work and to Malcolm Dean for sending me interesting papers.

References

1. Ainsztein, A.M., Purich, D.L. (1994). *J Biol Chem.* **269(45)**:28465–71.
2. Al-Bassam, J., Ozer, R.S., Safer, D., Halpain, S., Milligan, R.A. (2002) *J Cell Biol.* **157(7)**:1187–96.
3. Alier, K.A., Morris, B.J. (2004). *Brain Res Mol Brain Res.* **122(1)**:10–6.
4. Amassian, V.E., Cracco, R.Q., Maccabee, P.J., Cracco, J.B., Rudell, A.P., Eberle, L. (1998). *J Clin Neurophysiol.* **15(4)**:288–304.
5. Antonova, I., Arancio, O., Trillat, A.C., Wang, H.G., Zablow, L., Udo, H., Kandel, E.R., Hawkins, RD. (2001). *Science* **294(5546)**:1547–50.
6. Audesirk, G., Cabell, L., Kern, M. (1997). *Brain Res Dev Brain Res.* **102(2)**:247–60.
7. Bell, JS. (1987). In: *Speakable and Unspeakable in Quantum Mechanics*. Cambridge University Press:14–21.
8. Bock, O., Abeele, S., Eversheim, U. (2003). *Aviat Space Environ Med.* **74(12)**:1256–62.
9. Braendgaard, H., Evans, S.M., Howard, C.V., Gundersen, H.J. (1990). *J Microsc.* **157**:285–304.
10. Brodmann, K. (1909). *Vergleichende Lokalisationslehre der Grosshirnrinde in ihren Prinzipien dargestellt auf Grund des Zellenbaues.*
11. Brown, J.R., Stafford, P., Langford, GM. (2004). *J Neurobiol.* **58(2)**:175–88.
12. Brown, M.E., Bridgman, PC. (2004). *J Neurobiol.* **58(1)**:118–30.
13. Bruzzone, R., Hormuzdi, S.G., Barbe, M.T., Herb, A., Monyer, H. (2003). *Proc Natl Acad Sci USA.* **100(23)**: 13644–9.
14. Buddle, M., Eberhardt, E., Ciminello, L.H., Levin, T., Wing, R., DiPasquale, K., Raley-Susman, KM. (2003). *Brain Res.* **978(1–2)**:38–50.
15. Buttner, B., Kannicht, C., Reutter, W., Horstkorte, R. (2003). *Biochem Biophys Res Commun.* **310(3)**:967–71.
16. Carlo, G.G., Benenti, G., Casati, G. (2003). *Phys Rev Lett.* **91(25)**:257903.
17. Carmena, J.M., Lebedev, M.A., Crist, R.E., O'Doherty, J.E., Santucci, D.M., Dimitrov, D., Patil, P.G., Henriquez, C.S., Nicolelis, MA. (2003). *PLoS Biol.* **1(2)**:E42
18. Castoldi, M., Popov, AV. (2003). *Protein Expr Purif.* **32(1)**: 83–8.
19. Chang, S., De Camilli, P. (2001). *Nat Neurosci.* **4(8)**:787–93.
20. Cohen, R.S., Kriho, V. (1991). *J Neurocytol.* **20(9)**:703–15.
21. Dehmelt, L., Halpain, S. (2004). *J Neurobiol.* **58(1)**:18–33.
22. Dehmelt, L., Smart, F.M., Ozer, R.S., Halpain, S. (2003). *J Neurosci.* **23(29)**: 9479–90.
23. Delon, J., Legendre, P. (1995). *Neuroreport* **6(14)**:1932–6.
24. Doubell, T.P., Stewart, MG. (1993). *J Neurosci.* **13(5)**:2230–6.
25. Edge, A.L., Marple-Horvat, D.E., Apps, R. (2003). *Eur J Neurosci.* **18(6)**: 1468–85.

26. Elston, GN. (2003). *Cereb Cortex*. **13(11)**:1124–38.
27. Falchier, A., Clavagnier, S., Barone, P., Kennedy, H. (2002). *J Neurosci*. **22(13)**:5749–59.
28. Fattal, D., Inoue, K., Vuckovic, J., Santori, C., Solomon, G.S., Yamamoto, Y. (2004). *Phys Rev Lett*. **92(3)**:037903.
29. Fischl, B., Dale, AM. (2000). *Proc Natl Acad Sci, USA*. **97(20)**: 11050–5.
30. Fu, K.M., Johnston, T.A., Shah, A.S., Arnold, L., Smiley, J., Hackett, T.A., Garraghty, P.E., Schroeder, CE. (2003). *J Neurosci*. **23(20)**:7510–5.
31. Fukazawa, Y., Saitoh, Y., Ozawa, F., Ohta, Y., Mizuno, K., Inokuchi, K. (2003). *Neuron* **38(3)**:447–60.
32. Ghosh, S., Rosenbaum, T.F., Aepli, G., Coppersmith, SN. (2003). *Nature* **425(6953)**:48–51.
33. Gibbons, F., Chauwin, J.F., Desposito, M., Jose, JV. (2001). *Biophys J*. **80(6)**:2515–26.
34. Giepmans, B.N., Verlaan, I., Moolenaar, WH. (2001). *Cell Commun Adhes*. **8(4–6)**:219–23.
35. Gizewski, E.R., Gasser, T., de Greiff, A., Boehm, A., Forsting, M. (2003). *Neuroimage* **19(3)**:968–75.
36. Glickstein, M. (2000). *Trends Neurosci*. **23(12)**:613–7.
37. Grafman, J., Wassermann, E. (1999). *Neuropsychologia* **37(2)**:159–67.
38. Grau, E., Felipo, V., Minana, M.D., Grisolia, S. (1992). *Neurochem Res*. **17(10)**:967–71.
39. Greenough, W.T., Larson, J.R., Withers, GS. (1985). *Behav Neural Biol*. **44(2)**:301–14.
40. Griffith, L.M., Pollard, TD. (1982). *J Biol Chem*. **257(15)**:9143–51.
41. Grutzendler, J., Kasthuri, N., Gan, WB. (2002). *Nature* **420(6917)**:812–6.
42. Guillaud, L., Setou, M., Hirokawa, N. (2003). *J Neurosci*. **23(1)**:131–40.
43. Hagan, S., Hameroff, S.R., Tuszynski, JA. (2002). *Phys Rev, E Stat Nonlin Soft Matter Phys*. **65(6 Pt 1)**:061901.
44. Halpain, S., Hipolito, A., Saffer, L. (1998). *J Neurosci*. **18(23)**:9835–44.
45. Halpain, S. (2000). *Trends Neurosci*. **23(4)**:141–6.
46. Hameroff, S. (1998). *Philos. Trans. R. Soc. London Ser. A* **356**:1869–1896.
47. Hameroff, S.R., and Penrose, R. (1996b). *J. Conscious. Stud*. **3**:36–53
48. Harada, A., Teng, J., Takei, Y., Oguchi, K., Hirokawa, N. (2002). *J Cell Biol*. **158(3)**:541–9.
49. Hasbani, M.J., Schlief, M.L., Fisher, D.A., Goldberg, MP. (2001). *J Neurosci*. **21(7)**:2393–403.
50. Hebb, DO. (1949). *The Organization of Behavior*. New York: John Wiley.
51. Hilgetag, C.C., Burns, G.A., O'Neill, M.A., Scannell, J.W., Young, MP. (2000). *Philos Trans, R Soc Lond, B Biol Sci*. **355(1393)**:91–110.
52. Hiller, G. and, K. Weber, (1978). *Cell* **14**:795–804.
53. Hobson, J.A. (1994). *The Chemistry of Conscious States: How the Brain Changes its Mind*. Little, Brown.
54. Hobson, J.A., McCarley, R.W. (1977). *Am, J Psychiatry*. **134(12)**:1335–48.
55. Hobson, J.A., Pace-Schott, E.F. (2002). *Nat Rev Neurosci*. **3(9)**:679–93.
56. Homma, N., Takei, Y., Tanaka, Y., Nakata, T., Terada, S., Kikkawa, M., Noda, Y., Hirokawa, N. (2003). *Cell* **114(2)**:229–39.
57. Huang, X.P., Hampson, DR. (2000). *J Neurochem*. **74(1)**:104–13.

58. Huang, Y.S., Carson, J.H., Barbarese, E., Richter, JD. (2003). *Genes Dev.* **17(5)**:638–53.
59. Hunter, A., Stewart, MG. (1989). *Exp Brain Res.* **78(2)**:425–34.
60. Infante, A.S., Stein, M.S., Zhai, Y., Borisy, G.G., Gundersen, GG. (2000). *J Cell Sci.* **113(Pt 22)**:3907–19.
61. Jasmin, B.J., Changeux, J.P., Cartaud, J. (1990). *Nature* **344(6267)**:673–5.
62. Kaech, S., Brinkhaus, H., Matus, A. (1999). *Proc Natl Acad Sci USA.* **96(18)**:10433–7.
63. Kasai, H., Matsuzaki, M., Noguchi, J., Yasumatsu, N., Nakahara, H. (2003). *Trends Neurosci.* **26(7)**:360–8.
64. Khuchua, Z., Wozniak, D.F., Bardgett, M.E., Yue, Z., McDonald, M., Boero, J., Hartman, R.E., Sims, H., Strauss, AW. (2003). *Neuroscience* **119(1)**:101–11.
65. Kim, C.H., Lisman, JE. (1999). *J Neurosci.* **19(11)**:4314–24.
66. Kim, C.H., Lisman, JE. (2001). *J Neurosci.* **21(12)**:4188–94.
67. Klein, Gr. J., Xia Teng, P.T. Schoenemann and, T.F. Budinger. (1998). In *Medical Imaging 98: Physiology and Function from Multidimensional Images, Proceedings of the Society of Photo-Optical Instrumentation Engineers*, E Hoffmann, (ed.), 3337.
68. Kotani, S., Nishida, E., Kumagai, H., Sakai, H. (1985). *J Biol Chem.* **260(19)**: 10779–83.
69. Kreitzer, G., Liao, G., Gundersen, GG. (1999). *Mol Biol Cell.* **10(4)**:1105–18.
70. Kyuhou, S., Okada, Y.C. (1993). *J Neurophysiol.* **70(6)**:2665–8.
71. Ladrech, S., Lenoir, M., Ruel, J., Puel, JL. (2003). *Hear Res.* **186(1–2)**:85–90.
72. Lagercrantz, H., Ringstedt, T. (2001). *Acta Paediatr.* **90(7)**:707–15.
73. Lakin, W.D., Stevens, S.A., Tranmer, B.I., Penar, PL. (2003). *J Math Biol.* **46(4)**: 347–83.
74. Lendvai, B., Zelles, T., Rozsa, B., Vizi, ES. (2003). *Brain Res Bull.* **59(4)**:257–60.
75. Leuner, B., Falduto, J., Shors, TJ. (2003). *J Neurosci.* **23(2)**:659–65.
76. Lewis, J.W., Van Essen, DC. (2000). *J Comp Neurol.* **428(1)**:112–37.
77. Li, W., Gilbert, CD. (2002). *J Neurophysiol.* **88(5)**:2846–56.
78. Liu, X.B., Jones, EG. (2003). *J Comp Neurol.* **466(4)**: 457–67.
79. Malan, D., Gallo, M.P., Bedendi, I., Biasin, C., Levi, R.C., Alloatti, G. (2003). *J Mol Cell Cardiol.* **35(2)**:195–206.
80. Matsumoto, G., Ichikawa, M., Tasaki, A., Murofushi, H., Sakai, H. (1984). *J Membr Biol.* **77(2)**:77–91.
81. Matus, A. (1994). *Trends Neurosci.* **17(1)**:19–22.
82. Matus, A. (2000). *Science* **290(5492)**:754–8.
83. Mednikova, Y.S., Karnup, S.V., Loseva, EV. (1998). *Neuroscience* **87(4)**:783–96.
84. Miyamoto, Y., Muto, E., Mashimo, T., Iwane, A.H., Yoshiya, I., Yanagida, T. (2000). *Biophys, J.* **78(2)**:940–9.
85. Mok, H., Shin, H., Kim, S., Lee, J.R., Yoon, J., Kim, E. (2002). *J Neurosci.* **22(13)**:5253–8.
86. Moran, O., Tammaro, P., Nizzari, M., Conti, F. (2000). *Biochem Biophys Res Commun.* **275(3)**:839–44.
87. Mountcastle, VB. (2003). *Cereb Cortex.* **13(1)**:2–4.

88. Mountcastle, VB. (1997). *Brain* **120**(Pt 4):701–22.
89. Mouton, P.R., Price, D.L., Walker, LC. (1997). *J Neurosci Methods* **75**(2):119–26.
90. Muresan, V. (2000). *J Neurocytol.* **29**(11–12):799–818.
91. Naito, E., Sadato, N. (2003). *Rev Neurosci.* **14**(4):387–99.
92. Olmsted, J.B., Borisy, GG. (1975). *Biochemistry* **14**(13):2996–3005.
93. O’Malley, A., O’Connell, C., Murphy, K.J., Regan, CM. (2000). *Neuroscience* **99**(2):229–32.
94. O’Malley, A., O’Connell, C., Regan, CM. (1998). *Neuroscience* **87**(3):607–13.
95. Ostroff, L.E., Fiala, J.C., Allwardt, B., Harris, KM. (2002). *Neuron* **35**(3):535–45.
96. Ozer, R.S., Halpain, S. (2000). *Mol Biol Cell.* **11**(10):3573–87.
97. Pakkenberg, B., Gundersen, H.J. (1997). *J Comp Neurol.* **384**(2):312–20.
98. Papaseit, C., Pochon, N., Tabony, J. (2000). *Proc Natl Acad Sci, USA* **97**(15):8364–8.
99. Parvizi, J., Damasio, AR. (2003). *Brain* **126**(Pt 7):1524–36.
100. Paus, T. (1999). *Neuropsychologia* **37**(2):219–24.
101. Poluch, S., Drian, M.J., Durand, M., Astier, C., Benyamin, Y., Konig, N. (2001). *J Neurosci Res.* **63**(1):35–44.
102. Portet, S., Tuszyński, J.A., Dixon, J.M., Sataric, MV. (2003). *Phys Rev, E Stat Nonlin Soft Matter Phys.* **68**(2 Pt 1):021903.
103. Qualmann, B., Boeckers, T.M., Jeromin, M., Gundelfinger, E.D., Kessels, MM. (2004). *J Neurosci.* **24**(10):2481–95.
104. Quinlan, E.M., Halpain, S. (1996). *Neuron* **16**(2):357–68.
105. Roberts, L.A., Large, C.H., Higgins, M.J., Stone, T.W., O’Shaughnessy, C.T., Morris, BJ. (1998). *Brain Res Mol Brain Res.* **56**(1–2):38–44.
106. Rockland, K.S., Ojima, H. (2003). *Int, J Psychophysiol.* **50**(1–2):19–26.
107. Saito, D.N., Okada, T., Morita, Y., Yonekura, Y., Sadato, N. (2003). *Brain Res Cogn Brain Res.* **17**(1):14–25.
108. Sanchez, C., Diaz-Nido, J., Avila, J. (2000). *Prog Neurobiol.* **61**(2):133–68.
109. Sataric, M.V., Tuszyński, JA. (2003). *Phys Rev, E Stat Nonlin Soft Matter Phys.* **67**(1 Pt 1):011901.
110. Schroeder, C.E., Foxe, JJ. (2002). *Brain Res Cogn Brain Res.* **14**(1):187–98.
111. Seitz, A., Kojima, H., Oiwa, K., Mandelkow, E.M., Song, Y.H., Mandelkow, E. (2002). *EMBO J.* **21**(18):4896–905.
112. Shah, J.V., Flanagan, L.A., Janmey, P.A., Leterrier, JF. (2000). *Mol Biol Cell.* **11**(10):3495–508.
113. Shcherbatko, A., Ono, F., Mandel, G., Brehm, P. (1999). *Biophys J.* **77**(4):1945–59.
114. Shea, TB. (2000). *J Neurocytol.* **29**(11–12):873–87.
115. Smart, F.M., Halpain, S. (2000). *Hippocampus* **10**(5):542–54.
116. Spence, C. (2002). *Behav Brain Res.* **135**(1–2):57–64.
117. Srinivasan, R., Russell, D.P., Edelman, G.M., Tononi, G. (1999). *J Neurosci.* **19**(13):5435–48.
118. Star, E.N., Kwiatkowski, D.J., Murthy, VN. (2002). *Nat Neurosci.* **5**(3):239–46.

119. Stepanova, T., Slemmer, J., Hoogenraad, C.C., Lansbergen, G., Dortland, B., De Zeeuw, C.I., Grosveld, F., van Cappellen, G., Akhmanova, A., Galjart, N. (2003). *J Neurosci.* **23**(7):2655–64.
120. Steward, O., Schuman, E.M. (2003). *Neuron* **40**(2):347–59.
121. Stukenberg, P.T. (2003). *Curr Biol.* **13**(21):R848–50.
122. Sugaya, T., Kitani, Y., Saito, S., Uehara, K., Morita, T., Fujita, T. (1994). *Masui* **43**(12):1812–7. (Japanese)
123. Tashiro, T., Komiya, Y., Kurachi, M., Kikumoto, M., Tashiro, H. (1997). *J Neurosci Res.* **50**(1):81–93.
124. Taylor-Clarke, M., Kennett, S., Haggard, P. (2002). *Curr Biol.* **12**(3):233–6.
125. Tegmark, M. (2000). *Phys. Rev. E* **61**:4194–4206.
126. Temple, M.D., Kosik, K.S., Steward, O. S(2002). *Neurobiol Learn Mem.* **78**(2):199–216.
127. Tuszyński, J.A., Trpisova, B., Sept, D., Brown, J.A. (1997). *J Struct Biol.* **118**(2):94–106.
128. Unal, B., Bradley, P.M., Sahin, B., Canan, S., Aslan, H., Kaplan, S. (2002). *Brain Res Dev Brain Res.* **136**(2):135–44.
129. Van der Zee, E.A., Luiten, P.G. (1999). *Prog Neurobiol.* **58**(5):409–71.
130. Van der Zee, E.A., Douma, B.R., Bohus, B., Luiten, P.G. (1994). *Cereb. Cortex* **4**(4):376–90.
131. Veral, V. (2003). *Nature* **425**(6953):28–29.
132. Wagner, O., Zinke, J., Dancker, P., Grill, W., Bereiter-Hahn, J. (1999). *Bioophys J.* **76**(5):2784–96.
133. Walaas, S.I., Nairn, A.C. (1989). *J Mol Neurosci.* **1**(2):117–27.
134. Wang, G.J., Jackson, J.G., Thayer, S.A. (2003). *J Neurochem.* **87**(1):85–94.
135. Ward, L.M. (2003). *Trends Cogn Sci.* **7**(12):553–559.
136. Werner-Reiss, U., Kelly, K.A., Trause, A.S., Underhill, A.M., Groh, J.M. (2003). *Curr Biol.* **13**(7):554–62.
137. Westermann, S., Weber, K. (2003). *Nat Rev Mol Cell Biol.* **4**(12):938–47.
138. Whatley, V.J., Harris, R.A. (1996). *Int Rev Neurobiol.* **39**:113–43.
139. Wing, A.M. (2000). *Curr Biol.* **10**(6):R245–8.
140. Withers, G.S., Greenough, W.T. (1989). *Neuropsychologia* **27**(1):61–9.
141. Wolff, J., Sackett, D.L., Knippling, L. (1996). *Protein Sci.* **5**(10):2020–8.
142. Wong, R.W., Setou, M., Teng, J., Takei, Y., Hirokawa, N. (2002). *Proc Natl Acad Sci USA.* **99**(22):14500–5.
143. Woolf, N.J., Hameroff, S.R. (2001). *Trends Cogn Sci.* **5**(11):472–478.
144. Woolf, N.J., Young, S.L., Johnson, G.V., Fanselow, M.S. (1994). *Neuroreport* **5**(9):1045–8.
145. Woolf, N.J., Zimmerman, M.D., Johnson, G.V. (1999). *Brain Res.* **821**(1):241–9.
146. Woolf, N.J. (1998). *Prog Neurobiol.* **55**(1):59–77.
147. Woolf, N.J. (1993). *J Chem Neuroanat.* **6**(6):375–90.
148. Woolf, N.J. (1996). *Neuroscience* **74**(3):625–51.
149. Wyszynski, M., Lin, J., Rao, A., Nigh, E., Beggs, A.H., Craig, A.M., Sheng, M. (1997). *Nature* **385**(6615):439–42.
150. Yang, S.D., Song, J.S., Liu, H.W., Chan, W.H. (1993). *J Protein Chem.* **12**(4):393–402. 75
151. Yuste, R., Bonhoeffer, T. (2001). *Annu Rev Neurosci.* **24**:1071–89.

4 Towards Experimental Tests of Quantum Effects in Cytoskeletal Proteins

Andreas Mershin, Hugo Sanabria, John H. Miller, Dharmakeerthna Nawarathna, Efthimios M.C. Skoulakis, Nikolaos E. Mavromatos, Alexandre A. Kolomenskii, Hans A. Schuessler, Richard F. Luduena, and Dimitri V. Nanopoulos

Summary. This volume is appropriately titled “The Emerging Physics of Consciousness” and much of it is focused on using some aspect of “quantum weirdness” to solve the problems associated with the phenomenon of consciousness. This is sometimes done in the hope that perhaps the two mysteries will somehow cancel each other through such phenomena as quantum coherence and entanglement or superposition of wave functions.

We are not convinced that such a cancellation can take place. In fact, finding that quantum phenomena are involved in consciousness, what we will call the “quantum consciousness idea” (QCI) (fathered largely by Penrose and Hameroff [40, 102, 103]), is likely to confound both mysteries and is of great interest.

In our contribution, we want to emphasize the “emerging” part of this volume’s title by pointing out that there is a glaring need for properly controlled and reproducible experimental work if any proposed quantum phenomena in biological matter, let alone consciousness are to be taken seriously.

There are three broad kinds of experiments that one can devise to test hypotheses involving the relevance of quantum effects to the phenomenon of consciousness. The three kinds address three different scale ranges associated roughly with tissue-to-cell (1 cm – $10\text{ }\mu\text{m}$), cell-to-protein ($10\text{ }\mu\text{m}$ – 10 nm) and protein-to-atom (10 nm – 1 \AA) sizes. Note that we are excluding experiments that aim to detect quantum effects at the “whole human” or even “society” level as these have consistently given either negative results or been plagued by irreproducibility and lack of appropriate controls (e.g. the various extra sensory perception and remote viewing experiments [72]).

The consciousness experiments belonging to the tissue-cell scale frequently utilize apparatus such as electroencephalographs (EEG) or magnetic resonance imaging (MRI) to track responses of brains to stimuli. The best example of such is the excellent work undertaken by Christoff Koch’s group at Caltech [61] sometimes in collaboration with the late Francis Crick [22], tracking the activity of living, conscious human brain neurons involved in visual recognition. These experiments are designed to elucidate the multi- and single-cellular substrate of visual consciousness and awareness and are likely to lead to profound insights into the working human brain. Because of the large spatial and long temporal resolution of these methods, it is unclear whether they can reveal possible underlying quantum behavior (barring some unlikely inconsistency with classical physics such as, for instance, nonlocality of neural firing).

The second size scale that is explored for evidence of quantum behavior related to aspects of consciousness (memory in particular) is that between a cell and a protein. Inspired by QCI, seminal experimental work has been done by Nancy

Woolf [142, 143] on dendritic expression of MAP-2 in rats and has been followed by significant experiments performed by members of our group on the effects of MAP-TAU overexpression on the learning and memory of transgenic Drosophila (summarized in Sect. 4.3). Such attempts are very important to the understanding of the intracellular processes that undoubtedly play a significant role in the emergence of consciousness but it is hard to see how experiments involving tracking the memory phenotypes and intracellular redistribution of proteins can show a direct quantum connection. It seems clear that experimentation at this size scale can at best provide evidence that is “not inconsistent with” and perhaps “suggestive of” the QCI [86].

The third scale regime is that of protein-to-atom sizes. It is well understood that at the low end of this scale, quantum effects play a significant role and it is slowly being recognized that even at the level of whole-protein function, quantum-mechanical (QM) effects may be of paramount importance to biological processes such as, for instance, enzymatic action [4] or photosynthesis [112].

In what follows, we give a brief overview of our theoretical QED model of microtubules and the extensive experimental work undertaken (belonging to the second and third size scales). We conclude by pointing towards directions of further investigation that can provide direct evidence of quantum effects in the function of biological matter and perhaps consciousness.

4.1 Introduction

4.1.1 Overview

In our contribution to the “Emerging Physics of Consciousness” volume, we will report on our efforts to address, in several different ways, the hypotheses concerning the existence and function of subcellular, protein-based information-processing elements with a special emphasis on ways to test the QCI as it pertains to cytoskeletal proteins.

Our system of interest is the neural cytoskeleton and specifically the tubulin polymers known as microtubules (MTs). This work was originally motivated by quantum-physics-based scenarios of brain function and consciousness that implicated these structures [40, 79, 82, 96, 102, 103]. As the vast majority of such proposals are purely speculative, with no experimental evidence mentioned or sought our first step was to show that at least some of the predictions of the more realistic and specific scenarios proposed, such as for instance the models put forth by Nanopoulos, Mershin, Skoulakis et al. [81, 88, 96], are in fact experimentally testable. In the first part of this contribution, we present the QED model of microtubules explored in [81] and showcase some of its predictions such as superefficient energy transport and quantum teleportation. Initially, this research concentrated on testing one prediction that was common to many of these exotic theories: that microtubules had a global role in neural function and were not merely the structural scaffolding of cells occasionally assisting in mobility and intracellular transport. To test this prediction, we decided to investigate what effects a minimal disruption

of the microtubular network of neural cells has on memory. Memory was selected because certain models, such as for instance the guitar string model (GSM) of the engram suggested an intracellular memory encoding and storage mechanism highly dependent on the precise stoichiometry of microtubules and microtubule-associated proteins (MAPs) such as TAU [88] (see Sect. 4.2).

In Sect. 4.3, we show how this stoichiometry can be manipulated in genetically altered organisms whose memory can then be tested to reveal any effects. Thus we ascertained that *Drosophila* olfactory associative memory does indeed suffer when the equilibrium of MAPs and MTs is disturbed [86] suggesting that the neural cytoskeleton plays a central role in memory encoding and retrieval beyond those that were traditionally reported.

The next step was investigating the properties of tubulin and MTs in depth since once experimentally implicated in information manipulation, it was not unreasonable to ask whether these protein structures do indeed work as biological and perhaps quantum binary digits (biobits or bioqubits). The dielectric constant and electric dipole moment of tubulin were chosen for closer study since these featured prominently in information manipulation schemes by naturally occurring or fabricated MT networks. In order to check the validity of previous computer simulations first done by the group of Jack Tuszyński [16] and later replicated by our group (giving virtually identical results [87]), an experimental determination of the dielectric constant of tubulin and MTs was needed. This was undertaken in the high-frequency (optical) region (using refractometry and surface plasmon resonance) [87] and the low-frequency region (using dielectric spectroscopy – previously unpublished data and reported here in Sect. 4.4) and it was found that the rather high dipole moment suggested by simulation is reasonable.

As a result of these efforts, novel experimental techniques and theoretical models have been developed that point to several directions of further experimental research from molecular electronics and proteomics to actually at least one way of directly testing for quantum coherence and entanglement in biological matter (Sect. 4.5). Finally, in Sect. 4.6 we summarize our results and attempt a unification of concepts.

4.1.2 Tubulin and Microtubules

Proteins are the ubiquitous living machines inside all cells performing everything from signal and energy transduction to movement, force generation and catalysis of reactions. It has also been suggested that information manipulation and storage is a possible role for proteins at least in the case of tubulin, microtubules and associated proteins.

Tubulin Biochemistry

Tubulin is a common polar protein found mainly in the cytoskeleton of eukaryotic cells and especially enriched in brain tissue. Many of its properties

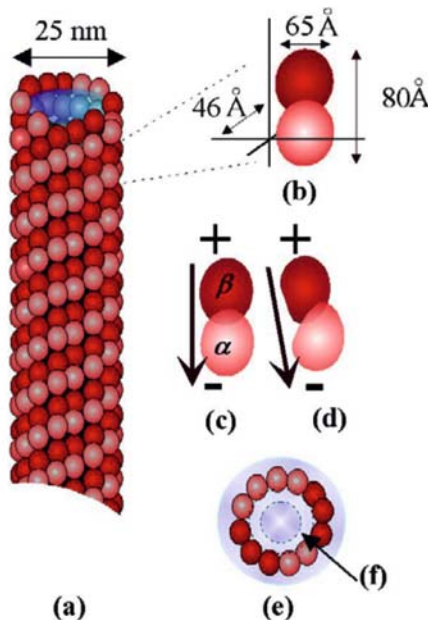


Fig. 4.1. Microtubules and tubulin. (Taken from [81]). MTs are hollow (averaging 25 nm outer diameter, 14 nm inner diameter) tubes forming the main component of the cytoskeleton (a) Typical microtubule made of 13 tubulin protofilaments. (b) dimensions of the $\alpha\beta$ -heterodimer. (c) GTP-tubulin. (d) GDP-tubulin (e) a cross section of the MT showing water environment (f) thin isolated region that has been theoretically suggested to possibly be equivalent to a quantum optical (QED) cavity [80]

have been studied both experimentally and theoretically because of its importance in mitosis, its role as the building block of microtubules and its relevance to the pathology of several neurodegenerative diseases including cancer and Alzheimer's. Although the structure of tubulin has been solved to better than 3.7 Å, by electron crystallography [97, 98] yielding data suggesting that the tubulin heterodimer has dimensions of $46 \times 80 \times 65$ Å (Fig. 4.1b), the dipole moment has so far only been calculated via computer simulations [16, 87].

Microtubules (MTs) are hollow (25 nm-outer diameter, 14 nm inner diameter) tubes (Fig. 4.1a); they constitute a major portion of the cytoskeleton. Apart from giving shape and support to the cell, they also play a major role in cellular transport and have been hypothesized to be central in cellular information processing. The structure of MTs has been the subject of a comprehensive study using electron and optical microscopy. The structure of the microtubule is 13-protofilament B-lattice. The helical pitch is 3 monomers per turn and there is a “seam” where adjacent protofilaments

join. The microtubule is thus an asymmetric structure [9, 135]. Under normal physiological conditions, tubulin is found as a heterodimer, consisting of two nearly identical monomers called α - and β -tubulin, each of molecular weight of about 50 kDalton [97]. GDP–GTP exchange (hydrolysis) releases approximately 0.42 eV per molecule and can be modeled by a conformational change resulting in a 27° angle [85] between the original line connecting the centers of the α and β monomers and the new center-to-center line as shown in Fig. 4.1d. Note that for free tubulin, the energy needed for this conformational change is roughly 200 times lower than a conventional silicon-based binary switch and about 30 times more than thermal noise at room temperature. Therefore, at least energywise, these two conformations can act as the basis for a naturally occurring or fabricated biabit.

There exists a large number of studies dealing with microtubule (MT) dynamics, and various scenarios have been proposed for explaining the dynamic behavior of MTs. At this point, however, there is controversy even as to the correct mechanism of polymerization with the “GTP cap” theory [94] facing alternatives such as those described in [48].

Unless otherwise specified, we will refer to the $\alpha\beta$ -dimer simply as tubulin. Tubulin binds to two molecules of guanosine 5'-triphosphate (GTP). One GTP binds irreversibly to the subunit; this is referred to as the “nonexchangeable” GTP. We will not concern ourselves further with this GTP. The subunit binds reversibly to another GTP molecule; this is referred to as the “exchangeable” GTP. If it is bound to GTP then the tubulin dimer exists in an energy-rich form that favors polymerization. Alternatively, it can bind guanosine 5' diphosphate (GDP-tubulin) in which case the dimer would be in an energy-poor form (GDP-tubulin) that favors dissociation [51, 140]. Above 0°C, free tubulin can self-assemble into MTs *in vitro* provided the buffer contains sufficient GTP and the concentration is above critical (about 1 mg/mL) so that sufficient nucleation sites exist. In tubulin from mammalian brains (the most commonly used source, and the one we have used in the experiments of Sect. 4.4) MTs do not assemble at 4°C while they start assembling at around 17°C. The lower the temperature, the more they disassemble, until by 4°C there are no microtubules left. Antarctic fish on the other hand have MTs that can assemble even at -1°C. The size of the minimum nucleus required to start polymerization is not exactly understood.

Certain interesting phenomena arise in microtubules such as length oscillations (known as dynamic instability), or treadmilling; these have been studied extensively [33, 54] but are not directly relevant to our analysis at this stage as such phenomena can be avoided *in vitro* by choosing appropriate environments.

Tubulin Biophysics

A measurement of the tubulin electric dipole moment will be useful in simulations of MTs that aim at understanding the polymerization mechanism, as it

can be incorporated into the various models as an experimentally determined parameter. For similar reasons, computer simulation of MT networks as cellular automata will also benefit from such a measurement. Furthermore, drug interactions with tubulin are currently under investigation and it has been theorized that electric dipole moment “flips” are responsible for London forces during interaction of tubulin with other molecules possessing dipole moments such as general anesthetic molecules [40]. A simplistic estimate of the tubulin dipole moment \mathbf{p} based on a mobile charge of 18 electrons multiplied by a separation of 4 nm gives a magnitude of $\mathbf{p} = 4 \times 10^{-27} \text{ C m}$ (or 1200 Debye) while using a more sophisticated molecular simulation, \mathbf{p} has been quoted at around 1700 Debye [16, 87]. At physiological pH (= 7.2) MTs are negatively charged [85, 115, 127] due to the presence of a 15-residue carboxyl terminus “tail” and there have been suggestions that this C-terminus is important in polymerization, protein interactions and perhaps charge conduction [115]. This had not been included in the original electron crystallography data of Nogales et al. [97] so all values concerning the dipole moment are quoted with the understanding that \mathbf{p} has been calculated ignoring the effect of the C-terminus. It is expected that posttranslational modifications such as polyglutamylation, polyglycation, tyrosination/detyrosination, deglutamylation, and phosphorylation (reviewed in [76]) will affect the electrostatics and electrodynamics of tubulin and MTs. For instance, the addition of 6 glutamates to the C-terminus of both and makes this region extraordinarily negatively charged. It is also known that at pH 5.6 MTs become neutral. Finally, there have been some preliminary experiments aimed at measuring the electric field around MTs [52, 107, 108] indicating that MTs could be ferroelectric.

Apart from the above observations, there exists little experimental evidence concerning the electrical properties of tubulin and MTs. On the other hand, there have been a large number of publications of theoretical work describing various electrical and optical properties that tubulin and MTs are expected to have based on their structure and function. Ferroelectricity (spontaneous abrupt orientation of dipoles for an above-threshold externally applied electric field) has been thoroughly explored and so far supported by the analysis in [79]. The MTs’ paracrystalline geometrical structure has been implicated in error-correcting codes [62]. Energy-loss-free transport along MTs has also been theoretically shown in [82] and the presence of “kink-like excitations” or solitons has also been suggested as an energy-transfer mechanism in MTs [81]. Many models exist regarding the exact nature of these excitations and waves but they all depend on the dipole moment of tubulin and its ability to flip while in the polymerized state so we will collectively call them “flip waves”. Depending on the model and the parameters assumed, the speed of such waves has been estimated to be $10^{2\pm 1} \text{ m/s}$. Note that although biochemically it seems MTs are made predominantly of GDP-tubulin, this does not mean that the dipole flips are “frozen-out” since intramolecular electron motion can still occur in the hydrophobic pockets of the tubulin heterodimer.

Detection of such waves would be a major step towards understanding the function of MTs and also towards using them as nanowires for bioelectronic circuits. We suggest several ways to test for the existence of flip waves in Sect. 4.5.

4.1.3 Motivation

Tubulin and Classical Molecular Electronics

Recent efforts have concentrated on identifying various chemical substances with appropriate characteristics to act as binary switches and logic gates needed for computation. While at present the size of the smallest conventional silicon-based devices is around 180 nm, molecular devices promise a one or two order of magnitude reduction in this minimum. For instance, rotaxanes have been considered as switches and/or fuses [21] and carbon nanotubes as active channels in field effect transistors [27]. Many of these are not suitable for placement on traditional chips [63] or for forming ordered networks, while virtually all of these attempt to hybridize some kind of electrical wires to chemical substrates in order to obtain current flows. This requirement adds a level of complexity to the task because of the need for appropriate nanomanufactured wires and connections. The work presented here is suggestive of a different approach. The role of the binary states can be played not by the presence or bulk movement of charge carriers but by naturally occurring conformational states of protein (tubulin) molecules. The external interaction with these states may be performed by coupling laser light to specific spots of the MT network. Signal propagation can be achieved by traveling electric dipole moment flip waves along protofilaments and MTs, while modulation can be achieved by MAP binding that creates “nodes” in the MT network. In this proposed scheme for information manipulation, there is no bulk transfer of charge or mass involved. Permanent information encoding can be achieved by creating geometrical arrangements via placing the MTs on chips spotted with appropriate chemicals (e.g. taxol, zinc, colchicine) to force specific features such as centers, sheets, spirals or elongated structures to emerge from the MT self-assembly.

The end products of tubulin polymerization can be controlled by temperature and application of chemicals and MAPs to yield closely or widely spaced MTs, centers, sheets, rings and other structures [29, 46] thus facilitating fabrication of nanowires, nodes and networks. Charge conduction by peptides/natural switches has been under investigation using femtosecond laser pulses and the results show that electron transfer exists in peptides even at low energies [139]. Femtosecond processes are taking place as charges jump across peptide backbones in certain favorable conformations that provide efficient conduction, or charges are stopped by those same peptides assuming a nonconducting conformation [121]. These general properties of peptides make proteins even more attractive as molecular-switch candidates. Finally,

these assemblies of protein are ideal for implementing fault-tolerant operation, as massive redundancy is possible due to the relative ease of obtaining large amounts of protein polymerized to specifications, e.g. on etched chips.

Quantum Computing and Quantum Consciousness Idea (QCI)

At the core of many “quantum brain” hypotheses lies a QCI that assumes that the tubulin electric dipole moment is capable of flips while in the polymerized state and starting from that assumption, predictions have been developed such as long-lived superposed and entangled states among tubulin dimers [81] and long-range non-neurotransmitter-based communication among neurons [40]. Interaction between water molecule dipoles and the tubulin dipole plays a central role in the models predicting ferroelectricity along MT protofilaments, emission of coherent photons, intracellular quantum teleportation of dipole quanta states [81] and other controversial yet fascinating features. As explained in Sect. 4.5, a minimally modified design of the surface plasmon resonance (SPR) apparatus built and used for the work presented here, coupled to an entangled photon source and a correlation device might be capable of detecting the often conjectured mesoscopic (of order micrometers) bulk coherence and partial quantum entanglement of dipole moment states, the existence of which will cast biomolecules as appropriate candidates for the implementation of bioqubits.

4.2 QED Model of Tubulin and its Implications

4.2.1 Introduction

Background

Observable quantum effects in biological matter such as proteins are routinely expected to be strongly suppressed, mainly due to the macroscopic nature of most biological entities as well as the fact that such systems live at near room temperature. These conditions normally result in a very fast collapse of the pertinent wave functions to one of the allowed classical states. However, we suggest that under certain circumstances it is in principle possible to obtain the necessary isolation against thermal losses and other environmental interactions, so that meso- and macroscopic quantum-mechanical coherence, and conceivably entanglement extending over scales that are considerably larger than the atomic scale, may be achieved and maintained for times comparable to the characteristic times for biomolecular and cellular processes.

In particular, it has been shown [82] how MTs [31] can be treated as quantum-mechanically isolated (QED) cavities, exhibiting properties analogous to those of electromagnetic cavities routinely used in quantum optics [1, 12, 41, 118]. Recently, this speculative model has been supported by some

indirect experimental evidence. It has been experimentally shown [57], that it is possible to maintain partial entanglement of the bulk spin of a macroscopic quantity of cesium (Cs) atoms ($N = 10^{12}$), at room temperature, for a relatively long time (0.5 ms). Note that in this experiment, the large quantity of atoms was of paramount importance in creating and maintaining the entanglement, and even though the gas samples were in constant contact with the environmental heat bath, Julsgaard et al. [107] managed to detect the existence of entanglement for a much longer time than one would intuitively expect. We stress that it was exactly the large amount of spins that was responsible for the long decoherence times. Fewer spins would have decohered faster. Here, we use the main features of the QED model of the quantum-mechanical properties of MTs (described in detail in [80, 81]), and we exhibit its relevance to the Julsgaard et al. experiment. A direct consequence of this model for MTs as QED cavities is that virtually every experimentally known QED-cavity-based observation may have an analog in living MTs and we show this analytically with the specific case of intra- and intercellular dissipation-less energy transfer and quantum teleportation of coherent (biologically relevant) quantum states.

Intracellular Energy Transfer

Energy transfer across cells, without dissipation, was first speculated to occur in biological matter by Fröhlich [34]. The phenomenon conjectured by Fröhlich was based on a onedimensional superconductivity model: a one-dimensional electron system with holes, where the formation of solitonic structures due to electron–hole pairing results in the transfer of electric current without dissipation. Fröhlich suggested that, if appropriate solitonic configurations are formed inside cells, energy in biological matter could also be transferred without any dissipation (superefficiently). This idea has led theorists to construct various models for cellular energy transfer, based on the formation of classical kink solutions [67].

In these early works, no specific microscopic models had been considered. In 1932, Sataric et al. suggested a classical physics model for microtubule dynamics [119], in which solitons transfer energy across MTs without dissipation. In the past, quantum aspects of this one-dimensional model have been analyzed, and a framework for the consistent quantization of the soliton solutions was developed [80]. That work suggested that such semiclassical solutions may emerge as a result of “decoherence” due to environmental interactions, echoing ideas in [147].

The basic assumption used in creating the model of [119] was that the building blocks of MTs, the tubulin molecule dimers, can be treated as elements of Ising spin chains (one-space-dimensional structures). The interaction of each tubulin chain (protofilament) with the neighboring chains and the surrounding water environment was accounted for by suitable potential

terms in the one-dimensional Hamiltonian. The model describing the dynamics of such one-dimensional substructures was the ferroelectric distortive spin chain model of [119].

Ferroelectricity is an essential ingredient of the quantum-mechanical mechanism of energy transfer that we propose. It has been speculated [79] that the ferroelectric nature of MTs will be that of hydrated ferroelectrics, i. e. the ordering of the electric dipole moment of the tubulin molecules will be due to the interaction of the tubulin dimers' electric dipoles with the water molecules in the interior and possibly exterior of the microtubular cavities. Ferroelectricity induces a dynamical dielectric "constant" $\varepsilon(\omega)$ that is dependent on the frequency ω of the excitations in the medium. Below a certain frequency, such materials are characterized by almost vanishing dynamical dielectric "constants", which in turn implies that electrostatic interactions inversely proportional to ε will be enhanced, and thus become dominant against thermal losses. In the case of microtubules, the pertinent interactions are of the electric-dipole type, scaling with the distance r as $1/(\varepsilon r^3)$. For ordinary water media, the relative dielectric constant $\kappa = \varepsilon/\varepsilon_0$ is of order 80. In the ferroelectric regime, however, ε is diminished significantly. As a result, the electric dipole-electric dipole interactions may overcome the thermal losses that are proportional to $k_B T$ (where k_B is Boltzmann's constant $= 1.38 \times 10^{-23}$ J/K and T is the temperature in degrees K) at room temperature inside the interior cylindrical region of MT bounded by the dimer walls of thickness of the order of a few Å [80] see Fig. 4.1.

Cavities

Once isolation from thermal noise is provided, one can treat the thin interior MT regions as electromagnetic cavities in a way similar to that of QED cavities. Note that the role of MT as waveguides was proposed by Hameroff already some time ago [39]. In this scenario, on the other hand, we are interested in isolated regions inside the MT that play the role of QED cavities not waveguides.

QED cavities are well known for their capacity to sustain in their interior coherent modes of electromagnetic radiation. Similarly, one expects that such coherent cavity modes will occur in the thin interior regions of MTs bounded by the protein dimer walls. Indeed, as was discussed in [80], these modes are provided by the interaction of the electric dipole moments of the ordered-water molecules in the interior of MT with the quantized electromagnetic radiation [25, 26]. Such coherent modes are termed dipole quanta. It is the interaction of such cavity modes with the electric dipole excitations of the dimers that leads to the formation of coherent (dipole) states on the tubulin dimer walls of MTs. A review of how this can happen, and what purely quantum effects can emerge from the QED nature of MTs, will be the main topic of this section.

A concise exposé of the mechanism described in detail in [79–82] is presented here that justifies the application of QM to the treatment of certain aspects of MT dynamics. An analogy of this mechanism to the experimental setup used by Julsgaard et al. [57] is drawn. A straightforward calculation of how quantum teleportation of states can occur in MTs, in direct analogy to the experimental quantum teleportation in optical cavities that has been observed recently [123, 126] is performed. A parallel between certain geometrical features of MTs such as their ordered structure, which obeys a potentially information-encoding code, is illustrated and suggestions to exploit this for (quantum) error correction and dense coding are put forth.

4.2.2 Quantum Coherence in Biological Matter?

Tubulin, Microtubules and Coherent States

Tubulin and MTs have been described in detail in Sect. 4.1. The interior of the MT, seems to contain ordered water molecules [80], which implies the existence of an electric dipole moment and an electric field. We stress here that the intracellular ordered water, which is full of proteins and other molecules, is different from ordinary water in various respects, e.g. as is implied in [117]. It has been put forward that each dimer has two hydrophobic pockets, containing 2×18 unpaired electrons [31] that have at least two possible configurations associated with the GTP and GDP states of tubulin, which we will call \uparrow and \downarrow electron (or equivalently electric dipole moment) conformations, respectively.

It is evident that an experimentally determined electric dipole moment for the tubulin molecule and its dynamics are important areas of study for this field. If we account for the effect of the water environment that screens the electric charge of the dimers by the relative dielectric constant of the water, $\kappa = \varepsilon/\varepsilon_0 \sim 80$, we arrive at a value

$$p_{\text{dimer}} = 3 \times 10^{-28} \text{ C m}. \quad (4.1)$$

Note that under physiological conditions, the unpaired electric charges in the dimer may lead to even further suppression of p_{dimer} .

Note that although the caps of the MT contain both GTP and GDP tubulin, it is well known experimentally [85] that the tubulin comprising the trunk of the MT is GDP-tubulin incapable of acquiring a phosphate and becoming GTP tubulin. However, this does not preclude electric-dipole moment flip wave propagation down the MT, as a flip at the cap can be propagated without phosphorylation but rather via the mechanism suggested below. In view of this, the value of the yet undetermined electric dipole moment direction flip angle θ_{flip} is much smaller than the $27^\circ 42'$ value for free tubulin and it is entirely unphysical to suggest a complete reversal of the dipole moment direction as some authors have recently done. The \uparrow and

\downarrow states still exist, but are hard to observe experimentally as they are not associated with a large-scale geometrical mass shift. Note that virtually all of the MT-based QCIs today fail to take this into account and instead wrongly suggest that θ_{flip} is of the order of 27° and that such large distortions occur in the trunk of the polymerized MT.

In standard models for the simulation of MT dynamics [119], the physical degree of freedom that is relevant for the description of energy transfer is the projection of the electric dipole moment on the longitudinal symmetry axis (x -axis) of the MT cylinder. The θ_{flip} distortion of the \downarrow -conformation leads to a displacement u_n along the x -axis. In this way, the effective system is one-dimensional (spatial), and one has the possibility of being quantum integrable [80].

It has been suggested for quite some time that information processing via interactions among the MT protofilament chains can be sustained on such a system, if the system is considered as a series of interacting Ising chains on a triangular lattice. For such schemes to work, one must first show that the electromagnetic interactions among the tubulin dimers are strong enough to overcome thermal noise. It is due to this problem that such models for intraneuronal information processing have been criticized as unphysical [129]. Classically, the various dimers can only be in the \uparrow and \downarrow conformations. Each dimer is influenced by the neighboring dimers resulting in the possibility of a transition. This is the basis for classical information processing, which constitutes the picture of a (classical) cellular automaton.

If we assume (and there is theoretical basis for such an assumption [80]) that each dimer can find itself in a QM superposition of \uparrow and \downarrow states, a quantum nature results. Tubulin can then be viewed as a typical two-state quantum-mechanical system, where the dimers couple to conformational changes with 10^{-9} – 10^{-11} s transitions, corresponding to an angular frequency $\omega \sim 10^{10}$ – 10^{12} Hz. In this approximation, the upper bound of this frequency range is assumed to represent (in order of magnitude) the characteristic frequency of the dimers, viewed as a two-state quantum-mechanical system:

$$\omega_0 \sim (10^{12}) \text{Hz}. \quad (4.2)$$

Let u_n be the displacement field of the n -th dimer in a MT chain. The continuous approximation proves sufficient for the study of phenomena associated with energy transfer in biological cells, and this implies that one can make the replacement

$$u_n \rightarrow u(x, t), \quad (4.3)$$

with x a spatial coordinate along the longitudinal symmetry axis of the MT. There is a time variable t due to fluctuations of the displacements $u(x)$ as a result of the dipole oscillations in the dimers.

The effects of the neighboring dimers (including neighboring chains) can be phenomenologically accounted for by an effective potential $V(u)$. In the model of ref. [119] a double-well potential was used, leading to a classical

kink solution for the $u(x, t)$ field. More complicated interactions are allowed in the picture of ref. [80] where we have considered more generic polynomial potentials.

The effects of the surrounding water molecules can be accounted for by a viscous force term that damps out the dimer oscillations,

$$F = -\gamma \partial_t u, \quad (4.4)$$

with γ determined phenomenologically at this stage. This friction should be viewed as an environmental effect, which, however, does not lead to energy dissipation, as a result of the nontrivial solitonic structure of the ground state and the nonzero constant force due to the electric field. This is a well-known result, directly relevant to energy transfer in biological systems [67]. The effective equation of motion for the relevant field degree of freedom $u(x, t)$ reads:

$$u''(\xi) + \rho u'(\xi) = P(u), \quad (4.5)$$

where $\xi = x - vt$, v is the velocity of the soliton, ρ is proportional to γ [119], and $P(u)$ is a polynomial in u , of a certain degree, stemming from the variations of the potential $V(u)$ describing interactions among the MT chains [80]. In the mathematical literature [101] there has been a classification of solutions of equations of this form. For certain forms of the potential [80] the solutions include kink solitons that may be responsible for dissipation-free energy transfer in biological cells [67]:

$$u(x, t) \sim c_1 (\tanh[c_2(x - vt)] + c_3), \quad (4.6)$$

where c_1, c_2, c_3 are constants depending on the parameters of the dimer lattice model. For the form of the potential assumed in the model of [119], there are solitons of the form $u(x, t) = c'_1 + \frac{c'_2 - c'_1}{1 + \exp[c'_3(c'_2 - c'_1)(x - vt)]}$, where again c'_i where $i = 1, 2, 3$ are appropriate constants. A semiclassical quantization of such solitonic states has been considered in [80]. The result of such a quantization yields a modified soliton equation for the (quantum corrected) field $u_q(x, t)$ [133]

$$\partial_t^2 u_q(x, t) - \partial_x^2 u_q(x, t) + M^{(1)}[u_q(x, t)] = 0, \quad (4.7)$$

with the notation $M^{(n)} = \exp \left[\frac{1}{2} (G(x, x, t) - G_0(x, x)) \frac{\partial^2}{\partial x^2} \right] U^{(n)}(z)|_{z=u_q(x, t)}$ and $U^n \equiv \frac{d^n U}{dz^n}$, where the quantity U denotes the potential of the original soliton Hamiltonian, and $G(x, y, t)$ is a bilocal field that describes quantum corrections due to the modified boson field around the soliton. The quantities $M^{(n)}$ carry information about the quantum corrections. For the kink soliton (4.6) the quantum corrections (4.7) have been calculated explicitly in [133], thereby providing us with a concrete example of a large-scale quantum coherent state.

A typical propagation velocity of the kink solitons (e.g. in the model of ref. [119]) is $v \sim 2$ m/s, although, models with $v \sim 20$ m/s have also been considered [120]. This implies that, for moderately long microtubules of length $L \sim 10^{-6}$ m, such kinks transport energy without dissipation in

$$t \sim 5 \times 10^{-7} \text{ s}, \quad (4.8)$$

Energy will be transferred superefficiently via this mechanism only if the decoherence time is of the order of, or longer than, this time. We shall see in fact that indeed such time scales are of order comparable to, or smaller than, the decoherence time scale of the coherent (solitonic) states $u_q(x, t)$. This then implies that fundamental quantum-mechanical phenomena may be responsible for frictionless, dissipationless superefficient energy (and signal) transfer and/or transduction across microtubular networks in the cell.

Microtubules as Cavities

In [80], a microscopic analysis of the physics underlying the interaction of the water molecules with the dimers of the MT was presented. This interaction is responsible for providing the friction term (4.4) in the effective (continuum) description. We briefly review this scenario here.

As a result of the ordered structure of the water environment in the interior of MTs, there appear collective coherent modes, the so-called dipole quanta [25]. These arise from the interaction of the electric dipole moment of the water molecule with the quantized radiation of the electromagnetic field [26], which may be self-generated in the case of MT arrangements [80, 120]. Such coherent modes play the role of “cavity modes” in the quantum optics terminology. These in turn interact with the dimer structures, mainly through the unpaired electrons of the dimers, leading to the formation of a quantum coherent solitonic state that may extend even over the entire MT network. As mentioned above, such states may be identified [80] with semiclassical solutions of the friction equations (4.5). These coherent, almost classical, states should be viewed as the result of decoherence of the dimer system due to its interaction/coupling with the water environment [147].

Such a dimer/water coupling can lead to a situation analogous to that of atoms interacting with coherent modes of the electromagnetic radiation in quantum optical cavities, namely to the so-called vacuum-field rabi splitting (VFRS) effect [118]. VFRS appears in both the emission and absorption spectra of atoms [1] in interaction with a coherent mode of electromagnetic radiation in a cavity. For our purposes below, we shall review the phenomenon by restricting ourselves to the absorption spectra case.

Consider a collection of N atoms of characteristic frequency ω_0 inside an electromagnetic cavity. Injecting a pulse of frequency Ω into the cavity causes a doublet structure (splitting) in the absorption spectrum of the atom–cavity system with peaks at:

$$\Omega = \Omega_0 - \Delta/2 \pm (1/2)(\Delta^2 + 4N\lambda^2)^{1/2}, \quad (4.9)$$

where $\Delta = \Omega_c - \Omega_0$ is the detuning of the cavity mode, of frequency ω_c , compared to the atomic frequency. For resonant cavities the splitting occurs with equal weights

$$\Omega = \omega_0/pm\lambda\sqrt{N}. \quad (4.10)$$

Notice here the enhancement of the effect for multiatom systems $N \gg 1$. The quantity $2\lambda\sqrt{N}$ is called the “Rabi frequency” [118]. From the emission-spectrum analysis an estimate of λ can be inferred that involves the matrix element, \underline{d} , of atomic electric dipole between the energy states of the two-level atom [118]:

$$\lambda = \frac{E_c \underline{d} \cdot \underline{p}}{\eta}, \quad (4.11)$$

where \underline{p} is the cavity (radiation) mode polarization, and

$$E_c \left(\frac{2\pi\eta\omega_c}{\varepsilon V} \right), \quad (4.12)$$

is the r.m.s. vacuum (electric) field amplitude at the center of a cavity of volume V , and of frequency ω_c , with ε being the dielectric constant of the medium inside the volume V . In atomic physics, the VFRS effect has been confirmed by experiments involving beams of Rydberg atoms resonantly coupled to superconducting cavities [12].

In the analogy between the thin cavity regions near the dimer walls of MTs with electromagnetic cavities, the role of atoms is played by the unpaired two-state electrons of the tubulin dimers [80] oscillating with a frequency (4.2). To estimate the Rabi coupling between cavity modes and dimer oscillations, one should use (4.11) for the MT case.

We have used some simplified models for the ordered-water molecules, which yield a frequency of the coherent dipole quanta (“cavity” modes) of order [80]:

$$\omega_c \sim 6 \times 10^{12} \text{ Hz}. \quad (4.13)$$

Notably this is of the same order of magnitude as the characteristic frequency of the dimers (4.2), implying that the dominant cavity mode and the dimer system are almost in resonance in the model of [80]. Note that this is a feature shared by atomic physics systems in cavities, and thus we can apply the pertinent formalism to our system. Assuming a relative dielectric constant of water with respect to that of vacuum ε_0 , $\varepsilon/\varepsilon_0 \sim 80$, one obtains from (4.12) for the case of MT cavities:

$$E_c \sim 10^4 \text{ V/m}. \quad (4.14)$$

Electric fields of such a magnitude can be provided by the electromagnetic interactions of the MT dimer chains, the latter viewed as giant electric

dipoles [119]. This suggests that the coherent modes ω_c , which in our scenario interact with the unpaired electric charges of the dimers and produce the kink solitons along the chains, owe their existence to the (quantized) electromagnetic interactions of the dimers themselves. The Rabi coupling for the MT case then is estimated from [80] to be of the order of:

$$\begin{aligned} \text{Rabi coupling for MT} &\equiv \lambda_{\text{MT}} \\ &= \sqrt{N} \lambda_0 \ 3 \times 10^{11} \text{ Hz}, \end{aligned} \quad (4.15)$$

which is, on average, an order of magnitude smaller than the characteristic frequency of the dimers (4.2).

In the above analysis, we have assumed that the system of tubulin dimers interacts with a *single* dipole-quantum coherent mode of the ordered water and hence we ignored dimer–dimer interactions. More complicated cases, involving interactions either among the dimers or of the dimers with more than one radiation quantum (which undoubtedly occur *in vivo*), may affect the above estimate.

The presence of such a coupling between water molecules and dimers leads to quantum coherent solitonic states of the electric dipole quanta on the tubulin dimer walls. To estimate the decoherence time we remark that the main source of dissipation (environment) comes from the imperfect walls of the cavities, which allow leakage of coherent modes and energy. The time scale, T_r , over which a cavity-MT dissipates its energy, can be identified in our model with the average lifetime t_L of a coherent-dipole quantum state, which has been found to be [80]: $T_r \sim t_L \sim 10^{-4}$ s. This leads to a first-order-approximation estimate of the quality factor for the MT cavities, $Q_{\text{MT}} \sim \omega_c$, $T_r \sim 10^8$ s. We note, for comparison, that high-quality cavities encountered in Rydberg atom experiments dissipate energy in time scales of 10^{-3} – 10^{-4} s, and thus have Q values that are comparable to Q_{MT} above. The analysis of [80] yields the following estimate for the collapse time of the kink coherent state of the MT dimers due to dissipation:

$$t_{\text{collapse}}: 10^{-7}\text{--}10^{-6} \text{ s}. \quad (4.16)$$

This is larger than the time scale (4.8) required for energy transport across the MT by an average kink soliton in the models of [80, 120]. The result (4.16), then, implies that quantum physics may be relevant as far as dissipationless energy transfer across the MT is concerned.

Therefore, this specific model is in stark disagreement with the conclusions of Tegmark in [129], i.e. that only classical physics is relevant to the energy and signal transfer in biological matter. Tegmark's conclusions did not take proper account of the possible isolation against environmental interactions, which seems to occur inside certain regions of MTs with appropriate geometry.

Ordered Water in Biological Systems

The above scenarios are consistent with independent studies of water in biological matter, which are summarized below.

Recent experimental spectroscopic studies of resonant intermolecular transfer of vibrational energy in liquid water [144] have established that energy is transferred extremely rapidly and along many water molecules before it dissipates. This energy is in the form of OH-stretch excitations and is thought to be mediated by dipole–dipole interactions in addition to a yet unknown mechanism that speeds up the transfer beyond that predicted by the so-called Förster expression for the energy transfer rate between two OH oscillators, k .

$$k = T_1^{-1} \left(\frac{r_0}{r} \right)^6, \quad (4.17)$$

where T_1 is the lifetime of the excited state, r the distance between the oscillators and r_0 the Förster radius. The Förster radius, which is a parameter experimentally determined for each material, characterizes the intermolecular energy transfer and has been determined by Woutersen et al. [144] to be $r_0 = 2.1 \pm 0.05 \text{ \AA}$, while the typical intermolecular distance (at room temperature) for water is 2.8 \AA . It is evident from these data that the energy transfer in pure water will be fast and yet experimentally it is determined to be even faster than that by one or even two orders of magnitude. Woutersen et al. speculate that this extremely high rate of resonant energy transfer in liquid water may be a consequence of the proximity of the OH groups that causes other, higher-order-uples to also exchange energy. Here, we propose another mechanism to explain the rapidity of the energy transfer, namely kink–soliton propagation. This is based on the phenomenological realization that it is exactly this kind of energy transfer that one would expect to see experimentally as a result of the existence of kink–solitons. Such a mechanism, regardless of exact origin, is ideal for loss-free energy transfer between OH groups located on either different biomolecules or along extended biological structures such as MTs that would be covered (inside and out) with water. Note also that this predicts that OH groups in hydrophobic environments would be able to remain in a vibrationally excited state longer than OH groups in a hydrophilic environment lending credence to our working assumption that the electrons inside the hydrophobic pockets of the tubulin molecules are sufficiently isolated from thermal noise.

It is quite possible that such solitonic states in water may not be quantum in origin in the case of microtubules. The 25 nm diameter of the MT is too big a region to allow for quantum effects to be sustained throughout, as we discussed above. Such solitons may be nothing other than the ones conjectured in [53], which may be responsible for the optical transparency of the water interior of MTs. Such classical solitons in the bulk of the water interior may coexist with the quantum coherent states on the dimer walls [80].

The Relevance of Superconductivity to Quantum Coherence in Biological Matter

As we have already seen, some of the principal objections to the quantum consciousness idea are that: (1) thermal fluctuations and interactions with the environment will destroy quantum coherence over distances greater than a few nanometers at biological temperatures, and (2) the total mass of the particles is too large. However, the discovery of high-temperature superconductivity [11] establishes the existence of large-scale quantum coherence at temperatures within a factor of three of biological temperatures. MRI magnets contain hundreds of miles of superconducting wire and routinely carry a persistent current. There is no distance limit – the macroscopic wave function of the superfluid condensate of electron pairs, or Cooper pairs, in a sufficiently long cable could maintain its quantum phase coherence for many thousands of miles.¹ Moreover, there is no limit to the total mass of the electrons participating in the superfluid state. The condensate is “protected” from thermal fluctuations by the BCS energy gap at the Fermi surface, and the term “quantum protectorate” has recently been coined [69] to describe this and related many-body systems.

A remarkable phenomenon displayed by superconductors is that of flux quantization [8], in which the magnetic flux Φ passing through a superconducting ring is quantized in multiples of $\Phi_0 = h/2e$ (in SI units, or $hc/2e$ in cgs units). This is because the Cooper pairs are condensed into the same macroscopic wave function, or condensate, whose phase must change by a multiple of 2π as one traces a closed path around the ring. One consequence is that the angular momentum of *each* Cooper pair is quantized in multiples of \hbar . Amazingly, the *total* angular momentum of the electron superfluid is also quantized, but in multiples of $N_p \hbar$, where N_p is the number of pairs. The magnetic flux is then proportional to the total angular momentum divided by the total circulating charge, i.e. $\Phi_0 = 2\pi \frac{N_p \hbar}{N_p(2e)} = \frac{\hbar}{2e}$. It is as though the effective quantum of angular momentum (or of action) and that of charge had been scaled up to macroscopic quantities. A similar phenomenon occurs in superfluid helium, where the circulation, defined as the integral of the velocity around a closed loop, is quantized.

Condensed-matter systems providing evidence for macroscopic quantum effects at *biological* temperatures include charge and spin density waves in quasi-1D conductors [38]. A Peierls gap opens up at the Fermi surface, thus creating a “quantum protectorate” below the transition temperature. For example, the quasi-1D compound NbS₃ forms a density wave (DW) at 340 K or 67°C, 30°C higher than the human body temperature, and the transition

¹ What is generally referred to as the “coherence length” ξ of a superconductor is actually the distance over which the amplitude of the order parameter can vary significantly. The phase coherence length is essentially infinite. Otherwise, flux quantization could not occur in a persistent-current mode.

temperatures are even higher in some quasi-2D compounds. A DW pinned by impurities can collectively transport an electric current when an applied electric field exceeds a threshold value. A simplified model represents the DW as an elastic string in a washboard, or sine-Gordon, pinning potential. In the classical picture, a sufficiently large field tilts the washboard potential enough for the DW to “slide.” (Real pinning potentials are disordered, but coherent voltage oscillations seen in high-quality crystals suggest that the simple sine-Gordon picture captures much of the essential physics.)

A number of experiments indicate that nucleation of soliton–antisoliton ($S\hat{S}$) domain wall pairs [92], via quantum tunneling [6, 7], or “decay of the false vacuum” [77] occurs for fields far below the classical depinning threshold in weakly pinned DWs. In particular, NMR experiments [113, 114] and an observed bias-independent ac response below threshold [145] show that the DW phase is displaced by only a fraction of its classically predicted value as the applied field approaches the threshold in some materials. These experiments are explained nicely by the quantum picture, in which the threshold for $S\hat{S}$ nucleation can be much smaller than the classical depinning field, and is a Coulomb blockade effect due to $S - \hat{S}$ electrostatic interactions [65, 89]. Moreover, rf linear response and mixing experiments [90, 91] show remarkable agreement with the predictions of photon-assisted tunneling theory and, indirectly at least, give a scaling between voltage and frequency that is consistent with the ratio \hbar/e [130]. Aharonov–Bohm-type oscillations in the magnetoconductance of DWs with columnar defects [68] and “soliton-tunneling transistor” experiments [92] provide further evidence for quantum effects, the latter showing evidence for macroscopically charged domain walls. Finally, the shapes of the current–field (I–E) characteristics of weakly pinned DWs show nearly precise agreement [130] with the form $I \sim [E - E_T] \exp[-E_0/E]$ predicted by the soliton tunneling model, where E_T is the Coulomb blockade threshold field for $S\hat{S}$ pair creation [20] and E_0 depends on the washboard pinning potential.

Some theoretical arguments for how topological soliton domain walls might suppress decoherence are as follows. The tunneling probability amplitude is governed by the action density rather than the total action for nucleating $S\hat{S}$ domain wall pairs, and is thus independent of the transverse dimensions of the domain walls (or “branes”) [28]. Even infinitely large domain walls would thus have a finite probability of nucleating via quantum tunneling. However, thermal fluctuations and decoherence effects will be suppressed by the topological stability and overall large mass-energy of the domain walls, thus allowing coherent quantum effects to dominate even at high temperatures. Perhaps biological systems use similar mechanisms to suppress decoherence, and thereby enable the utilization of large-scale quantum coherence. These systems are of potential relevance to biology because: (1) quasi-1D structures, including microtubules, actin filaments, the DNA helix, etc., are pervasive in biological systems, (2) the transition temperatures can be

comparable to or higher than biological temperatures, (3) the mechanisms by which decoherence is suppressed may be similar in biological systems, and (4) soliton models have been proposed for several biological systems, including DNA and microtubules.

A type of learned behavior, known as the pulse-duration memory effect, is another phenomenon especially pertinent to the QCI. It has been found that, by applying a series of rectangular current pulses of identical width, one can “train” a DW to remember the widths of the previous pulses, such that a voltage oscillation minimum produced by the DW response coincides with the end of the next applied pulse, apparently defying causality [55]. What is especially intriguing is that just a few pulses (in some cases only one!) are required for the DW to “learn”, whereas classical simulations predict that many (often hundreds) of pulses should be needed. This suggests that a driven DW may operate as a rudimentary quantum computer operating at relatively high temperatures. The key may be the redundancy provided by soliton domain walls, each of which contains identical kinks along many parallel chains. The price paid is the increased size of each elementary unit of information, but the gain is that the domain walls are protected from decoherence and thermal fluctuations. Perhaps biological systems also use some degree of redundancy and/or topological objects to suppress decoherence. Clearly, further experiments, as well as more detailed theoretical work on possible mechanisms, are strongly warranted.

Error Correction and Quantum Entanglement of a Macroscopic System

As we have seen above, under appropriate environmental isolation, it is theoretically conceivable to obtain quantum coherence of macroscopic populations of tubulin dimers in microtubule systems, which can be sustained for long enough times so that dissipationless energy and signal (information) transfer can occur in a cell.

We would now like to discuss the feasibility of the above, admittedly speculative, ideas by making a brief report on recent progress made in experimentally demonstrating macroscopic quantum entanglement at room temperature in atomic physics.

In a recent article, Julsgaard et al. [57] describe the macroscopic entanglement of two samples of Cs atoms at room temperature. The entangling mechanism (see Sect. 4.5 for more on entanglement) is a pulsed laser beam and although the atoms are far from cold or isolated from the environment, partial entanglement of bulk spin is unambiguously demonstrated for 10^{12} atoms for 0.5 ms. The system’s resilience to decoherence is in fact facilitated by the existence of a large number of atoms as even though atoms lose the proper spin orientation continuously, the bulk entanglement is not immediately lost. Quantum informatics, the science that deals with ways to encode, store and retrieve information written in qubits has to offer an alternative

way of interpreting the surprising resilience of the Cs atoms by implicating redundancy. Simply stated, information can be stored in such a way that the logical (qu)bits correspond to many physical (qu)bits and thus are resistant to corruption of content. Yet another way of looking at this is given in the work by Kielpinski et al. [58] where a decoherence-free quantum memory of one qubit was built by encoding the qubit into the “decoherence-free subspace” (DFS) of a pair of trapped beryllium ${}^9\text{Be}^+$ ions. They achieved this by exploiting a “safe-from-noise-area” of the Hilbert space for a superposition of two basis states for the ions, thus encoding the qubit in the superposition rather than one of the basis states. By doing this they achieved decoherence times on average an order of magnitude longer than regular. Both of the above works show that it is possible to use DFS, error correction and high redundancy to both store information and to keep superpositions and entanglements intact for biologically relevant times in macroscopic systems at high (room) temperature. Thus, it may not be entirely inappropriate to imagine that in biological *in vivo* regimes, one has, under certain circumstances such as specified above, entanglement of tubulin/MT arrangements.

4.2.3 Implications for Cell Function

The above raises the question of how such phenomena can affect the functioning of cells. In other words, would the existence of such coherent states and the emergence of quantum-mechanical entanglement be somehow useful or beneficial to biological function? Is it then reasonable to propose that in certain cases, natural selection may have favored molecules and cellular structures that exhibited and sustained such phenomena? If we accept the notion that according to the laws of quantum physics certain macroscopic arrangements of atoms will exhibit such effects, is it not reasonable then to expect that biomolecules and (by extension) cellular structures and whole cells have “found” a use for such phenomena and have evolved to incorporate them? We stress that at a given instant in time, the different microtubule coherent states participating in a specific bulk entanglement would be almost identical due to the fact that they are related/triggered by a specific “external agent” (e.g. the passing of a specific train of action potentials in the case of a neural cell). This is of importance since it increases the system’s resilience to decoherence (by entangling a large number of nearly identical states), in addition to facilitating “sharp decision making” (i.e. rapid choice among a vast number of very similar states) as explained in [96] which is presumably a trait favored by natural selection. More and more, physicists are exploring the quantum mechanics behind such important biological processes as enzyme action [4] or photosynthesis [112]. Below, we digress to investigate one possible way teleportation of coherent quantum states across and between cells can play a biologically relevant role as the mechanism behind some of the information storage, retrieval and processing done by cells.

Biological Quantum Teleportation

We define teleportation as the complete transfer of the coherent state of an MT *without any direct transfer of mass or energy*. This means that the “receiver” MT finds itself in an identical state to the “sender” MT. We will demonstrate the way in which, given the possibility for entangled states, teleportation between microtubule A and microtubule C can occur. The use of pure state vectors, $|\Psi\rangle$, to describe the coherent states along a MT arrangement is justifiable since they do not obey the ordinary Schrödinger evolution equation. Instead, they obey the stochastic equations of open systems, of the form discussed in [37]. Nowhere in the proof of teleportation below are the precise forms of the evolution equations used. As argued in [37], by using appropriate stochastic (Langevin-type) equations one may recover, for instance, the standard Lindblad form of evolution equations for the corresponding density matrices $\rho = \text{Tr}_M |\Psi\rangle\langle\Psi|$, where M is an appropriate subset of environmental degrees of freedom, nonaccessible to the observer.

A coherent state in microtubule A (referred to as simply A and designated as $|\Psi(A)\rangle$) of the (collective) dipole moment(s) being in either of the two classically allowable states with probability amplitude ω_0 and ω_1 can be written as:

$$|\Psi(A)\rangle = \omega_0|0\rangle + \omega_1|1\rangle. \quad (4.18)$$

Step 1: The cell finds itself with microtubule B and microtubule C – which can be parallel or collinear – in an entangled state written as:

$$|\Psi(B, C)\rangle = (1/\sqrt{2})|1_B, 0_C\rangle + |0_B, 1_C\rangle. \quad (4.19)$$

The combined state of A, B, C can be written as:

$$|\Psi(A, B, C)\rangle = |\Psi(A)\rangle \otimes |\Psi(B, C)\rangle, \quad (4.20)$$

which upon expanding the outer product can be written as:

$$\begin{aligned} |\Psi(A, B, C)\rangle &= \frac{1}{\sqrt{2}}[(\omega_0|0_A, 1_B, 0_C\rangle + |0_A, 0_B, 1_C\rangle) \\ &\quad + (\omega_1|1_A, 1_B, 0_C\rangle + |1_A, 0_B, 1_C\rangle)]. \end{aligned} \quad (4.21)$$

We can also express the combined state $|\Psi(A, B, C)\rangle$ in a different basis, known as the “Bell basis”. Instead of $|0\rangle$ and $|1\rangle$, the basis vectors will now be,

$$|\Psi^\pm(A, B)\rangle = \frac{1}{\sqrt{2}}(|0_A, 1_B\rangle \pm |1_A, 0_B\rangle), \quad (4.22)$$

and

$$|\Phi^\pm(A, B)\rangle = \frac{1}{\sqrt{2}}(|0_A, 0_B\rangle \pm |1_A, 1_B\rangle). \quad (4.23)$$

In this new basis, our state of the three microtubules $|\Psi(A, B, C)\rangle$ is written as:

$$\begin{aligned} |\Psi(A, B, C)\rangle &= \frac{1}{2}(|\Psi^+(A, B)\rangle \otimes (\omega_0|0_C\rangle + \omega_1|1_C\rangle) \\ &\quad + (|\Phi^+(A, B)\rangle \otimes (\omega_0|1_C\rangle + \omega_1|0_C\rangle)) \\ &\quad + (|\Psi^-(A, B)\rangle \otimes (\omega_0|0_C\rangle + \omega_1|1_C\rangle)) \\ &\quad + (|\Phi^-(A, B)\rangle \otimes (\omega_0|1_C\rangle + \omega_1|0_C\rangle)). \end{aligned} \quad (4.24)$$

This concludes the first step of teleporting the state of MT A to MT C .

Step 2: Notice that so far, MT A has not interacted with the environment or cell, i.e. the coherent state of A that we designated as $|\Psi(A)\rangle = \omega_0|0_C\rangle + \omega_1|1_C\rangle$ has not been touched. Now the part of the cell containing A and B (the “sender part”) makes a “measurement” – which in our case can be an electromagnetic interaction with a passing action potential or the binding of a MAP molecule. If this measurement or forced collapse is done in the Bell basis, on $|\Psi^\pm(A, B)\rangle$ it will project the state in MT C (!) to:

$$|\Psi^\pm(C)\rangle = \langle\Psi^\pm(A, B)|\Psi(A, B, C)\rangle = \omega_0|0_C\rangle \pm \omega_1|1_C\rangle, \quad (4.25)$$

similarly,

$$|\Phi^\pm(A, B)\rangle = |\Phi^\pm(C)\rangle = \omega_0|1_C\rangle \pm \omega_1|0_C\rangle. \quad (4.26)$$

This effectively concludes the teleportation of the state of MT A to MT C with one caveat.

Step 3: There is a probabilistic nature to this process, which means that MT C may receive the exact copy of the state of MT A , i.e. $|\Psi^+(C)\rangle$ or it may receive a state that is a unitary transformation away from the original $|\Psi(A)\rangle$ (one of the other three possibilities: $|\Psi^-\rangle$ or $|\Phi^\pm\rangle$). MT C can reproduce the state of MT A if there is a “hardwired” condition so that when MT C receives $|\Psi^+(C)\rangle$ it does nothing further, yet if it receives one of the other three, it performs the correct unitary transformation to obtain the correct state from A . This “hardwired” behavior can be implemented through the use of codes, not unlike the Koruga bioinformation [62] code that MTs seem to follow. In principle, the exact state correspondence may not even have any significance and instead the information could be encoded in the frequency of transferred states, similar to information being encoded in the frequency of action potentials and not their shapes.

Teleportation is an entirely nonclassical phenomenon and has been experimentally demonstrated in matter and light states and combinations of these (see Sect. 4.5). Currently, the scientific consensus is that teleportation is impossible without entanglement although this may change in the future. Biological teleportation as described above, can be imagined as the basis of intra- and intercellular correlation that leads to yoked function (e.g. intracellularly during translation and intercellularly during yoked neuron firing). Experiments to check for such teleportation of states can be designed based on the surface plasmon resonance (SPR) principle [105] as applied to sheets of polymerized tubulin immobilized on a metal film (Sects. 4.4 and 4.5).

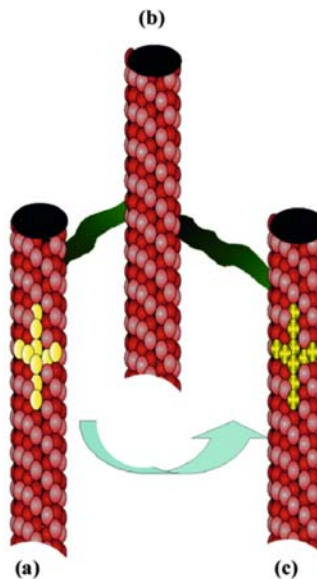


Fig. 4.2. Schematic of quantum teleportation of dipole states. (Taken from [81]) MT (a) sends its state (represented by the yellow cross) to MT (c) without any transfer or mass or energy. Both MT (a) and MT (c) are entangled with MT (b). Entanglement represented by the presence of connecting MAPs (green)

A graphical representation of biological quantum teleportation of dipole moment states is presented in Fig. 4.2.

Information Processing by Biopolymers and the Guitar String Model (GSM)

In the quantum-mechanical scenario for MT dynamics discussed above, as suggested in [80], a quantum-hologram picture for information processing of MT networks emerges. Further, the existence of solitonic quantum-coherent states along the MT dimer walls implies a role for these biological entities as logic gates [82]. Consider, for instance, a node (junction) of three MTs connected by microtubule-associated proteins (MAPs) see Fig. 4.3. The quantum nature of the coherent states makes the junction interaction probabilistic. Therefore, at tube junctions one is facing a probabilistic Boolean interaction. The probability of having a solitonic coherent state in a MT branch does depend on its geometric characteristics (such as length). By modulating the length of the tubes and the binding sites of the MAPs a bias can be introduced between bit states that can affect the probabilistic final outcomes. This has obvious implications for information processing by MT networks.

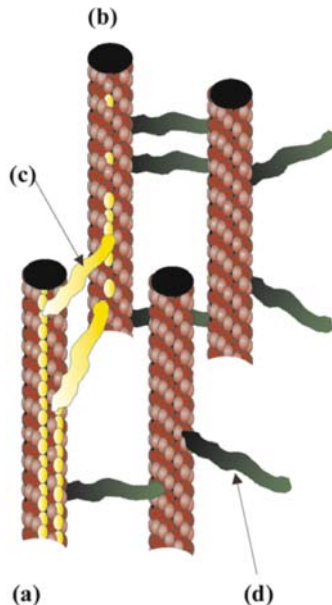


Fig. 4.3. An XOR (exclusive-or) logic gate. (Taken from [81]) “0” (“1”) is represented by absence (presence) of solitonic kink wave of dipole moment flips indicated in yellow. (a) Input MT, (b) Output MT, (c) A MAP transmitting a solitonic kink wave, (d) a “quiet” MAP. MT (a) has two solitons traveling, encountering two MAPs that transmit both solitons to MT (b). In this hypothetical scenario, the solitons arrive out of phase at MT (b) and cancel each other out. The truth table for XOR reads: $0,0 \rightarrow 0$; $0,1 \rightarrow 1$; $1,0 \rightarrow 1$, $1,1 \rightarrow 0$ and can be realized by an MT arrangement if the MAPs are arranged such that each can transmit a soliton independently but if they both transmit the solitons cancel out, i.e. the two MAPs must be an odd number of dimers apart on MT(a)

Such a binary information system can then provide the basic substrate for quantum information processing inside a (not exclusively neural) cell. In a typical MT network, there may be about 10^{12} tubulin dimers. Although such a number is large, as discussed earlier there may be subtle “shielding” mechanisms at play. The above scenario is not necessarily *quantum* in nature. An essentially identical argument can be made for information processing via waves of dipole flips or just momentum transfer as a result of propagating conformational changes.

This suggests an obvious model for encoding information in a network of MTs that we shall call the “guitar string model” to emphasize the analogy to the way six guitar strings (the MTs) can be clamped by four fingers (MAPs) at different nodes to generate hundreds of different chords (engrams). If propagating dipole moment flips are indeed carrying signals inside the cell then the nodes in the network can affect this propagation in a large variety of

ways. A limited set of MTs with a limited set of MAP binding sites can have a very large set of engrams. This also suggests a way for new memories to form and old ones to be erased by simply changing the distribution of MAPs.

4.2.4 Conclusions

If it is experimentally confirmed that treating MTs as QED cavities is a fair approximation to their behavior, one can propose that nature has provided us with the necessary structures (microtubules) to operate as the basic substrate for quantum computation either *in vivo*, e.g. intracellularly, or *in vitro*, e.g. in fabricated bioqubit circuits. Such a development would pave the way to construct quantum computers by using quantum computers by using microtubules as building blocks, in much the same way as QED cavities in quantum optics are currently being used in successful attempts at implementing qubits and gates [126]. Detecting quantum behavior at this level would undoubtedly advance attempts at implicating quantum physics.

4.3 Tau Accumulation in *Drosophila* Mushroom Body Neurons Results in Memory Impairment

4.3.1 Introduction

In this section we summarize and attempt a “physicist-friendly” account of the neurobiological results obtained by our group and published in [86].

In order to test some of the predictions of the models discussed in Sects. 4.1 and 4.2, an *in-vivo* neurobiological behavioral study was undertaken. The goal was to experimentally investigate whether memory is affected by perturbations in the microtubular (MT) cytoskeleton. Associative olfactory learning and memory were the types of memory accessible to us with the transgenic *Drosophila* fruitfly behavior analysis system. We tried disturbing the fly MTs as little as possible, avoiding perturbing the cytoskeleton by formation of such large protein aggregates as neurofibrillary tangles (NFTs) that could effectively “strangle” the neuron, disrupting or even stopping intracellular (axonal) transport. In addition, NFTs and/or amyloid or senile plaques (APs or SPs) have been unequivocally shown to contribute to neurodegeneration and eventual neuronal death and it is reasonable to expect a dying neuron to dysfunction, regardless of the state of its MTs. We also avoided causing any developmental problems by selecting gene promoters (drivers) with appropriate temporal activity.

Since this is a contribution addressed mostly to physicists an effort has been made to explain potentially unfamiliar biological terms and procedures. Following established standards in genetics, small case italics such as *tau* indicate the *gene* that codes for the protein TAU indicated in capitals. Strains or lines of transgenic animals (animals that have been genetically manipulated

and contain extra genes) are named somewhat arbitrarily so here we use *b*-, *h*-, or *d*-, indicating bovine- human- or *Drosophila*- (native) derived-genes, while a few letters identify the source.

Microtubule-associated protein (MAP) TAU has long been implicated in the encoding of human memory and it has been shown that mutations in the human NC-17 *tau* gene are one of the causes of Alzheimer's Disease [95, 99, 138]. For this reason, NFT and SP/AP formation have been the main focus of studies of tauopathies in animal models. For instance, transgenic mice with frontotemporal dementias with Parkinsonism (FTDP 17) mutations develop NFTs and neurodegeneration accompanied by motor deficits [47, 71]. Expression of human wild type and FTDP-17-linked mutations in *Drosophila* results in age-dependent neurodegeneration without NFTs [141] except when wild-type TAU was phosphorylated by overexpressed *Drosophila* glycogen synthase kinase-3 [50]. Mice carrying mutated *tau*, *presenilin 1* and *alpha-beta peptide precursor (APP)* transgenes show synaptic dysfunction before the development of NFTs or amyloid plaques. From these and other studies it seems that tauopathy-caused deficits in memory appear even without NFTs or SPs/APs although frequently, at least NFTs do eventually appear in the late stages of the disease.

For NFTs to form there must be a situation of elevated TAU accumulation (in a nonfilamentous or "pretangle" state) in the affected neurons. Such a condition has been suggested as the underlying cause of pre-neurodegeneration cognitive symptoms such as memory loss [15, 47] and our research experimentally addresses the question of the effect of elevated pretangle state TAU in *Drosophila* mushroom bodies and we propose a connection between the observed effects and theoretical models of cytoskeletal function.

4.3.2 Drosophila

The *Drosophila Melanogaster* fruit fly has long been a favorite of experimental behavioral neurobiologists for numerous reasons including its relatively simple genetic makeup and quick generation time, powerful classical and molecular genetics and the animal's ability to learn and remember a variety of tasks.

To illustrate our approach and choice of *Drosophila* more fully, our initial experimental design will be briefly described here. *Drosophila* was selected as the ideal system for investigating cytoskeletal involvement in learning and memory because we were to attempt to track an intraneuronal *redistribution* of MAP-2 and/or MAP TAU as a result of conditioning. This is a prediction of the GSM described in Sect. 4.2. In order to track a redistribution of MAPs inside neurons one must be able to differentiate between the various parts of the neuron such as the dendrites, axons, axonal projections and somata. In humans and other mammals, the neuronal organization is such that multiple neurons and neuronal types are involved in a given process forming an extensive complex network of axons and dendrites. As a result, it is particularly difficult to locate individual neurons' specific parts and stain selectively to

track changes in distribution of a particular protein. In *Drosophila*, on the other hand, the neuronal organization is such that differentiation of subneuronal parts is facilitated. For instance, neurons belonging to mushroom bodies (MBs are prominent structures in the *Drosophila* brain essential for olfactory learning and memory) represent a highly ordered, tightly and sequentially packed neuronal system where axonal projections (i. e. synaptic fields), dendrites and somata are macroscopically (on the order of μm) separated in ordered fiber bundles, see Fig. 4.4.

This provides a strong advantage for analysis of the results of expression of microtubule-associated proteins in specific neurons (e. g. those associated with a specific type of memory) but also *within* different parts of such neurons. For instance, a bulk redistribution of a certain MAP from the axons to the dendrites of the MB, presumably as a result of memory formation can, in principle, be tracked. This is in fact a prediction of the GSM for memory encoding since if the MAPs play the role of fingers on the guitar fret board and the various chords correspond to encoded information, acquisition of new information and memory would result in a redistribution of MAPs. Unfortunately, our preliminary experiments utilizing directed expression of chicken MAP-2 in MBs showed that either the resolution offered by existent anti-MAP antibodies was insufficient to decipher appreciable MAP redistribution and/or no such redistribution took place as a result of learning. The latter would be inconsistent with results obtained in rodents [143] that suggest a redistribution of MAP-2 resulting in accumulation in dendrites as a result of learning an auditory associative task.

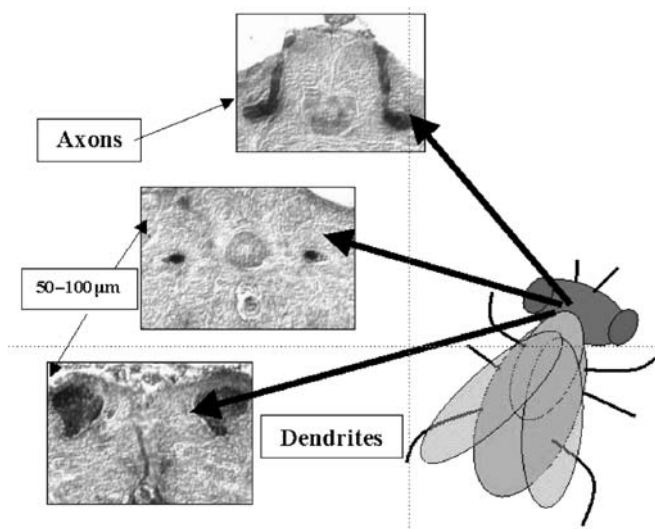


Fig. 4.4. Fly mushroom bodies (MBs). Fly mushroom bodies are shown in paraffin frontal sections 5 μm thick, stained for LEO, a MB-specific protein

We therefore shifted our approach to determining the impact of MAP TAU overexpression on the ability of the animals to learn and retain memories. Although this is not as direct a test of the GSM it does provide a solid link between the microtubular cytoskeleton and memory retrieval and stability as will be argued in this section.

4.3.3 Genetic Engineering

We induced the expression of vertebrate (human and bovine) *tau* genes, producing TAU protein in *specific* tissues and at specific *times* in *Drosophila* using the method of directed gene expression.

Directed Expression

Directed gene expression rests on the principle of obtaining two genetically manipulated (transgenic) lines, the first of which contains the gene to be expressed, fused to and under the direction of an *upstream activating sequence* (UAS). This UAS promoter is activated by the presence of its unique, selective and specific activator protein GAL4. To generate transgenic lines expressing GAL4 in a cell or tissue specific pattern, the GAL4 gene is inserted randomly into the fly's genome, thus driven in its expression from various genomic enhancers. A GAL4 target gene (UAS-tau) will remain silent in the absence of GAL4. To activate the target gene, the flies carrying the UAS-tau are crossed to flies expressing GAL4 at specific tissues and at specific times in the animal's development (see Fig. 4.5). To eliminate potential complications arising from expression of TAU in the embryonic and developing nervous system, we selected strains expressing GAL4 in late pupal and adult mushroom body neurons [3] only by utilizing the MB drivers c492 and c772.

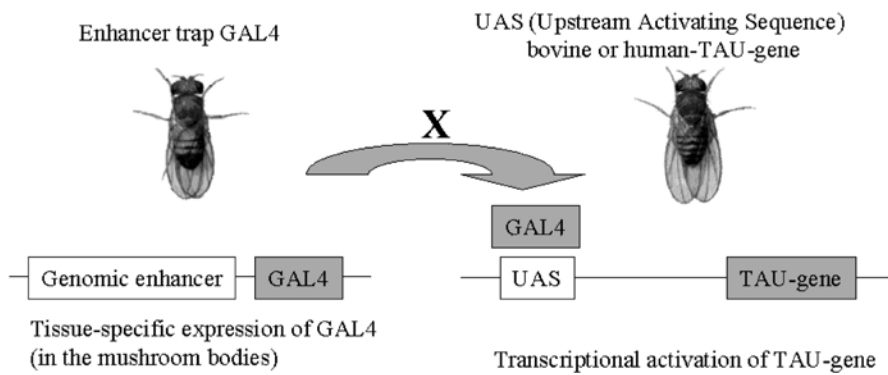


Fig. 4.5. Upstream activating sequence and target gene

Coimmunoprecipitation

Note that past studies have shown that mere accumulation of non-*Drosophila* proteins such as β -galactosidase [124, 125], and GAL4, or *Drosophila* proteins [30, 83] that are not MT specific in MB neurons, do not cause any behavioral deficits. Therefore, once TAU is shown to bind to MB MTs, any effects of TAU accumulation in MBs can be taken as specific to TAU. Also note that the mere presence of two proteins in the same tissue does not necessarily mean they are bound together so although we expected h- and b- TAU to bind to MTs we performed a coimmunoprecipitation study. The *Drosophila* protein (dTau), contains four putative tubulin-binding repeats [43]. They exhibit 42% and 46% identity (62% and 66% similarity)² with the respective sequence of bTAU and hTAU [43–45]. To determine whether this sequence conservation among vertebrate and *Drosophila* TAU also signals a functional conservation (i. e. if all types retain their MT binding sites intact), antitubulin antibodies were used in immunoprecipitation experiments from head lysates of *btau*-expressing animals and controls. We found that bTAU coimmunoprecipitates with *Drosophila* tubulin, indicating that the vertebrate protein is capable of binding *Drosophila* microtubules. Figures and extensive details are presented in [86].

There is one obvious problem in assuming that we have just substituted “more of the same” in the fly’s mushroom bodies because dTau lacks the amino-terminal extension of vertebrate TAU and this suggests that the conformation of vertebrate TAU will be somewhat different from the *Drosophila* protein despite its microtubule-binding ability. This, however, does not affect the conclusions of this study, as will be illustrated later.

Collectively, the ability to bind *Drosophila* tubulin in head lysates and its preferential accumulation within the mushroom bodies indicate that bTAU, and by virtue of its high degree of identity hTAU, bind to the microtubular cytoskeleton within these neurons. Therefore, in the mushroom body neurons of the three *tau* transgenics investigated, the microtubular cytoskeleton is likely burdened with excess TAU.

All strains were normalized to an isogenic (i. e. genetically identical) w¹¹¹⁸ strain.³ To obtain flies for behavioral analyses, c772 and c492 homozygotes were crossed to UAS-*btau*, UAS-*htauwt1*, UAS-*dtau* 4 and UAS-*dtau1* homozygotes (see separate section on *dtau* below) and the progeny was collected and tested 3–5 days after emergence. Similarly, the UAS-*btau*, UAS-*htauwt1*,

² Identity is defined as absolute conservation of the amino acid sequence between two proteins, while similarity is conservation of type (e. g. exchanging one acidic amino acid for another acidic preserves similarity)

³ Isogenic lines are strains of identical genetic background. w¹¹¹⁸ was chosen to represent the wild-type genotype. The transgene of interest was bound to red-eye phenotype and the transgenic flies were crossed to w¹¹¹⁸ for seven generations (keeping only the red eyes) thus normalizing the genetic background and avoiding contamination.

UAS-*dtau* 4 and UAS-*dtau1* homozygotes were crossed to w¹¹¹⁸, the line not containing any drivers (and thus one does not expect to see any extra tau expression) to obtain heterozygotes used as controls.

In addition to the pattern of expression of a gene, it is important to also quantify the amount of protein that is being created. To investigate the relative level of TAU accumulation within adult fly heads we performed semiquantitative Western blot analyses (see [86] for details). We determined that bovine TAU was present in head lysates of animals that had the *tau* transgenes and the MB drivers, but not in parental strains as was expected. The level of bTAU protein did not appear to change significantly over a three-

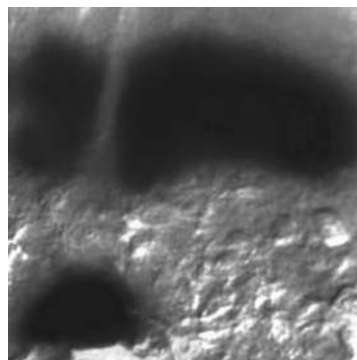


Fig. 4.6. (Taken from [86]) To determine whether the vertebrate (bovine) TAU binds onto *Drosophila* microtubules, extracts were prepared from the brains of flies that express UAS-*btau* under the c772 (lanes 2 and 3) and the c492 (lane 5) drivers under mild conditions that would not disrupt TAU/tubulin complexes. A monoclonal antibody against tubulin was added to the mix and then precipitated using standard techniques (coimmunoprecipitation). The resulting complexes were resolved in a denaturing polyacrylamide gel blotted onto a nylon membrane and the presence of bovine TAU was investigated using a monoclonal antibody. Lane 1 does not contain bTAU because the extracts were prepared from heads of animals that contained only the *btau* transgene without the driver and therefore do not accumulate the vertebrate protein. Lane 2 represents extracts from bTAU accumulating animals under the c772 driver that were not subjected to coimmunoprecipitation. Therefore the characteristic bTAU band serves as a marker of the size and the amount of total bTAU in the extract. Lane 3 represents that products of coimmunoprecipitation from an equal amount of protein as in lane 2. Detection of a bTAU-specific band demonstrates that most of the vertebrate protein (compare the intensities the band in lane 2 indicating the total amount of bTAU in the head extract with the intensity of the band in lane 3 indicating the amount of bTAU that is complexed with *Drosophila* tubulin in the extract) exists in a complex with the *Drosophila* tubulin. Similar results were obtained with the c492 driver (lane 5). Notably, these bTAU specific bands were absent in the negative controls (extracts from animals not expressing bTAU because they do not carry the UAS-*btau* transgene, but only the drivers (lanes 4 and 6)

week period, indicated by densitometric quantification of results from three independent experiments. Similarly, the level of hTAU appeared relatively constant (data not shown).

Although it would be desirable to know exactly how much more TAU than normal is present, the techniques we used for quantifying the presence of b and h protein relied on mono- or polyclonal antibody binding and densitometry and thus are inherently difficult to normalize.

In principle, it would be possible to refine these findings with such elaborate methods as ion trapping and matrix-assisted laser-directed ionization and time-of-flight spectroscopy. Even though we did not attempt such a high degree of quantification, we are confident that the transgenic animals did express a significantly higher level of TAU in their mushroom bodies and this is sufficient for the scope of our study.

4.3.4 Conditioning

Drosophila fruit flies are naturally attracted or repulsed with a variety of affinities by different odors. We followed two standard negatively reinforced associative learning paradigms that essentially generalize the Pavlovian conditioning protocol by coupling aversive odors as conditioned stimuli (CS+ and CS−), and electric shock as the unconditioned stimulus (US). In this way, olfactory cues are coupled with electric shock to condition the flies to avoid the odorant associated with the negative reinforcer. These conditioning protocols for *Drosophila* were initially developed by Tully and Quinn [134] and modified by Skoulakis et al. [106, 125]. We used two aversive odorants: 3-octanol (OCT) and Benzaldehyde (BNZ). The conditioning apparatus consists of a training chamber and a selection maze (see Fig. 4.7). The maze is normalized by adjusting the concentration of odorants. Once normalized, both wild-type (control) and transgenic naïve (i.e. untrained) flies choose to enter one of two identical tubes smelling of OCT and BNZ, respectively, with a probability of 50% (as they avoid both odors equally). Because the earliest possible time that we can test the animals past the CS+ and US presentation is 180–200 s, our measurements cannot differentiate between “acquisition” and “3-minute memory”. This earliest performance assessment will be referred to as “learning”.

Conditioning of the flies in the LONG training protocol takes place as follows. A batch of wild-type, naïve flies (numbering between 50 and 60) are collected under light anesthesia (using CO₂) and 12–24 h later are left in the dark for one to two hours. The entire conditioning procedure takes place in a temperature- and humidity-controlled darkroom under red illumination in order to isolate the effects of olfactory stimulation from visual stimulation (flies have been shown to react least to red light). Once the flies have been acclimated to the darkroom, half are inserted into conditioning chamber A. The cylindrical wall of the chamber is covered by a grid of two interspersed conducting electrodes spaced such that at least two of the fly’s six legs must be

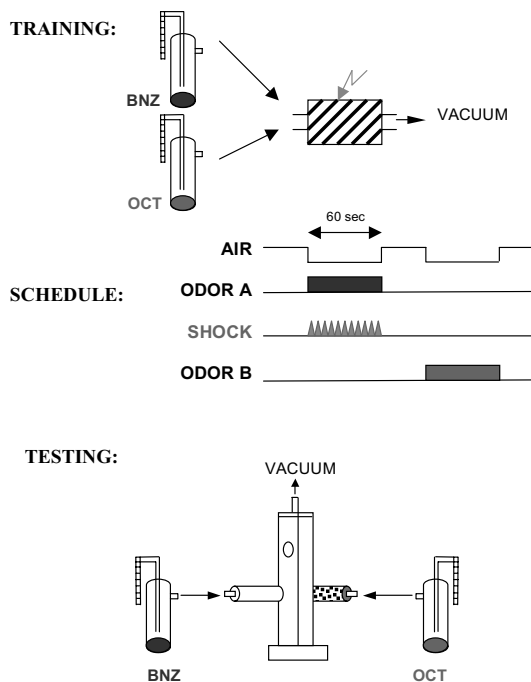


Fig. 4.7. Conditioning apparatus and training schedule. (Taken from [88])

in contact with two opposite voltage electrodes. The diameter of the chamber is chosen such as to prevent flies from hovering midair. In this way, the fly necessarily completes the circuit making it the path of least resistance. The electrodes are electrified by a signal generator set to 92.0 V. The flies receive eleven electric shocks once every five seconds. During this time, the chamber is filled with air containing OCT. The flies are given 30 s to rest while the air is being cleared of odorants and are then given the opposite (control) odorant (in this case BNZ) for another minute in the absence of electrical shocks. A rest period of 30 s follows after which the flies are tested for acquisition of memory by being inserted into the selection maze and given the choice of entering a chamber smelling of OCT or an identical one smelling of BNZ. For control and consistency purposes, the experiment is done simultaneously in an identical apparatus B with the shock-associated and control odors reversed. We define a conditioned or “trained” fly as one that has chosen to go into the chamber filled with the control odor after given the choice for 90 s.

It is observed that following training, a large percentage of wild-type flies choose to avoid the smell that was present when they received the electric shocks. The percentage is calculated as a normalized *performance index* (PI) where $PI = \frac{\text{trained-untrained}}{\text{total}} \times 100\%$. Typical PI values for wild-type flies were between 75 and 90%, giving us confidence that the flies have learned to

associate the stimuli. The general procedure described above is a typical associative learning Pavlovian conditioning paradigm for behavioral experiments appropriate for a variety of animals and more details can be found in the literature [106, 125]. One improvement that was discovered (and increased wild-type PI to about 90%) was that it was possible to collect the flies without subjecting them to CO₂ anesthesia after conditioning by simply tapping the chambers sharply so that the flies entered a test tube through a funnel by their own inertia. The mechanical shock associated with such tapping was shown to have no effect on the flies' PI, while the (light) anesthesia immediately following conditioning as well as the presence of a naturally leaky CO₂ tank in the darkroom was known to compromise PI scores.

4.3.5 Controls

During physics experimentation, background measurements play a significant role in determining the signal. Similarly, a dominant theme in biological behavioral research of the type described here is that of a set of measurements collectively called controls. When results such as, for instance, a decrement in learning and memory exhibited by transgenic animals are presented, they must always be quantified with respect to the equivalent in the control (nontransgenic or wild-type animal).

For our behavioral analyses to have any significance we had to first determine that the flies expressing foreign TAU or overexpressing native TAU were not affected in ways unrelated to learning and memory. Thus we had to assess the experimental flies' task-relevant sensory behaviors and olfactory acuity to an attractive odor in addition to testing their ability to feel and avoid electric shock and to detect and avoid aversive odorants. Experience-dependent nonassociative behavior was also tested by examining the effects of *pre-exposure* to odorant plus shock since pre-exposure to electric shock and one odorant tends to decrease the animals' ability to perform well in associative learning tasks that depend on electric shock and another odorant.

We also had to determine that our flies were viable and no neurodegeneration took place as the result of expression of the transgenes. Note that in all these control experiments, the main principle is to test the transgenic against the control, for instance, an absolute decrement in PI is not indicative of a TAU-mediated effect if it is mirrored identically in control animals.

Finally, one must be certain that the observed effects are TAU specific, i.e. that other proteins that do not bind the microtubular cytoskeleton and are (over)expressed with the same drivers, result in no memory effects. This was done and was discussed in Sect. 4.3.4.

Mechanosensory

Sensory control experiments to ascertain that the transgenic flies retained their mechanosensory abilities (to feel and avoid pain caused by electric

shock) were performed as described in [106, 125]. Avoidance of electrified grids kept at 92 V (normal US stimulus), or 45 V was not different between *tau*-expressing animals and controls, indicating lack of mechanosensory deficits due to TAU accumulation. The two levels of voltage were used as a further refining mechanism to help find any mechanosensory effects that our transgene expression may have had (e.g. it may have made the flies less sensitive but still able to sense 92 V).

Olfactory Acuity

Pre-Exposure

Although, as expected CS+/US pre-exposure significantly reduced subsequent avoidance of the complementary odor, *tau*-expressing animals and controls exhibited equal decrements (Fig. 4.8A). Therefore, TAU accumulation did not cause differential responses to odor-shock pre-exposure and we can conclude that TAU accumulation does not affect experience-dependent, nonassociative tasks.

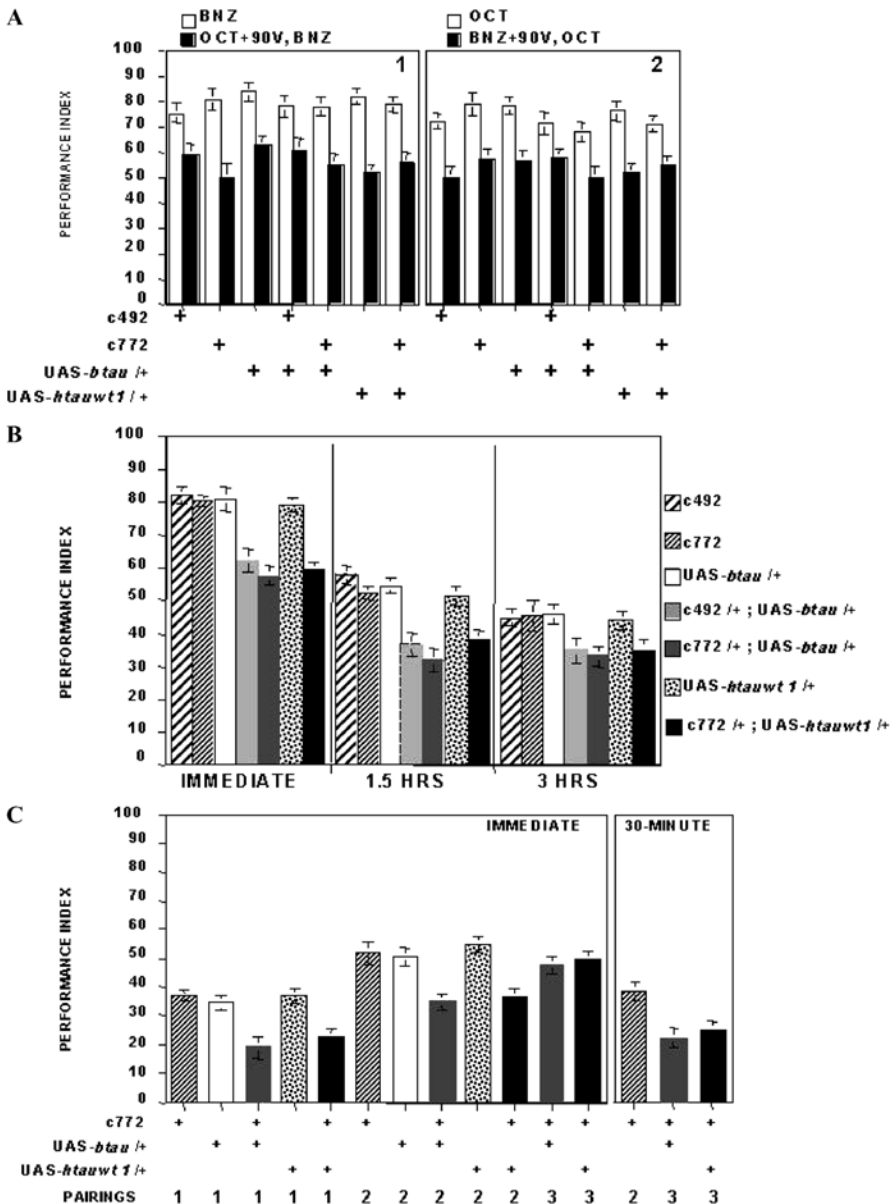
Attractive and Aversive Odors

Both control and transgenic *tau*-expressing animals avoided equally the aversive odors benzaldehyde and 3-octanol (CS) at two different odor concentrations given the choice of fresh air. These results indicate that TAU accumulation in mushroom body and other central brain neurons described above, did not result in deficits in sensory abilities necessary for olfactory conditioning. In addition, we tested the response of *btau* and *htau*-expressing animals relative to controls to the attractive odor geraniol (GER) in olfactory trap assays [125]. Though this odor is not task relevant, it provided an independent measure of olfactory acuity towards a qualitatively different odor.

As shown in Table 1 of [86] the performance of *tau*-expressing animals was not significantly different from controls for these tasks. Collectively, the results of these olfactory control experiments support the conclusion that despite the accumulation of TAU in antennal lobe neurons (that are used as olfactory sensors by the fly) *btau*- and *htau*-expressing animals retained their normal olfactory responses to the odors tested [86].

Viability of Transgenics

To assess the effects of extra TAU in MBs on the learning and memory capabilities of flies convincingly, we had to establish that our flies would be reasonably healthy during their conditioning and testing. We hypothesized that accumulation of TAU within the mushroom bodies would not affect survival because these neurons are dispensable for viability [24]. However, the



effect on fly longevity of TAU accumulation in additional neurons where *c772* and *c492* drivers were determined to be active was unknown. In addition, it has been recently shown that expression of human wild-type and mutant TAU proteins in the entire *Drosophila* nervous system (pan-neuronal expression), or targeted expression in cholinergic neurons, results in neurodegeneration and

Fig. 4.8. Results (taken from [86]) **(A)** Nonassociative pre-exposure effect. 1. Avoidance of benzaldehyde after pre-exposure to full strength octanol and 90-V electric shock (filled bars) in comparison to avoidance without such pre-exposure (open bars) ($n \geq 7$). ANOVA revealed significant effects of treatment ($F_{(1,78)} = 13.784, p < 0.005$), but not for genotype, both in pre-exposed and non-pre-exposed animals. 2. Avoidance of octanol after pre-exposure to benzaldehyde and 90-V electric shock (filled bars) in comparison to octanol avoidance without pre-exposure (open bars) ($n \geq 7$). ANOVA revealed significant effects of treatment ($F_{(1,84)} = 14.026, p < 0.005$), but not for genotype, both in pre-exposed and non-pre-exposed animals. **(B)** Olfactory memory after LONG paradigm conditioning. The mean performance index \pm SEM of c492/+; c772/+; UAS-dtau4/+ (open bars) and c492/+; UAS-dtau4/+ and c772/+; UAS-dtau4/+ (filled bars) are shown ($n \geq 9$). Two-way ANOVA revealed significant effects of genotype [$(F_{(4,52)} = 14.687, p < 0.005)$ immediate (3-minute), and $(F_{(4,49)} = 9.327, p < 0.005)$ 1.5 h]. Subsequent Dunnett's tests for each time interval did not reveal significant differences in performance among the c492/+; c772/+; UAS-dtau4/+ control strains or between the c492/+; UAS-dtau4/+ and c772; UAS-dtau4/+ heterozygotes. However, the differences between c492/+; UAS-dtau4/+ and c772; UAS-dtau4/+ heterozygotes and the control strains were highly significant ($p < 0.001$) for immediate memory and 1.5 h memories. **(C)** Performance of c492/+; UAS-dtau1/+ and c772; UAS-dtau1/+ heterozygotes with or without induction at 29°C after LONG conditioning. The average performance (PI \pm SEM) of animals raised at 23–24°C for control strains (c492/+; c772/+; UAS-dtau1/+) is indicated by open bars and c492/+; UAS-dtau1/+ and c772; UAS-dtau1/+ heterozygotes with gray filled bars. The performance of animals raised at 23–24°C and subsequently induced at 29°C for 48–52 h prior to behavioral experiments is indicated by the stippled bars for controls and the black-filled bars for c492/+; UAS-dtau1/+ and c772; UAS-dtau1/+ heterozygotes. Two-way ANOVA indicated significant effects of genotype [$(F_{(4,44)} = 8.287, p < 0.005)$ for 23–24°C animals and $(F_{(4,48)} = 10.016, p < 0.005)$ for animals induced at 29°C]. Subsequent Dunnett's tests revealed significant differences between the performance of c772; UAS-dtau1/+ heterozygotes and all control strains, as well as c492/+; UAS-dtau1/+ when uninduced ($p < 0.001$). In contrast, both c772; UAS-dtau1/+ and c492/+; UAS-dtau1/+ heterozygotes were different from controls when the animals were induced at 29°C

premature death of adult flies [141]. In order to determine whether TAU expression in adult mushroom bodies and the other brain neurons described above affects the flies' viability, we evaluated the survival of *btau*-, *htauwt1*- and *dtau*-expressing flies over a period of 21 days posteclosion.⁴

Because both male and female animals are used for our behavioral experiments, we used mixed-sex populations to evaluate survival, unlike previous studies [17, 141]. We concluded that expression of vertebrate or *Drosophila tau* in adult mushroom body and other brain neurons did not result in decreased survival [86]. No overt differences between control strains and transgenics were observed for a limited set of animals that were evaluated for

⁴ Eclosion refers to the adult fly emerging from the pupal case (cocoon).

viability for two additional weeks (data not shown). Furthermore, TAU accumulation did not appear to result in gross morphological differences, or decreased fecundity and vigor from control strains.

These results indicate that TAU accumulation within the MB and other neurons of the adult brain does not precipitate the neurodegeneration-dependent decrease in survival observed with pan-neural expression of human mutant TAU proteins throughout development [141].

Neuroanatomy and Histology

Although the mushroom bodies are not essential for viability, we expected that degeneration of these neurons would severely impair behavioral neuroplasticity [24]. To determine whether TAU accumulation in adult mushroom bodies causes their degeneration, we histologically investigated the brain neuroanatomy of animals that expressed the tau transgenes. Because in past studies the severity of neurodegeneration was observed to increase with age and accumulation of TAU [24], we focused on 21-day-old animals. Using a semiquantitative western blot [86] we concluded it is unlikely that any degeneration in older flies is the result of progressively increasing amounts of TAU in mushroom body neurons. Note here that although as previously mentioned, densitometry and immunohistochemistry are by nature hard to normalize, they do give reasonably accurate relative results. Thus we were able to determine that no more TAU was present in older flies even though we could not tell exactly how much overall TAU there was. Staining with various mushroom body antigenic markers [23] did not reveal detectable morphological anomalies in 21-day-old transgenic tau-expressing flies compared to similarly aged, or 2–3-day-old controls.

4.3.6 Results

The results of this study can be summarized as follows. Vertebrate (bovine and human) as well as native TAU accumulation in mushroom bodies (implying TAU bound to MTs) of adult flies results in associative olfactory learning and memory deficits.

Vertebrate TAU-Expressing Flies

We had determined that transgenic animals under the c772 MB driver express higher levels of TAU so we used *c772/+; htauwt1/+* heterozygotes in the analysis presented below, and similar results were obtained for *c4922/+; htauwt1/+* heterozygotes in a limited set of experiments (data not shown).

To determine whether TAU accumulation in the mushroom bodies affected associative processes, we trained *btau-*, *htau-* and *dtau*-expressing animals and controls in the long version of a negatively reinforced, olfactory

associative learning task as described above. *c492/+; UAS-btauI/+; c772/+*; *UAS-btauI/+ and c772/+*; *UAS-htauwt1/+ heterozygotes* exhibited a highly significant 25–30% impairment in learning compared to controls (Fig. 4.8B, immediate). Similar results were obtained for *driver X dtau* and they are described in the literature [86]. These results demonstrated that TAU accumulation in the mushroom bodies strongly compromised behavioral neuroplasticity underlying associative olfactory learning and memory.

To more closely examine the learning and memory deficits of *btau-*, *htau-* and *dtau*-expressing animals, we utilized the SHorT variant of associative olfactory training [10] performed by E.M.C. Skoulakis. Because the LONG paradigm utilizes a 60-s CS+ presentation concurrent with 11, 92 V electric shocks, the flies' performance represents learning from multiple rounds of what is referred to as "massed" CS/US pairing. On the other hand, in the SHorT paradigm, a 10-s CS+ presentation is coupled to a single 1.25-s, 92-V shock, allowing assessment after a single CS/US pairing [10, 19]. Furthermore, performance in SHorT training improves upon multiple pairings with a 15-min intertrial interval [10, 19]. This allows for a very fine-tuned experimental manipulation to produce equivalent learning in control and experimental animals, a necessary condition to investigate memory stability and retrieval properties.

The results in Fig. 4.8C demonstrate that a single CS/US pairing in *btau-* and *htau*-expressing animals yielded losses in learning scores of the order of nearly 50% relative to controls. As with controls, the performance of tau-expressing animals improved upon multiple CS/US pairings, indicating that the basic neuroplasticity mechanisms were at least operating in the right direction, but three CS/US pairings were necessary for *tau*-expressing animals to perform at the level reached by controls after only two pairings (Fig. 4.8C). This suggests that TAU accumulation causes either an impairment in the learning resulting by each CS/US pairing, or a compromise of memory stability, retrieval, or a combination of the two.

To distinguish between these three possibilities, we trained *c772; UAS-btau* and *c772; UAS-htauwt1* heterozygotes to the same performance level as controls (3 pairings for *tau*-expressing animals and 2 for controls) and measured memory of the association after 30 min. The *tau*-expressing animals exhibited a significant decrease in 30-min memory, despite performing equivalently to controls immediately after training. This indicates that memory retrieval and/or stability were compromised in TAU-expressing animals. This result implicates TAU within mushroom body neurons to mechanisms that are key to memory stability and/or retrieval.

Since our coimmunoprecipitation experiments showed that all TAU tested did bind to MTs we can conclude that the behavioral deficits observed are the effect of burdening MTs with excessive TAU. This is in accord with what one would expect if the MTs were the first (or at least near the "front lines") of intercellular information-manipulation elements.

Integrating Results from *h*-, *b*-, *dtau*-Expressing Animals

Combining the results summarized above and those in [86] we are led to the conclusion that the decrements in learning and memory observed in *btau*- and *htau*-expressing animals were not caused by accumulation of a vertebrate protein, but rather by increasing the level of TAU in these neurons. Low levels of *dtau* transcription did not affect the performance of c492/+; UAS-*dtau1*/+ animals. However, elevation of *dtau* transcription precipitated learning deficits similar to those observed with vertebrate *tau* and *dtau4* transgenics [86]. These results strongly indicate that the associative learning and memory deficits in vertebrate *tau*- and *dtau*-expressing animals are very likely the direct result of elevated TAU accumulation within mushroom body neurons and not because of the conformational differences between vertebrate and *Drosophila* proteins.

Finally, another unlikely scenario that fits the data is that since the native and overexpressed *dtau* genes were in different parts of the genome, some role was played by the directed expression on the conformation of the extra dTAU resulting in a perturbation that made dTAU behave like its b and h analog. One way to rule this out would be to entirely knock out the native TAU gene and replace it with *htau* or *btau*, thus testing whether these will take up the role meant for *dtau* and thus possibly refining the findings reported here and also determining whether the hypothesis behind the “fetal, 4R” TAU versus the “adult 3R” TAU in Alzheimer’s disease is correct.

4.3.7 Conclusions

Collectively, the results of the behavioral analyses suggest that the level of TAU within mushroom body neurons is essential for both olfactory learning elicited by each CS/US and memory retrieval or stability. The areas of significant homology between the vertebrate and *Drosophila* TAU are confined to the tubulin binding sites and the vertebrate protein appears to bind microtubules in a way similar to the way the fly protein does. Taken together, the results strongly suggest that excess TAU binding to the neuronal microtubular cytoskeleton causes mushroom body neuron dysfunction exhibited as learning and memory deficits. This also indicates that although excessive TAU may not result in (immediate or medium-term) neurodegeneration, it is sufficient to cause significant decrements in associative learning and memory that may underlie the cognitive deficits observed early in human tauopathies such as Alzheimer’s.

4.3.8 Discussion

The pretangle state of elevated tau has been the topic of limited study in the past (e.g. loss of TAU in axons and elevation in the somatodendritic compartment of neurons prior to tangle formation shown in humans and

animal models [5, 15] but the possible effect of this state on neuroplasticity and possibly consciousness (if one is willing to make the leap of faith and extend these findings from fly to human), had not been previously explored. Similarly, splicing mutations that increase the level of 4R (fetal) TAU are the hallmark of many human tauopathies [35, 70]. It has been argued that accumulation of unbound TAU and subsequent NFT formation in human tauopathies may be the result of conformational changes [93]. However, the conformational differences between dTAU and its vertebrate homologs did not appear important in affecting learning and memory deficits in our study, at least at the level of resolution we could obtain. In contrast, the overall level of TAU, i.e. the MAP:MT stoichiometry within mushroom body neurons appeared to be of primary importance.

TAU accumulation in mushroom body neurons caused robust associative learning and memory deficits. It is surprising that within the resolution limits of our techniques, the deficits appeared confined to associative learning and memory and not to other experience-dependent olfactory processes. These results suggest that normal cytoskeletal-mediated processes, likely disrupted by excess TAU are necessary for neuroplasticity underlying associative functions. One possible overarching explanation of our findings involves the disruption of axonal transport of vesicles and is explored fully in [86]. An alternative, of interest to us as explorers of the QCI involves the roles for neuronal microtubules and their dynamic interaction with the proper ratio of MAPs in learning and memory discussed in Sect. 4.2 and [142, 143], or as neuronal computational elements proposed in [81]. These data are consistent with specific predictions of these models, including the GSM model that predicts that perturbations in the ratio of microtubule-binding proteins will precipitate learning and memory dysfunction and also with the general approach behind the dipole-dipole logic suggestion where extra TAU would alter the local dielectric constant κ by virtue of its increased density.

In summary, these results strongly suggest that the stoichiometry of TAU and microtubules within neurons is essential for behavioral neuroplasticity. Increasing the level of TAU within neurons precipitates deficits possibly due to inhibition of microtubule-dependent intraneuronal traffic, microtubule stability or interactive capacity. The strong behavioral effects indicate that directed TAU-accumulation within neurons can be used as a tool to disrupt and study neuronal function in general.

4.4 Refractometry, Surface Plasmon Resonance and Dielectric Spectroscopy of Tubulin and Microtubules

4.4.1 Theory of Dielectrics

Dielectric Properties of Polar Molecules

The dipole moment \mathbf{p} is defined as a vector associated with a separation of two identical point charges. Its magnitude is defined as the (positive) charge times the displacement vector between the positive and the negative charge and its direction is from the negative to the positive

$$\mathbf{p} = q \cdot \mathbf{d}, \quad (4.27)$$

where q is the charge (in Coulombs) and \mathbf{d} the displacement vector pointing from $-$ to $+$. Units of “Debyes” are customarily used where $1\text{D} = 3.338 \times 10^{-30}$ Coulomb · meters. For N dipoles, in volume V , we define the total electric polarization vector \mathbf{P} as the total electric dipole moment per unit volume

$$\mathbf{P} = \frac{N\mathbf{p}}{V}. \quad (4.28)$$

The (time-invariant) displacement electric field D in isotropic media is defined as

$$\mathbf{D} = \epsilon \mathbf{E} = \epsilon_0 \mathbf{E} + \mathbf{P}, \quad (4.29)$$

where ϵ_0 and ϵ are the permittivities of free space and sample, respectively, and \mathbf{E} is the external electric field and thus

$$\mathbf{P} = (\kappa - 1)\epsilon_0 \mathbf{E}, \quad (4.30)$$

where we have defined $\kappa = \epsilon/\epsilon_0$ the optical frequency *dielectric constant* of the material, which is related to the refractive index n via

$$\kappa = n^2. \quad (4.31)$$

The dielectric permittivity ϵ of a substance is a measure of its ability to “neutralize” part of a static electric field by responding to it with a displacement of some of its localized charge. This charge displacement is referred to as polarization and is not dependent on a material having excess charge. Even for a static electric field, but most importantly when the incident field is time varying, the dielectric permittivity will also depend on time. Because the capacitance (ability to store charge for a given potential difference) C of a medium is directly proportional to its ϵ (as in the elementary case of the parallel plate capacitor where $C = \epsilon A/d$ with A the area and d the separation of the plates in the limit $d^2 \ll A$), ϵ can be measured by inserting the medium between the plates of a capacitor and noting the ratio of the capacitance with (C) and without (C_0)

the medium so that $\varepsilon = C/C_0$. This general basic principle holds even for a fluctuating field but with certain modifications, as will be illustrated later.

Molecular electric polarizability α is a scalar of proportionality that quantifies the polarization of a sample as a result of application of an electric field that in general can have four components: electronic α_e (sensitive even to high-frequency fields), ionic or atomic α_i (medium frequency), orientational or dipolar α_d (low frequency) and interfacial α_{dc} (very low to dc frequencies). For simplicity, we will assume that α is an isotropic characteristic of a protein solution sample, which is justifiable at low concentrations. The total polarizability as a function of frequency $\alpha(\omega) = \alpha_e(\omega) + \alpha_i(\omega) + \alpha_d(\omega) + \alpha_{dc}(\omega)$ is a good parameter to use when describing a system such as a protein in solution since, unlike the total dipole moment it does not change as a result of solvation, changes in pH, or local electric field (\mathbf{E}_{loc}) amplitude or direction. We define the total dipole moment as the sum of the permanent dipole moment added to the polarizability-dependent dipole moment

$$\mathbf{p} = \mathbf{p}_{perm} + \alpha \mathbf{E}_{loc}. \quad (4.32)$$

It can be shown [49] that a molecule in a spherical cavity surrounded by a medium of volume polarization \mathbf{P} will experience a local electric field

$$\mathbf{E}_{loc} = \mathbf{E} + \mathbf{P}/3\varepsilon_0. \quad (4.33)$$

The above is known as the Lorentz field approximation and is applicable in the case of simple dipolar rotor molecules. Combining (4.28), (4.30), and (4.33) one finds that the average electric dipole moment is

$$\mathbf{p}_{av} = \frac{\alpha}{3\varepsilon_0} \left(\frac{\kappa+2}{\kappa-1} \right) \mathbf{P}, \quad (4.34)$$

where $\kappa = \varepsilon$ = relative dielectric constant, and one arrives at the Clausius–Mossotti relation for electric polarizability

$$\alpha = \left(\frac{\kappa-1}{\kappa+2} \right) \left(\frac{3\varepsilon_0 V}{N} \right) \quad (4.35a)$$

$$\mathbf{P} = \frac{p_N}{V}$$

$$\text{and by extension, } \mathbf{P} = (\kappa-1)\varepsilon_0 \mathbf{E} \quad (4.35b)$$

$$\Rightarrow \mathbf{p} = \frac{V}{N}(\kappa-1)\varepsilon_0 \mathbf{E}.$$

Note that (4.35a) and (4.35b) can give α and \mathbf{p} in terms of macroscopic, measurable parameters such as the dielectric constant κ and volume and number of molecules in the sample, while (4.34) is not easily applicable to an experimental determination of \mathbf{p} as it contains the difficult-to-measure \mathbf{P} . However, (4.35) is not applicable to cases where the local field cannot

be approximated by the simple field assumed by (4.33). These cases include water, where, if the measured permanent dipole moment (6.1×10^{-30} C m) is inserted into the Clausius–Mossotti equation one arrives at a negative value for κ .

Dielectric in a Nonpolar Solvent

Noting that antiparallel orientations between the local field and the dipole moment of a molecule in a sample will have higher interaction energies U (where $U = -\mathbf{p} \cdot \mathbf{E} = -|\mathbf{p}||\mathbf{E}| \cos \theta$) than parallel ones, we can find the contribution of the permanent electric dipole of a molecule to the volume electric dipole moment of a bulk sample as follows: consider an equilibrium situation where the thermal energy $k_B T \gg U$ and we can expand the probability of each dipole's orientation (determined by Boltzmann statistics $\propto \exp^{-U/k_B T}$) keeping only the zeroth and first-order terms. This gives the average dipole moment as

$$\mathbf{p}_{\text{ave}} = |\mathbf{p}|^2 E' / (3k_B T), \quad (4.36)$$

and the volume polarizability ignoring high frequencies can be written as

$$\alpha = \alpha_e + \alpha_i + \alpha_d = \alpha_i + |\mathbf{p}|^2 / (3k_B T), \quad (4.37)$$

so volume polarizability varies inversely with temperature as expected (at lower temperatures it is easier to reorient dipoles as $k_B T$ is closer to $\mathbf{p} \cdot \mathbf{E}$). In the case of a dilute liquid, for instance when a protein is present at low concentration inside a nonpolar buffer, and assuming the properties of the solution are the sum of the properties of the components, we can write the effective molar polarizations of each component in terms of their mole fractions. For instance, by replacing V/N in (4.35a) by V_m the molar volume of the material, we can write the molar polarizability $\alpha_m = 3\varepsilon_0(\frac{\kappa-1}{\kappa+2})V_m$ and also the molar polarization $P_m = \frac{\alpha_m}{3\varepsilon_0} = P_0 + P_p$ where P_0 and P_p are the induced and permanent dipole moments respectively. $P_0 = \alpha_0/3\varepsilon_0$ and $P_p = |\mathbf{p}|^2/(9\varepsilon_0 k_B T)$. In this dilute approximation, the molar polarization

for an N -component solution would be given by $P_m = \sum_i X_i P_{mi}$, where X_i

is the mole fraction of the i -th component and P_{mi} is its polarization. By performing an experiment in a stepwise fashion where all the ingredients are added one at a time (e.g. starting with the buffer base added to a nonpolar solvent) one can determine all the P_{mi} s. In the case of a binary solution with nonpolar solvent (i.e. one with only induced polarization) we can approximate the molar polarization of the solvent P_{m1} as that of the pure solvent and using only the first term of (4.37) arrive at: $P_{m1} = \frac{(\kappa_1-1)M_1}{(\kappa_1+2)\rho_1}$ where M_1 is the mass and ρ_1 the density of the solvent. Thus to determine the solute

molar polarization at each concentration we can use:

$$P_{m2} = P_{m1} + (P_m - P_{m1}) \left(\frac{1}{X_2} \right), \quad (4.38)$$

where P_m stands for the measured “bulk” molar polarization of the binary solution. Note here that according to this simplistic formalism one would expect the result of (4.38) to be independent of concentration since it is supposed to be uniquely determined by the molecular structure. However, it is frequently observed that the polarization increases as the concentration decreases due to significant solvent–solute interactions. As a result, it is customary to report the molar polarization extrapolated to an infinite dilution, i. e. P_{m2} as $\lim(X_2 \rightarrow 0)$ [117]. We address further limitations of this approach below.

Hedestrand’s procedure [42] for determining polarizabilities of solutions is based on the above approach plus assumptions that the dielectric constant and the density of the solution are linear in the solute mole fraction, i. e. in our case $\kappa = \kappa_1 + aX_2$ and $\rho = \rho_1 + bX_2$ where a and b are the derivatives of the dielectric constant and density with respect to mole fraction. Substituting these into (4.38) one obtains:

$$P_{m2} = \left(\frac{3M_1}{(\kappa_1 + 2)^2 \rho_1} \right) a - \left(\frac{(\kappa_1 - 1)M_1}{(\kappa_1 + 2)\rho_1^2} \right) b + \left(\frac{(\kappa_1 - 1)M_2}{(\kappa_1 + 2)\rho_1} \right), \quad (4.39)$$

where M_1 and M_2 are the molar masses of the solvent and solute and ρ_1 is the density of the solvent. It can be seen then that we only need to know the limiting slopes of the κ and ρ versus mole fraction slopes to determine P_{m2} and these we can obtain by measuring a number of solutions of increasing dilution.

Dielectric in Polar Solvent and Generalized Case

When dealing with a protein it is important to realize that modeling it as a dipolar rigid rotator is only justified in very specific cases. In general, proteins have many rigid dipoles, polar substituents such as backbone amides, polar side chains and C-termini. Although constrained to be part of the protein, these have significant freedom and can rotate and translate at low incident field frequencies to give very large dielectric constant to proteins. The generalized Kirkwood–Fröhlich theory gives a way to combine the high-frequency dielectric constant with the complicated dipolar contributions to obtain our desired static or dc dielectric constant of the protein in a polar solution. In this approach the sample of dielectric constant ε is approximated to a collection of permanent rigid dipoles embedded in surroundings of dielectric constant ε_∞ that represents the sample’s high-frequency dielectric constant (which can be easily determined from a measurement of the refractive index). Focusing on a spherical region of volume V , of the order of the

size of a molecule of sample and using classical continuum theory the effective aligning field is calculated (E_{eff}) as a function of the average field in the medium E that results in the following relation [59, 60]:

$$\frac{3V\varepsilon_0(\varepsilon - \varepsilon_\infty)(2\varepsilon + \varepsilon_\infty)}{\varepsilon(\varepsilon_\infty + 2)^2} = \left(\frac{\partial}{\partial E_{\text{eff}}} \langle \mathbf{M} \bullet \hat{\mathbf{E}}_{\text{eff}} \rangle \right)_0, \quad (4.40)$$

where $\mathbf{M} = \sum_i \rho_i$ is the total instantaneous dipole moment of the spherical volume V , the vector sum of the individual dipoles ρ_i , and it is dotted into the unit vector pointing in the direction of $\hat{\mathbf{E}}_{\text{eff}}$. The angled brackets denote the statistical thermodynamic average and the derivative is evaluated at zero field strength. Note that the ρ_i have the magnitude of the dipole moments in a theoretical “gas” phase. A relationship between the thermal fluctuation term can be derived from statistical mechanics and one finally arrives [36] at:

$$\frac{3V\varepsilon_0(\varepsilon - \varepsilon_\infty)(2\varepsilon + \varepsilon_\infty)}{\varepsilon(\varepsilon_\infty + 2)^2} = \frac{\langle (\mathbf{M} \cdot \hat{\mathbf{E}}_{\text{eff}})^2 \rangle_0 - \langle \mathbf{M} \cdot \hat{\mathbf{E}}_{\text{eff}} \rangle_0^2}{k_B T}, \quad (4.41)$$

by including the correction term g [59] in the right-hand side of the Kirkwood–Frölich theory $N g \frac{p^2}{3k_B T}$ (N is the number density of dipole molecules, \mathbf{p} as before is b the “gas” phase moment of one molecule) one can account for the correlation between dipoles. If $g = 1$ moments are entirely free from interaction with each other. For $g > (<) 1$ we have positive (negative) correlation, both physical in the case of polar liquids. So g is, in a sense, the ratio of actual fluctuations to theoretical “gas” uncorrelated fluctuations and it has been shown [36] to be $g = \sum_{j=1}^{n_d} \langle \cos \theta_{ij} \rangle_0$, where θ_{ij} is the angle between dipoles \mathbf{p}_i and \mathbf{p}_j and n_d is the number of dipoles in the sample. Gilson and Honig [36] generalized this to the case of proteins in polar or nonpolar environments and *constrained* dipoles arriving at:

$$g' = \frac{\langle (\mathbf{M} \cdot \hat{\mathbf{E}}_{\text{eff}})^2 \rangle_0 - \langle \mathbf{M} \cdot \hat{\mathbf{E}}_{\text{eff}} \rangle_0^2}{\sum_{i=1}^{n_d} \left[\langle (\mathbf{p}_i \cdot \hat{\mathbf{E}}_{\text{eff}})^2 \rangle_0 - \langle \mathbf{p}_i \cdot \hat{\mathbf{E}}_{\text{eff}} \rangle_0^2 \right]}, \quad (4.42)$$

and also introduced a constraint factor C that accounts for the reduction of the freedom of individual dipoles

$$C = \frac{n_d p^2}{3 \sum_{i=1}^{n_d} \left[\langle (\mathbf{p}_i \cdot \hat{\mathbf{E}}_{\text{eff}})^2 \rangle_0 - \langle \mathbf{p}_i \cdot \hat{\mathbf{E}}_{\text{eff}} \rangle_0^2 \right]}. \quad (4.43)$$

So, finally we have that:

$$\frac{3V\varepsilon_0(\varepsilon - \varepsilon_\infty)(2\varepsilon + \varepsilon_\infty)}{\varepsilon(\varepsilon_\infty + 2)^2} = \frac{g'}{C}N\frac{p^2}{3k_BT}. \quad (4.44)$$

As seen above, by measuring the dielectric constant of a tubulin solution at various concentrations (and incident frequencies) one can experimentally deduce the dipole moment of the free tubulin dimer. This is not straightforward since even though an ideal dielectric contains no free charge, parts of its constituent units (individual molecules, polymer filaments, etc.) can suffer a localized separation of charge as a result of application of an external electric field. By using a solution with above-critical concentration it is also possible to monitor the changes in the dipole moment as tubulin dimers polymerize into MTs. At high frequencies where only α_e will contribute, one can use the Clausius–Mossotti equation with the substitution $\kappa = n^2$ and by measuring the refractive index of the solution arrive at the value of $|\mathbf{p}_{\text{ave}}|$.

4.4.2 Optics

The two basic laws of optics are the law of reflection: $\theta_i = \theta_r$ (the angle of incidence is equal to the angle of reflection) and the law of refraction, also known as Snell's law: $n_1 \sin \theta_1 = n_2 \sin \theta_2$ where n_i refers to the refractive index of medium i and θ_i is the angle between the normal and the incident and refracted beams see Fig. 4.9. Both these laws refer to specular processes (i.e. the boundary between the media can be assumed smooth) and can be derived from Maxwell's equations for electromagnetic waves incident on a boundary [49].

Using Snell's law for $n_2 > n_1$ in Fig. 4.9b above, it can be easily shown that there will be a critical angle $\theta_c = \sin^{-1}(n_1/n_2)$ for a beam incident from n_2 such that the emergent beam will make an angle of $\theta_1 = 90^\circ$ and will be just grazing the surface. By exceeding this critical angle the beam is reflected back into the material (total internal reflection) and this is of importance

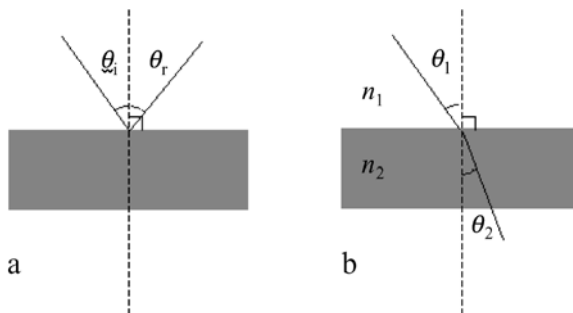


Fig. 4.9. Laws of optics. (a) Law of reflection (b) Snell's law

in many applications including light guidance by optical fibers, sensing by surface plasmon resonance and refractometry. Note also that the refractive index is a slow function of temperature: $n_{T=25^\circ\text{C}} = n_T - (25.0 - T)(0.00045)$.

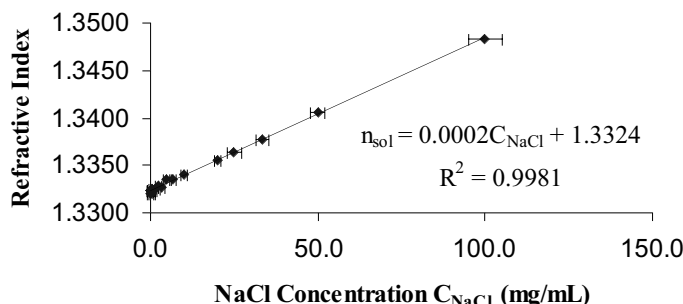
Refractometry

The easiest way to measure n would be to pass a laser beam at some angle (other than the normal) through a sample of known thickness and measure the beam's deviation from the original path. This presents obvious problems with liquid sample containment, etc., so practical refractometers are instead based on the phenomenon of total internal reflection and utilize high-quality prisms that can be tilted to compensate for wavelength-dependent dispersion and thus ordinary sunlight or white light can be used as the source. The machine used for these experiments [Abbe refractometer, Vista C10] was of exceptional accuracy and particularly elegant design requiring no electrical power. Briefly, light was allowed to enter and be reflected into a prism that was coated with the material of interest and covered. The prism's refractive index was known and the beam's incident angle was tilted until total internal reflection was reached (seen as a dark band in the eyepiece). The refractive index of the sample was then read on a precalibrated scale. This method depends on the prism having a higher refractive index than the material. Our machine was capable of measuring refractive indices between 1.3000 and 1.7000. After standard calibration and prior to measurement of tubulin solutions a number of different NaCl solutions of varying concentration were used as additional calibration. Determining the exact concentration was the main source of error in this measurement so high-precision electronic scales and precision micropipettes were used. The prism was cleaned after each measurement with ethanol soaked cotton and left to dry before applying the next sample. It was found that 30 to 50 μL of solution were adequate to deposit a thin film on the prism such that there was virtually no noise (indicated as colors). This small volume is comparable to the requirements of the sophisticated BIAcore 3000 SPR machine for a single injection.

The refractive index of a series of concentrations of NaCl (in 18.1 $\text{M}\Omega/\text{cm H}_2\text{O}$) and tubulin in buffer (0.1 M 4-Morpholinoethane sulphonic acid (MES), 1 mM EGTA, 0.1 mM EDTA, 0.5 mM MgCl₂, 1 mM GTP at pH 6.4) was measured. Three measurements were taken for each data point and the average is shown in Table 4.1. Errors are estimated at $\sim 5\%$ for concentration (shown). The refractometer was scale limited with an error of 0.00005 for n (not shown, represented as the size of the data points. In Figs. 4.10 and 4.11 a least-squares fit linear regression yields straight lines with R factors 0.9981 and 0.9928, respectively. The intercepts were manually set to the zero-point concentration averages. A limited second set of data points was taken ($n_{\text{tub}2}$) at several times after the first but as it was practically impossible to keep the timing consistent it is only shown here for qualitative purposes. The results at dif-

Table 4.1. Refractometry data

NaCl (mg/mL)	n_{NaCl}	Tub (mg/mL)	n_{tub1}	n_{tub2}	time (min)
0.000	1.3324	0.00	1.3352	1.3352	40
0.084	1.3321	0.00	1.3351	1.3353	51
0.167	1.3324	3.55	1.3415		
0.208	1.3324	2.37	1.3386	1.3380	15
0.333	1.3325	1.18	1.3370	1.3371	17
0.416	1.3321	0.789	1.3364	1.3364	25
0.833	1.3323	0.592	1.3357	1.3360	25
1.67	1.3325	7.10	1.3478	1.3489	29
2.50	1.3329	7.10	1.3482		7
3.33	1.3327	0.592	1.3357	1.3360	42
5.00	1.3335	1.183	1.3372	1.3370	45
6.67	1.3335	2.37	1.3390	1.3390	47
10.0	1.3341	0.473	1.3358	1.3358	55
20.0	1.3356				
25.0	1.3364				
33.3	1.3377				
50.0	1.3406				
100.	1.3484				

NaCl conc. VS Refractive Index**Fig. 4.10.** NaCl concentration vs refractive index. (Taken from [87].) Note the low value of the slope (compared to tubulin)

ferent times did not deviate appreciably, suggesting that at this wavelength range tubulin dimers and microtubules have similar refractive indices.

Note how a very small change in concentration of tubulin results in a large jump in the index of refraction (Fig. 4.11) giving a slope of $\Delta n / \Delta C = 1.800 \pm 0.090 \times 10^{-3}$ (strongly corroborated by the SPR measurement of the same value that gave $1.80 \pm 0.20 \times 10^{-3}$). Compare this to $\Delta n / \Delta C \sim 0.0002$ for the NaCl solution.

Tubulin conc. VS Refractive Index

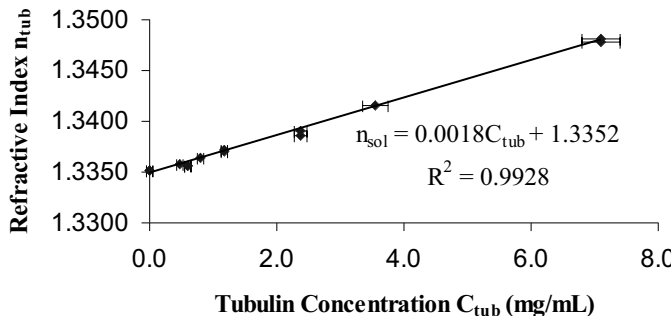


Fig. 4.11. Tubulin concentration vs refractive index. (Taken from [87])

A physiological concentration is assumed at $15.0 \mu\text{M}$ (i.e. $1.50 \times 10^{-5} \text{ mol/L}$) [137]. Since the molecular weight of a tubulin dimer is 110 kD this gives a proportionality of $1.00 \text{ mg/mL} \sim 9.10 \mu\text{M}$ so $15.0 \mu\text{M}$ is equivalent to 1.60 mg/mL and this gives a molecular density of $N = 9.03 \times 10^{18}$ tubulin molecules per liter or 9.03×10^{21} per m^3 . Note that the concentration necessarily varies across cell types, intracellular position and cell condition. For instance, although a TAU-burdened cell may have unchanged overall tubulin density, it has much higher local axonal and dendritic density of tubulin when MTs have deteriorated into neurofibrillary tangles.

The partial contribution to the refractive index of the solution by tubulin can be found if the density dependence on concentration of the solution is known (see Fig. 4.11). Assuming that the contributions from the various components are linearly additive, we have for the total index of refraction of the solution $n_{\text{sol}} = \sum_i C_i n_i$ where C_i and n_i are the fractional concentration of the i -th component with refractive index n_i and i runs over all components. Lumping the contribution from all the buffer components we can write

$$n_{\text{sol}} = (1 - \chi_{\text{tub}})n_{\text{buffer}} + \chi_{\text{tub}}n_{\text{tub}} \Rightarrow n_{\text{tub}} = \frac{n_{\text{sol}} - (1 - \chi_{\text{tub}})n_{\text{buffer}}}{\chi_{\text{tub}}}, \quad (4.45)$$

where $\chi_{\text{tub}} = C_{\text{tub}}/\rho$ the mass fraction and ρ is the density of the solution. It could be argued that using a volume fraction is more appropriate here but for our purposes a mass fraction is adequate and simpler. At $C_{\text{tub}} = 1.60 \text{ mg/mL}$, $n_{\text{sol}} = 1.8000 \times 10^{-3}C_{\text{tub}} + 1.3352$ (from Fig. 4.11) gives $n_{\text{sol}} = 1.34 \pm 0.07$ and using the measured value for the solution density ρ at $C_{\text{tub}} = 1.60 \text{ mg/mL}$ we arrive at the value for n_{tub}

$$n_{\text{tub}} = 2.90 \pm 0.10, \quad (4.46)$$

which can be used in

$$\kappa = n^2 \quad (4.47)$$

to give the high-frequency tubulin dielectric constant

$$\kappa = 8.41 \pm 0.20. \quad (4.48)$$

A thorough search of the literature suggests that this is likely the first time these two quantities have been experimentally determined for tubulin.

Both n and κ are at the very top of the range of what is usually assumed for proteins, as expected since tubulin seems to have such a high dipole moment in molecular dynamics simulations.

The refractive index n of an optically dense material is related to the high-frequency polarizability α via:

$$n^2 = 1 + \frac{N\alpha}{\varepsilon_0} \frac{1}{\left(1 - \frac{n\alpha}{3\varepsilon_0}\right)}, \quad (4.49)$$

where N is the molecular concentration, which for our chosen concentration is 9.03×10^{21} molecules/m³. Solving the above equation for α gives

$$\alpha = \frac{\varepsilon_0}{N} \frac{3(n^2 - 1)}{(n^2 + 2)}, \quad (4.50)$$

and therefore the high-frequency tubulin polarizability is

$$\alpha = 2.1 \pm 0.1 \times 10^{-33} \text{ C m}^2/\text{V}. \quad (4.51)$$

A very large number owing to the evidently large dipole moment of tubulin. Note that the generally accepted value of the density of proteins is 1.45 g/mL [109].

4.4.3 Surface Plasmon Resonance (SPR)

SPR basics

The technique of surface plasmon resonance (SPR) [64, 110] allows measurement of changes in the optical properties of a medium adjacent to a thin metal film. Practical applications of the SPR method include chemical sensors [78, 136] and biosensors [32]. Specifically, the SPR technique is by now a well-established method for the analysis of interactions among biomolecules [13]. SPR curves (sensograms) can be measured either by varying the angle or the wavelength of the incident light [56, 84, 132]. Here, we discuss our application of the SPR technique to measurement of the dielectric properties of the bovine cytoskeletal protein tubulin. A surface plasmon (SP) is an electromagnetic wave that can propagate along the surface of a dielectric-metal interface [110]. Surface plasmons can be excited by shining light on a layered

system consisting of a transparent medium on one side, a metal film (most often gold or silver) and a dielectric on the other. When the light is incident at an angle greater than the critical angle of total internal reflection, an evanescent wave is produced and penetrates into the adjacent medium to a depth of the order of one wavelength. The maximum coupling between the evanescent wave and the surface plasmon takes place when their phase velocities coincide, at which point the surface plasmon is excited at resonance. Thus, the surface plasmon resonance (SPR) occurs at a characteristic angle of incidence. This angle depends on the thickness as well as the dielectric permittivities of the layers of the adjacent media. Since the effective permittivities depend on the frequency of the exciting laser light, the resonance angle does too. The most convenient geometry for the development of a sensor is the Kretschmann–Raether configuration that consists of a glass prism, a metal film and the adjacent medium that is to be probed [74, 122].

The SPR Sensor

Fig. 4.12 shows the experimental arrangement of our custom-built SPR sensor [74, 87, 122]. In addition to the experimental arrangement shown, we used the commercial SPR-based BIAcore 3000 and 1000 sensors, which furnished the additional convenience of automated injection of very small volumes of analyte solutions and allowed for crosschecking of results.

Optics and Data Acquisition

A helium-neon laser provided the incident illumination at 633 nm (or 760 nm in the BIAcore). A p-polarized light beam convergent in an angular interval was produced with an arrangement of lenses and a polarizer. A prism provided the coupling of the laser beam to the SPs that were excited in the gold film, and a multiple-channel custom-built (see below) flow cell allowed solution access to the gold film. The angular distribution of the reflected light was measured with a photodiode array and its electrical output was read with a data acquisition (DAQ) board and transferred to a PC using software developed in-house by the author. The readout rate of the DAQ board set the time resolution to 67 ms. The spatial resolution was determined by the dimensions of the laser beam spot at the surface: 0.5 mm × 0.3 mm. The angular resolution for the configuration used was ~ 1 resonant unit (RU); this angular unit, commonly used in SPR measurements, corresponds to 10^{-4} degrees. The change of the SPR angle by this quantity occurred when the change of the refractive index was only approximately 10^{-6} [21].

Fluidic Cell

One of the serious challenges in an SPR measurement is the management and routing of the samples. In commercial devices, such as the BIAcore 3000,

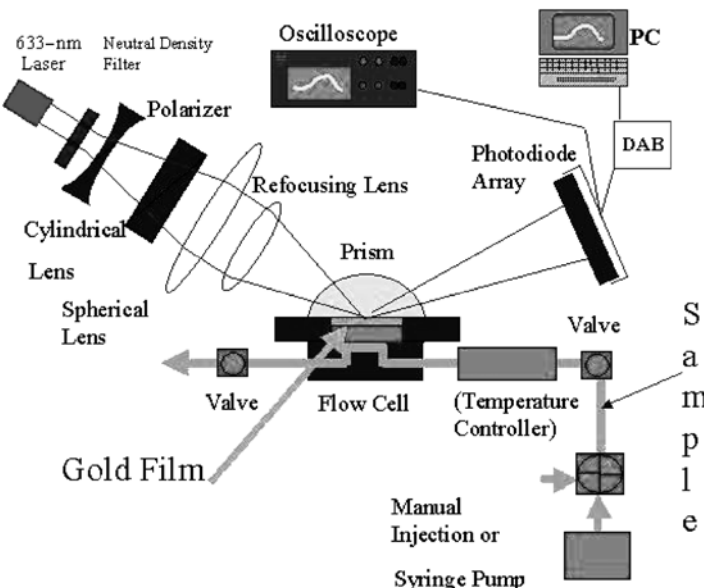


Fig. 4.12. Experimental setup of the SPR sensor. Sample flow is indicated with light blue. The prism provides the coupling of the excitation light to the surface plasmon. The polarizer is used to produce the p-polarized light, since only this component interacts with the surface plasmon. The angular distribution of the reflected light intensity is detected by the photodiode array that can be replaced by just two photodiodes with differential lockin detection. The sample medium is injected into a small flow cell adjacent to the gold film. The fluidic cell presented a serious challenge and is described separately below

proprietary microfluidic technology based on a lithography casting method is used and injections require robot-arm handling and sophisticated electronics, raising the cost of the device to several hundred thousand dollars. Previous methods used for in-house SPR measurements used hand-cut rubber and micromachined Plexiglas cells and manual injection using microsyringes. In both rubber and Plexiglas cell designs, significant errors were introduced as a result of misalignment of the various cell parts, evaporation of sample and presence of air bubbles. In our custom-built apparatus, to bring a series of 30–100 µL sample injections into close contact with a vertical gold film, avoiding air bubbles and mixing of samples, a casting technique was developed as follows. Using AutoCAD software, channels of precise dimensions (3 mm × 0.5 mm and 3 mm × 0.3 mm) were laser printed on thin plastic sheets (overhead transparencies). Those were then cut by hand under a dissecting stereoscope and pushed against modeling clay. The clay was pliable enough to follow the contours imposed by the plastic sheet positive and after oven curing became the negative mold. Poly-di-methyl-siliconate (PDMS) was used as the material for a fluidic cell. PDMS was found to be ideal for this application because it

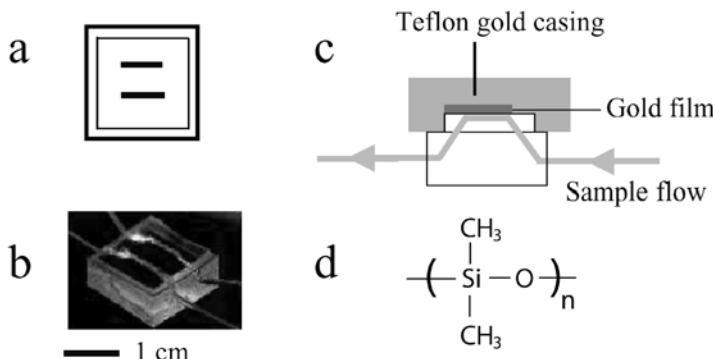


Fig. 4.13. PDMS fluidic cell. (a) Top view (b) photograph of a two-channel cell (c) side view (d) PDMS chemical composition formula. The parenthesis is repeated n times (polymer)

is biologically inert and virtually indestructible. Unfortunately, the material is nonmachinable as holes drilled tend to self-seal but this was eventually advantageous for our purposes facilitating channel/syringe interfaces. None of the chemicals tried (ethanols, xylenes, acetone, hydrochloric acid) left any trace of abrasion, and freezing in liquid nitrogen and heating with an acetylene torch produced no effect. The material is transparent and we also found that this polymer is nonhomogeneous in its fluorescence properties. Seemingly random parts of a large piece of PDMS would fluoresce strongly when exposed to UV laser illumination, while others would be entirely transparent. This may be the result of domains of specially oriented polymer strands in the bulk of the material and would be interesting to investigate in a separate project. Stainless steel tubes (outer diameter 0.002 in, inner 0.001 in) were used to interface with the channels and provided a way to inject and clear sample (see Fig. 4.13). The mold and PDMS were degassed in a low-vacuum (200 mTorr) custom-built chamber and left to dry for 24 h. The elasticity of the final product was of importance as if too elastic it would deform under pressure during sample injection and if too stiff it would not form the close contact needed to avoid evaporation. Elasticity was controlled by addition of curing and viscosity agents (Sylgard 186/184 and D.C. 200, respectively) and finding the optimum ratio. The technique described above allowed us to comfortably have up to four independently addressable channels, while previously only one or at most two were possible. The limiting factor for the number of channels is the accuracy of the human hand in cutting the positives under a stereoscope. Delegating this task to a metal-deposition circuit board machine such as the T-Tech 700 would make it possible to obtain up to 8 channels before encountering problems with self-sealing.

Theoretical Model

To obtain quantitative data, we use a five-layer model that is based on Maxwell's equations describing reflection of light from a layered system. This enabled us to calculate SPR curves, estimate SPR response from protein immobilization and estimate changes in dielectric permittivity. We consider a structure with five layers: layer 1 consists of a prism with dielectric permittivity $\varepsilon_1 = 2.30$, layer 2 consists of a gold film of thickness $d_2 = 47\text{ nm}$ with complex permittivity $\varepsilon_2 = -13.2 + i1.25$, layer 3 consists of a dextran layer filled with high relaxation (HR) solution of thickness $d_3 = 140\text{ nm}$ [128] and $\varepsilon_3 = 1.78$ in the case of the sarcomeres, and with buffer in the case of tubulin, layer 4 consists of our sample medium (tubulin) with thickness d_4 and layer 5 consists of only solution. The fifth layer is assumed to be semi-infinite with respect to surface plasmon penetration depth. One can obtain the intensity reflection coefficient R for this system with the following recursive formula [14] by calculating each input impedance $Z_{\text{in},m}$ and each layer impedance Z_m .

$$R = \left| \frac{Z_{\text{in},2} - Z_1}{Z_{\text{in},2} + Z_1} \right|^2. \quad (4.52)$$

The input impedance at layer m ($Z_{\text{in},m}$) and layer impedance (Z_m) are obtained from,

$$Z_{\text{in},m} = Z_m \left| \frac{Z_{\text{in},m+1} - iZ_m \tan(k_{z,m} d_m)}{Z_m - iZ_{\text{in},m+1} \tan(k_{z,m} d_m)} \right|, \quad m = 2, 3, 4, \quad (4.53)$$

where,

$$\begin{aligned} Z_{\text{in},5} &= Z_5, Z_m = \frac{k_{z,m}}{\varepsilon_m k_0}, k_{z,m} \\ &= \sqrt{\varepsilon_m k_0^2 - k^2}, \quad k = k_0 \sqrt{\varepsilon_1} \sin(\theta), \quad k_0 = \frac{2\pi}{\lambda}. \end{aligned} \quad (4.54)$$

The wavelength of the laser in vacuum is λ . The incidence angle θ of light onto the prism/gold interface determines the component of the wave vector k that is parallel to the interface. A change in dielectric permittivity of sarcomeres or tubulin solution (ε_4) will alter the reflection coefficient R . Once the change in the SPR angle $\Delta\theta_{\text{SPR}}$ for different media is experimentally determined, the corresponding change in the dielectric constant ($\Delta\varepsilon_4$) can be calculated from (4.2) and (4.3) and the change in the refractive index n inferred from $\varepsilon = n^2$.

The decrease of the SPR sensitivity to changes in the dielectric permittivity with depth z starting from the boundary between 3rd and 4th layers into the protein sample was calculated. This decrease can be approximated as $\sim e^{-(z/d_p)}$ and the characteristic penetration depth d_p can be calculated to be 110 nm [14]. For BIAcore, and $\lambda = 760\text{ nm}$, $d_p \geq 110\text{ nm}$ and therefore we do not expect to see saturation of the signal due to sensitivity degradation.

This can also be seen if one considers that each free tubulin dimer occupies one binding site on the dextran surface, thus saturation is achieved when the total mass of immobilized protein reaches that of a monomolecular layer (with thickness of ≤ 10 nm).

Tubulin and Immobilization

Following established protocols [18], tubulin was purified from bovine cerebra (provided by R.F. Luduena). Our SPR measurements took place at 24°C and the time between injection and measurement was of the order of 10 s. Measurements were taken for times up to 5 min. Tubulin does not polymerize at 0°C and although 10 s is adequate time for our sample of 50 μ L to reach room temperature and start polymerizing, we are confident that in our measurements mainly free tubulin dimers were present and not MTs since (using spectrophotometry and monitoring the absorption curve) we had previously determined that the characteristic time for our tubulin to polymerize into MTs was of the order of 45 min at room temperature (data not shown) agreeing with the literature [73].

Gold film chips (CM5) coated with carboxymethylated dextran were obtained from BIACore (BIACore AB, Sweden). Using standard chemical activation/deactivation protocols [75], we introduced N-hydroxysuccinimide esters into the surface matrix of the chip by modifying the carboxymethyl groups with a mixture of N-hydroxysuccinimide (NHS) and N-ethyl-N'-(dimethylaminopropyl)-carbodiimide (EDC). These esters then form covalent bonds with the amine groups present in the ligand molecules, thus immobilizing them on the surface. Effective immobilization requires that the pH be lower than the isoelectric point of the protein; however, lowering pH below 4.9 eliminates tubulin function and was avoided. The temperature controller raised and maintained the temperature of the inflow at 26°C.

Surface Plasmon Resonance Results

In this setup, a 1 ng/mm² surface immobilization yields a signal of 1 kRU and the laser spot size on the gold chip is 1.2 mm². As shown in Fig. 4.14, after tubulin immobilization and application of a high flow rate (20 nL/min) of running buffer to wash away any weakly bound protein, the average response was ~ 4 kRU, which means 4.8 ng of protein (i.e. 2.6×10^{10} individual tubulin dimers) were captured by the dextran. A reference cell on the same chip without any immobilized tubulin was used as control and any nonimmobilization relevant signals (such as due to refractive index changes) were automatically subtracted.

As discussed earlier, electron crystallography measurements on zinc-induced tubulin protofilament sheets have shown that the tubulin heterodimer has dimensions $46 \times 80 \times 65$ Å [16, 97, 98] so the footprint of the

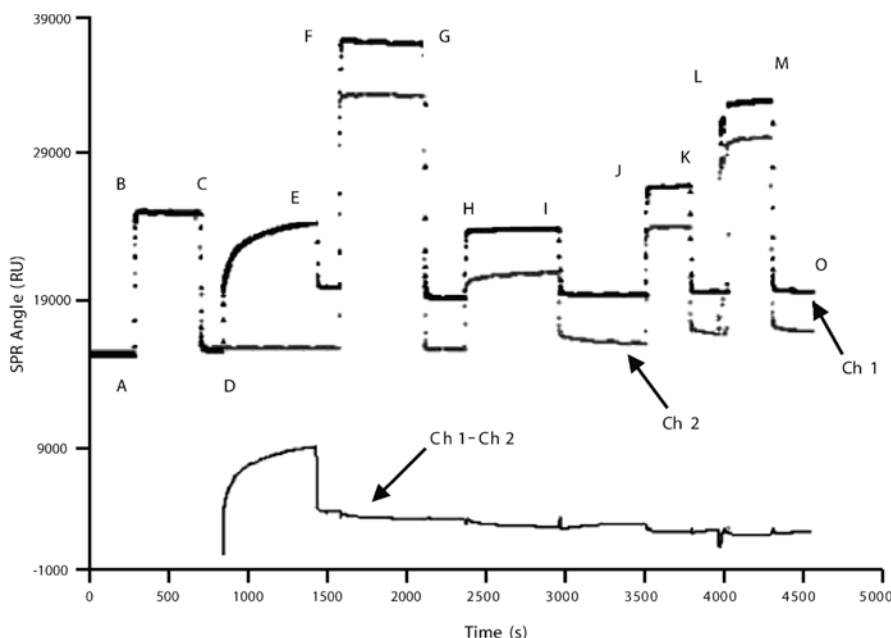


Fig. 4.14. Tubulin sensogram on BIAcore3000 (taken from [122]). Tubulin was immobilized on Channel 1. Channel 2 was treated identically to Channel 1 but had no tubulin. Ch. 1–Ch. 2 shows tubulin signal–background. A→B: running buffer. B→C: EDC/NHS dextran-activating complex injected, note identical response of both channels. C→D: running buffer. D→E: Ch. 1 shows tubulin immobilization with a clear tendency towards saturation, Ch. 2 remains at running buffer baseline level. E→F: high flow rate running buffer. Difference between Ch. 1. and Ch. 2 shows amount of immobilized tubulin ~4000 RU. F→G: ethanolamine blocking (dextran-deactivation). G→H: running buffer. H→I: 0.51 mg/ml tubulin in Ch. 1. Since both channels exhibit same signal, all signal is due to refractive index change, not tubulin–tubulin binding (there is slight nonspecific binding to Ch. 2). I→J: running buffer. J→K: 1.70 mg/ml tubulin in Ch. 1, all signal is due to refractive index change. K→L: running buffer, L→M: 5.1 mg/ml tubulin in Ch. 1, all signal is due to refractive index change. Slight noise in the forms of bumps in Ch. 1–Ch. 2 is due to 0.5 s delay between measurement of Ch. 1 and Ch. 2 and subsequent subtraction. Bump at around 4000 s is due to the temporary presence of a bubble in the 5.1 mg/ml tubulin sample

molecule on the surface can be between 30 nm^2 minimum and 52 nm^2 maximum depending on orientation. Using the average of these two values, it can be seen that a monomolecular layer covering the 1.2 mm^2 spot would require 3.0×10^{10} individual tubulin molecules, leading us to believe that we have achieved 87% coverage, an observation corroborated by the immobilization part of the sensogram where a tendency towards saturation can be clearly seen (Fig. 4.14 D→E).

In vitro polymerization happens spontaneously at room temperature (also at 37°C, only faster) if the protein concentration is above critical and the buffer contains adequate GTP. The critical concentration varies for different tubulin preparations. By using spectrophotometry, we determined that our tubulin started polymerizing at room temperature when the concentration exceeded 1.0 mg/ml (data not shown). In order to determine the dielectric constant of tubulin we first had to be sure that the shift in SPR angle was due to the change in the refractive index of the solution floating over the gold chip and not due to further immobilization of protein or perhaps tubulin–tubulin binding (polymerization).

To address the first concern, we performed the experiment in parallel, utilizing a reference channel on the same chip but without any tubulin in it. The reference signal was automatically subtracted from the tubulin signal thus also addressing concerns related to nonspecific binding to deactivated dextran. To eliminate the possibility that our signal was due to further tubulin–tubulin interactions on the surface (polymerization) we tried both below-critical (0.51 mg/ml) and above-critical (1.7 mg/ml and 5.1 mg/ml) concentrations and saw a return to baseline in all cases showing that in this environment tubulin was incapable of polymerization, a fact that may be due to dextran binding and/or insufficient nucleation sites. Using the sensogram of Fig. 4.14 we calculated the changes of the refractive index and dielectric constant with tubulin concentration:

$$\frac{\Delta n}{\Delta c} = (1.85 \pm 0.20) \times 10^{-3} \text{ (mg/mL)}^{-1} \Rightarrow \frac{\Delta \varepsilon}{\Delta c} = (5.0 \pm 0.5) \times 10^{-3} \text{ (mg/mL)}^{-1}, \quad (4.55)$$

where Δn and Δc are the changes in the refractive index n and dielectric constant ε ; Δc is the change in concentration c .

Since saturation occurs at only ~ 4 kRU (nearly a monomolecular layer of tubulin), our assertion that we are dealing with free tubulin dimers is supported as each dimer must occupy one dextran binding site and there is no tubulin–tubulin binding or aggregation/polymerization into MTs.

As the dielectric constant and refractive index of a solution are intimately connected to the polarizability and consequently to the dipole moment of its constituents, these measurements show that SPR can be used to further elucidate the dielectric properties of “live” proteins in solution.

Refractometry–SPR Comparison

Both refractometry and SPR, two methods based on the same underlying physical principles yet very far apart in implementation, gave a $\Delta n/\Delta c$ of 1.8×10^{-3} , a strong indication that these methods are consistent, our apparatus is properly calibrated and our analysis is correct. In summary, refractometry and SPR gave consistent results for the dielectric constant and polarizability of tubulin. These methods alone cannot provide the permanent

dipole moment of the molecule since they address only the high-frequency region where the permanent dipole is “frozen out”.

4.4.4 Dielectric Spectroscopy

Earlier, we described obtaining the dielectric constant of tubulin at high frequencies. In order to probe lower frequencies we performed dielectric spectroscopy experiments.

Simplified Case

To illustrate the main principles behind the method used, consider the simplest way to measure the low-frequency dielectric constant of a solution: a capacitor-resistor (RC) circuit. The capacitance C of a flow cell with conducting parallel-plate walls can be measured first filled with air and then filled with the tubulin-buffer solution for various tubulin concentrations. R_1 is assumed to be infinite in the case of air and some finite but very large value (of the order of $10\text{ M}\Omega$) in the case of solution. R_2 is set to a known value (e.g. $5\text{ k}\Omega$) and is needed to overwhelm any small conductance due to the presence of liquid between the plates. This ensures that the equivalent resistance in the circuit is nearly identical for all measurements. The inductance-resistance-capacitance (LRC) bridge performs the measurement at several low to medium frequencies (e.g. 1 Hz to 32 MHz) by measuring the RC time constant and displaying the total equivalent resistance and capacitance for the circuit. The ratio C'/C for the tubulin/air capacitances then gives κ and from (4.9) the dipole moment can be inferred. Unfortunately, a simple RC circuit with low inductance connected to a bridge such as the one described above and shown in Fig. 4.15 is not ideal for our case because aqueous solutions containing molecules with large dipole moments tend to

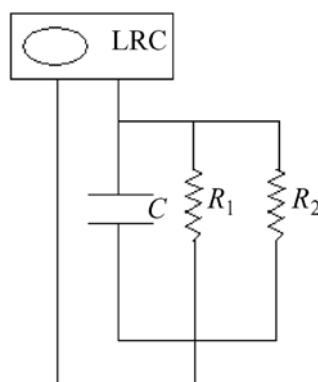


Fig. 4.15. LRC Bridge

form double layers at the electrodes giving extremely high values for κ at low frequencies (the polarization effect). A further complication arises from the requirement that the sample volumes be as small as possible as purified proteins and especially tubulin are expensive.

Capacitor and Impedance Analyzer

We performed a dielectric spectroscopy measurement on liquid samples contained in a custom-made holder. A commercial impedance analyzer (Solartron 1260 from Solatron Inc.) was used that sampled the real and imaginary parts of the impedance from 1 Hz to 32 MHz. The device was calibrated with polar and nonpolar molecules such as water, benzene and ethanol. By employing the distance-variation polarization-removal technique it was possible to extract dielectric information in the lower limit of the frequency range even though individual scans were swamped by the electrode polarization effects below about 10 kHz. The experimental setup is shown in Fig. 4.16. Note that the sample holder had a guard ring to reduce fringe-field effects and allow use of a simple parallel-plate capacitor theoretical model.

The impedance analyzer provides a sinusoidal voltage to the capacitor. As a result, alternating current I exists in the sample and produces a voltage drop V where $V = IZ$. Giving the impedance Z as

$$Z = \frac{V}{I}. \quad (4.56)$$



Fig. 4.16. Capacitor cell. The capacitor had stainless steel plates 20 mm diameter, with a precision digital micrometer controlling the plate separation (to 3 μm precision), and a Teflon sample holder. Sample volume was $\sim 1 \text{ mL}$

The ratio of the output of channel 1 (Hi) to that of channel 2 (Lo) is recorded as a function of frequency. The real and imaginary parts of the ratio were stored separately for additional processing. The main source of error in measuring biological impedances is due to electrode polarization. This effect becomes very strong when measurements are carried out at low frequencies. We minimized this effect as follows. The measured impedance Z^0 is the sum of the sample impedance and the polarization impedance Z^P . We took two measurements of each sample at slightly different plate separations yielding Z_1^0 and Z_2^0 where

$$\begin{aligned} Z_1^S + Z^P &= Z_1^0 \\ Z_2^S + Z^P &= Z_2^0. \end{aligned} \quad (4.57)$$

Assuming the polarization effect to be the same in both cases (justifiable for similar separations), subtracting the two measurements gives

$$Z_1^S - Z_2^S = Z_1^0 - Z_2^0. \quad (4.58)$$

Our parallel plate capacitor had capacitance $C = \frac{\varepsilon A}{d}$, where ε is the dielectric permittivity of the suspension and A is the plate area and d is the electrode separation and since the capacitor impedance is given by $Z = \frac{1}{Y} = \frac{1}{G - i\omega C}$, where G is the conductance and Y is the admittance so that $G = \frac{1}{R} = \frac{\sigma A}{d}$. From (4.58) we obtain

$$Z_1^0 - Z_2^0 = \frac{d_1 - d_2}{(\sigma + i\omega\varepsilon)A}, \quad (4.59)$$

leading to the two dispersion curves:

$$\sigma(\omega) = \text{Re}(Z_1^0 - Z_2^0) = \text{Re} \frac{d_1 - d_2}{A(Z_1 - Z_2)}, \quad (4.60)$$

$$\varepsilon(\omega) = \text{Im}(Z_1^0 - Z_2^0) = \text{Im} \frac{d_1 - d_2}{\omega A(Z_1 - Z_2)}, \quad (4.61)$$

where $\sigma(\omega)$ and $\varepsilon(\omega)$ are the frequency-dependent conductivity and permittivity of the sample, respectively. It is thus seen that by obtaining the imaginary part of the transfer function, one can deduce $\varepsilon(\omega)$.

Calibration and Errors

Several substances including polar and nonpolar molecules were used for calibration, as shown in Figs. 4.18 and 4.19.

Polar materials show a high polarization effect at frequencies higher than 10 kHz, while gases and nonpolar liquids such as benzene do not show this error. We measured the dielectric constant of a holder filled with plain air to corroborate that the obtained geometric capacitance has a κ of 1 as shown in Fig. 4.19.

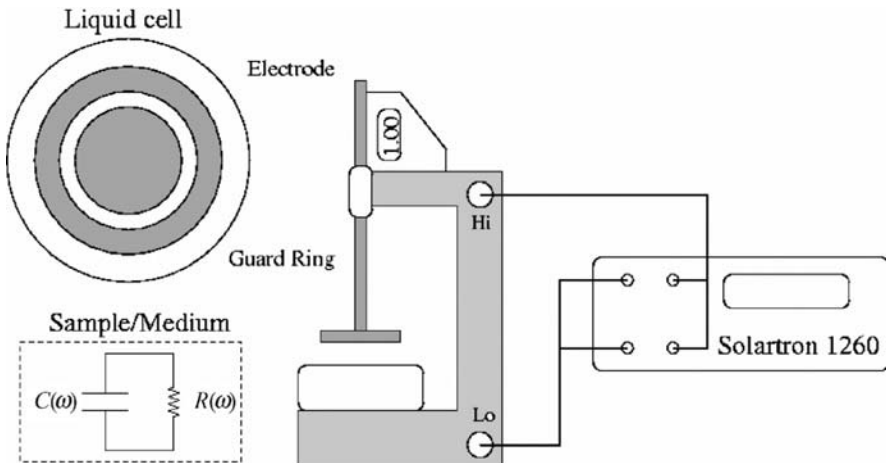


Fig. 4.17. Experimental setup. Solartron dielectric interface was connected to the impedance analyzer. Sample holder had a guard ring to reduce fringe-field effects

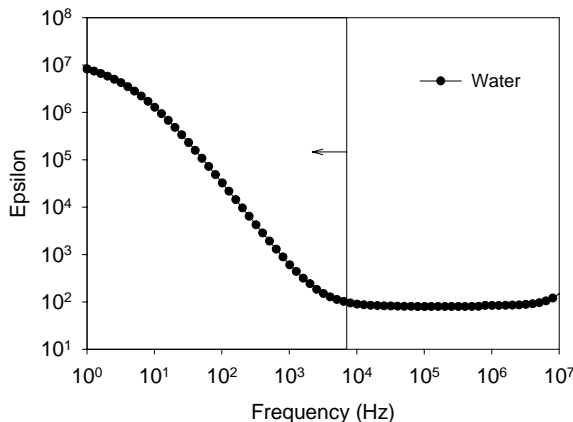


Fig. 4.18. Water calibration. Pure, deionized water ($18.0 \text{ M}\Omega/\text{cm}$) tends to a relative permittivity of $\epsilon = \kappa \sim 80$ at high frequency in accordance with values well established in the literature. The sharp rise in the lower frequencies (shown by the arrow) illustrates the polarization effect

Note that using a four-electrode technique would further reduce the polarization effect as would any electrodeless method if they could be adapted to small sample volumes.

Dielectric Spectroscopy Results

Purified tubulin of various concentrations was measured in standard buffer: 0.1 M 2-morpholinoethanesulfonic acid (MES) 1 mM ethylene glycol-bis (2-

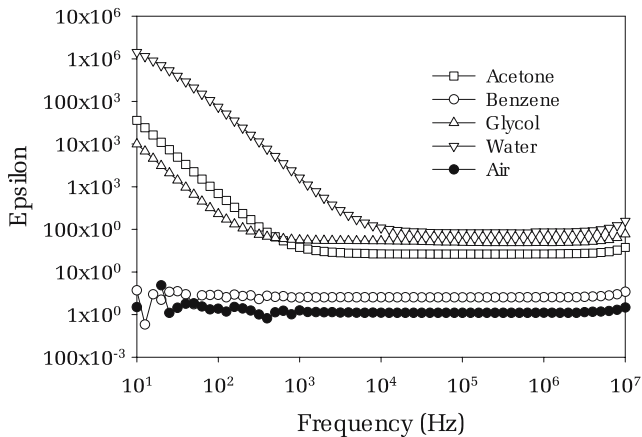


Fig. 4.19. Dielectric spectrum of various substances. For polar molecules like water and acetone we observed a strong polarization effect at frequencies lower than 10 kHz, while for nonpolar substances such as benzene with dielectric constant of $\kappa = 2.5$ we do not observe this effect. Also for calibration we are able to read the dielectric constant of the air gap between the plates with $\kappa = 1$

aminoethylether)-N,N,N',N'-tetraacetic acid (EGTA), 0.1 mM ethylenediaminetetraacetic acid, 0.5 mM MgCl₂ and 1 mM of guanosine 5'-triphosphate (GTP). The results for concentrations of 0.1 mg/ml and 1.1 mg/ml are summarized in Figs. 4.20 and 4.21 below.

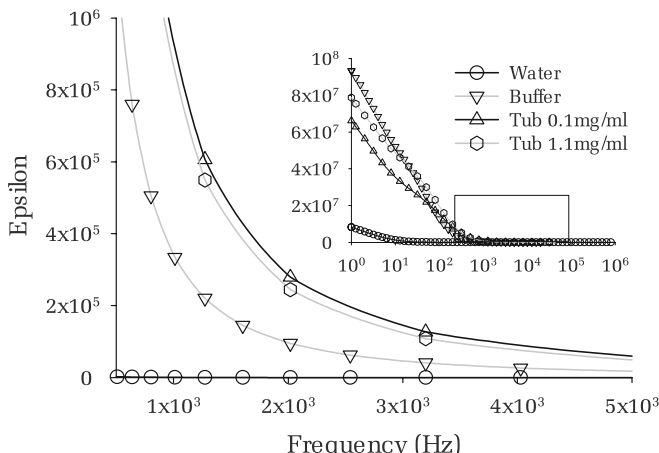


Fig. 4.20. Combination graph. Composite graph of two indicative tubulin concentrations. The inset shows the entire frequency range behavior and the main graph is the close-up

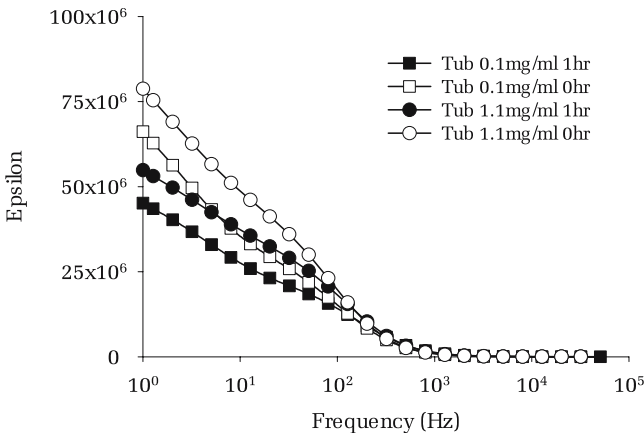


Fig. 4.21. Time dependence. Time dependence of relative permittivity at different concentrations (\circ : 1.1 mg/mL, \square : 0.1 mg/mL). Solid symbols correspond to $t = 1$ h, while open symbols correspond to 0 h. after starting measurements. Differences may be attributable to polymerization of tubulin dimers into microtubules that is known to have a characteristic time of ~ 45 min at room temperature. Time-dependence measurements were taken to show polymerization of tubulin dimers at concentrations higher than the critical concentration of 1 mg/ml. We noticed some sedimentation of our sample at rates faster than the characteristic microtubule polymerization time

Discussion of Dielectric Spectroscopy Results

It is stressed that currently, the preliminary dielectric spectroscopy results obtained by our group and summarized here are only shown as proof of principle. We have shown that it is possible, by taking data at a range of concentrations, to obtain the characteristic curves of concentration VS dielectric permittivity for tubulin and other samples of biological interest. In principle, by adding the components of a sample one by one it is possible to extract an accurate value for the dipole moment of a large protein molecule (and the rest of the components) at around 50 kHz. Below this frequency a sophisticated error-reduction technique is required, which is currently under development. From the preliminary data shown here, an order of magnitude calculation for the dipole moment of tubulin can be performed from (4.35) of this section to yield $|\mathbf{p}| \sim 10^3$ Debye assuming no interaction of buffer and tubulin dipole moments. This value is purely qualitative but can be refined with further experimentation.

4.5 Emerging Directions of Experimental Tests of the Quantum Consciousness Idea

4.5.1 Entanglement

Since 1935 when Erwin Schrödinger coined the word “entanglement” to refer to a state where the wave function describing a system is unfactorizable, much has been learned about this peculiar phenomenon and it has turned out to be very useful in quantum information science, quantum cryptography and quantum teleportation. Entanglement has been experimentally realized in light [104, 131], in matter [116] and in combinations of those [57, 111]. One way to produce entangled states in light is via type-II phase-matching parametric downconversion that is a process occurring when ultraviolet (UV) laser light is incident on a non-linear beta-barium borate (BBO) crystal at specific angles. A UV photon incident on a BBO crystal can sometimes spontaneously split into two correlated infrared (IR) photons (each of half the energy of the incident photon). The infrared photons are then emitted on opposite sides of the UV pump beam, along two cones, one of which is horizontally polarized and the other vertically. The photon pairs that are emitted along the intersections of the two cones have their polarization states entangled. This means that each photon is individually unpolarized, but the photons necessarily have perpendicular polarizations to each other. The state Ψ of the outgoing entangled photons can be written as: $|\Psi\rangle = (|\leftarrow, \beta\rangle + e^{i\alpha} |\beta, \leftarrow\rangle)$ where the arrows indicate polarizations for the (first, second) IR photon and can be controlled by inserting appropriate half-wave plates, while the phase factor $e^{i\alpha}$ can be controlled by tilting the crystal or using an additional BBO crystal in a setup similar to the one depicted in Fig. 4.22, modified from [66].

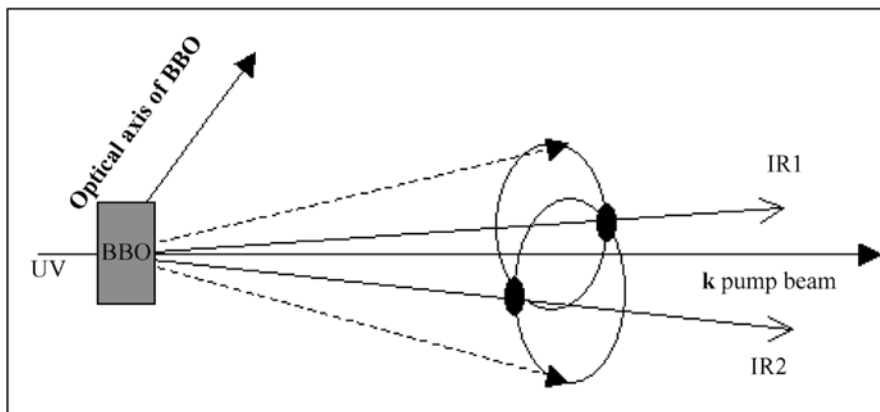


Fig. 4.22. Type-II phase-matching parametric downconversion. For certain orientations, a UV photon is absorbed by the BBO crystal and re-emitted as two entangled IR photons (IR1, IR2)

Measuring the state of one of the outgoing photons – say IR1, immediately determines the state of the other (IR2) regardless of their separation in space. This counterintuitive phenomenon is referred to as the Einstein–Podolsky–Rosen (EPR) paradox and such pairs are called EPR pairs.

4.5.2 Molecular Electronics

Today's conventional silicon-based devices are of order 180 nm in size, while future molecular devices promise a further order of magnitude reduction to this minimum. As a result, there have been considerable efforts concentrated on identifying various chemical substances with appropriate characteristics to act as binary switches and logic gates. For instance, rotaxanes have been considered as switches/fuses [21] and carbon nanotubes as active channels in field effect transistors [27]. Many of these substances are unsuitable for placement on traditional chips [63] or for forming networks, while virtually all of these efforts attempt to hybridize some kind of electrical wires to chemical substrates in order to obtain current flows. This complicates the task because of the need for appropriately nanomanufactured wires and connections.

We re-emphasize that the work presented here is suggestive of a different approach where the role of the binary states in an information encoding system is not played by the presence or bulk movement of charge carriers, but by naturally occurring conformational states of tubulin molecules and their self-assembled polymers – microtubules (MTs). Moreover, the external interaction with these states is to be performed by coupling laser light to specific spots of a microtubular network. Signal propagation is via traveling electric dipole moment flip waves such as those stipulated in Sect. 4.2 along MTs, while modulation may be achieved by microtubule-associated-protein (MAP) binding that creates “nodes” in the MT network. In our proposed scheme for information manipulation, there is no bulk transfer of (charged) mass involved. Tubulin polymerization can be controlled by temperature and application of chemicals and MAPs to yield closely or widely spaced MTs, centers, sheets, rings and other structures [29, 46], thus facilitating fabrication of *nanowires, nodes and networks* and even structures capable of long-term information storage (*biomolecular computer memory*).

4.5.3 Proposed Further Research

On-Demand Entangled-Photon Source

An on-demand entangled-photon source (OD EPS) can be built and utilized to do spectroscopic analysis of proteins and other biomolecules. Such a device would greatly facilitate studies of the fundamental quantum properties of entangled objects, possible quantum properties of living matter, quantum information science and more. It would also provide an opportunity to test and

identify the problems associated with the construction of a portable entanglement source to be taken “into the field” when entangled photons become indispensable to secure communications. For instance, tolerances of entangled photon generation to vibration and temperature changes could be studied. A minimally modified design of the SPR apparatus developed for the work already done and presented here, coupled to a source of entangled photons would be capable of detecting the often-conjectured mesoscopic bulk coherence and partial quantum entanglement of electric dipole moment states, the existence of which will cast biomolecules as appropriate candidates for the implementation of *bioqubits*. One could follow a protocol similar to that developed by Oberparleiter et al. [100], capable of producing brightness in excess of 360 000 entangled photon pairs per second, coupled to a setup similar to the that developed by Altewischer et al. [2] where entangled photons are transduced into (entangled) surface plasmons and reradiated back as entangled photons. The essential difference would be that the insides of the perforations in the gold film of Altewischer et al. would be covered with dextran to which a monolayer of tubulin dimers or microtubules would be immobilized by amine coupling (as described in detail in Sect. 4.4). The evanescent wave of the (entangled) surface plasmon generated at resonance will interact with the electric dipole moment of the immobilized protein complexes and presumably transfer the entanglement to a dipole state in a manner similar to the transfer of the photon polarization entanglement to surface plasmons. At the end of the tunnel, the surface plasmons would be reradiated having undergone the interaction with the protein electric dipole moment. If partial entanglement with the partner photon (that underwent none of these transductions) is found, then this would suggest that the protein is capable of “storing” the entanglement in its electric dipole moment state and characteristic decoherence times could be derived.

There are obvious objections to suggestions of long decoherence times for quantum properties of large molecules at room temperature and we have discussed possible ways to avoid early decoherence in Sect. 4.2. Here we note that these objections usually come from the application of equilibrium principles to the quantum-mechanical aspects of the constituent atoms. We hope to investigate deeper, as although, for instance the tubulin molecule consists of some 17 000 atoms that are subject to considerable thermal noise, the electric dipole moment state depends crucially on only a few electrons that can be in two sets of orbitals. In addition, tubulin is not an equilibrium system, rather it is a dynamic dissipative system where energy is being pumped in and out constantly. In fact, our theoretical work has suggested that for a certain set of parameters (such as the value of the dipole moment, the pH, etc.) tubulin could indeed sustain a quantum-mechanically coherent state for times of the order of microseconds [80].

Ways to Detect Quantum Coherence in Microtubules

In Sect. 4.2 and [80] comprehensive model conjecture treating certain regions inside MTs as isolated high-Q(uality) QED cavities was put forth as well as a scenario according to which the presence of ordered water in the interior of MTs results in the appearance of electric dipole quantum coherent modes, which couple to the unpaired electrons of the MT dimers via Rabi vacuum field couplings. The situation is analogous to the physics of Rydberg atoms in electromagnetic cavities [118]. In quantum optics, such couplings may be considered as experimental proof of the quantized nature of the electromagnetic radiation. In our case, therefore, if experimentally detected, such couplings would indicate the existence of coherent quantum modes of electric dipole quanta in the ordered water environment of MT, as conjectured in [25, 26], and used here.

To experimentally verify such a situation, one must first try to detect the emergent ferroelectric properties of MTs, which are predicted by this model and are potentially observable. Measurement of the dipole moment of the tubulin dimers is also an important step (see Sect. 4.4). A suggestion along these lines has been put forward in [79]. In addition, one should verify the aforementioned vacuum field Rabi coupling (VFRS), λ_{MT} , between the MT dimers and the ordered water quantum coherent modes. The existence of this coupling could be tested experimentally by the same methods used to measure VFRS in atomic physics [12], i. e. by using the MTs themselves as cavity environments, and considering tunable probes to excite the coupled dimer–water system. Such probes could be pulses of (monochromatic) light coupling to MTs. This would be the analog of an external field in the atomic experiments mentioned above. The field would then resonate, not at the bare frequencies of the coherent dipole quanta or dimers, but at the Rabi-split ones, leading to a double peak in the absorption spectra of the dimers [12]. By using MTs of different sizes one could thus check on the characteristic \sqrt{N} -enhancement of the (resonant) Rabi coupling as described by (4.10) of Sect. 4.2 for MT systems with N dimers.

Other Ways to Measure Dipole Moments

Although the most direct approach to determine this quantity would be to measure the acceleration of evaporated single molecules with dipole moment in the gradient of an electric field in vacuum, this may prove a difficult task. Even though it is possible to keep tubulin from polymerizing in solution (e. g. by lowering the temperature and concentration), evaporating individual tubulin molecules may be very difficult due to tubulin’s affinity towards polymerization and aggregation. In other words the protein is naturally “sticky” and will be hard to corpusculize. Furthermore, tubulin’s electric dipole moment in vacuum is not directly relevant to its physiological value (although such

a measurement would facilitate crosscheck of theoretical molecular dynamics simulation calculations). In addition to the techniques described in detail above, the dipole moment can also be experimentally determined in a manner similar to that used in “optical tweezers”. A thin gold chip is bathed in a solution of purified depolymerized tubulin. A small spot (1 mm^2) is illuminated with a continuous-wave laser beam of known wavelength and power. The laser beam’s diameter can be modulated creating a gradient in the intensity of the beam. The dielectric moment of tubulin will interact with this gradient and the molecule will feel a ponderomotive electric force towards higher beam intensity. This, over a period of time, will concentrate the tubulin molecules at the center of the laser spot. The concentration of tubulin along the chip can be monitored in real time using a second laser beam exciting a SPR. Thus, by measuring the redistribution of molecules in response to the interaction with the intensity gradient and accounting for Brownian motion, one can evaluate the force exerted on tubulin and therefore the electric dipole moment.

4.6 Unification of Concepts and Conclusions

4.6.1 Putting It All Together

In our contribution to “The Emerging Physics of Consciousness”, we have summarized roughly six years of theoretical and experimental work in physics, biophysics, biochemistry and neurobiology of tubulin and microtubules. Under the orchestration of Andreas Mershin (currently at the Center for Biomedical Engineering of the Massachusetts Institute of Technology) who did most of this work as part of his PhD at Texas A&M University (TAMU) Physics Department and the expert guidance of Dimitri V. Nanopoulos, we have organized a wide collaboration between experimental physicists (H.A. Schuessler’s group at TAMU), theoretical physicists (the group of N.E. Mavromatos at King’s College London), neurobiologists (the group of E.M.C. Skoulakis at TAMU and currently at the A. Fleming Institute in Greece) biochemists (the group of R.F. Luduena at the University of Texas, San Antonio) and dielectric spectroscopists (the group of J.H. Miller Jr. at the University of Houston) to study the notion that cytoskeletal proteins could be used in biomolecular-based electronic and/or quantum information-processing devices.

To this end and to aid in further theoretical study of tubulin and microtubules, our work concentrated on investigating the electric properties of this molecule. Supercomputer-based molecular dynamics simulations were performed to study geometrical, energetic and electric properties of tubulin *in silico* determining the electric dipole moment (this computational answer agreed closely with similar simulations performed by others) and for the first time the dipole moments of the alpha and beta tubulin monomers were individually determined. In order to provide an experimental value to check the simulation results, precision *in vitro* refractometry with two independent

methods (direct refractometry and surface-plasmon resonance sensing) was performed yielding the optical frequency polarizability and refractive index of tubulin for the first time. Furthermore, a custom-built dielectric spectroscopy apparatus was developed to demonstrate a method of obtaining the low (~ 50 kHz) dielectric constant and as proof of principle a preliminary run was performed. This paves the way for more precise measurements of tubulin and other proteins and it is shown that the low-frequency dielectric response of proteins can be used as an additional handle in proteomics as it depends strongly on the dipole moment of the protein. The latest theoretical approaches were described, yet currently there is not an adequate theory to analytically and accurately describe the dipole–dipole interactions of a protein molecule in a polar solvent so only order-of-magnitude values for the dipole moment of tubulin were obtained based on simplifying assumptions. In order to establish a connection between the microtubular cytoskeleton and information processing *in vivo*, the effects of overexpression of microtubule-associated protein TAU in the associative olfactory memory neurons of *Drosophila* were determined. Future directions of research concentrating on establishing the possible quantum nature of tubulin were developed theoretically.

Putting all of the above together makes for a wide-scope study that impinged upon many aspects of tubulin. This work aims to show the way for focusing future efforts in a number of directions that will, hopefully, lead to a deeper understanding of proteins and the role that the dielectric and possibly quantum properties of biomolecules play in their function.

4.6.2 Conclusions

It has become increasingly evident that fabrication of novel biomaterials through molecular self-assembly is going to play a significant role in material science [146] and possibly the information technology of the future [104]. Tubulin, microtubules and the dynamic cytoskeleton are fascinating self-assembling systems and we asked whether their structure and function contain the clues on how to fabricate biomolecular information-processing devices. Our work with the neurobiology of transgenic *Drosophila* [86] strongly suggests that the cytoskeleton is near the “front lines” of intracellular information manipulation and storage. We also established that straightforward spectroscopic techniques such as refractometry, surface plasmon resonance sensing and dielectric spectroscopy, coupled with molecular dynamic simulations and (quantum) electrodynamic analytical theory are useful tools in the study of electrodynamic and quantum effects in cytoskeletal proteins.

Implicit in our driving question is the possibility that if tubulin and MTs can indeed be made into the basis for a classical or quantum computer, then perhaps nature has already done so and tubulin and MTs already play such a role in living neural and other cells. If quantum mechanics is found to be important in cellular function (through its involvement in proteins) it is natural to ask whether there are indeed quantum effects in consciousness –

if one reasonably assumes that the phenomenon of consciousness depends on cellular processes.

Acknowledgement. The experimental work described here was undertaken mainly at Texas A&M University, the University of Houston and the University of Texas at San Antonio. We are indebted to the help and encouragement of Dr. Mita Desai of the National Science Foundation (NSF) and Prof. Jack A. Tuszyński. We wish to thank D. Chana, A. Michette, A.K. Powell, I. Samaras and E. Unger for discussions. We appreciate the technical support of Veena Prasad, Rita L. Williamson and Dr. Lisa Perez. The work presented here has been supported in part by NSF (grant No. 021895) and the Texas Informatics Task Force (TITF). In addition, AM was partially supported by the A.S. Onassis Public Benefit Foundation (Greece) and an Interdisciplinary Research Initiative grant from Texas A&M University. JHM is supported by the Texas Center for Superconductivity at the University of Houston, the Robert A. Welch Foundation (E-1221) and the Institute for Space Systems Operations (ISSO). RFL is supported by the Welch Foundation (grant No. AQ-0726). NEM is partly supported by the Leverhulme Trust (UK).

References

1. Agarwal, G.S. (1984). *Phys. Rev. Lett.* **53**:1732–1742.
2. Altewischer, E.T. (2002). *Nature* **418**:304–306.
3. Armstrong, J.D., deBelle, J.S., Wang, Z. & Kaiser, K. (1998). *Learning & Memory* **5**:102–114.
4. Ball, P. (2004). *Nature* **431**:397.
5. Bancher, C., Brunner, C., Lassmann, H., Budka, H., Jellinger, K., Wiche, G., Seitelberger, F., Grundke-Iqbali, I. & Wisniewski, H.M. (1989). *Brain Res.* **477**:90–99.
6. Bardeen, J. (1979). *Phys. Rev. Lett.* **42**:1498–1500.
7. Bardeen, J. (1980). *Phys. Rev. Lett.* **45**:1978–1980.
8. Bardeen, J. (1990). *Physics Today December*:25–31.
9. Bayley, P.P., Sharma, K.K. & Martin, S.R. (1994). In *Microtubules*, Hyams, J.S., Lloyd, C.W., (eds.) Wiley-Liss, New York: 111–137.
10. Beck, C.D.O., Scrhoeder, B. & Davis, R.L. (2000). *J. Neuroscience* **20**:2944–2953.
11. Bednorz, J.G.M. (1988). *Rev. Mod. Phys* **60**:585–600.
12. Bernadot, F. (1992). *Electrophysics Letters* **17**:34–44.
13. BIACore, I.B.A.
14. Brekhovskikh, L.M. (1980). *Waves in Layered Media*. New York: Academic Press.
15. Brion, N.J., Tremp, G. & Octave, N.J. (1999). *Am, J Pathol* **154**:255–270.
16. Brown, J.A. (1999). University of Alberta, Canada: Edmonton.
17. Buchanan, R.L.B., S. (1993). *Neuron* **10**:839–850.
18. Chaudhur, A.R., Tomita, I., Mizuhashi, F., Murata, K. Potenziano, J.L. & Luduena, R.F. (1998). *Biochemistry* **37(49)**:17157–17162.
19. Cheng, Y., Endo, K., Wu, K., Rodan, A.R., Heberlein, U., and Davis, R.L. (2001). *Cell* **105**:757–768.

20. Coleman, S. (1976). *Ann. Phys.* **101**:239–267.
21. Collier, C.P., wong, E.W., Belohradsky, M., Raymo, F.M., Stoddart, J.F., Kuekes, P.J., Williams, R.S. & Heath, J.R. (1999). *Science* **285**:391–394.
22. Crick, F.C., Koch, C., Kreiman, G., and Fried, I (2004). *Neurosurgery* **55**:273–282.
23. Crittenden, J.R., Skoulakis, E.M.C., Han, K-A., Kalderon, D., and Davis, R.L. (1998). *Learning & Memory* **5**:38–51.
24. deBelle, S.J.H., M. (1994). *Science* **263**:692–695.
25. del Guidice, E., Doglia, S., Milani, M., and Vitiello, G. (1986). *Nucl. Phys. B* **275**:185–195.
26. del Guidice, E., Preparata, G., and Vitiello, G. (1988). *Phys. Rev. Lett.* **61**:1085.
27. Derycke, V.M., R., Appenzeller, J., and Avouris, Ph. (2001). *Nano Lett* **1(9)**:453–456.
28. Dias, O.J.C.L., J.P.S. (2001). *J. Math. Phys* **42**:3292–3299.
29. Diaz, J.F., Pantos, E., Bordas, J., and Andreu, M.J. (1994). *J. Mol. Biol.* **238**:213–225.
30. Dubnau, J., Grady, L., Kitamoto, T., and Tully, T. (2001). *Nature* **411**:476–480.
31. Dustin, P. (1992). *Microtubules*. Berlin: Springer-Verlag.
32. Earp, R.L.D., R.E. (1998). *Surface Plasmon Resonance in Commercial Biosensors: Applications to Clinical Bioprocesses and Environmental Samples*, (ed.) G. Ramsay. New York: John Wiley & Sons Inc.
33. Flyvbjerg, H., Holy, T.E., and Leibler, S. (1994). *Phys. Rev. Lett.* **73(17)**: 2372–2375.
34. Fröhlich, H. (1986). *Bioelectrochemistry*, (ed.) F.K. Guttman, New York: Plenum Press.
35. Garcia, M.L.C. (2001). *Current Opinion in Cell Biology* **13**:41–48.
36. Gilson, M.K.H. (1986). *Biopolymers* **25**:2097–2119.
37. Gisin, N.P. (1993). *J. Phys. A* **26**:2233–2239.
38. Grutner, G. (1994). *Density Waves in Solids*. Vol. Advanced Book Program. 1994, Reading, Mass: Addison-Wesley Publication Co.
39. Hameroff, S.R. (1974). *Am. J. Clin. Med.* **2**:163–173.
40. Hameroff, S.R. (1998). *Toxicology Letters* **100–101**:31–39.
41. Harcoche, S.R. (1994). *Cavity Quantum Electrodynamics*, (ed.) P. Berman. New York: Academic Press.
42. Hedstrand, G. (1929). *J. Phys. Chem.* **B2**:428–438.
43. Heidary, G.F., M. (2001). *Mech. Development* **108**:171–178.
44. Himmller, A. (1989). *Mol. Cell. Biol.* **9**:1389–1396.
45. Himmller, A., Drechsel, D., Kirschner, M.W., and Martin, J.D.W. (1989). *Mol. Cell. Biol.* **9**:1381–1388.
46. Hirokawa, N., Shiomura, Y., and Okabe. S. (1988). *J. Cell Biol.* **107**:1449–1459.
47. Hutton, M., Lewis, J., dickson, D., Yen, S-H., and McGowan, E. (2001). *Trends in Mol. Medicine* **7**:467–470.
48. Hyman, A.A., Chretien, D., Arnal, I., and Wade, R.H. (1995). *J. Cell Biol.* **128(1/2)**:117–125.

49. Jackson, J.D. (1999). *Classical Electrodynamics*. 3rd edn. 1999, New York: John Wiley & Sons Inc.
50. Jackson, G.R., Wiedau-Pazos, M., Wagle, N., Brown, C.A., Massachi, S., and Geschwind, D.H. (2002). *Neuron* **43**:409–519.
51. Jacobs, M. (1979). In *Microtubules*, K.H. Roberts, J.S., (ed.). 1979, Academic Press: London.
52. Jelinek, F., Pokorny, J., Saroch, J., Trkal, V., Hasek, J., and Palan, B. (1999). *Bioelectrochemistry and Bioenergetics* **48**:261–266.
53. Jibu, M., Hagan, S., Hameroff, S.R., Pribram, K., and Yasue, K. (1994). *Biosystems* **32**:195–214.
54. Jobs, E., Wolf, D.E., and Fylyvbjerg, H. (1997). *Phys. Rev. Lett.* **29**(3):519–522.
55. Jones, T.C., Wu, X., Simpson, C.R. Jr., Clayhold, J.A., and McCarten, J.P. (2000). *Phys. Rev. B* **61**:10066–10075.
56. Jorgenson, R.C., Jung, C., Yee, S.S., and Burgess, L.W. (1993). *Sensors and Actuators* **B13–14**:721–722.
57. Julsgaard, B., Kozhekin, A., and Polzik, E. (2001). *Nature* **413**:400–412.
58. Kielpinski, D., Meyer, V., Rowe, M.A., Sackett, C.A., Itano, W.M., Monroe, C., and Wineland, W.M. (2001). *Science* **291**:1013–1033.
59. Kirkwood, J.G. (1939). *J. Chem. Phys.* **7**:911–919.
60. Kirkwood, J.G. (1939). *J. Phys. Chem.* **7**:919–924.
61. Koch, C. (2004). *Current Biology* **14**:497–97.
62. Koruga, D.L. (1985). *Ann. NY Acad. Sci* **466**:953–957.
63. Kozhuma, T., Dennison, C., McFarlane, W., Nakashima, S., Kitagawa, T., Inoue, T., Kai, Y., Nishio, N., Shidara, S., Suzuki, S. & Sykes, A.G. (1999). *J. Biol. Chem.* **270**:25733–25738.
64. Kretschmann, E., Z. (1971). *Physik* **241**:313–324.
65. Krive, I.V.R., A.S. (1985). *Solid State Commun.* **55**:691–694.
66. Kwiat, p., Matle, P., Weirfurter, P., and Zeilinger, K. (1996). *Phys. Rev. Lett.* **75**:4337–4343.
67. Lal, P. (1985). *Phys. Lett.* **111**(A):389–400.
68. Latyshev, y.I., Laborde, O., Monceau, P., and Kaumunzer, S. (1997). *Phys. Rev. Lett.* **78**:919–922.
69. Laughlin, R.B.P. (2000). *Proc. Nat. Acad. Sci., USA* **97**:28–31.
70. Lee, V., Goedert, M., and Trojanowski, J.Q. (2001). *Ann. Rev. Neuroscience* **24**:1121–1159.
71. Lewis, J., McGowan, E., Rockwood, J., Melrose, H., Nacharaju, P., Van Slegtenhorst, M., Gwinn-Hardy, K., Paul-Murphy, M., Baker, M., Yu, X., Duff, K., Hardy, J., Corral, A., Lin, W.L., Yen, S.H., Dickson, D.W., Davies, P., and Hutton, M. (2000). *Nat. Genet.* **1**:127–158.
72. Lilienfeld, S., O. (1999). *Skeptical Inquirer Magazine Online*, Nov/Dec.
73. Liliom, K., Wagner, G., Pacz, A., Vascante, M., Kovacs, J., and Ovadi, J. (2000). *Eur. J. Biochem.* **267**:4731–4739.
74. Lioubimov, V., Kolomenski, A.A., Mershin, A., Nanopoulos, D.V., and Schuessler, H.A. (2004). *Applied Optics* **43**(17).
75. Lofas, S., Johnsson, B., Edstrom, Al. Hansson, A., Lindquist, G., Muller, H., and Stigh, L. (1995). *Biosensors and Bioelectronics* **10**:813–822.
76. Luduena, R.F. (1998). *Int. Rev. Cytol.* **178**:207–275.

77. Maki, K. (1977). *Phys. Rev. Lett.* **39**:46–48.
78. Matsubara, K., Kawata, S., and Minami, S. (1988). *Applied Optics* **27**:1160–1163.
79. Mavromatos, N.E., Nanopoulos, D.V., and Zioutas, K. (1998). *Advances in Structural Biology* **5**:127–137.
80. Mavromatos, N.E.N. and Nanopoulos, D.V. (1998). *Int. J. of Mod. Physics B* **B12**:517–527.
81. Mavromatos, N.E., Mershin, A., and Nanopoulos, D.V. (2002). *Int. J. of Mod. Physics B* **16(24)**:3623–3642.
82. Mavromatos, N.E. (1999). *Bioelectrochemistry and Bioenergetics* **48**:100–123.
83. McGuire, S.E., Le, P.T., and Davis, R.L. (2001). *Science* **293**:1330–1333.
84. Melendez, J., Carr, R., Bartholomew, D.U., Kukanskis, K., Elkind, J., Yeee, S., Furlong, C., and Woodbury, R. (1996). *Sensors and Actuators* **B35**:1–5.
85. Melki, R., Carlier, M.F., and Pantaloni, D., and Timasheff, S.N. (1989). *Biochemistry* **28**:9143–9152.
86. Mershin, A., Pavlopoulos, E., Fitch, O., Braden, B.C., Nanopoulos, D.V., and Skoulakis, E.M.C.S. (2004). *Learning & Memory* **11(2)**:277–287.
87. Mershin, A., Kolomenskii, A.A., Schuessler, H.A., Nanopoulos, D.V. (2004). *Biosystems* **77**:73–85.
88. Mershin, A., Nanopoulos, D.V., and Skoulakis, E.M.C.S. (1999). *Proceedings of the Academy of Athens* **74**:123–173.
89. Miller, J.H.J., Ordonez, C., and Prodan, E. (2000). *Phys. Rev. Lett.* **84**:1555–1558.
90. Miller, J.H.J., Richard, J., Tucker, J.R., and Brandeen, J. (1983). *Phys. Rev. Lett.* **51**:1592–1595.
91. Miller, J.H.J., Thorne, R.E., Lyons, W.G., Tucker, J.R. (1985). *Phys. Rev. B* **31**:5229–5243.
92. Miller, J.H.J., Cardenas, G., Garcia-Perez, A., More, W., and Beckwith, A.W. (2003). *J. Phys A:Math Gen.* **36**:9209–9221.
93. Mitchison, J.K., M.W. (1984). *Nature* **312**:237–242.
94. Mitchison, J. (1997). *Annu. Rev. Cell. Dev. Biol.* **13**:83–117, 99–100.
95. Mori, H. (1989). *Biochemical and Biophysical Research Communications* **159(3)**:1221–1226.
96. Nanopoulos, D.V. (1995). October 4–8, 1994, invited talk at the “Physics Without Frontiers Four Seas Conference”, Trieste, Italy, June 25–July 1, 1995. also in, XV Brazilian National Meeting on Particles and Fields. 1995. Angra dos Reis, Brazil. <http://xxx.lanl.gov/abs/hep-ph/9505374>.
97. Nogales, E., Whittaker, M., Milligan, R.A., and Downing, K.H. (1999). *Cell* **96**:79–88.
98. Nogales, E., Wolf, S.G., and Downing, K.H. (1998). *Nature* **291**:199–203.
99. Novak, M. (1999). *PNAS (USA)* **88**:5837–5841.
100. Oberparleiter, B.W., P. (2001). *Phys. Rev. A* **64**:23–28.
101. Otwinowski, M., Paul, R., and Laidlaw, W.G. (1988). *Phys. Lett. A* **128**:483.
102. Penrose, R. (1989). *The Emperor’s New Mind*. 1st edn., Oxford: Oxford University Press.
103. Penrose, R. (1994). *Shadows of the Mind*. Oxford: Oxford University Press.
104. Pereira, A.k., A. & Peng, A. (1992). *Phys. Rev. Lett.* **68**:3663–3666.
105. Peterlinz, K.A. (1996). *Optics Communications* **130**:260.

106. Philip, N., Acevedo, S., and Skoulakis, E.M.C. (2001). *J. Neuroscience* **21**:8417–8425.
107. Pokorny, J., Jelinek, F., and Trkal, V. (1998). *Bioelectrochemistry and Bioenergetics* **45**:239–245.
108. Pokorny, J. (1999). *Bioelectrochemistry and Bioenergetics* **48**:267–271.
109. Quillin, M.L.M. (2000). *Acta Crystallogr. D Biol. Crystallogr.* **56**(7):791–794.
110. Raether, H. (1988). *Springer Tracts in Modern Physics* **111**. New York: Springer-Verlag.
111. Rauschenbeutel, E. (2000). *Science* **288**:2024–2028.
112. Ritz, T., Damjanovic, A., and Schulten, K. (2002). *Chem. Phys. Chem.* **3**:243–248.
113. Ross, J.H., Jr., Wang, Z., and Slichter, C.P. (1986). *Phys. Rev. Lett.* **56**:663–666.
114. Ross, J.H., Jr., Wang, Z., and Slichter, C.P. (1990). *Phys. Rev. B.* **41**:2722–2734.
115. Sackett, D.L. (1995). In *Subcellular Biochemistry*, B.B.R. Biswas, S., (ed.). Plenum Press: New York.
116. Sackett, L. (2000). *Nature* **404**:256–259.
117. Samal, S.G., K.E. (2001). *Chemical Communications*:2224–2225.
118. Sanchez-Mondragon, J.J., Narozhny, N.B., and Eberly, J.H. (1983). *Phys. Rev. Lett.* **51**:550–560.
119. Sataric, M.V., Tuszyński, J.A., and Zakula, R.B. (1993). *Physical Review E* **48**(1):589–597.
120. Sataric, M.V., Zekovic, S., Tuszyński, J.A., and Pokorny, J. (1998). *Phys. Rev. E* **58**:6333–6340.
121. Schlag, E.W., Sheu, S-Y., Yang, D-Y., Sezle, H.L., and Lin, S.H. (2000). *PNAS (USA)* **97**:1068–1072.
122. Schuessler, H.A., Mershin, A., Kolomenskii, A.A., and Nanopoulos, D.V. (2003). *J. Modern Optics* **50**(15–17):2381–2391.
123. Scully, M.O.Z., S. (2001). *PNAS (USA)* **98**(17):9490–9493.
124. Skoulakis, E.M.C.K., D., and Davis, R.L. (1993). *Neuron* **11**:197–208.
125. Skoulakis, E.M.C.D., R.L. (1996). *Neuron* **17**:931–944.
126. Song, K.-H.Z., W-J. (2001). *Physics Letters A* **290**:214–218.
127. Stebbins, H.H., C. (1982). *Cell. Tissue Res.* **227**:609–617.
128. Stenberg, E., Persson, B., Roos, H., and Urbaniczky, C. (1991). *Journal of Colloid and Interface Science* **143**:513–526.
129. Tegmark, M., (2000). *Phys. Rev. E* **61**:4194–42000.
130. Thorne, R.E., Miller, J.H. Jr., Lyons, W.G., Lyding, J.W., and Tucker, J.R. (1985). *Phys. Rev. Lett.* **55**:1006–1009.
131. Togerson, T., Branning, S., Monken, M., and Mandel, A. (1995). *Phys. Lett. A.* **204**:323–328.
132. Tong, C., Kolomenskii, A.A., Lioubimov, V.A., Muthuchamy, M., Schuessler, H.A., Trache, A., and Granger, H. (2001). *Biochemistry* **40**:13915–13924.
133. Tsue, Y.F., Y. (1991). *Prog. Theor. Phys.* **86**:469.
134. Tully, T.Q., W. (1985). *J. Comp. Physiol.* **157**:263–277.
135. VanBuren, V., Odde, D.J., and Cassimeris, L. (2002). *PNAS (USA)* **99**: 6035–6040.

136. Van Gent, J., Lambeck, P.V., Kreuvel, J.J.M., Gerritsma, G.J., Sudhoelter, E.J.R., Reunhoudt, D.N., and Popma, T.J.A. (1990). *Applied Optics* **29**:2843–2849.
137. Vater, W., Bohm, K.J., and Unger, E. (1997). *Cell Mobility and the Cytoskeleton* **36**:76–83.
138. Vogel, G. (1998). *Science* **280**:123.
139. Weinkauf, R., Schanen, P., Yang, D., Soukara, S., and Schlag, E.W. (1995). *J. Phys. Chem.* **99**:11255–11265.
140. Weisenberg, R.C. (1981). *Cell Motility* **1**:485–498.
141. Wittman, C.W., Wszolek, M.F., Shulman, J.M., Salvaterra, P.M., Lewis, J., Hutton, M., and Feany, M.B. (2001). *Science* **293**:711–714.
142. Woolf, N.J., Young, S.L., Johnson, G.V.W., and Fanselow, M.S. (1994). *NeuroReport* **5**:1045–1048.
143. Woolf, N.J., Zinnerman, M.D., and Johnson, G.V. (1999). *Brain Res.* **821**(1):241–249.
144. Wouternsen, H.B. (1999). *Nature* **402**:507–510.
145. Zettl, A.G., G. (1984). *Phys. Rev. B* **29**:755–767.
146. Zhang, S. (2003). *Nature Biotechnology* **21**(10):1171–1178.
147. Zurek, W.H. (1991). *Physics Today* **44**(10):36–56.

5 Physicalism, Chaos and Reductionism

Alwyn Scott

Summary. In addition to ignoring the severe practical problems posed by decoherence phenomena, quantum mind hypotheses are motivated by a misunderstanding of the nature of classical (i. e. nonquantum) dynamics. As presently understood, nonlinear dynamical systems – of which the brain is clearly one – exhibit the twin phenomena of chaos and emergence. The first of these impedes reductionist formulations as does quantum theory, and the second leads to hierarchical structures in biological organisms and cognitive systems, which are difficult to analyze reductively. Thus a quantum mind theory must rest on empirical evidence rather than philosophical speculation.

5.1 Introduction

Although it is suggested in other chapters of this book that quantum phenomena play important roles in neuroscience, arguments to the contrary are compelling [30]. Due to a disruptive process called decoherence, a large-scale quantum state in a biological brain would become disorganized by random thermal motions in a very short time, leaving a system that can be accurately described by classical dynamics, as is widely assumed by the neuroscience community [26].

One of the reasons that supporters of “quantum mind” hypotheses advance for assuming that quantum theory must play a key role in neuroscience – I suspect – is philosophical. Classical dynamics seems to imply that high-level brain processes can be reduced, in principle if not in practice, to a description that is based on the classical laws of physics and chemistry, leaving no room for the subjective experiences that we confirm in our daily lives. To avoid this unwelcome conclusion, it is asserted that quantum theory must be an essential component in the dynamics of biological brains, and various arguments are advanced to show that large-scale quantum states can indeed survive long enough to play functional roles in living organisms.

The primary aim of this chapter is to show that classical neuroscience cannot be reduced to fundamental descriptions; thus quantum theory is not needed to provide theoretical space for those phenomena that we know exist but don’t understand.

The chapter opens with a brief review of the basic facts of quantum decoherence and an introduction to current perspectives on classical nonlinear

dynamics, including the concept of emergence. It is then shown that we humans are exceptionally intricate organisms with many levels of functional activity, some biological and others cognitive. In other words, we comprise both a biological hierarchy and a cognitive hierarchy, both governed by nonlinear dynamics. Under the assumption of physicalism, arguments supporting the concept of reductionism are presented as a prelude to a survey of its problematic aspects. Among these are the immense numbers of higher-order structures that can emerge at each level of the biological and cognitive hierarchy, and the phenomenon of dynamical chaos that leads to the “butterfly effect” (formally termed a “sensitive dependence on initial conditions”). The nature of causality is then considered from an Aristotelian perspective, recognizing how complicated this notion can be in the context of nonlinear systems. Finally, the concept of downward causation is introduced, which leads to the emergence of intricate networks of positive feedback in open systems. As these networks can span many levels of both the biological and cognitive hierarchies, ample scope for challenging the claims of reductionism become apparent.

5.2 Quantum and Classical Dynamics

The dynamics of atomic particles are necessarily described by quantum theory because these particles also exhibit wave properties. As was first proposed by Louis de Broglie in his 1924 doctoral thesis and soon confirmed experimentally, an electron has a wavelength equal to Planck’s constant (\hbar) divided by its momentum (mass times velocity). De Broglie’s suggestion inspired Erwin Schrödinger to formulate his famous wave equation, which provides a theoretical basis for chemical bonding among many important applications. Yet the particles that we deal with in our daily lives (golf balls, for example) do not exhibit wave properties – they are entirely particle-like in nature. How can we decide whether to use quantum or classical mechanics to study a particular problem?

In considering the relevance of quantum phenomena at a temperature (T), an important number to keep in mind is the *thermal de Broglie wavelength*

$$\lambda_T = \frac{\hbar}{\sqrt{2mkT}}, \quad (5.1)$$

which is the wavelength of a particle that is moving with thermal velocity. (In this equation, k is the Boltzmann constant, which indicates the thermal energy per unit of absolute temperature.) Notice that as the temperature and particle mass (m) increase, λ_T gets smaller. For a sufficiently large product of mass and temperature, $\lambda_T \ll \Delta x$ (where Δx is the precision to which the particle position is carried in measurements or theoretical analyses), and the results of quantum calculations will be identical to those of nonlinear classical (nonquantum) calculations.

Consider a golf ball, which according to international agreement has a mass of 45.9 g. At 300 K, a golf ball has a thermal de Broglie wavelength of $\lambda_T = 3.4 \times 10^{-23}$ m, which is many orders of magnitude smaller than the size of an atomic nucleus and so far smaller than any conceivable Δx . Thus there is no point in using quantum theory to describe a golf ball as it sits on a tee, moving about with random thermal motion while waiting to be struck. After it is struck and is soaring down the fairway, the wavelength of a golf ball is even smaller, and quantum theory is even less relevant. Suppose we ignore this insight and ask how long an initially constructed quantum state can exist before being scattered by the myriad influences of random thermal vibrations. The time scale on which an initial quantum state decays into a corresponding classical description is called the *decoherence time* (τ_D), and Wojciech Zurek has shown that [37]

$$\tau_D \sim \tau_R \left(\frac{\lambda_T}{\Delta x} \right), \quad (5.2)$$

where τ_R is the time scale for corresponding classical processes and Δx can be interpreted as the distance between two virtual locations of the particle. Evidently, the condition $\lambda_T \ll \Delta x$ implies $\tau_D \ll \tau_R$, which means that classical processes dominate the dynamics.

Returning to our golf ball and taking Δx to be about the size of an atom (10^{-10} m), we see that any initial quantum state would decay (decohere) into a corresponding classical state in about 10^{-13} times the classical time constant, rendering meaningless any quantum corrections to the classical formulation.

To show how well the electrodynamics of neuroscience can be described in classical terms, Max Tegmark has recently estimated the decoherence time in biological brains under a variety of assumptions, finding that $\tau_D \sim 10^{-13}$ to 10^{-20} s [30], which is many orders of magnitude less than the times that are empirically relevant [26]. Thus – as with the golf ball – the classical representation of dynamic variables in neuroscience is on a firm theoretical footing: adding quantum corrections won't tell us anything.

To see how classical dynamics are able to represent the strongly nonlinear phenomena observed in biological brains, we shall assume in the following discussion that quantum effects can be neglected and see what difficulties and opportunities arise.

5.3 What Are Classical Nonlinear Phenomena?

The short answer to this question – suitable for a cocktail party response – is that nonlinear phenomena are those for which the whole is greater than the sum of its parts. Going beyond this slogan, one can point to an impressive array of dynamic effects currently studied under the aegis of nonlinear science, including but not limited to the following:

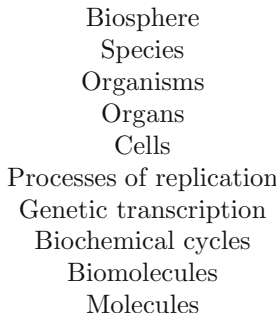
- *emergent structures* (tornadoes, tsunamis, lynch mobs, optical solitons, black holes, schools of fish, cities, Jupiter's Great Red Spot, nerve impulses)
- *filamentation* (rivers, bolts of lightning, woodland paths, optical filaments)
- *chaos* (sensitive dependence on initial conditions or the “butterfly effect”, strange attractors, Julia sets, turbulence)
- *threshold phenomena* (an electric wall switch, the trigger of a pistol, flip-flop circuits, tipping points, the all-or-nothing property of a neuron)
- *spontaneous pattern formation* (natural languages, fairy rings of mushrooms, the Gulf Stream, fibrillation of heart muscle, ecological domains)
- *harmonic generation* (digital tuning of radio receivers, conversion of laser light from red to blue, musical overtones)
- *synchronization* (Huygens's pendulum clocks, electric power generators connected to a common grid, circadian rhythms, hibernation of bears, flashing of Indonesian fireflies, human empathy), and
- *shock waves* (sonic booms of jet airplanes, the sound of a cannon, bow waves of a boat, sudden pileups in smoothly flowing automobile traffic)

For a broad view of this area, see the recently published *Encyclopedia of Nonlinear Science* [29]. All of these striking phenomena and more can play roles in the nonlinear dynamics of hierarchical systems.

A yet deeper answer to the above question recognizes that the definition of nonlinearity involves a statement about the nature of causality. This perspective is presented below after we look at the hierarchical nature of living organisms.

5.4 The Biological and Cognitive Hierarchies

Before taking up philosophical issues, consider the following biological hierarchy of a living organism.



In thinking about this formulation, five comments are appropriate.

First, it is only the general nature of the hierarchy that is of interest to us here, not the details. One might include fewer or more levels in the diagram or account for branchings into (say) flora and fauna or various phyla. Although such refinements may be useful in particular discussions, the present aim is to study the general nature of a nonlinear dynamic hierarchy, so a relatively simple diagram is appropriate.

Second, the nonlinear dynamics at each level of description generate emergent structures, and nonlinear interactions among these structures provide a basis for the dynamics at the next higher level [27].

Third, the emergence of new dynamic entities stems from the presence of closed causal loops, in which positive feedback leads to exponential growth that is ultimately limited by nonlinear effects.

Fourth, these closed causal loops also provide a basis for the phenomenon of dynamical chaos, fortuitously discovered by the eminent French mathematician Henri Poincaré near the end of the nineteenth century. In his words [24]:

“If we knew exactly the laws of nature and the situation of the universe at the initial moment, we could predict exactly the situation of that same universe at a succeeding moment. But even if it were the case that the natural laws had no longer any secret for us, we could still only know the initial situation approximately. If that enabled us to predict the succeeding situation with the same approximation, that is all we require, and we should say that the phenomenon had been predicted, that it is governed by laws. But it is not always so; it may happen that small differences in the initial conditions produce very great ones in the final phenomena. A small error in the former will produce an enormous error in the latter. Prediction becomes impossible, and we have the fortuitous phenomenon.”

The possibility of such fortuitous phenomena was largely ignored by the scientific world until the 1960s, when a clear example was observed numerically by an MIT meteorologist named Edward Lorenz. He was using the newly available digital computer to develop atmospheric models for weather prediction – a challenging task.

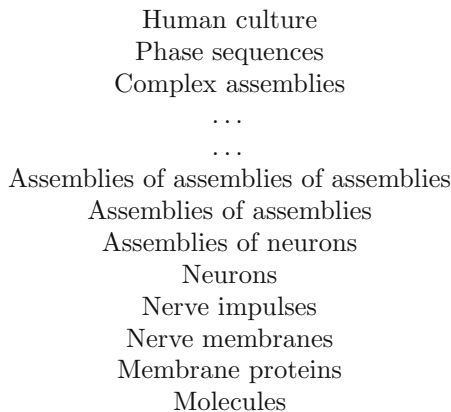
At the outset of a difficult study, scientists often consider simple versions of their real problems, but even after paring his model down to only three dynamic variables, Lorenz found a geometric growth of small errors, just as Poincaré had theoretically predicted for errors in the three-body problem of planetary motion. Weather prediction beyond a certain limited time was thus shown to be impossible, a result that Lorenz emphasized in a 1972 talk famously entitled: “Predictability: Does the flap of a butterfly’s wings in Brazil set off a tornado in Texas?”

Thus the term “butterfly effect” entered our language as a graphic metaphor for Poincaré’s fortuitous phenomenon, but the concept of a sharp

division between possible futures is much older; in geography there is a divide (or watershed), where water runs either east to one sea or west to another, and in mathematics, such a sharp dividing line is called a separatrix. Less formally, politicians and social scientists speak of a “tipping point” and of the “straw that broke the camel’s back”, and we are all familiar with a light switch – which is either on or off – and a coin toss. Such switches are the essential elements of modern electronics, and a computer can be viewed as a system of many interconnected switches. Some believe that the human brain can be similarly described as it parses the future in unanticipated ways.

Finally, the number of possible entities that can emerge at each level is immense, implying that all possibilities cannot be physically realized in a finite universe. Thus only a small subset of the possible emergent and chaotically interacting entities actually occur.

In addition to the biological hierarchy, each of us also comprises a cognitive hierarchy with the following structure.



Although this diagram differs from the biological hierarchy in some ways, the previous comments apply. In particular, each cognitive level has its own nonlinear dynamics, involving closed causal loops of positive feedback, out of which can emerge an immense number of chaotically interacting entities. A necessarily small subset of these possibilities does in fact emerge, providing a basis for the nonlinear dynamics of the next higher level.

Perhaps the most significant difference between the biological and cognitive hierarchies stems from the internal levels, which involve assemblies of neurons described by Donald Hebb as follows [16–18].

“Any frequently repeated, particular stimulation will lead to the slow development of a ‘cell-assembly,’ a diffuse structure comprising cells . . . capable of acting briefly as a closed system, delivering facilitation to other such systems and usually having a specific motor facilitation. A series of such events constitutes a ‘phase sequence’ – the thought process.”

Because an assembly shares the threshold (all-or-nothing) properties of individual neurons, this concept is hierarchical. Thus these internal levels range from assemblies of neurons to the phase sequence, but their existence is deduced from theoretical speculation and circumstantial evidence rather than direct observation [26].

Importantly, philosophers disagree about the ontological nature of emergent entities. Do the various levels of the biological and cognitive hierarchies differ merely by their labels, convenient for academic organization, or are some of them qualitatively different aspects of reality? In attempting to answer this question, it is necessary to understand how the upper levels are related to lower levels, which brings us to the doctrine of reductionism.

5.5 Reductionism

Since the seventeenth century, the reductive program has been surprisingly successful in prising out explanations for the behavior of the natural world. This perspective is now widely accepted by the scientific community as the fundamental way to pose and answer questions. Basically, the reductive approach to understanding natural phenomena proceeds in three steps.

- *Analysis.* Assuming some higher-level phenomenon is to be explained, separate the dynamics of that phenomenon into components, the behaviors of which are individually investigated.
- *Theoretical formulation.* Guided by empirical studies and imagination, develop a theoretical formulation of how the components interact.
- *Synthesis.* In the context of this formulation, derive the higher-level phenomenon.

Among the many aspects of nature that have fallen to this approach, one can mention planetary motion (based on the concepts of mass and gravity and on Newton's laws of motion), electromagnetic radiation (based on the concepts of electric charge, electric fields, and magnetic fields related through Maxwell's electromagnetic equations), atomic and molecular structures (based on the concepts of mass, electric charge, Planck's constant, and Schrödinger's equation for the dynamics of quantum probability amplitudes), and nerve impulse propagation (based on the concepts of voltage, membrane permeability, ionic current, and the Hodgkin–Huxley equations for the dynamics of current flow through a voltage-sensitive membrane).

Generalizing from such specific examples, some believe that all natural phenomena can be understood in this way [33]. Others maintain that there exist natural phenomena that cannot be completely described in terms of lower-level entities – life and the human mind being outstanding examples. In its more extreme form, this latter position is called substance dualism: the view of René Descartes that important aspects of the biological and

cognitive realms do not have a physical basis. A less extreme position is property dualism, which accepts a physical basis but asserts aspects of biology and social science that cannot be explained in terms of atomic or molecular dynamics. Under property dualism, higher-level phenomena are thought to be divided between those that can be understood and explained in terms of physics and chemistry and those that cannot.

To statements of belief there is no scientific response, but if we can agree on the physical basis of life and mind, the scope of the discussion narrows. Let us agree, therefore, that all biological and mental phenomena supervene on the physical in the following sense. If the constituent matter is removed, the phenomenon in question disappears, or as philosopher Jaegwon Kim puts it in the context of cognitive phenomena [20]: “Any two things that are exact physical duplicates are exact psychological duplicates as well.” This position is called physicalism, and among biologists it is now widely accepted for the phenomenon of life. In other words, there is no Bergsonian “life force” or elan vital that exists independent of the molecules comprising a living organism. Similarly, most neuroscientists believe that a person’s mind (or consciousness) would not survive removal of the molecules of his or her brain. Under this assumption, two questions arise.

- Does reductionism follow from physicalism?
- Does physicalism allow property dualism?

Over the past two decades, these questions have been considered by Kim [20], who reluctantly concludes that physicalism does indeed imply reductionism and sits uneasily with property dualism. Let us review his argument with reference to Fig. 5.1.

This figure represents higher-level mental phenomena (M_1 and M_2) that supervene on lower-level physical descriptions (P_1 and P_2), where supervenience is indicated by the vertical dashed lines. In other words, if the properties P_1 are removed, then the phenomenon M_1 will disappear, with a similar relationship between P_2 and M_2 .

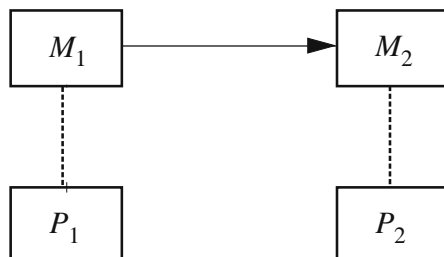


Fig. 5.1. The causal interaction of higher-level phenomena (M_1 and M_2) that supervene on lower-level properties (P_1 and P_2)

Now suppose that studies in experimental psychology have established a causal relationship between M_1 and M_2 (indicated by the horizontal arrow in Fig. 5.1), under which the initial upper-level observation of M_1 always leads to a corresponding upper-level observation of M_2 . Because under the assumption of physicalism P_1 (P_2) must be present to provide a basis for M_1 (M_2), we could as well say that P_1 causes P_2 , which is a formulation of the upper-level causality in terms of the corresponding lower-level properties. In other words, one could reduce the causal relation between phenomena M_1 and M_2 to a corresponding relation between P_1 and P_2 , thereby supporting reductionism and undercutting property dualism. There is no claim that this reduction is convenient or even feasible, but that it is possible “in principle”.

In addition to this logic, there is a practical argument for the reductive view. Even if reductionism were not to hold for all aspects of biological or mental organization, it is still a prudent strategy for the majority of biologists and cognitive scientists to take as a working hypothesis. Why? Often the riddles of one generation become standard knowledge of the next; thus the dualist (substance or property) is ever in danger of giving up too soon on the search for reductive formulations. One might say that it is the duty of a scientist to search for reductive explanations of natural phenomena.

5.6 Objections to Reductionism

As we have seen, reductionism based on physicalism is a serious philosophical position meriting careful response. Those who disagree on intuitive grounds must offer substantial objections. Let us consider some.

5.6.1 Constructionism versus Reductionism

Although many elementary particle physicists (often those who seek a “theory of everything”) are reductionists [33], condensed-matter physicists (who study aggregates of atoms and molecules) tend to question such claims. Thus Philip Anderson has asserted [2]:

“The reductionist hypothesis does not by any means imply a ‘constructionist’ one: The ability to reduce everything to simple fundamental laws does not imply the ability to start from those laws and reconstruct the universe. In fact the more the elementary-particle physicists tell us about the nature of the fundamental laws, the less relevance they seem to have to the very real problems of the rest of science, much less to those of society. The constructionist hypothesis breaks down when confronted with the twin difficulties of scale and complexity.”

What is it about “scale and complexity” that creates problems for the constructionist hypothesis?

5.6.2 Immense Numbers of Possibilities

Severe computational difficulties arise in life science because the number of possible emergent structures at each level of the biological hierarchy (although finite) is too large to be counted. To sharpen such ideas in theoretical biology, physicist Walter Elsasser introduced the term *immense* to characterize a number that is finite but greater than a *googol* (10^{100}), and thus is inconveniently large for numerical studies [7, 9].

To grasp Elsasser's concept, consider the proteins. These workhorses of biochemistry are valence-bonded strings of amino acids, each designated by an underlying DNA code. Because there are 20 different amino acids and a typical protein is composed of some 200 of them, the number of possible proteins is about 20^{200} , which is greater than a googol. As the number of possible proteins grows very rapidly with the length of the amino-acid string, mathematicians call this a "combinatorial explosion."

The number of possible protein molecules is therefore immense, meaning that all the matter in the universe falls far short of that required to construct but one example of each possible protein molecule [9, 25]. Throughout the eons of biological evolution, most of the possible protein molecules have never been constructed and never will be. Those particular proteins that are presently known and used by living creatures were selected in the course of evolution through a succession of historical accidents that are consistent with the laws of physics and chemistry but not determined by them.

So it goes at all levels of the biological and cognitive hierarchies. Combinatorial explosions abound, and the number of entities that might emerge from each hierarchical level – to form a basis for the dynamics of the next level – is immense, suggesting that happenstance guides the evolutionary process [15].

It follows that biological science differs fundamentally from physical science, which deals with homogeneous sets having identical elements. Thus a physical chemist has the luxury of performing as many experiments as are needed to establish laws governing the interactions among (say) atoms of carbon and hydrogen as they form molecules of benzene. In the biological, cognitive, and social sciences, on the other hand, the numbers of possible members in most interesting sets are typically immense, so experiments are necessarily performed on heterogeneous subsets of the classes of interest. Because the elements of heterogeneous subsets are never exactly the same, it follows that experiments cannot be precisely repeated. Thus causal laws cannot be determined with the same degree of certainty in the biological, cognitive and social sciences as in the physical sciences.

In other words, psychologists establish rules rather than laws for interpersonal interactions, and your doctor can only estimate the probability that a certain pill will cure you. At the levels of biology, neuroscience, and social science, therefore, the horizontal arrow from M_1 to M_2 in Fig. 5.1 should better be drawn fuzzy or labeled with an estimate of its reliability, to indicate this deviation from strict causality.

5.6.3 Sensitive Dependence on Initial Conditions

Nonlinear dynamics offer many examples of the sensitive dependence on initial conditions, leading to the “fortuitous phenomena” noted by Poincaré and dubbed “the butterfly effect” by Lorenz, but such effects have long been informally recognized. Among computer engineers and neuroscientists, the corresponding idea of a threshold level at the input of an information processor – below and above which different outcomes transpire – is an essential concept.

In neuroscience, threshold phenomena are becoming increasingly important. Although the linear dendritic dynamics assumed for neurons until the 1980s helped the analyst follow the strands of theoretical causality, real dendrites are now known to be highly nonlinear, offering many additional tipping points to the dynamics of every neuron [26]. How are these twisted skeins of causality to be sorted out?

5.6.4 The Nature of Causality

Whether one is concerned with establishing dynamic laws in the physical sciences or seeking rules in the biological and social sciences, the notion of causality requires careful consideration [6]. As was noted above, a study of causality is essential for appreciating nonlinear phenomena, but it is not a new issue. Some twenty-three centuries ago, Aristotle noted that “We have to consider in how many senses because may answer the question why” [3]. As a “rough classification of the causal determinants of things,” he suggested four types of causes.

- *Material cause.* Material cause stems from the presence of some physical substance that is needed for a particular outcome. Aristotle suggested that bronze is an essential factor in the making of a bronze statue, but the concept is more general. Obesity in the United States, for example, is materially caused by the overproduction of corn (maize), just as Russian alcoholism is materially caused by the abundance of vodka.
- *Formal cause.* The material necessary for some particular outcome must be available in the appropriate form. The blueprints of a house are necessary for its construction, the DNA sequence of a particular gene is required for synthesis of the corresponding protein, and a pianist needs the score to play a concerto.
- *Efficient cause.* For something to happen, according to Aristotle, there must be an “agent that produces the effect and starts the material on its way.” Thus, a golf ball moves through the air in a certain trajectory because it was struck at a particular instant of time by the head of a club. Similarly, a radio wave is emitted into the ether in response to the current that is forced to flow through an antenna. Following Galileo, this is the standard sense in which physical scientists use the term causality [6].

- *Final cause.* Events may come about because they are desired by some intentional organism. Thus a house is built – involving the assembly of materials, reading of plans, sawing of wood, and pounding of nails – because someone wishes to have shelter from the elements. Such purposive answers to the question “why?” are problematic in the biological sciences, and they emerge as central issues at upper levels of the cognitive hierarchy.

For those familiar with the jargon of mathematics, the following paraphrasing of Aristotle’s definitions may be helpful.

- At a particular level of the biological hierarchy, a material cause might be a time or space average over dynamic variables at lower levels of description and enter a hierarchical formulation as a slowly varying parameter at the level of interest.
- Again, at a particular level of the biological hierarchy, formal causes might arise from the more slowly varying values of dynamic variables at higher levels of description, which enter as boundary conditions at the level of interest.
- An efficient cause is represented by a stimulation–response relationship, which is usually formulated as a differential equation with a dependent variable that responds to a forcing term. Fledgling physical scientists spend their formative years solving such problems, with the parameters (material causes) and boundary conditions (formal causes) specified. This educational experience may explain why physical scientists tend to assume that everything that transpires in nature can be described in terms of efficient causes.
- In mathematical terms, it is not clear (to me, at least) how one might formulate a final cause.

Although this classification seems tidy, reality is usually more intricate. Thus Aristotle noted that causes may be difficult to sort out in particular cases, with several of them often “coalescing as joint factors in the production of a single effect” [3]. Such interactions among component causes are a key property of nonlinear phenomena.

Distinctions among Aristotle’s “joint factors” are not always easy to make. A subtle difference between formal and efficient causes appears in the metaphor for Norbert Wiener’s cybernetics: the steering mechanism of a ship [34]. If the wheel is connected directly to the rudder (via cables), then the forces exerted by the helmsman’s arms are the efficient cause of the ship executing a change of direction. For larger vessels, however, control is established through a servomechanism in which the position of the wheel merely sets a pointer that indicates the desired position of the rudder. The forces that move the rudder are generated by a feedback control system (or servomechanism) that minimizes the difference between the actual and desired positions of the rudder. In this case, one might say that the position of the

pointer is a formal cause of the ship's turning, with the servomotor of the control system acting as the efficient cause.

Another example is provided by the conditions needed to cause the firing of a neuron. If the synaptic weights and firing threshold are supposed to be constants, they can be viewed as formal causes of a firing event. On a longer time scale associated with learning, however, these parameters can be viewed collectively as a weight vector that is governed by the learning dynamics and might be classified as efficient causes of neuron ignition. Although the switching of a real neuron is far more intricate than this simple picture suggests, the point remains valid – neural switching is a nonlinear dynamic process, melding many contributing factors.

Finally, when a particular protein molecule is constructed within a living cell, sufficient quantities of appropriate amino acids must be available to the messenger RNA as material causes. The DNA code, controlling which amino acids are to be arranged in what order, is a formal cause, and the chemical (electrostatic and valence) forces acting among the constituent atoms are efficient causes.

For applied mathematicians, it is not surprising to find several different types of causes involved in a single event. We expect that parameter values, boundary conditions, and forcing functions will all combine to influence the outcome of a given computation. What other complications of causality are anticipated?

5.6.5 Nonlinear Causality

In applied mathematics, the term “nonlinear” is defined in the context of relationships between efficient causes and effects. Suppose that a series of experiments on a certain system have shown that cause C_1 gives rise to effect E_1 ; thus

$$C_1 \rightarrow E_1 ,$$

and similarly

$$C_2 \rightarrow E_2$$

expresses the relationship between cause C_2 and effect E_2 . This relation is *linear* if

$$C_1 + C_2 \rightarrow E_{12} = E_1 + E_2 . \quad (5.3)$$

If, on the other hand, E_{12} is not equal to $E_1 + E_2$, the effect is said to be a *nonlinear* response to the cause.

Equation (5.3) indicates that for a linear system any efficient cause can be arbitrarily divided into components (C_1, C_2, \dots, C_n) , whereupon the effect will be correspondingly divided into (E_1, E_2, \dots, E_n) . Although convenient for analysis – providing a basis for Fourier analysis and Green function methods – this property is not usually found in the realms of biological, cognitive, and social sciences [25, 27, 29].

Far more common is the nonlinear situation, where the effect from the sum of two causes is not equal to the sum of the individual effects. The whole is not equal to the sum of its parts. Nonlinearity is less convenient for the analyst because multiple causes interact among themselves, allowing possibilities for many more outcomes, obscuring relations between cause and effect and confounding the constructionist. For just this reason, nonlinearity plays a key role in the course of biological evolution and the organization of the human mind.

5.6.6 The Nature of Time

Causality is intimately connected with the way we view time – thus, the statement “ C causes E ” implies (among other things) that E does not precede C in time [6] – yet the properties of time may depend on the level of description [12, 13, 35, 36]. Thus, the dynamics underlying molecular vibrations are based on Newton’s laws of motion, in which time is bidirectional. In other words, the direction of time in Newton’s theoretical formulation can be changed without altering the qualitative behavior of the system. At the level of a nerve impulse, on the other hand, time is unidirectional, with a change in its direction making an unstable nerve impulse stable and vice versa. In appealing to Fig. 5.1, therefore, the reductionist must recognize that the nature of the time used in formulating the causal relationship between P_1 and P_2 may differ from that relating M_1 and M_2 .

5.6.7 Downward Causation

Reductionism assumes that causality acts upward through the biological hierarchy, where the causality can be interpreted as both efficient and material. Formal causes, on the other hand, can also act downward because variables at the upper levels of a hierarchy can place constraints (boundary conditions, for example) on the dynamics at lower levels [1].

A dramatic example of downward causation occurred eons ago when certain bacteria began to harvest and store energy from the sun, creating atmospheric oxygen as a poisonous waste [22]. The presence of oxygen in the atmosphere, in turn, led to the emergence of the animal kingdom, in which we humans participate. Other examples of downward causation include modifications of DNA codes caused by interactions among species, germination of an ovum following sexual activity, and the disintegration of an organism upon death.

Although such examples provide convincing evidence of downward causation, the means through which it acts are not widely understood. To sort things out, Claus Emmeche and his colleagues have recently defined three types of downward causation [10].

- *Strong downward causation* (SDC). Under SDC, it is supposed that upper-level phenomena can act as efficient causal agents in the dynamics of lower levels. In other words, upper-level organisms can modify the physical and chemical laws governing their molecular constituents. Presently, there is no empirical evidence for the downward action on efficient causation, so SDC is almost universally rejected by biologists.
- *Weak downward causation* (WDC). WDC assumes that the molecules comprising an organism are governed by some nonlinear dynamics in a phase space, having attractors (which include the living organism) each with a corresponding basin of attraction. Under WDC, a higher-level phenomenon might move certain lower level variables from one basin of attraction to another. With this formulation, for example, death is but another of the attractors shared by the interacting molecules of your body, and your physician's job is to keep your molecules within the basin of the living state. (Unfortunately, the basin shrinks with age, making the task ever more difficult.)

Because many examples of such nonlinear systems have been studied both experimentally and theoretically [27, 29], there is little doubt about the scientific credibility of this means for downward causation. Building on a seminal suggestion of Alan Turing [31], biologists Stuart Kauffman [19] and Brian Goodwin [14], among others, have presented detailed discussions of ways that WDC can influence the development and behavior of living organisms.

- *Medium downward causation* (MDC). Accepting WDC, proponents of MDC go further in supposing that higher-level dynamics (e.g., the emergence of a higher-level structure) can modify the local features of an organism's lower-level phase space through the downward actions of formal causes. In the modern biology, MDC is a key aspect of evolutionary theory, and in neuroscience, the phenomenon of learning is an example of MDC, in which higher-level experiences (or training) of an organism alter the ways that neurons interact, changing its behavioral spectrum.

5.6.8 Open Systems

In contrast with the conservative formulations of classical physics, biological organisms are open systems, requiring a steady input of energy and matter (sunlight or food) to maintain their metabolic activities. A familiar example of an open system is provided by the flame of a candle – the heat of the flame releases vaporized wax that provides the energy to keep the flame hot.

From the size and composition of the flame and the candle, it is possible to compute the (downward) propagation velocity of the flame (v) whereby establishing a rule for where the flame will be located at a particular time [27].

Corresponding to

$$M_1 \rightarrow M_2$$

in Fig. 5.1, such a rule is the following. If the flame is at position x_1 at time t_1 , then it will be at position

$$x_2 = x_1 + v(t_2 - t_1)$$

at time $t_2 > t_1$. Because the flame is an open system, it follows that a corresponding relation

$$P_1 \rightarrow P_2$$

cannot be written – not even “in principle” – for the physical substrate. Why not? Because the atoms comprising the physical substrate are *continually changing* [5]. The flame’s heated molecules of air and wax vapor at time t_2 are entirely different from those at time t_1 . Thus, knowledge of the detailed positions and speeds of the molecules present in the flame at time t_1 tells us nothing about those at time t_2 . What remains constant is the flame itself – a higher-level process.

Although it might be asserted that “in principle” one could compute the dynamics of all the matter and all the radiation of the universe, this would require an “omniscient computer,” which is similar to the Calvinist notion of God. Such speculation tells us nothing about reductionism.

5.6.9 Closed Causal Loops

In his analysis of reductionism, Kim misses the concept of a closed causal loop, asking: “How is it possible for the whole to causally affect its constituent parts on which its very existence and nature depend?” [21]. Causal circularity, he claims, is unacceptable because it violates the following “causal-power actuality principle.”

“For an object, x , to exercise, at time t , the causal/determinative powers it has by virtue of having property P , x must already possess P at t . When x is being caused to acquire P at t , it does not already possess P at t and is not capable of exercising the causal/determinative powers inherent in P .”

There are two replies to this assertion, one theoretical and the other empirical.

From a theoretical perspective, Kim errs in supposing that an emergent structure somehow pops into existence at time t , which would indeed be surprising. An emergence entity (or coherent structure), however, begins from an infinitesimal seed (noise) that appears at a lower level of description and develops through a process of exponential growth (instability). Eventually, this growth is limited by nonlinear effects, and a stable entity comes into existence. Think of lighting a candle. Upon being barely lit, a tiny flame grows rapidly before settling down to its natural size.

Similarly, in Kim's notation, both x and P should be viewed as functions of time (t), which may be related by ordinary differential equations as

$$\begin{aligned}\frac{dx}{dt} &= F(x, P) , \\ \frac{dP}{dt} &= G(x, P) ,\end{aligned}$$

where F and G general nonlinear functions of both x and P . (The time scales of F and G can be very different, allowing P to remain approximately constant during the dynamics of x .) The emergent structure is not represented by $x(t)$ and $P(t)$ (which are functions of time and can be infinitesimally small), but by x_0 and P_0 satisfying

$$\begin{aligned}0 &= F(x_0, P_0) , \\ 0 &= G(x_0, P_0) .\end{aligned}$$

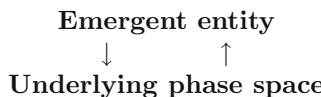
Assuming that x_0 and P_0 are an asymptotically stable solution of this system,

$$\begin{aligned}x(t) &\rightarrow x_0 , \\ P(t) &\rightarrow P_0 ,\end{aligned}$$

as $t \rightarrow \infty$ exemplifying the establishment of a dynamic balance between downward and upward causations.

Thus, Kim's causal-power actuality principle is recognized as an artifact of his static analysis of an essentially dynamic situation.

Empirically, there is much evidence for closed causal loops. Going back to James Watt in the eighteenth century, engineers have used negative feedback to "govern" the speed of engines. Since the 1920s, negative feedback loops are invariably used to stabilize the performance of electronic amplifiers, making long-distance telephone communications possible, and they play key roles in Wiener's science of cybernetics [34]. Such closed causal loops can be represented as



a positive feedback diagram. Over two decades ago, biochemists Manfred Eigen and Peter Schuster suggested that closed causal loops around at least three levels of dynamic description were necessary for the emergence of living organisms from the oily foam of the Hadean oceans [8].

In engineering applications of closed causal loops, a signal from the output is brought back to the input, as shown in Fig. 5.2a. Here **A** causes **B**, which in turn causes **A**, confounding the concepts of cause and effect. Occasionally, the net gain around the loop exceeds unity, leading to oscillations (called "singing"), for which cause and effect are indistinguishable. Oscillations are

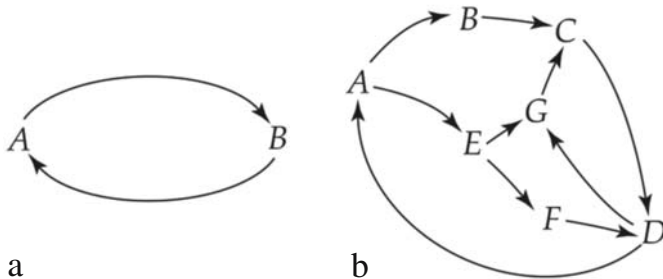


Fig. 5.2. Feedback diagrams in which the arrows indicate the actions of causality. (a) A simple loop. (b) A complex network

unwanted emergent structures in amplifiers, but for systems that are intended to oscillate, positive feedback is an essential element of the design.

Journals of nonlinear science offer many examples of positive feedback and the subsequent emergence of coherent structures [27]. In the physical sciences, structures emergent from positive feedback loops include tornadoes, tsunamis, optical solitons, and Jupiter's Great Red Spot, among many others. Biological examples include the nerve impulse, cellular reproduction, flocks of birds and schools of fishes, and the development of new species, in addition to the emergence of life itself. In the social sciences, there are lynch mobs, natural languages, and the founding of a new town or city [29]. In hierarchical systems, downward causation (WDC, MDC, or both) leads to additional opportunities for more intricate closed causal loops (or networks), as is suggested in Fig. 5.2b. Here the network comprises the following closed loops of causation: **ABCD**, **CDG**, **AEGD**, and **AEGCD**, where the letters correspond to coherent entities at various levels of the biological and cognitive hierarchies. In the context of modern nonlinear science, each such diagram would correspond to the presence of an attractor in the phase space describing the system dynamics, and it could lead to the emergence of a new coherent entity of theoretically unbounded complexity.

5.7 Concluding Comments

As we have seen, there are several reasons for questioning reductionism in the context of classical (nonquantum) dynamics. First, although the reductive program asserts that all higher-level dynamics can "in principle" be causally explained in terms of physics and chemistry, reductionism does not imply constructionism. This is because there is an immense number of possible emergent entities at each level of both the biological and the cognitive hierarchies, so what actually occurs depends largely on happenstance (Poincaré's "fortuitous phenomena") that is consistent with but not constrained by the laws of physics and chemistry.

Second, reductionism does not explain how the various types of Aristotelian causality (material, formal, efficient, and final) are to be sorted out. Under nonlinear dynamics, even the threads of efficient cause become interwoven, and downward action of formal causes makes lower-level dynamics depend on higher-level phenomena, at variance with reductive assumptions.

Third, from an operational perspective, the nature of time differs at higher and lower levels – the “arrow of time” being bidirectional under energy conservation and unidirectional under the energy-consuming dynamics of biology. This is problematic for biological reductionism because a system with unidirectional time is asked to be described in terms of bidirectional time.

Fourth, living creatures are open systems, regularly replacing their atomic and molecular constituents. Thus exact knowledge of the speeds and positions of these constituents at one time cannot be used for making higher-level predictions at later times.

In biological and cognitive systems, finally, myriad closed causal loops and networks with positive feedback obscure the relationships between cause and effect, leading both to the emergence of new dynamic entities with unanticipated properties and to chaotic interactions among them.

In describing a human being from the perspective of nonlinear science, the possibility of causal interactions among the various levels of both the cognitive and biological hierarchies must be included in the overall theoretical formulation. At lower levels, this is evident because the physiological condition of a neuron clearly affects the manner in which it relates incoming and outgoing streams of information, but higher cognitive levels also have causal biological effects. Cultural imperatives to ingest a psychoactive substance, for example, can alter the dynamics of membrane proteins, leading to mental changes that influence bodily health with subsequent psychological effects in a wending path of branching causes and effects that staggers the imagination and daunts analysis. Thus one can easily imagine corresponding feedback diagrams that are far more intricate than in Fig. 5.2b.

The types of phenomena that could emerge from such intricate networks of closed causal loops – spanning several levels of both the biological and cognitive hierarchies – are yet only dimly imagined, but some theoretical work is underway. Building on the seminal work of Eigen and Schuster on the emergence of life [8], several scientists are attempting to formulate relationships among levels of a nonlinear dynamic hierarchy in a manner that is suitable for mathematical analysis [4, 11, 23, 32]. This is not a trivial matter because the time and space scales for models of living creatures differ by many orders of magnitude as one goes from the biochemical levels to the whole organism, creating a challenge for the numerical modeler. Are there ways to evade such computational constraints? Might hierarchically organized functions be defined on nested sets of points, with different rules of averaging at various stages of the computations? Is it possible to resolve key issues without resorting to mind-numbing numerical computations?

In conclusion, consider two questions.

- Can one comprehend the nature of life without lapsing into nineteenth-century (Bergsonian) vitalism?
- Is it possible to provide a credible explanation of human consciousness without resorting to Cartesian dualism?

In response to the first question, few biologists now doubt that the phenomena of life – including both its emergence from the chemical scum of the Hadean seas and its subsequent evolution – will eventually be understood as a complex process comprising many closed causal loops and networks of positive feedback that thread through several levels of nonlinear dynamics.

Although the answer to the second question is less clear, I have these comments. Accepting physicalism and rejecting substance dualism (as I do) does not require me to accept reductionism; indeed, the burden of proof lies with the reductionist. In other words, reductionism is not a conclusion of science but a belief of many scientists, leaving the door open to a property dualism that is rooted in physicalism. As well as substance dualism, this property dualism may allow the phenomena of human consciousness to emerge from interactions among myriad positive feedback networks that engage many levels of both the biological and the cognitive hierarchy.

Understanding the nonlinear dynamics of such intricate emergent structures is a central task for twenty-first century science.

Acknowledgement. It is a pleasure to thank the organizers and participants of the (October 2003) conference on “Reductionism and Emergence: Implications for the Science/Theology Dialogue” at the University of San Francisco for providing an environment in which these ideas were critically evaluated. A somewhat different version of this chapter has recently appeared in the *Journal of Consciousness Studies* [28].

References

1. Andersen, P.B.; Emmeche, C.; Finnemann, N.O.; and Christiansen, P.V. (2000). *Downward Causation: Minds, Bodies and Matter*, Aarhus University Press, Aarhus, Denmark.
2. Anderson, P.W. (1972). *Science* **177**:393–396.
3. Aristotle. (1953). *The Physics* (translated by PH Wicksteed and FM Cornford), Harvard University Press, Cambridge, and William Heinemann Ltd, London.
4. Baas, N.A. (1994). In *Artificial Life III*, Langton, C.G. (ed.), Addison-Wesley, Reading.
5. Bickhard, M.H. and Campbell, D.T. (2000). In [1].
6. Bunge, M. (1979). *Causality and Modern Science*, 3rd edn, Dover, New York.
7. Crandall, R.E. (1997). *Sci. Am.* February:72–78.

8. Eigen, M. and Schuster, P. (1979). *The Hypercycle: A Principle of Natural Self-Organization*, Springer-Verlag, Berlin.
9. Elsasser, W.M. (1998). *Reflections on a Theory of Organisms: Holism in Biology*, The Johns Hopkins University Press, Baltimore (first published in 1987).
10. Emmeche, C.; Køppe, S. and Stjernfelt, F. (2000). In [1].
11. Fontana, W. and Buss, L.W. (1994). *Bulletin of Mathematical Biology* **56**:1–64.
12. Fraser, J.T. (1982). *The Genesis and Evolution of Time*, Harvester Press, Brighton, England.
13. Fraser, J.T. (1990). *Of Time, Passion, and Knowledge: Reflections on the Strategy of Existence*, 2nd edn, Princeton University Press, Princeton.
14. Goodwin, B. (1994). *How the Leopard Changed its Spots: The Evolution of Complexity*, Scribner's, New York.
15. Gould, S.J. (1989). *Wonderful Life: The Burgess Shale and the Nature of History*, W.W. Norton & Co., New York.
16. Hebb, D.O. (1949). *Organization of Behavior: A Neuropsychological Theory*, John Wiley & Sons, New York.
17. Hebb, D.O. (1980). In *The Nature of Thought*, Jusczyk, P.W. and Klein, R.M., (eds.), Lawrence Erlbaum Associates, Hillsdale, NJ:19–35.
18. Hebb, D.O. (1980). *Essay on Mind*, Lawrence Erlbaum Associates, Hillsdale, NJ.
19. Kauffman, S. (1993). *The Origins of Order: Self-Organization and Selection in Evolution*, Oxford University Press, Oxford.
20. Kim, J. (2000). *Mind in a Physical World*, MIT Press, Cambridge.
21. Kim, J. (2000). In [1].
22. Margulis, L. and Sagan, D. (1995). *What Is Life?* Simon & Schuster, New York.
23. Nicolis, J.S. (1986). *Dynamics of Hierarchical Systems: An Evolutionary Approach*, Springer-Verlag, Berlin.
24. Poincaré, H. (2001). *Science and Method*, St. Augustine's Press, Chicago (first published in 1903).
25. Scott, A.C. (1995). *Stairway to the Mind*, Springer-Verlag, New York.
26. Scott, A.C. (2002). *Neuroscience: A Mathematical Primer*, Springer-Verlag, New York.
27. Scott, A.C. (2003). *Nonlinear Science: Emergence and Dynamics of Coherent Structures*, 2nd edn, Oxford University Press, Oxford.
28. Scott, A.C. *Journal of Consciousness Studies* **11**(2):51–68.
29. Scott, A.C. (ed.), (2004). *Encyclopedia of Nonlinear Science*, Taylor and Francis (Routledge), New York.
30. Tegmark, M. (2000). *Physical Review E* **61**:4194–4206.
31. Turing, A.M. (1952). *Philosophical Transactions of the Royal Society London B* **237**:37–72.
32. Voorhees, B.H. (1983). *Behavioral Science*. **28**:24–34.
33. Weinberg, S. (1992). *Dreams of a Final Theory: The Search for the Fundamental Laws of Nature*, Pantheon Books, New York.
34. Wiener, N. (1961). *Cybernetics*, John Wiley & Sons, New York.
35. Winfree, A.T. (1987). *When Time Breaks Down: The Three-Dimensional Dynamics of Electrochemical Waves and Cardiac Arrhythmias*, Princeton University Press, Princeton.
36. Winfree, A.T. *The Geometry of Biological Time*, Springer-Verlag, New York.
37. Zurek, W.H. (1991). *Physics Today*, October:36–44.

6 Consciousness, Neurobiology and Quantum Mechanics: The Case for a Connection

Stuart Hameroff

Summary. Consciousness is generally considered to emerge from synaptic computation among brain neurons, but this approach cannot account for its critical features. The Penrose–Hameroff “Orch OR” model suggests that consciousness is a sequence of quantum computations in microtubules within brain neurons, shielded from decoherence to reach threshold for objective reduction (OR), the Penrose quantum gravity solution to the measurement problem. The quantum computations are “orchestrated” by neuronal/synaptic inputs (hence “Orch OR”), and extend throughout cortex by tunneling through gap junctions. Each Orch OR is proposed as a conscious event, akin to Whitehead’s philosophical “occasion of experience”, occurring in concert with brain electrophysiology. This chapter discusses the need for such an approach and its neurobiological requirements.

6.1 Introduction: The Problems of Consciousness

Consciousness involves phenomenal experience, self-awareness, feelings, choices, control of actions, a model of the world, etc. But what is it? Is consciousness something specific, or merely a byproduct of information processing? Whatever it is, consciousness is a multifaceted puzzle. Despite enormous strides in behavioral and brain science, essential features of consciousness continue to elude explanation. Unresolved problems include:

1. Neural correlates of conscious perception apparently occur too late – 150 to 500 milliseconds (ms) after impingement on our sense organs – to have causal efficacy in seemingly conscious perceptions and willful actions, often initiated or completed within 100 ms after sensory impingement. For example, in the color phi and cutaneous rabbit anomalies, the brain apparently fills in conscious sensory information that is not yet available [130, 71, 40]. Preparation of speech can precede conscious identification of heard words to which one is responding [247, 248, 241]. And in tennis, specific movements to return a fast-moving ball precede conscious identification of ball location and trajectory [157, 81].¹ Nonetheless, sub-

¹ Visual information apparently flows from V1 in two streams [239, 160]. The dorsal stream from V1 to posterior parietal cortex is thought to provide visual

jectively (i.e. we feel as though) we consciously perceive and respond to these perceptions (e.g. [247, 81, 129]).

2. How does the brain provide binding: fusion of a) aspects in one modality (e.g. visual shape, color and motion), b) different modalities (e.g. sight and sound), c) temporal binding of synchronous events sensed asynchronously (e.g. sight and touch) and d) allocentric (simulated external world), egocentric (personal point of view) and enteroceptive (bodily sensation) spaces into unified conscious moments [81]?
3. Electrophysiological correlates of consciousness and attention (e.g. gamma EEG/coherent 40 Hz) may be incompatible with the presumed neural-level correlate of consciousness—trains of axonal action potentials (spikes)—and network-level correlate of consciousness—Hebbian assemblies of axonal-dendritic neurotransmitter-mediated synaptic networks.
4. The vast majority of brain activity is nonconscious. What distinguishes nonconscious activity from consciousness?
5. The hard problem: how does the brain produce qualia, the raw components of phenomenal experience—the smell of a rose, the felt qualities of emotions and the experience of a stream of conscious thought? Why is there conscious experience associated with the brain at all (e.g. [28])?

Prevalent approaches assume that consciousness arises from information processing in the brain, with the level of relevant detail varying among philosophical stances. Generally, all-or-none firings of axonal action potentials (spikes) are seen as the fundamental currency of brain function and equated to roles performed by unitary information states and switches in computers [31]. Consciousness is said to emerge from complex computation: nonlinear dynamics of axonal-dendritic neuronal networks sculpted by modulation of spike-mediated chemical synapses (Hebbian assemblies) form metastable patterns—attractors—identified with conscious experience (e.g. [198, 55, 56]).

I will refer to all contemporary approaches (perhaps unfairly) as classical functionalism. The implication is that if a robot were precisely constructed to mimic the brain activities that orthodox neuroscience assumes to be relevant to consciousness and perform functions that in a human being are associated with consciousness, then the robot would be conscious regardless of the material from which it was made.

Classical functionalist explanations of the problems stated above are (roughly):

1. Near-immediate conscious perception and volition are illusions; nonconscious processes initiate many actions (e.g. [247, 128, 256]).

information for online, nonconscious control of many kinds of actions. This pragmatic representation for immediate goal-directed behavior is created faster than the ventral stream semantic representation that corresponds with consciousness. The assumption is that the brain creates an illusion of conscious control of such dorsal stream-mediated actions.

2. Binding, e.g. temporal binding in Dennett's [39] multiple drafts model, results from edited memory, rather than real-time unified conscious perception.
3. Electrophysiological activities measured from scalp, brain surface or within brain extracellular spaces (e.g. gamma EEG/coherent 40 Hz, Sect. 6.3.4) that seem to correlate with cognition and consciousness are discredited, apparently because axonal spikes fail to account for synchrony [204, 34].
4. Nonconscious processes compete, with the content of the most active (or optimally synchronized) neuronal groups winning to gain consciousness (e.g. [39]).
5. Conscious experience is an emergent property of functional information processing (e.g. [198, 55]).

Consequently, classical functionalism deconstructs consciousness into an out-of-the-loop, after-the-fact illusory set of epiphenomena.² While this might prove true, the view is a default position due to lack of credible alternative and (I will argue) faulty assumptions. Neuronal activities presumed to be relevant are tailored to fit the computer analogy, omit essential neurobiological ingredients and miss the target³. Specifically, I will argue that axonal spikes and chemical synaptic transmissions are not the primary currency of consciousness, that electrophysiological correlates of consciousness derive from dendritic activities linked by window-like gap junctions, that glia are involved and that quantum processes in intradendritic cytoskeletal microtubules are the actual substrate for consciousness.

Twelve years ago Roger Penrose and I put forth a model called orchestrated objective reduction (Orch OR) based on quantum computation in cytoskeletal microtubules inside the brain's neurons⁴ [174, 89–92, 264]. Orch OR has been viewed skeptically by mainstream scientists and philosophers. One apparently valid reason to discount Orch OR is that technological quan-

² Epiphenomenal in this case refers to the type of immediate actions that may be reflexive (e.g. dorsal stream-mediated) but seem conscious to the one performing them. Those who ascribe such actions to nonconscious activities (e.g. [129, 81, 142]) argue that consciousness plays important causal roles in other functions, e.g. veto, comparisons and longer-term planning and behaviors.

³ Some scientists and philosophers do consider finer-grained details. For example, Koch [129] raises the issue of intracellular calcium ions in the context of the neural correlate of consciousness, but maintains that axonal spike are the primary medium. Chalmers [28] points out that even if the precise activity and state of every receptor, ion and molecule in the brain were known, the cause of conscious experience would not be explained. However, I will argue that certain types of organized quantum processes in the brain can account for conscious experience based on a Whiteheadian pan-protopsychist philosophy tied to modern physics.

⁴ The original motivation put forth by Penrose [170, 171] was based on noncomputability (i.e. nonalgorithmic processes) of human thoughts and choices, as argued through Gödel's theorem.

tum computation is designed to occur in isolation at extremely low temperatures to avoid decoherence – disruption of seemingly fragile quantum states by thermal/environmental interactions. Thus quantum computing at brain temperature in an apparently liquid medium appears impossible. However, quantum processes in biological molecules not only occur, but are enhanced at higher temperature [167]. Furthermore, the neuronal interior can exist in an isolated, nonliquid gelatinous ordered state ([179], Sect. 6.5.2). Another objection – that quantum states inside one neuron could not extend to others across cellular boundaries – prompted the suggestion that quantum tunneling through window-like gap junctions (which essentially fuse neurons into hyperneurons, Sect. 6.3.5) could enable such extension. Gap-junction networks are now shown to be widely prevalent in the brain and to mediate gamma EEG/coherent 40-Hz neuronal activity, the best electrophysiological correlate of consciousness (Sect. 6.3.4). Finally, Orch OR has been discounted because it differs so markedly from conventional approaches, despite 1) the lack of progress by conventional explanations, and 2) Orch OR being perfectly consistent with neurobiology. Ten years after, known neurobiology has moved toward Orch OR.

In this chapter connections among consciousness, neurobiology and quantum mechanics are proposed. They are previewed here:

Consciousness and neurobiology (Sect. 6.3): Consciousness occurs in dendrites of cortical neurons interconnected by gap junctions, forming Hebbian “hyperneurons”. Chemical synapses and axonal spikes convey inputs to, and outputs from, conscious processes in hyperneuron dendrites, consistent with gamma EEG/coherent 40 Hz and the postsynaptic mechanism of general anesthesia. The molecular correlate of consciousness is the intradendritic cytoskeleton, specifically microtubules and related proteins whose information processing triggers axonal spikes and regulates synapses.

Neurobiology and quantum mechanics: Quantum superposition, entanglement and other effects (Sects. 6.4.3 and 6.4.4) are considered to wash out at supramolecular levels due to environmental interactions (decoherence). However, certain proteins act as quantum levers whose functional conformational states are governed by weak quantum forces. Such proteins mediate effects of anesthetic gases that impair the quantum forces, erasing consciousness, while sparing other brain activities. Thus, only proteins directly involved in consciousness are quantum levers (which can function as quantum bits, or qubits in quantum computation). Evidence suggests that mechanisms have evolved to counter decoherence and enable large-scale quantum states in the brain at 37.6 °C.

Quantum mechanics and consciousness (Sect. 6.5.1): The conscious observer has been implicated in quantum mechanics since its inception. Experiments show that quantum superpositions (particles/systems existing in multiple states or locations simultaneously, governed by a quantum wave function) persist until measured or observed, then reduce/collapse to definite states and

locations. Interpretations vary: in one form of the Copenhagen interpretation the conscious observer causes collapse/reduction of quantum superpositions, placing consciousness outside physics. David Bohm (e. g. [20]) proposed that the wave function contains active information that guides the movement of particles, and that consciousness was associated with active information. Like Bohm, the multiple-worlds hypothesis [50] avoids collapse/reduction but requires an infinity of minds for each individual⁵. Decoherence theory avoids isolated superpositions (and consciousness). Henry Stapp's view [221] identifies consciousness with collapse/reduction but doesn't specify a cause or distinction. The objective reduction (OR) of Roger Penrose identifies consciousness with collapse/reduction, specifies a cause and threshold, and connects consciousness to fundamental space-time geometry, introducing mechanisms for noncomputable Platonic influences and protoconscious qualia. And like Stapp's view, Penrose OR connects to Whitehead's philosophical approach to consciousness.

We begin with a consideration of the timing of conscious experience.

6.2 Time and Consciousness

6.2.1 Is Consciousness Continuous or a Sequence of Discrete Events?

William James [112] initially considered consciousness as a sequence of specious moments but then embraced a continuous stream of consciousness. Alfred North Whitehead [257, 258] portrayed consciousness as a sequence of discrete events: occasions of experience. As motion pictures – in which sequential frames are perceived as continuous – became increasingly popular, so did the notion of consciousness as discrete events, e. g. the perceptual moment theory of Stroud [205, 224]. Evidence in recent years suggests periodicities for perception and reaction times in the range of 20 to 50 ms (gamma EEG) and another in the range of hundreds of ms (alpha and theta EEG), the latter consistent with saccades and the visual gestalt [242, 243]. Based on a proposal for memory by Lisman and Idiart [145], VanRullen and Koch [242] suggested a multiplex for visual perception in which a series of fast gamma waves (each corresponding to specific components of vision) rides on a slower, e. g. theta wave (corresponding to an integrated visual perception). A similar, previous model of gamma/theta complex waves supporting quantum mechanisms underlying conscious vision [264] will be discussed in Sect. 6.8.1. Freeman [57] has shown cinematographic effects in neural excitations in the brain, supporting the notion of discrete conscious frames.

If consciousness is a sequence of events, what is its rate or frequency? Can it vary? In the midst of a car accident, victims often report that time

⁵ Or a single universal mind. See Squires [219].

seems to slow down. Does this excited state involve an actual increase in the rate of subjective conscious moments per objective time? What *are* conscious moments, why are they subjective and how do they relate to neurobiology?

6.2.2 The Timing of Conscious Experience

Many behaviors apparently happen too quickly to be initiated by consciousness. Max Velmans [247] lists examples: analysis of sensory inputs and their emotional content, phonological and semantic analysis of heard speech and preparation of one's own spoken words and sentences, learning and formation of memories, and choice, planning and execution of voluntary acts. Consequently, subjective feeling of conscious control of these behaviors is deemed illusory [256].

In speech, evoked potentials indicating conscious word recognition occur at about 400 ms after auditory input, however, semantic meaning is appreciated (and response initiated) after only 200 ms. As Velmans points out, only two phonemes are heard by 200 ms, and an average of 87 words share their first two phonemes. Even when contextual effects are considered, semantic processing and initiation of response occurs before conscious recognition [241].

Jeffrey Gray [81] observes that in tennis “The speed of the ball after a serve is so great, and the distance over which it has to travel so short, that the player who receives the serve must strike it back before he has had time consciously to see the ball leave the server’s racket. Conscious awareness comes too late to affect his stroke”. John McCrone [157]: “[for] tennis players... facing a fast serve ... even if awareness were actually instant, it would still not be fast enough ...”

Visual recognition of an object’s shape, color, motion and semantic meaning occur in different parts of visual cortex, and at different times [270, 269]. Yet we consciously perceive these features simultaneously (the temporal binding problem).

Touch also involves temporal binding. If you tap your foot with your finger, the foot and finger sensations occur simultaneously. Yet the sensory signal from your foot requires significantly longer to reach sensory cortex than does that from your finger. How does the brain provide synchrony?

In the cutaneous rabbit experiment [71, 72] a subject’s arm is mechanically “tapped” at three locations along the arm, e. g. 5 taps at the wrist followed by 2 at the elbow then 3 more on the upper arm. However, subjects report a regular sequence of taps traveling in equidistant increments, as if a small animal were hopping along their arm. The “departure” from the wrist begins with the second tap, yet if the upper taps are not delivered, all 5 wrist taps are felt at the wrist. It is as if the brain knows in advance there will be (or not be) taps further along the arm.

In the “color phi” effect [130] a red spot appears briefly on the left side of a screen, followed after a pause by a green spot on the right side. Ob-

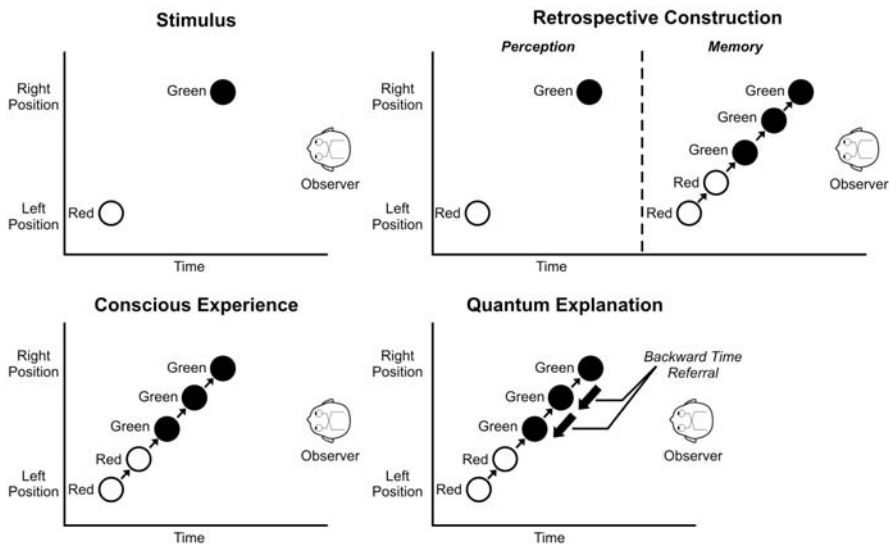


Fig. 6.1. The “color phi” phenomenon [130]. *Top left:* an observer views a screen on which a red circle appears on the left, disappears, and then a green circle appears on the right. *Bottom left:* the observer’s conscious (reported) experience is of a red circle moving from left to right, changing to green half-way across. *Upper right:* the retrospective construction explanation is that the observer’s real time perception is of two separate circles, subsequently revised and recorded in (delayed) memory as the red circle moving and changing to green half-way across. *Bottom right:* Quantum explanation in which the brain sends subconscious quantum information backward in time, filling in the red circle changing to green half-way across

servers report one spot moving back and forth, changing color half-way across (Fig. 6.1). Does the brain know in advance to which color the dot will change?

Perhaps the most perplexing experiments regarding time and mental events were done by Benjamin Libet and colleagues in the 1960s and 1970s. They studied awake, cooperative patients undergoing brain surgery with local anesthesia so that the patients’ brains were exposed (e.g. [136, 138, 142]). In these patients Libet was able to access, identify, record from and stimulate specific areas of somatosensory cortex (postcentral gyrus) corresponding to the skin of each patient’s hand (Fig. 6.2). He found that direct electrical stimulation of the somatosensory “hand” area of cortex resulted in brain electrical activity (DCR: direct cortical response due to neuronal dendritic activity). This in turn caused conscious sensation referred to the hand, but only after a train of threshold-level pulses (and DCR activity) lasting about 500 ms. This requirement of ongoing, prolonged electrical activity from direct cortical stimulation to produce conscious experience (“Libet’s 500 ms”) was confirmed by Amassian et al. [5], Ray et al. [187], Pollen [180] and others.

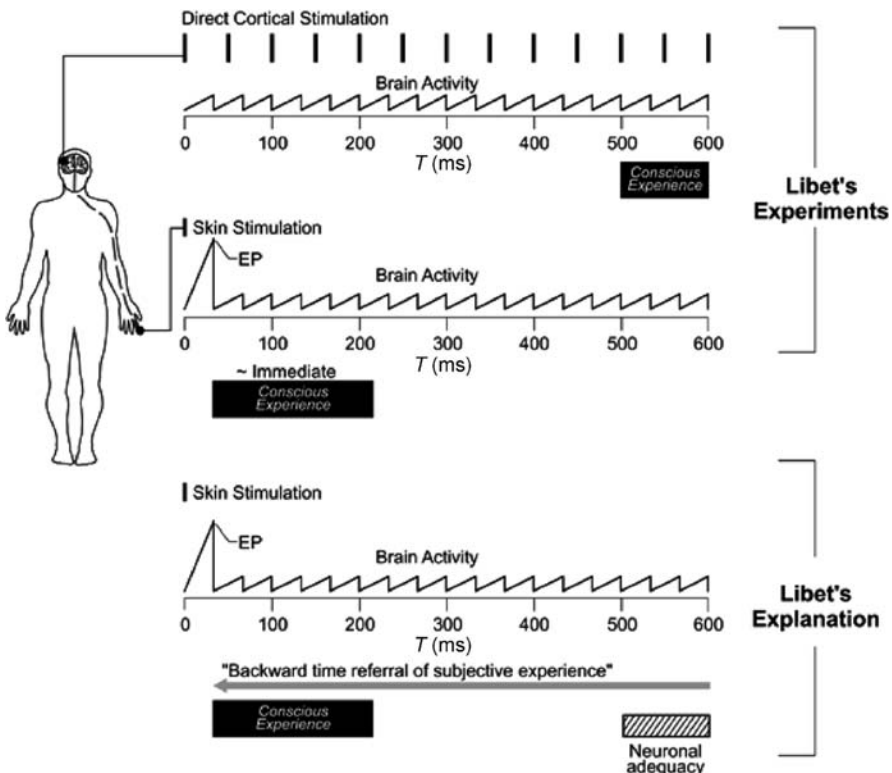


Fig. 6.2. Libet's experiments and explanation [138, 142]. Patient (*left*) was accessed 1) at hand area of somatosensory cortex, and 2) skin of corresponding hand. *Top:* Direct cortical stimulation of electrical pulses every 50 ms caused cortical brain activity that was required to proceed for 500 ms to cause conscious experience of a sensation in the hand. *Middle:* Single pulse to the skin of the hand caused primary evoked potential (EP) after 10 to 30 ms and ongoing brain activity for at least 500 ms. Conscious experience occurred concomitant with primary EP. *Bottom:* Libet's explanation – 500-ms ongoing activity required for neuronal adequacy, which refers subjective experience backward in time to the primary EP

But what about normal sensory perception? Single, threshold-level stimuli to the hand or elsewhere are seemingly perceived consciously almost immediately; no 500-ms delay occurs when we touch something. In the brain somatosensory cortex, threshold level stimuli at the skin of the hand cause a primary evoked potential (EP) 10 to 30 ms after skin stimulation, followed by ongoing activity of several hundreds of ms, very much like Libet's DCR.

But the primary EP is not sufficient for conscious experience:

- A single stimulus delivered to subcortical brain regions in the sensory pathway causes a primary EP without conscious experience or prolonged activity [139, 113]⁶.
- Subthreshold skin stimulation causes a primary EP, but no prolonged cortical activity nor conscious experience.
- Under general anesthesia, skin stimulation of any kind can cause a primary EP but no ongoing cortical activity nor conscious experience.
- On the contrary, prolonged cortical activity (“Libet’s 500 ms”) is both necessary and sufficient for conscious experience, but in the absence of a primary EP produces only delayed conscious experience.
- Libet’s DCR patients (also Amassian et al. [5], Ray et al. [187]) had 500-ms delayed conscious experience of skin stimulation without a primary EP caused by a train of pulses delivered to the cortex. Pollen [180] showed a similar delay with visual phosphenes after occipital cortex stimulation.

Libet’s conclusion was that the 500-ms prolonged cortical activity is the *sine qua non* for conscious experience – the NCC, or neural correlate of consciousness. The primary EP is necessary (but not sufficient) for near-immediate conscious experience⁷. Primary EP and prolonged activity together produce near-immediate conscious experience.

But if the neural correlate of conscious experience is delayed for 500 ms, how/why do we seem to perceive sensory events almost immediately? Are we living in the past, but remembering (falsely) being in the here and now, as Dennett suggests (next section)? To address the question, Libet and colleagues proposed and tested a rather outrageous hypothesis – that the perception of a stimulus was indeed delayed for 500 ms of brain activity but subjectively referred backward in time to the primary evoked potential 10 to 30 ms after stimulus.

Experiments were performed in which patients received both direct cortical stimulation of the hand area and stimulation of the actual skin of the hand. Although both were perceived in the hand, the two were qualitatively different so the subjects could distinguish them. Stimulation of the two sites were given in close, but varying temporal proximity (i. e. within one second), and the patients asked which stimulus was felt first. The patients reported that the sensations generated at the skin appeared before the cortically induced sensation, even when the skin pulse was delayed by some hundreds of ms after the start of the cortical stimulation. Only when the skin pulse

⁶ Repetitive subcortical stimulation does cause a primary EP, prolonged activity and conscious experience.

⁷ Libet contended that the duration per se of the pulse train and DCR was the critical factor in reaching threshold for consciousness, and that the delay was useful for psychic modification. Freud and many others have recognized that conscious experience may differ from raw sensory perception (or be repressed entirely). The delay would permit such modification (e. g. retrospective construction – Sect. 6.2.3).

was delayed for about 500 ms after the cortical stimulation did the subjects report feeling the two stimuli simultaneously. The skin-induced experience appeared to have no delay. The cortically induced experience was delayed 500 ms relative to the skin-induced sensation.

So both skin-induced and cortically-induced sensations required 500 ms of cortical processing, but the skin-induced sensation was experienced almost immediately. Unlike the cortically-induced experience the skin-induced sensation was marked by a primary EP. Was that the difference?

To investigate this question, Libet also studied patients with electrodes implanted (for therapeutic purposes) in the medial lemniscus below the thalamus, i. e. in the brain's sensory pathway en route from hand to cortex. He determined that stimulation of the medial lemniscus could produce a conscious experience only after 500 ms of stimulation and cortical activity. But unlike direct cortical stimulation (and like skin stimulation) medial lemniscus stimulation caused primary EPs. Libet and his colleagues then performed another set of experiments comparing stimulation of the hand with stimulation of medial lemniscus, coupling the two stimuli at varying time intervals. They found no delay of the medial lemniscus stimuli compared to skin stimuli. But the patients felt nothing if medial lemniscus stimulation was interrupted prior to the full 500-ms stimulation. So prolonged cortical activity was necessary for conscious experience, and the primary EP was necessary for near-immediate subjective experience.

Libet came to the following conclusions:

- Conscious perception requires brain activity for 500 ms to achieve neuronal adequacy.
- Information is referred up to 500 ms backward in time to the primary evoked potential – 10 to 30 ms after peripheral stimulation – for near-immediate conscious perception.

Libet's results and conclusions have been repeatedly challenged but never refuted [140, 141]¹⁸.

6.2.3 Taking Backward Time Referral Seriously

How do we resolve these temporal anomalies? The color phi effects apparently "... leave us a choice between a retrospective construction theory and a belief in clairvoyance" [76].

Daniel Dennett [39, 40] chose retrospective construction in the context of a multiple drafts model in which sensory inputs and cognitive processing

¹⁸ For example Pockett [177], Breitmeyer [22], Pollen [180] and others argued that some type of facilitated buildup, or inhibition followed by excitation delayed the onset of effective cortical activity until late in the 500 ms, suggesting the delay in conscious experience was artifactual. However, Libet [140, 141] successfully rebutted these contentions and defended his results and conclusions.

produce tentative contents under continual revision. A definitive, final edition is inserted into memory, overriding previous drafts. A key feature is that consciousness (e.g. of a particular perception) occurs not at any one specific moment, but arbitrarily in time, like the onset of fame, or end of a war. The brain retrospectively creates content or judgment, e.g. of intervening movement in the color phi experiment⁹.

According to retrospective construction (I presume): 1) tennis players see and hit balls unconsciously, but remember seeing and hitting consciously.¹⁰ 2) Sensory components of objects or events are perceived asynchronously but remembered as being synchronous. 3) In the cutaneous rabbit experiment, the subjects feel wrist taps, then elbow taps, then upper arm taps, but remember a sequence of evenly spaced taps. 4) In the color phi phenomenon the observer sees the left-side red spot, then the right-side green spot, but remembers the red spot moving and changing colors midstream.

Thus according to Dennett and many others, smooth, real-time conscious experience is an edited construction – an illusion. Dennett and Kinsbourne [40] have a more difficult time dispensing with Libet's findings, describing them as “interesting but inconclusive”.

Libet performed other experiments related to volition. Kornhuber and Deecke [131] had recorded over premotor cortex in subjects who were asked to move their finger randomly, at no prescribed time. They found that electrical activity preceded finger movement by 800 ms, calling this activity the readiness potential. Libet et al. [143] repeated the experiment except they also asked subjects to note precisely when they consciously decided to move their finger. This decision came approximately 200 ms before movement, hundreds of ms after onset of the readiness potential. Libet concluded that many seemingly conscious actions are initiated by nonconscious processes.

Libet didn't consider backwards referral in volition because antedating in his sensory experiments was pinned to the primary sensory EP, and no such marker existed in the spontaneous finger movement experiments. However,

⁹ Dennett describes two possible methods of disinformation the brain might utilize in resolving temporal anomalies. The first is the Stalinesque show trial, in which the brain modifies sensory information before it reaches consciousness. For example, in the color phi experiment the red spot and the green spot are unconsciously perceived, and interstitial moving spots that change midway are inserted before the sequence reaches consciousness. In Orwellian revisionism, both the red spot and green spot are consciously perceived, but intervening movement and color change are inserted into the final draft for memory. Dennett claims that because of the arbitrary timing in multiple drafts, no distinction between the two methods need be made. However, if the time factor in consciousness is not arbitrary, Dennett's choice of retrospective construction becomes equivalent to Orwellian revisionism.

¹⁰ The actual contact of ball against racket or bat is rarely, if ever, seen. I am referring to conscious recognition of the ball, its approach and initiation of the stroke or swing.

voluntary acts in response to stimuli (hitting a ball, choosing a word in a sentence) do have such markers, as would binding of temporally asynchronous perceptual components of synchronous events. Nor did Libet consider backward referral as implying an actual reversal in time, but a phenomenon akin to retrospective construction. Libet [137, p.7] says:

“...the timing of a sensation is subjectively referred...not that the conscious sensation itself jumped backwards in time...the content of the subjective experience...is modified by the referral to the earlier timing signal.”

But consciousness lagging a half second behind reality would render it largely epiphenomenal (and illusory)¹¹. We would be (in the words of T.H. Huxley) “helpless spectators”. Perception would be a jangle of disconnected events edited for memory, too late for conscious control of many seemingly conscious actions. Perhaps so, but is there a possible alternative?

Yes. To account for Libet’s results, Roger Penrose ([170], cf. [259]) suggested that the brain sends unconscious quantum information backward through time. In the quantum world, time is symmetrical, or bidirectional (as it also appears to be in unconscious dreams – Sect. 6.6)¹². Aharonov and Vaidman [1] proposed that quantum-state reductions send quantum information backward in time; backward time referral is the only apparent explanation for experimentally observed EPR effects in quantum entanglement (Fig. 6.3, Sect. 6.5.1, Penrose [173], cf. [15]).

Quantum information cannot actually convey information, and is thus a misnomer (Penrose now calls it “quanglement” because of its role in quantum entanglement). Quanglement can only modify classical information, but mere modification is highly significant in EPR experiments and quantum technology (Sect. 6.5). Quantum information/quanglement going backward in classical time is also constrained by possible causality violations, i. e. causing an observable change resulting in a paradox like going back in time to kill your ancestor, thereby preventing your birth. Any effect that could be even possibly measured or observed may be prohibited. However, nonconscious backward referral of quantum information/quanglement that modifies existing information in the brain at the moment of consciousness (e. g. adding qualia to primary evoked potentials, influencing choices) would not violate causality because the effects are unobservable before they occur.¹³

¹¹ Gray [81] suggests that consciousness serves a longer-term review and planning function, and Libet [142] suggests a veto role for consciousness. Thus consciousness would not be useless. But in terms of real-time executive actions, consciousness would indeed be epiphenomenal.

¹² The second law of thermodynamics may not operate in the quantum world.

¹³ The problem of qualia has been framed in the well-known “knowledge argument” put forth by philosopher Frank Jackson [111]. He described a hypothetical color-blind visual neuroscientist named Mary who knew all facts related to color vision but had never experienced color. If Mary then received a retinal

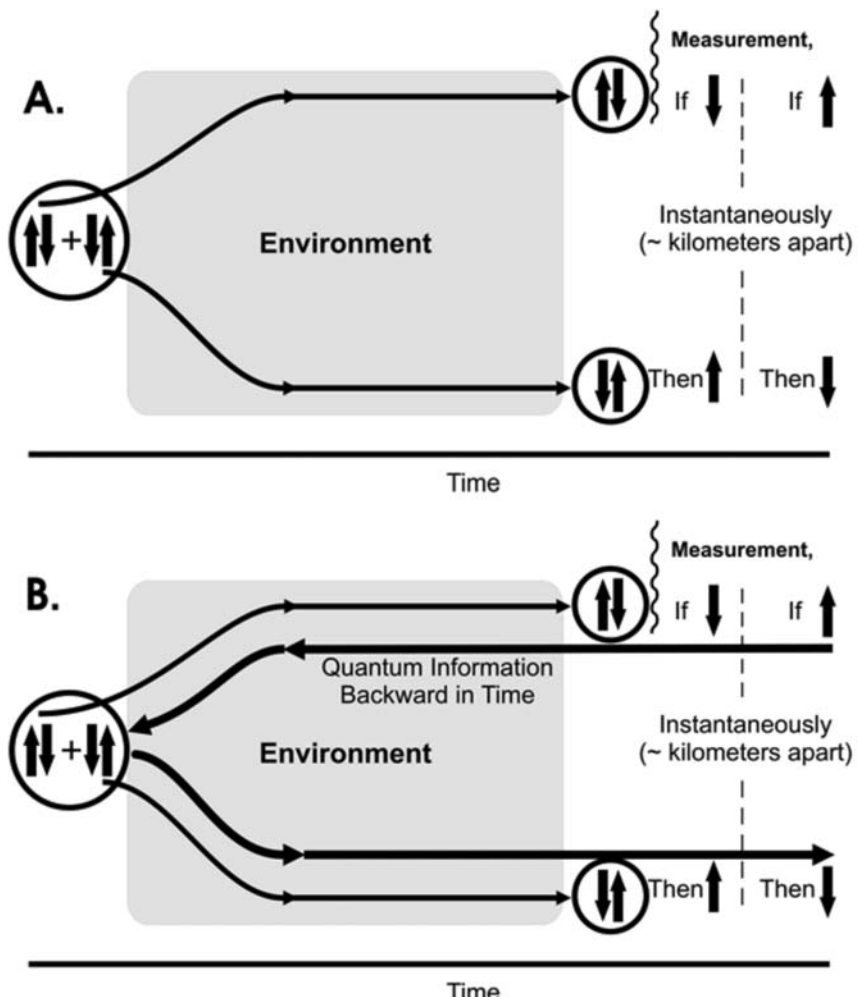


Fig. 6.3. Backward time in the EPR effect. A. The Einstein–Podolsky–Rosen (EPR) experiment verified by Aspect et al. [10], Tittel et al. [232] and many others. On the left is an isolated entangled pair of superpositioned complementary quantum particles, e.g. two electrons in spin-up and spin-down states. The pair is separated and sent (through environment but unmeasured) to different locations/measuring devices kilometers apart. The single electron at the top (in superposition of both spin-up and spin-down states) is measured, and reduces to a single classical state (e.g. spin-down). Instantaneously, its complementary twin kilometers away reduces to the complementary state of spin-up (or vice versa). The effect is instantaneous over significant distance, hence appears to be transmitted faster than the speed of light. B. The explanation according to Penrose ([173], cf. [15]) is that measurement/reduction of the electron at the top sends quantum information backward in time to the origin of the unified entanglement, then forward to the twin electron. No other reasonable explanation has been put forth

Backward time referral of unconscious quantum information/quanglement in the brain could provide temporal binding and near-immediate perception and volition, rescuing consciousness from illusory epiphenomenon (i.e. enabling near-immediate conscious decisions based on sensory information referred from the near future). How this could actually happen will be discussed in Sect. 6.7, but we next turn to where it could happen – the neural correlate of consciousness.

6.3 The Neural Correlate of Consciousness

6.3.1 Functional Organization of the Brain

Most brain activities are nonconscious; consciousness is a mere “tip of the iceberg” of neural functions. Many brain activities – e.g. brainstem-mediated autonomic functions – never enter consciousness. While consciousness is erased during general anesthesia, nonconscious brain EEG and evoked potentials continue, although reduced.¹⁴

Functional units corresponding to particular mental states are generally considered as networks or assemblies of neurons, originally described by Donald Hebb ([100], see also [199]). Hebb described assemblies as closed causal loops of neurons that could be ignited by particular inputs and remain active for hundreds of ms, following which another related assembly would ignite, then another and so on in a phase sequence. Hebb described assemblies as “three-dimensional fishnets” of many thousands of neurons. At any one time a single particular assembly would be the neural correlate of consciousness (NCC).

Why would a particular assembly be conscious? Dennett’s multiple-drafts model proposes, as does Susan Greenfield’s [82] epicenter model, that brain

transplant, or gene therapy or brain implant to gain color vision, would she be acquiring new facts about color? If so, qualia are facts and no different from information in a computer (as materialists so argue). But quantum information/quanglement could modify the nonconscious (nonqualia) facts/information about color in Mary’s brain to provide the phenomenal experience of color while not conveying classical information. Thus, qualia as quanglement avoids causality violation and can defeat the materialist interpretation of the knowledge argument.

¹⁴ There are unfortunate cases of intraoperative awareness. There can also be implicit learning/memory during light anesthesia. Some authors have conflated these two situations to suggest that anesthesia involves awareness with amnesia, not loss of consciousness. Because consciousness is unobservable there is no absolute resolution of this question. However, there is no reason to believe that intraoperative awareness occurs except during rare instances due to inadequate anesthesia. Clinical signs of pain/awareness (pupillary size, heart rate and blood pressure, lacrimation, diaphoresis, mucus secretion, EEG power spectrum/40 Hz, etc.) are used to indicate adequate anesthesia and lack of consciousness.

activity accompanying consciousness is the same in kind as unconscious brain activity, except more so. Regardless of location, if activity of a neural assembly representing a specific set of content exceeds all other in some type of competition, it takes the prize of entering into consciousness.

The precise neural activity accompanying consciousness remains to be elucidated. Global workspace theory describes *where* it is likely to occur: multiple specialized brain areas interconnected in a coordinated, though variable manner. Bernie Baars [12] introduced the concept that was elaborated anatomically by Changeux and Dehaene [29] (see also [38]). Crick and Koch [33], and Edelman and Tononi [48] have similar approaches.

Global workspace describes a horizontal layer of interconnected cortical neurons sandwiched between ascending, bottom-up inputs from thalamus and basal forebrain, and top-down executive functions from prefrontal cortex.¹⁵ Bottom-up inputs convey sensory information, as well as general arousal and highlighted saliency such as emotional context from basal forebrain inputs [261, 263]. Top-down influences categorize and manipulate unexpected features [129], e.g. those associated with danger, reward, etc. Acting together, bottom-up and top-down activations select a neural assembly – a specific subset of cortical-cortical projections – for attention and consciousness, prompting sufficient activity for the assembly to become the NCC. Over time, the NCC and its contents change with dynamically shifting, temporary alliances of neurons and assembly makeup. Global workspace models demonstrate a functional architecture that could accommodate consciousness.

Placing consciousness between bottom-up and top-down neuronal pathways agrees with Ray Jackendoff's [110] intermediate level theory, which notes we are not normally aware of pure sensation, nor of pure conceptual structures, but an optimized admixture of the two. The intermediate level is also consistent with Jeffrey Gray's [79, 80] comparator hypothesis in which consciousness is the output of a process that compares available (e.g. incoming, bottom up) information against anticipatory (executive, top down) schemata.

Evidence from vision supports both Jackendoff's contention and the global workspace theory. Visual inputs synapse in thalamus and project raw data mostly to primary visual area V1 in the posterior occipital cortex. V1 then sends information forward to other regions of visual cortex¹⁶, e.g. V2, where shape and contour are recognized, V4, where color is perceived and V5, where motion is detected. These and other secondary visual areas project to prefrontal cortex for categorization and planning. Prefrontal cortex then projects back toward V1 and other visual areas. Crick and Koch [34] have argued the NCC of vision lies not in V1 or prefrontal cortex but in intermediate areas. In Jackendoff's terms, V1 houses "pure sensation unaffected by conceptual in-

¹⁵ Some accounts include thalamocortical projections as part of the workspace, and parietal cortex in the top-down influences. Also, top-down influences from prefrontal or parietal cortex may loop through the thalamus.

¹⁶ Apparently in two streams: See Footnote 1.

terpretation". Visual consciousness occurs in the middle-shifting assemblies of cortical-cortical projections sandwiched between (but possibly including) V1 and prefrontal cortex.

However, Zeki [268] has shown that excessive activity in any feature-selective region may be sufficient on its own for that feature to enter consciousness. Thus, activity in V4 alone can result in the experience of color.

Other NCC candidates include the hippocampus in Jeffrey Gray's comparator hypothesis, and the brainstem in Antonio Damasio's [35] and Jaak Panksepp's [168] separate views of emotional core consciousness. Thus, while consciousness occurs generally in what is termed a global workspace, it may also arise in more localized and perhaps separate regions. The question remains how/why consciousness arises in any region. What aspect of neural activity gives rise to consciousness?

6.3.2 Cerebral Cortex and Neuronal Assemblies

Cerebral cortex is hierarchical in two different ways [129]. Microscopically, layer 4 receives primary sensory inputs from the thalamus and is thus on the bottom. Geography aside, layers 1–3 and 6 are more or less in the middle. In layer 5 giant pyramidal cells (which convey the verdicts of cortical processing to subcortical regions) are at the top of the hierarchy. This arrangement is nested in a larger-scale anatomical hierarchy with primary sensory areas (such as V1 for vision) at the bottom, and prefrontal executive cortex at the top. Consistent with Jackendoff's intermediate theory, shifting assemblies of many types of neurons sandwiched throughout numerous cortical regions appear to act as the NCC.

Particular Hebbian assemblies may be formed and strengthened primarily by alterations in dendritic morphology leading to enhanced synaptic activity and lowered threshold for specific circuits. Assemblies sculpted by postsynaptic changes – synaptic plasticity – are the cornerstone of theoretical mechanisms for learning, memory and the NCC. The mechanisms of plasticity include altered number, sensitivity and clustering of postsynaptic receptors, optimal geometry of dendritic spines and branchings, dendro-dendritic connections, and changes in decremental conductance of postsynaptic potentials (e.g. Hausser et al. [98]). All these changes are mediated by structures within neuronal dendritic interiors, namely the cytoskeleton (e.g. Dayhoff [37]).

6.3.3 Axons and Dendrites

Since Cajal, the neuron doctrine has been that information flows from an incoming axon across a chemical synapse to a dendrite or cell body of another neuron. When a postsynaptic threshold is met from accumulation of excitations (offset by inhibitions), the second neuron's axon fires and an action potential or spike is triggered at the proximal axon hillock. Mediated

by sodium ion fluxes across membrane channels, spikes propagate along the axon to reach another synapse where they influence release of neurotransmitters. Each neuron has only one axon, though they may branch downstream. Thus multiple postsynaptic inputs are integrated to lead to one output, the all-or-none firing of a spike.¹⁷

Spikes can be quantified by electrodes that traverse or pass near axonal membranes. Thus we know that spike frequency (and possibly patterns) correlates with intensity of stimulus and/or behavior (e.g. Britten et al. [23]). Spikes travel rapidly and are robust, not degrading over long distances. They are widely assumed to be the primary means of signaling and information transfer in the brain, and thus the currency – the neural code – of consciousness. The notion of multiple inputs integrated to a threshold leading to a single output lends itself well to computer analogies. Spike = bit!

However, there are other cellular-level candidates for the NCC. Electrodes on scalp or brain surface detect mostly dendritic dipole potentials from pyramidal cells with axial symmetry, i.e. oriented perpendicular to the brain surface [55]. Electrodes implanted into the brain detect mainly local field potentials (LFPs) generated from cortical interneurons with radial symmetry, linked mostly by dendrodendritic gap junctions and inhibitory chemical synapses. Thus synchrony in the EEG and LFPs derives not from axonal spikes but from dendritic activities. Moreover, the BOLD signal used in fMRI, widely assumed to represent neural metabolic activity related to consciousness, corresponds more closely with LFPs than axonal spikes [147].

Some have argued (e.g. Libet [142], McFadden [156], Pockett [176]) that the brain's complex electromagnetic field (global LFPs and surface potentials) constitutes the NCC. However, as Koch [129] points out, the brain's electromagnetic field per se is a crude and inefficient means of communication. On the other hand, dendritic activities that generate LFPs and/or surface potentials may indeed best represent the NCC. Eccles [47] as well as Pribram [182] suggested that dendrites host consciousness, with axonal spikes conveying the results of consciousness.

Neurotransmitter binding at synaptic receptors changes voltage potentials across dendritic or cell-body membranes, causing either excitatory or inhibitory postsynaptic potentials (IPSPs, EPSPs) and in some cases dendritic action potentials [27, 201]. These are then presumed to summate as membrane potentials to reach threshold for spike initiation at the proximal axon hillock.

However, integration of membrane potentials to trigger spikes is not the full extent of dendritic function. Some cortical neurons have no axons, den-

¹⁷ Axonal sodium channels are activated by membrane voltage potentials and modulated by intracellular cytoskeletal proteins [109, 223]. Sodium channels clustered at the axon hillock are connected to, and regulated by proteins ankyrin and spectrin that link them to underlying microtubules and other cytoskeletal proteins [220, 21].

drites interact with other dendrites (e.g. Isaacson and Strowbridge [108], Sassoè-Pognetto and Ottersen [196]) and extensive dendritic activity may occur without causing spikes. Evidence shows complex logic functions in local dendritic compartments, signal boosting (e.g. at branch points), filtering and changing axon hillock sensitivity [217, 178, 207, 208, 209]. Dendritic membrane fluctuations below spike threshold (generally considered noise) may oscillate coherently across wide regions of brain [9, 51]!

Nor is dendritic processing limited to membrane potentials. Many postsynaptic receptors are metabotropic, sending signals internally into the dendritic cytoskeleton, activating enzymes,¹⁸ causing conformational signaling and ionic fluxes along actin filaments and dephosphorylating microtubule-associated protein 2 (MAP2) that links microtubules into cytoskeletal networks. MAP2 activity is necessary for learning and memory, and is the largest

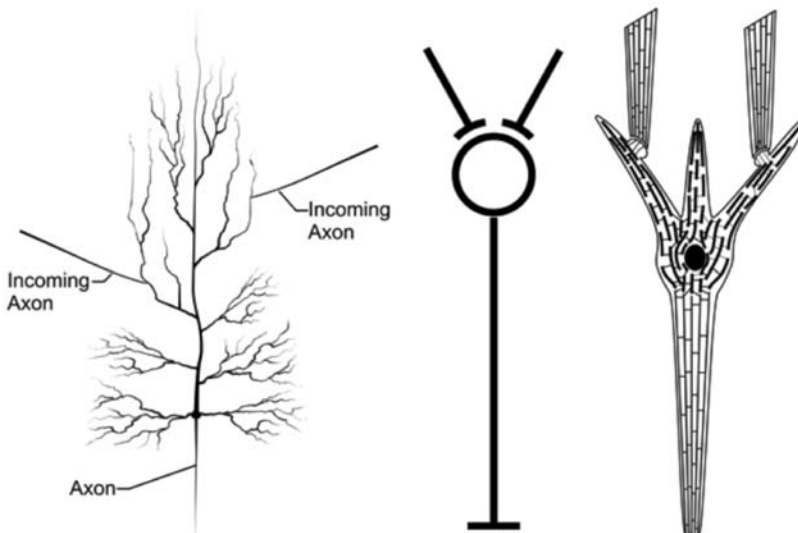


Fig. 6.4. Characterizing neurons. *Left:* Illustration of an actual pyramidal neuron with multiple apical and basilar dendrites (*top and middle*) and a single axon heading downward. Two incoming axons are shown synapsing on apical dendrites. *Middle:* A cartoon neuron as depicted in neural network and functionalist models. Two incoming axons are shown synapsing on the cell body/dendrite. *Right:* A cartoon neuron as utilized in this chapter, showing three dendrites, cell body and a single axon heading downward. The internal cytoskeleton – microtubules interconnected by microtubule-associated proteins – is shown schematically; in dendrites and cell body the microtubules are short, interrupted (and of mixed polarity, not visibly apparent). In the axon the microtubules are continuous (and of uniform polarity, not visibly apparent). Two incoming axons synapse on dendritic spines

¹⁸ For example, calcium-calmodulin protein kinase and protein kinase C.

consumer of dendritic metabolic energy [230, 8, 118]. Changes in the cytoskeleton regulate synaptic plasticity [86, 240, 262, 165, 255, 265, 53, 195, 155, 125].

Dendritic processing is assumed to be constrained by global all-or-none output through the axon, and to exist merely to trigger axonal spikes. But neither assumption is substantiated. The full extent of dendritic internal processing is unknown but its capabilities are enormous. For example, synaptic activity causes glycolytic production of ATP in dendritic spines, energy that may be used for ion channels as well as protein synthesis and signal transduction into the dendritic cytoskeleton [266, 211]. Accordingly, Kasischke and Webb [124] suggested that brain function might be "...more refined on a higher temporal and smaller spatial scale".

Figure 6.4 shows 1) an actual pyramidal neuron with multiple dendrites; two incoming axons synapse on two different dendrites (a pyramidal neuron is likely to have many thousands of such incoming synapses), 2) a cartoon neuron with two axonal inputs synapsing on a cell body (as presumed in

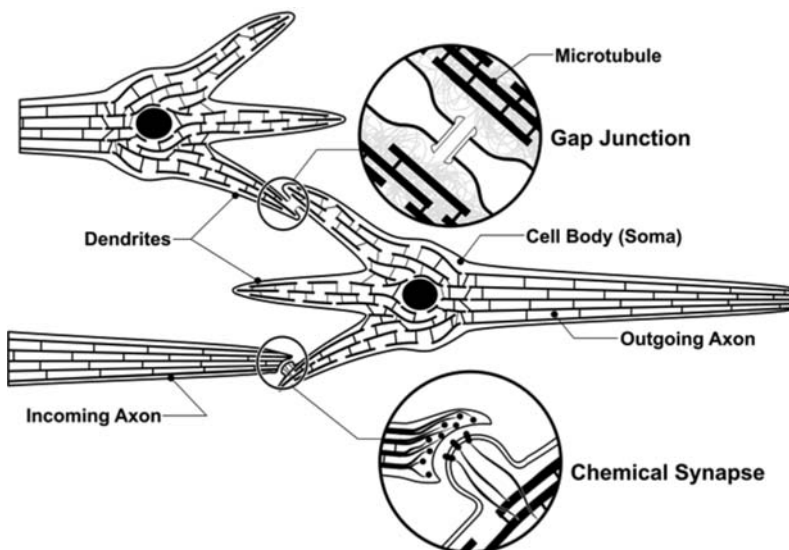


Fig. 6.5. Cartoon neuron with two types of connections. Internal structure represents nucleus (dark circle) and cytoskeletal microtubules (MTs) connected by strut-like microtubule-associated proteins (MAPs). MTs in axons are continuous (and unipolar) whereas dendritic MTs are interrupted (and of mixed polarity). *Lower left:* An incoming axon forms a chemical synapse on a dendritic spine. Close-up shows neurotransmitter vesicles in presynaptic axon terminal, and postsynaptic receptors on spine connected to intraspine actin filaments that link to MTs. *Upper left:* Dendritic-dendritic gap junction is a window between the two neurons. Both the membranes and cytoplasmic interiors of the two cells are continuous

functionalist models), and 3) a more elaborate cartoon neuron with three dendrites (and two incoming synapses) showing the internal cytoskeleton. Figure 6.5 shows this type of cartoon neuron with a chemical synapse and dendritic-dendritic gap junction.

6.3.4 Neural Synchrony

Evidence supports a correlation between consciousness and synchronous brain activity. Electrical recording from scalp, brain surface or implanted electrodes reveal synchrony at various frequencies of the electroencephalogram (EEG) due to LFPs or surface potentials. Among these, the so-called gamma frequency range between 30 and 70 Hz correlates best with attention and consciousness. Gray and Singer ([77], cf. [78]) found coherent gamma oscillations in LFPs of cat visual cortex that strongly depended on specific visual stimulation. Though the synchrony occurred in the gamma EEG range between 30 and 70 Hz, the phenomenon became known as coherent 40 Hz.

Following a suggestion by von der Malsburg [251] that synchronous neural excitations could solve the binding problem, von der Malsburg and Singer [252], Crick and Koch [33]¹⁹, Varela [244] and others proposed that the neural correlate of any particular conscious content was an assembly of neurons excited coherently at 40 Hz or thereabouts. Varela [244] succinctly observed that neural synchrony operated whenever component processes subserved by spatially separate brain regions were integrated into consciousness.

Neural synchrony in the gamma frequency range has been observed in many animal studies using multiunit scalp, surface and implanted electrodes. They demonstrate synchrony within and across cortical areas, hemispheres and sensory/motor modalities that reflects perceptual gestalt criteria and performance (for a review: Singer and Gray [212], Singer [213]). Among human studies using scalp EEG and MEG, most support a role for synchrony in integration and binding [119, 213, 245, 236]. Gamma synchrony correlates with perception of sound and linguistic stimuli [161, 169, 190], REM dream states [146], attention [60, 231], working memory [225, 226], face recognition [162], somatic perception [42] and binding of visual elements into unitary percepts, with the magnitude of synchrony diminishing with stimulus repetition [83]. Loss of consciousness associated with onset of general anesthesia is characterized by a decrease in gamma EEG activity that returns when patients awaken [117]²⁰.

¹⁹ Crick and Koch subsequently retreated from this contention, maintaining that 40-Hz synchrony alone is insufficient for consciousness but may boost assemblies of neurons (in competition with other assemblies) into consciousness [129].

²⁰ Anesthesia is also marked by an increase in slower bands and a marked “anteriorization” of power. Additionally, prefrontal and frontal regions of each hemisphere become more closely coupled. Uncoupling occurs between anterior and posterior regions on each hemisphere, as well as homologous regions between the two hemispheres [117].

Some human studies have failed to support neural synchrony in perception and cognition. Menon et al. [159] found gamma synchrony restricted to less than 2 cm regions of cortical surface, arguing against long-range coherence. However, the study only examined a 7 cm \times 7 cm region and other studies show that synchrony drops off at intermediate ranges but then reappears at long-range distances [164]. Some discrepancies have ensued from differences in methodology [236]. Overall, synchronous gamma EEG/coherent 40 Hz is the best electrophysiological correlate of consciousness.

How is gamma synchrony mediated? Coherence over large distances, in some cases multiple cortical areas and both cerebral hemispheres, shows zero, or near-zero phase lag. Significant phase lags would be expected from the speed of axonal conduction and delays in synaptic transmission [233].

There is no evidence to support coordinated axonal spiking as the source of gamma synchrony. As Koch [129] states:

“Gamma oscillations can be routinely observed in the local field potential and, less frequently, when recording multi neuron activity

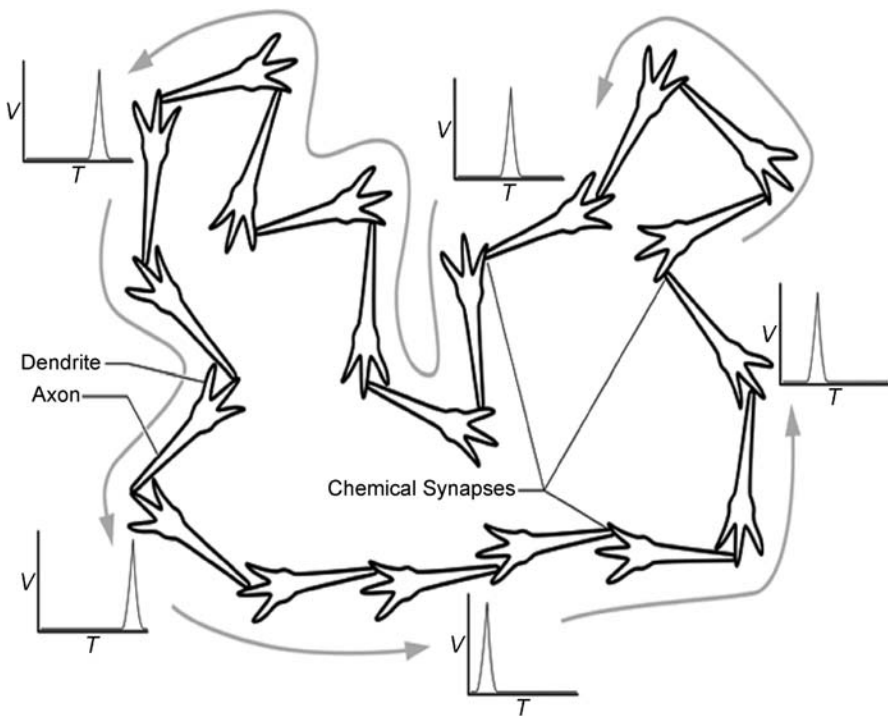


Fig. 6.6. Neural network/Hebbian assembly of cartoon neurons linked by axonal-dendritic chemical synapses. Information/excitation flows unidirectionally from axon to dendrite through the network. Electrical recordings at various points show single voltage spike potential propagating through the network

(that is, the summed spikes of neighboring cells). Detecting these rhythms in the spiking patterns of individual neurons has proven to be more problematic . . .”.

A critical review [204] rejects the relevance of synchrony to temporal binding (and consciousness) based on the lack of coherence of spike activity, perhaps throwing away the baby with the bathwater. However, many studies have shown gamma frequency synchronized by dendritic gap junction electrical synapses. Measuring both spikes and dendritic LFPs in multiple regions of cat visual cortex, Fries et al. [60] showed that visual recognition corresponded with gamma-frequency EEG emanating from LFPs, not with spikes.

Figure 6.6 shows a cartoon neuronal network based on axonal spikes and chemical synapses. Excitation/information flows through the network; there is no coherence. Figure 6.7 shows a gap-junction-linked neuronal network (a hyperneuron, including glial cells) with continuous membrane and cytoplasm. Dendritic membrane throughout the hyperneuron is excited coherently.

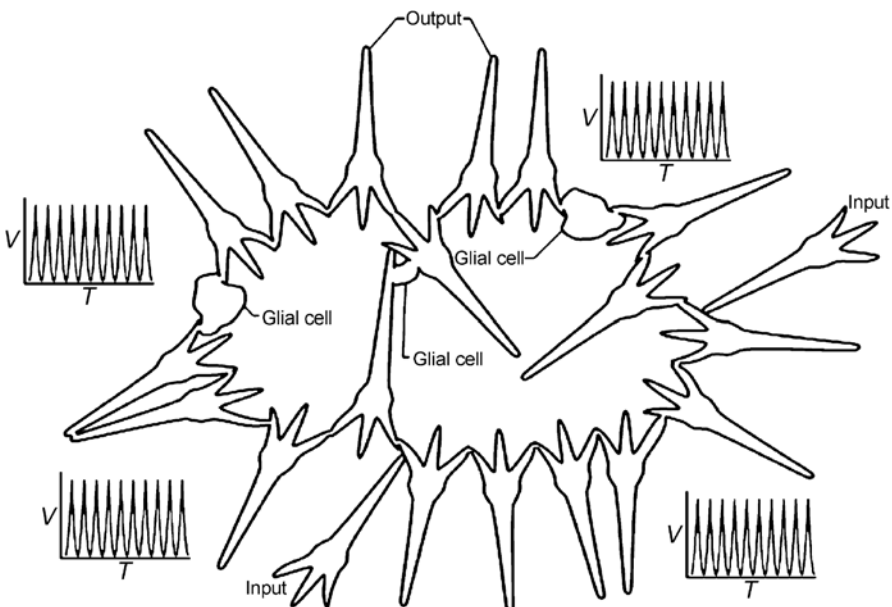


Fig. 6.7. Neural network/Hebbian assembly (“hyperneuron”) linked by window-like gap junctions, mostly dendritic–dendritic but also by glial cell gap junctions. Inputs to the hyperneuron are from axonal–dendritic chemical synapses. Outputs from the hyperneuron are from axons of hyperneuron components. Because gap-junction-connected neurons depolarize synchronously like “one giant neuron”, electrical recordings at various points show synchronous voltage depolarizations, e.g. at coherent 40 Hz. Both membranes and cytoplasmic interiors are continuous throughout the hyperneuron

6.3.5 Gap-Junction Assemblies – “Hyperneurons”

Gap junctions, or electrical synapses, are direct open windows between adjacent cells formed by paired collars consisting of a class of proteins called connexins [101, 193]. Gap junctions occur between neuronal dendrites, between axons and axons, between neurons and glia, between glia, and between axons and dendrites – bypassing chemical synapses [234, 61, 235, 17]. Ions, nutrients and other material pass through the open gaps, so gap-junction-connected neurons have both continuous membrane surfaces and continuous cytoplasmic interiors. Neurons connected by gap junctions are electrically coupled, depolarize synchronously and “behave like one giant neuron” [121].

In early development gap junctions link pyramidal cells with each other, with nonpyramidal neurons, and with glia during formation of cortical circuits [18]. The number of cortical gap junctions then declines so gap junctions were considered irrelevant to cognition or consciousness. However, many studies show that gap junctions persist significantly in the adult mammalian brain. Moreover, gap-junction circuits of cortical interneurons in adult brains mediate gamma EEG/coherent 40 Hz and other synchronous activity [41, 45, 105, 16, 135, 59, 26, 194, 175, 68, 75].

At least ten different connexins are found in mammalian brain, and their placement and function are dynamic [25, 16]. A single neuron may have numerous gap-junction connections, only some of which are open at any one time, with rapid openings and closings regulated by cytoskeletal microtubules, and/or phosphorylation via G-protein metabotropic receptor activity [97]. Thus gap-junction networks are at least as dynamic and mutable as those crafted by chemical synapses, and may include glial cells [62]. They fulfill the criteria for Hebbian assemblies with the added advantage of synchronous excitations. Networks of gap-junction-linked neurons (and glia) have been termed hyperneurons [116]²¹.

Cortical inhibitory interneurons are particularly studded with gap junctions, potentially connecting each cell to 20 to 50 others [6]. Many have dual synapses – their axons form inhibitory GABA chemical synapses on another interneuron’s dendrite, while the same two cells share dendrodendritic gap junctions [227, 66, 67, 69]. Within each cortical hemisphere there is no apparent limit to the extent of interneuron gap junction networks – hyperneurons – in which they may form a “large, continuous syncytium” [6].

The case for gap-junction hyperneurons involving primary neurons such as pyramidal cells in mature brains, and extending to both hemispheres is less clear. However, Venance et al. [249] showed gap junctions between interneurons and excitatory neurons in juvenile rat brain. Pyramidal cells in hippocampal slices show axo-axonal gap-junction coupling [235], and glial

²¹ Ironically, prior to Santiago Ramon-y-Cajal’s [184] determination that the brain was composed of individual neural cells, Camille Golgi had proposed that the brain was a syncytium – a threaded reticulum of fibers.

cells envelope both axons and dendrites in many chemical synapses. Neuron–glia–neuron gap junctions could thus provide chemical synapses with alter egos as links in hyperneurons. Thalamocortical cells generating synchronous alpha and theta cortical activity are linked by gap junctions in thalamus [106], so thalamocortical projections (or trans-corpus callosum pathways) could couple both hemispheres in hyperneurons to account for bilateral synchrony.

In principle, all the brain's neurons and glia could be linked together by gap junctions. However, too many active gap junctions and near total synchrony (e.g. as in seizures) would reduce the brain's information-processing capacity. More than three active gap junctions per neuron (i.e. with three different neurons or glia) would connect the entire brain into a single hyperneuron topology.²² Thus pruning and sparseness are necessary. For the purpose of this chapter, hyperneurons will imply gap-junction-linked cortical interneurons, glia, primary cortical neurons such as pyramidal cells and perhaps others such as thalamocortical neurons that can extend throughout both cerebral hemispheres and subcortical areas.

Brain-wide gamma synchrony mediated by gap-junctions is the best electrophysiological NCC. A logical conclusion is that gap-junction networks – hyperneurons – are the cellular-level NCC. Can that help explain consciousness?

A key feature of gap-junction hyperneurons is continuous dendritic membranes that depolarize coherently. Another key feature is continuous cytoplasmic interiors.

6.3.6 The Next NCC Frontier – Neuronal Interiors and the Cytoskeleton

Membrane-based neuronal input–output activities involve changes in synaptic plasticity, ion conductance, neurotransmitter vesicle transport/secretion and gap-junction regulation – all controlled by intra-neuronal networks of filamentous protein polymers known as the cytoskeleton. If simple input–output activities fully described neural function, then fine-grained details might not matter. But simple input–output activities – in which neurons function as switches – are only a guess, and most likely a poor imitation of neurons' actual activities and capabilities.

To gauge how single neuron functions may exceed simple input–output activities, consider the single-cell organism paramecium. Such cells swim about gracefully, avoid obstacles and predators, find food and engage in sex with partner paramecia. They may also learn; if placed in capillary tubes they escape, and in subsequent attempts escape more quickly. As single cells with no synaptic connections, how do they do it? Pondering the seemingly intelligent

²² Personal communication from Roger Penrose.

activities of such single-cell organisms, famed neuroscientist C.S. Sherrington [206] conjectured:

“of nerve there is no trace, but the cytoskeleton might serve”.

If the cytoskeleton is the nervous system of protozoa, what might it do for neurons?

6.4 The Neuronal Cytoskeleton

6.4.1 Microtubules and Networks inside Neurons

Shape, structure, growth and function of neurons are determined by their cytoskeleton, internal scaffoldings of filamentous protein polymers that include microtubules, actin and intermediate filaments. Rigid microtubules (MTs) interconnected by MT-associated proteins (MAPs) and immersed in actin form a self-supporting, dynamic tensegrity network. The cytoskeleton also includes MT-based organelles called centrioles that organize mitosis, membrane-bound MT-based cilia, and proteins that link MTs with membranes. Disruption of intraneuronal cytoskeletal structures impairs cognition, such as tangling of the MAP tau linking MTs in Alzheimer’s disease [153, 107].

Actin is the main component of dendritic spines and also exists throughout the rest of the neuronal interior in various forms depending on actin-binding proteins, calcium, etc. When actin polymerizes into a dense meshwork, the cell interior converts from an aqueous solution (sol state) to a quasisolid, gelatinous (gel) state. In the gel state, actin, MTs and other cytoskeletal structures form a negatively charged matrix on which polar cell water molecules are bound and ordered [179]. Glutamate binding to NMDA and AMPA receptors triggers gel states in actin spines [53].

Neuronal MTs self-assemble, and with actin enable growth of axons and dendrites. Motor proteins transport materials along MTs to maintain and regulate synapses. Direction and guidance of motor proteins and synaptic components (e.g. from cell body through branching dendrites) depends on conformational states of MT subunits [132]. Thus MTs are not merely passive tracks but appear to actively guide transport. Among neuronal cytoskeletal components, MTs are the most stable and appear best suited for information processing. Wherever cellular organization and intelligence are required, MTs are present and involved.

MTs are cylindrical polymers 25 nanometers ($\text{nm} = 10^{-9} \text{ m}$) in diameter, comprised of 13 longitudinal protofilaments that are each chains of the protein tubulin (Fig. 6.8). Each tubulin is a peanut-shaped dimer (8 nm by 4 nm by 5 nm) that consists of two slightly different monomers known as alpha and beta tubulin, (each 4 nm by 4 nm by 5 nm, weighing 55 000 daltons). Tubulin subunits within MTs are arranged in a hexagonal lattice that is slightly twisted, resulting in differing neighbor relationships among each

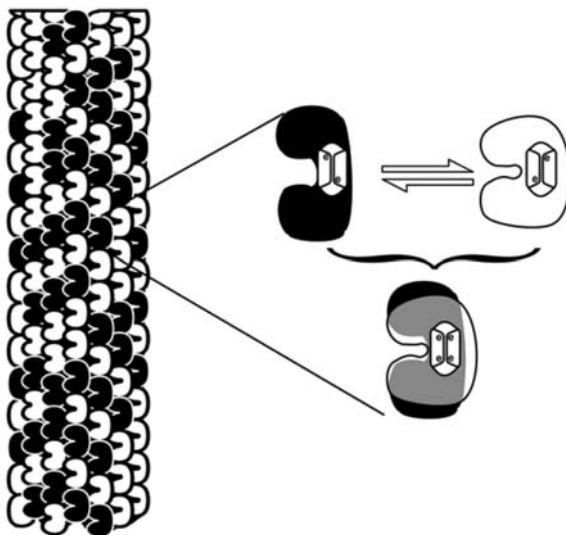


Fig. 6.8. Microtubule (*left*) is a cylindrical polymer of subunit proteins known as tubulin arranged in a skewed hexagonal lattice. Each tubulin can exist in two or more conformational states, e.g. open (*black*) or closed (*white*). *Right*: Each tubulin state is governed by quantum-mechanical London forces – collective positions of hundreds of electrons (represented here as two electrons) in nonpolar hydrophobic regions within the protein. Because of governance by quantum forces, it is proposed that tubulins can exist in quantum superposition of both conformations (*black* and *white* = *gray*). The actual displacement in the superposition separation need only be the diameter of a carbon atom nucleus, but is illustrated here as roughly 10% of the protein volume

subunit and its six nearest neighbors (Fig. 6.9). Thus pathways along contiguous tubulins form helical patterns that repeat every 3, 5, 8, etc. rows (the Fibonacci series). Alpha tubulin monomers are more negatively charged than beta monomers, so each tubulin (and each MT as a whole) is a ferroelectric dipole with positive (beta monomer) and negative (alpha monomer) ends²³.

In non-neuronal cells and in neuronal axons, MTs are continuous and aligned radially like spokes of a wheel emanating from the cell center. MT negative (alpha) ends originate in the central cell hub (near the centrioles, or MT-organizing-center adjacent to the cell nucleus) and their positive (beta) ends extend outward in the case of axons, where the negative ends of continu-

²³ The skewed lattice symmetry matches the polarity. Thus in the “alpha (positive) up” orientation, the 3-start and 5-start helical windings go to the left, and the 8-start helical windings go to the right. The intervals on any protofilament between the tubulins on which the various windings repeat match the mathematical Fibonacci series (Figs. 6.8 and 6.9).

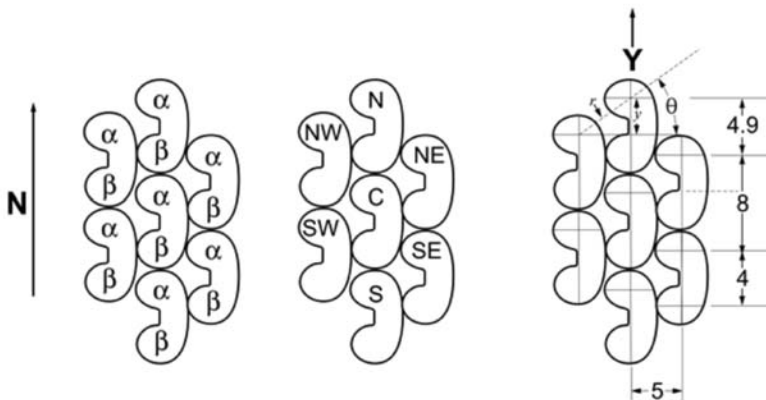


Fig. 6.9. The lattice of tubulins in microtubules. *Left:* The lattice showing the tubulin dimers as (negatively charged) alpha monomers and (positively charged) beta monomers. *Middle:* A tubulin neighborhood is defined by identifying the central tubulin C and its 6 surrounding neighbors by compass points: N (north), NE (northeast), SE (southeast), S (south), SW (southwest), NW (northwest). *Right:* The spacings (in nanometers) and definition of angle theta. y is the vertical distance between (the same points on) any two neighboring dimers and r the absolute distance. While y varies, the horizontal distance is always 5 nanometers. Curvature around the cylinder is ignored and the dipole force between dimers is related to y/r^3 . From [185]

ous MTs originate in the axon hillock, and positive ends reach the presynaptic region.

However, the dendritic cytoskeleton is unique. Unlike axons and any other cells, MTs in dendrites are short, interrupted and mixed polarity. They form networks interconnected by MAPs (especially dendrite-specific MAP2) of roughly equal mixtures of polarity. There is no obvious reason – from a structural standpoint uninterrupted MTs would be preferable, as in axons. Networks of mixed polarity MTs connected by MAPs may be optimal for information processing.

Intradendritic MT-MAP networks are coupled to dendritic synaptic membrane and receptors (including dendritic spines) by calcium and sodium flux, actin and metabotropic inputs including second messenger signaling, e. g. dephosphorylation of MAP2 [86]. Alterations in dendritic MT-MAP networks are correlated with locations, densities and sensitivities of receptors (e. g. Woolf et al. [265]). Synaptic plasticity, learning and memory depend on dendritic MT-MAP networks.

Since Sherrington's observation in 1957, the idea that the cytoskeleton – MTs in particular – may act as a cellular nervous system has occurred to many scientists. Vassilev et al. [246] reported that tubulin chains transmit signals between membranes, and Maniotis et al. [148, 149] demonstrated that

MTs convey information from membrane to nucleus. But MTs could be more than wires. The MT lattice is well designed to represent and process information, with the states of individual tubulins playing the role of bits in computers. Conformational states of proteins in general (e.g. ion channels opening/closing, receptor binding of neurotransmitter, etc.) are the currency of real-time activities in living cells. Numerous factors influence a protein's conformation at any one time, so individual protein conformation may be considered the essential input–output function in biology.

6.4.2 Microtubule Automata

The peanut-shaped tubulin dimer switches between two conformations in which the alpha monomer flexes 30 degrees from vertical alignment with the beta monomer. These are referred to as open and closed states (Fig. 6.8, [158, 104, 186])²⁴.

Atema [11] proposed that tubulin conformational changes propagated as signals along MTs in cilia. Hameroff and Watt [87] suggested the MT lattice acted as a two-dimensional computer-like switching matrix with tubulin states influenced by neighbor tubulins, and input/output occurring via MAPs²⁵. MT information processing potential came to be viewed in the context of cellular automata [214, 185].

Cellular automata are self-organizing information systems based on lattices of fundamental units (cells) whose states interact with neighbor cells at discrete time steps. In a two-dimensional checkerboard lattice, each cell has eight neighbors (corner neighbors included) and exists in two (or more) possible states. Neighbor-interaction rules determine each cell's state at the next time step.

²⁴ Pharmacological studies suggest five possible ligand-induced conformations. In addition to these dynamical states, more permanent variability in tubulin within microtubules depends on genetics (22 different tubulin isozymes in brain) and post-translational modification, addition or removal of amino acids to specific tubulins. Thus, intact MTs may be mosaics of slightly different tubulins, allowing for a baseline memory or programming upon which dynamical changes can occur.

²⁵ Other proposals include the following: Roth et al. [192] proposed that conformational gradients among tubulins created patterns that dictated function, Puck and Krystosek [183] suggested that waves of phosphorylation/dephosphorylation along tubulins conveyed information, and Wang and Ingber [254] described a tensegrity communication structure among MTs and actin filaments. Nonlinear soliton waves along MTs have been proposed [197, 30], and Lader et al. [133] suggested that ion transfer along actin conveyed functional signals [237]. Tuszynski et al. [238] predicted MT ferroelectric effects and “spin glass” behavior, Albrecht-Buehler [2, 3] suggested MTs convey infrared photons as the “nerves of the cell”, and Jibu et al. [114, 115] proposed MTs as quantum optical waveguides. For a review of classical models of cytoskeletal information processing see Hameroff [88] and Rasmussen et al. [185]

A well-known example is the game of life in which two possible states of each cell whimsically represent either alive or dead on a checkerboard lattice [70]. There are three neighbor rules:

- If the number of live neighbors is exactly two, the cell maintains the status quo into the next generation. Thus a live cell stays alive, a dead cell stays dead.
- If the number of live neighbors is exactly three, the cell will be alive in the next generation. A dead cell is “born”, a live cell lives on.
- If the number of live neighbors is 0, 1, or 4–8, the cell will be dead in the next generation due to not enough support (0 or 1) or overcrowding (4–8).

The generations are synchronized by a universal clock mechanism. Starting from random initial patterns, complex behaviors emerge, for example chaotic dynamics [260, 134]. However, common types of patterns generally appear: stable objects, oscillators/blinkers and gliders that move through the grid. Streams of gliders can perform all logic and memory functions on which computers are based. The game of life and cellular automata in general are universal computers.

MTs were modeled as automata in which tubulin conformational states (open, closed) interacted with neighbor tubulin states by dipole interactions. Dipole strengths in open and closed conformations were used to generate interaction rules. Thus the dipole-coupled conformation for each tubulin was determined at each generation by the sum of the dipoles of its six surrounding neighbors²⁶. Because of the skewed hexagonal geometry, contributions from each of the six neighbors differed (Fig. 6.9). The generations, or time steps were assumed to be nanoseconds, following Fröhlich’s suggestion of coherent excitations.

Herbert Fröhlich [63–65] proposed that a set of dipoles constrained in a common geometry and electric field would oscillate in phase, coherently like a laser²⁷ if biochemical energy were supplied. Membrane proteins and tubulins in MTs are predicted to oscillate in the range of 10^{-9} to 10^{-11} s²⁸.

²⁶ In which $f_{\text{net}} = \frac{e^2}{4\pi\epsilon} \sum_{i=1}^6 \frac{y_i}{r_i^3}$ is the sum of the six neighbor dipole forces on each

tubulin dimer, e is the electron charge, ϵ is the average permittivity for proteins, typically ten times the vacuum permittivity, y is the vertical offset between (identical points in each of the) dimer pairs, and r is the absolute distance between (identical points in each of the) dimer pairs. We assumed that only the y -component of the interaction forces is effective and neglected any net force around the MT circumference. Absolute values of the forces may be found in Rasmussen et al. [185].

²⁷ Essentially forming a Bose–Einstein condensate.

²⁸ Fröhlich pointed out that living systems should be sensitive to effects of specific microwave frequencies, and indeed many such effects have been reported. Vos et al. [253] showed coherent nuclear motions of membrane proteins.

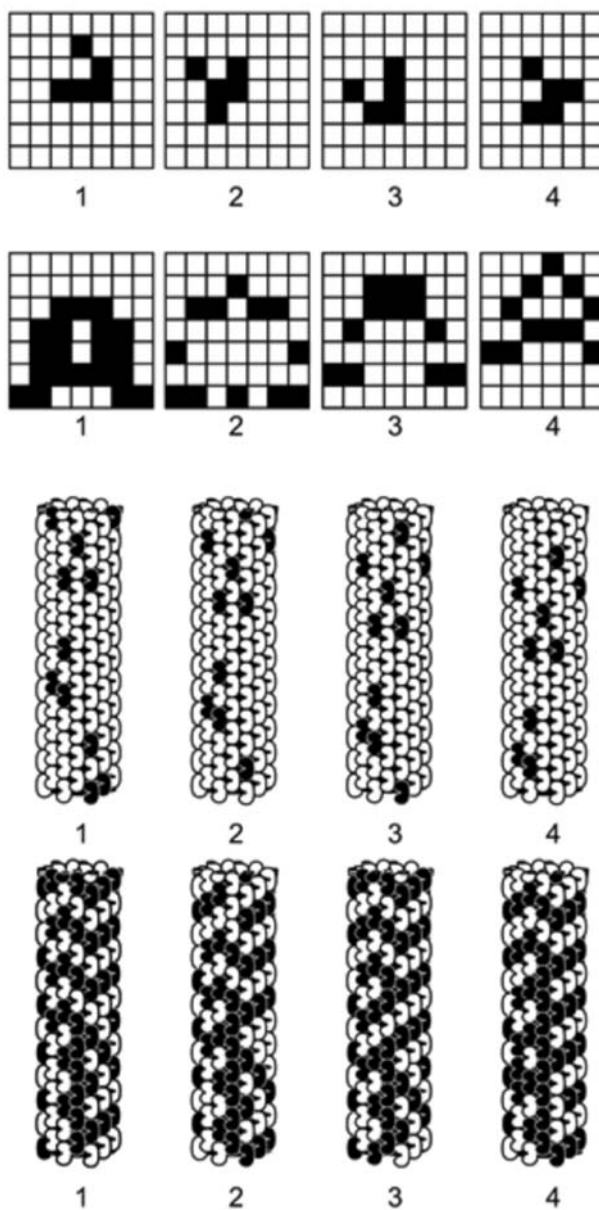


Fig. 6.10. Cellular automata. *Top two rows:* Two different sequences of gliders moving in the game of life. In the *first row* the glider moves downward; in the *second row* the glider moves upward. *Bottom two rows:* Two different sequences of gliders moving and patterns evolving in microtubule automata. In the *third row*, gliders move downward through the microtubule; in the *fourth row*, patterns move both upward (black column, 4th protofilament) and downward (white column, 2nd protofilament)

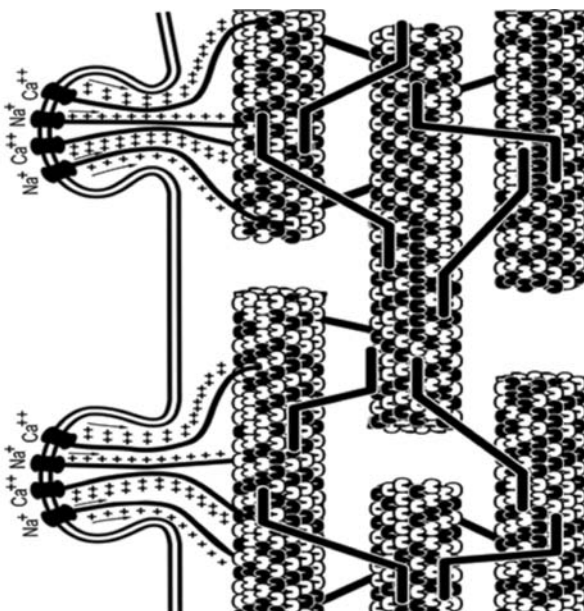


Fig. 6.11. Interior schematic of dendrite showing unique mixed polarity networks of microtubule automata interconnected by microtubule-associated proteins (MAPs). Inputs to microtubule automata (orchestration) from, e.g. glutamate activation of dendritic spine receptors are conveyed by sodium and calcium ion flux along actin filaments. MAPs convey information between MTs to form an automaton network. Output/results of MT automaton network processing can trigger axonal spikes, regulate synapses and hardwire memory

Simulations of MT automata showed stable patterns, blinks and propagating gliders (velocity 8 to 800 m/s²⁹, Fig. 6.10). Two MT automata interconnected by MAPs exhibited recognition and learning (Fig. 6.11; [185]).

MT automata potentially increase cellular and brain-wide information processing enormously. Neurons each contain at least 10^7 tubulins [267]; switching in nanoseconds (10^9 /s) predicts roughly 10^{16} operations per second per neuron.³⁰ But enhanced information processing per se fails to answer fundamental questions about consciousness. A clue lies in the mechanism of state switching present in proteins.

²⁹ Using the Fröhlich oscillation time of 10^{-9} to 10^{-11} s, gliders move one tubulin dimer length (8 nm) per oscillation, hence 8 to 800 nm/ns, or 8 to 800 m/s. This is essentially the range of velocities for action potentials.

³⁰ Conventional approaches focus on synaptic switching (roughly 10^{11} brain neurons, 10^3 synapses/neuron, switching in the millisecond range of 10^3 operations per second) and thus predict about 10^{17} bit states per second for a human brain. Nanosecond MT automata offer about 10^{27} brain operations per second for a human brain.

6.4.3 Protein Conformational Dynamics – Nature’s Bits and Qubits

Proteins are the engines of life, dynamically changing conformational shape at multiple scales [123]. Functional changes occur in 10^{-6} s to 10^{-11} s transitions. Proteins have large energies with thousands of kiloJoules per mole (kJ mol^{-1}) but are only marginally stable against denaturation by 40 kJ mol^{-1} . Consequently, protein conformation is a “delicate balance among powerful countervailing forces” [250].

Individual proteins are linear chains of amino acids that fold into three-dimensional conformations.³¹ The driving force in folding is attraction of uncharged nonpolar amino acid groups, repelled by solvent water. These hydrophobic groups attract each other by van der Waals forces, avoiding water and burying themselves within protein interiors forming (in some proteins) hydrophobic pockets.³² Volumes of pockets (0.4 cubic nanometers) are 1/30 to 1/250 the volume of single proteins. Though tiny, hydrophobic pockets are critically important in the determination of protein conformation both in folding and regulation of conformational dynamics. Hydrophobic pockets may act as the brain of a protein.

Nonpolar (but polarizable) amino acid side groups within hydrophobic pockets interact by van der Waals London forces. Electrically neutral atoms and nonpolar molecules can have instantaneous dipoles in their electron-cloud distribution. Electrons in clouds from neighboring nonpolar amino acid side groups repel each other, inducing mutual fluctuating dipoles that then couple to each other like oscillating magnets. As high energy forces cancel out, weak but numerous (thousands per protein) London forces govern protein conformation (Fig. 6.8).³³

³¹ The precise folding depends on attractive and repellent forces among various amino acid side groups, and a current view is that many possible intermediate conformations precede the final one. Predicting the final three-dimensional folded shape using computer simulation has proven difficult if not impossible. This conundrum is known as the “protein-folding problem” and so far appears to be “NP complete”: the answer can be calculated in theory, but the space and time required of any classical computer is prohibitive. Klein-Seetharaman et al. [127] showed nonlocal interactions among nonpolar groups in protein folding, suggesting a form of quantum computation.

³² Such as leucine, isoleucine, phenylalanine, tryptophan, tyrosine and valine.

³³ Due to the Mossbauer effect [24] electronic motions in tubulin should be coupled to nuclear motions via a recoil phenomenon, connecting protein conformation to London forces. The movement would be slight due to the disparity in mass between single electrons and the mass of protons – a one-nanometer shift in location of a single electron would shift the nuclear mass, and hence protein conformation, by only 10^{-8} nm. However, such a shift per electron (thousands of electron London forces per protein) would be significant if all nuclei were affected collectively. The conformational superposition/separation distance in Orch OR is precisely 2.5 fermi lengths (carbon atom nuclear diameter) of 10^{-6} nm. So ~ 250

Due to inherent uncertainty in electron localization, London forces are quantum-mechanical effects. Thus proteins governed by London forces in hydrophobic pockets are quantum levers, amplifying quantum forces to govern conformational changes and physical effects. Prevention of quantum leverage accounts for the action of anesthetic gases.

6.4.4 Anesthesia

Millions of people every year undergo general anesthesia for surgery with complete and reversible loss of consciousness. At a critical concentration of anesthetic drug, consciousness is erased while many nonconscious functions of brain and other organs continue (e.g. EEG, evoked potentials, control of breathing). How does this happen?

The situation seems confusing, with many different types of anesthetic drugs acting on many different types of brain molecules. Purely inhalational anesthetic gases that travel through the lungs and blood to the brain constitute a variety of types of molecules: halogenated hydrocarbons, ethers, the inert element xenon, nitrous oxide, etc. However, there is one important unifying feature.

All anesthetic gas molecules are nonpolar, and thus poorly soluble in water/blood, but highly soluble in a particular lipid-like, hydrophobic environment akin to olive oil. The potency of anesthetic gases in erasing consciousness correlates perfectly with solubility in such an environment. The brain has a large lipid-like (olive oil-like) domain, both in lipid regions of neural membranes and hydrophobic pockets within certain proteins. Anesthetics were originally thought to act in lipid regions of membranes, but protein hydrophobic pockets were determined to be their primary sites of action [54]. Anesthetic gases bind to nonpolar amino acid groups in the pockets (e.g. the benzene-like ring in phenylalanine, and the indole ring in tryptophan) by van der Waals London forces, the same quantum forces that form the pockets and govern conformational dynamics.

Why do weak quantum forces have such profound and selective effects? Anesthetic gas molecules form their own London force interactions with nonpolar amino acid groups, preventing or altering normally occurring London forces necessary for protein conformational dynamics and consciousness. Anesthetic gases prevent quantum leverage.

Most protein conformational changes are unaffected by general anesthetics – muscle contractility, enzyme function and most brain activities (as evidenced by EEG and evoked potentials) continue during anesthesia. Axonal action potentials are also relatively unaffected by general anesthetics. Pro-

London forces (among thousands per protein) would be required. The charge shift of a single electron, equal to a proton charge, is even more likely to exert an effect on conformation [32]. Roitberg et al. [191] and Tejada et al. [229] also suggest quantum states in proteins.

teins that are affected include postsynaptic receptors for acetylcholine, serotonin, GABA and glycine [54], connexins in gap junctions [151, 99], tubulin in microtubules [4] and actin, which disassembles in dendritic spines when exposed to anesthetics [120].

Anesthetics act (and consciousness occurs) not in any one brain region, or in any one type of neuron or particular protein. Rather, anesthesia and consciousness occur in hydrophobic pockets of a class of proteins in dendrites throughout the brain [93]. In these pockets, quantum London forces govern protein function responsible for consciousness. Does that imply that consciousness is a quantum process?

6.5 Quantum Information Processing

6.5.1 Quantum Mechanics

Reality is described by quantum physical laws that reduce to classical rules (e.g. Newton's laws of motion) at certain large-scale limits. According to quantum physical laws:

- Objects/particles may exist in two or more places or states simultaneously – more like waves than particles and governed by a quantum wave function. This phenomenon of multiple coexisting possibilities is known as quantum superposition.
- Multiple objects/particles can be unified, acting as a single coherent object governed by one wave function. If a component is perturbed, others feel it and react. This is called nonlocality and is the main difference between classical and quantum physics. If the objects remain together, nonlocality is known as Bose–Einstein condensation.
- If unified objects are spatially separated they remain unified. This nonlocality is also known as quantum entanglement.

Why don't we see quantum superpositions in our world? How are quantum particles connected over distance?

Experiments show that quantum superpositions persist until they are measured, observed or interact with the classical environment (decohere). If such interactions occur, quantum superpositions reduce, collapse or decohere to particular classical states, with the particular choice of states apparently random. What actually constitutes the act of measurement/observation is unclear, as is the fate of isolated, unmeasured quantum superpositions. Interpretations of quantum mechanics address this issue:

- The Copenhagen interpretation (measurement or conscious observation collapses the wave function)³⁴ puts both consciousness and fundamental reality outside physics.

³⁴ This is one form of the Copenhagen interpretation, parodied in Schrödinger's famous thought experiment of the dead-and-alive cat [200].

- The multiple-worlds view suggests each superposition is amplified, leading to a new universe. There is no collapse, but an infinity of realities (and conscious minds) is required.
- David Bohm's interpretation avoids reduction/collapse but requires another layer of reality. Objects are guided by complex waves of possibility (active information, associated with consciousness).
- Henry Stapp views the universe as a single quantum wave function. Reduction of part of it within the brain is a conscious moment (akin to Whitehead's "occasion of experience" – [257, 258]. Reduction/collapse is consciousness.
- In decoherence theory any interaction (loss of isolation) of a quantum superposition with a classical system (e. g. through heat, direct interaction or information exchange) erodes the quantum system. But 1) the fate of isolated superpositions is not addressed, 2) no quantum system is ever truly isolated, 3) decoherence doesn't actually disrupt superposition, just buries it in noise, 4) some quantum processes are enhanced by heat and/or noise.
- An objective threshold for reduction (objective reduction, or) exists due to, e. g., the number of superpositioned particles (GRW theory [73, 74]) OR quantum gravity as in the OR proposals of Károlyházy et al. [122], Diosi [44] and Roger Penrose [170].

How can objects actually be in multiple locations or states simultaneously? Penrose [170, 171] takes superposition as an actual separation in underlying reality at its most basic level (fundamental space-time geometry at the Planck scale of 10^{-33} cm).³⁵ This is akin to the multiple-worlds view (superpositions/separations are amplified to form a separate universe), however, according to Penrose the separations are unstable and (instead of branching off completely) spontaneously reduce (self-collapse) due to an objective threshold in space-time geometry.³⁶ Accordingly, the larger the superposition, the more rapidly it reduces. For example an isolated one kilogram object in superposition would meet OR quickly, in only 10^{-37} s. An isolated superpositioned electron would undergo OR only after 10 million years. Penrose OR is currently being tested experimentally [150].

³⁵ Penrose brings in general relativity in which matter equates to space-time curvature. An object in any particular location is a specific curvature in underlying space-time geometry; the same object in a slightly different location is curvature in a different (e. g. opposite) direction. Hence superposition (object in two places) implies a separation, bubble or blister in fundamental space-time geometry.

³⁶ By $E = \hbar/t$ where E is the gravitational self-energy, \hbar is Planck's constant over 2π , and t is the time until or occurs. E is the amount, or degree of superposition given for superposition/separation at the level of atomic nuclei by $E = Gm^2/a_c$ where G is the gravitational constant, m is the superpositioned mass, and a_c is the distance of separation, i. e. the diameter of a carbon nucleus equal to 2.5 fermi distances (2.5×10^{-6} nm). See [89] and [172] for details.

In *The Emperor's New Mind* Penrose [170] suggested that choices resulting from OR were not random, but influenced by Platonic information embedded at the Planck scale, the fundamental level of the universe. Moreover, this particular type of nonrandom, nonalgorithmic (noncomputable) selection is characteristic of conscious choices, differing in a basic way from the output of classical computers. Penrose proposed that OR-mediated quantum computation must be occurring in the brain. Quantum computation (see next section) relies on both superposition and entanglement.

Entanglement is stranger than superposition. Quantum theory predicted that complementary quantum particles (e.g. electrons in coupled spin-up and spin-down pairs) would remain entangled even when separated. Einstein, Podolsky and Rosen [49] described a thought experiment intended to disprove this notion (Fig. 6.3). An entangled complementary pair of superpositioned electrons (EPR pairs) would be separated and sent in different directions along two different wires, each electron remaining in superposition. When one electron was measured at its destination and, say, spin-up was observed, its entangled twin miles away would correspondingly reduce instantaneously to spin-down, which would be confirmed by measurement. This would require a faster-than-light signal that Einstein's special relativity had precluded. Nonetheless since the early 1980s [10, 232] this type of experiment has been performed through wires, fiber optic cables and via microwave beams through the atmosphere. Entanglement has been repeatedly confirmed. The mechanism of instantaneous communication remains unknown, seeming to violate special relativity.

To explain entanglement, Penrose ([173], cf. [15]) suggested backward time referral of quantum information, i.e. from the measurement back in time to the unified complementary pair, then forward in time to the opposite twin (Fig. 6.3). In the quantum world, time is symmetric (bidirectional), or the flow of time doesn't exist.

Although poorly understood, entanglement and superposition are used in quantum computing and related technologies.

6.5.2 Quantum Computation

Initially proposed by Benioff [14], Deutsch [43] and Feynman [52], quantum computers (and quantum cryptography and teleportation) are being developed in a variety of technological implementations.

The basic idea is this. Conventional computers represent digital information as binary bits of either 1 or 0. Quantum computers can represent quantum information as superpositions of both 1 and 0 (quantum bits, or qubits). While in superposition (isolated from environment) qubits interact with other qubits by nonlocal entanglement, allowing interactions to evolve³⁷ resulting in computation of enormous speed and near-infinite parallelism.

³⁷ Linearly and deterministically according to the Schrödinger equation.

After the interaction/computation is performed, qubits reduce/collapse to specific classical bit states by measurement, giving the output or solution.³⁸

The major hurdle to quantum computing is the sensitivity of fabricated superpositioned qubits to disruption by thermal vibration or any interaction with the environment – decoherence. Consequently, quantum-computing prototypes have been built to operate at extremely low temperatures to avoid thermal noise, and in isolation from the environment.

In the mid-1990s quantum error-correcting codes were developed that could detect and correct decoherence, preserving the quantum information [222]. Topological quantum error correction was developed in which the geometry of the quantum computer lattice was inherently resistant to decoherence. For example, a quantum computer could utilize the Aharonov–Bohm effect in which alternate possible paths of a quantum particle are considered as a superposition of paths [126]. So lattice pathways (rather than individual components of those pathways) can be global qubits resistant to decoherence.

6.5.3 Quantum Computing with Penrose OR

Technological qubits reduce/collapse by measurement, introducing randomness averaged out by redundancy. According to Penrose [170] quantum computation that self-collapses by OR avoids randomness, instead providing a noncomputable influence stemming from Platonic values embedded at the Planck scale. Such quantum computation would be algorithmic up to the instant of OR, with an added modification then occurring.

The Penrose argument for noncomputability using Gödel's theorem was harshly criticized but not refuted. For consciousness, OR also provides explanations for:

³⁸ Qubits may be manifest as switches that utilize superpositions of various quantum states including electron spins, photon polarization, ionic states, nuclear spin, magnetic flux in a Josephson junction superconducting loop, or “quantum dots” – confined spaces in that single electrons or atoms are mobile but can occupy only discrete sites. Many other possibilities for qubits have also been suggested including some that could be mass produced in silicon. Quantum computers remained largely theoretical curiosities until 1994. Bell Labs mathematician Peter Shor developed a quantum algorithm that would be capable of factoring large numbers into their primes exponentially faster than conventional computers, assuming a quantum computer could be built to run it. Factoring large numbers into primes is the basis for banking and military cryptography, and so governments and industry became extremely supportive of efforts to build quantum computers. A functional quantum computer would make all classically supported cryptography obsolete. The race was on. Subsequently, other algorithms for quantum computers were developed that would provide exceedingly faster search capabilities. There is no doubt quantum computers will be revolutionary if technical obstacles to their construction and operation can be overcome.

- Transition from nonconscious (superpositioned quantum information) to classical information, with consciousness the transition itself.
- Binding via quantum coherence, condensation and/or entanglement.
- Libet's backward time referral and other temporal anomalies.
- The hard problem of conscious experience via Whitehead pan-protopsychism connected to fundamental space-time geometry (Sect. 6.8.4, [90]).

Penrose initially suggested the possibility of superpositions of neurons both firing and not firing as qubits. Microtubules seemed ideal for the type of quantum computation Penrose was suggesting.

Penrose implied that nonconscious processes capable of becoming conscious utilize quantum information. What do we know about nonconscious processes?³⁹

6.6 The Quantum Unconscious

German psychologist Frederic Meyer in 1886 described subliminal consciousness, followed by William James' transmarginal consciousness or fringe, a region of the mind just outside consciousness but accessible to it (e.g. access consciousness, [19]).

Sigmund Freud saw dreams as the “royal road to the unconscious” whose bizarre character was due to censorship and disguise of thwarted drives. Freud’s ideas became downplayed, and dreams characterized as mental static (e.g. [102, 103]). However, recent brain imaging shows dream-associated REM sleep activity in regions associated with emotion and gratification [215, 216].

Chilean psychologist Ignacio Matte Blanco ([154], cf. [188]) compared logic structure in dreams to the Aristotelian logic of waking consciousness in which, for example, the logic statement:

If x, then y

does not imply the statement:

If y then x.

This is obvious to our conscious minds. For example:

If the light turns green, then I go

³⁹ I equate nonconscious, unconscious, subconscious and preconscious processes as potentially capable of consciousness. That is, they utilize both classical processes and quantum superposition. However, there are clearly brain processes that are almost exclusively nonconscious and utilize classical processing. But in principle such processes could become conscious. For example, practitioners of certain types of yoga gain conscious control over normally nonconscious processes such as intestinal peristalsis.

Does not imply:

If I go, then the light will turn green.

However, from decades of dream analysis Matte Blanco determined two non-Aristotelian axioms of the logic of the unconscious: symmetry and generalization. In dreams:

If x then y

(according to symmetry) implies that also:

If y then x .

In dreams, according to Matte Blanco:

If the light turns green, then I go

implies that also:

If I go, then the light turns green.

Generalization means that any entity is a part of a whole, and when symmetry and generalization are combined, paradox occurs. For example:

If a hand is part of the body

then also:

The body is part of the hand.

The seeming contradiction of any set being a subset of itself defines an infinite set, and is also holographic (and fractal). Any part of a whole also contains the whole within the part.⁴⁰

Symmetry also means that:

If event a happened after event b,

then also:

Event b happened after event a.

From this Matte Blanco concluded: "...the processes of the unconscious ...are not ordered in time".

Another implication of unconscious logic is that apparently negating propositions (e.g. p and not p) may be true, resulting in coincidence of con-

⁴⁰ According to neuroscientists Karl Lashley and Karl Pribram, memory is holographic. Multiple overlapping homunculi in both the central and peripheral nervous systems also suggest holography. Finally, there are serious suggestions that the universe is holographic.

tries. For example (to use Matte Blanco's example):

x is alive

and

x is dead

are both true (e.g. when time is removed). More generally, according to Matte Blanco, "the unconscious is unable to distinguish any two things from each other".

The unconscious utilizes multiple coexisting possibilities, inseparability and timelessness, very much like quantum information. Matte Blanco summarized the unconscious as "where paradox reigns and opposites merge to sameness", also an apt description of the quantum world.

6.7 Quantum Computation in Microtubules – The Orch OR Model

6.7.1 Specifics of Orch OR

In a proposal for the mechanism of consciousness, Roger Penrose and I suggested that microtubule (MT) quantum computations in neurons are orchestrated by synaptic inputs and MT-associated proteins (MAPs), and terminate (e.g. after 25 ms, 40 Hz) by Roger's objective reduction (OR) mechanism. Hence, the model is known as orchestrated objective reduction, Orch OR. Complete details may be found in Penrose and Hameroff [174], Hameroff and Penrose [89, 90] and Hameroff [91]. The key points are:

1. Conformational states of tubulin protein subunits within dendritic MTs interact with neighbor tubulin states by dipole coupling such that MTs process information in a manner analogous to cellular automata that regulate neuronal activities (trigger axonal spikes, modify synaptic plasticity and hardwire memory by MT-MAP architecture, etc.).
2. Tubulin conformational states and dipoles are governed by quantum-mechanical London forces within tubulin interiors (nonpolar hydrophobic pockets) so that tubulins may exist as quantum superpositions of differing conformational states, thus acting as quantum levers and qubits.⁴¹

⁴¹ Proteins may be optimally leveraged as qubits in terms of being 1) large enough to exert causal efficacy in the macroscopic world, and 2) small enough/delicately balanced to be regulated by quantum forces. In Hameroff and Penrose [89] the gravitational self-energy E was calculated for tubulin superpositions at the level of 1) entire tubulin protein separation, 2) separation at the level of atomic nuclei, and 3) separation at the level of nucleons, i.e. protons and neutrons. The dominant effect is for separation at the level of atomic nuclei, the Fermi length of 10^{-6} nm. The eigenstates (differing possible classical positions) of such slight

3. While in superposition, tubulin qubits communicate/compute by entanglement with other tubulin qubits in the same MT, other MTs in the same dendrite, and MTs in other gap-junction-connected dendrites (i.e. within a hyperneuron). Thus quantum computation occurs among MTs throughout macroscopic regions of brain via tunneling through gap junctions or other mechanisms.⁴²
4. Dendritic interiors alternate between two phases determined by polymerization of actin protein: a) In the liquid (solution: sol) phase, actin is depolymerized and MTs communicate/process information classically (tubulin bits) with the external world. During this phase synaptic activities provide inputs via MAPs that orchestrate MT processing. After reduction, sol-phase MT output states regulate axonal firing and synaptic plasticity. b) As actin polymerizes (e.g. triggered by glutamate binding to receptors on dendritic spines), dendritic cytoplasm enters a quasisolid gelatinous (gel) phase, MTs become isolated from environment and enter quantum superposition mode in which tubulins function as quantum bits or qubits (Fig. 6.12). The two phases alternate, e.g., at 40 Hz (Fig. 6.13).
5. Quantum states of tubulin/MTs in gel phase are isolated/protected from environmental-decoherence by biological mechanisms that include encasement by actin gelation, ordered water, Debye screening, coherent pumping and topological quantum error correction (Sect. 6.7.2).
6. During quantum gel phase, MT tubulin qubits represent preconscious (unconscious, subconscious) information as quantum information – superpositions of multiple possibilities, of which dream content is exemplary.
7. Preconscious tubulin superpositions reach threshold for Penrose OR (e.g. after 25 ms) according to $E = \hbar/t$ in which E is the gravitational self-energy of the superpositioned mass (e.g. the number of tubulins in superposition), \hbar is Planck's constant over 2π , and t is the time until OR. Larger superpositions (more intense experience) reach threshold faster. For $t = 25$ ms (i.e. 40 Hz) E is roughly 10^{11} tubulins, requiring a hyperneuron of minimally 10^4 neurons per conscious event (Hameroff and Penrose [89]). The makeup of the hyperneuron (and content of consciousness) evolves with subsequent events.
8. Each 25 ms OR event chooses 10^{11} tubulin bit states that proceed by MT automata to govern neurophysiological events, e.g. trigger axonal spikes, specify MAP binding sites/restructure dendritic architecture, regulate synapses and membrane functions. The quantum computation is algo-

shifts will be significant if they are collective for all nuclei in a protein, tipping into basins of attraction upon reduction. Thus superposition of conformations need involve only separation at the level of atomic nuclei. The delicate balance of powerful countervailing forces determining protein conformation lends itself to functioning as a qubit.

⁴² Centriole entanglement [96], quantum optical photons, Bose–Einstein condensation.

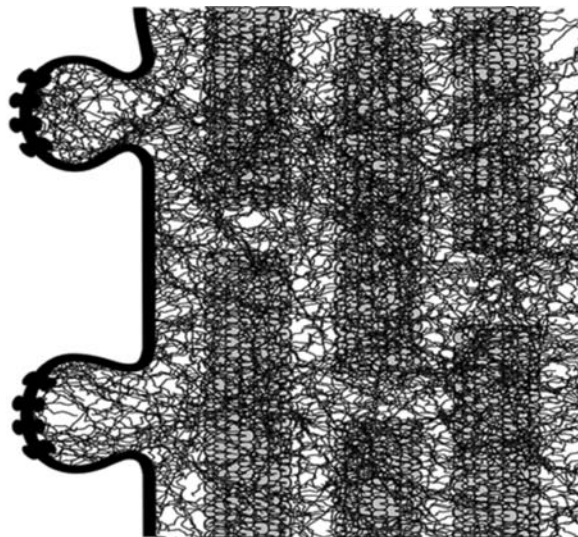


Fig. 6.12. Interior schematic of dendrites in quantum isolation phase. Actin has polymerized into the gel meshwork and MAPs detached, shielding and isolating MTs whose tubulins have evolved into quantum superposition

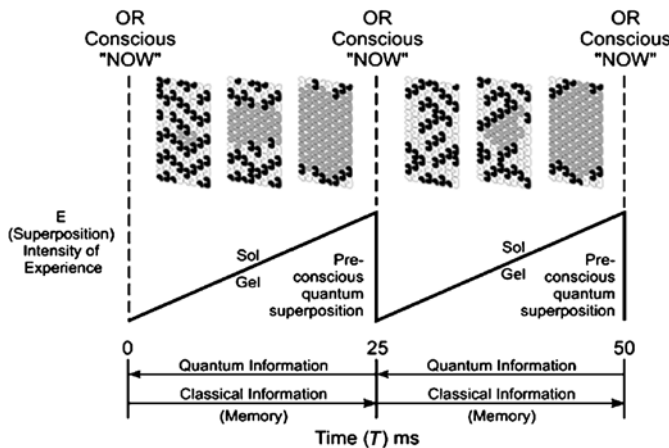


Fig. 6.13. Conscious events. *Top:* Microtubule automata enter preconscious quantum superposition phase (gray tubulins) until threshold for OR is met after 25 ms (this would involve superposition of 10^{11} tubulins in tens of thousands of neurons interconnected by gap junctions). A conscious moment (NOW) occurs, new classical states of tubulins are chosen and a new sequence begins. *Middle:* Phase diagram of increasing superposition in gel phase that meets threshold after, e.g., 25 ms. A conscious event (NOW) occurs, and the cycle repeats. *Bottom:* After each OR event, quantum information is sent backward in time to influence previous event. Classical information (memory) goes forward in time

rithmic, but at the instant of OR a noncomputable influence (i.e. from Platonic values in fundamental space-time geometry) occurs.

9. Each OR event ties the process to fundamental space-time geometry, enabling a Whiteheadian pan-protopsychist approach to the “hard problem” of subjective experience. A sequence of such events gives rise to our familiar stream of consciousness.

Applications of Orch OR to aspects of consciousness and cognition will be considered in Sect. 6.8.

6.7.2 Decoherence

Decoherence is the disruption of quantum superposition due to energy or information interaction with the classical environment. Consequently, quantum technology is generally developed in ultracold isolation, and physicists are skeptical of quantum computing in the “warm, wet and noisy” brain.

However, biological systems may delay decoherence in several ways [36]. One is to isolate the quantum system from environmental interactions by screening/shielding. Intraprotein hydrophobic pockets are screened from external van der Waals thermal interactions; MTs may also be shielded by counterion Debye plasma layers (due to charged C-termini tails on tubulin) and by water-ordering actin gels [95]. Biological systems may also exploit thermodynamic gradients to give extremely low effective temperatures [152].

Another possibility concerns decoherence-free subspaces. Paradoxically, when a system couples strongly to its environment through certain degrees of freedom, it can effectively “freeze” other degrees of freedom (by a sort of quantum Zeno effect), enabling coherent superpositions and entanglement to persist [163]. Metabolic energy supplied to MT collective dynamics (e.g. Fröhlich coherence) can counter decoherence (in the same way that lasers avoid decoherence at room temperature). Finally, MT structure seems ideally suited for topological quantum error correction by the Aharonov–Bohm effect [95].

Attempting to disprove the relevance of quantum states in consciousness, Max Tegmark ([228], cf. [203]) calculated MT decoherence times of 10^{-13} s, far too brief for neural activities. However, Tegmark did not address Orch OR nor any previous proposal, but his own quantum MT model, which he did indeed successfully disprove. Hagan et al. [85] recalculated MT decoherence times with Tegmark’s formula⁴³ but based on stipulations of the Orch OR model. For example, Tegmark used superposition of solitons “separated from

⁴³ The time tau to decoherence due to the long-range electromagnetic influence of an environmental ion is $\tau \simeq \frac{4\pi\epsilon_0 a^3 \sqrt{mkT}}{Nq_e^2 s}$ where T is the temperature, m is the mass of the ionic species, a is the distance from the ion to the position of the superposed state, N is the number of elementary charges comprising that superposed state, and s is the maximal separation between the positions of the tubulin mass in the alternative geometries of the quantum superposition.

themselves” along MTs by a distance of 24 nm. In Orch OR, superposition separation distance is the diameter of a carbon atom nucleus, 6 orders of magnitude smaller. Since separation distance is in the denominator of the decoherence formula, this discrepancy alone extends the decoherence time 6 orders of magnitude to 10^{-7} s. Additional discrepancies (charge versus dipole, correct dielectric constant) extend the calculated decoherence time to 10^{-5} to 10^{-4} s. Shielding (counterions, actin gel) extends the time into physiological range of tens to hundreds of ms⁴⁴. Topological (Aharonov–Bohm) quantum error correction may extend MT decoherence time indefinitely [181].

Is the brain truly “wet and noisy”? In gel phase MTs are in a quasisolid environment with ordered water. As for “noisy”, electrophysiological background fluctuations show ongoing “noise” to actually correlate over distances in the brain [9, 51].

Quantum spin transfer between quantum dots connected by organic benzene molecules is more efficient at room temperature than at absolute zero [167]. The same structures are found in amino acids (phenylalanine, tyrosine, tryptophan) in hydrophobic pockets of proteins. Other experiments have shown quantum wave behavior of biological porphyrin molecules [84], and still others that noise can enhance some quantum processes [13]. Evolution has had billions of years to solve the decoherence problem (Sect. 6.8.6).

6.7.3 Testability and Falsifiability

In 1998 twenty testable predictions of Orch OR were published [91]. Among them, the following have been validated: signaling along MTs [148, 149], correlation of synaptic function/plasticity with cytoskeletal structure [125, 262, 165], actions of psychoactive drugs involve MTs [7], and gap junctions mediate gamma synchrony/40 Hz (numerous references cited in Sect. 6.3.5). Others are currently being tested, and all are listed in Appendix 1. None have as yet been proven wrong. With the possible exception of the link to Planck-scale geometry, all are imminently testable. Orch OR is falsifiable – it need only be shown that consciousness can occur without dendrites, gap junctions (or some other mechanism for brain-wide quantum coherence), microtubules or quantum computation and Orch OR is falsified.

6.8 Applications of Orch OR to Consciousness and Cognition

6.8.1 Visual Consciousness

Visual components (e. g. shape, color, motion) are processed in separate brain areas and at different times but integrated into unified visual gestalts. How does this occur? And how do 40-Hz excitations relate to longer periods as

⁴⁴ The decohering effects of radiative scattering on microtubules is negligible.

sociated with the visual gestalt (e.g. 250 to 700 ms)? Thalamic inputs to V1 are fed-forward to areas V2, V3, V4 and LO for shape recognition, then to V8 and V4v for color, to V5, V3A and V7 for motion, then back to V1 and prefrontal cortex. In Woolf and Hameroff [264] we suggested that each component step corresponded with a 40-Hz excitation, and microconsciousness as proposed by Zeki [269]. To unify components in a visual gestalt after hun-

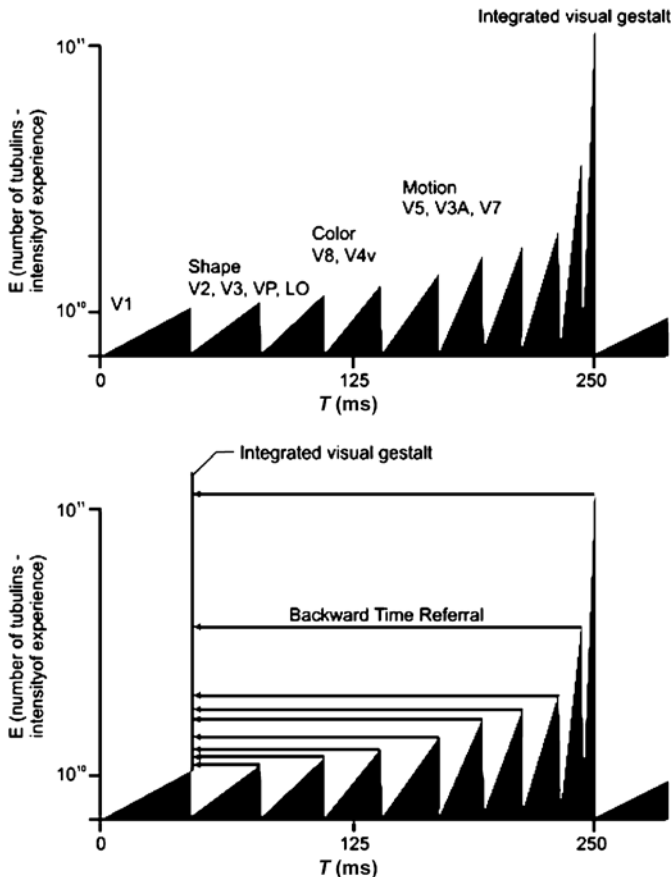


Fig. 6.14. A visual gestalt. *Top:* A crescendo sequence of 25-ms/40-Hz quantum computations/conscious events of components of conscious vision culminating in an integrated visual gestalt after, e.g. 250 to 700 ms (modified from Woolf and Hameroff [264]). The intensity (y -axis) is related to the amount of superposition represented by $E = \hbar/t$. Thus the slope/intensity for each event is inversely proportional to time to OR. *Bottom:* Modified version in which components are referred backward in time as nonconscious quantum information. The duration backward in classical time is related to slope/intensity of each component event. Thus an integrated visual gestalt occurs early in visual processing

dreds of ms, a cumulative snowball effect – a crescendo of crescendos – occurs (corresponding with the growth of a hyperneuron, Fig. 6.14). Commenting on this proposal Gray [81] points out that we are conscious only of the visual gestalt, not incremental components. This suggests that each Orch OR event refers quantum information/qualia of visual components backward in time (the duration proportional to E) to the initial V1 potential, resulting in an integrated visual gestalt early in the integration process. Consequently tennis and baseball players consciously see and recognize the ball's shape, color and motion early enough to respond successfully. In the color phi phenomenon the brain fills in the gap by backward referral from the subsequent location. Thus unlike retrospective construction, conscious sensation actually occurs in transit between the two locations.⁴⁵

6.8.2 Volition and Free-Will

Volition and free-will raise two major issues. One is time, in which we apparently act prior to processing the relevant inputs to which we respond. Backward time referral of unconscious quantum information can solve this problem. The other issue is determinism. If brain processes (including non-conscious processes) and events in our environment are algorithmic – even if highly nonlinear/chaotic – then our actions are deterministic products of genetic influences and experience. Wegner [256] concludes that free-will is the (illusory) conscious experience of acting deterministically. The noncomputable aspect of Penrose OR can help.

Suppose I am playing tennis about to return my opponent's ground stroke. As I begin to get my racket in position, I consider hitting a) to his forehand, b) to his backhand, c) a drop shot. A quantum superposition of these three possibilities (manifest as tubulin qubits) in a premotor cortical hyperneuron evolves and reaches threshold for OR, at which instant one set of tubulin states corresponding with one action (e.g. hit to his forehand) is chosen resulting in the appropriate set of axonal spikes to execute the choice.

Could such actions be completely algorithmic and classical? Yes, but in addition to the beneficial time effect, the noncomputable influence in Penrose OR can provide intuition, tipping the balance to the appropriate choice.⁴⁶ Sometimes (it seems to me at least) we do things and we're not quite sure why we do them.

⁴⁵ The same effect can account for tactile binding (we feel our foot strike the ground, and refer the sensation backwards in time to match the visual input) and the cutaneous rabbit (we feel the upper-arm, elbow and wrist sensations after the first tap and refer them to the appropriate spatial location). If no elbow or upper-arm sensations occur, no referral of the second and subsequent wrist sensations occur.

⁴⁶ From either Platonic influences embedded at the Planck scale, entangled quantum information from my opponent or an image from the near future, e.g. my opponent leaning the wrong way.

This is not free-will in the sense of complete agency because the non-computable influence is ultimately deterministic.⁴⁷ What we experience as free-will is algorithmic processes influenced by noncomputable factors. This differs from Wegner's [256] view in that 1) our actions are not completely algorithmic, and 2) because of backward time referral, decisions are made consciously, concomitantly with the experience of the choice and action, and 3) consciousness is not epiphenomenal.

6.8.3 Quantum Associative Memory

Evidence suggests memory is hard-wired in dendritic cytoskeletal structure [125, 262, 165]. Woolf and Hameroff [264] suggested that perception of a stimulus precipitates conscious awareness of associated memory via EPR-like OR of entangled (associated) information. This implies that disparate contents of unified consciousness remain entangled in memory [96].

6.8.4 The Hard Problem of Conscious Experience

How the brain produces phenomenal experience composed of qualia – the smell of a rose, the felt qualities of emotions, and the experience of a stream of conscious thought – is the “hard problem” [28].

Broadly speaking, there are two scientific approaches: 1) emergence (experience arises as a novel property from complex interactions among simple components in hierarchical, recursive systems), and 2) some form of panpsychism, pan-protopsychism, or pan-experientialism (essential features or precursors of conscious experience are fundamental components of reality, accessed and organized by brain processes).

Emergence derives from the mathematics of nonlinear dynamics, e. g. describing weather patterns, candle flames and self-organizing computer programs. Is consciousness an emergent property of interactions among neurons (or among tubulin proteins in microtubules)? Perhaps, but emergent phenomena generally have predictable and testable transition thresholds, and none are evident for consciousness.

Panpsychism, pan-protopsychism, and pan-experientialism view consciousness as stemming from fundamental, irreducible components of physical reality, like electrical charge, or spin. These components just are. Panpsychism holds that primitive consciousness is a quality of all matter: atoms and their subatomic components having subjective, mental attributes (e. g. [218], [189]). Whitehead [257, 258] eschewed panpsychism (as do I), arguing for processes rather than objects and properties. In Whitehead's pan-experientialism, consciousness is a sequence of events – occasions of experience – occurring in what he described as a wider, basic field of protoconscious experience. Philosopher

⁴⁷ One could say that free-will involves the choice of whether or not to allow oneself to be influenced by noncomputable factors.

Abner Shimony [210] observed that Whitehead occasions could be construed as quantum state reductions, consistent with Penrose OR. If so, what is Whitehead's basic field of protoconscious experience?

Penrose OR describes events in fundamental space-time geometry, the foundational level of the universe. Going down in scale below the size of atoms (10^{-8} cm) space-time is smooth until the Planck scale at 10^{-33} cm where coarse granularity (i.e. information) occurs.⁴⁸ The Planck scale is approached in modern physics through string theory, quantum gravity, twistor theory, spin networks, etc. Although the correct description is unknown, it is known that the Planck scale is quantized and nonlocal, and the level at which Penrose suggests quantum superpositions occur as separations, and where Platonic values exist. It is also at this ubiquitous level that protoconscious qualia are proposed to be embedded [90], hence pan-protopsychism.

If so, Whitehead's occasions of experience may be Orch OR events occurring in a pan-protopsychist field manifest at the Planck scale. Quantum computations with OR in microtubules connect our brains to the fundamental level of reality. Each Orch OR event accesses and selects a particular set/pattern of proto-conscious qualia that manifests as consciousness at the instantaneous moment of reduction – an occasion of experience.⁴⁹ A sequence of such events gives rise to our stream of consciousness.

6.8.5 What is Consciousness?

Orch OR is a threshold-based event, fulfilling Freeman's [58] criterion for consciousness: self-organized criticality occurring in the brain. Consciousness is OR. OR is consciousness. To be consistent: 1) all quantum superpositions are protoconscious, and 2) any Penrose OR must be conscious, regardless of where or how it occurs. Are brains the only site?⁵⁰

⁴⁸ The quantum world is generally considered to be random, however, EPR entanglement demonstrates that order exists. Measurement and decoherence may introduce randomness and indeterminacy avoidable through Penrose OR.

⁴⁹ Protoconscious qualia are presumed to exist in Planck scale geometry everywhere, including the space-time geometry within the brain. Because space-time at the Planck-scale is nonlocal (e.g. as evidenced by entanglement according to Penrose) the Planck scale configurations manifesting a particular set of qualia would exist both in the external world and in the brain. This is perhaps akin to the sensorimotor account of consciousness put forth by O'Regan and Noe [166].

⁵⁰ What about quantum superpositions in nonbiological systems? Technological quantum computers presently use superpositions of qubits with low mass separation/low E (e.g. ions, electrons, or photons) and reduction occurs by measurement well before OR threshold could be met. Hence these systems will not be conscious by the criteria of Orch OR. However, in principle, quantum computers using superpositions of larger mass qubits such as perhaps fullerene technology could reach the threshold for OR and have conscious moments.

Superpositions are common (ubiquitous at the Planck scale, hence pan-protopsychism) but Penrose OR requires stringent conditions. The time to reach threshold for OR is inversely related to the amount of superpositioned mass ($E = \hbar/t$, the larger the superposition, the more quickly it reaches threshold). Decoherence (i. e. by interaction with the environment) must be avoided by isolating the superposition until threshold is met. Small superpositions are easier to isolate/avoid decoherence but require longer times to reach threshold. Large superpositions reach threshold quickly but are more difficult to isolate. Conscious brain activities occur in the range of tens to hundreds of ms (e. g. 25 ms for 40 Hz), requiring nanograms of superpositioned proteins. Only in the brain can relatively large superpositions be isolated (e. g. in dendrites of hyperneurons) and linked to cognition.

Proteins are optimal quantum levers, large enough to exert causal efficacy in the macroscopic physical world but small (and delicately balanced) enough to be in superposition and mechanically governed by quantum London forces. Protein-based OR/consciousness is a self-organizing process on the edge between the quantum and classical worlds.

6.8.6 Consciousness and Evolution

Has evolution favored consciousness? The functionalist view of consciousness as illusory epiphenomenon seems to offer few advantages for adaptation and survival. However, Orch OR offers the following: 1) Quantum computing (e. g. search algorithms) offers faster (near-infinitely parallel) processing than conventional computing, 2) Penrose noncomputability would confer intuitive unpredictability, e. g. in predator-prey relationships, and 3) Backward time referral and near-instantaneous semantic perception and response would also be beneficial, e. g. in predator-prey relationships. Thus evolution would favor quantum isolation mechanisms for progressively larger superpositions, e. g. proteins, assemblies of proteins, assemblies of assemblies of proteins (neurons), assemblies of neurons/hyperneurons ... brains, resulting in faster and more useful times to OR⁵¹. There is also the possibility that biology evolved and adapted to a pre-existing protoconsciousness.

Large-scale quantum superpositions may exist naturally in the universe, for example in the cores of neutron stars, or the very early universe [271], able to reach OR threshold quickly. Such OR events would presumably lack organized information and cognition (OR without Orch). But to be consistent with the Orch OR criteria, yes, they would be conscious/have conscious experience, perhaps as flashes of meaningless awareness. This issue is faced by any theory: are all emergent phenomena conscious? Are all information processing systems such as computers and thermostats conscious? Functionalists often obfuscate this issue by saying, e. g., a thermostat is conscious in a thermostat-like way whereas humans are conscious in a human-like way, cats in a cat-like way, etc.

⁵¹ The onset of consciousness in the course of evolution is speculated upon in Hameroff [94].

6.9 Conclusion

The Penrose–Hameroff Orch OR theory “goes out on a limb” to address the puzzling facets of consciousness. It has engendered criticism because 1) it differs markedly from conventional wisdom, and 2) significant quantum processes seem unlikely in the warm brain milieu. But conventional wisdom fails to address puzzling facets of consciousness, and evidence suggests that biology has evolved mechanisms for brain-temperature quantum processes. Orch OR is consistent with all known neuroscience, cognitive science, biology and physics although it extends these disciplines theoretically. Moreover, unlike conventional theories Orch OR is testable and falsifiable. Spanning neurobiology, physics and philosophy, it is the most complete theory of consciousness.

Acknowledgement. Dedicated to the memory of Jeffrey Gray. I am grateful to Sir Roger Penrose for collaboration and insight, to Dave Cantrell for artwork, Patti Bergin for manuscript preparation and to the following friends and colleagues (none of whom necessarily endorse my position) for manuscript review and suggestions: Samuel Braunstein, Samantha Clark, Walter Freeman, Uriah Kriegel, Steve Macknik, Susana Martinez-Conde, Mitchell Porter, Paavo Pylkkanen, Logan Trujillo, Jack Tuszyński, Fred Alan Wolf and Nancy Woolf.

Appendix

Testable predictions of the Orch OR model [91]. Major assumptions are in bold, specific predictions are numbered in lower case and pertinent supportive references are in brackets.

Neuronal microtubules are directly necessary for consciousness

1. Synaptic sensitivity and plasticity correlate with cytoskeletal architecture/activities in both presynaptic and postsynaptic neuronal cytoplasm [125, 120, 155, 165].
2. Actions of psychoactive drugs including antidepressants involve neuronal microtubules [7].
3. Neuronal microtubule stabilizing/protecting drugs may prove useful in Alzheimer’s disease, ischemia, and other conditions [107].

Microtubules communicate by cooperative dynamics of tubulin subunits [148, 149, 246].

4. Laser spectroscopy (e.g. Vos et al. [253]) will demonstrate coherent GHz Fröhlich excitations in microtubules. (Preliminary work using surface plasmon resonance, see Lioubimov et al. [144].)
5. Dynamic vibrational states in microtubule networks correlate with cellular activity.
6. Stable patterns of microtubule cytoskeletal networks (including neurofilaments) and intramicrotubule diversity of tubulin states correlate with memory and neural behavior [125, 262, 165].

7. Cortical dendrites contain largely “A lattice” microtubules (compared to “B lattice” microtubule, A lattice microtubules are preferable for information processing).

Quantum coherence occurs in microtubules

8. Studies similar to the famous “Aspect experiment” in physics (which verified nonlocal quantum correlations [10] will demonstrate quantum correlations between spatially separated microtubule subunit states a) on the same microtubule, b) on different microtubules in the same neuron, c) on microtubules in different neurons connected by gap junctions.
9. Experiments with SQUIDS (Superconducting Quantum Interference Device) will detect phases of quantum coherence in microtubules.
10. Coherent photons will be detected from microtubules.

Microtubule quantum coherence requires isolation by cycles of surrounding actin gelation.

11. Neuronal microtubules in cortical dendrites and other brain areas are intermittently surrounded by tightly crosslinked actin gels. (Glutamate binding to NMDA and AMPA receptors causes actin polymerization in dendritic spines: [53].)
12. Cycles of gelation and dissolution in neuronal cytoplasm occur concomitantly with membrane electrical activity (e.g. synchronized 40-Hz activities in dendrites).
13. The sol gel cycles surrounding microtubules are regulated by calcium ions released and reabsorbed by calmodulin associated with microtubules.

Macroscopic quantum coherence occurs among MT in hundreds/thousands of distributed neurons and glia linked by gap junctions.

14. Electrotonic gap junctions link synchronously firing networks of cortical neurons, and thalamocortical networks [68, 75, 227].
15. Quantum tunneling occurs across gap junctions.
16. Quantum correlation occurs between microtubule subunit states in different neurons connected by gap junctions – the microtubule EPR experiment in different neurons (proposal by Andrew Duggins).

The amount of neural tissue involved in a conscious event is inversely proportional to the event time by $E = \hbar/t$.

17. The amount of neural mass involved in a particular cognitive task or conscious event (as measurable by near future advances in brain-imaging techniques) is inversely proportional to the preconscious time (e.g. visual perception, reaction times).

An isolated, unperturbed quantum system self-collapses according to $E = \hbar/t$.

18. Isolated technological quantum superpositions will self-collapse according to $E = \hbar/t$ (being tested – Marshall et al. [150]).

Microtubule-based cilia/centriole structures are quantum optical devices.

19. Microtubule-based cilia in rods and cones directly detect visual photons and connect with retinal glial cell microtubule via gap junctions.

A critical degree of cytoskeletal assembly (coinciding with the onset of rudimentary consciousness) had a significant impact on the rate of evolution.

20. Fossil records and comparison with present-day biology will show that organisms which emerged during the early Cambrian period with onset roughly 540 million years ago had critical degrees of microtubule-cytoskeletal size, complexity and capability for quantum isolation (e.g. tight actin gels, gap junctions; see Hameroff [94]).

References

1. Aharonov, Y., & Vaidman, L. (1990). *Physical Reviews A*. **41**:11.
2. Albrecht-Buehler, G. (1992). *Proceedings of the National Academy of Sciences USA*, **89** (17):288–92.
3. Albrecht-Buehler, G. (1998). *Cell Motility and the Cytoskeleton*. **40**(2):183–92.
4. Allison, A.C., & Nunn, J.F. (1968). *Lancet* **II**:1326–29.
5. Amassian, V.E., Somasunderinn, M., Rothswell, J.C., Crocco, J.B., Macabee, P.J., & Day, B.L. (1991). *Brain* **114**:2505–20.
6. Amitai, Y., Gibson, J.R., Beierlein, M., Patrick, S.L., Ho, A.M., Connors, B.W., & Golomb, D. (2002). *The Journal of Neuroscience* **22**(10): 4142–52.
7. Andrieux, A., Salin, P.A., Vernet, M., Kujala, P., Baratier, J., Gory-faure, S., Bose, C., Pointu, H., Proietto, D., Schweitzer, A., Denarier, E., Kamperman, & J., Job, D. (2002). *Genes and Development* **16**(18):2350–64.
8. Aoki, C., & Siekevitz, P. (1988). *Scientific American December*: 34–42.
9. Arieli, A., Sterkin, A., Grinvald, A., & Aertsen, A. (1996). *Science*. **273**:1868–74.
10. Aspect A, Grangier P, & Roger, G. (1982). *Phys. Rev. Lett.* **48**:91–94.
11. Atema, J. (1973). *Journal of Theoretical Biology* **38**:181–90.
12. Baars, B.J. (1988) *A Cognitive Theory of Consciousness*. Cambridge University Press, Cambridge.
13. Beige, A., Cable, H., Marr, & C., Knight, P. (2004). *arXiv.quant-ph/0405186v1*.
14. Benioff, P. (1982). *Journal of Statistical Physics* **29**:515–46.
15. Bennett, C.H., & Wiesner, S.J. (1992). *Physical Reviews Letters* **69**:2881–84.
16. Bennett, M.V., & Zukin, R.S. (2004). *Neuron*. **41**(4):495–511.
17. Bezzi, P., & Volterra, A. (2001). *Current Opinion in Neurobiology*. **11**(3):387–94.
18. Bittman, K., Becker, D.L., Cicirata, F., & Parnavelas, J.G. (2002). *Journal of Comparative Neurology*. **443**(3):201–12.
19. Block, N. (1995). *Behavioral and Brain Sciences* **18**:227–87.

20. Bohm, D. & Hiley, B.J. (1993) *The Undivided Universe*. Routledge, New York.
21. Braun, N., Schikorski, T., & Zimmerman, H. (1993). *Neuroscience* **52**(3):745–56.
22. Breitmeyer, B.G. (2002). *Consciousness & Cognition*. **11**(2):280–83.
23. Britten, K.H., Shadlen, M.N., Newsome, W.T., & Movshon, A. (1992). *Journal of Neuroscience* **12**:4745–65.
24. Brizhik, L., Scordino, A., Triglia, A. and Musumeci, F. (2001). *Phys. Rev. E* **64**:031902.
25. Bruzzone, R., Hormuzdi, S.G., Barbe, M.T., Herb, A., & Monyer, H. (2003). *Proceedings of the National Academy of Sciences of the USA* **100**(23):13644–9.
26. Buhl, D.L., Harris, K.D., Hormuzdi, S.G., Monyer, H., & Buzsaki, G. (2003). *Journal of Neuroscience*. **23**(3):1013–8.
27. Buzsáki, G., & Kandel, A. (1998). *Journal of Neurophysiology* **79**:1587–91.
28. Chalmers, D.J., (1996) *The Conscious Mind: In Search of a Fundamental Theory*. Oxford University Press, New York.
29. Changeux, J.-P. & Dehaene, S. (1989). *Cognition* **33**:63–109.
30. Chou, K.C., Zhang, C.T., & Maggiore, G.M., (1994). *Biopolymers*, **34**:143–53.
31. Churchland, P.S. (1981). *Philosophy of Science* **48**:165–81.
32. Conrad, M. (1994). *Chaos, Solitons and Fractals* **4**:423–38.
33. Crick, F., & Koch, C., (1990). *Seminars in the Neurosciences* **2**:263–75.
34. Crick, F.C. & Koch, C. (2001). *Nature Neuroscience* **6**:119–26.
35. Damasio, A. (1999) *The Feeling of What Happens*. Harcourt, San Diego.
36. Davies, P.C.W. (2004) *Biosystems* **78**(1–3):69–79.
37. Dayhoff, J., Hameroff, S., Lahoz-Beltra, R., & Swenberg, C.E. (1994). *Europe Biophysics Journal* **23**:79–83.
38. Dehaene, S. & Naccache, L. (2001). *Cognition* **79**:1–37.
39. Dennett, D.C. (1991) *Consciousness Explained*. Little, Brown, Boston.
40. Dennett, D.C. & Kinsbourne, M. (1992). *Behavioral and Brain Sciences* **15**:183–247.
41. Dermietzel, R. (1998). *Brain Research Reviews*. **26**(2–3):176–83.
42. Desmedt, J.D. & Tomberg, C. (1994). *Neuroscience Letters* **168**:126–29.
43. Deutsch, D. (1985). *Proceedings of the Royal Society (London)* **A400**:97–117.
44. Diçsi, L. (1989). *Physica Reviews A*. **40**:1165–74.
45. Draguhn, A., Traub, R.D., Schmitz, D., & Jefferys, J.G. (1998). *Nature*. **394**(6689):189–92.
46. Dustin, P. (1985) *Microtubules* 2nd edn, New York, Springer-Verlag.
47. Eccles, J.C. (1992). *Proceedings of the National Academy of Sciences* **89**:7320–24.
48. Edelman, G.M. & Tononi, G. (2000) *A Universe of Consciousness: How Matter Becomes Imagination*. Allen Lane, London.
49. Einstein, A., Podolsky, B. & Rosen, N., (1935). *Physical Review* **47**:777–80.
50. Everett, H. (1957). In *Quantum Theory and Measurement*, J.A. Wheeler and W.H. Zurek (eds.) Princeton University Press, 1983; originally in *Reviews of Modern Physics*. **29**:454–62.
51. Ferster, D. (1996). *Science* **272**:1812.
52. Feynman, R.P. (1986). *Foundations of Physics* **16**(6):507–31.
53. Fischer, M., Kaech, S., Wagner, U., Brinkhaus, H., & Matus, A., (2000). *Nature Neuroscience*. **3**(9):887–94.

54. Franks, N.P., & Lieb, W.R. (1982). *Nature* **316**:349–51.
55. Freeman, W.J. (2001) *How Brains Make up their Minds*. New York, Columbia University Press.
56. Freeman, W.J. (2003). *Journal of Integrative Neuroscience* **2**(1):3–30.
57. Freeman, W.J. (2004a) *Clinical Neurophysiology* **115**(9):2077–88.
58. Freeman, W.J. (2004b). *Clinical Neurophysiology* **115**(9):2089–107.
59. Friedman, D., & Strowbridge, B.W. (2003). *Journal of Neurophysiology* **89**(5):2601–10.
60. Fries, P., Schroder, J.H., Roelfsema, P.R., Singer, W., & Engel, A.K. (2002). *Journal of Neuroscience*. **22**(9):3739–54.
61. Froes, M.M. & Menezes, J.R. (2002). *Neurochemistry International*. **41**(5):367–75.
62. Froes, M.M., Correia, A.H., Garcia-Abreu, J., Spray, D.C., Campos de Carvalho, A.C., & Neto, M.V. (1999). *Proceedings of the National Academy of Sciences USA* **96**(13):7541–6.
63. Fröhlich, H. (1968). *International Journal of Quantum Chemistry*. **2**:641–9.
64. Fröhlich, H. (1970). *Nature* **228**:1093.
65. Fröhlich, H. (1975). *Proceedings of the National Academy of Sciences USA* **72**:4211–15.
66. Fukuda, T., & Kosaka, T. (2000). *Neuroscience Research* **38**(2):123–30.
67. Fukuda, T., & Kosaka, T. (2000). *Journal of Neuroscience* **20**(4):1519–28.
68. Galarreta, M., & Hestrin, S. (1999). *Nature* **402**, 72–75.
69. Galarreta, M., & Hestrin, S. (2001). *Nature Reviews Neuroscience*. **2**(6):425–33.
70. Gardner, M. (1970). *Scientific American* **223**(4):120–123.
71. Geldard, F.A. & Sherrick, C.E. (1972). *Science* **178**:178–9.
72. Geldard, F.A. & Sherrick, C.E. (1986). *Scientific American* **254**:90–95.
73. Ghirardi, G.C., Rimini, A., & Weber, T. (1986). *Physica Reviews D* **34**:470.
74. Ghirardi, G.C., Grassi, R., & Rimini, A. (1990). *Physica Reviews A* **42**:1057–64.
75. Gibson, J.R., Beierlein, M., & Connors, B.W. (1999). *Nature*, **402**:75–79.
76. Goodman, N. (1978) *Ways of Worldmaking*. Harvester Brighton, U.K.
77. Gray, C.M., & Singer, W. (1989). *Proceedings of the National Academy of Sciences USA* **86**:1698–702.
78. Gray, C.M., Konig, P., Engel, A.K., & Singer, W. (1989). *Nature* **338**:334–37.
79. Gray, J.A. (1995). *Behavioral and Brain Sciences* **18**:659–722.
80. Gray, J.A. (1998). In: *Toward a Science of Consciousness II? The Second Tucson Discussions and Debates*. (eds.) S. Hameroff, A. Kaszniak, A. Scott. Cambridge, MA. MIT Press:279–291.
81. Gray, J.A. (2004) *Consciousness: Creeping up on the Hard Problem*, Oxford, Oxford University Press.
82. Greenfield, S. (2000) *The Private Life of the Brain*. Allen Lane, London.
83. Gruber, T., & Muller, M.M. (2002). *Cognitive Brain Research* **13**(3):377–92.
84. Hackermüller L, Uttenhaller, Hornberger K, Reiger E, Brezger B, Zeilinger A, & Arndt (2003). *Physical Review Letters*, **91**:090408.
85. Hagan S, Hameroff S, & Tuszyński J, (2002). *Physical Reviews E*, **65**:061901.
86. Halpain, S., & Greengard, P. (1990). *Neuron* **5**:237–46.
87. Hameroff, S.R., & Watt, R.C. (1982). *Journal of Theoretical Biology* **98**:549–61.

88. Hameroff, S.R. (1987). *Ultimate Computing: Biomolecular Consciousness and Nanotechnology* (Amsterdam S Hameroff – The Netherlands: North Holland).
89. Hameroff, S.R., & Penrose, R., (1996a). In: *Toward a Science of Consciousness The First Tucson Discussions and Debates*. Hameroff, S.R., Kaszniak, and Scott, A.C., (eds.):507–540, MIT Press. Also published in *Mathematics and Computers in Simulation* (1996) **40**:453–480.
<http://www.quantumconsciousness.org/penrose-hameroff/orchor.html>
90. Hameroff, S.R., & Penrose, R. (1996b). *Journal of Consciousness Studies* **3(1)**:36–53. <http://www.quantumconsciousness.org/penrose-hameroff/consciousevents.html>
91. Hameroff, S. (1998a). *Philos. Trans. R. Soc. London Ser. A* **356**, 1869–96.
<http://www.quantumconsciousness.org/penrose-hameroff/quantumcomputation.html>
92. Hameroff, S. (1998b). *Trends in Cognitive Science* **2**:119–127.
93. Hameroff, S. (1998c). *Toxicology Letters* **100/101**:31–39.
94. Hameroff, S. (1998d). In: *Toward a Science of Consciousness II: The Second Tucson Discussions and Debates*. (eds.) Hameroff, S.R., Kaszniak, A.W., & Scott, A.C., Cambridge, MA: MIT Press:421–437.
95. Hameroff, S., Nip, A., Porter, M., & Tuszyński, J. (2002). *Biosystems* **64(13)**:149–68.
96. Hameroff, S.R. (2004). *Biosystems* **77(103)**:119–136.
97. Hatton, G.I. (1998). *Cell Biology International* **22**:765–780.
98. Hausser, M., Spruston, N., Stuart, G.J. (2000). *Science* **290**:739–750.
99. He, D.S., Burt, J.M. (2000). *Circulation Research* **86(11)E**:104–9.
100. Hebb, D.O. (1949) *Organization of Behavior: A Neuropsychological Theory*, New York, John Wiley and Sons.
101. Herve, J-C. (2004). *Biomembrane* **1662(1–2)**,1–2.
102. Hobson, J.A. (1988) *The Dreaming Brain*. New York, Basic Books.
103. Hobson, J.A. (2004). *Scientific American* **290(5)**:89.
104. Hoenger, A., Milligan, R.,A., (1997). *Journal of Molecular Biology* **265(5)**:553–564.
105. Hormuzdi, S.G., Filippov, M.A., Mitropoulou, G., Monyer, H., Bruzzone, R. (2004). *Biochimica Biophysica Acta*. **1662(1–2)**:113–3.
106. Hughes, S.W., Lorincz, M., Cope, D.W., Blethyn, K.L., Kekesi, K.A., Parri, H.R., Juhasz, G., & Cruneli, V. (2004). *Neuron* **42(2)**:253–268.
107. Iqbal, K., Grundke-Iqbali, I. (2004). *Current Drug Targets* **5(6)**:495–501.
108. Isaacson, J.S., & Strowbridge, B.W. (1998). *Neuron* **20(4)**:749–61.
109. Issom, L.L. (2002). *Novartis Foundation Symposium* **241**:124–38.
110. Jackendoff, R. (1987) *Consciousness and the Computational Mind*. MIT Press, Cambridge, Mass.
111. Jackson, F., (1982). *Philosophical Quarterly* **32**:127–36.
112. James, W. (1890). *The Principles of Psychology*. Vol. 1, Holt. New York N.Y.
113. Jasper, H., & Bertrand, G. (1966). *Journal of Neurosurgery* **24**:219–44.
114. Jibu, M., Hagan, S., Hameroff, S.R., Pribram, K.H., & Yasue, K. (1994). *BioSystems* **32**:195–209.
115. Jibu, M., Pribram, K.H., & Yasue, K. (1996). *International Journal of Modern Physics B* **10 (13&14)**:1735–54.
116. John, E.R., Tang, Y., Brill, A.B., Young, R. & Ono, K. (1986). *Science* **233**:1167–75.

117. John, E.R. (2001). *Consciousness & Cognition*. **10**(2):184–213.
118. Johnson, G.V.W., & Jope, R.S. (1992). *Journal of Neuroscience Research* **33**:505–12.
119. Joliot, M., Ribary, U., & Llinas, R. (1994). *Proceedings of the National Academy of Sciences USA* **91**(24):11748–11751.
120. Kaech, S., Brinkhaus, H., & Matus, A. (1999). *Proceedings of the National Academy of Sciences USA*. **96**(18):10433–10437.
121. Kandel, E.R., Schwartz, J.S., & Jessell, T.M. (2000) *Principles of Neural Science*, 4th edn, New York, McGraw-Hill.
122. Károlyházy, F., Frenkel, A., & Lukacs, B. (1986). In *Quantum Concepts in Space and Time*, R. Penrose and C.J. Isham (eds.), Oxford University Press. Oxford, U.K.
123. Karplus, M., & McCammon, J.A. (1983). In: *Dynamics of Proteins: Elements and Function, Annual Reviews of Biochemistry*, J. King (ed.), Benjamin/Cummings, Menlo Park. pp 263–300.
124. Kasischke, K.A., & Webb, W.W. (2004). *Science* **306**:411.
125. Khuchua, Z., Wozniak, D.F., Bardgett, M.E., Yue, Z., McDonald, M., Bero, J., Hartman, R.E., Sims, H., & Strauss, A.W. (2003). *Neuroscience* **119**(1):101–11.
126. Kitaev, A.Y., (1997). *ArXiv.org preprint quant-ph/9707021*.
127. Klein-Seetharaman, J., Oikawa, M., Grimshaw, S.B., Wirmer, J., Duchardt, E., Ueda, T., Imoto, T., Smith, L.J., Dobson, C.M., & Schwalbe, H. (2002). *Science* **295**(5560):1719–22.
128. Koch, C. & Crick, F.C.R. (2001). *Nature* **411**:893.
129. Koch, C.K. (2004) *The Quest for Consciousness: A Neurobiological Approach*. Englewood, Colorado, Roberts and Company.
130. Kolers, P.A., & von Grunau, M. (1976). *Vision Research* **16**:329–35.
131. Kornhuber, H.H., & Deecke, L. (1965). *Pflugers Archiv* **284**:1–17.
132. Krebs, A., Goldie, K.N., & Hoenger, A. (2004). *Journal of Molecular Biology* **335**:139–53.
133. Lader, A., Woodward, H., Lin, E., and Cantiello, H. (2000). *METMBS'00 International Conference*:77–82.
134. Langton, C.G. (1990). *Physica D* **42**:12–37.
135. LeBeau, F.E., Traub, R.D., Monyer, H., Whittington, M.A., & Buhl, E.H. (2003). *Brain Research Bulletin* **62**(1):3–13.
136. Libet, B., Alberts, W.W., Wright, W., Delattre, L., Levin, G., & Feinstein, B. (1964). *Journal of Neurophysiology* **27**:546–78.
137. Libet, B. (2000). *Consciousness and Cognition* **9**(1):1–12(12).
138. Libet, B., Wright, E.W. Jr., Feinstein, B., & Pearl, D.K. (1979). *Brain* **102**:193–224.
139. Libet, B., Alberts, W.W., Wright, E.W., & Feinstein, B. (1967). *Science* **158**:1597–1600.
140. Libet, B., (2002). *Consciousness and Cognition* **11**:291–99.
141. Libet, B., (2003). *Consciousness and Cognition* **12**:321–31.
142. Libet, B. (2004) *Mind Time: The Temporal Factor in Consciousness*. Cambridge, Mass., Harvard University Press.
143. Libet, B., Gleason, C.A., Wright, E.W., & Pearl, D.K. (1983). *Brain* **106**:623–42.

144. Lioubimov, V., Kolomenskii, A., Mershin, A., Nanopoulos, D.V., Schuessler, H.A. (2004). *Appl Opt.* **43**(17):3426–32.
145. Lisman, J.E., & Idiart, M.A., (1995). *Science* **267**: 1512–15.
146. Llinas, R. & Ribary, U. (1993). *Proceedings of the National Academy of Sciences USA* **90**:2078–81.
147. Logothetis, N.K., (2002). *Philosophical Transactions of the Royal Society B* **357**:1003–37.
148. Maniotis, A.J., Bojanowski, K., & Ingber, D.E. (1997a). *Journal of Cellular Biochemistry* **65**:114–30.
149. Maniotis, A.J., Chen, C.S., & Ingber, D.I. (1997b). *Proceedings of the National Academy of Science USA* **94**:849–54.
150. Marshall, W., Simon, C., Penrose, R., & Bouwmeester, D. (2003). *Physical Reviews Letters* **91**:13.
151. Masaki, E., Kawamura, M., Kato, F. (2004). *Anesthesia & Analgesia* **98**(3):647–52.
152. Matsuno, K. (1999). *Biosystems* **51**:15–19.
153. Matsuyama, S.S., & Jarvik, L.F. (1989). *Proceedings of the National Academy of Sciences USA* **86**(20):8152–56.
154. Matte Blanco, I. (1975) *The Unconscious as Infinite Sets*. London, Duckworth.
155. Matus, A. (2000). *Science* **290**:754–58.
156. McFadden, J. (2000) *Quantum Evolution: The New Science of Life*. New York, W.H. Norton.
157. McCrone, J. (1999) *Going Inside: A Tour Round a Single Moment of Consciousness*. Faber and Faber, London.
158. Melki, R., Carlier, M.F., Pantaloni, D., & Timasheff, S.N., (1989). *Biochemistry* **28**:9143–52.
159. Menon, V., Freeman, W.J., Cutillo, B.A., Desmond, J.E., Ward, M.F., Bressler, S.L., Laxer, K.D., Barbaro, N., & Gevins, A.S. (1996). *Electroencephalography and Clinical Neurophysiology* **98**:89–102.
160. Milner, A.D., & Goodale, M.A. (1995) *The Visual Brain in Action*. Oxford, U.K., Oxford University Press.
161. Miltner, W.H.R., Braun, C., Arnold, M., Witte, H. & Taub, E. (1999). *Nature* **397**:434–36.
162. Mouchetant-Rostaing, Y., Giard, M.-H., Bentin, S., Aguera, P.A. & Pernier, J. (2000) Neurophysiological correlates of face gender processing in humans. *European Journal of Neuroscience* **12**:303–10.
163. Nielson, M. & Chuang, I.L. (2001) *Quantum computation and quantum information*, Cambridge, UK, Cambridge University Press.
164. Nunez, P.L., Srinivasan, R.A., Westdorp, F., Wijesinghe, R.S., Tucker, D.M., Silberstein, R.B., & Cadusch, P.J. (1997). *Electroencephalography and Clinical Neurophysiology* **103**:499–515.
165. O'Connell, C., O'Malley, A., & Regan, C.M. (1997). *Neuroscience* **76**(1):55–62.
166. O'Regan, J.K., & Noe, A. (2001). *Behavioral and Brain Sciences* **24**:939–1031.
167. Ouyang, M., & Awschalom, D.D. (2003). *Science* **301**:1074–78.
168. Panksepp, J. (1999) *Affective Neuroscience*. Oxford University Press, Oxford.
169. Pantev, C. (1995). *Brain Topography* **7**:321–330.
170. Penrose, R. (1989) *The Emperor's New Mind*, Oxford University Press. Oxford, U.K.

171. Penrose, R. (1994) *Shadows of the Mind: A Search for the Missing Science of Consciousness*, Oxford University Press. Oxford, U.K.
172. Penrose, R. (1996). *General Relativity and Gravitation* **28**(5):581–600.
173. Penrose, R. (2004) *The Road to Reality: A Complete Guide to the Laws of the Universe*. London, Jonathan Cape.
174. Penrose, R. and Hameroff, S.R. (1995). *Journal of Consciousness Studies*. **2**:98–112.
175. Perez Velazquez, J.L., & Carlen, P.L. (2000). *Trends in Neurosciences*. **23**(2):68–74.
176. Pockett, S. (2000) *The Nature of Consciousness: A Hypothesis*, Writers Club Press, San Jose.
177. Pockett, S. (2002). *Consciousness and Cognition* **11**:144–161.
178. Poirazi, P.F. & Mel, B.W. (2001). *Neuron* **29**(3):779–796.
179. Pollack, G.H. (2001) *Cells, Gels and the Engines of Life*. Ebner and Sons, Seattle.
180. Pollen, D.A. (2004). *Consciousness and Cognition* **13**(3):626–645.
181. Porter, M. (2001). At <http://www.consciousness.arizona.edu/hameroff/topqcomp.htm>.
182. Pribram, K.H. (1991) *Brain and Perception*. Lawrence Erlbaum, New Jersey.
183. Puck, T., Krystosek, A. (1992). *International Reviews in Cytology*, **132**:75–108.
184. Ramón y Cajal, S. (1909). *Histologie du System Nerveux de L'homme & des Vertebrates*.
185. Rasmussen, S., Karampurwala, H., Vaidyanath, R., Jensen, K.S., & Hameroff, S. (1990). *Physica D* **42**:428–49.
186. Ravelli, R.B.G., Gigant, B., Curmi, P.A., Jourdain, I., Lachkar, S., Sobel, A., Knossow, M. (2004). *Nature* **428**:198–202.
187. Ray, P.G., Meador, K.J., Smith, J.R., Wheless, J.W., Sittenfeld, M., & Clifton, G.L. (1999). *Neurology* **52**(2):1044–49.
188. Rayner, E (1995) *Unconscious Logic: An Introduction to Matte-Blanco's Bi-Logic and its Uses*. London, Routledge.
189. Rensch, B. (1960) *Evolution Above the Species Level*. New York, Columbia University Press.
190. Ribary, U. Ioannides, A.A., Singh, K.D., Hasson, R., Bolton, J.P.R., Lado, F., Mogilner, A., & Llinas, R. (1991). *Proceedings National Academy of Sciences USA* **88**:11037–11041.
191. Roitberg, A., Gerber, R.B., Elber, R. & Ratner, M.A. (1995). *Science* **268**(5315): 1319–22.
192. Roth, L.E., Pihlaja, D.J. & Shigenaka, Y. (1970). *Journal of Ultrastructural Research* **30**:7–37.
193. Rouach, N., Avignone, E., Meme, W., Koulakoff, A., Venance, L., Blomstrand, F., & Giaume, C. (2002). *Biology of the Cell* **94**(7–8):457–75.
194. Rozental, R., Giaume, C. & Spray, DC. (2000). *Brain Research Reviews* **32**(1):11–5.
195. Sánchez, C., Diaz-Nido, J., Avila, J. (2000). *Progress in Neurobiology* **61**:133–68.
196. Sassoè-Pognetto, M., & Ottersen, O.P. (2000). *Journal of Neuroscience* **20**(6):2192–201.

197. Sataric, M.V., Zakula, R.B., & Tuszyński, J.A. (1992). *Nanobiology* **1**:445–6.
198. Scott, A.C. (1995) *Stairway to the Mind*, New York, Springer-Verlag.
199. Scott, A.C. (2004). *Journal of Consciousness Studies* **11**(2):51–68.
200. Schrödinger, E. 1935. (1983). *Naturwissenschaften*, **23**:807–812, 823–828, 844–849. (Translation by, J.T. Trimmer (1980) in *Proceedings of the American Philosophical Society* **124**:323–338.) In *Quantum Theory and Measurement* (eds.) J.A. Wheeler and W.H. Zurek). Princeton University Press.
201. Schwindt, P.C., & Crill, W.E. (1998). *Journal of Neurophysiology* **79**(5):2432–46.
202. Seck, M., Michel, C.M., Mainwaring, N., Cosgrove, R., Blume, H., Ives, J., Landis, T. & Schomer, D.L. (1997). *NeuroReport* **8**(12):2749–54.
203. Seife, C. (2000). *Science*, **287**:791.
204. Shadlen, M.N., & Movshon, J.A. (1999). *Neuron* **24**:67–77.
205. Shallice, T. (1964). *British Journal of Mathematical & Statistical Psychology* **17**:113–135.
206. Sherrington, C.S. (1957) *Man on His Nature*, 2nd edn, Cambridge University Press.
207. Shepherd, G.M. (1994) *Neurobiology*, 3rd edn, Oxford University Press, New York.
208. Shepherd, G.M. (1996). *Journal of Neurophysiology* **75**:2197–2210.
209. Shepherd, G.M. (2001) *The Synaptic Organization of the Brain*. 4th edn, New York, Oxford University Press.
210. Shimony, A., (1993) *Search for a Naturalistic World View?* Volume II. Natural Science and Metaphysics. Cambridge University Press, Cambridge, UK.
211. Siekevitz, P., (2004). *Science* **306**:410–411.
212. Singer, W., & Gray, C.M. (1995). *Annual Review of Neuroscience* **18**:555–86.
213. Singer, W. (1999). *Neuron* **24**:111–125.
214. Smith, S., Watt, R.C., & Hameroff, S.R. (1984). *Physica D*, **10**:168–174.
215. Solms, M. (2000). *Behavioral & Brain Sciences* **23**(6):843–50.
216. Solms, M. (2004). *Scientific American* **290**(5):82–88.
217. Sourdet, V., & Debanne, D. (1999). *Learning and Memory* **6**(5):422–47.
218. Spinoza, B. (1677) *Ethica in Opera quotque reperta sunt*. 3rd edn, (eds.) J. van Vloten and J.P.N. Land, Netherlands: Den Haag.
219. Squires, E.J. (1998). In: *Toward a Science of Consciousness The Second Tucson Discussions and Debates*. Hameroff, S.R., Kaszniak, & Scott, A.C. (eds.) Cambridge, MA., MIT Press:609–618.
220. Srinivasan, Y., Elmer, L., Davis, J., Bennett, V., & Angelides, K. (1988). *Nature* **333**(6169):177–80.
221. Stapp, H.P. (1993) *Mind, Matter and Quantum Mechanics*. Berlin, Springer-Verlag.
222. Steane, A. (1998). *Philosophical Transactions of the Royal Society London A*, **356**:1739–58.
223. Strege, P.R., Holm, A.N., Rich, A., Miller, S.M., Ou, Y., Sarr, M.G., & Far-rugia, G. *American Journal of Physiology – Cell Physiology* **284**(1):C60–66.
224. Stroud, J.M. (1956). In: *Information Theory in Psychology*, (ed.) H. Quastler, Free Press:174–205.
225. Tallon-Baudry, C., Bertrand, O., Delpuech, C., & Pernier, J. (1996). *Journal of Neuroscience* **16**:4240–49.

226. Tallon-Baudry, C., Bertrand, O., Delpuech, C., & Pernier, J. (1997). *Journal of Neuroscience* **17**:722–34.
227. Tamas, G., Buhl, E.H., Lorincz, A., & Somogyi, P. (2000). *Nature Neuroscience* **3**:366–71.
228. Tegmark, M. (2000). *Physica Rev E* **61**:4194–4206.
229. Tejada, J., Garg, A., Gider, S., Awschalom, D.D., DiVincenzo, D.P., & Loss, D. (1996). *Science* **272**:424–26.
230. Theurkauf, W.E. & Vallee, R.B. (1983). *Journal of Biological Chemistry* **258**:7883–86.
231. Tiitinen, H., Sinkkonen, J., Reinikainen, K., Alho, K., Lavikainen, J., & Naatanen, R. (1993). *Nature* **364**:59–60.
232. Tittel, W., Brendel, J., Gisin, B., Herzog, T., Zbinden, H., & Gisin, N., (1998). *Phys. Rev. A*, **57**:3229–32.
233. Traub, R.D., Whittington, M.A., Stanford, I.M., & Jefferys, J.G. (1996). *Nature* **383(6601)**:621–4.
234. Traub, R.D., Kopell, N., Bibbig, A., Buhl, E.H., LeBeau, F.E. & Whittington, M.A. (2001). *Journal of Neuroscience* **21(23)**:9478–86.
235. Traub, R.D., Draguhn, A. Whittington, M.A., Baldeweg, T., Bibbig, A., Buhl, E.H., Schmitz, D. (2002). *Reviews in the Neurosciences* **13(1)**:1–30.
236. Trujillo, L.T., Peterson, M.A., Kaszniak, A.W., & Allen, J.J.B. (2004). *Clinical Neurophysiology* (in press).
237. Tuszyński, J.A., Portet, S., Dixon, J.M., Luxford, C., & Cantiello, H.F. (2004). *Biophysical Journal* **86**:1890–1903.
238. Tuszyński, J.A., Hameroff, S., Sataric, M.V., Trpisova, B., & Nip, M.L.A. (1995). *Journal of Theoretical Biology* **174**:371–80.
239. Ungerleider, L.G. & Mishkin, M. (1982) Two cortical visual systems. In: *Analysis of Visual Behavior*. (eds.): Ingle, D.J., Goodale, M.A., & Mansfield, R.J.W.:549–586, Cambridge MA, MIT Press.
240. Van der Zee, E.A., Douma, B.R., Bohus, B., & Luiten, P.G. (1994). *Cerebral Cortex*. **4(4)**:376–90.
241. Van Petten, C., Coulson, S., Rubin, S., Plante, E., & Parks, M. (1999). *Journal of Experimental Psychology: Learning, Memory and Cognition* **25(2)**:394–417.
242. VanRullen, R. & Koch, C. (2003). *Trends in Cognitive Sciences* **7(5)**:207–13.
243. VanRullen, R., & Thorpe, S.J., (2001). *Journal of Cognitive Neuroscience* **13(4)**:454–61.
244. Varela, F.J. (1995). *Biological Research* **28**:81–95.
245. Varela, F., Lachaux, J.P., Rodriguez, E., & Martinerie, J., (2001). *Nature Reviews in Neuroscience* **2**:229–39.
246. Vassilev, P., Kanazirska, M., & Tien, H.T. (1985). *Biochemical and Biophysical Research Communications* **126**:559–65.
247. Velmans, M. (1991). *Behavioral and Brain Sciences* **14**:651–69.
248. Velmans, M. (2000) *Understanding Consciousness*. Routledge, London.
249. Venance, L., Rozov, A., Blatow, M., Burnashev, N., Feldmeyer, D., & Monyer, H. (2000) *Proceedings National Academy of Sciences USA* **97(18)**:10260–10265.
250. Voet, D., Voet, J.G. (1995). *Biochemistry*, 2nd edn, Wiley, New York.
251. Von der Malsburg, C., (1981). *MPI Biophysical Chemistry, Internal Reports 81–2*. Reprinted in *Models of Neural Networks II*, Domany E, van Hemmen, J.L., & Schulten, K., (eds.) Berlin, Springer (1994).

252. Von der Malsburg, C., & Singer, W., (1988). In: P. Rakic & W. Singer, (eds.), *Neurobiology of the Neocortex: Proceedings of the Dahlem Conference*, Wiley, Chichester:69–99.
253. Vos, M.H., Rappaport, J., Lambry, J.C., Breton, J., & Martin, J.L. (1992). *Nature* **363**:320–25.
254. Wang, N. & Ingber, D.E. (1994). *Biophys. J.* **66**:2181–2189.
255. Whatley, V.J., & Harris, R.A. (1996). *International Review of Neurobiology*. **39**:113–143.
256. Wegner, D.M. (2002) *The Illusion of Conscious Will* Cambridge, MA, MIT Press.
257. Whitehead, A.N., (1929) *Process and Reality*. New York, Macmillan.
258. Whitehead, A.N. (1933) *Adventure of Ideas*, London, Macmillan.
259. Wolf, F.A. (1989). *Journal of Theoretical Biology* **136**:13–19.
260. Wolfram, S. (1984). *Physica D* **10**:1–35.
261. Woolf, N.J. (1997). *Consciousness and Cognitive* **6**:574–96.
262. Woolf, N.J. (1998). *Progress of Neurobiology* **55**:59–77.
263. Woolf, N.J. (1999). *Trends in Neuroscience* **22**:540–41.
264. Woolf, N.J. & Hameroff, S.R. (2001). *Trends in Cognitive Science* **5**:472–78.
265. Woolf, N.J., Zinnerman, M.D., & Johnson, G.V.W. (1999). *Brain Research* **821**:241–49.
266. Wu, K., Aoki, A., Elste, A., Rogalski-Wilk, P., & Siekevitz P (1997). *Proceedings of the National Academy of Sciences USA* **94**:13273.
267. Yu, W., & Baas, P.W. (1994). *Journal of Neuroscience* **14(5)**:2818–29.
268. Zeki, S. (1999). *Inner Vision*. Oxford, Oxford University Press.
269. Zeki, S. (2003). *Trends in Cognitive Sciences* **7**:214–18.
270. Zeki, S., and Bartels, A., (1998). *Proceedings Royal Society of London, B.* **265**:1583–85.
271. Zizzi, P. (2002). <http://arxiv.org/abs/gr-qc/0007006>.

7 Life, Catalysis and Excitable Media: A Dynamic Systems Approach to Metabolism and Cognition

Christopher James Davia

Summary. This chapter examines the remarkable property that life has to maintain its organization in order to determine if there is a hitherto undiscovered principle that unites all living processes, including microprocesses, such as protein folding, and macroprocesses. The hypothesis is that at every scale, living processes are processes of catalysis, and that all biological processes mediate transitions in their environments, employing the same mechanism as enzymes.

Enzyme catalysis is a prototype process that elucidates the way in which living processes maintain their organization by mediating transitions via the structure in the environment (in this case, the substrate) leading to energy dissipation. Enzyme catalysis may involve solitons or traveling waves, nondissipative and robust waves that maintain their energy and structure in environments that embody invariance or symmetry. Solitons and/or traveling waves are ubiquitous in biological processes; it has been proposed that they are involved in a variety of biological processes including muscle contraction, protein folding, DNA “zipping” and “unzipping”, action potentials and crucially, in the brain itself. The chapter examines the relationship between microscopic instances of catalysis and traveling waves (solitons) in excitable media. It is then suggested that the brain is an excitable medium, and that cognition (and all mental processes) correlates with the spatiotemporal evolution of traveling waves in the brain.

This theory offers an alternative to the functionalist perspective that underlies much of current theoretical biology, by grounding biology and neuroscience within a general understanding of the process of catalysis. By instantiating the same principle at multiple scales, the theory suggests how the many biological processes that comprise an organism work and “cooperate”. Also, if living processes are catalytic, this leads to a better reconciliation between living processes and thermodynamics.

7.1 Life and Robustness

Whatever the contemporary paradigm of a field of study, its effect is to organize that field into components and relations and so influence how it is perceived and interacted with, both theoretically and practically. Our understanding of the evolutionary process, with its emphasis on mutation and natural selection, permits no absolute in terms of a common theme by which any living process may be identified and understood as such. The consequence is that there is no definition of the living process. Aside from reproduction and mutation, the often-cited fact that all living organisms feed, excrete and

metabolize does not provide what is necessary for a definitive understanding. The terms “feed”, “excrete”, etc. are so loosely defined and find expression in so many diverse ways that to suggest that these are definitive of life seems simply to suggest that life is a process. To list the numerous disciplines associated with the attempt to understand life underscores the lack of a unified theory of metabolism.

This state of affairs has left us with a set of difficult problems. What is the relationship between relatively simple processes, such as catalyzed chemical reactions, that are consistent with a basic understanding of thermodynamic principles, and processes that are understood to involve information in the form of codes, symbols or representations? These latter processes seem to require levels of organization that are more difficult to reconcile with thermodynamic considerations. In short, how do we reconcile the epistemological or functional variations of living processes with ontological considerations within a unified framework?

The challenge for an ecological theory is that it should provide a clear, definitive understanding of the living process that distinguishes living from nonliving processes. It must be consistent with our basic understanding of thermodynamic principles; and it should enable us to understand complex processes, such as cognition, as variations of a basic metabolic theme. If an encompassing theory of metabolism could be discovered, it would greatly simplify what is at present, a diverse and highly complex set of disciplines. It could rationalize our approach to the diagnosis and treatment of disease and provide a useful theoretical approach to complex biological problems such as cognition.

It might be argued that there is little reason to suppose that there is a common principle underlying biological processes; that evolution, via mutation and natural selection, provide all that is necessary to explain the diversity of living forms and processes. However, the growing realization that dynamic systems play a central role in practically every living process has placed life firmly in the nonlinear domain. This has introduced a unique set of problems. Nonlinear dynamic systems are extremely difficult to quantify. Their behavior is difficult to predict given even a detailed knowledge of the basic elements that comprise them. How do the many complex nonlinear processes that comprise an organism “cooperate” to the benefit of the organism as a whole? How do specific biological processes, such as mental development and indeed the whole evolutionary process itself, “ride” upon such unpredictable and sensitive processes? Does life “utilize” the properties of dynamic systems, implying that the relationship between life and nonlinear dynamic systems is contingent – a chance evolutionary discovery, or else, is life to be understood as essentially a dynamic system? Do the properties of nonlinear dynamic systems themselves hold the key to understanding life? In this respect, this chapter attempts to provide not only a definition of living processes, but also, a deeper understanding of nonlinear processes.

The structure of the chapter is as follows: I first examine some problems associated with the contemporary paradigm. Then I shall propose a unified theory of metabolism, a scale-invariant catalytic model, and argue that the model resolves these problems. Finally, I will apply the model to the complex problem of the brain and cognition.

Problems

The traditional approach requires us to understand the commonly observed properties of living systems as being consequent upon the process of natural selection. Within this framework, reproduction and mutation are the only “givens”; all other properties of biological processes are subsequent evolutionary developments. In this chapter I will explore the alternative proposition – specifically, that there is a common theme to living processes, and that reproduction and natural selection were subsequent developments. This alternative position seems difficult to rationalize, given that there would seem to be no mechanism by which a fundamental living process could perpetuate itself for a sufficient period of time in order to then incorporate reproduction and natural selection. However, even a single cell replaces the basic physical components of its constitution and is also (or consequently) a very robust process. From an abstract perspective, it may be argued that this replacement is actually a primitive form of reproduction. More central to the ideas to be developed, however, is the property of robustness itself. I suggest that life may have developed from a process that was naturally robust. If life is an essentially robust process, then the specific “mechanisms” of reproduction may have evolved subsequently. The complex chemical environments that gave rise to life would have inevitably involved the constant replenishment of raw materials and energy necessary for the continuation of the process. I suggest that what we understand as reproduction is an evolutionary development of an essentially robust process¹.

Life maintains its organization in highly complex and changing environments. The Bristlecone pine may live for 4600 years. A bacterium may represent a continuous process of metabolism stretching back to the beginning of life on this planet. We might point to a mountain as an example of a robust phenomenon. However, its apparent robustness is simply a function of the limited time frame in which it is observed. Speed the film up and we note that it is actually in a perpetual state of change, at the mercy of environmental forces. Nothing suggests that there is a “tendency” for the mountain to maintain its organization. On the other hand, we can count the tiny digits of the mouse when it is born and count them again when eventually it dies, and

¹ A similar argument in favor of focusing on the robustness of living processes was made by Maturana and Varela [44], who argued that it was a better starting point for insights into the possible ontogenetic and evolutionary transformations of biological systems, rather than starting with diversity and reproduction.

we note that there is the same number. Life exhibits a remarkable tendency to maintain its organization.

Before advancing the alternative model, I shall first briefly describe four problems in our attempt to understand the robustness of living processes within the contemporary paradigm.

1. Function and metabolism

Within the context of a complex organism, a cell or organ is understood to have a function that facilitates the survival of the organism as a whole. However, a cell or organ must survive in order to perform that function. But this raises a difficulty: How does a cell or organ reconcile the seemingly different tasks of functionality and self-maintenance? Why don't these different aspects of biological process compromise each other? When we use the term "function", we often mean a machine-like process that is designed or evolved to perform some task that is specific to some requirement. This implies a property schism. Machines are usually compromises between its functional requirements and the properties of the materials that instantiate that function; machines must be maintained. This problem can be illustrated by examining the brain. The brain is thought (by some) to be a computer of some sort, which entails the use of symbols and/or representations. The functional behavior of a computer is dependent upon the significance of these symbols/representations within a logical schema. However, there is no necessary relationship between functions that run within the schema and the properties of the materials upon which the schema operates. Thus, we can build a computer out of silicon or coke cans. In an ordinary computer, functions are expressed as tiny voltages in a larger robust structure. We attribute the robustness of a computer to the properties of the materials of which it is made, rather than to the functions that run on it. In the brain, by contrast, functional changes are linked to large-scale structural changes, suggesting an intimate entanglement between its functions and the structure of the material substrate that supports those functions. Do we assume that the robustness of the millions of dynamic neural relationships that constitute the working mind, when considered as a collection of diverse functional processes, is consequent on a complex set of maintenance functions? If so, we would encounter the same difficulty if we wish to understand the integrity of the maintenance functions.

If we consider a simple bacterium in functional terms (leaving aside the question of reproduction), we might claim that the function of the metabolism of a bacterium is to maintain the bacterium itself – that the "object" of its functionality is itself. This maneuver cannot so easily be applied to the brain, however. Mental functions cannot be argued to support the integrity of the brain itself – the brain is not the object of its functionality in the same way as may be claimed of a bacterium. It would seem to be quite clear that the physical principles that determine

the robustness of behavioral states of complex organisms, such as ourselves, cannot be the same principles that determine the robustness of the neural states that give rise to the behavior.

2. Structure and energy

Biological processes involve a complex interplay between energy and structure. Energetic forces invariably impose stresses on structures. How does life achieve the careful management of structure and energy in so many diverse biological processes?

3. Organism and environment

The environment is not static; it is dynamic and changing. Living organisms are exposed to constant variations in the thermodynamics of the environment. How does life manage to change its metabolic processes to account for variations in the thermodynamics of its environment?

4. Dynamic systems: Emergence and cooperation

The fact that life is a highly dynamic ensemble of nonlinear processes raises questions concerning the evolution and integrity of living organisms. “Emergence” is a term used to describe the fact that a complex system gives rise to dynamics that cannot be predicted from their basic constituents. Yet, living organisms are comprised almost exclusively of such complex systems. How do these dynamic systems “cooperate” to the benefit of the organism as a whole?

Function and Living Processes: Is “Function” a Redundant Term?

To address the first of these problems, we shall critically examine the concept of “function” as it applies to living processes. “Function” is such a commonly used term in biology that it is rarely questioned. If we wish to understand an organ or cell that forms part of a larger organism, we ask ourselves what function it performs. However, “function” is a problematic term because it is only meaningful within a generally understood context. The function of an engine can only be understood if we are already aware of the vehicle that the engine powers.

A stronger reason for rejecting the concept of “function” in living processes is the intimate relation between “function” and metabolism. For example, consider the effect that rabbits have on their environment. By keeping the grass short, rabbits help create environments that facilitate the emergence of plants and animals that would otherwise have difficulty finding a foothold. From an ecological perspective, it might be claimed that the rabbits are performing a function. But, the rabbits are only interested in their food supply. Their effect on their environments is not a function that is explicit in the rabbits other than as a consequence of their basic metabolic needs. Another example is the heart. It might seem quite clear that heart has a function – to provide oxygen and nutrients for the rest of the organism. It is often overlooked that the heart is also providing energy and nutrients for itself.

If function were an explicit aspect of the biological process, then we would expect a division in the workload. If a brain cell had to maintain its own organization in addition to the functional role that it plays, then we should see this reflected in its metabolism. However, “function” seems to be so deeply entwined with metabolism (or how the biological process maintains itself) that they appear to be identical. Indeed, subsequent to trauma, brain cells may die that were not directly affected. The cells that die as a direct consequence of trauma actually comprise the environment that sustains other cells, which then subsequently die as a consequence of the fact that their “environment” can no longer support them.

Following on from these two arguments, I suggest that there is no distinction between function and metabolism. Indeed, we can abandon the concept of “function” as redundant and focus on the relationship between the biological process (whether cell, organelle, organ or organism) and its environment in order to understand the metabolic process and how the metabolic process maintains its organization.

If we can abandon the concept of “function”, we can resolve the first set of problems enumerated above, namely, that of reconciling function and metabolism, because there is no distinction to be made between them. The heart’s pumping is its metabolism. Also, we eliminate the potential problem of a property schism that arises as a result of instantiating functional schemas with their own set of logical properties and relations, within metabolic processes.

We shall now examine the hypothesis that life exhibits the same type of process at every level of scale and attempt to define this process. At this stage we are principally interested in finding an explanation for the robustness of living processes. Once a hypothetical model has been proposed, we can examine if the model provides solutions to the remaining problems.

7.2 Life and Catalysis

The proposition that there is a principle common to all living processes, suggests that life may be organized fractally (or scale invariantly) in terms of process [15]². The proposal is that the physical principle that enables a cell to maintain its organization is the same principle that enables a collection of cells, a whole organ, and even the tiny structures within cells, to maintain their organizations. Indeed, there is much evidence of fractal structures in biology, such as the vascular structure of the brain and the structure of the lungs. Although fractal structures may be evidence of underlying scale invariant processes, more direct evidence may be found in biological processes

² In this chapter, the phrase “scale invariant” is used in lieu of “fractal” because not all scale-invariant processes and structures are fractals. The strong claim of this chapter is that there is a single process that defines life in a scale-invariant organization. Whether this is truly fractal is not currently known.

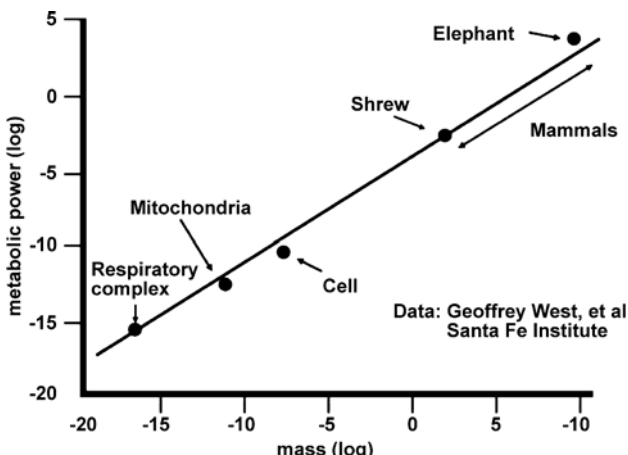


Fig. 7.1. The linear relation between metabolic rate and mass across biological scales (from [11])

themselves. A significant source of data is the existence of biological relations that hold across multiple scales. Figure 7.1 illustrates one such relation, the scaling law between the rate of metabolism of a living process and its mass. This relation holds from the scale of the elephant down to the level of the enzyme. In addition, universal scaling laws can be used to predict the structural and dynamic properties of vertebrate cardiovascular and respiratory systems, plant vascular systems, and insect tracheal tubes [11, 10].

If life is fractally organized in terms of process, then this may help us to identify the “prototype” process. The enzyme is the smallest working component of a living system. Enzymes are biological catalysts that can accelerate reactions by factors of many millions, they are the most efficient catalysts known. Catalysts participate in chemical reactions and emerge unchanged³.

This is a significant fact considering the central theme of this analysis – the robustness of living processes. If we consider a simple far-from-equilibrium environment that contained just two reagents, then a catalyst that mediated the predominant course of the chemistry would “survive” indefinitely. This follows from our basic understanding of catalyzed chemistry. The only active chemicals in the environment are the reagents. The catalyst mediates the reaction between them to produce products and then emerges unchanged to repeat the process. It is assumed here that the environment is maintained in a constant state. Thus, products are removed and the reagents are replaced as

³ A distinction must be made between enzyme catalysis and some forms of catalysis that work in a quite different way, by providing a reaction path to the products via a set of intermediary reactions. In this latter type, the catalyst may actually be transformed as a consequence of the reaction pathways and subsequently reformed via another reaction.

quickly as they are used up. If we extend this idea and introduce the concept of nonspecificity, then we can increase the complexity of the environment. A nonspecific catalyst may mediate a number of different reactions involving different reagents. The robustness of the catalyst depends upon the fact that its environment only contains reagents for which it may act as a catalyst. This may simply be a consequence of the limited number of chemicals in the environment. Alternatively, if we introduce a barrier, the effect of which is to limit access to the catalyst to only those reagents for which it may mediate reactions (in the same way that a cell membrane may limit access to the interior of a cell), then again, the catalysts will “survive” indefinitely. Of course, random quantum fluctuations may destroy a catalyst, chance chemicals may arise that react with a catalyst and so destroy it. This analysis serves only to illustrate the strong connection that exists between robustness, catalysts, and the process of catalysis itself.

If we consider the catalyst as a prototype of the living process, we find elements that correlate with our basic understanding of metabolism – the reagents can be considered as food and the principle source of energy that drives the process. The products can be considered as waste. Also, there is a strong relationship between catalysis and life when considered in terms of robustness. If we change the environment a catalyst may be destroyed or denaturized; change the environment of a life form and it may die.

The central proposition, then, is that life evolved as a scale-invariant process of catalysis; that is, each organelle, cell, organ, etc., up to and including the entire organism, maintains its organization by mediating transitions in its environment in the same way that an enzyme does. That life may have evolved from interacting catalysts has been previously proposed [33, 34]. Also, research increasingly points to the catalytic properties of DNA itself [12, 21, 40, 41, 70]. Although these instances of catalysis involve single-strand DNA rather than the double-strand variety, this may be evidence that DNA may have once acted as a catalyst in the early evolution of life [9]. Indeed, DNA still shares fundamental characteristics with enzymes. DNA undergoes conformational changes (a characteristic of enzymes) and participates in many reactions associated with transcription and emerges unchanged. Although, the transcription process of DNA involves many chemical processes, this does not preclude the possibility that this is essentially a catalytic process. It will be argued that complex interactions of enzyme-mediated reactions may give rise to macroscopic catalytic processes.

But, can a seemingly microscopic chemically based process – catalysis, be applied to macroscopic living processes? In order to address this question we shall examine the process of enzyme catalysis more closely.

Thermodynamics and Chemical Reactions: An Abstract View

Chemical reactions proceed according to the laws of thermodynamics. There is a tendency for the entropy of a chemical system to increase; this equates

to a decrease in the free energy (energy that is available to do work or enthalpy) and a decrease in the order of the system. (An increase in entropy may involve an increase in structure at the expense of a greater reduction in free energy.) In calculating the course of chemical reactions, the basic factors that are considered are chemical bond types, level of free energy, temperature, etc. However, not all chemical reactions proceed spontaneously; this is because of the existence of what is termed an “energy barrier”. Molecules have complex three-dimensional structures, forces and dynamics that may hinder the progress of the reaction.

When we observe a chemical reaction, we are observing the interplay between two different physical principles. The laws of thermodynamics, as they apply to an overall analysis of the chemistry, are quite independent of physical laws that govern how molecules dynamically interact depending upon their structures and the forces involved, how they collide, and how the kinetic energy is distributed among them. In a simplified way, the rate of a chemical reaction can be understood as being consequent on two components:

1. Thermodynamics – an analysis of which can indicate how far a system is away from thermodynamic equilibrium and thus, how the reaction is likely to proceed.
2. Factors that constitute a hindrance to the progress of the reaction: a major one being structure. Molecules have shapes and three-dimensional dynamics that are purely contingent factors, as far as the thermodynamics of the chemistry is concerned, but that influence the rate of the reaction, because molecules may have to come together at particular energies and orientations for the reaction to proceed.

This is essentially a story about energy and structure.

Enzyme Catalysis: The Classical View

Enzymes effectively overcome the structural hindrance to the progress of chemical reactions. They are said to reduce the “energy of activation” (i.e. the amount of energy required for the reaction to proceed).

A key feature of the process of enzyme catalysis is structural complementarity. Enzymes have binding sites that are shaped so that reagents may be positioned very specifically with respect to one another or, according to the theory of “induced fit”, approximately complementary such that the enzyme conforms to the shape of reagents. Early theories of enzyme catalysis argued that the reduction of entropy, resulting from the reduction of the ways in which the reagents could move with respect to one another, was the key to understanding the acceleration of the reaction. Subsequently, it has been discovered that enzyme catalysis involves dynamic structural changes (or conformational changes) of the enzyme–substrate complex. So, although complimentary structural features play an important role, the actual mechanism of the catalytic process is still a subject of research [43]. The compli-

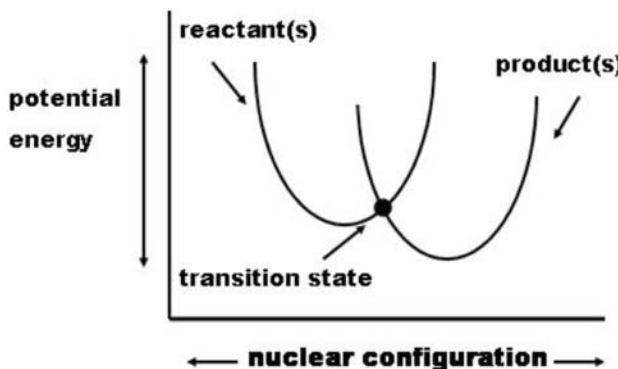


Fig. 7.2. A graph of the potential energy associated with particular molecular configurations, indicating the overlap between reagent(s) and product(s) at the transition state. Transition-state stabilization refers to the action of the enzyme stabilizing the reagents at the transition state facilitating a transition from the potential-energy surface of the reagents to that of the products

mentary structural features may limit access to the enzyme to molecules of a particular structure and chemical make up (hence their specificity); but, this is not the principle agent of the catalytic process.

According to the transition state theory (TST) the acceleration of the reaction results from the action of the enzyme in facilitating a “path” to the transition state and stabilizing the reagent(s) at that state. The transition state is an intermediate conformational state that occurs between the reagent(s) and product(s). Stabilizing the reagents at the transition state was thought to facilitate a transition from the potential energy surface of the reagent(s) to that of the product(s).

An Alternative Perspective

In the last quarter century TST has been found to be inadequate in accounting for observations resulting from improved methods of analysis. It is possible to create molecules in which specific atoms are replaced with heavier or lighter isotopes – i. e. with different numbers of neutrons in the nucleus. Differences in the rates of reaction reveal how critical the mass, or wave function, of the nucleus is in determining the rate of the reaction.

Kinetic isotope effects (KIEs) revealed discrepancies between the observed kinetics of enzyme-catalyzed reactions and the kinetics predicted by TST [25]. Initially, it was thought that these discrepancies could be accounted for by introducing a correction factor [7]. Transition-state stabilization was still thought to be the principle mechanism of catalysis. However, to account for the discrepancies, it was theorized that the energy barrier to the reaction was not overcome entirely classically. Quantum tunneling of a hydrogen nucleus was thought to occur just below the peak of the energy barrier.

This classical/quantum theory of enzyme catalysis itself came under scrutiny as a consequence of experimental data from a number of research groups in the mid- to late 1990s. These data suggested that, instead of a classical TST mechanism providing a path to, or near, the transition state prior to tunneling, the reaction proceeds entirely as a consequence of quantum tunneling. Furthermore, the underlying mechanism that is thought to achieve this is a vibrational mode of the enzyme/substrate complex [37]. This represents a move away from the view of enzyme catalysts as a collection of molecules with differing chemical mechanisms evolved to achieve transition state stabilization dependant upon the class of reaction being catalyzed and the structure of the reagents/products. The number of enzymes and the differing classes of chemical reaction in which this mechanism is implicated suggests that vibrationally assisted quantum tunneling may be the principle mechanism for a significant percentage, if not all, enzyme-catalyzed reactions that involve hydrogen transfer ([68]minireview, see also minireview papers [36, 2] for discussion on vibrationally assisted hydrogen tunneling in enzyme catalysis).

One variation of this theoretical approach to enzyme catalysis involves a unique type of nonlinear vibrational mode in the form of a soliton wave,⁴ [58]. Soliton waves (originally identified in water by J. Scott Russell in the nineteenth century) are nonlinear, localized, nondissipative waves that occur at the boundary between different tendencies of waves, depending upon the type of medium [53, 63]. In water they occur at the boundary between low-amplitude linear waves and high-amplitude nonlinear waves. Solitons can be formed using light by carefully balancing refraction and diffraction. If the medium is uniform and the boundary conditions embody symmetry, their complex dynamics form a localized self-sustaining solution to those boundary conditions, which, in principle at least, will persist as long as the boundary conditions do.

Understanding how solitons are instrumental in the process of catalysis involves understanding a little of the quantum world. Quantum mechanics is a statistical discipline that does not treat objects as exactly definable in space and time. The Uncertainty Principle portrays a world where a particle may inhabit a range of possible states involving parameters such as momentum, position, etc. To handle this “uncertainty”, quantum mechanics treats a particle as a wave function that encompasses its possible states. One of the surprising consequences of quantum theory is a phenomenon termed quantum tunneling. In the classical world if an object does not have enough

⁴ The transition state occurs at a point of invariance. Although this particular state cannot be linked to the dynamics of solitons directly, nevertheless, it may be strongly related to solitonic dynamics. The process of catalysis may not simply be a matter of providing sufficient energy at the right place. Rather, the relationship between the symmetry embodied by solitons and the symmetry of the transition state may be of primary importance.

momentum to traverse a barrier, then the barrier will not be traversed. However, in the quantum world there are circumstances when this rule is broken. Imagine a barrier; because of the wave description of quantum phenomena, a particle cannot exist near a barrier without its wave function extending, to a degree, into the barrier itself. If the barrier is narrow enough, the probability wave function may actually extend through the barrier entirely. Consequently, there is a chance that the particle will “disappear” from one side of the barrier and “reappear” on the other side.

Biologically based reactions often involve the transfer of an electron and/or a hydrogen nucleus (a proton) from one state (or position) to another. However, the bonds or forces that bind a proton or electron must first be broken, which requires energy, and hence, an energy barrier. Somehow, the enzyme overcomes this energy barrier. According to the solitonic theory, the mechanism that effects this transition is quantum tunneling facilitated by a vibrational mode of the enzyme, a soliton wave. The soliton, as described earlier, does not dissipate its energy; it can transfer a coherent, localized “lump” of energy from one place in the enzyme to another. Because the soliton is expressed as movement among the molecular chains that comprise an enzyme, the effect is to cause the enzyme to change shape (described as a conformational change); that change, in turn, causes movement among any molecules bound to the enzyme. The effect of this movement is to contract the distance between parts of the molecules bound to the enzyme. Consequently, the wave function of a hydrogen atom may overlap with the wave function corresponding to the product configuration thereby greatly increasing the possibility of quantum tunneling. This increases the rate of the reaction. This mechanism has also been suggested for catalytic events theorized to take place on the surfaces of cell membranes [58].

Generalizing the Concept of Catalysis

Questions of structure play a dominant role whichever theoretical approach to enzyme catalysis is adopted. For example, a major question for vibrationally assisted tunneling models, is how the energy is specifically targeted along the reaction coordinate [36, 68, 2]. The interplay between energy and structure, which forms the basic physical theme of chemical transitions, may also be generalized and understood to play a role at the macroscopic scale. Energy, in a variety of forms, is often “trapped” in the structures of the environment and rarely dissipates via the most efficient route to more favorable thermodynamic states. If the essential theme of catalysis involves overcoming structural constraints to achieve transitions to more favorable thermodynamic states, there is no reason in principle why the term “catalysis” could not be equally applied to macroscopic processes that achieve the same result. The chief question to be addressed is whether a similar mechanism is employed at both the microscopic and macroscopic scales in living processes.

So, does life utilize the mechanism of the soliton in a variety of biological processes at different levels of scale, and can these processes be understood as catalytic? Although enzyme catalysis may specifically involve solitons, there are many related waves with a variety of names – scroll waves, spiral waves, conformons, instantons, traveling waves, [23, 31, 51]. The principle characteristics that are important for the current argument are that they are localized, nonlinear, highly robust, and there is a relation (to be discussed) between the possibility of their formation and persistence and the structure of their environment or boundary conditions.

Localized nonlinear traveling waves, of which solitons are an example, are known or theorized to play a role in a variety of biological processes at different levels of scale (see the references in Table 7.1). It is generally thought that they represent an efficient way of transferring energy. I suggest that this represents evidence of a scale-invariant catalytic theme. Some examples are microscopic processes, including not just enzyme catalysis, but also the action potential of nerves. Other examples are macroscopic processes. For example, an analysis of the relative timing and power output of muscles in eels indicates that they correspond to a traveling wave [3]. Petroukhov [48] argues that the locomotions of many species, such as fish, snakes and millipedes, manifest solitons.

The enzyme is the smallest working component of the living cell. I would suggest that the next significant identifiable biological process is what is termed an autocatalytic cycle. The living cell is comprised of many interrelated autocatalytic cycles [73, 33, 34]. A living autocatalytic cycle is a self-reinforcing cycle of catalyzed reactions. If life is a scale-invariant process of catalysis, then we should be able to find evidence of solitons or traveling waves at this level of metabolism. Calcium waves, which form the basis of many cellular processes are autocatalytic processes [65]. The action potential is another example of a self-perpetuating autocatalytic cycle that exhibits

Table 7.1. Biological processes where nonlinear traveling waves have been observed or theorized

Microscopic processes	Macroscopic processes
Enzyme catalysis [58]	Basilar membrane [17]
Muscle function [16]	Population dynamics [47]
DNA [19, 75]	Locomotion of snails, worm-like organisms, millipedes, snakes, fish [48]
Microtubules [59]	
Cell membranes [58]	Nonmuscle motor systems (<i>ibid.</i>)
Protein folding [14]	Conformations of biological bodies (<i>ibid.</i>)
Nerve action potential [5]	The retina [76]
Purkinje fibres [4]	The brain [38]
Calcium waves [65]	Heart function [4]

soliton-like behavior [5]. In fact there are many examples of self-organizing traveling waves associated with autocatalytic cycles in excitable media. The presence of robust traveling waves and soliton-like behavior associated with autocatalytic cycles that mediate transitions within cellular metabolism suggests the possibility that the traveling wave or soliton) associated with an autocatalytic cycle may be behaving as a catalyst. In fact, it is suggested that the entire cell may be understood as an autocatalytic cycle [73].

Autocatalytic cycles are often instrumental in “amplifying” reaction rates, but this does not provide sufficient evidence that they are indeed catalysts. Better evidence may be found by analyzing the relationship between nonlinear traveling waves and structure.

Traveling Waves and Structure

The relationship between structure and solitons, or nonlinear localized waves generally, is crucially important. Soliton waves embody a great deal of symmetry in their dynamics. For soliton-wave formation there must be symmetry in the medium and boundary conditions. For example, canals (such as the type in which J. Scott Russell first identified a soliton wave) have a regular depth and width, regularity that is ideal for soliton formation. Also, solitons that are predicted to occur on membrane surfaces require topological transformations that leave key geometric features unchanged [56, 57]. Mathematical analyses of equations with solitonic solutions use Lie groups or other mathematical techniques that involve invariance under transformation. These examples illustrate the importance of regularities or symmetries in structure and the formation and persistence of solitons and nonlinear traveling localized waves generally.

The relationship between solitons or traveling waves and structural regularity is also evident in instances where solitons have been implicated in biological processes, such as the Davydov model of muscle contraction [16]. At the subcellular level, muscle contraction results from the dynamic interaction between microfilaments, myosin and actin. Energy released by the hydrolysis of ATP at the binding site of a myosin molecule would normally be expected to dissipate. However, Davydov noted that the regular spacing of the oxygen and carbon atoms that comprised the myosin molecule (an alpha helix protein) would give rise to a “compressive” force that would exactly cancel out the dissipative tendency of the wave. Consequently, a highly localized “lump” of energy would progress as a deformation of the myosin molecule in the form of a soliton. Davydov reasoned that this would provide sufficient energy such that the myosin molecules would slide and rebind with the surrounding actin molecules and thus decrease the overall length of the sarcomere (see Fig. 7.3).

The similarities between enzyme catalysis and the Davydov model of muscle function at the subcellular level are striking. Both may involve a soliton-mediated conformational change of a protein to effect a transition. Enzymes

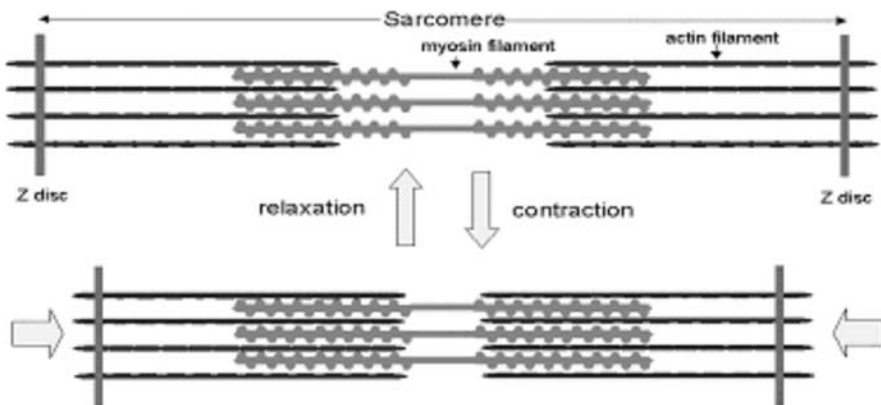


Fig. 7.3. A diagram of the relation between myosin and actin during muscle contraction

may also be activated by the hydrolysis of ATP. I suggest that the myosin molecule is acting as a catalyst and is employing the same mechanism as the enzyme, the soliton, to achieve this transition. Other examples of symmetries (or invariance) in biological structures associated with solitons and/or traveling waves include the regular crystalline structure of DNA, which is theorized to support traveling waves associated with the local unwinding of DNA in preparation for transcription [42, 49, 75, 74]. Soliton waves may also be supported by the uniform diameter and structure of microtubules [28]. These symmetries determine the particular solutions of solitons and/or nonlinear waves that can exist in those environments.

Nonlinear traveling waves in biology represent a unique synthesis between energy and the structure associated with their material substrate and/or boundary conditions. If we consider the problem of providing energy to do work at a particular location in a biological structure, such as DNA, it might initially seem that we would require a complex external system to deliver the energy where it is required, as machines do. However, if solitons are a principle means of energy transport in DNA then it is the structure (symmetry, invariance) of DNA itself that provides the means for energy to be delivered where it is required.

This point can be further strengthened by considering what happens when biological processes go wrong. A condition termed arrhythmia may occur when there is a small defect in the excitable tissues of the heart. The beating of the heart is associated with a traveling wave of excitation that moves through these tissues. The traveling-wave is a continuous phenomenon. The defect represents a discontinuity that cannot be “integrated” into the overall traveling-wave solution. The consequence of such defects is to give rise to irregular heart rhythms. One such irregularity results in a form of spiral-wave. What is interesting to note, is that the defect itself represents an invariance

or symmetry. It is theorized that spiral-type waves of excitation organize around the defect – it is described as an “organizing center” [6, 20]. Such spiral waves of activity, share characteristics of traveling waves generally and may be extremely robust.

Because of the intimate relation between traveling waves and their supporting structures, life combines energy and structure in such a way that they work together in the most efficient and least potentially damaging way. The possibility exists that the process of catalysis works, not simply by providing a path for energy so that it can be delivered where it is required, but by removing the discontinuity between energy and structure. Although this does not constitute a formal definition of what is happening, it is nevertheless clear that solitons and traveling waves represent a unique synthesis between energy and structure. At the molecular level, solitons are necessarily quantum coherent structures – a unified state of energy/matter. Even at the macroscopic scale the behavior of solitons and nonlinear traveling waves are noted as having characteristics shared by quantum processes. Traveling waves may combine both wave (continuous) and particle (discrete) characteristics [8]. Solitons theorized to move through crystal structures are modeled as quantum particles.

The Davydov soliton is a continuous phenomenon that is expressed as movement amongst the atoms that comprise the myosin molecule. The atoms behave, not as individual components contributing to an emergent wave, rather, the individual molecules become unified in a continuous, i. e. coherent traveling phenomenon. I suggest that a deeper understanding of the relationship between solitons and structure will reveal that the soliton may be understood as essentially unifying energy and structure.

Thus, the current proposal provides a potential solution to the second problem raised in the introduction, namely, the interplay of energy and structure in biology. I suggest that we should not consider biological structures independently of the traveling-wave forms that they support. Biological processes represent a unique synthesis between energy and structure such that there is no discontinuity between them.

Furthermore, if life is a catalytic process, we are closer to understanding how life maintains its organization in dynamic environments with changing thermodynamic conditions, the third problem discussed in the introduction. If we think of life as machine-like, then an organism would be faced with the problem of maintaining its functionality dependent upon the local conditions. Alternatively, from a catalytic perspective, the changing thermodynamic conditions are what determine the metabolic state of the organism. The organism changes its metabolism to a state that can mediate the predominant tendency of the local environment. Of course, an organism cannot mediate any tendency. If we change an environment drastically, then life will die. Thus, I would define the range of thermodynamic conditions in which an organism can mediate transitions as a catalyst to be its “environmental sur-

vival space". This argument holds true if we are considering the organism in an environment, or a biological process that forms part of a larger organism.

7.3 Catalysis, Traveling Waves and Excitable Media

To complete the analysis of living processes as catalytic, we need to consider the living process in the context of an environment that is maintained in a far-from-equilibrium state [50]. For life to be sustained and evolve, not only must there be energy in the environment that can be released, but there must be a means by which energy can be put back into the environment. This basic physical requirement may be simulated in the form of an excitable medium. An excitable medium is a substrate with energy associated with it. Once the energy has been depleted, as a consequence of a living process (or autocatalytic reaction), there is a system to replenish the energy. A familiar natural excitable medium is a field of grass; the energy may be depleted as a consequence of herd grazing, this leaves an area of the medium that can no longer support grazing, termed a refractory zone. Grazing can resume once the grass has replenished itself. This feature of excitable media plays an important role in the formation of traveling waves. Just as herd animals vacate an area that can no longer support grazing, so autocatalytic reactions or traveling waves of bacteria in excitable media are characterized by waves separating "active" areas of the medium from those depleted of refractory areas. To cite the importance of the relationship between life and excitable media, may seem to be simply underscoring the fact that life requires a constant supply of energy – a far-from-equilibrium environment. However, it is often overlooked, that a key feature of all laboratory experiments involving excitable media, and indeed, in instances that involve excitable media in biological processes, is the structure of the medium itself. For example, studies that involve the emergence of traveling waves or dissipative structures invariably also involve a medium that is uniformly structured. I suggest then, that it is not sufficient to define an excitable medium simply in terms of its potential energy content and its ability to renew itself. It must necessarily be defined in terms of a structural component.

Many of the examples of solitons and traveling waves in biology that have been cited so far are associated with excitable media. For example, the nerve and muscle fibers of animals are excitable media. As has been discussed, energy is released from these tissues as a result of the action of traveling waves. At a larger scale, the locomotion of animals such as fish and snakes, is also associated with traveling waves, specifically soliton waves that move through these tissues [48].

Traveling-wave forms that are observed in biological media resemble those that are observed associated with coupled catalyzed reactions in excitable media. There is a variety of traveling-wave forms in excitable media – spiral, branching, and circular forms are common. For example, spiral forms have

been observed in calcium waves at the cellular level [39] and in isolated chicken retinas and the brain tissue of rats [76].

In laboratory studies robust traveling-wave solutions in excitable media are often found by careful control of crucial parameters that comprise the system. However, there is much evidence that robust wave forms emerge quite spontaneously, especially in living systems. For example, studies of the spatiotemporal evolution of traveling waves of bacteria [60], comparing them to a reaction–diffusion model, a coupled pair of partial differential equations [35], demonstrated that the traveling-wave forms of the bacteria conformed to the only long-term solution supported by the problem. Traveling waves are also observed in the spatiotemporal evolution of herd grazing animals, moth migrations, measles epidemics, and so forth [26, 27, 46, 47, 64]. The similarity in the spatiotemporal evolution of these traveling waves provides additional evidence that a common dynamic theme occurs as a consequence of the chemistry of catalysis and also of living processes in excitable media, both at the microscopic scale and the macroscopic scale.

From these examples we can generalize the key elements of scale-invariant biological catalysis at the microscopic and macroscopic levels, as illustrated in Table 7.2. The substrate corresponds to the reagents of a molecular reaction, or, at the macroscopic scale, an excitable medium such as a field of grass. The structural constraint is the structure of the substrate, such as the structure of the molecules that comprise the medium or the structure of the medium at the macroscopic level. The catalyst itself is the dynamic self-sustaining traveling wave associated with the depletion of the energy stored in the medium.

The structural constraint at the molecular level is overcome by the robust wave form associated with the enzyme, the soliton. At higher levels of scale, structural constraints are overcome as a consequence of large-scale traveling waves. Thus, from the level of molecular reagents to the classical world, energy dissipation is constrained by structure. A scale-invariant catalytic process extends the basic process of catalysis to overcome structural constraints at greater and greater levels of scale.

Table 7.2. Generalizing the concept of catalysis across scales

	Microscopic	Macroscopic
Substrate	Molecular reagents	Excitable media, e.g. the agar in a Petri dish or the environment that supports an organism
Structural constraint	Structure of molecular reagent(s)	Macroscopic structure of the excitable medium or the structure of the environmental survival space of an organism
Catalytic agent	Soliton associated with the enzyme	Large-scale soliton or robust traveling wave – e.g. traveling waves formed by bacteria in an excitable medium

Many internal biological processes that form parts of complex organisms illustrate the relation between excitable media, traveling waves and structure. For example, certain heart tissues are excitable media, and heart contractions are associated with robust traveling waves that move through these tissues. It is a shared characteristic of solitons and traveling waves that they require a threshold perturbation, after which the wave evolves according to its own internal dynamics. Thus the method by which we stimulate heart action after a cardiac arrest is to provide an initial perturbation, an electric shock, after which the heart begins to beat according to its own internal dynamics. The evolution of the traveling wave in the heart is dependent upon the structure of the heart itself [22, 18].

Microscopic biological processes also reveal the twin themes of excitable media and traveling waves. For example, a solitonic mechanism has been proposed as the principle agent in protein folding and conformational changes in proteins generally [13, 14, 29]. These researchers, using toy models of protein folding, suggested that solitons might assist in protein folding by overcoming energy barriers to achieve transitions from metastable configurations to configurations of lower energy. The unfolded protein embodies energy because it is in a metastable configuration and can therefore be considered as an excitable medium. Indeed, the toy model studies suggest the soliton may replenish its energy from the energy released as the protein folds to a more thermodynamically favorable configuration. Similar mechanisms have been suggested to explain DNA functioning, as mentioned earlier. Energy can be put into DNA as a consequence of torsional forces, effectively increasing the enthalpy, such that DNA itself can be considered an excitable medium. There is energy associated with the structure that can be potentially released. DNA “unzipping” is thought to result as the consequence of a soliton progressing along the DNA strand, releasing this energy as it goes [42].

The themes of excitable media and traveling waves play an important role in the auditory system as well. The basilar membrane is an excitable medium, and Von Bekesy [72, 71] demonstrated that its motion, consequent on a sound stimulus, is a traveling wave [17]. The basilar membrane is not a passive “receiver” of sound stimuli. Its frequency responses are highly non-linear, and its sensitivity is increased by active feedback processes [54, 55]. Specialized hair bundles have the effect of altering the dynamic response of the basilar membrane and thus altering its sensitivity to particular frequencies in real time ([45] pp. 32–36). This process is similar to what happens when a child makes a swing go higher by timing his/her pulling of the swing ropes with the upward motion of the swing. The dynamic feedback mechanisms associated with the basilar membrane not only respond to a stimulus but also “anticipate” it.

Traveling waves and excitable media can be discovered at every scale of biological. For example, the ocean, with energy stored in the millions of microscopic animals that it supports, can be considered an excitable medium.

The whale shark feeds exclusively on plankton and small sea creatures. If the locomotion of the whale shark is indeed a soliton or traveling wave, then we have a beautiful example of a complex biological process that exhibits the same fundamental dynamics as bacteria in a petri dish. This represents a move away from a mechanistic view of living processes. The emphasis is placed instead on the relationship between robust, nonlinear waves, excitable media and structure.

To summarize, the surface of this planet can be considered as a collection of excitable media that are maintained in a far-from-equilibrium state as a result of geothermal and solar energy combined with the rotation of the earth. Within these environments, plant growth and bacteria plumes in the ocean deplete this energy that is then replaced. These biological processes may take the form of traveling waves and can also be considered examples of excitable media. They support more complex animal life processes that themselves represent further excitable media and also give rise to complex nonlinear dynamics in the form of traveling waves. For example, the complex dynamics of predator-prey relations give rise to traveling waves. What is being suggested, is that excitable media and robust traveling waves, not only form essential biological processes, but are also its central components. Indeed, it has also been argued that robust autocatalytic processes may have played a crucial role in the prebiotic stages of evolution [67].

To test this idea we shall examine the possibility that the most complex of biological processes, the nervous system, which is often considered to be a unique evolutionary development, may be understood simply as an excitable medium that supports traveling waves [66].

7.4 The Brain as an Excitable Medium

The problems associated with the functionality of living processes outlined at the beginning of this chapter included the observation that the brain is not the “object of its functionality”. From this it would seem to follow that successful (i. e. robust) modes of behavior must take precedence over the neural states that gave rise to them. It would seem to be obvious that whatever principle determines that a particular behavioral state is successful in terms of survival cannot be the same principle that determines the robustness of the neural state associated with that behavior. Behavioral modes of animals take place in physical contexts that appear quite removed from the physical context of neural activity.

The aim of this section is not only to examine the possibility that the brain is essentially an excitable medium that supports traveling waves, but, when applied to neural states and their corresponding behavioral states specifically, it will be possible to show that there is no primacy of successful behavioral states over neural states. Successful (i. e. robust) behavioral states are necessarily correlated with robust neural states and these instances of robustness

are consequent upon the same dynamic principle. It will therefore be argued that although the brain is apparently not the “object of its own functionality”, no additional or specific mechanism is required to maintain neural states that give rise to successful modes of behavior.

Neural Structure and Catalysis

In addition to studies that point to traveling waves in the brain similar to those observed in excitable media [66, 38], further evidence can be found by considering the interface between the brain and the body and senses. As has been discussed, the locomotion of animals, such as snakes and millipedes, exhibits traveling waves. Also, there is good evidence that the auditory system involves traveling waves at the basilar membrane. Given that the brain “interfaces” with these motor and sensory systems, it is reasonable to speculate that it does so by utilizing similar dynamic processes, traveling waves. It would be more difficult to control the evolution of a traveling wave associated with the locomotion of a fish, for example, if the brain had to convert from some other “format” to a nonlinear traveling wave.

Perceiving the brain as an excitable medium may offer an insight into its basic structure. As has been discussed, the spatiotemporal evolution of traveling waves is strongly influenced by the structure of the medium itself. This is useful in situations where the structure of the medium represents the catalytic problem to be solved, as in the case of the heart. But this would represent an unwanted contingency for a system that has evolved to overcome structural constraints (i. e. the environment) other than those that are already implicit in the structure of the medium.

If we wished to design an excitable medium that could allow for the spatiotemporal evolution of traveling waves to be dependent upon a variety of structures (symmetries, invariance) in real time, we would require a medium that could be structured in real time. Furthermore, we may wish to allow for the spatiotemporal evolution of traveling waves to be dependent upon structures (symmetries/invariance) that do not necessarily translate to proximate areas of the medium. For example, when we speak, we coordinate the movement of our lips and tongue and the shape of our mouths with the sounds that we hear. I suggest that this synchrony is achieved as a consequence of traveling waves uniting the neural activity in different parts of the brain. The brain may be arranged in the way that it is both to eliminate its own structure from playing a determining role in how traveling waves evolve, and also to allow traveling waves to evolve according to complex spatiotemporal relations (symmetries, invariance), facilitated by the brain’s complex network of interrelations. If we imagine an ordinary excitable medium in which each part of the medium was isolated and then connected to other parts of the medium with excitable fibers – we would have a simple brain.

To pursue the catalytic hypothesis, we can explicitly cast the brain in catalytic terms. Glucose supplied by the bloodstream maintains a potential

energy gradient in the brain – as an excitable medium. The consequence of stimulation by the senses activates or suppresses areas of the brain and thus structures the medium (the brain). How the available energy dissipates is determined by these structures. We can consider the excitable medium of the brain as the substrate, and the way in which the medium is structured by the senses and the body as the structural constraint. The spatiotemporal evolution of traveling waves in the brain overcomes the structural constraint by providing paths for energy dissipation via the invariance or symmetries that are implicit in the structure of the medium (and that are activated and thus able to provide energy), in the same way that a catalyst does utilizing a solitonic or traveling-wave mechanism⁵. This hypothesis represents a move away from the idea that the senses are providing information. The senses, I suggest, are simply structuring the medium in real time.

Of course, the act of perception does not bring about a change in the environment as an enzyme does. To understand the catalytic effect of neural activity we must also consider perception in conjunction with behavior or “action”. This will be discussed shortly.

Emergence

Emergent structures in far-from-equilibrium-systems, of which traveling waves in excitable media are an example, have been cited as evidence that dynamic systems may give rise to complex patterns of behavior [50, 66]. Furthermore, it is claimed that these structures cannot be understood from a consideration of the basic constituents, processes, etc. that comprise the system, that is, that they are “emergent”. It is hoped that the “emergence” of these structures may offer an insight into biological processes that increase their level of complexity – the brain being the most significant example. Implicit in this approach is the idea that far-from-equilibrium systems may “give rise” to structure – order for free! While the current hypothesis builds on this body of research on dynamic systems, it provides an importantly different perspective on emergence. It suggests that the complex processes that emerge associated with dynamic systems are instances of catalysis, but catalysis with wider and different domains of mediation that involve overcoming structural constraints at higher levels of scale or more complex levels of structure implicit in the medium (what this means will be more apparent when we apply this idea to mental development shortly), and it is this aspect that makes them irreducible to their constituents. This perspective has the added advantage that it can address the questions of why and how “emergent” processes or structures cooperate in the context of complex organisms to benefit the organism as a whole, problem four in the introduction.

⁵ Although I have not explored quantum issues at length in this chapter, I am of the opinion that the traveling waves described earlier may well be associated with quantum coherent states.

Processing in the Plane of the Problem

This approach to understanding the brain can be clarified by considering research that illustrates how processing occurs “in the plane of the problem”, that is, how the evolution of traveling waves relates directly to the structure of the medium itself. Research of Rambidi et al. [52], Adamatzky [1] and others uses a variation of the Belousov–Zhabotinsky (BZ) reaction to examine how the spatiotemporal evolution of traveling waves relates to the structure of the medium. Adamatzky uses a photosensitive medium. The reaction is initiated by projecting a light image onto the medium, the effect of which is to suppress or excite areas of the medium. Surprisingly, the spatiotemporal evolution of the traveling waves performs basic image processing; contrast is enhanced, edges become more defined, and broken contours are repaired, as shown in Fig. 7.4. The effect of activating and/or suppressing areas of the excitable medium amounts to structuring the medium. If an area of the medium is suppressed or inhibited, then there may as well be no medium there at all. Also, structures that are not normally associated with continuous

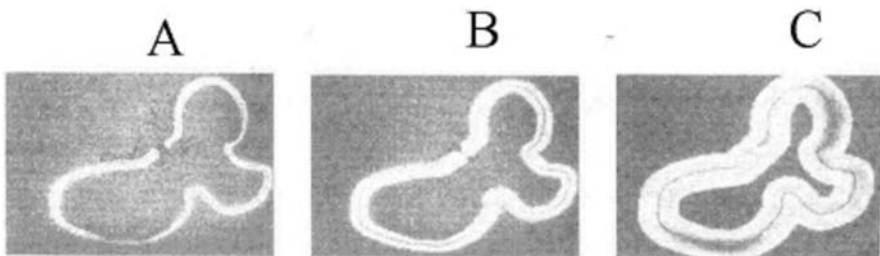


Fig. 7.4. Examples of how traveling waves of a BZ reaction in a photosensitive medium have the effect of completing broken contours (adapted from Rambidi et al. [52] in Adamatzky [1])

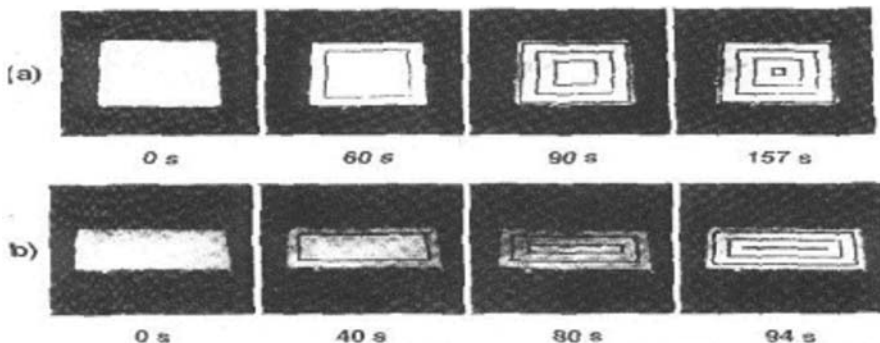


Fig. 7.5. A rectangular traveling wave, demonstrating the remarkable variety of forms that traveling waves in excitable media and the BZ reaction can adopt (adapted from Jinguji et al. [32])

phenomena, such as rectangular traveling waves, can be generated, as shown in Fig. 7.5.

This proposal challenges the assumption that neurons communicate with each other via some, as yet, undeciphered code. It suggests instead that the significance of a neural event is that it occurs at a certain place and at a certain time within an overall context of neural events taking place in space and time. It is the direct correspondence between the relative position and timing of events in the perceptual field and the brain that is of primary importance. Indeed, there is a direct topological mapping between the retina and the V1 layer in the visual cortex [76]. What this means is that a triangle in the visual field, for example, translates to a triangle of neural excitability and/or suppression in the V1 layer. The relative spatial and temporal relationships implicit in the triangle are preserved in terms of how the medium is structured. The mapping of spatial and temporal relationships in the visual system may be seen as parallel to the frequency mapping of sound in the auditory system, as described earlier in reference to the research of Von Bekesy and others. The basilar membrane responds at the frequency of the stimulus. This response is translated directly to neural activity. If neural processing involved the use of codes, then this would be difficult to reconcile with the fact that the brain preserves essential spatiotemporal characteristics of the perceptual domain.

Traveling Waves and Cognition

Because the suggested mechanism of brain processing is the soliton (or traveling wave), the relationship between soliton formation and the structure (invariance or symmetry) of the environment may offer an insight into how the brain unifies aspects of the environmental stimulus into the familiar objects and events of perception. For an object or event to become an object of cognition it must embody invariance or symmetries, what is being called “structure”, in space and/or time [24]. If the potential object or event of perception embodies structure, then via the senses, that structure translates to excitable areas in the brain that embody invariance or symmetries in space and/or time. Traveling waves in the brain sustain themselves by releasing this energy, hence, they constitute a process of catalytic mediation. Thus, the particular solitonic or traveling-wave solution is dependent upon the structure (invariance, symmetry) of the object or events of perception.

To understand how cognition, as a process of catalytic mediation, might give rise to perception, we might consider a soliton moving down a canal. We can choose to observe this soliton in more than one way. We can imagine the canal moving in the opposite direction to the soliton, such that the soliton remains in a fixed position. From this equally valid perspective, the soliton is observed to maintain its organization while mediating a set of transitions that correspond to the regular structure of the water determined by the structure of the canal. The basilar membrane and the proposed traveling waves

in the V1 layer associated with visual perception may be doing something very similar. The traveling wave in the basilar membrane can maintain its organization while mediating transitions (pressure changes) from the sound stimulus to neural activity, releasing energy in the brain as it does so. The basilar membrane, via nonlinear feedback processes, “anticipates” where energy is available in the brain at the interface between the basilar membrane and the nervous system. Similarly, the traveling wave in V1 that is associated with visual perception, such as the perception of a rotating cube, also releases energy in the brain by mediating transitions embodied by the visual stimulus. The traveling wave in the visual cortex “anticipates” where energy will be available, such that areas of the brain that are excited by the stimulus release their energy as a consequence of the dynamic activity of the traveling wave.

It may seem that what is proposed is that traveling waves progress through the brain in much the same way as they progress through an excitable medium. This is not the case. As was mentioned previously, we can choose to observe a soliton such that the soliton remains in a fixed position, maintaining its organization, while mediating a set of transitions. The brain is posed with a similar problem. Whatever neural activity corresponds to the perception of an event, it must maintain its integrity, given the set of transformations in space and time imposed upon the brain as a consequence of the transformations in space and time embodied by the stimulus. As Gibson [24] and other perception psychologists have emphasized, we should think of the act of perception as dynamic, not static. There is a constant stream of stimuli, much like the constant stream of water moving through the soliton in the canal, and the essential geometric and temporal relations are preserved as an aspect of neural activity.

To illustrate this point, we can visualize a simplification of a “data stream” imposed upon the visual cortex by a triangular stimulus, schematically depicted in Fig. 7.6. If we imagine the situation of a child who is too young to recognize a triangle, the same set of transformations is imposed upon the

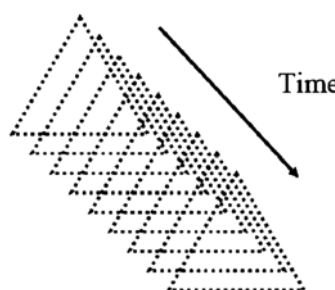


Fig. 7.6. A simplified representation of the data stream in the visual cortex as a result of looking at a triangle

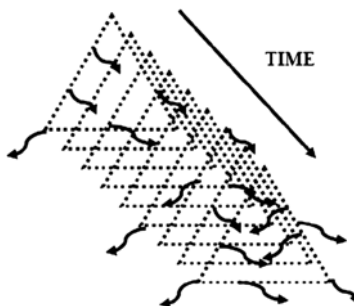


Fig. 7.7. A simplified representation of activity in the visual cortex of a child who is too young to recognize a triangle

visual cortex as in the case of an older child who is able to recognize the triangle. However, the energy that is released as a result of the stimulus disperses in a chaotic way (see Fig. 7.7). Feedback relationships among neurons that fire as a consequence of stimulus may be formed momentarily among aspects of the triangle and other objects in the visual field. These cannot be sustained, however, because there is no ordered relationship among these different stimuli; there are no invariants or symmetries. They may be moving quite randomly with respect to one another, and so any relationships that may be formed quickly become unstable. However, solitons or traveling-wave solutions depend upon symmetries or invariance within the medium and its boundary conditions. It is the order that is implicit in the stimulus, the symmetries or invariance, that facilitates the emergence of traveling-wave solutions.

The only stable dynamic that is possible is one that unites the stimulus in terms of its own implicit spatiotemporal invariance (see Fig. 7.8). In this respect, the soliton or traveling wave is an ideal candidate to form the basis of cognition. The soliton is robust and can maintain its organization while

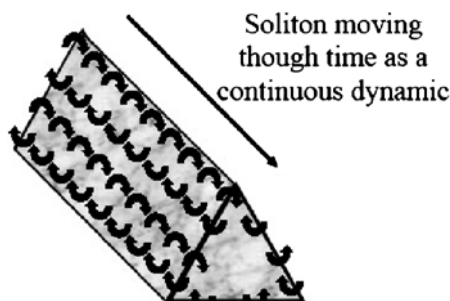


Fig. 7.8. A simplified representation of activity in the visual cortex of a person looking at a triangle

mediating a set of ordered transitions. This is because a soliton is always continuous with its boundary conditions; it is a completely integrable solution to those boundary conditions. Essentially, there is no “conflict” between the soliton and its environment. The soliton represents an autopoietic, self-sustaining dynamic. Thus, if solitons (or traveling waves) form the basis of cognition, we can understand how the solution to a cognitive problem and the robustness of that solution are necessarily related.

Representations vs. Ontology

The implications of this theory in terms of how we understand cognition are subtle and surprising. Conventionally, cognition is thought to involve representations. However, this view is problematic. In order to understand why, we must first analyze the stimulus itself. This is because we can often take for granted aspects of the world revealed to us by our minds as being meaningful beyond the world of perception. For example, we have no doubt that a mountain exists whether we are looking at it or not. Although trivially true, this basic assumption must be critically examined. Exactly what do we mean by the statement that “A mountain exists”? Although there is a collection of implicit invariant relationships in space and time in the overall arrangement of rock strata, boulders, and stones, molecules, etc., there is nothing that unifies the mountain in terms of those implicit relations and invariance. The mountain, then, is only implicit in a set of geometric invariance in space and time. Likewise, the unformed mind of the child is presented with stimuli from all the entire visual field. There is nothing that suggests that a particular stimulated neuron in the retina belongs with any other neuron that fires. The world is presented to the senses in discrete, discontinuous events. The discontinuous set of events that are imposed upon the nervous system can be thought of as representative of the implicit triangle as it exists in the world. It is false to claim that there is an object to be represented; the object is only implicit in a discrete set of statistical invariance. Therefore, we cannot claim that the brain represents an object when the object itself is only implicit in a set of discrete events. The question then, is how to establish a criterion by which we may define and distinguish both the implicit object and the mental state associated with the perception of that implicit object without invoking the concept of representation? Figure 7.6 depicts the triangle as it exists implicitly in the world; Fig. 7.8 depicts the mental state that corresponds to the perception of the triangle. The triangle, as it exists in the world, is a discontinuous set of events in space and time. The neural activity that corresponds to the observation of the triangle is a phenomenon that relates the invariance of the triangle, that is, the set of geometric spatial and temporal symmetries that the triangle embodies implicitly, into a single unified dynamic – a traveling wave or soliton. I suggest that the solitonic triangle is not a representation, but an ontological phenomenon. That is to say, the act of observation unites the boundary conditions (the invariance

in space and time that forms the implicit triangle) into a continuous, self-sustaining dynamic. The triangle of observation exists and persists because it is a triangle – this represents an ontological state of structure and energy that is rarely discovered at the macroscopic level.

“Ontology” is a philosophical term that deals with issues of being or existence. The term, as it is used here, simply refers to the defining characteristics of the objects and phenomena around us. Thus, the ontology of a triangle may include the fact that it has three sides and three angles. The ontology of a raindrop may include the fact that it falls from the sky. Just as in the case of the triangle that, I argue, is only implicit in a set of invariance in space and time, so too, the ontology of objects and phenomena, their form and defining characteristics, constitutes an implicit ontology. If we take the example of a pool of water, its behavior is the result of a great many discontinuous interactions among water molecules. Its macroscopic behavior is an emergent phenomenon that may appear to be evidence that the properties of the water are intrinsic to water itself. However, these observed properties (and therefore conscious properties) cannot be demonstrated to exist other than as implicit characteristics that are actually comprised of a great many discontinuous events, none of which can be claimed to embody the property in question.

I suggest, then, that cognition does not involve representations; rather the brain makes explicit the implicit ontology of the objects and phenomena around us. For example, consider a hypothetical object with a dynamic property associated with it. The object and its behavior cannot be claimed to comprise a continuous unified dynamic that exhibits its form and behavior as a result of its own unified internal dynamics. However, when we observe the object in question, the soliton or traveling wave corresponding to the perception of the object would exhibit the same ontology, but, in this case, that ontology would be as a direct result of its unified internal dynamics, a continuous solution to the boundary conditions imposed upon the excitable medium of the brain as a consequence of stimulus that embodies the ontology implicitly. Thus, perception makes explicit the implicit ontology of the objects and phenomena of the world around us.

From the current perspective, cognition is not consequent upon representation; rather it is to be correlated with ontology – phenomenology equals ontology. So, for example, when we experience a face, we experience each aspect of the face in a dynamic relationship with the rest. We don’t “see” individual features (unless we choose to); we experience the dynamic relations (invariance and symmetries) that were implicit in the many faces that we have seen. With the traditional representational viewpoint of perception, it has been difficult to correlate the qualitative (or phenomenological) aspect of the conscious experience with objects of perception quantitatively. However, by correlating the conscious experience with dynamic and relational properties of nonlinear traveling waves, we are a little closer to understanding the qualitative nature of consciousness.

Dynamic Ontological Induction

We can now understand how “solutions” to problems of perception and the robustness of those solutions are necessarily related. Also, we can understand the process of mental development as an essentially inductive process. That is to say, it is the implicit order of the objects and phenomena of the world around us, their patterns, symmetries and invariance in space and time, that form the necessary conditions for the formation of solitons or traveling waves in the brain. The persistence of these solutions depends upon the persistence of the implicit “order” associated with the objects of perception. Thus, the robustness of cognitive states and all biological processes is a complimentary aspect of the fact that they make explicit the implicit ontology of the environment that they mediate as part of the catalytic process. It is not what can be calculated from the structure of the environment that is important, but rather, what can persist by uniting energy and structure (invariance, symmetry) in the form of a nonlinear continuous dynamic. The brain strengthens synaptic junctions according to how often they are stimulated (Hebbian learning). Once a dynamic solution to a perceptual “problem” is established, the consequence of synaptic strengthening will ensure the emergence of a similar dynamic given the same stimulus. So, similar to the way that a bacterium may change its metabolic state depending upon the availability of raw materials and the changing thermodynamics of its environment, the brain changes its cognitive state depending upon the stimulus.

This general approach is to be applied to all mental processes including behavioral processes. For example, the “solution” to the problem of co-ordination for an animal is implicit in the structure of the animal itself. The symmetries or invariance implicit in the structure of an animal enable traveling-wave solutions that both provide paths for energy dissipation and also make explicit these invariance as a continuous solution. For evidence of this, we can look to the locomotion of creatures like millipedes to observe solitonic solutions. As a millipede crawls, the waves of activity of its many legs represent a continuous solution to the boundary conditions embodied by its structure. There is evidence that these waves are solitons [48].

The Catalytic Model, Ecological Theory and the Perception/Action Cycle

A growing group of theorists are attempting to reconcile living processes with the laws of thermodynamics within a unified theory. For example, in ecosystems that have been perturbed as a consequence of species reduction, the gradual process by which animal and plant species reintegrate into the ecosystem correlates with an increase in the paths for energy dissipation [61, 62]. Also, it is argued that the perception-action cycle of com-

plex animals allows for an increase in the available paths for energy dissipation [69].

To demonstrate how the scale-invariant catalytic model rationalizes and unifies the catalytic theme in living processes when we consider the nervous system specifically, we may consider a particular evolutionary development. The early stages of the evolutionary process would have started where there was a constant supply of raw materials and energy that could support an ongoing and robust catalytic process involving many catalysts in a dynamic relationship. However, when we observe the behavior of a complex organism, for example, a whale shark, we note that it is no longer necessary for there to be a constant supply of energy and raw materials in the environment. The fact that complex living organisms can escape the necessity of a continuously excited medium may seem to imply that complex behavior mediated by the nervous system represents a development that cannot be fully accommodated by the catalytic model as it has been described. The question is: can the complex behavior of the shark, for example, be understood in the same way that we understand a traveling wave of bacteria in an excitable medium?

The brain of the whale shark is structured according to a set of boundary conditions. These include the spatiotemporal symmetries or invariance that are implicit in the shark's body, the dynamic interaction between the shark and its environment, and the relative spatial relationships in the sensory field. In this case, the energy constraint is not associated with the environment per se, but is determined by the internal energy reserve of the shark. It is within this set of boundary conditions that a traveling-wave solution emerges. Because of the intimate relationship between the nervous system and the shark's musculature, a traveling-wave solution corresponds to the macroscopic motion of the shark. Not only is energy released as a consequence of energy being used to drive the musculature of the shark, but the traveling-wave solution is also releasing energy in the shark's nervous system. In this way we see that there is no real precedence of behavioral states over neural states. The reason for the robustness of each is identical. The effect of internalizing an excitable medium that can be structured in real time, is that it facilitates the emergence of catalytic processes that do not rely on the constant availability of energy and raw materials in the environment; we observe this as complex behavior. Consequently, the perception/action cycle of complex animals can be understood as resulting from exactly the same dynamic principles that operate at the level of the enzyme.

The scale-invariant catalytic model is essentially an ecological theory that places the emphasis on the relationship between entropy production and the structure in the environment that is effected as a result of a soliton or traveling-wave mechanism. We can observe this at the macroscopic scale in the perception/action cycle of animals. Animal behavior invariably involves the structure of the environment. The perception/action cycle is essentially an

extension of the catalytic process made possible by internalizing an excitable medium. This is an inevitable consequence of the scale-invariant model.

Catalysis and Mental Development

Given there is a common theme to all biological processes, we should be able to establish a developmental model of the brain rooted in the catalytic process that leads to an increase in the available paths for entropy production in a similar way that perturbed ecosystems do. As a direct consequence of the scale-invariant catalytic structure of the living processes, we can consider the excitable medium of the brain as an environment in its own right and the development of the brain as providing paths for greater energy dissipation.

The example of a triangle imposed upon the medium of the brain and the emergence of a unifying dynamic (Fig. 7.8) can be taken a stage further to understand the “emergence” of language and “meaning”. A hypothetical child who has recently learned to recognize the triangle is also learning to speak. Her mother uses the word “triangle” whenever the child is looking at the triangle. At this early stage of development words are simply “sound objects”, no different in principle to visual objects. The child learns to recognize these “sound objects” in the same way that she learns to recognize visual objects. There is sufficient implicit order in the frequency components and repeated use of words to facilitate the emergence of a traveling-wave dynamic to unite these components into a single continuous process. There is, of course, a second level of order implicit in the mother’s use of the word “triangle” and the appearance of the actual triangle in the visual field. This facilitates the emergence of a dynamic that unites the word object “triangle” and the triangle. I suggest that it is this “union” that forms the basis of conceptual cognitive states.

In as far as the brain makes explicit the implicit invariance (order) of the triangle, we can claim that the experience of the triangle (what might be described as triangleness) was implicit in the invariance exhibited by the stimulus – its implicit ontology. Conceptuality, then, is implicit in the relationship between the use of language in the context of recognizable objects and events to which that use refers. “Meaning”, in so far as this term refers to the experience that we have when we hear a word, cannot be derived as a consequence of an epistemological analysis. Rather, meaning is a catalytic phenomenon consequent on a nonlinear dynamic that makes explicit the invariance in the relationship between the word and the object. If we consider words and language simply as a set of events in the world, no different in kind to any other phenomenon, then we may claim that words and language generally embody an implicit ontology, just as a triangle embodies an implicit ontology. Meaning is the experience that we have when that implicit ontology becomes explicit.

We can now propose a model for mental development. At the most fundamental level, the brain is structured as a consequence of stimuli. This takes

the form of neural events in space and time that correspond to the spatiotemporal relationships implicit in the stimulus. Areas of the brain are “excited” and others, suppressed. If the stimulus embodies invariance, then these may support solitons (or traveling waves) that unite the stimulus in terms of the invariance. When these implicit orders (invariance/symmetries) become explicit as a consequence of the spatiotemporal evolution of traveling waves, then basic object recognition is the result. Once this basic level of cognition is established, the implicit relationships between these objects of recognition may become explicit as higher levels of cognition, such as language, conceptuality, self, etc. Consistent with the ecological perspective, these higher levels of cognition are actually providing paths for energy dissipation via the solitonic mechanism in the brain. These higher levels of structure correspond to the implicit structure of the world around us. Each new level of cognitive development represents a new level of mediation between established cognitive and behavioral processes. At each level of the organism, biological structures

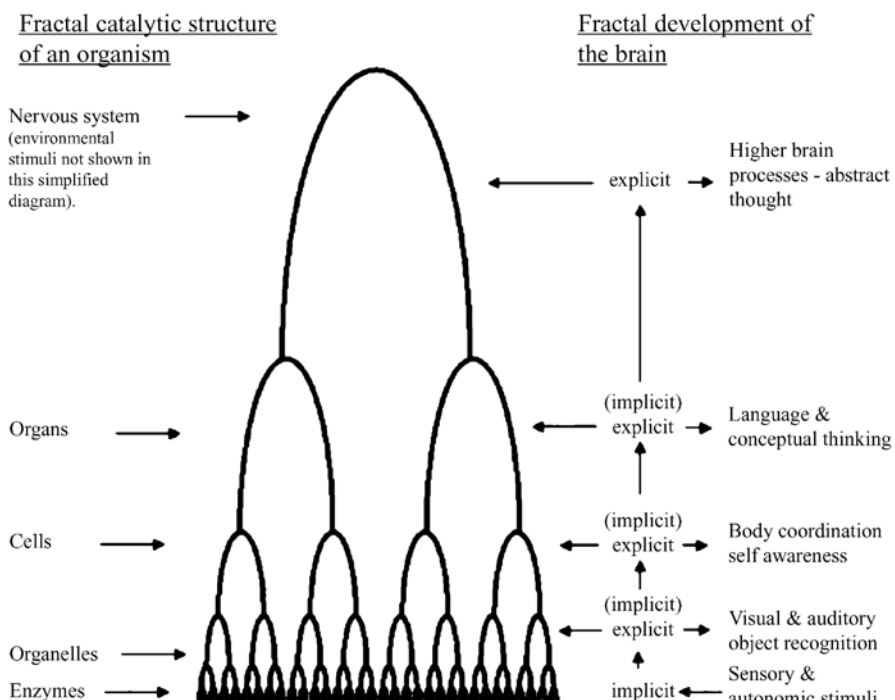


Fig. 7.9. A graphic depiction of how the same principle (catalysis) that combines metabolism/ function and structure/energy, as a process of catalytic mediation, exhibits robustness at every level of scale, whether we are considering the robustness of the organism or the robustness of its cognitive processes. Also, mental development may be seen as a succession of steps that mediate implicit relationships between established cognitive processes

maintain their organization by mediating transitions via structure in a unified way. Figure 7.9 uses the principle of the arch to illustrate how the same principle applies at multiple levels of scale. Therefore, life facilitates entropy production, not only via the structure of the brain consequent upon stimuli, but also via the structure that is implicit in the environment via cognition and the perception-action cycle.

Philosophical Issues

The scale-invariant catalytic model has characteristics that are relevant with respect to the philosophical issues on the mind/brain relation. One problem, that of “intentionality”, concerns the “aboutness” of conscious states. Specifically, how is it that there is a phenomenon (cognition) associated with a subject (a brain) that is “about” something else (the “object” of perception)? The key components to this problem are as follows:

- There must be a “subject” (a brain) to which the intentional state is attributed.
- There must be an “object” (the object or process that is being observed) to which the intentional state refers.
- The “subject” and the “object” are nonidentical objects/processes.

There is a significant correlation between these necessary conditions and the conditions associated with enzyme catalysis. The “subject” of the catalytic process can be correlated with the enzyme. The “object” of the catalytic process is the reaction of the reagent(s) leading to product(s). The problem of intentionality centers on the difficulty of correlating the “intentional state” with the properties of the subject. Similarly, the reaction that an enzyme mediates is primarily determined by the properties of the reagent(s) rather than the enzyme. The enzyme does not alter the thermodynamics of a reaction. The enzyme facilitates a path for the reaction that is determined by the structure of the reagents. We cannot determine any particular properties of a catalyst from an analysis of the reaction that it mediates.

This proposal is also significant with respect to what is termed “identity theory”, a philosophical position proposing that conscious states are understood to be identical to neural states (for a discussion, see Hesslow [30]). The scale-invariant catalytic model implies an identity between neural and conscious states. However, in my opinion a major problem with “identity theory” stems from a lack of criteria by which we may distinguish, in a significant way, a neural state from any other process that may occur in the world. It has been generally assumed that it is appropriate to consider objects and phenomena in the world as embodying an ontology explicitly. Thus, the idea that we can correlate consciousness states to the ontology of mental phenomena – their form, behavior etc., has implied that a similar correlation could be applied to any phenomenon – not just neural phenomenon. Consequently,

an explanation for the phenomena of consciousness, its essential qualities, has been attributed to some as yet, undiscovered ingredient.

The catalytic model implies an identity between the solitons or traveling waves associated with cognition or behavior and conscious states. It is also claimed that these dynamics embody a macroscopic unified ontology, whereas the objects of perception do not. This establishes a criterion by which we may clearly distinguish the mental state associated with the observation of an object from the object of cognition in terms of ontology. We can correlate the “quality” of a cognitive state to the “implicit” ontology of the object of perception. Establishing a correlation between the phenomena of consciousness and ontology does not solve the so-called “hard problem” of why there should be any experience at all. This question, I believe, goes to the very heart of physics and cosmology.

The hallmark of complex life is complex behavior. But, how do we quantify and distinguish the complex behavior associated with living organisms from the behavior of nonliving processes, for example a waterfall? I suggest that the answer to this question lies in probability. Complex living organisms can make previously unlikely events more likely. In fact, it is difficult to envisage any other criteria by which we could confidently determine that a living process was occurring without waiting for reproduction to occur. If the hallmark of life lies in its effect of bringing about previously unlikely events, then we can draw another parallel between life and enzyme catalysis. Enzyme catalysis may be defined as a process that increases the probability of a chemical event.

7.5 Conclusion

Within the scale-invariant catalytic model, catalysis occurs under particular conditions that facilitate the emergence of nonlinear dynamics that involve the bringing together of energy and structure. By creating such conditions, life plays a central role in entropy production by dissipating energy via structure within living organisms themselves and also via the structures implicit within the environment. Thus, life is not a machine-like process that requires the constant management of energy and structure within thermodynamic and functional constraints. Rather, every biological process is a process of mediation to a more favorable thermodynamic state that involves the seamless union of energy and structure.

Within this model, the brain is not a vastly complex machine; rather, it expresses the simple requirements of life itself, energy and structure combined within an excitable medium. The development of our minds is governed by the same principles that give rise to the multitude of creatures in the forest. In the ecology of the forest, plants and animals evolve over millions of years, shoulder to shoulder, and thus define each other’s environments. The ecology of our minds evolves in the short period of our lives and is constrained by the spatiotemporal geometric relations implicit in the complex world around us.

If the brain is an example of macroscopic catalysis, then consciousness and all living processes are to be associated with the transition state or tunneling condition of the catalytic process. This would seem to be consistent with the fact that life is a far-from-equilibrium process.

The proposal integrates living processes with the laws of thermodynamics. It also reintegrates the “organism” with its environment at all levels, by proposing that the cell, organ, organism, and so forth are each mediators of their environments, rather than independent agents acting in or on their environments. The theory also addresses the issue of coordination within an organism, that is, how the many complex nonlinear processes that comprise an organism “cooperate” to the benefit of the organism as a whole. “Cooperation” is the natural reflection of successfully mediating an environment that itself may be a dynamic process. The theme of mediation provides a criterion by which we may define the healthy from the sick. The healthy process is the process that mediates an existing tendency of the environment and maintains its organization as a direct consequence of making explicit the implicit ontology of the environment as an aspect of the process of catalysis.

This theory embraces the perspective of dynamic systems in biology, with the important reconstrual of the phenomena that is called “emergence”, the appearance of complex processes that are not reducible to their constituents. It suggests that such complex processes are indeed not reducible, but are nevertheless instances of catalysis, albeit with wider and different domains of mediation.

Many questions remain unanswered. Much of this argument has been based upon empirical observations. The relationship between structure (symmetries/invariance) and solitons has not been formalized. Indeed, the process of enzyme catalysis is still a matter of research. I suggest then, that the most pressing task facing theoretical biology, neurobiology, and psychology is to solve the riddle of enzyme catalysis.

Acknowledgement. I would like to gratefully acknowledge my friend and mentor, Paul Gray, whose help, inspiration and guidance in developing these ideas has been constant along an uncertain path. I would also like to thank Patricia Carpenter whose invaluable insight and experience has helped shape a loose collection of ideas into a coherent theory, and also Drs. Ron Chrisley, Clark Glymour, Indira Nair, Robert Ulanowicz, and especially Benoit Morel, for their encouragement and comments on earlier drafts of the manuscript. Also, I want to acknowledge Carnegie Mellon University and funding from the National Institute for Neurological Diseases and Stroke (Grant # P01NS35949 to P. Carpenter) for giving me the opportunity to research these ideas.

References

1. Adamatzky, A. (2001). *Computing in Nonlinear Media and Automata Collectives*. Philadelphia, Pa.: IOP Publishing Ltd.

2. Antoniou, D., Caratzoulas, S., Kalyanaraman, C., Mincer, J.S., and Schwartz, S.D., (2002). *Eur. J. Biochem.* **269**: 3103–3112. (MINIREVIEW)
3. Août, K.D., Curtin, N.A., Williams, T.L., and Aerts, P. (2001). *J. Experimental Biology* **204**, 2221–2230.
4. Aslanidi, O.V. and Mornev, O.A. (1999). *J. of Biological Physics* **25**, 149–164.
5. Aslanidi, O.V. and Mornev, O.A. (1996). *International Conference on Mathematical Models of Nonlinear Excitation Processes*, Tver, Russia, July 2–5, 1996.
6. Beaumont, J., Davidenko, N., Davidenko, J.M., and Jalife, J. (1998). *Biophys J* **75**(1):1–14.
7. Bell, R.P. (1980). In *The Tunnel Effect in Chemistry*:51–140. Chapman and Hall, London.
8. Biktsheva, I.V. and Biktshev, V.N., (2003). *Phys. Rev. E*, **67**:026221.
9. Breaker, R.R. (1997). *Nature Biotechnology*, **15**(5):427–430.
10. Brown, J.H., Enquist, B.J., and West, G.B. (1999). *Science* **284**:1677–1678.
11. Brown, J.H., Enquist, B.J., and West, G.B. (1997). *Science* **276**:122–126.
12. Carmi, N. and Breaker, R.R. (2001). *Bioorg. Med. Chem.* **9**:2589–2600.
13. Caspi, S. and Ben-Jacob, E. (1999). *Europhysics Letters* **47**:522–527.
14. Caspi, S. and Ben-Jacob, E. (2000). *Physics Letters A* **272**:124–129.
15. Davia, C.J. (2002). Presentation at the International Conference on Complex Systems. The New England Complex Systems Institute. June 9, 2002, Nashua, N.H.
16. Davydov, A.S. (1982). *Biology and Quantum Mechanics*. Oxford: Pergamon Press.
17. Duke, T. and Jülicher, F. (2003). *Physics Review Letters* **90**:158101.
18. Echebarria, B. and Karma, A. (2000). *Chaos* **12**:923–930.
19. Englander, S.W., Kallenbach, N.R., Heeger, A.J., Krumhansl, J.A., and Litwin, A. (1980). *Proc Natl Acad Sci USA*, **77**:7222–7226.
20. Fagen, Xie., Zhilin, Qu., J.N. Weiss, and, A. Garfinkel, (1998). *Phys. Rev. E* **58**:6355–8.
21. Feldman, A. and Sen, D. (2001). *J Molecular Biol.* **313**:283–294.
22. Fenton, F. and Karma, A. (1998). *Chaos* **8**:20–47.
23. Filippov, A.T. (2000). *The Versatile Soliton*. Boston: Birkhauser.
24. Gibson, J.J. (1979). *The Ecological Approach to Visual Perception*. Boston: Houghton Mifflin Co.
25. Glickman, M.H., Wiseman, J.S., and Klinman, J.P. (1994). *J. Am. Chem. Soc.* **116**:793–794.
26. Grendel, B.T., Bjornstad, O.N., and Kappey, J. (2001). *Nature* **414**:716–723.
27. Gueron, S. and Liron, N. (1989). *J Mathematical Biology* **27**:595–608.
28. Hameroff, S., Nip, A., Porter, M., and Tuszynski, J. (2002). *BioSystems* **64**:149–168.
29. Hermon, Z., Caspi, S., and Ben-Jacob, E. (1998). *Europhysics Letters* **44**:482–487.
30. Hesslow, G. (1994). *J. Theor. Biol.* **171**:29–39.
31. Infeld, E. and Rowlands, G. (1990). *Nonlinear Waves, Solitons and Chaos*. Cambridge: Cambridge University Press.
32. Jinguji, M., Ishihara, M., Nakazawa, T., and Nagashima, H. (1995). *Physica, D (Nonlinear Phenomena)* **84**:246–252.

33. Kauffman, S. (1993). *The Origins of Order: Self-Organisation and Selection in Evolution*, Oxford University Press. New York
34. Kauffman, S. (1995). *At Home in the Universe: The Search for the Laws of Self-organisation and Complexity*. New York: Oxford University Press.
35. Kawasaki, K., Mochizuchi, A., Matsushita, M., Ueda, T., and Shigesada, N. (1997). *J. Theor. Biol.* **188**:177185.
36. Knapp, M.J. and Klinman, J.P., (2002). *Eur. J. Biochem.* **269**:3113–3121 (MINREVIEW).
37. Knapp, M.J., Rickert, K., and Klinman, J.P. (2002). *Journal of the American Chemical Society* **V124(N15)**:3865–74.
38. Koroleva, V.I. and Bures, J. (1979). *Brain Res.* **173**:209–215.
39. Lechleiter, J.L., Girard S., Peralta, E.G., and Clapham, D.E., (1991). *Science* **252**:123–126.
40. Li, Y. and Sen, D. (1996). *Nature Structural Biology* **3**: 743–747.
41. Li, Y. and Breaker, R.R. (1999). *Proc Natl Acad Sci, USA*. **96**:2746–2751.
42. Lipniacki, T. (1999). *Physics Review E*. **60**:7553–7561.
43. Ma, B., Kumar, S., Tsai, C., Hu, Z., and Nussinov, R. (2000). *J. Theor. Biol.* **203**:383–397
44. Maturana, H.R. and Varela, F.J. (1980). *Autopoiesis and Cognition: The Realization of the Living*. Vol. 42: Boston Studies in the Philosophy of Science. Dordrecht: D. Reidel.
45. Moore, B.C.J. (2003). *An Introduction to the Psychology of Hearing*. Boston: Academic Press (An imprint of Elsevier Science).
46. Murray, J.D. (1993). *Mathematical Biology* (2nd edn). Springer-Verlag.
47. Odell, G.M. (1980). In, L.A. Segal (ed.). *Mathematical Models in Molecular and Cellular Biology*:523–567. Cambridge University Press.
48. Petoukhov, S. (1999). *Biosolitons - One Secret of Living Matter-The Bases of Solitonic Biology*. Mechanical Engineering Research Institute, Russian Academy of Sciences, Malii Haritonievskii Pereulok, Moscow, Center, 101830, Russia.
49. Polozov, R.V. and Yakushevich, L.V. (1988). *J. Theor. Biol* **130**:423–430.
50. Prigogine, I. and Stengers, I. (1984). *Order Out of Chaos: Man's New Dialogue with Nature*. New York: Bantam Books.
51. Rajaraman, R. (1982). *Solitons and Instantons: An Introduction to Solitons and Instantons in Quantum Field Theory*. New York: North-Holland.
52. Rambidi, N.G., Maximychev, A.V., and Usatov, A.V. (1994). *Biosystems* **33**:125–137.
53. Remoissenet, M. (1999). *Waves called Solitons: Concepts and Experiments* (3rd edn). New York: Springer-Verlag.
54. Rhode, W.S. and Recio, A. (2001). *J. Acoust. Soc. Am.* **110**:3140–3154.
55. Rhode, W.S. and Robles, L. (1974). *J. Acoust. Soc. Am.* **55**:588–596.
56. Rogers, C. and Shadwick, W.F. (1982). *Bäcklund Transformations and Their Applications*. New York: Academic Press: 107–110.
57. Rogers, C. and Schief, W.K. (2002). *Bäcklund and Darboux Transformations: Geometry and Modern Applications in Soliton Theory*. Cambridge: Cambridge University Press.
58. Sataric, M.V., Zakula, R.B., Ivic, Z., and Tuszynski, J.A. (1991). *J. Molecular Electronics* **7**:39–46.

59. Sataric, M.V., Zakula, R.B., and Tuszynski, J.A. (1992). *Nanobiology* **1**:445–456.
60. Satnoianu, R.A., Maini, P.K., Garduno, F.S., and Armitage, J.P. (2001). *Discrete and Continuous Dynamical Systems - Series B* **1**:339–362.
61. Schneider, E.D. (1988). In Weber, B., Depew, H., David, J. and Smith, J.D., (eds.) *Entropy, Information, and Evolution - New Perspectives on Physical and Biological Evolution*. MIT, MA: A Bradford Book, The, MIT Press.
62. Schneider, E.D. and Kay, J.J. (1994). *Futures* **26**:626–647.
63. Scott, A. (1999). *Nonlinear Science: Emergence and Dynamics of Coherent Structures*. Oxford: Oxford University Press.
64. Sharov, A.A. (1996). In Korpilahti, E., Mukkela, H., and Salonen, T., (eds.) *Caring for the Forest: Research in a Changing World*. Congress Report, Vol. II:293–303. IUFRO XX World Congress, 6–12 August 1995, Tampere, Finland. Gummerus Printing, Jyvaskyla (Finland).
65. Sneyd, J. and Sherratt, J., (1997). *SIAM Journal on Applied Mathematics*, **57**:73–94 21.
66. Solé, R. and Goodwin, B. (2000). *Signs of Life: How Complexity Pervades Biology*. New York: Basic Books.
67. Stassinopoulos, D., Colombano, S.P., Lohn, J.D., Haith, G.L., Scargle, J., and Liang, S., (1998). *Proc. of the 1998 International Conference of Complex Systems*, Nashua, NH.
68. Sutcliffe, M.J., and Scrutton, N.S., (2002). *Eur. J. Biochem.* **269**:3096–3102 (MINREVIEW)
69. Swenson, R. and Turvey, M.T. (1991). *Ecological Psychology* **3**:317–348.
70. Travascio, P., Bennet, A.J., Wang, D.Y., and Sen, D. (1999). *Chemistry and Biology* **6**:779–787.
71. Von Békésy, G. (1960). *Experiments in Hearing*. New York: McGraw-Hill.
72. Von Békésy, G. (1947). *J. Acoust. Soc. Am.* **19**:452–460.
73. Weber, B.H. and Depew, D.J., (2001). In *Cycles of Contingency: Developmental Systems and Evolution*. Oyama, S., Griffiths, P., and Gray, R., (eds.), A Bradford Book. MIT Press, Cambridge MA.
74. Yakushevich, L.V. (2001). *J. Bioscience* **26**:101–109.
75. Yakushevich, L.V. (1998). *Nonlinear Physics of DNA*. Chichester, England: John Wiley and Sons.
76. Zeki, S. (1992). *Scientific American* **267**:69–72.

8 The Dendritic Cytoskeleton as a Computational Device: An Hypothesis

Avner Priel, Jack A. Tuszynski, and Horacion F. Cantiello

Summary. This chapter presents a molecular-dynamical description of the functional role of cytoskeletal elements within the dendrites of a neuron. Our working hypothesis is that the dendritic cytoskeleton, including both microtubules (MTs) and actin filaments plays an active role in computations affecting neuronal function. These cytoskeletal elements are affected by, and in turn regulate, ion-channel activity, MAPs and other cytoskeletal proteins such as kinesin. A major hypothesis we advance here is that the C-termini protruding from the surface of a MT can exist in several conformational states, which lead to collective dynamical properties of the neuronal cytoskeleton. Further, these collective states of the C-termini on MTs have a significant effect on the ionic condensation and ion-cloud propagation that have physical similarities to those recently found in actin filaments. Our objective is to provide an integrated view of these phenomena in a bottom-up scheme. We outline substantial evidence to support our model and contend that ionic wave propagation along cytoskeletal structures impact channel function, and thus the computational capabilities of the dendritic tree and neuronal function at large.

8.1 Introduction

8.1.1 Neurobiological Introduction

The neuron is the quintessential communicating cell. The strength of information processing performed by a neural circuit depends on the number of interneuronal connections or synapses. Neurons are highly polarized cells, whose level of morphological complexity increases during maturation into distinct subcellular domains. Morphologically speaking, a typical neuron presents three functional domains. These are the cell body or “soma” containing the nucleus and all major cytoplasmic organelles, a single axon, which extends away from the soma and takes cable-like properties, a variable number of dendrites, varying in shape and complexity, which emanate and ramify from the soma. The axonal terminal region, where the synapse or contact to other cells takes place, displays a wide range of morphological specializations, depending of the target area.

Turning morphology into a functional event, the soma and dendritic tree are the major domains of receptive (synaptic) inputs. Thus both the dendritic arborization and the axonal ramifications confer a high level of subcellular

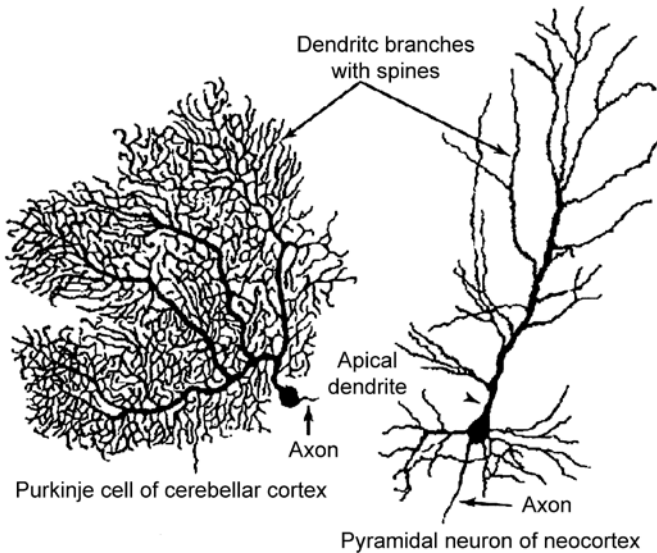


Fig. 8.1. Typical morphology of projection neurons. Reproduced from Fig. 3.1, Fundamental Neuroscience Book. High degree of polarization in neurons, with an extensive degree of branching, including spiny apical dendrite, shorter basal dendrites, and a single axon emerging from the basal pole of the cell. The complexity in the level of arborization is associated with the number and complexity of connections to which a neuron is associated

specificity in the localization of particular synaptic contacts on a given neuron. The extent to which a neuron may be interconnected largely depends on the three-dimensional spreading of the dendritic tree (see Fig. 8.1).

Dendrites are the principal element responsible for both synaptic integration and for the changes in synaptic strengths that take place as a function of neuronal activity [101, 46, 81]. While dendrites are the principal sites for excitatory synaptic input, little is still known about their function. The activity patterns inherent to the dendritic tree-like structures such as in integration of synaptic inputs, is likely based on the wide diversity of shapes and sizes of the dendritic arborizations [101, 49]. The size and complexity of dendritic trees increase during development [105], which has been, in turn, associated with the ability of the neural system to organize and process information, such as when animals are reared in complex sensory environments [35]. Thus, dendritic size and branching patterns (see Fig. 8.2) are important features of normal development and function. Most synapses, either excitatory or inhibitory, terminate on dendrites, so it has long been assumed that dendrites somehow integrate the numerous inputs to produce single electrical outputs. It is increasingly clear that the morphological functional properties of dendrites are central to their integrative function [79, 53]. Branching in this context is essential to the increasingly complex ability of the neuron to

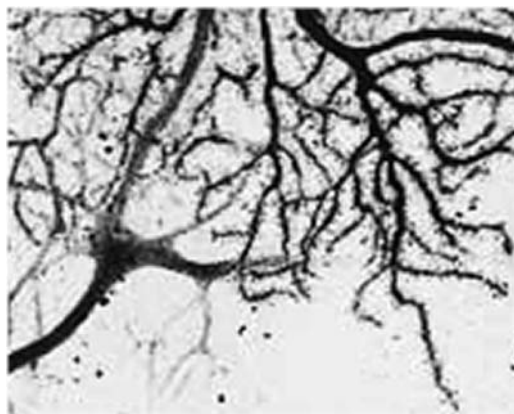


Fig. 8.2. Visualization of individual dendrites. Complex branching of the dendritic tree in Purkinje cell.

respond to developmental complexity [49]. The dendritic cytoskeleton plays a central role in the process of ramification, filopodia formation, and more specialized neuronal activity such as long-term potentiation (LTP) and long-term depression (LTD), circuit dynamics, including memory formation, and the response to pathological conditions.

Synaptic contacts take place in dendritic spines, which are small sac-like organelles, projecting from the dendritic trunk. Dendritic spines are more abundant in highly arborized cells such as pyramidal neurons and scarcer in lowly interconnected smaller-sized dendritic tree interneurons. The number of excitatory inputs can be linearly correlated with the number of spines present in the dendrite. How information is processed in a dendritic spine, is still a matter of current study [78, 141]. Dendritic spines contain ribosomes and cytoskeletal structures, including actin, and α - and β -tubulin. As in other parts of the neuronal structure, cytoskeletal components are highly relevant in the structure/function of the neuron. The axonal hillock contains large “parallel” bundles of microtubules. Axons are also located with other cytoskeletal structures, such as neurofilaments, which are more abundant in axons than in dendrites. The axon hillock is the region where the action potential is generated. The dynamics in cytoskeletal structures is central to our contention that information can be processed and “delivered” to the synaptic function by changes in the cytoskeleton structures.

It is widely accepted that chemical and structural modifications in dendritic spines underlie much of the plastic changes in the brain in response to learning and experience [142, 39]. Morphological changes in the dendritic spine are key to its plasticity and processing [78, 122]. Conversely, electrical stimulation leading to LTP, leads to the formation of new dendritic spines [27, 132]. In this regard, dynamic changes of the actin cytoskeleton have long been implicated in a number of neuronal functions, including the development and

stability of dendritic spines [28, 79, 63, 29]. Twitching of dendritic spines [29, 24] for example, which has been hypothesized to encode ultrashort memory [18], is a phenomenon that involves actin dynamics, and is blocked by cytochalasin treatment [29, 24]. The actin cytoskeleton plays a central role in synapse formation and maintenance [117]. Treating of cultured hippocampal neurons with the actin polymerization inhibitor latrunculin, for example, modifies synapse formation and stability [144]. Conversely, neuronal function also helps remodel the actin cytoskeleton. Repeated tetanic stimulation of hippocampal neurons causes remodeling of presynaptic actin, which results in the formation of potential new synapses capable of active vesicle recycling. Interestingly, even a single tetanus results in rapid translocation of actin in both presynaptic and postsynaptic compartments, such that presynaptic actin advanced towards and postsynaptic actin moved away from stimulated synapses [15]. Pruning is also associated with actin dynamics [110, 88, 138]. This process where exuberant axonal and dendritic ramification are effectively

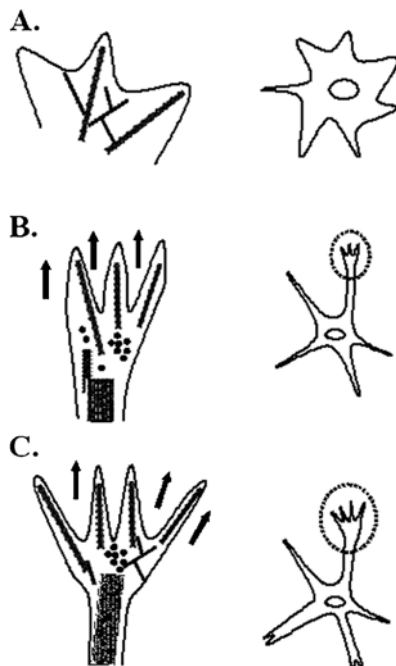


Fig. 8.3. Cytoskeletal dynamics in neurite initiation (A), neuritogenesis (B), and ogenesis (C). Reorganization of the lamellipodia with accumulation of microtubules into an ordered array results in formation of a neurite with a growth cone. The differentiation of a neurite growth cone (B) into an axon growth cone (C) requires depolymerization and reorganization of actin networks. Microtubules invade to form the characteristic central core. Actin filament dynamics is essential to all these stages of differentiation. Reproduced from [111]

eliminated is observed in developmental stages in insects where reorganization of their nervous system between larval and adult life takes place [133, 129, 64].

Thus, cytoskeletal alterations may reflect changes of neural circuits in response to learning and experience, and they must involve both destructive and constructive mechanisms (see Fig. 8.3).

8.1.2 Neuro computational Introduction

The prevailing view of long-term memory and information processing in the central nervous system continues to be heavily influenced by Hebb's conjecture [37]. The idea, which is based on the processing of information in a network of neurons, involves activity-dependent strengthening of synaptic connections between neurons. Thus, the biological steps that coordinate and strengthen synaptic activity are essential to better modeling of biological neural-based networks. McCullough and Pitts [80] showed that a sufficiently large network of simple neurons (modeled by point-like nodes – with linear threshold units) is capable of universal computation, i. e. is equivalent to a Turing machine. In this model, synaptic inputs are linearly added into a single threshold function. In the remainder of this chapter, we shall review two main routes in neural modeling, both relevant to our proposed revised model. The first deals with biologically realistic models of electrical (and chemical) signaling in the neural membrane and its implications on the way neurons respond to synaptic activity. The second approach focuses on constructing abstract models and deriving general results regarding their computational capabilities using analytic and simulative methods.

Several variants of the point-like neuron model exist (see [82, 60]). The simplest is the “integrate and fire” (IF) in which charges are accumulated across the membrane (modeled by a capacitor) via synaptic inputs (positive or negative) until a certain threshold is reached, causing an instantaneous discharge and a pulse generating along the axon. The next variant, known as the “leaky IF” (LIF), modeled as an “RC” circuit, includes a resistance in parallel to the membrane capacitor. In this case there is a certain discharge at all times, such that the membrane potential undergoes an exponential decay over time. Again, the neuron generates an impulse upon the event of (voltage) threshold crossing. While the variants described above are operating in an “all-or-none” fashion, the “rate neuron” has a continuous activation function that is monotonically increasing as a function of the membrane’s electrical activity, reaching a saturating constant value for high-activity regimes. This squashed function represents the average firing rate of a group of connected neurons.

This highly restrictive picture effectively models as the whole dendritic arbor as a single-point compartment. However, an application of the linear cable theory to dendrites [99, 41] gave rise to several interesting insights regarding the distribution of the membrane potential, which clearly challenge

this naive model. According to the one-dimensional passive cable equation analysis, dendrites:

1. Impose a large conductance load on the soma,
2. Low-pass filter postsynaptic potentials (PSPs),
3. Change the response at the soma to various combinations of synaptic activities [100].

However, while most of these models assume passive membrane properties, it is clear that the dendritic electrical properties change dynamically by modulation of a variety of voltage-gated ion channels [44, 20], and by dynamic changes in its cytoskeletal components [30, 73, 5, 32]. Dendritic channels provide this compartment with the ability to perform nonlinear operations on PSPs, at least locally. This means that synapses may interact in a nontrivial way, a fact that gives rise to a completely new set of possibilities regarding the operation and the function of dendrites [81, 119, 60]. Several types of experimental evidence support this view, hence weakening the relation between stable synaptic weights and long-term memory, as well as learning, namely:

- Neurons demonstrate significant morphological plasticity both by growing dendritic branches (even in mature cells) and by rapidly developing new dendritic spines [39]. This type of evidence supports alternative mechanisms for memory acquisition and handling that extend beyond the classical Hebbian conjecture.
- Experiments have revealed significant fluctuations of synaptic efficacy over short periods of time in response to a recent burst of activation, e. g. [135, 38]. This type of evidence questions the conventional assumption of stable synaptic strength whose fine resolution is obtained via repeated presentation of a set of training examples. This assumption is also one of the building blocks of most connectionist models [7].
- The dendritic membrane expresses a variety of active ion channels (NMDA receptors, Na^+ and Ca^{2+} and other voltage-dependent channels [115, 49] that can significantly affect the electrical properties, and hence integrative behavior of this compartment. Dendrites thus exhibit a capability to amplify their synaptic input. At the same time, nonlinear responses have been localized to specific dendritic arbors and even to single branches within a dendritic domain, clearly pointing to compartmentalization mechanisms capable of confining certain inputs to a specific dendritic region.

The above findings have triggered a revised view of information processing in dendrites. Rather than having a passive membrane, nonlinear models were proposed to incorporate the above evidence [60]. These adaptive models demonstrate that a novel and wider repertoire of capabilities than previously expected from large networks of simple integrating units (even with passive dendrites) are required, which are not supported by conventional models. Among these new capabilities one can count, multiplication, fast correlation/coincidence, which is beyond the capabilities of interneuron

transmission due to long temporal delays, and reduced sensitivity of somatic excitatory-PSP to the spatial distance from the dendrite [60]. In this context, dynamic cytoskeletal remodeling and functional interactions between cytoskeletal structures and synaptic ion-channel activity may be at the center of this revised model of neuronal adaptability [56, 32].

8.1.3 Dendritic Channel Function

Although action potentials can initiate and propagate in dendrites of various neurons, very little information was available until recently concerning the ion channels that sustain them. Ca^{2+} -dependent action potentials have been observed in hippocampal neurons and dendrites [116, 6]. Firing of action potentials elicits characteristic M-shaped Ca^{2+} profiles across the neuron. These spatially constrained Ca^{2+} signals are essential to distinct neuronal function. The Ca^{2+} rise is small in the soma, highest in the proximal apical and basal dendrites, and small again in distal apical dendrites [43, 83, 102–104]. Interestingly, addition of the K^+ -channel blocker TEA renders the Ca^{2+} distribution more uniform, with large increases that can be observed at the very tips of the dendrites [43]. These findings originally suggested the presence of voltage-gated Ca^{2+} channels in the dendritic tree. The spatial distribution of Ca^{2+} channels may reflect the propagation into the dendrites of trains of action potentials. Imaging with Na^+ -sensitive dyes has also yielded similar M patterns, suggesting that Ca^{2+} influx into the dendrites is driven by Na^+ -dependent action potentials [43, 44]. Both Na^+ -channel inactivation and K^+ -channel activation during action potentials would only allow a first few spikes, not necessarily sufficient to actively propagate the entire extent of the dendrites [43].

8.1.4 Actin–Microtubule Cytoskeletal Connections

Classically, F-actin and microtubular cytoskeletal networks are thought to fulfill separate, independent cellular roles. Highly dynamic actin networks are known for their role in cell spreading and contraction. The more stable microtubular cytoskeleton is best known for its importance in cell division and organelle trafficking. However, recent studies provide a more unified role, ascribing important roles for the actin cytoskeleton in cell division and trafficking and conversely, important roles for microtubules in the generation and plasticity of cellular morphology. Coordination between the actin- and microtubule-based cytoskeletons has also been observed during the process of neurite initiation [67, 21], which shares similarities with cellular migration and morphogenesis. A direct physical association between both cytoskeletons has been suggested, because microtubules often preferentially grow along actin bundles and transiently target actin-rich adhesion complexes. In neurons, certain plakins and neuron-specific microtubule-associated proteins (MAPs), including MAP1B and MAP2, play a role linking microtubules and F-actin, and

helping the transition from an undifferentiated state to neurite-bearing morphology [21]. Studies on contact-induced neurite formation in chick cortical neurons, however, suggested that microtubule polymerization is not required for the generation of neurites [123]. In this study, neurite-like protrusions were formed by the occasional contact of filopodia between two neurons on a coverslip. Upon contact, these filopodia grew in diameter and became filled with microtubules. Inhibition of microtubule dynamics by the combined application of the microtubule-stabilizing drug taxol and the destabilizing drug nocodazole did not prevent protrusion formation, which became filled with microtubules. This suggests that microtubules do not grow, but instead are transported into such locations. Depolymerization of most pre-existing microtubules with nocodazole induced cytosol flow into filopodia; which resulted in short and thick protrusions that did not resemble neurites in many respects. Thus, polymerization of new microtubules may not be a requirement for microtubule reorganization during contact-mediated neurite formation. In spontaneous neurite initiation, in contrast, microtubule polymerization does appear to be essential. Both taxol [67] and nocodazole [21], treatment, which inhibit microtubule polymerization and depolymerization, respectively, affected neurite formation without affecting pre-existing microtubules [143, 106, 68]. However, in the absence of normal microtubule polymerization, processes fail to form growth cones and fail to generate a thin neurite shaft. This suggests that key events in spontaneous neurite initiation, such as the separation of the lamellipodium from the cell soma to become a growth cone, are dependent on both the presence and the dynamic properties of microtubules. Paradoxically, experimental evidence suggests that actin filaments can both inhibit and promote neurite initiation and outgrowth [31]. Robust neurite-like induction was observed in neuroblastoma cells incubated with a variety of actin-disrupting drugs such as cytochalasin D, latrunculin A, and jasplakinolide, in combination with microtubule stabilizing concentrations of taxol [22]. These observations and others [26, 57] indicate that the actin cytoskeleton may be dispensable in process initiation, and in some cases the actin network is actually inhibitory. One observation that has emerged in studies of growth cones [114] is that actin filaments and microtubules are in intimate contact at the cell periphery. This suggests that membrane-associated complexes may directly tether both cytoskeletal systems. Growth cones are organized into distinct domains: a microtubule-rich central domain (C-domain) and an actin-rich peripheral domain (P-domain) [66, 69]. Although microtubules are only rarely observed within the P domain, over time many microtubules alternately advance into and retreat from the P-domain [127]. This can be observed in the lamellipodia of morphologically undifferentiated neurons prior to neurite initiation [22]. Certain perturbations, like exposure to actin assembly inhibitors, result in microtubular invasion into the P-domain [31]. Thus, it is possible that actin filaments restrain the microtubule cytoskeleton, as well as organelles and cytoplasm, from advancing toward the leading edge, such as in the actin-based retrograde flow [136, 109, 114].

Thus, dynamic interactions between both actin and microtubular cytoskeletons may be central to neuronal cell morphology and function. Only recently have clear functional interactions between those cytoskeletal structures become apparent. Association of microtubules with actin cables in filopodia appears to guide microtubule growth along the most efficient path antiparallel to retrograde flow [114]. Thus, specific coupling between microtubules and actin bundles possibly promotes microtubule advance. Association of microtubules with actin cables in lamellipodia of neuroblastoma cells expressing recombinant MAP2c, further suggests direct actin–microtubule interactions would play a key role in neurite initiation [22]. Actin–microtubule interactions might also be important for growth cone turning underlying axonal path-finding mechanisms. Both actin filament bundles [11] and dynamic microtubules [12] are required for growth-cone turning to avoid inhibitory cues. Increased microtubule invasion into neuronal lamellipodia might be essential for axon branching [23] and neurite initiation [22]. This is further evidenced by the presence in neurons of proteins capable of interacting with both microtubules and F-actin, and proteins that can mediate signaling between both cytoskeletons, which are thus likely to control microtubular invasion. The microtubule-associated proteins MAP1B and MAP2, for example, are known to interact with actin in vitro [96, 131, 113, 120, 17]. The C-terminal domain of the L2 subunit of MAP1B was shown to bind to F-actin and interact with stress fibers in transfected cells [131, 87]. Furthermore, MAP2 binds to F-actin efficiently, and induces actin bundle formation [113, 36]. MAP2 has also been found to localize in regions devoid of microtubules in neurons [84, 9]. Under certain conditions such as PKA activation, for example, MAP2 is found to be associated with the actin cytoskeleton [92]. This suggests that actin-related functions of MAP2 are regulated by phosphorylation. The MAP2-related MAP tau has been proposed to interact and bundle F-actin as well [36]. It is likely that by crosslinking, MAP2 and/or MAP1B associates with both cytoskeletons, and could thus be involved in guidance of microtubules along actin filament bundles.

8.2 Collective Modes of Behavior of C-Termini in Microtubules

In the following section we focus our attention on a specific dynamic mode of behavior within the MT cytoskeleton of a dendrite. MTs are long hollow cylinders made of $\alpha\beta$ -tubulin dimers [25]. These structures have outer diameters measuring 25 nm and inner diameters of 15 nm. During cell division, tubulin can account for as much as 10% of the cell's protein. MTs form by polymerization of tubulin dimers in a GTP-dependent process. In some cases, strands or protofilaments are formed first. MTs typically consist of 13 such protofilaments. Each μm of MT length consists of 1650 heterodimers. Recently, it has become apparent that neurons utilize MTs in cognitive processing. Both

kinesin and MAP2 have been implicated in learning and memory [139, 54, 140]. Dendritic MTs are implicated in particular, and it is highly probable that precisely coordinated transport of critical proteins and mRNAs to the postsynaptic density via kinesin along MT tracks in dendrites is necessary for learning, as well as for long-term potentiation (LTP) [55, 126]. As shown schematically in Fig. 8.4, presynaptic axon terminals make synaptic contact onto postsynaptic spines. Within the shaft of the dendrite, MTs act as tracks for kinesin motor protein propagation [2]; thus enabling them to transport proteins such as receptors. MTs also transport mRNA that translates proteins critical to synaptic activity.

In the following section we focus on the C-termini of neighboring tubulins, whose biophysical properties have a significant influence on the transport of material to activated synapses, thus affecting the capability of signal transduction and processing at the cytoskeleton on the one hand, and synapses undergoing LTP on the other hand. Using molecular dynamics modeling we calculated conformation states of the C-termini located on the outside of the MT, strongly interacting with other proteins, such as MAP2 and kinesin [108]. The processivity of kinesin appears to critically involve an interaction with the C-termini of tubulin, although MAP2 may temporarily uncouple to avoid interfering with the movement of kinesin along the MT [130]. On the other hand, removal of the C-terminus of tubulin profoundly affects kinesin processivity. Cleavage by subtilisin, for example, decreases the rate of kinesin transport by four-fold [137].

To elucidate the biophysical properties of C-termini and gain insight into the role it plays in the functioning of dendrites, we developed a quantitative computational model based on the currently available biophysical and

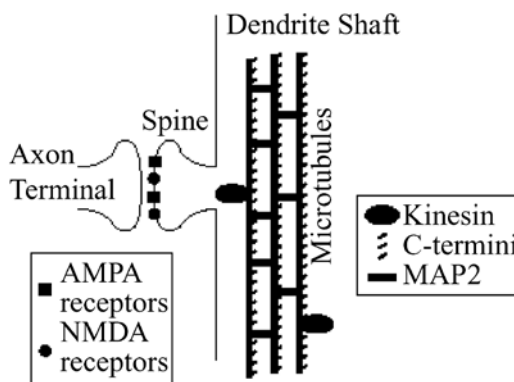


Fig. 8.4. Diagram of C-termini on the tubulin dimers of microtubules in relation to incoming synapses. Axon terminals typically input to spines, many of which contain AMPA and NMDA glutamate receptors. Kinesin motors transport cargo along microtubules. C-termini states affect the transport of kinesin along microtubules and this affects transport of materials to active synapses

biochemical data regarding the key macromolecular structures involved, including tubulin, their C-termini, and associated MAP2. In the following we describe the potential configurations of C-termini based on:

- The interactions between C-termini and the tubulin dimer,
- The interactions between nearest-neighbor C-termini, and
- The interactions between C-termini and MAP2 that lead to a model of wave propagation through counterions bounded to MAP2.

Our bead-spring model of the C-termini extends the static results, providing a finer picture of the dynamic behavior, the conformation states and their distribution.

8.2.1 Potential Configurations of Microtubular C-Termini

Based on the assumption that C-termini dynamics plays an important role in the functioning of a dendrite, we developed a simplified model of a C-terminus and its interactions with neighboring structures. The proposed model of the C-termini microtubular network is schematically illustrated in Fig. 8.5, where the tubulin dimer is considered to be the basic unit. Each dimer is decorated with two C-termini that may either extend outwardly from the surface of the protofilament or bind to it in one of few possible configurations (see next section).

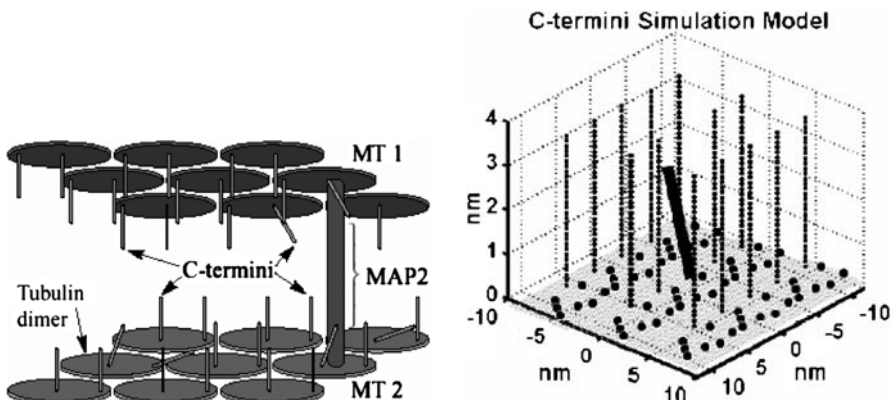


Fig. 8.5. *Left:* A schematic diagram of portions of two microtubules connected by a MAP2. Each portion shows the outer face of a tubulin dimer covered by two C-termini. Each C-terminus can be in one of two metastable states, perpendicular or parallel to the dimer surface. *Right:* A portion of the microtubule composed of a few tubulin dimers with their C-termini used as a model for the static simulation (right). Also shown are a few of the positively charged regions (circles) on the surface of a tubulin dimer. The test C-terminus is slanted (bold)

The most dynamic structural elements of the system (i.e. its elastic and electric degrees of freedom) can be best understood in terms of the conformational states of the C-termini. Each state of the unbound C-terminus is assumed to evolve such as to minimize the overall interaction energy of the system. According to our model, the C-termini, which are negatively charged, interact electrostatically with (a) the surface of the dimer, (b) the neighboring C-termini and (c) an adjacent MAP. Note that while the surface of the dimer is highly negatively charged on the average, it exhibits regions of positive charge that attract the C-termini causing them to bend and bind in what we generally denote as the “downward” state. The energy difference between the two major metastable states is relatively small, on the order of a few $k_B T$ at room temperature.

A MAP of the interaction energy of a C-terminus and its major neighbors reveals its static properties (the dynamic properties will be revisited later). For this purpose we studied numerically the interaction energy surface as experienced by a C-terminus. The details of the model and the terms involved are given in [98]. Fig. 8.6 shows a surface plot of the energy. It transpires that the “up” state has the lowest energy (corresponding to the C-terminus being perpendicular to the tubulin’s surface). However, the cone angle created by the constraint $E - E_0 < 50$ meV (where $E_0 = E$, $\theta = 90^\circ$) is about 40° . This means that the C-termini can move freely within this cone due to thermal fluctuations (with $k_B T$ approximately equal to 25 meV at physiological temperature). The important result is the existence of local minima associated

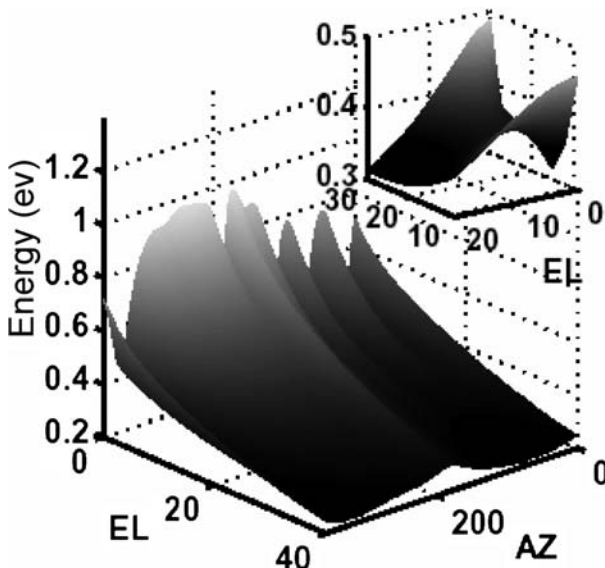


Fig. 8.6. Energy surface of the interaction between the test C-terminus and the environment. The inset shows a saddle point on the surface

with the “downward” state, which is only 100 meV higher than the straight-up state. The saddle point found is 160 meV above the “up-state”. What we deduce here is that, at least under the assumptions of the model, there are two major metastable states with a moderate energy barrier separating them. The inset in Fig. 8.6 shows a close-up view around the saddle point. In the next section we shall see that a more detailed model reveals the availability of multiple configurations associated with the “downward” state.

8.2.2 Dynamic Model of the C-Termini

To enable exhaustive simulations, we modeled the C-terminus as a sequence of beads with flexible connections, instead of the rigid rod, in what is known as a bead–spring model. The model takes into account the electric field exerted by the dimer, the external field generated by the environment, and various short-range interactions within the simulated C-terminus, including interactions between the beads (i. e. Lennard–Jones potential, angular forces, etc.). Our simulation indicates the ability of an ionic wave to trigger a corresponding wave of C-termini state changes from their upright to downward orientations as predicted by the simplified model discussed above.

Four views of C-termini states produced by this model are shown in Fig. 8.7, each has different conformation with examples of the “up” and “down” states evident. The position distribution showed in Fig. 8.8 describes the minimal energy positions of beads representing the constituent residues of a C-terminus. Calculations of the energy-minimized positions of the individual beads representing the amino acids of the C-termini in two equivalent

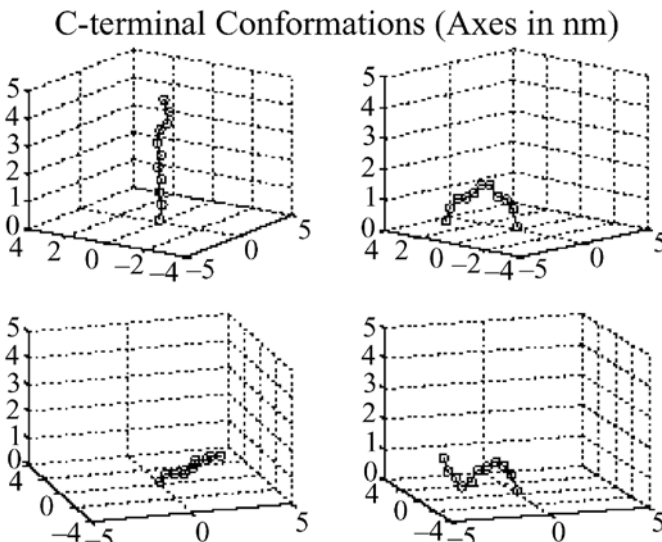


Fig. 8.7. Various C-terminal conformations observed with the dynamic model

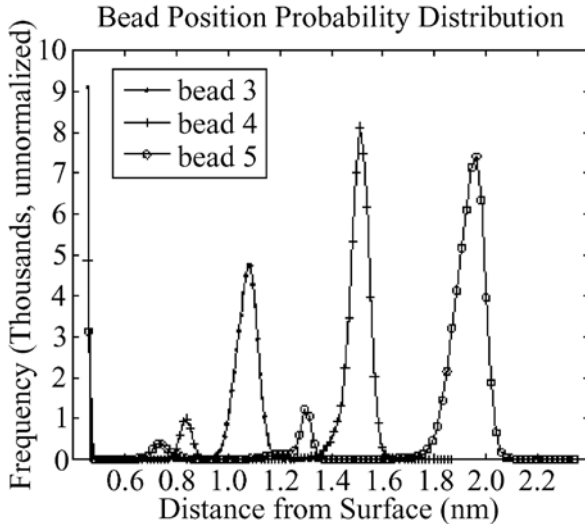


Fig. 8.8. Probability distribution describing minimal energy positions of beads representing a C-terminus ranging from 3 to 5 obtained at the end of each run after relaxation. The energy-minimized value can come from each of the beads at positions from 3 to 11. The first bead is permanently connected to the surface and hence has no freedom to move

forms reveals that the probability of the down position that includes all cases of full or partial attachment is 15%. This means that the system has indeed two major states with a strong bias towards the stretched-up state. In other words, the system tends to be mostly in the “up-state” unless driven towards one of the surface binding sites where the probability of attraction increases.

8.2.3 Ionic Wave Propagation along MAP2

Years ago, Manning [77] postulated an elegant theory, which stated that polyelectrolytes in solution may have condensed ions in their surroundings. According to Manning’s hypothesis, counterions “condense” about the polymer’s length, provided that a sufficiently high linear charge density is present on its surface. Thus, a linear polymer may be surrounded by counterions from the saline solution such that counterions are more closely surrounding the polymer’s surface, and salt co-ions in the solution are repelled such that a depletion region is also created [77, 93]. Although this theory was originally postulated for such polyelectrolytes as DNA, the same applies to highly charged one-dimensional polymers such as MAPs.

In an effort to investigate the ability of MAP2 to function as a “wave-guide” that transfers the conformational change in a C-terminus state to an adjacent MT, we studied a simplified model of the interaction between MAP2 and its ionic environment via counterions. While the 3D structure of MAP2 is

unknown since this protein has not been crystallized, it has been investigated for its binding with MTs. Although it is still uncertain whether a single MAP2 makes direct physical contact with a MT, it is apparent that it at least reaches its immediate vicinity. Our calculations of the charge distribution on the surface of the projecting domain of MAP2 resulted in a total negative charge of 150 e and a very close to linear charge distribution. To simplify the model we assumed that the counterion-attracting sites are equidistant and are

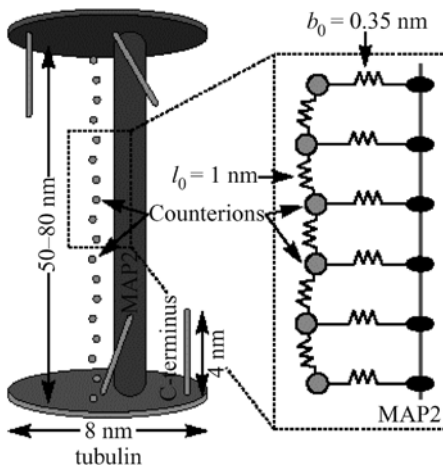


Fig. 8.9. Schematic model of a MAP2 interacting with positive counterions (*circles*). Also seen are two dimers at either end of the MAP2 and a slanted C-terminus. The zoomed region depicts the springs model used to describe the interactions between the MAP2 and the counterions

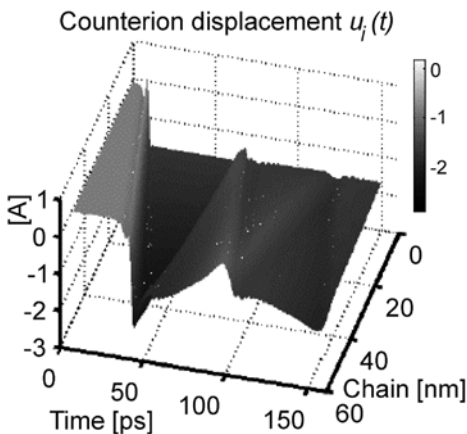


Fig. 8.10. Results of the MAP2 model simulation describing the counterions displacement (the chain-axis denotes the discrete indices of the counterions). The color bar is given in [Å]

arranged on a straight chain along the MAP2, schematically shown in Fig. 8.9. Hence we envisage that the counterions move only in a plane perpendicular to a cylinder representing the MAP2. We show that a perturbation applied to the counterions at one end of the MAP2 will drive them out of equilibrium and initiate a wave that travels along the MAP2. Details of the model are given elsewhere [98].

Fig. 8.10 depicts the main result of this analysis for a localized perturbation applied for a few picoseconds to the counterions near the binding site of the MAP2. The wave propagation along the chain of $N = 50$ counterions is represented by the counterion displacement parallel to the MAP2, u_i , where i denotes the i -th counterion. The profile of the displacement reveals that the perturbation along MAP2 propagates almost as a “kink”. Measurements of the phase velocity give values in the order of $v_{\text{ph}} \approx 2 \text{ nm ps}^{-1}$.

8.3 Ion Waves along Actin Filaments

8.3.1 Ionic Condensation along the Actin Filament

Motivated by several intriguing experiments [10, 70] indicating the possibility of ionic wave generation along actin filaments, we have also developed a physical model that provides a framework for the analysis of these waves. Actin filaments are highly charged one-dimensional polymers with an uneven distribution of charges along the polymer’s length. As a consequence, spatially dependent electric fields could be present and arranged in peaks and troughs as originally postulated by Oosawa [90]. This might imply large changes in the density of small ions around the polymer with a large dielectric discontinuity in the ionic distribution [51, 42, 3]. This uneven ionic distribution along a short stretch of the polymer (likely the average pitch 35–40 nm) may be considered a linear unit of an electrical circuit to be modeled with nonlinear electrical components. First, there is a nonlinear capacitor, which is associated with the spatial charge distribution between the ions located in the outer and inner regions of the polymer. Secondly, any charge movement tending to dissipate this local gradient (reversibly) generates a secondary electromotive force due to the charge movement, namely a local current. This is the main contribution to the inductance of the single stretch of polymer. F-actin, being a highly charged polyelectrolyte contains a fraction of its surrounding counterions in the form of a condensed cloud about its surface. Such a cloud may be highly insensitive to large changes in the ionic strength of the surrounding saline solution [89, 76, 145]. The Bjerrum length, λ_B , describes the distance beyond which thermal fluctuations are stronger than the electrostatic attraction or repulsion between charges in solution whose dielectric constant is $[\varepsilon]$. It is defined by

$$\frac{e^2}{4\pi\varepsilon\varepsilon_0\lambda_B} = k_B T, \quad (8.1)$$

for a given temperature T in Kelvin. Here e is the electronic charge, ε_0 the permittivity of the vacuum and k_B is Boltzmann's constant. For a temperature of 293 K it is readily found that $\lambda_B = 7.13 \times 10^{-10}$ m. Counterion condensation occurs when the mean distance between charges, b , is such that $\lambda_B/b = S > 1$. Each actin monomer carries an excess of 14 negative charges in vacuum, and accounting for events such as protonation of histidines, and assuming there to be 3 histidines per actin monomer, there exist 11 fundamental charges per actin subunit [128]. Assuming an average of 370 monomers per μm we find that there is approximately $4e/\text{nm}$ in agreement with an earlier statement. Thus we expect a linear charge spacing of $b = 2.5 \times 10^{-10}$ m, such that $S = 2.85$. As the effective charge, q_{eff} , or renormalized rod charge is the bare value divided by S we find $q_{\text{eff}} = 3.93e/\text{monomer}$.

Assuming for simplicity a linear charge distribution about the actin filament, the linear charge density, ξ , is much greater than $1/z$ where z is the valence of the counterions in solution. The parameter, ξ , is given by

$$\xi = \frac{e^2}{4\pi\varepsilon_0\varepsilon_r\lambda_B k_B T b}, \quad (8.2)$$

where e is the electronic charge, ε_r the dielectric constant of water, and b the average axial spacing of charges on the polyelectrolyte [145]. The parameter, ξ , was calculated to be 110 for actin filaments (with $z = 1$ for H^+ and K^+ ions) and so $\xi \gg 1/z$ [70]. Thus approximately 99% of the counterion population is predominantly constrained within a radius of 8 nm [97] round the polymer's radial axis [145]. Significant ionic movements within this "tightly bound" ionic cloud are therefore allowed along the length of the actin (Fig. 8.11) provided that it is shielded from the bulk solution [89, 93].

Bearing in mind the sheath of counterions around the actin filament we see that effectively actin polymers may act as biological "electrical wires" [70], which can be modeled as nonlinear inhomogeneous transmission lines. Such electrical devices are able to propagate nonlinear dispersive solitary waves [61, 91] in the form of solitons [86, 71, 72]. It has been proposed that such solitons, localized traveling waves, exist in many biological systems and, in fact, have earlier been postulated in linear biopolymers such as MTs [112] and DNA [4]. Interestingly, both solitary waves [70] and liquid crystal formation [16, 33] have been observed in actin filaments possibly providing a potentially fruitful environment for innovative biotechnological applications.

8.3.2 Electrical Modeling of Actin

We developed a model based on the transmission-line analogy with inductive, resistive and capacitive components. The physical significance of each of the components, for each section of the electrical network, as well as additional details is described in [134]. As the counterion condensation cloud separates the filament core from the rest of the ions in the bulk solution, we expect

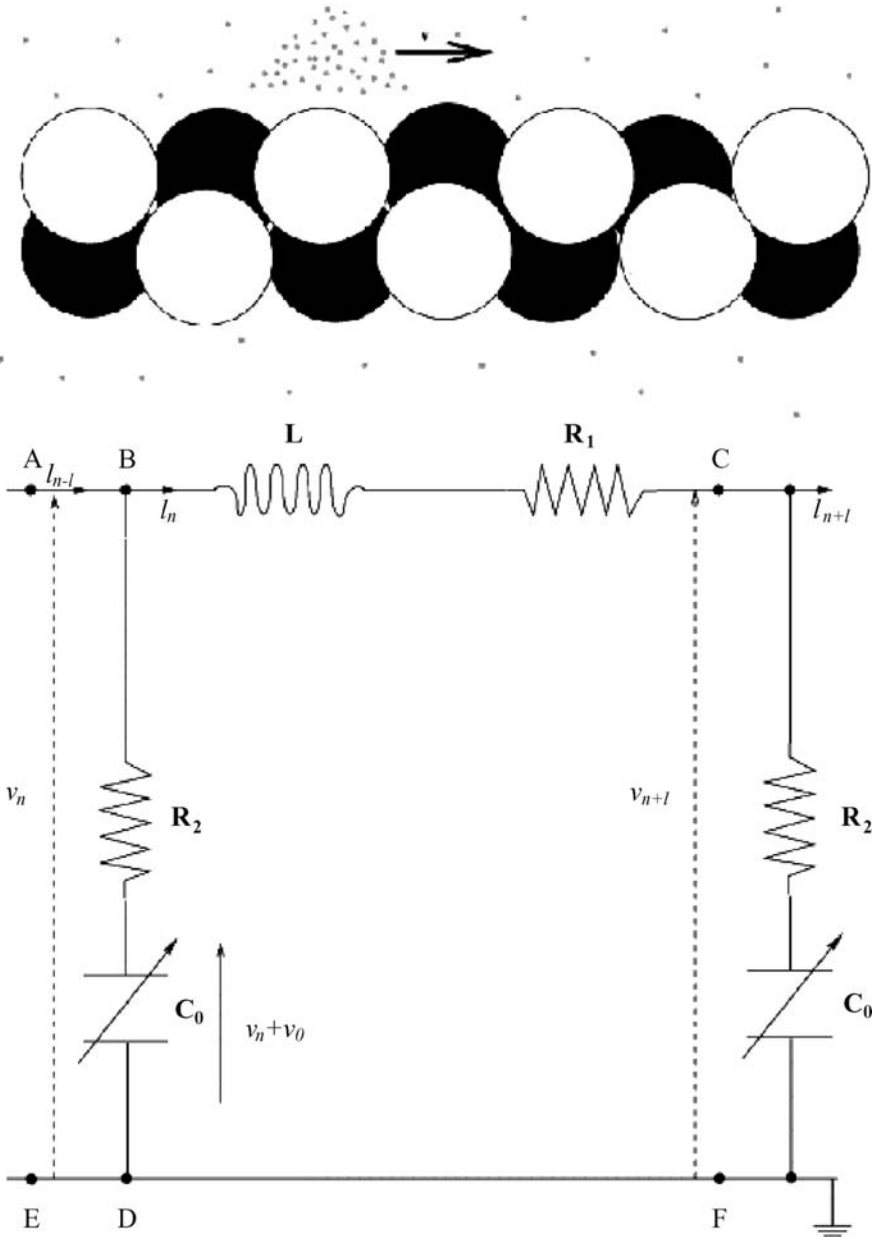


Fig. 8.11. Nonlinear dispersive solitary waves traveling along an actin filament. Positive counterionic charges in the bulk form a cylinder around the actin filament. The distance between this cylinder and the actin filament is one Bjerrum length. There are also some counterions that condense to the actin filament. An effective circuit diagram for the n -th monomer between the dotted lines. I_n is the current through the inductance L and resistance R_1

this cloud to act as a dielectric medium between the two. This cloud provides both resistive and capacitive components for the behavior of the monomers, which make up the actin filament. Ion flow is expected at a radial distance from the center of the filament, which is approximately equal to the Bjerrum length. The inductive component is due to the actin's double-stranded helical structure that induces the ionic flow in a solenoidal manner.

For actin in solution, a key feature is that the positively charged end assembles more quickly than the negatively charged end [121]. This results in an asymmetry in the charges at the ends of the filaments and F-actin's electric polarization. Actin monomers arrange themselves head to head to form actin dimers resulting in a probable alternating distribution of electric dipole moments along the length of the filament [58, 59]. We assume, therefore, that there is a helical distribution of ions winding around the filament at approximately a radial distance equal to one Bjerrum length. This may be thought of as a solenoid in which a fluctuating current is flowing as a result of voltage differences generated at each end. The number of turns, $N = a/r_h$, is approximated by simply working out how many ions could be lined up along the length of a monomer. We would then be approximating the helical turns as circular rings lined up along the axis of the F-actin. This is surely an overestimate of the number of helical turns per monomer, but it is certainly within reason for our purposes as an initial approximation. We also take the hydration shell of the ions into account in our calculation. This shell results when an ion is inserted into a water configuration, changing the structure of the hydrogen-bond network. A water molecule will reorient such that its polarized charge concentration faces the opposite charge of the ion. As the water molecules orient themselves towards the ion, they break the hydrogen bonds to their nearest neighbors. The hydration shell is then the group of water molecules oriented around an ion. A rough estimate for the size of a typical ion in our physiological solution, with a hydration shell, is $r_h = 3.6 \times 10^{-10} \text{ m}$. This is the approximate radius of the first hydration shell of sodium ions. For a filament containing n monomers, we would get an effective resistance, inductance, and capacitance, respectively, such that:

$$R_{\text{eff}} = \left(\sum_{i=1}^n \frac{1}{R_{2,i}} \right)^{-1} + \sum_{i=1}^n R_{1,i}, \quad (8.3)$$

$$L_{\text{eff}} = \sum_{i=1}^n L_i, \quad (8.4)$$

and

$$C_{\text{eff}} = \sum_{i=1}^n C_{0,i}, \quad (8.5)$$

where $R_{1,i} = 6.11 \times 10^6 \Omega$, and $R_{2,i} = 0.9 \times 10^6 \Omega$, such that $R_{1,i} = 7R_{2,i}$. The reader should note that we have used $R_{1,i} = R_1$, $R_{2,i} = R_2$, $L_i = L$, and $C_{0,i} = C_0$. For a 1-μm length of actin filament we find therefore

$R_{\text{eff}} = 1.2 \times 10^9 \Omega$, $L_{\text{eff}} = 340 \times 10^{-12} \text{ H}$ $C_{\text{eff}} = 0.02 \times 10^{-12} \text{ F}$. The electrical model of the actin filament is basically an application of Kirchhoff's laws to that section of the effective electrical circuit for one monomer, M , which involves coupling to neighboring monomers. We then take the continuum limit, assuming a large number of monomers along an actin filament. The application of Kirchhoff's laws and using the continuum approximation the following equation is derived [134], which describes the spatiotemporal behavior of the potential along the actin filament:

$$LC_0 \frac{\partial^2 V}{\partial t^2} = a^2 (\partial_{xx} V) + R_2 C_0 \frac{\partial}{\partial t} (a^2 (\partial_{xx} V)) - R_1 C_0 \frac{\partial V}{\partial t} + R_1 C_0 2bV \frac{\partial V}{\partial t}. \quad (8.6)$$

As a result of applying an input voltage pulse with an amplitude of approximately 200 mV and a duration of 800 μs to an actin filament, electrical signals were measured at the opposite end of the actin filament [62]. This experiment indicates that actin filaments can support ionic waves in the form of axial nonlinear currents. The current measured in the process lasted approximately 500 μs , and reached a peak value of approximately 13 nA. In a related earlier experiment [70], the wave patterns observed in electrically stimulated single actin filaments were remarkably similar to recorded solitary waveforms from experimental studies on electrically stimulated nonlinear transmission lines [61, 71, 86]. Considering the actin filament's highly nonlinear complex physical structure [97] and thermal fluctuations of the counterionic cloud from the average distribution [89, 90], the observation of soliton-like ionic waves is consistent with the idea of actin filaments functioning as biological transmission lines.

Indeed the soliton conformation theory for proteins, involves charge displacement for "resonant" states within a particular structure as predicted by Davydov (see [19]). However, in the case of actin in solution, the soliton behavior envisaged in our model is constrained to the ion clouds and represents the "convective movement of ions" along a one-dimensional polymer.

Analysis of the nonlinear equations using two different approaches resulted in two possibilities. The first ansatz resulted in a zero dissipation state (due to the absence of resistive terms) corresponding to an absolute maximum velocity of propagation. This, however, implies a purely electromagnetic disturbance propagating resonantly from node to node in the circuit. A more physically realistic case involved mapping our equation onto the Fisher–Kolmogoroff equation with the attendant elliptic and topological solitonic solutions. The elliptic waves were stationary in time and may lead to the establishment of spatial periodic patterns of ionic concentration.

8.3.3 Implications of Actin Filament's Electrical Activity

Successful application of electrical circuit components indicates the existence of a traveling kink wave, which describes a moving transition region between high and low ionic concentrations due to the corresponding intermonomeric

voltage gradient. The velocity of propagation was estimated to range between 1 and 100 ms^{-1} depending on the characteristic properties of the electrical circuit model. Interestingly, these values overlap with action potential velocities in excitable tissues [40]. Considering the abundance of actin filaments in axons and dendritic trees, our findings may have important consequences for our understanding of the signaling and ionic transport at the intracellular level. Extensive new information (see [45]) indicates that actin filaments are both directly [13] and indirectly linked to ion channels in both excitable and nonexcitable tissues, providing a potentially relevant electrical coupling between these current generators (i.e. channels), and intracellular transmission lines (i.e. actin filaments). Furthermore, actin filaments are crucially involved in cell motility and, in this context, they are known to be able to rearrange their spatial configuration. It is tantalizing to speculate that ionic waves surrounding these filaments may participate or even trigger the rearrangement of intracellular actin networks. In nerve cells actin filaments are mainly located in the synaptic bouton region. Again, it would make sense for electrical signals supported by actin filaments to help trigger neurotransmitter release through voltage-modulated membrane deformation leading to exocytosis [118]. Actin is also prominent in postsynaptic dendritic spines, and its dynamics within dendritic spines has been implicated in the postsynaptic response to synaptic transmission. Kaech et al. [52] have shown that general anesthetics inhibit this actin-mediated response. Incidentally, it is noteworthy that Claude Bernard showed also that the anesthetic gas chloroform inhibited cytoplasmic movement in slime mold. Actin structural dynamics plays a significant role in synaptic plasticity and neuronal function. Among functional roles of actin in neurons, we mention in passing glutamate receptor channels, which are implicated in long-term potentiation. It is therefore reasonable to expect ionic wave propagation along actin filaments to lead to a broad range of physiological effects.

8.4 Dendritic Cytoskeleton Computation – Vision of Integration

In previous sections we discussed novel properties of the main components of the neuronal cytoskeleton, in particular ionic wave propagation along actin filaments, and interacting MAPs and C-termini in microtubular tubulins. This is the core of our current hypothesis. The cytoskeletal biopolymers, including actin filaments and microtubules, constitute the backbone, through possible wave propagation via those structures, which in turn interact with membrane components, including ion channels thus rendering novel modulatory effects to synaptic connections. The basic experimental finding that actin filaments support wave propagation [70] suggests the possibility of nonlinear, soliton-type propagation along “one-dimensional” biopolymers [93], provided that ionic condensation is supported [76, 89, 77]. The molecular dynamics mod-

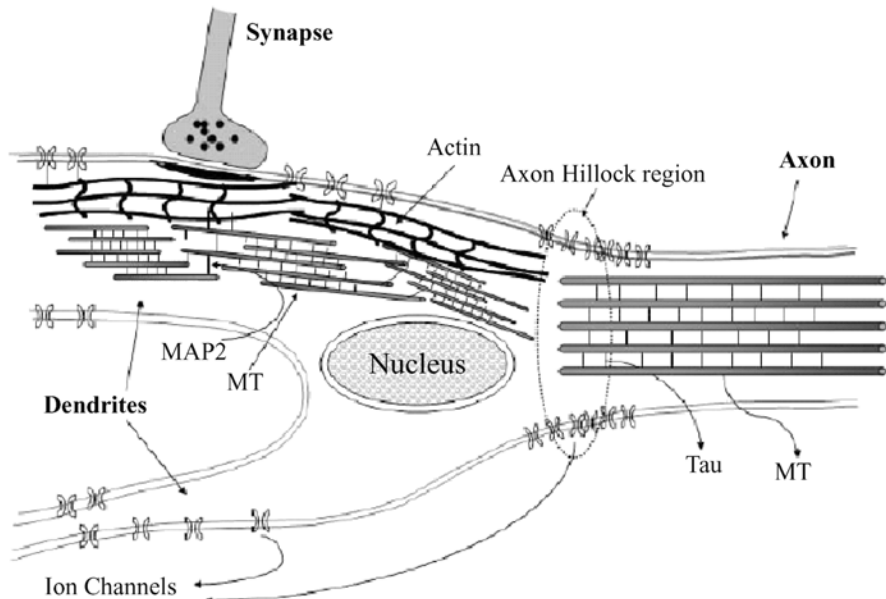


Fig. 8.12. Basic scheme of a neuron showing dendrites, the soma and an axon. Depicted within the dendrites are microtubule networks (MTs interconnected by MAP2), actin filaments and a synapse. Actin bundles and microtubules are interconnected. Actin filaments are also connected to ion channels

eling of microtubules also raises the possibility that these polymeric structures are capable of transmitting electrostatic perturbations both collectively among neighboring carboxy-termini and from these, to adjacent MTs via linking proteins such as MAP2 [95, 1]. Before we begin to describe our hypothesis, let us illustrate the basic relations between the main components of the model. Fig. 8.12 shows a general scheme of the neuron, emphasizing the main components to be discussed later. Some of the basic morphological features include the Tau-MAP inter-connected bundles of microtubules (MTs) present in the axon, and the axon hillock, a region rich in ion channels. The dendritic shaft contains microtubule networks (MTN), MAP2-interconnected MTs, and actin filaments and synapses. Microtubules and actin filaments are inter-connected, and actin filaments are connected to ion channels.

Fig. 8.13 focuses on the dendritic shaft. The MTs are decorated by C-termini and interconnected by MAP2 (thick line). Connections between MTs and actin filaments are shown as well. Two types of synaptic bindings are depicted. On the upper left side, actin bundles bind to the postsynaptic density (PSD) of a spineless synapse. On the lower right hand, a spiny synapse is shown where the actin bundle enters the spine neck and binds to the PSD, which at the other end, is connected to the MTN. This is further detailed in Fig. 8.13, right, showing the actin bundle linked to the PSD.

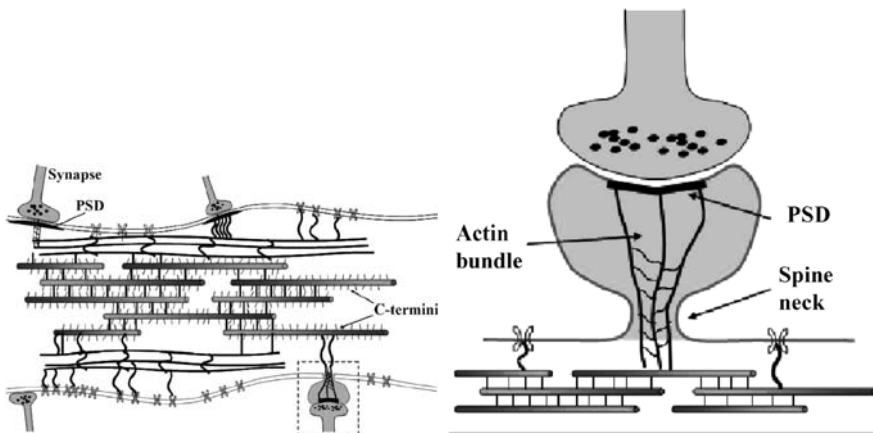


Fig. 8.13. *Left:* A scheme of the dendritic shaft. Depicted at the dendrite is a microtubule network, actin filaments, synapses and ion channels. Actin filaments enter the postsynaptic density (PSD). In the case of a spiny synapse (*lower right*) the actin bundle enters the spine neck. MTs are decorated by C-termini and interconnected by MAP2 (**bold lines**). The marked synapse is enlarged in the next figure. *Right:* Close-up view of the marked synapse in the *left figure*. Actin filaments enter the spine neck and connect to the PSD. The filaments are also connected to MTs (or MAP2s) at the dendritic shaft

We envision a mechanism in which a direct regulation of ion channels and thus synaptic strength by actin filaments and associated cytoskeletal structures controls and helps modify the electrical response of the neuron. In this picture, MTs arranged in networks of mixed polarity, receive signals in the form of electrical perturbations, from synapses via actin filaments connected to MTs by MAP2 [107], or via direct MT connections to postsynaptic density proteins by molecules such as CRIPT [94]. Due to the characteristics discussed earlier, the MTN may be viewed as a high-dimensional dynamic system where the main degrees of freedom are related to the (conformational) state of the C-termini. The input signals perturb the current state of the system that continues to evolve.

Hypothetical integration of the above ideas is outlined as follows:

1. Incoming (electrical) signals arrive at the postsynaptic density via synaptic transmission, which in turn elicit ion waves along the associated actin filaments at the synaptic spine (Fig. 8.14A).
2. These dendritic input signals propagate through actin filaments to the microtubules network (MTN) where they serve as input signals (Fig. 8.14B).
3. The MTN, operating as a large high-dimensional state machine, evolves these input states, e. g., by dynamically changing C-termini conformation (Fig. 8.14C).

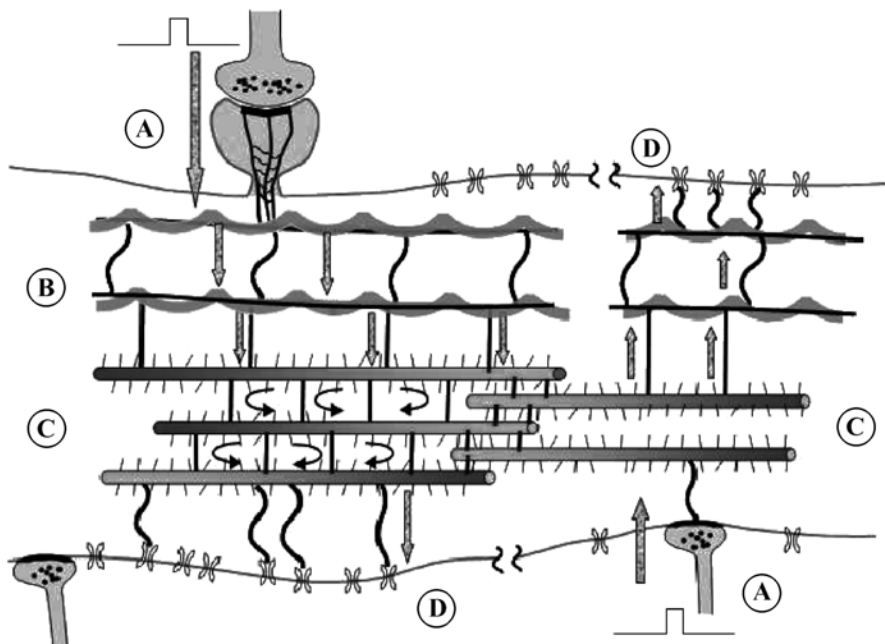


Fig. 8.14. Schematic picture of our model. **A** Incoming signal from the synapse is propagated via the actin bundle within the synaptic neck to the dendritic shaft, or directly to the MTN (see *lower-right* synapse). **B** The wave propagates along actin filaments (*thick wavy line*) and to a microtubule network (MTN). **C** The MTN operates as a high-dimensional dynamic system, which continuously processes the incoming perturbation. The curved arrows symbolize recurrent operations due to MAP2 coupling between adjacent MTs. **D** The current state of the “MTN state machine” is used as readout at certain areas, either directly to ion channels or mediated/propagated by the actin network, interacting with ion channels

4. The output from the MTN is the state of the system at some time “T” that is being “read” (sensed) in certain areas, again by actin filaments, and propagated to remote ion channels. These output functions are assumed to regulate the temporal gating state of voltage-sensitive channels (Fig. 8.14D).
5. This process subsequently regulates the membrane conductive properties as well as controlling the axon hillock behavior by changing the distribution and topology of open/closed channels. The overall function of the dendrite and neuron are thus regulated in this manner.

To understand how this integrative view may serve as a regulatory (adaptive) mechanism, let us elaborate on the main issues raised. The input level denoted by A in Fig. 8.14 is associated with external perturbations arriving through membrane processes. We mainly consider synaptic inputs arriving from other

neurons. These signals arrive at the cytoskeleton as electric perturbations, which either directly affect MTNs, and/or actin filaments (bundles), in spiny synapses. However, the actin cytoskeleton is responsible for the propagation of signals to the MTN (see level B). These propagated signals (level C) are in turn used as inputs to the MTN, which may be viewed as a dynamic system. The model further proposes that the MTN is capable of generating diverse phase-space trajectories in response to different input vectors. The requirements from such a system are in fact not too restrictive since the output state is not an attractor of the system. In other words, information processing at this level is not necessarily based on attractor dynamics but rather on real-time computations. This proposition relies on the observations regarding the ability of the MTN to propagate signals, on the one hand, and on the special (spatial) topological features of MTNs in dendrites, in which shorter MTs of mixed polarity are interconnected by MAP2s. The output from the MTN would be some function of the evolved state vector in certain areas accessed by actin filaments and/or directly linked to ion channels (see both possibilities at level D). These output signals may modify the temporal channel activity, either by directly arriving from the MTN to the channels, or mediated by actin filaments. Hence, the channel-based synaptic membrane conductance is regulated, in particular in the axon hillock region, which is, in most cases, responsible for the generation of action potentials.

The idea that a nonspecific high-dimensional dynamical system may serve as a reservoir of trajectories in the context of liquid state machines (LSM), has recently been suggested as a possible explanation for the existence of microcircuits in the brain [85]. The basic structure of an LSM is an excitable medium (hence “liquid”) and an output function that maps the current liquid state. The liquid must be sufficiently complex and dynamic to guarantee universal computational power. This may be sufficient to ensure that different input vectors will lead to separate trajectories. A network of spiking neurons, a recurrent neural network, and even real water have been used as a “liquid”, whereas the output (readout) function has been implemented by either simple perceptrons, threshold functions or even linear regression functions. Clearly, simpler readout functions restrict the ability of the whole system to capture complex nonlinear dependencies.

The attractiveness of the concept that the cytosol, with its cytoskeletal structures may behave as an LSM is obvious in the context of our model, because it provides a means for real-time computation without the need for stable attractors. Moreover, the output is relatively insensitive to small variations in the MTN (cytoskeletal networks!) or input vectors. Figure 8.15 depicts the functional scheme of the model described above and in Fig. 8.14. One should note that the MTN state evolves continuously, even without external inputs. Recent perturbations, however, have a long-term effect on the MTN trajectories, i. e. there is a memory effect inherent to this system (not to be mistaken with synaptic LTP, which possesses a much longer time scale).

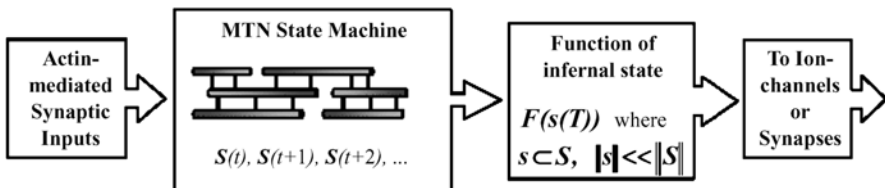


Fig. 8.15. Functional scheme of the model steps. Synaptic inputs are transferred to the MTN via actin filaments. These inputs perturb the MTN state machine that continuously evolves through time. The current state of the MTN in time “T” at certain areas is mapped by a function F and transmitted to its target, e.g., ion channels

The output from the MTN may be linear regression functions that converge at (or near) ion channels to regulate their temporal behavior. The issue of adapting the readout requires some sort of feedback mechanism that will, at least locally, enable the change in output function. In the context of neuronal function, with focus on processivity, synaptic strengthening, LTP, and memory enhancement, the output function may simply reflect an effect of the MTN on synaptic channel function, such that the desired state of the channel appears in a higher open probability. One possibility is a Hebbian-based response in which more frequent activity of certain subdomains of the MTN output states will give rise to higher (or lower, depending on the desired response) density of actin filaments connecting to corresponding channels.

8.4.1 MTN Control of Synaptic Plasticity, Modulation, and Integration

The above may reflect a most prominent feature of dendritic ion-channel regulation, with the potential boosting and enhancement of distal synaptic events, namely the interaction between channel activity and its regulation by cytoskeletal structures (Fig. 8.16). Voltage-gated Na^+ and Ca^{2+} channels play an important role in amplifying the magnitude of EPSPs towards the soma. Thus, channel regulation may also be important for dendritic interactions in the immediate vicinity of the synaptic input. Voltage-gated channels may alter the local input resistance and time constant, which in turn would influence both spatial and temporal summation of EPSPs and IPSPs, thus, conveying highly nonlinear interactions [122]; including signal amplification [46, 124]. The nonlinear properties of dendrites may act as amplification/modulation devices. In addition to providing an output, the action potentials elicited by synaptic input, whether initiated at the local synaptic sites or at the axon hillock and backpropagated into the dendrites, would essentially reset the dendritic membrane potential. This change in membrane potential would modify synaptic summation. Action potentials might also provide a feedback or an associative signal to other synapses active just before or just after the

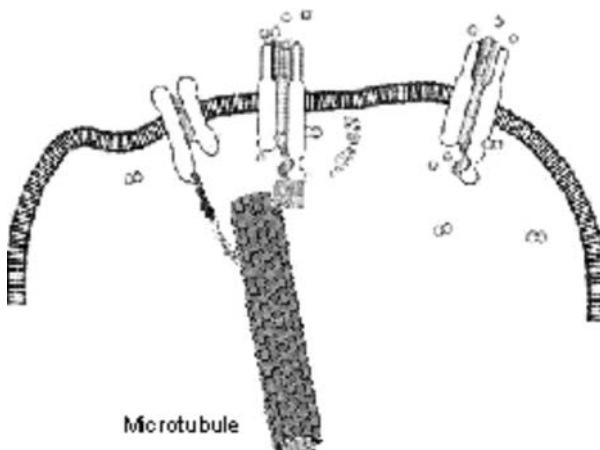


Fig. 8.16. MTs and actin filaments and interactions between the two (MTNs) elicit channel regulation in neurons. Conversely, synaptic channel function may also control cytoskeletal structures, thus structurally modifying the environment, and helping the dynamics of synaptic plasticity

action potential. Glutamate-activated NMDA receptors for example, could be rapidly opened by a backpropagating action potential that removes the voltage-dependent Mg^{2+} block of the channel [65, 125], thus producing Ca^{2+} influx through NMDA receptors. Feedback mechanisms between cytoskeletal structures (i.e. MTN) and synaptic signals may strengthen the adaptive behavior of the entire system.

Johnson and Byerly originally determined that agents that modify cytoskeletal organization alter Ca^{2+} -channel activity in Lymnaea neurons [47, 48]. Cytoskeletal disrupters such as colchicine and cytochalasin B were found to speed Ca^{2+} -channel decline in ATP, whereas the cytoskeletal stabilizers, taxol and phalloidin, were found to prolong Ca^{2+} -channel activity without ATP. In addition, cytoskeletal stabilizers reduced Ca^{2+} -dependent channel inactivation. Thus, both channel metabolic dependence and Ca^{2+} -dependent inactivation in neurons might be controlled by cytoskeletal interactions. Further, Ca^{2+} -channel inactivation in acutely isolated rat hippocampal pyramidal neurons [48] is modified by drugs that stabilize (taxol and phalloidin) and destabilize (colchicine and cytochalasin B) the actin and microtubular cytoskeletons, respectively. Voltage-gated K^+ channels from retinal bipolar neurons of the tiger salamander [74] were also found to be controlled by acute disruption of endogenous actin filaments with cytochalasin D, which was largely prevented by intracellular perfusion with the actin filament-stabilizer agent, phalloidin. Thus, acute changes in actin-based cytoskeleton dynamics also regulate voltage-gated ion-channel activity in bipolar neurons. This may be indicative of a more general and quite appealing mechanism by which cytoskeletal structures control feedback mechanisms in neuronal channels. Cy-

toskeletal remodeling may help sort, or otherwise deliver ion channel subunits to several neuronal locations. Cytoskeletal control of neuronal channels may also target channel localization and clustering. The discrete location of Na^+ channels to subdomains of the nerve, suggested that the Nav1.2 voltage-gated Na^+ channel contains axonal sorting and/or clustering signals [34]. Evidence indicated that addition of the cytoplasmic carboxy-terminal region of Nav1.2 restricted the distribution of a dendritic–axonal reporter protein to axons of hippocampal neurons. Interestingly, this motif was also sufficient to redirect somatodendritic K^+ channels to the axonal initial segment, a process involving association with ankyrin G.

Conversely, electrical synaptic activity may have the opposite effect in the control of subjacent cytoskeletal structures [30] (Fig. 8.16). Afferent back-propagating action potentials provide a feedback to dendritic synapses after a neuronal output has occurred. Ca^{2+} channels are implicated in postsynaptically induced synaptic plasticity such as short-term potentiation (STP) [75], long-term potentiation (LTP) (both NMDA-receptor dependent and NMDA-receptor independent), and long-term depression (LTD) [8, 14, 50]. This, in turn, is highly dependent on the control of the cytoskeletal structures involved in their vicinity [78, 79]. LTP induction is associated with a long-lasting increase in actin filament content within dendritic spines. This phenomenon, however, is dependent on NMDA receptor channel activity [32]. Similarly, long-term facilitation, and the response to cAMP-induced synaptic enhancement are both dependent on I_h -induced presynaptic current regulation of the actin cytoskeleton [5]. Thus, electrical synaptic activity is an essential component of structural stability and dynamic function of cytoskeletal structures, which in turn feedback the membrane components of the dendritic spine, to name a central player in synaptic plasticity. It is obvious that other neuronal regions are similarly affected, and may be dynamically regulated by such dual interactions.

8.5 Final Statement

In this report we provide extensive evidence for new roles of the actin and microtubule-based cytoskeletons in the control of dendritic function and morphological features. The most novel information relies on our findings that both structural elements of their respective cytoskeletons; namely actin filaments, and microtubular structures (MT-MAPs), support ionic waves, which may provide a new dimension to the control of neural function.

References

1. Al-Bassam, J., R.S. Ozer, D. Safer, S. Halpain, and, R.A. Milligan. (2002). *J. Cell Biol.* **157**:1187–1196.

2. Alberts, B., A. Johnson, J. Lewis, M. Raff, K. Roberts, and, P. Walter. (2002). *Molecular Biology of the Cell*. Garland Science Publishing, New York.
3. Anderson, C.F. and Record, M.T.Jr. (1990). *Ann. Rev. Biophys. Biophys. Chem.* **19**:423–465.
4. Baverstock, K.F. and Cundall, R.B. (1988). *Nature*. **332**:312–313.
5. Beaumont, V., N. Zhong, R.C. Froemke, R.W. Ball, and, R.S. Zucker. (2002). *Neuron*. **33**:601–613.
6. Bernardo, L.S., L.M. Masukawa, and D. Prince. (1982). *J. Neurosci.* **2**:1614–1622.
7. Bishop, C. (1995). *Neural Networks for Pattern Recognition*. Oxford University Press, Oxford.
8. Bliss, T.P. and G. Collingridge. (1993). *Nature*. **361**:31–39.
9. Caceres, A., M.R. Payne, L.I. Binder, and O. Steward. (1983). *Proc Natl Acad Sci USA*. **80**:1738–1742.
10. Cantiello, H.F., C.R. Patenaude, and K.S. Zaner. (1991). *Biophys. J.* **59**:1284–1289.
11. Challacombe, J.F., D.M. Snow, and P.C. Letourneau. (1996). *J. Cell Sci.* **109**:2031–2040.
12. Challacombe, J.F., D.M. Snow, and P.C. Letourneau. (1997). *J. Neurosci.* **17**:3085–3095.
13. Chasan, B., N.A. Geisse, K. Pedatella, D.G. Wooster, M. Teintze, M.D. Carattino, W.H. Goldmann, and H.F. Cantiello. (2002). *Eur. Biophys. J.* **30**:617–624.
14. Christie, B.R., D.S. Kerr, and W. Abraham. (1994). *Hippocampus*. **4**.
15. Colicos, M.A., B.E. Collins, M.J. Sailor, and Y. Goda. (2001). *Cell*. **30**:605–616.
16. Coppin, C. and P. Leavis. (1992). *Biophys J.* **63**:794–807.
17. Correas, I., R. Padilla, and J. Avila. (1990). *Biochem. J.* **269**:61–64.
18. Crick, F. (1982). *Trends Neurosci.* **5**:44–46.
19. Davydov. (1982). In *International Series in Natural Philosophy*. D. Haav, (ed.) Pergamon, Oxford, UK.
20. de Schutter, E. (1998). *J. Neurophysiol.* **80**:504–519.
21. Dehmelt, L. and S. Halpain. (2004). *J. Neurobiol.* **58**:18–33.
22. Dehmelt, L., F.M. Smart, R.S. Ozer, and S. Halpain. (2003). *J. Neurosci.* **23**:9479–9490.
23. Dent, E.W. and K. Kalil. (2001). *J. Neurosci.* **21**:9757–9769.
24. Dunaevsky, A., A. Tashiro, A. Majewska, C. Mason, and R. Yuste. (1999). *Proc. Natl. Acad. Sci. USA*. **96**:13438–13443.
25. Dustin, P. (1984). *Microtubules*. Springer-Verlag, Berlin.
26. Edson, K., B. Weisshaar, and A. Matus. (1993). *Development*. **117**:689–700.
27. Engert, F. and T. Bonhoeffer. (1999). *Nature*. **399**:66–70.
28. Fifkova, E. and R.J. Delay. (1982). *J. Cell Biol.* **95**:345–350.
29. Fischer, M., S. Kaech, D. Knutti, and A. Matus. (1998). *Neuron*. **20**:847–854.
30. Fischer, M., S. Kaech, U. Wagner, H. Brinkhaus, and A. Matus. (2000). *Nature Neurosci.* **3**:887–894.
31. Forscher, P. and S.J. Smith. (1988). *J. Cell Biol.* **107**:1505–1516.
32. Fukazawa, Y., Y. Saitoh, F. Ozawa, Y. Ohta, K. Mizuno, and K. Inokuchi. (2003). *Neuron*. **38**:447–460.

33. Furukawa, R., R. Kundra, and M. Fechheimer. (1993). *Biochem.* **32**:12346–12352.
34. Garrido, J.J., F. Fernandes, A. Moussif, M.-P. Fache, P. Giraud, and B. Dargent. (2003). *Biology of the Cell*. **95**:437–445.
35. Greenough, W. (1975). *Am. Sci.* **63**:37–46.
36. Griffith, L.M. and T.D. Pollard. (1982). *J. Biol. Chem.* **257**:9143–9151.
37. Hebb, D.O. (1949). *The Organization of Behavior: A Neuropsychological Theory*. John Wiley, New York.
38. Hempel, C.M., K.H. Hartman, X.J. Wang, G.G. Turrigiano, and S.B. Nelson. (2000). *J. Neurophysiol.* **83**:3031–3041.
39. Hering, H. and M. Sheng. (2001). *Nat. Rev. Neurosci.* **2**:880–888.
40. Hille, B. (1992). *Ionic Channels of Excitable Membranes*. Sinauer Associates Inc., Sunderland, MA.
41. Hodgkin, A.L. and A.F. Huxley. (1952). *J. Physiol.* **117**:500–544.
42. Holmes, K.C., D. Popp, W. Gebhard, and W. Kabsch. (1990). *Nature*. **347**:44–49.
43. Jaffe, D.B., D. Johnston, N. Lasser-Ross, E. Lisman, H. Miyakawa, and W. Ross. (1992). *Nature*. **357**:244–246.
44. Jaffe, D.B., W.N. Ross, J.E. Lisman, N. Lasser-Ross, H. Miyakawa, and D. Johnston. (1994). *J. Neurophysiol.* **71**:1065–1077.
45. Janmey, P. (1998). *Physiol. Rev.* **78**:763–781.
46. Jaslove, S. (1992). *Neurosci.* **47**:495–495I499.
47. Johnson, B.D. and L. Byerly. (1993). *Neuron*:797–804.
48. Johnson, B.D. and L. Byerly. (1994). *Pflügers Arch.* **429**:14–21.
49. Johnston, D., J.C. Magee, C.M. Colbert, and B.R. Christie. (1996). *Annu. Rev. Neurosci.* **19**:165–186.
50. Johnston, D., S. Williams, D. Jaffe, and R. Gray. (1992). *Annu. Rev. Physiol.* **54**:489–505.
51. Kabsch, W., H.G. Mannherz, D. Suck, E.F. Pai, and K.C. Holmes. (1990). *Nature*. **347**:37–44.
52. Kaech, S., H. Brinkhaus, and A. Matus. (1999). *Proc. Natl. Acad. Sci. USA*. **96**:10433–10437.
53. Kaech, S., H. Parmar, M. Roelandse, C. Bornmann, and A. Matus. (2001). *Proc. Natl. Acad. Sci. USA*. **98**:7086–7092.
54. Khuchua, Z., D.F. Wozniak, M.E. Bardgett, Z. Yue, M. McDonald, J. Boero, R.E. Hartman, H. Sims, and A.W. Strauss. (2003). *Neurosci.* **119**:101–111.
55. Kiebler, M.A. and L. DesGroseillers. (2000). *Neuron*. **25**:19–28.
56. Kim, C.-H. and J.E. Lisman. (1999). *J. Neurosci.* **19**:4314–4324.
57. Knowles, R., N. LeClerc, and K.S. Kosik. (1994). *Cell Motil. Cytoskeleton*. **28**:256–264.
58. Kobayasi, S. (1964). *Biochim. Biophys. Acta*. **88**:541–552.
59. Kobayasi, S., H. Asai, and F. Oosawa. (1964). *Biochim. Biophys. Acta*. **88**:528–540.
60. Koch, C. and I. Segev. (2000). *Nature Neurosci.* **3**:1171–1177.
61. Kolosick, J.A., D.L. Landt, H.C. S. Hsuan, and K.E. Lonngren. (1974). *Proc. IEEE*. **62**:578–581.
62. Lader, A.S., H.N. Woodward, E.C. Lin, and H.F. Cantiello. (2000). In *MEMTMBS*. Faramaz, V., (ed.) CRA, Las Vegas, NV. 77–82.

63. Landis, D.M. and T.S. Reese. (1983). *J. Cell Biol.* **97**:1169–1178.
64. Lee, T., S. Marticke, C. Sung, S. Robinow, and L. Luo. (2000). *Neuron*. **28**:807–818.
65. Lester, R.J., J.D. Clements, G.L. Westbrook, and C. Jahr. (1990). *Nature*. **346**:565–567.
66. Letourneau, P.C. (1996). *Perspect Dev. Neurobiol.* **4**:111–123.
67. Letourneau, P.C. and A.H. Ressler. (1984). *J. Cell Biol.* **98**:1355–1362.
68. Liao, G., T. Nagasaki, and G.G. Gundersen. (1995). *J. Cell Sci.* **108**:3473–3483.
69. Lin, C.H., C.A. Thompson, and P. Forscher. (1994). *Curr. Opin. Neurobiol.* **4**:640–647.
70. Lin, E. and H.F. Cantiello. (1993). *Biophys. J.* **65**:1371–1378.
71. Lonngren, K.E. (1978). In *Solitons in Action*. K.E. Lonngren and A. Scott (eds.) Academic Press, New York. 127–152.
72. Lonngren, K.E., D.L. Landt, C.M. Burde, and J.A. Kolosick. (1975). *IEEE Trans. Circuits and Systems*. **CAS-22**:376–378.
73. Luo, L. (2002). *Annu. Rev. Cell Develop. Biol.* **18**:601–635.
74. Maguire, G., Connaughton, V., Prat, A.G., Jackson Jr., G.R. and H.F. Cantiello. (1998). *NeuroReport*. **9**:665–670.
75. Malenka, R. (1991). *Mol. Neurobiol.* **5**:289–295.
76. Manning, G.S. (1969). *J. Chem. Phys.* **51**:924–933.
77. Manning, G.S. (1978). *Quarterly Rev. Biophys.* **2**:179–246.
78. Matus, A. (2000). *Science*. **290**:754–758.
79. Matus, A., M. Ackermann, G. Pehling, H.R. Byers, and K. Fujiwara. (1982). *Proc. Natl. Acad. Sci. USA*. **79**:7590–7594.
80. McCulloch, W.S. and W. Pitts. (1943). *Bull. Math. Biophys.* **5**:115–133.
81. Mel, B.W. (1999). In *Dendrites*. G. Stuart, N. Spruston, and M. Häusser (eds.) Oxford University Press, Oxford.
82. Meunier, C., I. Segev, and D. Zytnicki. (1999). *J. Physiol. (Paris)*. **93**:261.
83. Miyakawa, H., W.N. Ross, D. Jaffe, J.C. Callaway, N. Laser-Ross, et al. (1992). *Neuron*. **9**:1163–1173.
84. Morales, M. and E. Fifkova. (1989). *Cell Tissue Res.* **256**:447–456.
85. Natschlger, T., W. Maass, and H. Makram. (2002). *Foundations of Information Processing of TELEMATIK (special issue)*. **8**:39–42.
86. Noguchi, A. (1974). *Elec. and Comm. in Japan*. **57-A**:9–13.
87. Noiges, R., R. Eichinger, W. Kutschera, I. Fischer, Z. Nemeth, G. Wiche, and F. Propst. (2002). *J. Neurosci.* **22**:2106–2114.
88. O’Leary, D.D.M. and S.E. Koester. (1993). *Neuron*. **10**:991–1006.
89. Oosawa, F. (1970). *Biopolymers*. **9**:677–688.
90. Oosawa, F. (1971). *Polyelectrolytes*. Marcel Dekker, Inc., New York.
91. Ostrovskii, L.A., V.V. Papko, and E.N. Pelinovskii. (1974). *Radiophysics and Quantum Electronics*. **15**:438–446.
92. Ozer, R.S. and S. Halpain. (2000). *Mol. Biol. Cell*. **11**:3573–3587.
93. Parodi, M., B. Bianco, and A. Chiabrera. (1985). *Cell Biophys.* **7**:215–235.
94. Passafaro, M., C. Sala, M. Niethammer, and M. Sheng. (1999). *Nature Neurosci.* **2**:1063–1069.
95. Pedrotti, B., R. Colombo, and K. Islam. (1994). *Biochemistry*. **33**:8798–8806.
96. Pedrotti, B. and K. Islam. (1996). *FEBS Lett.* **388**:131–133.

97. Pollard, T.D. and J.A. Cooper. (1986). *Ann. Rev. Biochem.* **55**:987–1035.
98. Tuszynski J.A., Priel, A. and Woolf, N. (2004). Submitted to *European Biophysics Journal*.
99. Rall, W. (1959). *Exp. Neurol.* **1**:491–527.
100. Rall, W. and J. Rinzel. (1973). *Biophys. J.* **13**:648–688.
101. Ramon-Moliner, E. (1968). In *The Structure and Function of Nervous Tissue*. G.H. Bourne (ed.) Academic Press, New York. 205–267.
102. Regehr, W.G., J.A. Connor, and D. Tank. (1989). *Nature*. **341**:533–536.
103. Regehr, W.G. and D. Tank. (1990). *Nature*. **345**:807–810.
104. Regehr, W.G. and D. Tank. (1992). *J. Neurosci.* **12**:4202–4223.
105. Rihn, L.L. and B. Claiborne. (1990). *Dev. Brain Res.* **54**:115–124.
106. Rochlin, M.W., K.M. Wickline, and P.C. Bridgman. (1996). *J. Neurosci.* **16**:3236–3246.
107. Rodriguez, O.C., A.W. Schaefer, C.A. Mandato, P. Forscher, W.M. Bement, and C.M. Waterman-Storer. (2003). *Nature Cell Biol.* **5**:599–609.
108. Sackett, D.L. (1995). In *Subcellular Biochemistry - Proteins: Structure, function and engineering*. B. Biswas, B. and Roy, S. (eds.) Kluwer Academic Publishers, Dordrecht. 255–302.
109. Salmon, W.C., M.C. Adams, and C.M. Waterman-Storer. (2002). *J. Cell Biol.* **158**:31–37.
110. Sanes, J.R. and J.W. Lichtman. (1999). *Annu. Rev. Neurosci.* **22**:389–342.
111. Sarmiere, P.D. and J.R. Bamburg. (2004). *J. Neurobiol.* **58**:103–117.
112. Sataric, M.V., J.A. Tuszynski, and R.B. Zakula. (1993). *Phys. Rev. E*. **48**:589–597.
113. Sattilaro, W. (1986). *Biochemistry*. **25**:2003–2009.
114. Schaefer, A.W., N. Kabir, and P. Forscher. (2002). *J. Cell Biol.* **158**:139–152.
115. Schiller, J., G. Major, H.J. Koester, and Y. Schiller. (2000). *Nature*. **404**:185–289.
116. Schwartzkroin, P.A. and M. Slawsky. (1977). *Brain Res.* **135**:157–161.
117. Scott, E.K. and L. Luo. (2001). *Nat. Neurosci.* **4**:359–365.
118. Segel, L. and H. Parnas. (1991). In *Biologically Inspired Physics*. Peliti, L. (ed.) Plenum Press, New York.
119. Segev, I. and M. London. (2000). *Science*. **290**:744–750.
120. Selden, S.C. and T. Pollard. (1983). *J. Biol. Chem.* **258**:7064–7071.
121. Sept, D., J. Xu, T. Pollard, and J. McCammon. (1999). *Biophys. J.* **77**:2911–2919.
122. Shepherd, G.M., R.K. Brayton, M.J.P., I. Segev, J. Rinzel, and W. Rall. (1985). *Proc. Natl. Acad. Sci. USA*. **82**:2192–2195.
123. Smith, C.L. (1994). *J. Cell Biol.* **127**:1407–1418.
124. Softky, W. (1994). *Neurosci.* **58**:13–41.
125. Spruston, N., D.B. Jaffe, and D. Johnston. (1994). *Trends Neurosci.* **17**:161–166.
126. Steward, O. and E.M. Schuman. (2001). *Annu. Rev. Neurosci.* **24**:299–325.
127. Tanaka, E.M. and M.W. Kirschner. (1991). *J. Cell Biol.* **115**:345–363.
128. Tang, J.X. and P.A. Janmey. (1996). *J. Biol. Chem.* **271**:8556–8563.
129. Technau, G. and M. Heisenberg. (1982). *Nature*. **295**:405–407.
130. Thorn, K.S., J.A. Ubersax, and R.D. Vale. (2000). *J. Cell Biol.* **151**:1093–1100.

131. Togel, M., G. Wiche, and F. Propst. (1998). *J. Cell Biol.* **143**:695–707.
132. Toni, N., P.A. Buchs, I. Nikonenko, C.R. Bron, and D. Muller. (1999). *Nature*. **402**:421–425.
133. Truman, J.W. and S.E. Reiss. (1976). *Science*. **192**:477–479.
134. Tuszyński, J.A., S. Portet, J.M. Dixon, C. Luxford, and H.F. Cantiello. (2004). *Biophys. J.* **86**:1890–1903.
135. Varela, J.A., K. Sen, J. Gibson, J. Fost, L.F. Abbott, and S.B. Nelson. (1997). *J. Neurosci.* **17**:7926–7940.
136. Wang, Y.L. (1985). *J. Cell Biol.* **101**:597–602.
137. Wang, Z. and M.P. Sheetz. (2000). *Biophys. J.* **78**:1955–1964.
138. Weimann, J.M., A. Zhang, M.E. Levin, W.P. Devine, P. Brulet, and S.K. McConnell. (1999). *Neuron*. **24**:819–831.
139. Wong, R.W., M. Setou, J. Teng, Y. Takei, and N. Hirokawa. (2002). *Proc. Natl. Acad. Sci. USA*. **99**:14500–14505.
140. Woolf, N.J., M.D. Zimmerman, and G.V.W. Johnson. (1999). *Brain Res.* **821**:241–249.
141. Yuste, R. and T. Bonhoeffer. (2001). *Annu. Rev. Neurosci.* **24**:1071–1089.
142. Yuste, R., M.J. Gutnick, D. Saar, K.R. Delaney, and D. Tank. (1994). *Neuron*. **13**:23–43.
143. Yvon, A.M., P. Wadsworth, and M.A. Jordan. (1999). *Mol. Biol. Cell*. **10**:947–959.
144. Zhang, W. and D.L. Benson. (2001). *J. Neurosci.* **15**:5169–5181.
145. Zimm, B.H. (1986). In *Coulombic Interactions in Macromolecular Systems*. Eisenberg, A. and Bailey, F.E. (eds.) American Chemical Society, Washington D.C.:212–215.

9 Recurrent Quantum Neural Network and its Applications

Laxmidhar Behera, Indrani Kar, and Avshalom C. Elitzur

Summary. Although the biological body consists of many individual parts or agents, our experience is holistic. We suggest that *collective response behavior* is a key feature in intelligence. A nonlinear Schrödinger wave equation is used to model collective response behavior. It is shown that such a paradigm can naturally make a model more intelligent. This aspect has been demonstrated through an application – intelligent filtering – where complex signals are denoised without any *a priori* knowledge about either signal or noise. Such a paradigm has also helped us to model eye-tracking behavior. Experimental observations such as saccadic and smooth-pursuit eye-movement behavior have been successfully predicted by this model.

9.1 Intelligence – Still Ill-Understood

Natural intelligence is what determines a normal thought process of a human. Artificial intelligence is a property of a machine that gives it the ability to mimic the human thought process. The foundational framework for intelligent computing lies in our proper understanding of mental processes. Though the term *intelligence* is still not completely defined, research in artificial intelligence has focused on five components of intelligence [35], as shown in Fig. 9.1. An intelligent system should have the abilities to understand, perceive, reason, solve problems and, moreover, learn from past experiences. The understanding of cognitive processes consists of the formulation and solution of three fundamental problems in the design of intelligent machines

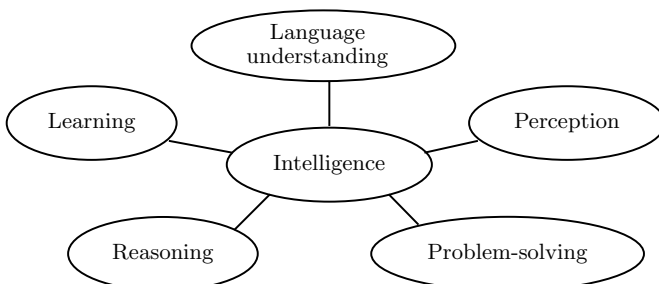


Fig. 9.1. What is intelligence? Alan Turing [35]

that “intelligently” observe, predict and interact with their surroundings. These problems are known as (i) the system-identification problem, (ii) the stochastic-filtering problem, and (iii) the adaptive-control problem.

Here we address the issue of the intelligent stochastic-filtering problem. The main question therefore is: *Can we design a method that allows us to estimate any signal embedded in noise without assuming any knowledge about the signal or noise behavior?*

Information processing in the brain is mediated by the dynamics of large, highly interconnected neuronal populations. The activity patterns exhibited by the brain are extremely rich; they include stochastic weakly correlated local firing, synchronized oscillations and bursts, and propagating waves of activity. Perception, emotion, etc., are supposed to be emergent properties of such complex nonlinear neural circuits.

Different architectures of interconnected neurons, such as feedforward and recurrent neural networks, have been explored to study global brain behavior [14, 1, 7, 8, 2]. Instead of considering one of these conventional neural architectures, an alternative neural architecture is proposed here for neural computing, namely, a recurrent quantum neural network (RQNN). This term entails that the individual neuronal response does not play a significant role when the collective behavior of a neural lattice is observed.

Population dynamics studies of “bird flocks” and “fish schools” [25] show that the individual dynamics does not play a role in group dynamics. Hence, ignoring individual neuron dynamics while considering average lattice behavior is sometimes a sound methodology. The proposed RQNN is quite different in spirit and objective from the QNN architecture available in the literature [10, 9, 32], as these QNNs synthesize a neural lattice using individual neural responses. The collective response model proposed in this chapter entails that there exists a quantum process that mediates the average behavior of a neural lattice. This collective response is described here using Schrödinger wave equation. We show that the closed-loop RQNN dynamics exhibits a soliton property. We exploit this property for stochastic filtering. The signal estimation is shown to be quite accurate. Moreover, filtering, using this approach, is done without any a priori knowledge of either signal or noise.

9.2 Intelligent Filtering – Denoising of Complex Signals

According to Bucy [13], every solution to a stochastic filtering problem involves the computation of the time-varying probability density function (pdf) on the state space of the observed system. Dawes [16, 17] proposed a novel model – a parametric avalanche stochastic filter – using this very concept. His work is the main impetus for the present work, which we hope will motivate others to explore this new approach.

For stochastic-filtering applications, we make the hypothesis that the average behavior of a neural lattice that estimates a stochastic signal is a probability density function that is mediated by a quantum process. We use the Schrödinger wave equation to track this pdf function since it is a known fact that the square of the modulus of the ψ function, the solution of this wave function, is also a pdf function. It will be explained in detail later in this chapter that the Schrödinger wave equation becomes nonlinear when its potential field is excited by a feedback signal that is a function of ψ , the state of the quantum process. It is known [11] that the nonlinear Schrödinger wave equation exhibits a soliton property, which is necessary to track nondispersing wave packets, representative of the time-varying pdf. This is a generic identity of a stochastic signal under observation.

The proposed model is an improvement over the model proposed by Dawes [17] in two respects: (i) the movement of wave packets as solitons and (ii) nonlinearly modulated spatial potential field. We also noted that it is very difficult to heuristically tune the parameters of the nonlinear Schrödinger wave equation while tracking the probability density function. This led us to make use of the evolutionary computation approach based on the univariate marginal distribution algorithm to identify these parameters in known cases of signals embedded in noise. In a recent work [6], we have shown that both Gaussian and non-Gaussian pdfs are learnt by the proposed recurrent quantum neural network (RQNN) and the signal estimation is quite accurate in the presence of a noise level up to 6 dB. The results were also compared with a classical filtering algorithm. In this work, we consider the stochastic-filtering of nonstationary signals including the speech signals. The speech-enhancement capability of the proposed RQNN is also established in real time. Thus this chapter provides a complete framework for learning a stochastic signal in terms of its probability density function.

The other important feature of our proposed model is the novelty of its application to signal processing. The popular Kalman filter assumes that the dynamic process is linear with Gaussian observation noise and the algorithm is too computationally intensive for a system of practical complexity [27]. The extended version, popularly known as EKF, makes many approximations to include nonlinear processes as well. However, in practical situations the stochastic noise can not be limited to a Gaussian or even a unimodal distribution. In contrast, the proposed RQNN estimates a signal without any a priori assumption on the shape and nature of the signal and the noise. In a nutshell, we propose a stochastic-filtering scheme that is a step forward towards intelligent filtering.

9.2.1 RQNN Architecture used for Stochastic-Filtering

The architecture of the RQNN for filtering a one-dimensional signal embedded in noise is shown in Fig. 9.2. The signal $y(t)$ is the actual signal ($y_a(t)$)

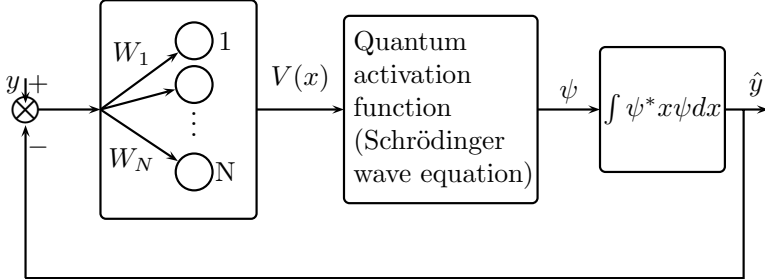


Fig. 9.2. A stochastic filter using RQNN with linear modulation

embedded in noise ($\mu(t)$), i.e. $y(t) = y_a(t) + \mu(t)$. The signal excites N neurons spatially located along the x -axis after being preprocessed by synapses. In the model the synapses are represented by time-varying synaptic weights $K(x, t)$. The unified dynamics of the one-dimensional neural lattice consisting of N neurons is described by the Schrödinger wave equation given as

$$i\hbar \frac{\partial \psi(x, t)}{\partial t} = -\frac{\hbar^2}{2m} \nabla^2 \psi(x, t) + \zeta(U(x, t) + G(|\psi|^2))\psi(x, t), \quad (9.1)$$

where $i, \hbar, \psi(x, t)$ and ∇ carry their usual meaning in the context of Schrödinger wave equation. The $\psi(x, t)$ function represents the solution of (9.1). The potential field of the Schrödinger wave equation given in (9.1) consists of two terms:

$$U(x, t) = -K(x, t)y(t), \quad (9.2)$$

$$G(|\psi|^2) = K(x, t) \int x f(x, t) dx, \quad (9.3)$$

where

$$f(x, t) = |\psi(x, t)|^2. \quad (9.4)$$

Since the potential field term in (9.1) is a function of $\psi(x, t)$, the Schrödinger wave equation that describes the stochastic filter is nonlinear. In contrast to artificial neural networks studied in the literature, in our model the neural lattice consisting of N neurons is described by the state $\psi(x, t)$ which is the solution of (9.1). Simultaneously, the model is recurrent as the dynamics consists of a feedback term $G(\cdot)$. The information about the signal is thus transferred to the potential field of the Schrödinger wave equation and the dynamics is evolved accordingly. Here we have used a linear neural circuit to set up the potential field where $K(x, t)$ s are the associated linear synaptic weights. The signal is then estimated using a maximum-likelihood estimator as

$$\hat{y}(t) = \int x f(x, t) dx. \quad (9.5)$$

When the estimate $\hat{y}(t)$ is the actual signal, then the signal that generates the potential field for the Schrödinger wave equation, $\hat{\nu}(t)$, is simply the noise that is embedded in the signal. If the statistical mean of the noise is zero, then this error-correcting signal $\hat{\nu}(t)$ has little effect on the movement of the wave packet. Precisely, it is the actual signal content in the input $y(t)$ that moves the wave packet along the desired direction that, in effect, achieves the goal of the stochastic-filtering. It is expected that the synaptic weights evolve in such a manner so as to drive the ψ function to carry the exact information of the pdf of the observed stochastic variable $y(t)$.

Learning and Estimation

The nonlinear Schrödinger wave equation given by (9.1) exhibits a soliton property, i. e. the square of $|\psi(x, t)|$ is a wave packet that moves like a particle. The importance of this property is as follows. Let the stochastic variable $y(t)$ be described by a Gaussian probability density function $f(x, t)$ with mean κ and standard deviation σ . Let the initial state of (9.1) correspond to zero mean Gaussian probability density function $f'(x, t)$ with standard deviation σ' . As the dynamics evolves with online update of the synaptic weights $K(x, t)$, the probability density function $f'(x, t)$ should ideally move toward the pdf, $f(x)$ of the signal $y(t)$. Thus the filtering problem in this new framework can be seen as the ability of the nonlinear Schrödinger wave equation to produce a wave packet solution that glides along with the time-varying pdf corresponding to the signal $y(t)$.

The synaptic weights $K(x, t)$, which is a $N \times 1$ -dimensional vector, is updated using the Hebbian learning algorithm

$$\frac{\partial K(x, t)}{\partial t} = \beta \nu(t) f(x, t), \quad (9.6)$$

where $\nu(t) = y(t) - \hat{y}(t)$. $\hat{y}(t)$ is the filtered estimate of the actual signal $y_a(t)$. We compute the filtered estimate according to (9.5). We will show later that the wave packet moves in the required direction in our new model.

9.2.2 Integration of the Schrödinger Wave Equation

The nonlinear Schrödinger wave equation is – from the mathematical point of view – a partial differential equation with two variables: x and t . In an abstract sense, receptive fields of N neurons span the entire distance along the x -axis. (9.1) is converted into the finite difference form by dividing the x -axis into N mesh points so that x and t are represented as follows:

$$x_j = j \Delta x \quad t_n = n \Delta t, \quad (9.7)$$

where j varies from $-N/2$ to $+N/2$. The finite-difference form of (9.1) is expressed as

$$\begin{aligned} i \frac{\psi(x, t + \Delta t) - \psi(x, t)}{\Delta t} = \\ - \frac{\psi(x + \Delta x, t) - 2\psi(x, t) + \psi(x - \Delta x, t)}{2m\Delta x^2} + V(x)\psi(x, t), \end{aligned} \quad (9.8)$$

where $V(x) = \zeta(U(x, t) + G(|\psi|^2))$. Here, we have assumed that $\hbar = 1$. For convenience, we represent $\psi(x_j, t_n + \Delta t)$ as ψ_j^{n+1} , $\psi(x_j, t_n)$ as ψ_j^n and $\psi(x_j - \Delta x, t_n)$ as ψ_{j-1}^n . With these representations, (9.8) reads

$$\psi_j^{n+1} = \psi_j^n + i\Delta t \frac{\psi_{j+1}^n - 2\psi_j^n + \psi_{j-1}^n}{2m\Delta x^2} - i\Delta t V_j \psi_j^n. \quad (9.9)$$

Rewriting this equation in a matrix form one gets

$$F^{n+1} = F^n - i\Delta t H' F^n, \quad (9.10)$$

where the Hamiltonian H' is defined as

$$H' = -\frac{\hbar^2}{2m} \frac{d^2}{dx^2} + V(x). \quad (9.11)$$

Subsequently,

$$F^{n+1} = UF^n \quad \text{where } U = I - i\Delta t H'. \quad (9.12)$$

Since it is required that the norm of F is $F^*F = 1$, U must be an orthonormal operator. Since U in (9.12) does not have such a property, in our simulation we impose the normalization after every step.

Selection of Parameters

The nonlinear equation (9.1) involves four external parameters: \hbar , m , ζ and β . The last parameter β is necessary to update the synaptic weight vector $K(x, t)$. For simplicity, the parameter \hbar is taken as unity and the other three parameters are tuned accordingly. Looking at the complexity of (9.1), we used a genetic algorithm (GA) based on the concept of the univariate marginal distribution algorithm (UMDA) [5, 29] to select near-optimal parameters. The details of the algorithm and its implementation are as follows:

The univariate marginal distribution algorithm estimates the distribution of gene frequencies using a mean-field approximation. Each string in the population is represented by a binary vector \mathbf{x} . The algorithm generates new points according to the following distribution:

$$p(\mathbf{x}, t) = \prod_{i=1}^n p_i^s(x_i, t). \quad (9.13)$$

The UMDA algorithm is given as follows:

- Step 1: Set $t = 1$, Generate $N(>> 0)$ binary strings randomly.
- Step 2: Select $M < N$ strings according to a selection method.
- Step 3: Compute the marginal frequencies $p_i^s(x_i, t)$ from the selected strings.
- Step 4: Generate N new points according to the distribution

$$p(\mathbf{x}, t) = \prod_{i=1}^n p_i^s(x_i, t).$$

- Set $t = t + 1$. If the termination criteria are not met, go to Step 2.

For infinite populations and proportionate selection, it has been shown [29] that the average fitness never decreases for the maximization problem (increases for the minimization problem).

In general, GA provided the parameter values where $m < 1, \beta < 1$ and $\zeta >> 1$. The significance of this finding can be understood in the following manner. Since β was the learning parameter in the Hebbian learning, it is natural to expect that $\beta < 1$. The less than unity value for m makes self-excitation larger. Similarly, a large value of ζ causes a larger input excitation since it appears as a multiplicand in the Schrödinger equation.

9.2.3 Simulation Results I

The proposed RQNN has been successfully applied to denoising of various signals like dc signals, sinusoids, shifted sinusoids, amplitude-modulated sine and square waves, speech signals, embedded in high Gaussian or non-Gaussian noise. Some selected results are presented in this section.

Amplitude - Modulated Sine and Square Waves

Amplitude-modulated and frequency-modulated signals are normally used in coding and transmission of data and appear corrupted at the receiver's end by channel noise [23]. For simulation purpose, we have selected the frequency of the carrier signal to be a sinusoid of frequency 5 Hz, although in reality they are very high frequency signals. The amplitude was modulated by superimposing a triangular variation of frequency 0.5 Hz. Thus the expression for the composite signal $y_a(t)$ is

$$y_a(t) = a(t) \cdot \sin(2\pi 5t); \quad a(t) = \begin{cases} 1.5t & 0 \leq t \leq 1 \\ 1.5(2-t) & 1 \leq t \leq 2, \end{cases} \quad (9.14)$$

where $a(t)$ is periodic with period 0.5 Hz. A similar strategy is applied in generating the amplitude modulated square wave, i.e., the amplitude of $a(t)$ is kept constant over every single period of the carrier sine wave in (9.14).

The expression for the actual signal $y_a(t)$ in this case is given below:

$$y_a(t) = \begin{cases} a(t) & 0 \leq t \leq 0.1 \\ -a(t) & 0.1 \leq t \leq 0.2 \end{cases} \quad \text{and} \quad a(t) = \begin{cases} 1.5t & 0 \leq t \leq 1 \\ 1.5(2-t) & 1 \leq t \leq 2 \end{cases}, \quad (9.15)$$

where $a(t)$ is periodic with period 0.5 Hz.

The amplitude-modulated sinusoid signal $y_a(t)$ in (9.14) was immersed in Gaussian noise. The variance of the Gaussian noise was set according to the 20 dB and 6 dB SNR measurement. The values selected for the parameters of the Schrödinger wave equation using UMDA are as follows:

$$\beta = 0.11 \quad m = 0.015 \quad \zeta = 84.31 \quad \hbar = 1.0. \quad (9.16)$$

The number of neurons along the x -axis are taken as $N = 400$. The parameters for the finite-difference equation used for integration are selected as

$$\Delta x = 0.1 \quad \Delta t = 0.001. \quad (9.17)$$

The parameter γ is selected as 100. The tracking of the desired signal $y_a(t)$ is shown in Fig. 9.3. It can be observed that the tracking is very smooth and accurate. Snapshots of wave packets are shown in the same figure corresponding to marker points shown in the left plot. It can be observed that the pdf does not split, sliding along the x -axis back and forth like a particle. Next, the amplitude-modulated square wave $y_a(t)$ in (9.15) is immersed in Gaussian noise. The variance of the Gaussian noise was set according to the 20 dB and 6 dB noise power with the instantaneous period amplitude of $y_a(t)$

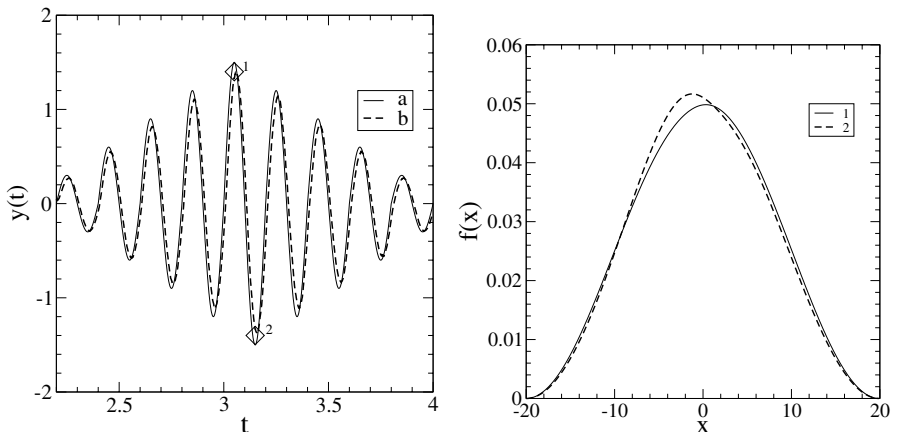


Fig. 9.3. (left) Tracking of amplitude-modulated sinusoid signal embedded in 20 dB Gaussian noise: “a” represents the actual signal and “b” represents the tracking by the RQNN; (right) Snapshots of wave packets corresponding to marker points are shown in the left plot

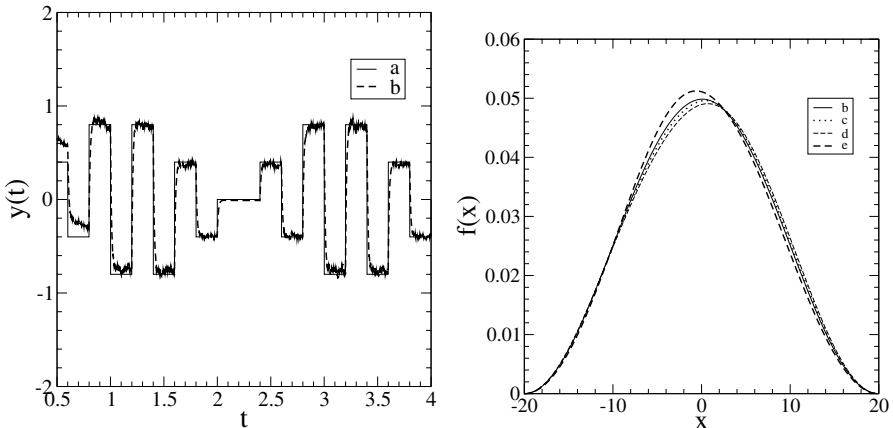


Fig. 9.4. (left) Tracking of amplitude-modulated square wave embedded in 20 dB Gaussian noise: “a” represents the actual signal and “b” represents the tracking by the RQNN. (right) Snapshots of wave packets: wave packet “b” at $t = 2.1\text{ s}$, the wave packet “c” at $t = 2.5\text{ s}$, wave packet “d” at $t = 2.9\text{ s}$ and the wave packet “e” at $t = 3.1\text{ s}$

as reference. The values selected for the parameters of the Schrödinger wave equation using UMDA are as follows:

$$\beta = 0.11 \quad m = 0.015 \quad \zeta = 84.31 \quad \hbar = 1.0. \quad (9.18)$$

This shows that the parameter γ influences the speed of response of the RQNN filter. The number of neurons along the x -axis is taken as $N = 400$. The parameters for the finite-difference equation used for integration are selected as

$$\Delta x = 0.1 \quad \Delta t = 0.001. \quad (9.19)$$

The tracking of the desired signal $y_a(t)$ and the movement of the wave packets are shown in Fig. 9.4. It can be observed that the tracking is accurate.

The pdf of the desired signal as estimated by the RQNN clearly exhibits a soliton property Fig. 9.4. The pdf does not split and slides along the x -axis like a particle.

Speech Signals

Speech signals are degraded in many ways that limit their effectiveness for communication. One major source of noise in the speech signal is *channel noise* that is a major concern, especially in speech-recognition systems. Since the RQNN estimates the pdf of the incoming signal at every instant, if the incoming signal is corrupted by zero-mean noise, then the RQNN must be able to filter out that noise. Working on this hypothesis, we added zero-mean Gaussian noise with variance equal to the square of the instantaneous

amplitude of the speech signal. The peak amplitude of the speech signal was normalized to 1.0. The original speech signals are recorded spoken digit utterances taken from the Release 1.0 of the Number Corpus. This corpus is distributed by the Center of Spoken Language Understanding of the Oregon Graduate Institute. The speech file names are mentioned in the captions, along with the respective plots for each of the speech signals.

For tracking the speech signals, the number of neurons along the x -axis is taken as $N = 400$. The parameters for the finite-difference equation used for integration are selected as

$$\Delta x = 0.1 \quad \Delta t = 0.001. \quad (9.20)$$

The values selected for the parameters of the Schrödinger wave equation using UMDA are as follows:

$$\beta = 0.16 \quad m = 0.015 \quad \zeta = 27.45 \quad \hbar = 1.0. \quad (9.21)$$

The parameter γ was selected as 800. The tracking for a particular period of the speech signals selected from the database are shown in Figs. 9.5 and 9.6. The snapshots of the wave packet at two time instants are also shown. It is evident from Figs. 9.5 and 9.6 that the RQNN does track the pdf of the input signal at every instant. The wave packet does not split and it maintains an approximate Gaussian nature. It moves slightly along the x -axis like a particle maintaining its soliton property. By estimating the actual signal as the mean of the pdf at every instant, we can filter out the corrupting noise added to the actual signal. In addition, we reconverted the tracked speech signal and the noisy speech signal to the WAV format. On listening to these signals, we

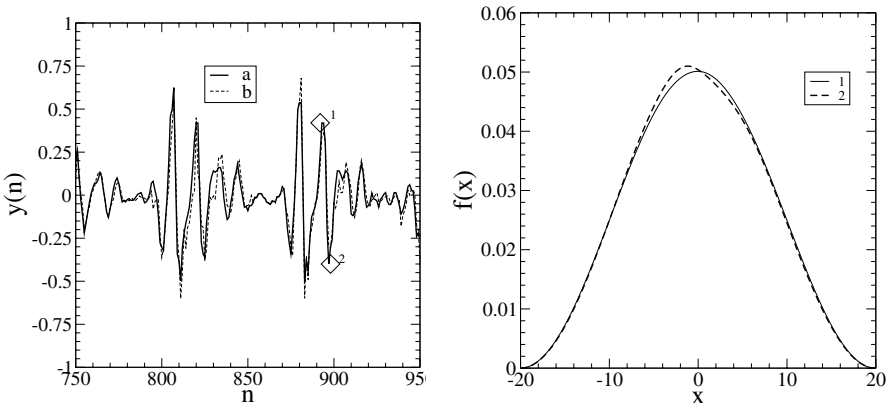


Fig. 9.5. Speech file NU_24streetaddr.wav: (*left*) Filtering of speech signal immersed in Gaussian noise: “a” represents the actual speech signal and “b” represents the tracking by the RQNN; (*right*) Snapshots of wave packets at marker points (1,2) shown in the *left* plot

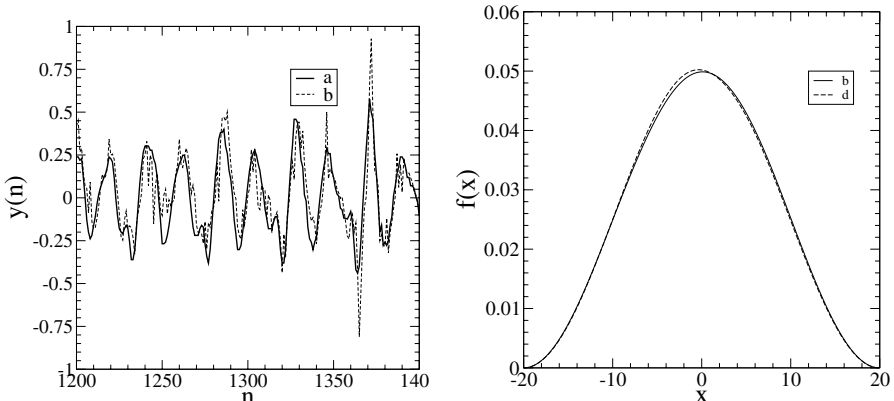


Fig. 9.6. (left) Filtering of speech signal immersed in Gaussian noise: “a” represents the actual speech signal and “b” represents the tracking by the RQNN. The x -axis represents the sample number n of the speech signal. (right) Movement of the wave packet: wave packet “b” at $t = 1.35$ s and wave packet “d” at $t = 1.45$ s

could verify that the RQNN filtering does improve the quality of the input noisy speech signal if corrupted by zero-mean Gaussian noise.

9.3 A Comprehensive Quantum Model of Intelligent Behavior

Biological organisms perform many complex tasks with ease. Although we may have supercomputers that have reached the level of computing power beyond our imagination, some of the tasks we perform, such as pattern recognition and language understanding, are still beyond the reach of such supercomputers. Can quantum-mechanical models better account for such complex behavior in biological organisms? The rest of this chapter is devoted to this question. We propose a theoretical quantum brain model to explain human eye movement behavior, where the same collective response attribute of natural intelligence plays the key role. While simulating the quantum brain model, two very interesting phenomena are observed. First, as eye-sensor data is processed in a classical brain, a wave packet is triggered in the quantum brain. This wave packet moves like a particle. Secondly, when the eye tracks a fixed target, this wave packet moves not in a continuous but rather in a discrete mode. This result reminds one of the saccadic movements of the eye consisting of “jumps” and “rests”. However, such a saccadic movement is intertwined with smooth-pursuit movements when the eye has to track a dynamic trajectory. In this sense, the proposed quantum brain concept is very successful in explaining the nature of eye movements that also accord with the experimental observations.

9.4 RQNN-based Eye-Tracking Model

There are certain aspects of brain functions that still appear to have no satisfactory explanation. As an alternative, researchers [36, 37, 21, 28] are investigating whether the brain can demonstrate quantum-mechanical behavior. According to a current hypothesis, microtubules, the basic components of neural cytoskeleton, are very likely to possess quantum-mechanical properties due to their size and structure. The tubulin protein, which is the structural block of microtubules, has the ability to flip from one conformation to another as a result of a shift in the electron-density localization from one resonance orbital to another. These two conformations act as two basis states of the system according to whether the electrons inside the tubulin hydrophobic pocket are localized closer to α or β tubulin. Moreover, the system can lie in a superposition of these two basis states, that is, being in both states simultaneously, which can give a plausible mechanism for creating a coherent state in the brain. Penrose [30] therefore argued that the human brain must utilize quantum-mechanical effects when demonstrating problem solving feats that cannot be explained algorithmically.

In this chapter, instead of going into the biological details of the brain, we propose a theoretical quantum brain model using the RQNN. The RQNN model proposed in Sect. 9.2.1 has been modified a little to cope with the present application. Instead of using a linear neural circuit to set up the potential field in which the quantum brain is dynamically excited, the present model uses a nonlinear neural circuit. This fundamental change in the architecture has yielded two novel features. The wave packets, $f(x, t) = |\psi(x, t)|^2$, are moving like particles. Here $\psi(x, t)$ is the solution of the nonlinear Schrödinger wave equation that describes the proposed quantum brain model to explain eye movements for tracking moving targets. The other very interesting observation is that the movements of the wave packets, while tracking a fixed target, are not continuous but discrete. These observations accord with the well-known saccadic movement of the eye [3, 18]. In a way, our model is the first of its kind to explain the nature of eye movements in static scenes that consists of “jumps” (saccades) and “rests” (fixations). We expect this result to inspire other researchers to further investigate the possible quantum dynamics of the brain.

9.4.1 A Theoretical Quantum Brain Model

An impetus to hypothesize a quantum brain model comes from the brain’s necessity to unify the neuronal response into a single percept. Anatomical, neurophysiological and neuropsychological evidences, as well as brain imaging using fMRI and PET scans, show that separate functional MAPs exist in the brain to code separate features such as direction of motion, location, color and orientation. How does the brain compute all these data to have a coherent perception? Here, a very simple model of a quantum brain is proposed, where

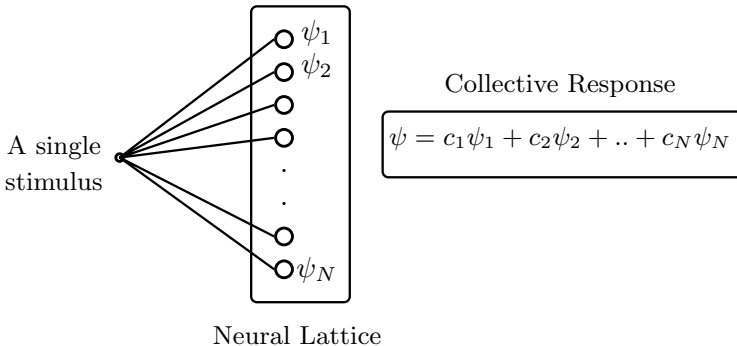


Fig. 9.7. Quantum brain – a theoretical model

a collective response of a neuronal lattice is modeled using a Schrödinger wave equation as shown in Fig. 9.7.

In this figure, it is shown that an external stimulus reaches each neuron in a lattice with a probability amplitude function ψ_i . This hypothesis suggests that the carrier of the stimulus performs quantum computation. The collective response of all the neurons is given by the superposition

$$\psi = c_1\psi_1 + c_2\psi_2 + \dots + c_N\psi_N = \sum_{i=1}^N c_i\psi_i. \quad (9.22)$$

We suggest that the time evolution of the collective response ψ is described by the Schrödinger wave equation

$$i\hbar \frac{\partial \psi(x, t)}{\partial t} = -\frac{\hbar^2}{2m} \nabla^2 \psi(x, t) + V(x)\psi(x, t), \quad (9.23)$$

where $2\pi\hbar$ is Planck's constant, $\psi(x, t)$ is the wave function (probability amplitude) associated with the quantum object at space-time point (x, t) , and m the mass of the quantum object. Further symbols such as i and ∇ carry their usual meaning in the context of the Schrödinger wave equation. Another way to look at our proposed quantum brain is as follows. A neuronal lattice sets up a spatial potential field $V(x)$. A quantum process described by a quantum state ψ , which mediates the collective response of a neuronal lattice, evolves in the spatial potential field $V(x)$ according to (9.23). Thus the classical brain sets up a spatiotemporal potential field, while the quantum brain is excited by this potential field to provide a collective response.

9.4.2 An Eye–Tracking Model using RQNN with Nonlinear Modulation of Potential Field

In this section we present an extension of RQNN, briefly described in the previous section. Here, the potential field of the Schrödinger wave equation is

modulated using a nonlinear neural circuit that results in a much pronounced soliton behavior of the wave packet. With this modification we now provide a plausible biological mechanism for eye tracking using the quantum brain model proposed in Sect. 9.4.1. The mechanism of eye movements, tracking a moving target consists of three stages as shown in Fig. 9.8: (i) stochastic-filtering of noisy data that impact the eye sensors; (ii) a predictor that predicts the next spatial position of the moving target; and (iii) a biological motor control system that aligns the eye pupil along the moving targets trajectory. The biological eye sensor fans out the input signal y to a specific neural lattice in the visual cortex. For clarity, Fig. 9.8 shows a one-dimensional array of neurons whose receptive fields are excited by the signal input y reaching each neuron through a synaptic connection described by a nonlinear MAP. The neural lattice responds to the stimulus by setting up a spatial potential field, $V(x, t)$, which is a function of external stimulus y and estimated trajectory \hat{y} of the moving target:

$$V(x, t) = \sum_{i=1}^n W_i(x, t)\phi_i(\nu(t)), \quad (9.24)$$

where $\phi_i(\cdot)$ is a Gaussian kernel function, n represents the number of such Gaussian functions describing the nonlinear MAP that represents the synaptic connections, $\nu(t)$ represents the difference between y and \hat{y} and W represents the synaptic weights as shown in Fig. 9.8. The Gaussian kernel function is taken as

$$\phi_i(\nu(t)) = \exp(-(\nu(t) - g_i)^2), \quad (9.25)$$

where g_i is the center of the i -th Gaussian function, ϕ_i . This center is chosen from input space described by the input signal, $\nu(t)$, through uniform random sampling.

Our quantum-brain model proposes that a quantum process mediates the collective response of this neuronal lattice that sets up a spatial potential field $V(x, t)$. This happens when the quantum state associated with this quantum

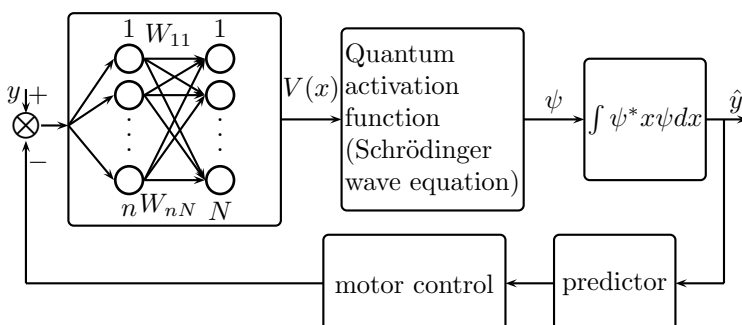


Fig. 9.8. Eye tracking-model using RQNN

process evolves in this potential field. The spatiotemporal evolution follows as per (9.23). We hypothesize that this collective response is described by a wave packet, $f(x, t) = |\psi(x, t)|^2$, where the term $\psi(x, t)$ represents a quantum state. In a generic sense, we assume that a classical stimulus in a brain triggers a wave packet in the counterpart “quantum brain”. This subjective response, $f(x, t)$, is quantified using the following estimate equation:

$$\hat{y}(t) = \int x(t)f(x, t)dx. \quad (9.26)$$

The estimate equation is motivated by the fact that the wave packet, $f(x, t) = |\psi(x, t)|^2$ is interpreted as the probability density function. Although computation of (9.26) using the nonlinear Schrödinger wave equation is straightforward, we hypothesize that this computation can be done through an interaction between a quantum and a classical brain, using a suitable quantum measurement operator. At this point we will not speculate about the nature of such a quantum measurement operator that will estimate the ψ function necessary to compute (9.26). Based on this estimate, \hat{y} , the predictor estimates the next spatial position of the moving target. To simplify our analysis, the predictor is made silent. Thus its output is the same as that of \hat{y} . The biological motor control is commanded to fixate the eye pupil to align with the target position, which is predicted to be at \hat{y} . Obviously, we have assumed that biological motor control is ideal.

After the above-mentioned simplification, the closed form dynamics of the model described by Fig. 9.8 becomes

$$i\hbar \frac{\partial \psi(x, t)}{\partial t} = -\frac{\hbar^2}{2m} \nabla^2 \psi(x, t) + \zeta G \left(y(t) - \int x |\psi(x, t)|^2 dx \right) \psi(x, t), \quad (9.27)$$

where $G(\cdot)$ is a Gaussian kernel MAP introduced to nonlinearly modulate the spatial potential field that excites the dynamics of the quantum object. In fact, $\zeta G(\cdot) = V(x, t)$, where $V(x, t)$ is given in (9.24).

The nonlinear Schrödinger wave equation given by (9.27) is one-dimensional with cubic nonlinearity. Interestingly, the closed-form dynamics of the recurrent quantum neural network (equation (9.27)) closely resembles a nonlinear Schrödinger wave equation with cubic nonlinearity studied in quantum electrodynamics [20]:

$$i\hbar \frac{\partial \psi(x, t)}{\partial t} = \left(-\frac{\hbar^2}{2m} \nabla^2 - \frac{e^2}{r} \right) \psi(x, t) + e^2 \int \frac{\psi(x, t) |\psi(x', t)|^2}{|x - x'|} dx', \quad (9.28)$$

where m is the electron mass, e the elementary charge and r the magnitude of $|x|$. Also, nonlinear Schrödinger wave equations with cubic nonlinearity of the form $\frac{\partial}{\partial t} \mathcal{A}(t) = c_1 \mathcal{A} + c_3 |\mathcal{A}|^2 \mathcal{A}$, where c_1 and c_3 are constants, frequently appear in nonlinear optics [12] and in the study of solitons [24, 11, 15, 33]. Application of the nonlinear Schrödinger wave equation for the study of quantum systems can also be found in [34].

In (9.27), the unknown parameters are weights $W_i(x, t)$ associated with the Gaussian kernel, mass m , and ζ , the scaling factor to actuate the spatial potential field. The weights are updated using the Hebbian learning algorithm

$$\frac{\partial W_i(x, t)}{\partial t} = \beta \phi_i(\nu(t)) f(x, t), \quad (9.29)$$

where $\nu(t) = y(t) - \hat{y}(t)$.

The idea behind the proposed quantum computing model is as follows. As an individual observes a moving target, the uncertain spatial position of the moving target triggers a wave packet within the quantum brain. The quantum brain is so hypothesized that this wave packet turns out to be a collective response of a classical neural lattice. As we combine (9.27) and (9.29), it is desired that there exist some parameters m , ζ and β such that each specific spatial position $x(t)$ triggers a unique wave packet, $f(x, t) = |\psi(x, t)|^2$, in the quantum brain. This brings us to the question of whether the closed form dynamics can exhibit soliton properties that are desirable for target tracking. As pointed out above, our equation has a form that is known to possess soliton properties for a certain range of parameters and we just have to find those parameters for each specific problem.

We would like to reiterate the importance of the soliton properties. According to our model, eye tracking means tracking of a wave packet in the domain of the quantum brain. The biological motor control aligns the eye pupil along the spatial position of the external target that the eye tracks. As the eye sensor receives data y from this position, the resulting error stimulates the quantum brain. In a noisy background, if the tracking is accurate, then this error-correcting signal $\nu(t)$ has little effect on the movement of the wave packet. Precisely, it is the actual signal content in the input $y(t)$ that moves the wave packet along the desired direction that, in effect, achieves the goal of the stochastic filtering part of the eye movement for tracking purposes.

9.4.3 Simulation Results II

In this section we present simulation results to test target tracking through eye movement where targets are either fixed or moving.

For fixed target tracking, we have simulated a stochastic-filtering problem of a dc signal embedded in Gaussian noise. As the eye tracks a fixed target, the corresponding dc signal is taken as $y_a(t) = 2.0$, embedded in Gaussian noise with SNR (signal-to-noise ratio) values of 20 dB, 6 dB and 0 dB.

We next compared the results with the performance of a Kalman filter [19] designed for this purpose. It should be noted that the operation of the Kalman filter is based on a priori information that the embedded signal is a dc signal, whereas the RQNN is not provided with this information. The Kalman filter also makes use of the fact that the noise is Gaussian and estimates the variance of the noise based on this assumption. Thus it is expected

that the performance of the Kalman filter will degrade as the noise becomes non-Gaussian. In contrast, the RQNN model does not make any assumption about the noise.

Notice that there are certain values of β , m , ζ and N for which the model performs optimally. A univariate marginal distribution algorithm was used to get near optimal parameters while fixing $N = 400$ and $\hbar = 1.0$. The selected values of these parameters are as follows for all levels of SNR:

$$\beta = 0.86; \quad m = 2.5; \quad \zeta = 2000. \quad (9.30)$$

The comparative performance of eye tracking in terms of rms error for all the noise levels is shown in Table 9.1. It is easily seen from Table 9.1 that the rms tracking error of RQNN is much less than that of the Kalman filter. Moreover, RQNN performs equally well for all the three categories of noise levels, whereas the performance of the Kalman filter degrades with the increase in noise level. In this sense we can say that our model performs the tracking with a greater efficiency compared to the Kalman filter. The exact nature of trajectory tracking is shown for 0 dB SNR in Fig. 9.9. In this figure, the noise envelope is shown, and obviously its size is large due to a high noise content in the signal. The figure shows the trajectory of the eye movement as the eye focuses on a fixed target.

To better appreciate the tracking performance, an error plot is shown in Fig. 9.10. Although Kalman-filter tracking is continuous, the RQNN model tracking consists of “jumps” and “fixations”. As the alignment of the eye pupil becomes closer to the target position, the “fixation” time also increases. Similar tracking behavior was also observed for the SNR values of 20 and 6 dB.

These theoretical results are very interesting when compared to experimental results in the field of eye-tracking. In eye-tracking experiments, it is known that eye movements in static scenes are not performed continuously, but consist of “jumps” (saccades) and “rests” (fixations). Eye-tracking results are represented as lists of fixation data. Furthermore, if the information is simple or familiar, eye movement is comparatively smooth. If it is tricky or new, the eye might pause or even flip back and forth between images. Similar results are given by our simulations. Our model tracks the dc signal that can be thought of as equivalent to a static scene, in discrete steps rather than in

Table 9.1. Performance comparison between Kalman filter and RQNN for various levels of Gaussian noise

Noise level in dB	RMS error for Kalman filter	RMS error for RQNN
20	0.0018	0.000040
6	0.0270	0.000062
0	0.0880	0.000090

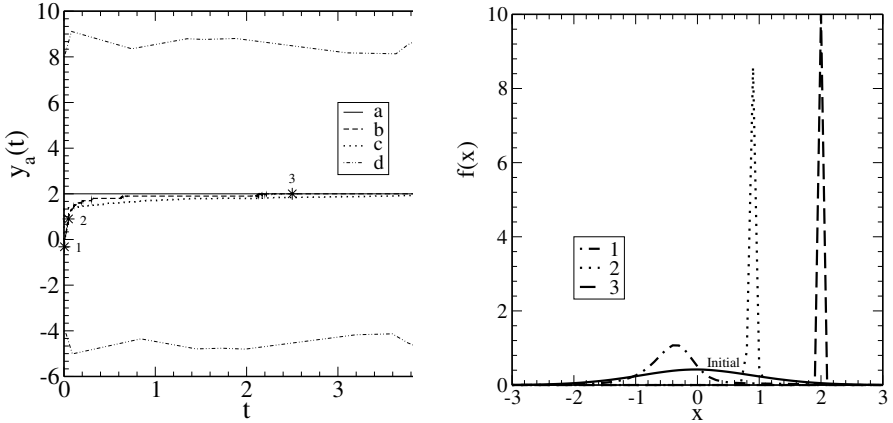


Fig. 9.9. (left) Eye tracking of a fixed target in a noisy environment of 0 dB SNR: “a” represents fixed target, “b” represents target tracking using RQNN model and “c” represents target tracking using a Kalman filter. The noise envelope is represented by the curve “d”; (right) The snapshots of the wave packets at different instances corresponding to the marker points (1,2,3) as shown in the *left figure*. The solid line represent the initial wave packet assigned to the Schrödinger wave equation

a continuous fashion. This is very clearly understood from the tracking error in Fig. 9.10.

The other interesting aspect of the results is the movement of wave packets. It is observed that these wave packets move in discrete steps, i.e. the movement is not continuous. In Fig. 9.9 (*right*), snapshots of wave packets

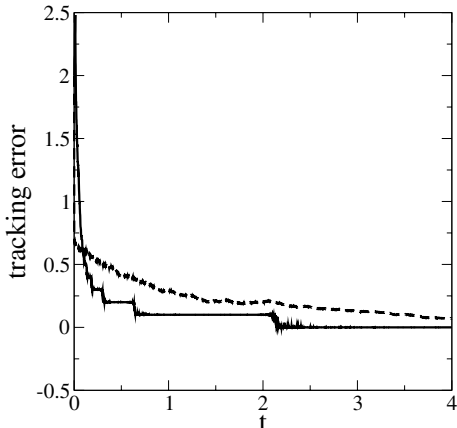


Fig. 9.10. The continuous line represents the tracking error using RQNN model, while the broken line represents the tracking error using a Kalman filter

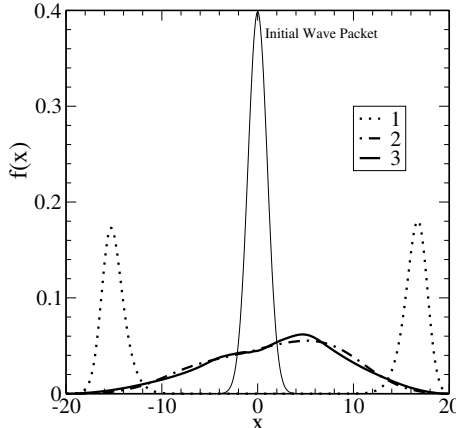


Fig. 9.11. Wave-packet movements for RQNN with linear weights

are plotted at different instances corresponding to marker points as shown along the desired trajectory. It can be noticed that a very flat initial Gaussian wave packet first moves to the left, and then proceeds toward the right until the mean of the wave packet exactly matches the actual spatial position. A similar pattern of movement of wave packets was also noticed in the case of 20 and 6 dB SNR. The wave-packet movement is compared with the same, when instead of nonlinear modulation of the potential field, we use a linear modulation as described in Sect. 9.2.1 in Fig. 9.11. The initial wave packet in the previous model first splits into two parts, then moves in a continuous fashion, ultimately going into a state with a mean of approximately 2 but with high variance. In contrast, in the present model there is no splitting of the wave packet, movement is discrete and variance is also much smaller. Thus the soliton behavior of the present model is highly pronounced.

To analyze the eye movement following a moving target, a sinusoidal signal $y_a(t) = 2\sin 2\pi 10t$ is taken as the desired dynamic trajectory. This signal is embedded in 20 dB Gaussian noise. The parameter values for tracking this signal were fixed at $\beta = 0.01$, $m = 1.75$ and $\zeta = -250$. It is observed that during the training phase, the wave packet jumps from time to time, thus changing the tracking error in steps until a steady-state trajectory following is achieved.

This feature can be better understood from the tracking-error plot that is shown in Fig. 9.12. In this figure we have plotted the tracking error between the actual sinusoidal signal and the predicted signal using the estimate (9.26). It is clearly seen that in the first stage of tracking, the error is fluctuating very frequently between its local maximum and minimum values in the negative region. Then this fluctuation settles down in the second stage. In the third stage this fluctuation starts again and the error is flipping between the local maxima and minima in the positive region. As the estimation (see (9.26)) of

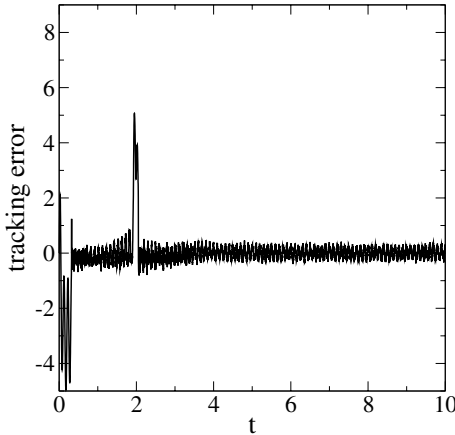


Fig. 9.12. Saccadic and pursuit movement of eye during dynamic trajectory following

the signal is very much dependent on the nature of the wave packet, the error dynamics is also correlated with the wave-packet movement. Discontinuities in error are reflected in the movement of the wave packet. It is obvious that the position of the wave packet is changing very frequently in the first stage, thus changing the mean value correspondingly, and it has no connection with the signal mean value. This means that there are a number of discontinuities or “jumps” in the wave-packet movement in the first stage. Then, in the second stage the movement becomes continuous with the mean values following the signal mean values. Again in the third stage the discontinuities take place several times, ultimately achieving a steady-state movement in the last stage.

Once a steady state is achieved, the tracking is efficient and the wave-packet movement is continuous, as shown in Fig. 9.13. In this figure, the snapshots of wave packets are plotted for three different instances of time indicated by the marker points (1,2,3) as shown in the trajectory tracking. When the signal is at position 1, the corresponding wave packet has a mean at 0. When the signal is at position 2, the corresponding wave packet has a mean at +2, and the mean of the wave packet moves to -2 when the signal goes to position 3. As seen in Fig. 9.13, during the continuous movement of the wave packets, trajectory tracking is smooth, which is similar to smooth-pursuit movement of biological eye tracking. Smooth pursuit is the eye movement that smoothly tracks slowly moving targets in the visual field. The purpose of smooth pursuit is partly to stabilize moving targets on the retina. It is a much slower movement than saccades. Eye-tracking experiments reveal that when pursuing a moving target, the smooth eye movements generally have a gain less than unity. The errors introduced by this are corrected by saccades that bring the target back on the fovea. Thus after one or two quick saccades to capture the target, the eye movement attains a steady-state velocity that

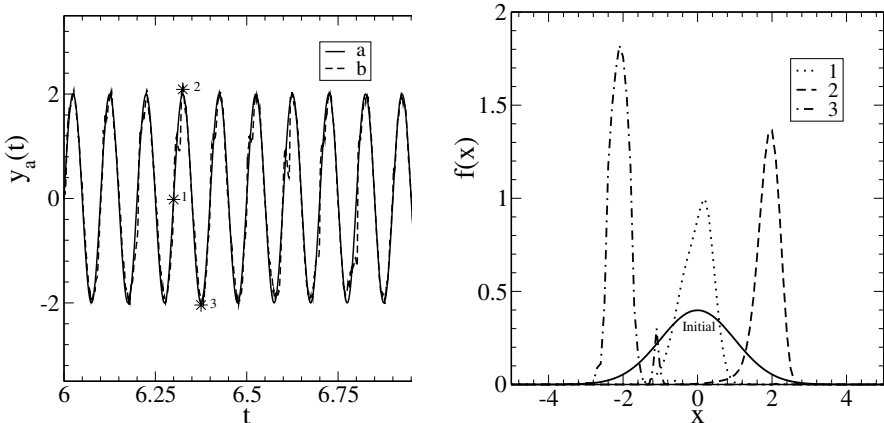


Fig. 9.13. (left) Eye tracking of a moving target in a noisy environment of 20 dB SNR: “a” represents a moving target, “b” represents target tracking using RQNN model; (right) The snapshots of the wave packets at different instances corresponding to the marker points (1,2,3) are shown in the figure. The solid line represents the initial wave packet assigned to the Schrödinger wave equation

matches the velocity of the target. In other words, during visual tracking of a moving object, saccadic and smooth-pursuit eye movements combine to keep the target image close to the fovea [26, 31]. This kind of movement is also called dual-mode tracking [4]. This experimental result completely agrees with the obeservation when our theoretical model tracks a smoothly varying trajectory.

9.5 Concluding Remarks

We presented an alternative neural information-processing architecture where a quantum process mediates the collective response of a neural lattice having spatial structure. The key feature of this model is *collective response behavior* that is identified as an attribute of intelligent behavior. The proposed RQNN is governed by a single-dimensional nonlinear Schrödinger wave equation. The nonlinear Schrödinger wave equation that emerged due to recurrent structure of the network exhibits soliton property – a property that defines the particle type of movement of the wave packet. Two types of RQNN-based applications have been considered here. The first application makes a model naturally more intelligent. In this application, complex signals such as amplitude-modulated signals and speech signals are denoised without making any assumption about the signal and noise as well. In contrast, all prevalent techniques use a priori information about the signal and noise before signals can be denoised.

The second application is a quantum brain model of eye tracking. The key concept here is that quantum-based models can be more predictive to explain complex biological phenomena such as eye-movement behavior. The interesting finding is that our theoretical model of eye tracking agrees with previously observed experimental results. The model predicts that eye movements will be of saccadic type while following a static trajectory. In the case of a dynamic trajectory, the eye movement consists of saccades and smooth pursuits. In this sense, the proposed quantum brain concept is very successful in explaining the nature of eye movements. Earlier explanations [3] for saccadic movement have been primarily attributed to a motor control mechanism, whereas the present model emphasizes that such eye movements are due to a decision-making process of the brain – albeit a quantum brain. Thus the contribution of this chapter for the explanation of biological eye movement as a neural information-processing event may inspire researchers to study quantum brain models from the biological perspective.

The other significant contribution is the prediction efficiency of the proposed model over the prevailing model. The stochastic-filtering of a dc signal using RQNN is 1000 times more accurate compared to a Kalman filter.

At this point we are silent about the exact biological connection between the classical and the quantum brain, as it is not clear to us. The model just assumes that the quantum brain is excited by the potential field set up by the classical brain. Another obvious question is that of decoherence. In this regard, we admit that the model proposed here is highly idealized since we have used the Schrödinger wave equation. In our future work we intend to replace the Schrödinger wave equation by a density matrix approach. Also, the phase-transition analysis of closed form dynamics, given in (9.27) with respect to various parameters m, ζ, β and N , has been kept for future work.

Finally, we believe that apart from the computational power derived from quantum computing, quantum learning systems may also provide a potent framework to study the subjective aspects of the nervous system [22]. The challenge to bridge the gap between physical and mental (or objective and subjective) aspects of matter may be most successfully met within the framework of quantum learning systems. In this framework, we have proposed a notion of a quantum brain, and a recurrent quantum neural network has been hypothesized as a first step towards a neural computing model.

References

1. Amari, S. (1983). *IEEE Trans SMC*, **SMC-13(5)**:741–748.
2. Amit, D.J. (1989). *Modeling Brain Function*. Springer-Verlag, Berlin/Heidelberg.
3. Bahill, A.T. and Stark, L. (1979). *Scientific American* **240**:84–93.
4. Bahill, A.T., Iandolo, M.J., and Troost, B.T. (1980). *Vision Research*, **20**:923–931.

5. Behera, L. (2002). *New Optimization Techniques in Engineering*, chapter Parametric Optimization of a Fuzzy Logic Controller for Nonlinear Dynamical Systems using Evolutionary Computation. McGraw-Hill. New York.
6. Behera, L. and Sundaram, B. (2004). *Proceedings, International Conference on Intelligent Sensors and Information Processing*.
7. Behera, L., Gopal, M., and Chaudhury, S. (1996). *IEEE Trans Neural Networks*, **7(6)**:1401–1414.
8. Behera, L., Chaudhury, S., and Gopal, M. (1998). *IEE Proceedings Control Theory and Applications*, **145(2)**:134–140.
9. Behrman, E.C., Chandrashekhar, V., Wang, Z., Belur, C.K., Steck, J.E., and Skinner, S.R. (2002). *Physical Review Letters*. Submitted.
10. Behrman, E.C., Nash, L.R., Steck, J.E., Chandrashekhar, V.G., and Skinner, S.R. (2000). *Information Sciences*, **128(3–4)**:257–269.
11. Bialynicki-Birula, I. and Mycielski, J. (1976). *Annals of Physics*, **100**:62–93.
12. Boyd, R.W. (1991). *Nonlinear Optics*. Academic Press. London.
13. Bucy, R.S. (1970). *IEEE Proceedings*, **58(6)**:854–864.
14. Cohen, M.A. and Grossberg, S. (1983). *IEEE Trans Syst, Man and Cybernetics*, **13**:815–826.
15. Davydov, A.S. (1982). *Biology and Quantum Mechanics*. Pergamon Press, Oxford.
16. Dawes, R.L. (1992). *IJCNN Proceedings*, 133.
17. Dawes, R.L. (1993). *Rethinking Neural Networks: Quantum Fields and Biological Data*, chapter – Advances in the theory of quantum neurodynamics. Erlbaum, Hillsdale, N.J.
18. Findlay, J.M. Brown, V., and Gilchrist, I.D. (2001). *Vision Research*, **41**:87–95.
19. Grewal, M.S. and Andrews, A.P. (2001). *Kalman Filtering: Theory and Practice Using MATLAB*. Wiley-Interscience. USA.
20. Gupta, S. and Zia, R.K.P. (2001). *Journal of Computer and System Sciences*, **63(3)**:355–383.
21. Hagan, S., Hameroff, S.R., and Tuszynski, J.A. (2002). *Physical Review E*, **65**:061901.
22. Atmanspacher, H. (2004). *Discrete Dynamics*, **8**:51–73.
23. Haykin, S. (2001). *Communication Systems*. John Wiley and Sons, Inc., 4th edn. New York.
24. Jackson, E. Atlee (1991). *Perspectives of Nonlinear Dynamics*. Cambridge. Cambridge University Press.
25. Kennedy, J. and Eberhart, R.C. (2001). *Swarm Intelligence*. Morgan Kauffman. USA.
26. Leung, H. and Kettner, R.E. (1997). *Vision Research*, **37(10)**:1347–1354.
27. Mendel, J.M. (1971). *IEEE Trans Automatic Control*, **AC-16**:748–758.
28. Mershin, A., Nanopoulos, D.V., and Skoulakis, E. (1999). *Proc. Acad. Athens*, **74**:148–179.
29. Muehlenbein, H. and Thilo Mahnig. (2001). *Foundations of Real-World Intelligence*, chapter – Evolutionary Computation and Beyond. CSLI Publications. Stanford.
30. Penrose, R. (1994). *Shadows of the Mind*. Oxford University Press. Oxford.
31. Pola, J., and Wyatt, H.J. (1997). *Vision Research*, **37(18)**:2579–2595.

32. Purushothaman, G. and Karayiannis, N.B. (1997). *IEEE Tran. on Neural Networks*, **8(3)**:679–693.
33. Scott, A.C., Chu, F.Y.F., and McLaughlin, D.W. (1973). *IEEE Proceedings*, **61(10)**:1443–1483.
34. Sulem, C., Sulem, P.L., and Sulem, C. (1999). *Nonlinear Schrödinger Equations: Self-Focusing and Wave Collapse*. Springer-Verlag. (Applied Mathematical Sciences/139). New York.
35. Turing, A.M. (1950). *Mind*, **59**:433–460.
36. Tuszyński, J.A., Hameroff, S.R., Sataric, M.V., Trpisova, B., and Nip, M.L.A. (1995). *Journal of Theoretical Biology*, **174**:371–380.
37. Vitiello, G. (1995). *International Journal of Modern Physics B*, **9**:973–989.

10 Microtubules as a Quantum Hopfield Network

Elizabeth C. Behrman, K. Gaddam, J.E. Steck, and S.R. Skinner

Summary. Penrose and Hameroff's orchestrated objective (Orch OR) theory [14] suggests the existence of quantum computation in microtubule protein assemblies inside living cells. To investigate this suggestion numerically, we model this system as a quantum Hopfield network (QHN) with qubits representing the tubulins and interacting coulombically with each other, at finite temperatures. The effects of energy losses, dissipation, and other environmental factors are not considered, or are considered to be screened. Simulations are carried out on this computational model, and we look for stable states (local minima) of the network. We find that quantum information processing in microtubules is feasible, though at temperatures (5.8 K) lower than physiological temperatures.

10.1 Introduction

There are two major architectures for computation: the centralized algorithmic, and the decentralized adaptive. Most everyday machine computing uses the former model, which is enormously successful in a number of applications. Everyday biological computing uses the latter. There are also a number of tasks that are less suited to the algorithmic approach: for example, pattern recognition, or the traveling salesman problem [12]. It can also happen, for a number of reasons, that an algorithm is very difficult to develop for a particular problem.

In fact, quantum computing in general may fall into this category [4, 5]. Despite now many years of intensive study by a large number of well-funded and very bright people, the number of truly quantum algorithms known is very small. We do not even know what problems it would be possible to solve were we to build a large-scale quantum computer, much less how to write algorithms to solve them. The full power of quantum computing may never be realized unless we discover a means of answering both kinds of questions.

In previous work, we have suggested the use of quantum neural computers to address at least the latter need [4, 1, 5]. An adaptive or neural computer in a sense constructs its own algorithm for the problem given from the training set supplied. (In addition, neural computers may be the answer to the extremely vexing problems [7] associated with error correction in quantum computers.)

Our own brains are clearly of the decentralized, adaptive type. Could they also be quantum mechanical, not just in their underlying chemical processes, but also in their processing of information? Hameroff and Penrose [14] have suggested that the process of human consciousness cannot be simulated classically. They have proposed an orchestrated objective reduction (Orch OR) model in which quantum computation takes place in the microtubule protein assemblies present in the neurons of the brain. On the face of it this seems unlikely: decoherence at physiological temperatures, one would guess, would be rapid. But it may be true that biology, as Hagan et al. suggest, “can take advantage of quantum modes in clever ways” [10] by building mechanisms to maintain coherence, even in the “warm, wet, and noisy” environment of the living brain.

In this chapter we take a step towards the exploration of this question, by simulating a quantum neural network with the structure of a microtubule. We use an extremely simplified model [18] of the tubulin dimers: each is represented simply as a qubit, a single quantum two-state system, the quantum analog of a classical bit. A qubit, unlike a bit, can exist in a superposition of the two states. We assume that environmental factors are negligible: for example, that the thermal fluctuations of the bath are screened by a Debye layer of counterions, as suggested in Hagan [10]. We do include Coulombic interactions between qubits, and thermal effects for the qubits themselves. This is a kind of quantum Hopfield network [4, 11]: Each of the individual processing elements or neurons (here, the qubits) interacts with each of the others (a fully interconnected network); the elements (qubits) are initialized in some state, and allowed to evolve towards a local minimum. These networks store information and are also called “associative memory” or “content addressable memory” models. The final stable state is a pattern that is recalled by the network. We will look for evidence of locally stable states that represent quantum information processing.

10.2 Microtubulin Model

Real biological neurons have a highly ordered internal network known as the cytoskeleton, a protein polymer that is responsible for cell movement and organization of the organelles within the cell. The cytoskeleton consists of microfilaments, microtubules, actin filaments, and intermediate filaments. Of these components, microtubules display the greatest structural versatility [17] by determining the cell shape and providing a set of tracks for the movement of cell organelles. Microtubules are conveyer belts inside the cells. With the help of special attachment proteins (MAPs), they move vesicles, granules, organelles like mitochondria and chromosomes. They form the skeleton (cytoskeleton) that gives shape to the cell and help in the transportation of materials inside the cell. The microtubules are linked to other microtubules through microtubule-associated proteins (MAPs). Microtubules

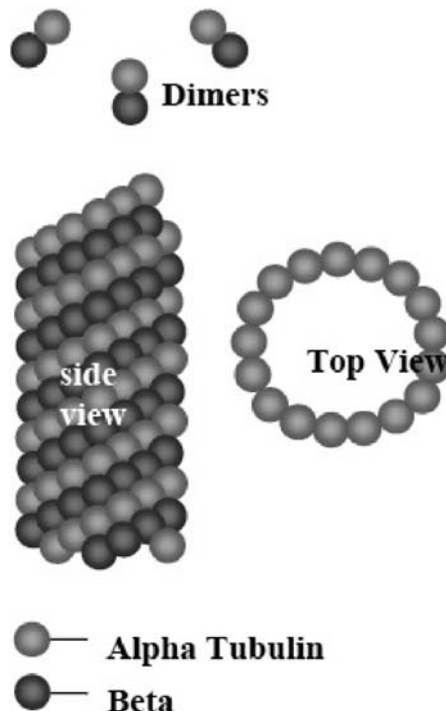


Fig. 10.1. Structure of a microtubule and the arrangement of its tubulins

are long, hollow cylinders that are 25 nm in diameter and their length may extend to macroscopic dimensions. They are composed of many smaller double molecules known as tubulin dimers. Fig. 10.1 shows the structure of a microtubule and the arrangement of its tubulins. The microtubules usually have 13 tubulins in circumference though there can be 12–16 tubulins depending on the environment, mainly ion concentrations. The tubulin dimers are arranged in a skewed hexagonal lattice. Each tubulin dimer is made up of two similar tubulin monomers called alpha tubulin and beta tubulin having slightly different properties. The tubulin dimers are 8 nm long and the monomers are 4 nm long with a molecular weight of 55 kDa. The dimers bind calcium ions and have a net electronegative charge due to the presence of acidic amino acids. This electronegative charge is predominant towards the alpha monomer that creates an oriented dipole in the tubulin dimer. The monomers bind together to form the microtubules.

Because each tubulin acts as an oriented dipole, the microtubule as a whole is an assembly of oriented dipoles. This is a kind of two-level system (TLS). The tubulins interact coulombically with their neighbors, and such a system exhibits some frustration in the ground state as it cannot satisfy all the dipole couplings with its neighbors. Couplings are created

due to the charge transfer within the dimers and their associated conformational changes. This coupling leads to the presence of piezoelectric properties that are very important in microtubule signaling, communication and assembly/disassembly behavior. Some experiments and simulations have shown that the microtubules can perform classical information processing.

Some of the functions of microtubules like assembly/disassembly, signaling and information processing could be related to the ground-state properties of the lattice of the dipoles [17]. Three kinds of classical arrangements of the dipoles are possible: (1) random arrangement where there is no order in the dipole arrangements; (2) ferroelectric arrangement, which is a long-range parallel-aligned order; and (3) intermediate or weak ferroelectric arrangement, where a short-range order is present. These three arrangements may exist under different conditions of temperature, electric field and microtubule length. A microtubule can switch among these arrangements. For assembly/disassembly and signaling processes, microtubules use a long-range ferroelectric arrangement, and a short-range weak ferroelectric arrangement for information processing. Are these arrangements influenced or perhaps produced by quantum effects?

10.3 Hopfield Model

The Hopfield neural network is a model of an associative content-addressable memory; it is capable of storing information as well as carrying out certain computational tasks such as error correction. In Hopfield neural networks the processing units, or neurons, are fully interconnected, i.e. each unit is connected to every other unit. Hopfield [11] demonstrated that an associative memory can be implemented with his network and hard optimization tasks such as the traveling salesman problem can be solved. A Hopfield network is initialized to a beginning state. Then each neuron's output is updated according to its weighted inputs. The updating of the neurons continues until the network converges to a stable state, or fixed point.

A *binary* Hopfield network has neurons that can be in one of two states: $S_i = +1$ (on) and $S_i = -1$ (off), where i is the number of the neuron. These are exactly analogous to bits 0 and 1. Each neuron is synaptically connected to other neurons with multiplicative weights that are real numbers. Each neuron is randomly selected and sums up its input and decides whether to turn itself on or off. Let W_{ij} be the synaptic strength from neuron ' j ' to neuron ' i ' and let I_i be the external input to unit ' i '. Each neuron takes a weighted sum of its inputs according to the following equation:

$$S_i = \text{sgn} \left(\sum_{j \neq i=1}^n W_{ij} S_j + I_i \right). \quad (10.1)$$

After repeated updating, the network may achieve a stable point, meaning, in the state space, all neurons remain in their current state after examining the inputs. The output is a stable vector-of-states that constitutes the recall of a stored pattern in the memory.

In the *continuous* Hopfield net, output values can be in the interval $(-1, +1)$. The governing equation of the i th neuron is

$$\begin{aligned}\frac{du_i}{dt} &= \sum_j W_{ij} S_j - \frac{u_i}{R_i} + I_i , \\ S_j &= \tanh(\gamma u_i) = f(u_j) ,\end{aligned}\tag{10.2}$$

where R_i is the decay rate ($R_i > 0$), S_j is the output of unit j after the activation function f is applied, and γ is the gain of the activation function. The Hopfield network considered in this chapter is in the high-gain limit where γ and R_i are large, and the tanh approximates the sgn function of the discrete network.

Each state in the high-gain Hopfield neural network has a Lyapunov function V , given by [13]

$$\begin{aligned}V &= L(\{S_i\}) - L(\{S_i^*\}) , \quad \text{where} \\ L &= -\frac{1}{2} \sum_i \sum_j W_{ij} S_j S_i - \sum_i S_j I_j .\end{aligned}\tag{10.3}$$

Here, L is a function of the states of all the neurons of the system $\{S_i\}$, and $\{S_i^*\}$ is the state of the system for which L is a minimum. V is a Lyapunov function for the dynamics of (10.2) since it is positive near the local stable state $\{S_i^*\}$, and it can be shown [11] that $dV/dt < 0$ except at the fixed points. Thus the Hopfield network is globally asymptotically stable and the stable states are the minima of the L function of the system. The processing of the Hopfield neural network, from an initial to a final steady state, is a process by which the L function of the system becomes smaller and eventually achieves a local minimum at the stable state. The weights, the external inputs, and the initial state determine which stable state, or pattern, is recalled by the network.

10.4 Quantum Model

The quantum system can be put into the Hopfield form to obtain the quantum Hopfield net (QHN) as follows. Consider an array of N qubits. We write the Hamiltonian, or energy function, for each qubit j as

$$H_j = K\sigma_{xj} + A\sigma_{zj} ,\tag{10.4}$$

where $\sigma_x = \begin{pmatrix} 0 & 1 \\ 1 & 0 \end{pmatrix}$ and $\sigma_z = \begin{pmatrix} 1 & 0 \\ 0 & -1 \end{pmatrix}$ are the Pauli matrices, and the full Hamiltonian $H = \sum H_j$. The first term represents the flipping of the qubit from one state to the other, with amplitude K . This term allows a quantum system to switch from one state to another without having the energy to climb the associated energy barrier and is therefore called “tunneling”. The effect of σ_x can be understood by looking at its operation on a state $\begin{pmatrix} \delta \\ \gamma \end{pmatrix}$. This state has probability amplitude δ of being found in the +1 state, $\begin{pmatrix} 1 \\ 0 \end{pmatrix}$, and γ of being found in the -1 state, $\begin{pmatrix} 0 \\ 1 \end{pmatrix}$; σ_x operating on this state gives us $\begin{pmatrix} 0 & 1 \\ 1 & 0 \end{pmatrix} \begin{pmatrix} \delta \\ \gamma \end{pmatrix} = \begin{pmatrix} \gamma \\ \delta \end{pmatrix}$, in which the amplitudes are flipped. In particular, the +1 state is flipped to the -1 state, and vice versa. The second term in (10.4) represents the energy difference $2A$ between the two states. This difference can be the result of external fields or interaction with other qubits. The Pauli matrix σ_z measures the state of the system; for example, $\begin{pmatrix} 1 & 0 \\ 0 & -1 \end{pmatrix} \begin{pmatrix} 0 \\ 1 \end{pmatrix} = (-1) \begin{pmatrix} 0 \\ 1 \end{pmatrix}$, telling us that the system is in the -1 state. The difference between the operation of σ_z on the +1 state and on the -1 state is $(+1 - (-1)) = 2$, so $A\sigma_z$ gives us an energy difference of $2A$ between the two states.

For the whole system we need to include all the qubits and their interactions. For a system at finite temperature we write the partition function $Q = \text{tr} e^{-\beta H}$, where tr is the trace of the matrix and β the inverse temperature in units of Boltzmann’s constant. The partition function contains information about all possible states of the quantum system, and how they depend functionally on each variable and each parameter. This will lead us to our definition of the quantum Hopfield net. Following [3] and [1], we write the trace in the basis set of state variables $\{S_j = \pm 1\}$, and use the Feynman path integral [8] formulation:

$$Q = \int \prod_{j=1}^N D[\sigma_{Zj}(t)] \exp \left\{ - \int_0^\beta dt \sum_{j=1}^N K \sigma_{xj}(t) + \int_0^\beta dt \int_0^\beta dt' \right. \\ \left. \sum_{j \neq j'=1}^N \sigma_{zj}(t) \alpha_{jj'}(t, t') \sigma_{zj'}(t') \right\}, \quad (10.5)$$

The path-integral formulation is one way of writing the trace: as a summation over all possible paths $\sigma_z(t)$ for each of the j qubits. Here, α is the Coulombic interaction between all the pairs of qubits of the array. The first term in (10.5) is the tunneling term that represents the probability amplitude that the qubit can make transition from one state to another. The second

term represents the coulombic interaction between the qubits. (10.5) can be thought of as propagation in imaginary time, because the Boltzmann factor $\exp\{-\beta H\}$ is the same as the expression for time evolution $\exp\{-itH/\hbar\}$ for $t = -i\beta\hbar$, where \hbar is Planck's constant divided by 2π .

To make progress in evaluating the path integral, we discretize the qubits of the QHN. This transforms the path integral over the continuous states of the N qubits, into a set of sums over states of the N qubits at n discrete times. Thus we can, for finite n , compute the state of the net by summing over all possible states of each of the discretized points of each of the qubits. If we let $n \rightarrow \infty$, the discretization is exact. The approximation of finite n will be good as long as $\beta H/n$ is small. Because the partition function is a trace, the state of each qubit at "time" $t = 0$ is constrained to be the same as its state at "time" $t = -i\beta H$. Thus we can picture each qubit as a loop, having n discretization points, propagating in imaginary time from 0 to β . A discretization point at any instant is the instantaneous state of the qubit at that corresponding value of inverse temperature. Figure 10.2 shows a qubit with 6 discretization points. While the loop is here drawn as a circle, it should not be imagined as being constrained so: all possible paths from the starting point to the ending point should be imagined as being included in the sum. The lines between discretization points represent the tunneling term in the Hamiltonian. (The analogous picture for a continuum position variable x is perhaps easier to understand; see, e. g., [6].) Qualitatively, we can think of the size of K , the tunneling amplitude, as indicating the floppiness of the bonds between adjacent discretization points: the larger it is, the less constrained is one point by its immediate neighbors, and thus, the more likely is the instantaneous state of the system at an intermediate imaginary time to flip from one state to the next.

Physically, the quantum-mechanical nature of the network increases as the discretization number n increases. In the picture, we can think of the amount of phase space (different states) the system is free to explore, as increasing when we increase the number of discretization points. That is, the loop can become floppier and floppier, for a given value of K , if the number of intermediate intervals is increased. On the other hand, if n is reduced, the loop will have less and less freedom to explore different states, and if we set $n = 1$ the loop must shrink to a single point, with no freedom to flip its state at all. This is the classical situation: no quantum-mechanical tunneling.

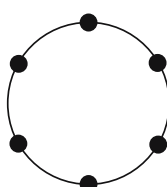


Fig. 10.2. A qubit with 6 discretization points

We can also think of this same situation in terms of the inverse temperature. The inverse temperature β is the total “length” of the path the qubit has to travel, from its initial point out into the world and then back. At low temperature, which is the quantum limit, β is large, which means the system can explore a large amount of the phase space (and we need to set n large in order to have a good approximation); at high temperature, $\beta \rightarrow 0$ and the loop necessarily shrinks to a point (the classical limit.)

Rewriting the path integral in terms of discretized sums, (10.5) becomes:

$$Q = \lim_{n \rightarrow \infty} \sum_{S_j=\pm 1} \exp \left\{ \zeta \sum_{j=1}^N \sum_{t=0}^{n-1} S_j(t) S_j(t+1) + \sum_{j \neq j'-1}^N \sum_{t=0}^{n-1} S_j(t) \alpha_{jj'}(t, t') S_{j'}(t') \right\}, \quad (10.6)$$

Here, ζ is the tunneling term that is given by the expression $\zeta = -\frac{1}{2} \ln[\tanh(\beta K/n)]$. Again, we use the variable t to label the inverse temperature ranging from 0 to β , but it is now a discrete variable, ranging from 0 to $n - 1$. The functions $\{S_j\}$ refer to the instantaneous values assumed by each of the qubits j ; i.e. the eigenvalues of the operators $\sigma_z(t)$ for each of the j qubits, frequently called “spins” in the literature. Thus, $\{S_j(t)\}$ is a microstate of the system; and the summation over all the microstates $\sum_{S_j=\pm 1}$

gives the partition function. The contribution of microstates to the partition function is large as their associated energy is low. For an infinite discretization value ($n \rightarrow \infty$), the discretization representation is exact, as indicated by the equality sign in (10.6) and as noted above, but since we do not have an infinite (or quantum) computer on which to do the simulation, we will make do with finite n . As long as $\beta H/n$ is much less than one, the discretization error should be small. Only infinite n and $n = 1$ have recoverable physical meaning, as corresponding to the quantum and classical cases, respectively; however, as we increase n we can investigate the role of increasing quantum-mechanical character of the network.

10.5 Quantum Hopfield Network

A quantum Hopfield network (QHN) has an enormously expanded range of states as the qubits can exist in any superposition of the two states. This is not the same as a continuum classical net, since the state of the system is not between the two states, but both states at the same time: the system carries information on as many channels as there are states contributing to the superposition. Under some circumstances that information is accessible, as in the operation of some quantum algorithms [16, 9].

Recall that the contribution of microstates to the partition function is large if their associated energy is low. In (10.6), the states that are more probable could be obtained by minimizing the argument of the exponential. We rearrange that argument to correspond with the L function for a Hopfield network. That is, we define the L function for the QHN as the integral of the Hamiltonian over the imaginary time loop, divided by β , i. e. the quantity in curly brackets in (10.6):

$$L_{\text{QHN}} = -\frac{1}{\beta} \left[\zeta \sum_{j=1}^N \sum_{t=0}^{n-1} S_j(t)S_j(t+1) + \sum_{j \neq j'=1}^N \sum_{t=0}^{n-1} S_j(t)\alpha_{jj'}(t, t')S_{j'}(t') \right] \quad (10.7)$$

This is the QHN. Classically, the high-gain Hopfield net replaces a continuum of possible values of each neuron with a finite number; in the QHN it becomes again a continuum, as described below. Information in the Hopfield net is stored as stable states. Classically the discrete net converges to the corners of an N -dimensional box [11], where the neuron outputs necessarily equal plus or minus 1. In a network of N classical neurons there are $2N$ possible states (corners of the box.) Once we discretize the quantum Hopfield net to discretization number n , there are $2Nn$ possible states: that is, each corner of the N -dimensional classical Hopfield box has $2n$ states. The greater the discretization n , the greater the number of possible states. When the temperature is lower we need a larger discretization number; thus, the lower the temperature the greater the storage capacity of the QHN. For infinite n we have the fully quantum-mechanical system, and have a fully faithful representation of the quantum dispersion – all possible superposition states.

To see how our quantum loop picture works with the Hopfield formulation, consider now the discretized path integral picture for more than one qubit, a QHN at finite n . Figure 10.3 shows a picture of the net for two qubits ($N = 2$) and two discretization points ($n = 2$). Each loop represents a qubit or two-level system (TLS), propagating in imaginary time (inverse temperature), from $t = 0$ to $t = \beta$. Each dot on a loop represents the instantaneous state of the qubit at a particular value of t , and these dots interact with their nearest neighbors along the loop (the first term in (10.6) or (10.7)). This is the tunneling term. The arrows show the direction of integration, from $t = 0$ to $t = \beta$. Each dot also interacts with other dots on other loops according to the second term in (10.6). In the simplest possible model, which we consider here, the two qubits interact only at equal imaginary times t , and the Lyapunov function from (10.7) becomes:

$$L_{\text{QHN}} = -\frac{1}{\beta} \left[\zeta \left(\sum_{i=1}^n S_i S_{i+1} + \sum_{i=1}^n S'_i S'_{i+1} \right) + \alpha \left(\sum_i S_i S'_i \right) \right], \quad (10.8)$$

where the (primed, unprimed) S functions refer to the two interacting loops.

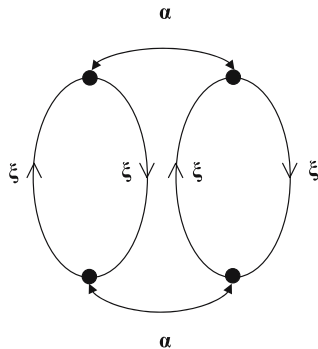


Fig. 10.3. Representation of two interacting qubits, with discretization $n = 2$. Each loop represents a qubit, propagating in imaginary time (inverse temperature) from 0 to β . The interactions between discretization points on the same loop have a strength of ξ ; the (bidirectional) interactions between points on different loops, of α

10.6 QHN as an Information Propagator for a Microtubules Architecture

The microtubule structure is cylindrical in shape consisting of a number of tubulins arranged in a hexagonal lattice structure, as shown in Fig. 10.1. The tubulin dimers are oriented as they have a net electronegative charge towards the alpha-monomer. There are 13 tubulins along the circumference of the microtubule. Each tubulin has six neighbors and interacts with its six neighbors. There can be propagation of information from one qubit to another in the network due to the (coulombic) interactions between each pair of qubits. The output is calculated as the lowest energy state of the qubit. Figure 10.4 shows the dipole-dipole interactions of a single dot with its neighbors, where a '+' sign represents a parallel arrangement and a '-' sign represents an antiparallel arrangement of the dipole moments.

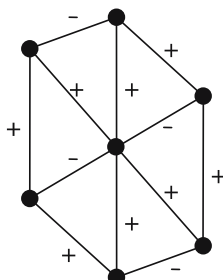


Fig. 10.4. Dipole-dipole interactions showing parallel or antiparallel arrangements of dipole moments

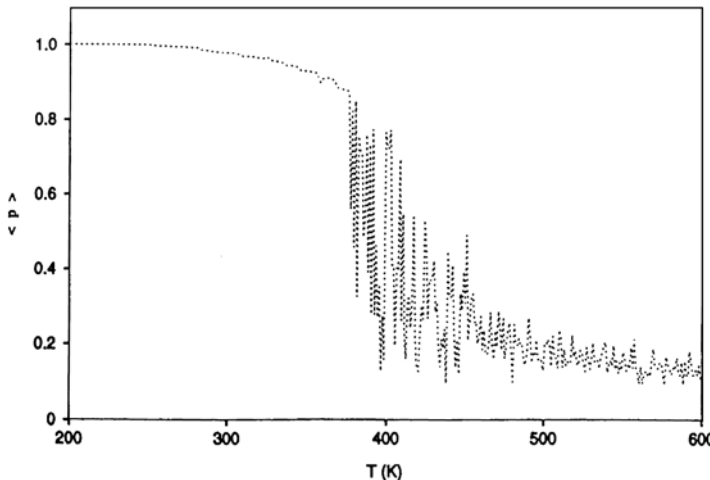


Fig. 10.5. Mean polarization per layer, as a function of temperature, for a 13×26 lattice, from [18], as calculated by classical Monte Carlo

We now apply our QHN methodology to the array of microtubules. The values of intra- and intermolecular distances, length of microtubule (based on the number of rows), tunneling amplitude, temperature, external field, leakage term, gain parameter, etc., are set, using experimental values where possible. The QHN is started out at some initial state after assigning values to all the parameters in the algorithm, by assigning an intial dipole value (orientation of the polarization) to each qubit. The output of each neuron is updated according to its weighted inputs. The updating procedure of the network minimizes the Hopfield energy or Lyapunov function and continues until the network converges to a stable state achieving a local minimum. This stable state is a pattern that is recalled by the network. This final state is the output of the network.

To test the validity of our method we first compare it to some published classical calculations on this model. Tuszynski, et al. [18], have performed some Monte Carlo computations to observe the size dependence of the phase behavior in microtubules. Figs. 10.5 and 10.7 are reproduced from that chapter. Figs. 10.5 and 10.6 show the mean polarization per site for a triangular lattice whose size is 13×26 (26 layers, 13 qubits in each row, 338 qubits), in the classical limit ($n = 1$). The initial values of spins Fig. 10.6 were taken from [18]. It can be seen that the QHN results are comparable to the Monte Carlo calculations. For the large-lattice limit, Tuszynski has a calculation of 5000 layers; due to computational capacity problems we were only able to do 3000 layers; nonetheless our results are comparable to theirs, as seen in Figs. 10.7 and 10.8. Again, Figs. 10.7 and 10.8 are in the classical limit.

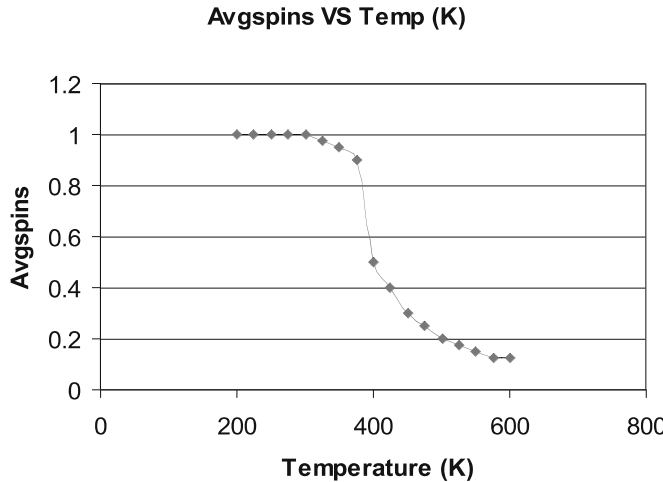


Fig. 10.6. Average polarization as a function of temperature, for a 13×26 lattice, using values for the parameters of [18], calculated by QHN, in the classical limit ($n = 1$)

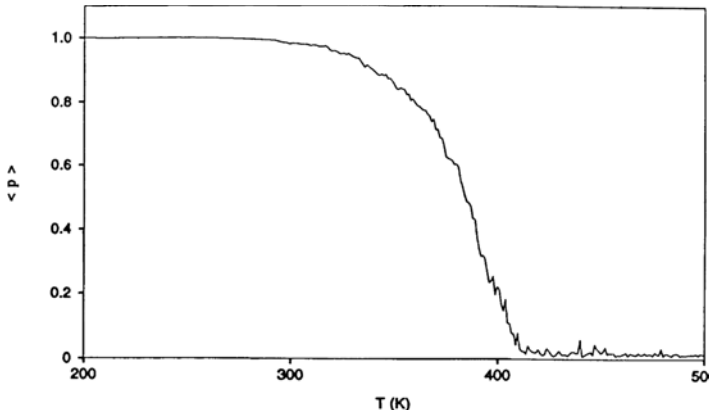


Fig. 10.7. The mean polarization for a 13×5000 lattice, as calculated by classical Monte Carlo [18]

With some confidence in our method we now move to nonzero quantum-mechanical effects, setting $n > 1$. In order that our discretization be valid we require $\beta E/n < 1$, where E is the energy of the system. Because of computational limitations we used only a 26-layer system, or 338 qubits. All other experimental parameters were kept as before, and we look for local minima for

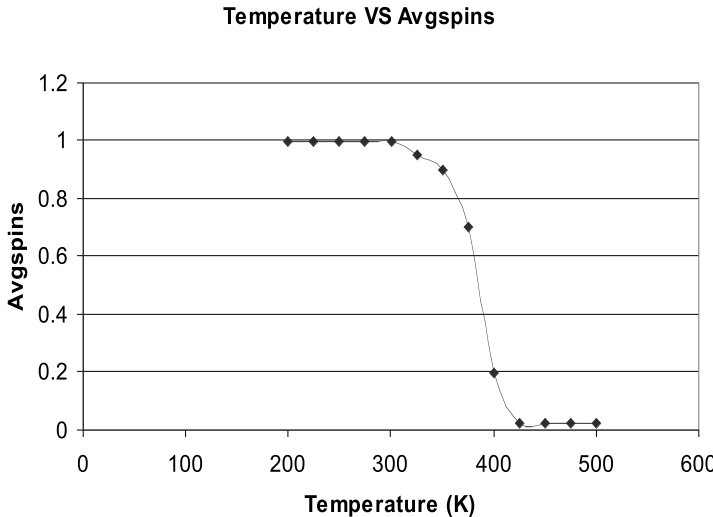


Fig. 10.8. Average polarization as a function of temperature for a 13×3000 lattice, calculated by QHN, in the classical limit ($n = 1$), using the parameters of [18]

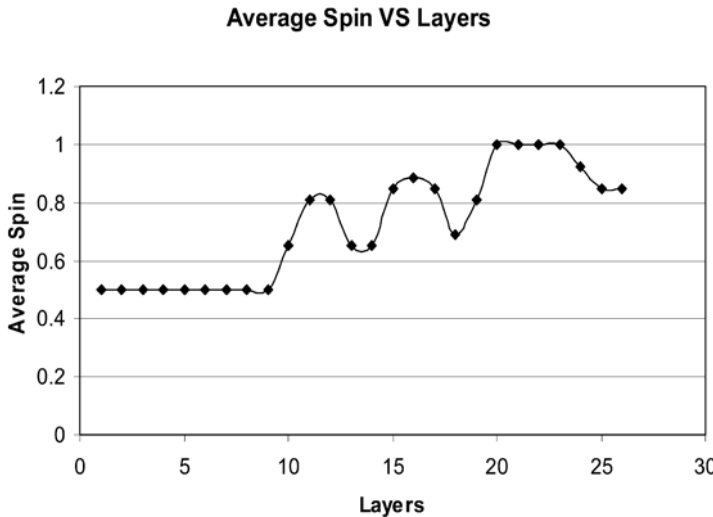


Fig. 10.9. The variation of average spins along the layers of the 13×26 microtubule for $n = 4$ with an initial configuration of 1 down, 3 up spins for each qubit, as calculated by QHN, at $T = 5.8$ K. This final configuration was stable at 100 000 passes

the QHN. Some interesting phenomena were observed. An example is shown in Fig. 10.9, where we see the variation of average spin along the layers of the microtubule, at a temperature of 5.8 K ($\beta = 2$ MeV), starting from an

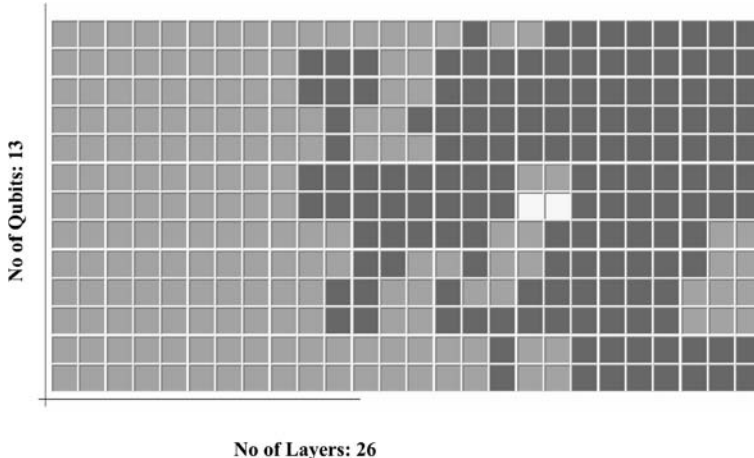


Fig. 10.10. Spin configuration, by qubit, of the system in Fig. 10.9

initialization of the qubits in a superposition state of 1 down and 3 up spins. The QHN was stable at 100 000 epochs.

It can be observed from the above graph that there is a locally stable configuration in which a nearly constant polarization at one end is transformed to a different one at the other, a kind of information processing effect. That is, we have found a stable configuration for which the “input” at one end of the microtubule is transformed to an “output” at the other, and both input and output are superposition states (i.e. the average spin (polarization) is between minus one and one). Since superposition states cannot be realized classically, the microtubule is acting as a quantum computer, with fully quantum-mechanical inputs and outputs. This is of course lower than physiological temperatures, and indeed no similar “processing” effect was observed at temperatures that high: the higher the temperature, the smaller the quantum loop, which represents the quantum dispersion, shrinks. At physiological temperatures the loop is essentially a single point, and no quantum effects (which are due to the spreading out of the loop) can be observed.

Figure 10.9 can be better understood by looking at each qubit, rather than only layer averages. In Fig. 10.10, each cell represents a qubit and its color represents its average spin value. The spin values vary from -1 to $+1$. The color for $+1$ is red, the color for 0.5 is orange, and the color for 1 is light yellow. There is a variation of color from red to light yellow as the spin value changes from $+1$ to -1 . So in fact though the average spin along a layer varies continuously from $+1$ to -1 , no single spin has any value other than $+1$, 0.5 , or -1 ; these seem to be the only stable values for the superposition states for these conditions. This may be an artifact of the discretization level: with only four discretization points per qubit there are only five possible distinguishable superposition states (1 , 0.5 , 0 , -0.5 , and 1 , which can be produced in 1 , 4 ,

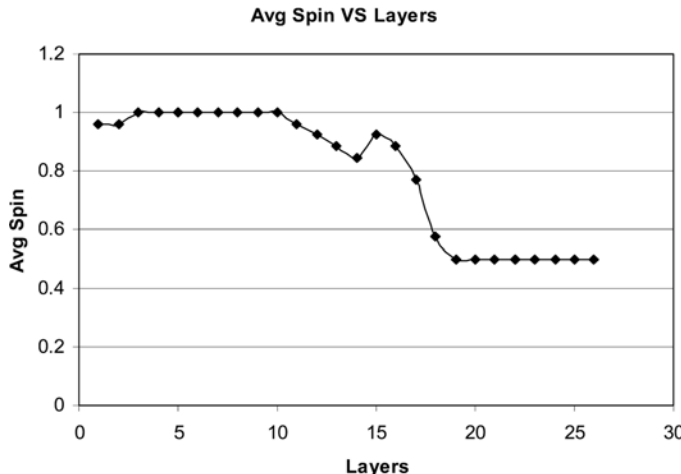


Fig. 10.11. The variation of spins along the layers of the microtubule for $n = 4$ where the initial spin configuration is the reversed final spins of the system whose initial configuration is 1 down, 3 up spins, as calculated by QHN, at $T = 5.8$ K. This final configuration was stable at 100,000 passes

6, 4, and 1 ways, respectively.) Different individual runs do produce different final averages for individual qubits; however, the overall pattern by layers is relatively stable.

Information processing of this type was fairly easy to produce, if the system was initialized in a superposition state of almost any kind. For example, an initial situation reversed from the one that produced Fig. 10.9, gives us a stable configuration like that shown in Fig. 10.11. That is, the initial spins for the qubits were the reversed final spin values obtained from the initial spin configuration of 1 down, 3 up spins for each qubit.

Another stable processing configuration was produced by setting the initial spins for the qubits to the final spin values obtained from the initial spin configuration of 1 down, 3 up spins for each qubit. The stable final configuration is shown in Fig. 10.12. Figure 10.12 is similar to the previous graph (but in the reverse direction) which has reversed final spins as initial spins.

Because our calculations are approximate (finite n) it behoves us to check that the discretization error is negligible. Thus we repeated our calculations for a discretization ten times the size, i.e $n = 40$. We took the initial spin configuration to be the final spin values of the $n = 4$ simulation (whose initial configuration was 1 spin down, 3 spins up), mapped to $n = 40$ such that the average was the same as for $n = 4$. Figure 10.13 shows the results, which while not identical are very much analogous to those for $n = 4$. We are thus confident that we are observing a real phenomenon, not an artifact of the discretization, at least in the overall information processing effect of the tubulin array.

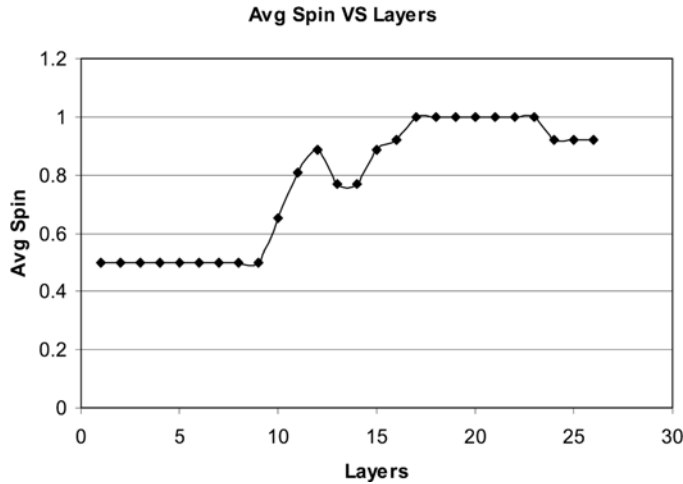


Fig. 10.12. The variation of spins along the layers of the microtubule for $n = 4$ where the initial spin configuration is the final spins of the system whose initial configuration is 1 down, 3 up spins, as calculated by QHN, at $T = 5.8$ K. This final configuration was stable at 100 000 passes

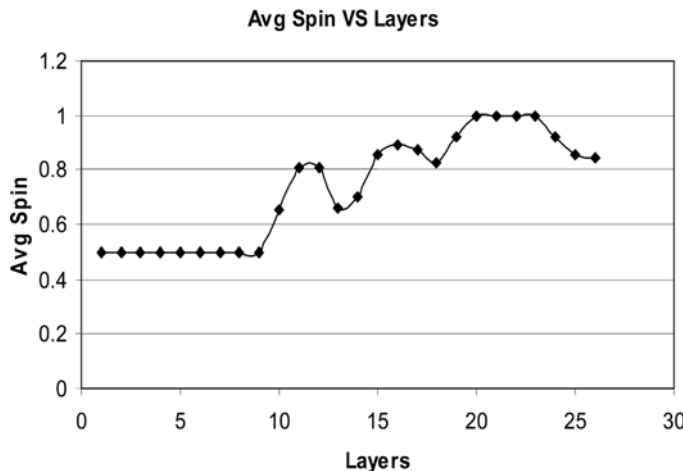


Fig. 10.13. The variation of spins along the layers of the microtubule for $n = 40$

Classical processing of information was even easier to produce. In Figs. 10.14–10.17 we show a number of classical switching configurations, produced with various different initial configurations, as detailed in the figure captions. All but one of the simulations shown stabilized at a classical switch configuration (± 1 at each end). A large number of other configurations were tried. Long-range ferroelectric configurations (no switching) were also easy to stabilize.

Average Spin VS Layers

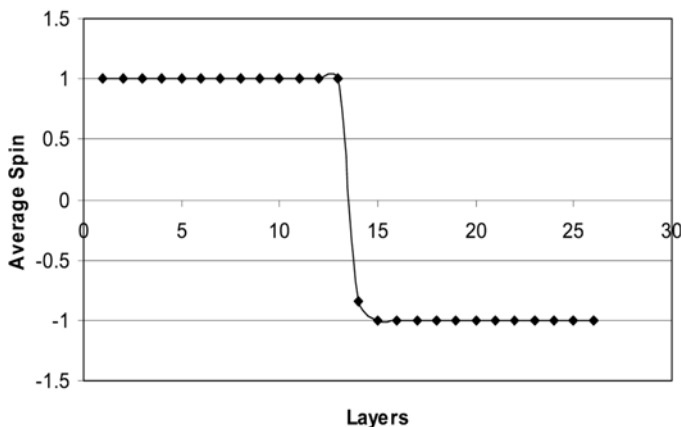


Fig. 10.14. Variation of spins along the layers of a microtubule for $n = 4$, starting from an initial spin configuration where half qubits (169) have all spins up and half qubits (169) have all spins down

Average Spin VS Layers

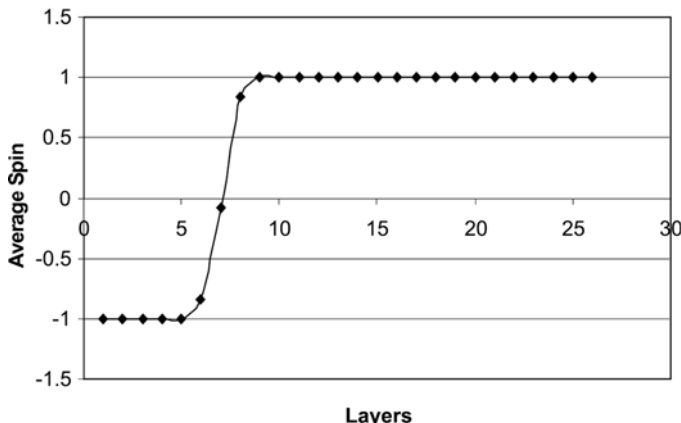


Fig. 10.15. Variation of spins along the layers of a microtubule for $n = 4$ having an initial spin configuration where a quarter of qubits (85) have all spins down and three-quarters of qubits (253) have all spins up

10.7 Conclusions and Future Work

We have shown that a simplified model of a microtubule, in which the tubulin dimers are represented as qubits, interacting with each other coulombically at finite temperature, can in fact exhibit quantum information processing, though at temperatures much lower than physiological temperatures. Still,

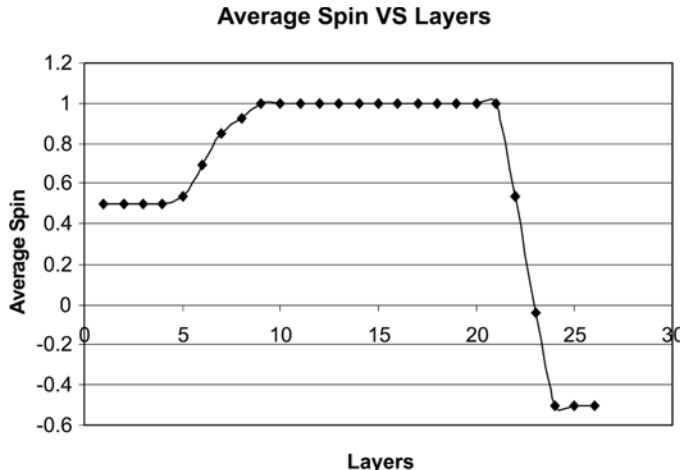


Fig. 10.16. Variation of spins along the layers of a microtubule for $n = 4$ having an initial spin configuration where all qubits in odd layers have 3 spins up and 1 spin down and all qubits in even layers have 3 spins down and 1 spin up

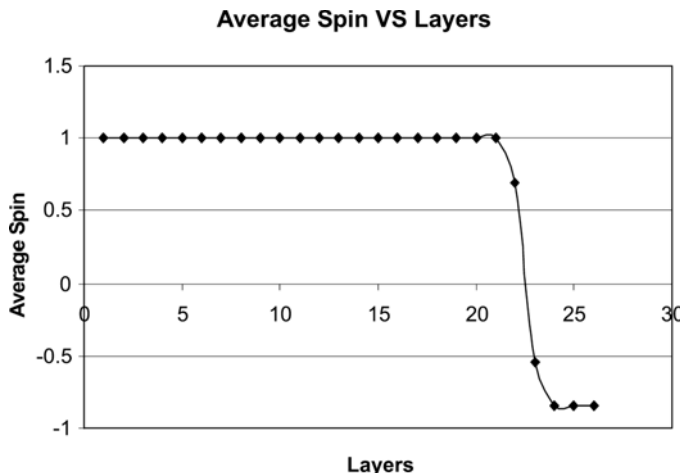


Fig. 10.17. Variation of spins along the layers of a microtubule for $n = 4$ having an initial spin configuration where the first 12 qubits in odd layers have all spins up and the 13th qubit has all spins down. The first 12 qubits in the even layers have all spins down and the 13th qubit has all spins down

all that is necessary for the temperature to be “low” is that it is small compared to the relevant energy scales in the problem; as is well known, quantum information processing has been successfully done at high temperatures [19]. While we have made every effort to ground the parameters for our simulations in experiment, some guesswork was necessary; if we are wrong in places

that could affect the scale at which our observed phenomena occur. We were also able to find stable classical switching configurations, and long-range ferroelectric configurations suitable for signaling or assembly/disassembly. Of course, the fact that quantum conditions can produce observed classical results does not show that those effects have in fact come from the simulated quantum conditions.

We have assumed a rather primitive model, due to computational capacity limitations; in particular, we have assumed most environmental effects to be screened. It would be interesting to do a detailed study to see if this is in fact the case. Another possible objection that could be made is that the simulations found only locally stable configurations: the Hopfield minimization procedure does not mimic the actual dynamics, and the configurations found are not necessarily kinetically accessible.

Another possible approach would be a larger-scale one: to determine what kinds of processing it is that we think a brain is doing, and try to train a quantum network (e.g., this model) to reproduce the training set and to generalize the result. Along those lines, we have developed a method [2] for training a spatial network like this model, based on Werbos's [20] earlier work; we have succeeded in training a small network (six qubits) to solve the controlled-NOT problem. Of much more interest would be the possibility of training the net to perform a truly quantum problem, like the calculation of entanglement; that work is in progress [5].

Acknowledgement. This work was supported by the National Science Foundation, grants #ECS-9820606 and 0201995. We thank J.A. Tuszynski for permission to reproduce Figs. 10.5 and 10.7 from his published work.

References

1. Allaardin, R., Gaddam, K., Behrman, E.C., Steck, J.E., and Skinner, S.R. (2002). *Proceedings of the International Joint Conference on Neural Networks* **3**: 2732–7.
2. Allaardin, R., Gaddam, K., Boehmer, S., Behrman, E.C., Steck, J.E., and Skinner, S.R. (2005). Submitted to *IEEE Transactions on Neural Networks*.
3. Behrman, E.C., Jongeward, G.A., and Wolynes, P.G. (1983). *Journal of Chemical Physics* **79**:6277–81.
4. Behrman, E.C., Nash, L.R., Steck, J.E., Chandrashekhar, V.G., and Skinner, S.R. (2000). *Information Sciences* **128**:257–269.
5. Behrman, E.C., Steck, J.E., Gagnebin, P.K., and Skinner, S.R. (2005). Submitted to Physical Review, A.
6. Chandler, D. and Wolynes, P.G. (1981). *Journal of Chemical Physics* **74**:4078.
7. Chuang, I.L. (2005). *Bulletin of the American Physical Society, March Meeting, 2005*, paper S33.00005.
8. Feynman, R.P. and Hibbs, A.R. (1965). *Quantum Mechanics and Path Integrals* (New York, McGraw-Hill)

9. Grover, L., (1997). *Physical Review Letters* **79**:325–8.
10. Hagan, S., Hameroff, S.R., and Tuszyński, J.A., (2002). *Physical Review E* **65**:061901–11.
11. Hopfield, J.J. (1982). *Proceedings of the National Academy of Sciences USA* **79**:2554–2558
12. Haykin, S. (1999) *Neural Networks: a Comprehensive Foundation* (Prentice Hall, New York):680–687.
13. Hassoun, M. (1995). *Fundamentals of Artificial Neural Networks*. (MIT Press, Cambridge, MA):345–362.
14. Hameroff, S.R. and Penrose, R. (1996). *Mathematics and Computers in Simulation* **40**:453–80.
15. Luenberger, D.G. (1984). *Linear and Nonlinear Programming*. (Addison-Wesley, New York.)
16. Shor, P., (1997). *SIAM Journal of Computing*, **26**:1484–1509.
17. Tuszyński, J.A., Hameroff, S., Sataric, M.V., Trpisova, B., and Nip, L.A. (1995). *Journal of Theoretical Biology* **174**:371–380.
18. Tuszyński, J.A., Hameroff, S., and Hurylak, P. (1998). *Philosophical Transactions of the Royal Society of London A* **356**:1897–1926.
19. Vandersypen, L.M.K., Steffen, M., Breyta, G., Yannoni, C.S., Sherwood, M.H., and Chuang, I.L. (2001). *Nature* **414**:883–7.
20. Werbos, P. *Handbook of Neural Computation*. release 97/1, A2.3:2

11 Consciousness and Quantum Brain Dynamics

Gordon Globus

Summary. The opposition to quantum brain theory is “deconstructed”. The quantum brain theory originated by Umezawa and coworkers is elaborated as a uni-mode quantum brain dynamics (QBD), a Hermitean dual-mode QBD and a non-Hermitean dual-mode QBD. The non-Hermitean version is applied to mathematics, where the Riemann hypothesis is seen in a fresh way. The philosophical implications of this approach turn out to be “monadological”.

11.1 Deconstruction

“Deconstruction” is a term of art in postmodernity (e. g. as stated by Derrida in [4, 5]). Note that I reserve “postmodernism” for the cult. Deconstruction covers various techniques directed against the conventional unthematized assumptions of modernity. Since nobody likes being deconstructed, practitioners of modernity have appropriated the term and it is found even in the daily newspaper. “Deconstruction” has been subverted to mean a clever analysis of a construction into its parts. Since modernity so permeates our language, postmodernity must resort to using modernity’s terms but then crossing them out, as in the present title.

The idea that the brain has quantum degrees of freedom in its functioning has been around for close to forty years, yet its revolutionary coterie remains small. Of course, quantum brain theory’s lack of cachet may be deserved, but what catches the deconstructionist eye is the emotional intensity of the opposition to quantum brain theory. Marginalia are the facts of deconstructionists. To see this emotional intensity one must look to the margins of a text, since science practitioners strive for an image of emotional neutrality. But here are two science writers – unlike scientists, writers are allowed more freedom of emotional expression – who clearly have an “attitude” toward quantum brain theory. Seife [24] sneers, in the highly respected journal Science, “The idea attracted a few physicists, some consciousness researchers, and a large number of mystics.” McCrone [18] opines it is “hard to report the various claptrap ideas with a straight face”. Such strong words in the margins of scientific discourse reveal a deeply felt conventional resistance to the quantum brain notion, which should encourage all quantum brain theorists that at least something deeply revolutionary is at stake!

Resistance to quantum brain theory has a number of sources, even personal. After all, if there is a deeper level of brain functioning that brain science has quite overlooked – a “cryptic brain”, as Jibu and Yasue [15] say – this will not sit well with successful practitioners, left barking up the wrong tree.

A typical tactic of threatened convention is to co-opt the threat. Here it is said that the brain processes information and the q-brain does too, but with a richer logic that admits superpositions (a qubit that is both zero and one). Ho-hum, from the conventional computational point of view. The brain is just a wet computer all the same, with bits and qubits. But what if the q-brain has novel powers beyond computation? The revolutionary imagination is stifled if the brain’s quantum powers only bring better computation. What else might quantum degrees of freedom offer? Quantum degrees of freedom, we shall see, can explain Being itself.

The conviction that the brain computes does not stand alone, but is part of a long and well-established philosophical framework, currently in a technoscientific rendition. This tradition of “metaphysics” goes back to the Socratic philosophers in ancient Greece. (The new dynamical powers of the q-brain are in contrast pre-Socratic in spirit, especially that of Heraclitus.) Plato’s “Demiurge” is literally a craftsman, shaping chaos to cosmos like the potter shapes clay into a pot or the programmer shapes information flow. To say that the brain does much more than compute is to go against the weight of the still-dominating tradition.

A more subtle co-opting also stands in the way of quantum brain theory. The most intriguing way that quantum brain theory has been put to use is in explaining consciousness. (Skeptics scoff that the only connection between consciousness and quantum brain functioning is that both are rather mysterious!) But “consciousness” is a central notion of traditional metaphysics and we should not expect a classical notion to fit easily with revolutionary quantum brain theory.

I confess that when someone uses the term “consciousness”, I am never really sure what is meant. Indeed, Natsoulas [20] long ago pointed out many different meanings of that term. Conscieri is etymologically to “know together”, but the meaning of social consensus has been lost over the centuries. Feigl [6] divided the consciousness problematic into sentience (qualia), sapience (intentionality) and selfhood, leaving “consciousness” quite nonspecific. Heidegger [12, 13] gets along fine without much mention of consciousness, which is replaced by world-thrownness, i.e., always finding ourselves undergrounded, always already amidst the world with its affordances.

My stance is completely contra to that of Tuszynski, who states in the Introduction to this volume,

“That the brain does give rise to consciousness is a key assumption of modern neuroscience and we will take it as a given, otherwise we would be compelled to seek these answers in the realm of religion or metaphysics.”

But what if we seek these answers in the realm of quantum brain theory? Quantum theory in physics provoked a profound revolution to common sense, and we have every reason to anticipate that quantum brain theory would also be deeply at odds with a common sense notion like consciousness. So quantum brain theory is co-opted by entangling it with the central problematic of metaphysics, that of consciousness. We should expect that revolutionary quantum brain theory will untangle it by decentering conventional consciousness in some fashion, even using it but then crossing it out.

A concerted critique of quantum brain theory has been made by a physicist, Max Tegmark [29]. This critique has been rebutted by Hagan et al. [11]. (It turns out that Tegmark demolishes a quantum brain theory that nobody holds.) It is widely believed, nonetheless, that coherence in quantum brain systems will ultrarapidly decohere by thermal interaction with outside systems, and so any quantum brain notions are plain silly. This belief fails to recognize that the coherent oscillations characterizing quantum brain systems are too rapid to be affected by ambient thermal noise.

Arguably the most extensively developed quantum theory of brain functioning was originated by Umezawa and coworkers [21, 25, 26] and extended by Jibu and Yasue [15], Vitiello [33], Globus [9] and others. Like all discourse, quantum brain theoretical discourse is a sheaf whose stalks may cross. The Umezawa stalk – itself a sheaf, discourse is a sheaf – fractal – is picked out here because of its ontological provenance, as we shall see.

11.2 Quantum Brain Dynamics

The development of quantum brain dynamics (QBD) has recently been described by Takahashi and Jibu [28] and Jibu and Yasue [16]. Jibu and Yasue emphasize the distinction between (1) nonliving systems whose fundamental elements are uncorrelated, completely disordered, “thermalized”, and (2) living systems whose fundamental elements are strongly correlated. Living “dissipative” systems are able to decrease entropy (increase order) even when supplied with thermalized energy, and later dissipate the order back to the environment. This has consequences for quantum theory “because complex systems of atomic ingredients with strong mutual correlation like living matter can not be treated by quantum statistical mechanics but only by quantum field theory” [16].

The anatomical organization of the brain relevant to QBD is at the nanolevel (10^{-9} m). Here there is a dense web of filamentous protein strands filling brain systems, easily passing through neuronal and neuroglial cell membranes, oblivious to the intracellular/extracellular distinction. This is a radically different picture from the classical one of neuronal networks supported by surrounding neuroglia. Instead the fundamental nanolevel web of protein strands is studded by neurons and neuroglia. The innermost region of this filamentous web is the one associated with microtubules, which are filled

with a lattice structure of water molecules. Here, in quasicrystalline water molecules, the quantum and the classical meet.

The nanolevel protein web is surrounded by (and in the case of microtubules, surrounds) water molecules with which it interacts. Because of the spatial configuration of the one oxygen and two hydrogen atoms of the water molecule, it is an electric dipole, with a pair of positive and negative charges that oscillate in polarity. The strength of this water dipole field is called the electric dipole moment. The electric dipole moment vector points from the positive pole to the negative pole

Dipolar solitons propagate along the protein filaments of the nanolevel web. Dipolar solitons [2] are a collective mode of many dipolar oscillations of nonlocalized electrons trapped on the filaments of the nanolevel web. Dipolar solitons are induced by input energy to the nanolevel web [7]. The creation and annihilation of dipolar solitons reflects the interaction between uncorrelated and correlated systems.

The initial work of Umezawa and coworkers [21] was directed toward memory traces, not consciousness, utilizing the resources of the quantum vacuum state (least-energy quantum state) and “condensations” there of coherent quanta. They called the quanta of the brain’s cortical fields “corticons”. Corticons undergo creation and annihilation dynamics by exchanging photons. Their proposal was that quasipermanent memory traces are laid down in the quantum vacuum states upheld by the living brain. The q-traces are traces that preserve symmetries broken by invariances in the input flux; these symmetry-preserving traces are called “symmetrons”. The symmetrons encode input invariances. Encoding of different traces is accomplished by different condensates of coherent Nambu–Goldstone (N–G) bosons [15].

A theory of recall of memory traces was also proposed. When a new input comes in carrying the same invariances as a symmetron trace, T, then T is recalled. Or the new input has invariances different from but in the past associated with T, bonded in virtue of past contiguity in time. Associated invariances of the same time slice are coherent. More basic than recall productivity from trace to remembrance, there is recognition in virtue of coherence. N–G symmetron traces recognize similar and associated inputs; memories are revived in recognition.

Jibu and Yasue [15] make this memory model into a theory of consciousness by expanding Umezawa’s q-physics – theoretical proposal of a quantum vacuum state repository for memories to a biologically based “quantum brain dynamics” (QBD). They identify consciousness with the creation and annihilation dynamics of corticons and photons.

The incoming energy triggers the creation and annihilation dynamics of corticons and photons. This dynamical event is regarded as the physical process of consciousness.

Consciousness is “constituted” in this quantum brain dynamics. So Jibu and Yasue supplement Umezawa’s account of memory with a theory of conscious-

ness, both grounded in QBD [31]. Consciousness lies in vacuum state dynamics. This does not resolve the consciousness/brain problem, however, which becomes a consciousness/q-brain problem. But the q-brain described by quantum brain dynamics has greater resources than classical neural networks, so the problematic, though not resolved, is greatly advanced by Jibu and Yasue.

11.3 Hermitean Dual-Mode Quantum Brain Dynamics

Umezawa's physics was not stagnant during the development of QBD (see [27, 30]). Now, quantum mechanics and quantum field theory do not strictly apply to living dissipative systems like the brain. Umezawa added thermodynamical degrees of freedom by developing "thermofield dynamics". He accomplished this by positing an unreachable alter quantum universe ("~mode") to our conventional quantum universe ("non~mode"). The alter universe is conceived as a heat bath for our non~universe. These dual quantum universes meet in the quantum vacuum state where energy exchange takes place.

In thermofield dynamics under the Hermitean assumption, the energy of the dual modes must be equal. Application of Hermitean thermofield dynamics to the brain was undertaken by Vitiello [32], who developed dual-mode QBD. The N-G memory traces in Vitiello's richly developed Hermitean thermofield QBD are dual-mode mirror images. (Now the original QBD of Jibu and Yasue [14] is seen to be unimode.)

Vitiello [33] emphasizes that the living brain is an open dissipative system in which consciousness emerges as a manifestation of q-brain dynamics. Consciousness is grounded in the dynamical matching relations between mirror-image modes. (The match of mirror images is insured by the Hermitean assumption.) The non~mode represents the environment and the ~mode has a (time-reversed) copy of the non~mode, and so a copy of the environment.

Consciousness for Vitiello [33] is not "centered exclusively on "first person" inner activity" but on an interaction between dual modes, an indivisible entre-deux in which duality is primary.

The conscious identity thus emerges at any instant of time, in the "present", as the minimum energy brain state [i.e. vacuum state] which separates the past from the future, that "point" on the "mirror of time" where the conjugate images ... join together ([33], bracket added).

... consciousness mechanisms might be involved in the continual "trade" (interaction) between the non-tilde and the tilde modes [34].

Consciousness is of a between that (by Hermitean assumption) is a dual-mode match of time-reversed mirror images. As with Jibu and Yasue's [15] identifying consciousness with corticon creation and annihilation dynamics, the consciousness/brain problem remains, now formulated as a consciousness/dual

q-modes problem. A correlation between consciousness and the dynamics of the dual-mode between is not at issue. But to say that consciousness is the \sim conjugate match in the dual-mode between appears to make a category mistake, like saying conscious states *are* brain states or conscious states *are* creation and annihilation corticon dynamics. To elide such category mistakes I have crossed out “consciousness” here.

The ontological significance of Vitiello’s proposal lies in the primacy of duality. The ontological bonus of duality’s primacy is its between.

11.4 Non-Hermitean Dual-Mode Quantum Brain Dynamics

So thermofield dynamics gives quantum field theory two modes and their vacuum state between. Further, the vacuum state in thermofield dynamics expands to an infinite number of independent “theta-vacua”. The ontological richness of dual-mode QBD derives from the between. The encounter between dual quantum modes meeting in the vacuum state is governed by a thermofield logic.

In an alternative non-Hermitean thermofield QBD, however, a peculiar trace may arise locally in addition to the dual-mode traces. Suppose a non \sim mode input comes in and is *recognized*. This means that quanta are excited out of the non \sim mode of a theta-vacuum, annihilated from the non \sim theta-vacuum state. It follows from the energy conservation law that an equal number of quanta must be created in the corresponding \sim mode. In the case of recognition, a non \sim mode *default* corresponds to a \sim mode quantum. After a time the excited quanta dissipate their energy and fall back into the non \sim mode of a different theta-vacuum, creating quanta there. But then an equal number of quanta must be annihilated from the \sim mode. So a \sim mode *default* corresponds to a non \sim mode quantum (and vice versa). Globally across theta-vacua, quanta are equal in number across dual-modes but locally in a particular theta-vacuum there may be dual-mode inequality, so long as the total energy remains constant, consistent with the energy conservation law.

So three theories of memory trace must be distinguished: 1) The unimode trace of QBD. 2) The dual-mode trace of thermofield QBD. 3) A dual-mode trace of recognition in which the trace in *our* thermofield mode is a default that “remarks” a trace in the alter mode. Each recognition further weights the \sim mode trace. Over time the recognition traces develop into a weighted attunement that has self-organized into an optimal attunement for typical kinds of input that might be expected based on past encounters.

In the non-Hermitean version the quantum brain attunement situates for the encounter with the flux of input invariances that represent physical reality. The special case of situating attunement and input invariance is when a “match” is made. What “match” means here will be explained next.

The dual-modes of thermofield dynamics are mathematically described by means of complex numbers of the form $a + bi$, $c - di$, etc. A match between complex numbers is of the form $a + bi$ and $a - bi$, the match of “complex conjugate” numbers. The complex conjugate match gives a real number.

$$(a + bi)(a - bi) = a^2 + b^2 , \quad (11.1)$$

(since the crossterms cancel and $i^2 = -1$). In the case of \sim conjugate match between $a + bi$ in the non- \sim mode and $a - bi$ in the \sim mode, the match is called the “ \sim conjugate match”. The \sim conjugate match gives real numbers that are associated with observables.

So when the \sim mode situating attunement makes a \sim conjugate match with the input flux from physical reality, the result is real, an observable, presence, *Being*. This is the ontological provenance of the vacuum state between-dual-modes: Being, in the \sim conjugate match between situatedness and reality [19].

Vitiello interprets the \sim conjugate match in the between-dual-modes as consciousness, whereas I interpret it as Being. Real numbers are associated with observable Being, not unobservable consciousness. Where Jibu and Yasue think that consciousness is related to the creation and annihilation dynamics of corticons, and where Vitiello thinks that consciousness is a function of the dual-mode match, I cross out consciousness and propose that Being/presence depends on the dual-mode \sim conjugate match.

The resources of dual-mode QBD are much greater than those of unimode QBD in virtue of the between that is an inseparable duality. Duality brings unity through the between. The fruit of unity here – the match – is not consciousness but Being. Consciousness is decentered, no longer perceptual (so no longer any “hard” qualia problem), but purely thought, res cogitans. The pernicious ontological twoness in Descartes is succeeded by the ontological oneness of two belonging together.

11.5 Application to Mathematics: The Riemann Hypothesis

The Riemann hypothesis (RH) – a guess made by Riemann in 1859 – is considered to be the greatest unresolved problem in mathematics. The precise prediction of RH (see below) has been calculated out to billions of instances and they all conform perfectly to RH, yet RH has not been proved. Furthermore, there is no clear understanding why RH should even be true.

RH deals with the infinite prime numbers that are the fundamental elements of arithmetic. Prime numbers cannot be factored into more basic components. They are divisible only by themselves and one: 2, 3, 5, 7, 11, 13, etc. The occurrence of prime numbers is unpredictable; they appear to be randomly scattered on the real number line. Riemann converts the chaotic disorderliness of prime numbers to a striking order, as we shall see.

The great intrigue of RH is that what appears to be a profound mathematical truth – relevant not only to arithmetic but to number theory, geometry, analysis, logic, and probability theory – elides proof. Furthermore, there are deep connections to quantum physics [3]. It has recently been suggested that quantum neurophysics provides an unexpected key to understanding RH [10]. A fresh look at RH will be undertaken here via non-Hermitean dual-mode QBD.

Considering the enormous variety and complexity of the mathematics that has been used in attempting to crack RH, it is surprisingly susceptible to an intuitive geometrical presentation. Recall the infinite harmonic series: $1 + 1/2 + 1/3 + 1/4 \dots$. The zeta-function adds a power to the denominator, specified by the argument, s , of the zeta-function.

$$\zeta(s) = 1 + 1/2^s + 1/3^s + 1/4^s \dots . \quad (11.2)$$

This can be rewritten as an Euler product of reciprocals of prime numbers, $1/p$, each p taken to the power specified by the argument, $1/ps$.

$$\zeta(s) = \prod_p (1 - p^{-s})^{-1} , \quad (11.3)$$

where \prod is the product ranging over all the primes, p .

Riemann envisioned the argument, s , of the ζ -function to be a complex number (c-number), from which it follows that the value is a c-number, too. (Zero is the c-number $0 + 0i$.) Specify different c-arguments and different c-values result.

Riemann envisioned a 3-dimensional geometry (R-3-space) for his hypothesis. The plane of Riemann's 3-dimensional zeta geometry is a complex plane (c-plane) whose points represent c-numbered arguments. Different c-arguments, s , are represented by different points on R-3-space's c-plane.

Now, the c-values of the ζ -function for the different c-arguments would take a c-plane, too, for their geometric interpretation, but Riemann has visually only one dimension left, a topography to sit on the argument c-plane. There is a facile mathematical maneuver that gets one dimension out of a c-plane. Just multiply the complex zeta value (for a specific argument) by its complex conjugate, then the imaginary dimension falls away, leaving a real-value (called the “modulus” of the c-number). By this mathematical trick the c-value can be geometrically realized as a real-value topography, mountains and valleys seated strangely on a complex argument plane. At certain points the real-value topography goes to sea level, where the value is zero, whereas at other points its peaks soar to infinity. There are both “trivial” and “nontrivial” zero values.

There is a “critical region” of the argument c-plane of R-3-space that lies between $\text{Re } 0$ and $\text{Re } 1$. When the real part of the argument is a negative number, the ζ -function is not well behaved, at $\text{Re} = 1$ the zeta value goes to infinity and for $\text{Re} > 1$ the zeta value quickly drops and plateaus. The

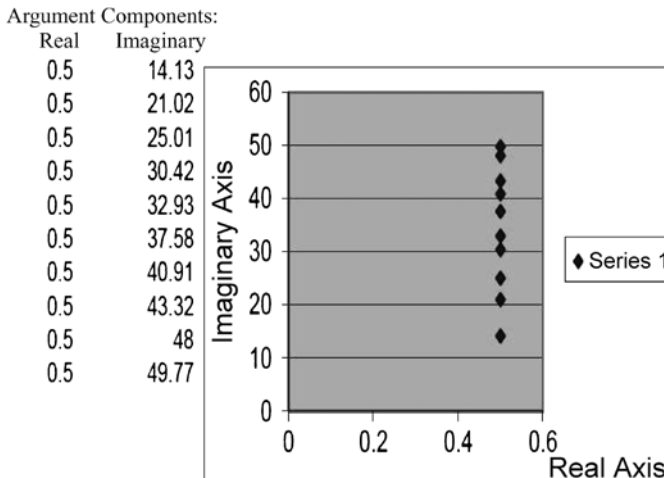


Fig. 11.1. The first ten nontrivial zeros (Series 1) of the Riemann zeta function (taken to two places) line up randomly on the “critical line” at Re 0.5, rather than being scattered about the complex argument plane

interesting region of the c-plane accordingly lies between 0 and 1 on the real axis.

Figure 11.1 shows a portion of the argument c-plane. The value topography is not represented, except for the nontrivial zeros. That is, only those c-arguments to the ζ -function whose c-values are nontrivially zero are marked. (Since the value topography goes to zero, it cannot be shown; instead the points on the argument c-plane where the value is nontrivially zero are marked.) As Fig. 11.1 shows, the nontrivial zeros are remarkably ordered, confined to the “critical line” at Re = 1/2. RH is that all nontrivial zero values of the ζ -function lie on this critical line. Billions of nontrivial zeros have been calculated and indeed all do lie on the critical line in the argument c-plane at Re = 1/2. The chaotic scattering of prime numbers on the real number line is retained as a chaotic scattering of nontrivial zeros. But instead of being scattered about the argument c-plane they are tightly ordered to the critical line. How might this be comprehended?

Riemann’s creativity cuts deeper than given thus far. Each value point can be conceived of as an oscillator with an amplitude and a frequency. Du Sautoy [23] interprets each point-oscillator as a *musical note* of a certain loudness and a certain pitch; geometry is transformed to music. As the real component of the argument increases from 0 to 1, the value note gets louder, and as the imaginary component of the argument increases, the value pitch goes higher. Equivalently, the amplitude of the value oscillation increases in going from Re 0 to Re 1 and the frequency of oscillation increases as the imaginary component increases. Geometrical and musical intuitions allow the discussion to climb with two hands.

There is another degree of freedom that du Sautoy brings out: *harmonics*. The value points/notes also vary in harmonics. Points with zero harmonics correspond to pure tones (as with a tuning fork). The nontrivial zero values of the ζ -function, all lined up on the critical line, are notes lacking harmonics. This means that the multiplied terms of the ζ -function (with their prime reciprocals taken to the power specified by the c -argument) are *balanced at the nontrivial zeros*. The overtones of unbalance do not arise there. At all other point-notes with nonzero values, there are harmonics. So now *the value topography becomes a musical landscape of harmonics*, with all points/notes having zero harmonics lined up perfectly on the critical line at $Re = 1/2$. Surely there is some profound significance to such a rigorously ordered state of affairs!

To review, the Riemann ζ -function takes reciprocals of primes, takes them to complex powers, and then multiplies them. Each value of the ζ -function can be considered a musical note with amplitude, frequency and harmonics. What sets nontrivial zero values apart is that their notes are pure, without harmonics, for certain c -arguments. Nontrivially zero values mean that the primes with certain c -exponents and multiplied achieve a perfect balance. An orchestra playing all the positive nontrivial zero values would be balanced, as du Sautoy brings out, in the sense that all notes are equally loud (having real part 0.5) and equally lack harmonics. Only the pitch would change across the nontrivial zeros. The “music of the primes”, then, is equally loud pure notes varying only in pitch. However, this picture does not explain why the real part is precisely 0.5. If the critical line passed through 0.75, the notes would still be equally loud and pure while varying in pitch.

Another degree of freedom can be added when quantum dual-mode considerations come into play: phase. Each point on the argument plane has a rotating phase arrow attached. Furthermore, the argument plane has dual-modes. Now the significance of the critical line being at $Re = 0.5$ comes into view.

Under thermofield logic, the real parts of dual-modes must add to one (due to energy conservation law). So as a non-Hermitean logic, when the real part of one mode increases, the real part of the other mode must decrease proportionally. It follows that the only place where the dual-modes can balance in amplitude is at $Re = 0.5$. Furthermore, the dual-modes are mirror images, so their frequencies must balance too.

But what of phase balance between dual-modes? This is the Heraclitean balance of polar opposites. The dual-modes are time reversed according to thermofield logic. As we move up the critical line, the phase arrow rotates clockwise in the non~mode and counterclockwise in the ~mode. Accordingly, the phase arrows come into the Heraclitean balance of polar opposites every 180 degrees of rotation.

The nontrivial zeros of the Riemann zeta function on the critical line at $Re = 0.5$, when considered in a dual q-mode framework, are points where

the dual-modes are equal in amplitude, mirror images in frequency, and polar opposites in phase. Points on the critical line that are not zero are expressions of dual-modes whose phases are not in Heraclitean balance.

Why are the nontrivial zeros scattered randomly on the critical line? The nontrivial zeros lie on a chaotic attractor due to nonlinearities of the ζ -function with phase introduced. The nontrivial zeros are instances of “Poincaré return”, when the chaotic attractor comes back aperiodically to its initial state. These concepts, then, can be thought together because they belong together: Prime numbers ... nontrivial zero values of the ζ -function ... pure tones (without harmonics) ... dual-mode \sim conjugate matches ... Being ... all stalks of a discourse sheaf. The dual-mode match at a point has three thermofield-logical criteria: 1) The dual amplitudes of oscillators at the point must be equal (which means it has to be somewhere on the critical line at $Re = 0.5$). 2) The dual frequencies at the oscillator-point are negative mirror images (reflected symmetrically about the real axis). 3) The dual phases at the oscillator-point must be polar opposites. The achievement of “balance” must meet all these criteria. Riemann’s hypothesis is about points of abstract Being, points of dual-mode belonging together, points that balance in amplitude, frequency and phase.

11.6 Monadological Implications of Non-Hermitean Dual-Mode QBD

The ontological richness offered by dual-mode QBD, hoisting Being in the match of the between, forces a profound change in the way that we view ourselves and the world in which we find ourselves. Common sense has it that our subjective consciousness is in some sense “immanent” and world is “transcendent”. Since the brain is part of this world, the more specific issue is that consciousness is immanent and its tightly correlated brain is transcendent [22]. The correlates are categorically distinct, and so any causal arrows are thrown into question. The correlates immanent consciousness and transcendent brain remain on different sides of an ontological divide to which common sense is committed.

Imagine that each brain is a windowless monad [19], rather than a wet computer. Weighted possibilities are interpenetrated in the monad’s fluctuating attunement. Actualities are continually unfolded within each monad in the match between the brain monad’s situatedness and input from reality. World-thrownness is continually disclosed in the \sim conjugate match between dual modes during waking and in dreaming too [8]. Monads with by and large the same attunement learned through local socialization practices, and by and large the same input, will constitute by and large the same world. There is no world-in-common transcendent to our consciousnesses but parallel monadic world-thrownnesses, hoisted by scattered monads that are entranced

by *maya*, the illusion of a world-in-common. Despite intense human involvement in social activity and our seeming prowess in the world, we are each confined to our solitary monad.

In quantum mechanics and quantum field theory the Hermitean assumption gets you ontologically to the general vicinity of Being/Presence/“is”, but only to probabilities of Being. What actually “is”, within the framework of classical quantum theory, requires an observer who stands outside and knows, after measurement, how things actually turned out. The observer gets quantum physics from probability to actuality. Without the observer quantum theory is completely blind to observables, having only mights and coulds, filled with probabilized possibility. The Hermitean assumption gets you to Being without fuss . . . any bother about Being, let the philosophers figure it out.

Dual-mode QBD has no need of any Hermitean assumption, because Being is already a quantum brain dynamical state, experienced as world-thrownness, the unique state of dual-mode match in the vacuum state of quantum brain dynamics. “Thrownness” is the groundlessness of our existence. We always find ourselves already thrown amidst the world along the particular world line of our existence. Our existence is abgrounded, and horrible dictu! This abgrounded existence is monadic. A monadic groundless existence . . . not a pretty picture!

The monad is filled with possibility. The possibilities are interpenetrated, a quantum superposition, a plenum of enfolded possibilia, a *holoworld* [8]. The possibilities are traces of actualities, all “enfolded” [1] to a holoworld of weighted (“tuned”) possibilia. Actualization of a possibility is an internal process of the monad. The monad’s holoworld meets representatives of physical reality . . . and world-thrownness unfolds in their vacuum state ~conjugate match. Unexpectedly, this is consistent with the perennial philosophy’s *maya* doctrine.

The monadic stalk of discussion and the stalk of *maya* intersect here. *Maya* is popularly interpreted in a superficial way: There is a true world reality around us, which until enlightened we each distort and, held rapt by *maya*, we believe in our own distortion. Here the illusion is a distortion. More deeply interpreting *maya*, there is no true world reality around us . . . the whole experience of being amidst world affordances is constituted within the monad. In the common interpretation *maya* is a potentially correctable cognitive illusion, whereas in the monadic interpretation *maya* is far scarier, an inescapable ontological illusion.

Co-monads agree about what’s now, so long as they have been similarly tuned by local social practices and have similar inputs, so similar world-thrownnesses are unfolded from co-monads’ similarly tuned holoworlds. This social consensus about the world powerfully reinforces *maya*, which narcotizes for each of us our true existential monadic state: scattered bubbles of lighted world disclosure, unfolded to presence from a dual-mode abground by the monad’s surrounding reality.

What happens to “consciousness” in this account? Consciousness is no longer perceptual, not an immanent consciousness-of-transcendent-Being, but pure thought, Descartes’ *res cogitans* deleted of all substantival properties. This is a consciousness blinded, confined to thought, a consciousness decentered, succeeded by world-thrownness. Finding oneself thrown amidst (*bei*) the world, as one always does, already thrown, is a monadic state of the dissipative quantum brain.

Consciousness, shorn of perception, becomes the Cartesian *cogito*. *Cogito* is linguistic; I think in words. A quantum brain theory of “consciousness” in the limited sense of the *cogito* awaits development.

11.7 Comment

The revolutionary potential of quantum brain theory has been overlooked because brain science is sanguine in its great success and because q-brain theory has been enlisted to the very familiar cause of computation. At its inception, quantum physics was extremely revolutionary for common sense, and this gives us reason to expect that quantum brain theory will be extremely revolutionary for the way we ordinarily think about the brain, too. The paradigm shift in the scientific revolution of quantum physics should not stop with physics. Quantum brain theory should be revolutionary for brain science too. “Scientific revolution” and “paradigm shift” (Kuhn [17]) are terms so widely applied that they have lost their shock value. Thus does convention sap the language of deep change. Quantum brain theory, if on the right track, is a scientific revolution if there ever was one. Common expectations about what the brain is doing ought to be overturned, if the brain really does have quantum degrees of freedom, as I have argued.

The preceding discussion has shown a way of thinking about the dissipative brain, initially developed by Umezawa and coworkers, and fleshed out to a dual-mode quantum brain dynamics whose operators are non-Hermitean. The quantum brain might supplement the classical brain’s computational abilities, but in addition the quantum brain, in virtue of its vacuum state between-two, has a revolutionary new ability: *de novo* generation of Being in the \sim conjugate vacuum state match.

Profound shock, sign of true revolution, can now be experienced in our thrown existential condition, once it is seen to be monadological. The Ab-ground’s indivisible duality is originary and our respective lives of monadic disclosure are strewn about in the case that the dual-modes match \sim conjugately. The shock of this is our thrown, existential isolation, once the chains of *maya* are broken by a monadological form of quantum brain theory. We are unable, in our usual “fallen” pragmatic mode, to break the chains of *maya*. One cannot help but believe in the transcendent world always already encountered, and this obligation soothes our wrenching monadic isolation. But once our true monadic state has been clearly recognized, we cannot forget; so we

must carry on paradoxically, with revolutionary thermofield-monadological brains, believing in the world without believing . . .

References

1. Bohm, D. (1980). *Wholeness and the Implicate Order*. London and Boston: Routledge and Kegan Paul).
2. Davydov, A.S. (1991). *Solitons in Molecular Systems*. (Dordrecht: Kluwer).
3. Derbyshire, J. (2003). *Prime Obsession*. Washington: Joseph Henry Press.
4. Derrida, J. (1981). *Dissemination* (B. Johnson Trans.). Chicago: University of Chicago Press.
5. Derrida, J. (1982). *Margins of Philosophy*, trans. A. Bass, (Chicago: University of Chicago Press).
6. Feigl, H. (1967). *The 'Mental' and the 'Physical'*. Minneapolis: University of Minnesota Press.
7. Fröhlich, H. (1968). *Journal of Quantum Chemistry*, **2**:641–649.
8. Globus, G. (1987). *Dream Life, Wake Life*. (Albany: State University of New York Press).
9. Globus, G. (2003). *Quantum Closures and Disclosures* (Amsterdam and Philadelphia: John Benjamins).
10. Globus, G. (2004). In *Brain and Being*, (eds.) G. Globus, K. Pribram & G. Vitiello (Amsterdam: John Benjamins).
11. S. Hagan, S.R. Hameroff, and J.A. Tuszyński (2002). *Physical Review E* **65**, 61901:1–10.
12. Heidegger, M. (1962 [1927]). *Being and Time*, trans. J. Macquarrie and E. Robinson, (New York: Harper and Row).
13. Heidegger, M. (1999), *Contributions to Philosophy* (from Enowning), P. Emad and, K. Maly, Trans. (Bloomington: Indiana University Press).
14. Jibu, M., Hagan, S., Hameroff, S.R., Pribram, K.H., and Yasue, K. (1994). *Biosystems* **32**:195–209.
15. Jibu, M. and Yasue, K. (1995). *Quantum Brain Dynamics and Consciousness* (Amsterdam and Philadelphia: John Benjamins).
16. Jibu, M. and Yasue, K. (2004). In *Brain and Being*, (eds.) G. Globus, K. Pribram, and G. Vitiello (Amsterdam: John Benjamins).
17. Kuhn, T. (1976). *The Structure of Scientific Revolution*. Chicago: University of Chicago Press.
18. McCrone, J. (2003). *The Lancet Neurology* **2**:450–452.
19. Nakagomi, T. (in press). In *Brain and Being*, (eds.) G. Globus, K. Pribram, and G. Vitiello (Amsterdam: John Benjamins).
20. Natsoulas, T. (1978). *American Psychologist* **33**:906–914.
21. Ricciardi, L.M. and Umezawa, H. (1967). *Kybernetik*, **4**:44–48.
22. Rorty, R. (1979). *Philosophy and the Mirror of Nature* (Princeton: Princeton University Press).
23. Sautoy, M. du (2003). *The Music of the Primes*. (New York: HarperCollins).
24. Seife, C. (2000). *Science* **287**, 791.
25. Stuart, C.I.J.M., Takahashi, Y., and Umezawa, H. (1978). *Journal of Theoretical Biology* **71**:605–618.

26. Stuart, C.I.J.M., Takahashi, Y., and Umezawa, H. (1979). *Foundations of Physics* **9**:301–327.
27. Takahashi, Y. and Umezawa, H. (1975). *Collective Phenomena* **2**:53–80.
28. Takahashi, Y. and Jibu. In *Brain and Being*, (eds.) G. Globus, K. Pribram, and G. Vitiello (Amsterdam: John Benjamins).
29. Tegmark, M. (2000). *Physical Review*, **E61**:4194–4206.
30. Umezawa, H. (1993). *Advanced Field Theory: Micro, Macro, and Therma Physics* (New York: American Institute of Physics).
31. Umezawa, H. (1995). *Mathematical Japonica*, **41**:109–124.
32. Vitiello, G. (1995). *International Journal of Modern Physics B*, **9**:973–989.
33. Vitiello, G. (2001). *My Double Unveiled* (Amsterdam and Philadelphia: John Benjamins).
34. Vitiello, G. (2004). In *Brain and Being*, (eds.) G. Globus, K. Pribram, and G. Vitiello (Amsterdam: John Benjamins).

12 The CEMI Field Theory: Seven Clues to the Nature of Consciousness

Johnjoe McFadden

Summary. In this chapter I examine seven clues to the nature of consciousness and explore what they reveal about the underlying physical substrate of consciousness. The consciousness clues are: it impacts upon the world; it is a property of living brains but no other structure; brain activity may be conscious or unconscious; the conscious mind appears to be serial; learning requires consciousness but recall doesn't; conscious information is bound; and consciousness correlates with synchronous firing of neurons. I discuss field theories of consciousness and introduce the conscious electromagnetic field (CEMI) theory that suggests that consciousness is a product of the brain's electromagnetic field. I show that the CEMI field theory successfully accounts for each of the seven clues to the nature of consciousness. Finally, I show that although current quantum mechanical theories of consciousness are also field theories, they are physical untenable and should be discarded.

12.1 Why Do we Need a Theory of Consciousness?

A theory of consciousness is only necessary if there is something that needs to be explained. With several journals, hundreds of books and ruminations of thousands of philosophers cogitating over various theories of consciousness, it may seem that this question must obviously be answered in the affirmative. I agree. But it is instructive to explore exactly why we need a theory, because the answer isn't as obvious as we may suppose.

Firstly, if what we are discussing is a scientific theory then such a theory is only of value if it explains facts in the world. This immediately drops out of consideration any steam whistle "theory" where it is supposed that the consciousness is merely an epiphenomenon. I don't for one moment believe that this is the case but there is a considerable body of opinion that asserts that consciousness has no impact on the way our brain works. If this is the case then consciousness makes no difference to the world; it generates no facts. Science can only deal with facts – data points, observations, phenomena. Scientific theories are a means to make sense of those facts in order to make predictions. Without the facts, there can't be any theories – at least none that are scientific. If consciousness is an epiphenomenon then, as scientists, we must turn aside and leave the topic to the philosophers and theologians to make sense of. It is not a subject for scientific theories.

But consciousness does of course generate phenomena. One of the most obvious is this chapter, and indeed this book, and all the other books and articles that have ever been written on the subject. If consciousness is an epiphenomenon locked inside our brain then why does our body write endless treatises on it? How does it even know it's there? The train isn't aware of the steam whistle; it has no impact on its function. But consciousness has had a major impact on the lives of philosophers, scientists and theologians who have studied the subject. It cannot be a steam whistle.

The approach in this chapter will be to examine seven clues to nature of consciousness and discuss how the conscious electromagnetic field theory (CEMI field theory) makes sense of those clues. Space constraints do not permit me to examine the other theories of consciousness against these clues, but it would be an interesting exercise for the reader to attempt this, at least for their favorite theory. The first clue, is what I have already discussed, the fact that consciousness has an effect on the world. Any theory must include a physical mechanism that allows our conscious mind to interact with the matter of our brain.

Clue 1: *Consciousness generates phenomena in the world. It is a cause of effects.*

The next clue to the nature of consciousness is the fact that it is associated with living flesh in particular configurations that we call brains. The type of brain that most clearly exhibits the phenomenon is a subtype of the basic design, called the human brain. We can (for the reasons discussed above) be pretty sure that our own brain and other people's brains are conscious (ignoring, because it is too unspeakably dull to even discuss, the solipsism argument) and most would make a case for the brains of higher animals, such as chimps, sharing that property, at least in some form. But not all living flesh is conscious. Our livers aren't conscious. Neither is our colon nor our kidneys. Only brains are conscious. So it must be something about the structure of brains that generates the phenomenon of consciousness. This fact requires an explanation.

Clue 2: *Consciousness is a property of living (human) brains. As far as we know, it is not a property of any other structure.*

Brains are of course involved in many activities but they share a common theme: information processing. But consciousness cannot simply be a property of information-processing systems. For a start, the brain isn't the only information processing system in the body. It's not even the most complex. With 10^{12} cells (compared to 10^{11} neurons in the brain), the immune system processes a vast amount of information concerning the interaction between the body and its environment. Like the brain, the components of the immune system (lymphocytes, macrophages, dendritic cells, etc.) communicate

via a complex network of chemical signaling pathways. But the system completely lacks awareness.

And of course, artificial information processing systems, thus far at least, are not conscious. Despite the heady predictions of artificial intelligence (AI) pioneers in the 1960s and 1970s, no computer has ever shown even the faintest glimmerings of either general intelligence or consciousness. Even Marvin Minsky, champion of AI and cofounder of MIT's Artificial Intelligence Laboratories recently complained, "There is no computer that has common sense. We're only getting the kind of things that are capable of making an airline reservation. No computer can look around a room and tell you about it." (Interview with WIRED magazine, August 2003 [45].) And although the computing power of any single computer is puny compared to the human mind, the internet links together millions of computers (volume is set to exceed 15 terabytes per second by 2008) yet no spark of awareness has ever emerged from all those computations. Any theory of consciousness must explain why, thus far at least, only the wet systems that process information through neurons possess awareness.

But even living human brains aren't always aware. Our brain remains very active in the state we call unconsciousness, and even when we are conscious, we are only aware of a very small trickle out of the vast quantity of information flowing through our brain. Activities (like driving a car) may be performed on "automatic pilot" while our conscious mind is engaged elsewhere. Any theory of consciousness that fails to account for the difference between conscious and unconscious brain activity is clearly incomplete.

Clue 3: *Brain activity may be conscious or unconscious.*

It is useful to compare lists of those brain activities that are always unconscious (obligate unconscious), brain activities that may or may not be performed consciously (facultative conscious) and those activities that are always accompanied by awareness (obligate conscious, Table 12.1). Examination of the list highlights several interesting features. Firstly, there is clearly a tendency for the more primitive activities – those we share with lower animals and even plants – to be performed unconsciously and the more specialist activity – the strictly human actions, like use of language – to be accompanied by awareness. Why should this be? A straightforward explanation based on complexity – the more complex the information processing going on in the brain the more likely it is to be conscious – doesn't work. Imagine driving, alone in your car, along a familiar route. Your conscious brain may be reviewing the day's activities, planning an evening's entertainment or considering the latest football scores. You are unlikely to be aware of the numerous adjustments to the car's direction and velocity that your body will be making to maintain the vehicle on the road and prevent collision. These operations must require the information-processing capabilities of millions of neurons in the brain's visual system and motor centers, but you will be aware of none of

Table 12.1. Brain activity

Brain activity		
<i>Obligate unconscious</i>	<i>Facultative unconscious</i>	<i>Obligate conscious</i>
Endocrine control	Breathing	Reading
Temperature homeostasis	Maintaining balance during locomotion	Writing Creative activity
	Learned activities, such as driving or riding a bicycle	Learning Conversing
	Eating	Arithmetic
	Recalling information	Memorizing information

it. And then you feel a tap on your shoulder. You are not alone! The information processing associated with the sensory perception of that tap is likely to be vastly simpler than those involved with your driving manipulations but you will be acutely aware of one and oblivious of the other. Complexity per se cannot account for why we are aware of some, but not all brain activity.

So, if it isn't complexity, how else do our conscious and unconscious minds differ? Does the list provide us with further clues? I believe it does. Firstly, there is a very clear and stark difference between conscious and unconscious brain activity. Our brain is clearly able to perform several operations in parallel, if they are all unconscious. Nobody has trouble riding a bike whilst whistling a familiar tune. We can all drive a car whilst chewing gum. But try reading a book whilst writing a letter; or add up two six figure numbers whilst chatting to a friend. These operations must be performed sequentially. Any theory of consciousness must explain why our unconscious mind appears to be massively parallel but our conscious mind is infuriatingly serial. The question, as Bernard J. Baars puts it [4], is how does "a serial, integrated and very limited stream of consciousness emerge from a nervous system that is mostly unconscious, distributed, parallel and of enormous capacity".

Clue 4. *The unconscious mind can perform parallel computations but consciousness appears to be serial.*

It is also interesting to consider why it is that the *higher* level activities that require consciousness, reading, writing (language use generally), arithmetic, etc., are all restricted to humans. The simplest explanation is that these capabilities evolved fairly recently and that they *require* the unique computation capabilities of the conscious mind: they simply can't be done with the unconscious mind, despite it having the same neuronal resources at its disposal. Any theory of consciousness must clearly delineate the operational difference between these systems.

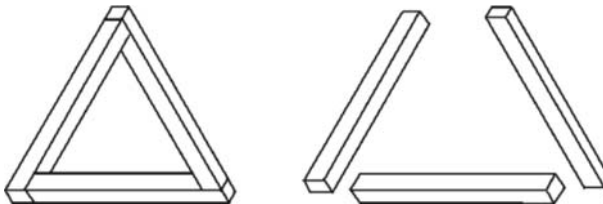
It is also intriguing that the obligate conscious activities include memorizing information and learning, but recall of memorized information (such as the motor actions required to perform a learnt task) does not require consciousness. When learning a task such as playing the piano, one's first plodding fingering of the keys is painfully conscious but, once learnt, a practised pianist can effortlessly play a familiar tune whilst singing the accompanying song. Indeed, learning a skill seems largely to be about driving its accomplishment into our unconscious mind. Another aspect of this dualism is the fact that our visual system is constantly analyzing the changing scenery as we go through our day, but we only recall those items that we thought about. The memory of everything else is lost. Any theory should explain why our conscious mind appears to be the conduit for delivering information to our memory but is not required for its retrieval.

Clue 5: *Learning and memory require consciousness but recall may be unconscious.*

The next clue to the nature of consciousness is usually known as the binding problem and is perhaps the most problematic, because it relies on introspection. Look at a tree. How many leaves do you see? Tens, hundreds, thousands? The problem for science is that the information encoding all those leaves – their colour, texture, position in space – is being processed in quite distinct regions of your brain. There is of course no problem in accounting for the functionality of such a system. So long as the multiple independent pathways in the brain come together at some point to provoke an appropriate response, “this is a tree”, then the system is functioning appropriately. A computer that similar dissects the complex scene and processes that information – perhaps in a set of quite independent but parallel processors – would generate the same response. But a computer would not be provoked into writing, “I think that I shall never see; a poem as lovely as a tree.” (Joyce Kilmer). To understand such a line, you need to see the whole tree. And that is of course what we all report. We do not see individual leaves or scattered contours; we see the tree in all its leafy glory, as a single percept. Where does all the information come together? As Valerie Hardcastle (1994) put it [23], “given what we know about the segregated nature of the brain and the relative absence of multimodal association areas in the cortex, how [do] conscious percepts become unified into single perceptual units?”.

It has of course been argued that the binding problem is a *pseudoproblem* since conceptual binding is part of the grand-illusion [5, 10]. According to the grand-illusion hypothesis, visual scenes (or any other bound aspect of consciousness) are actually as fragmented as the neuronal information within our brains but our minds somehow fool us into thinking the information is all stuck together. I fully accept that our visual experience is not as rich as we naively assume and the stream of consciousness may actually be closer to a dribble. However, despite this, binding remains a problem even within the

grand-illusion hypothesis. “Change blindness”, “inattentional blindness” and other cognitive effects indicate that our conscious mind can attend to only five or six objects within a visual scene but each attended object is a complex item whose informational content must be bound within consciousness. This can be illustrated by considering optical illusions, such as the familiar “impossible triangle”.



The geometric inconsistencies of the object are a property of the percept corresponding to the whole object, not a collection of its parts. During the information processing performed first by the retina and then by neurons in the visual cortex, information corresponding to various properties of the object (in this case just lines and angles but normally including color, texture, shading, etc.) is stripped, separated, handled and processed by thousands of distinct neurons. However, the illusion only makes sense if this disparate information is somehow bound together again within our conscious minds to generate a unified percept of the triangle.

Clue 6: *Information that is encoded by widely distributed neurons in our brain is somehow bound together to form unified conscious percepts.*

There is of course no center of the brain where all this information is put together, but it is well established that there are a number of *correlates of consciousness* – dynamic activity that is usually associated with attention and awareness. The best studied of these is synchronous firing of neurons [8, 27, 11–15, 19]. For instance, Wolf Singer and colleagues at the Max Planck Institute for Brain Research in Frankfurt [27] demonstrated that neurons in the monkey brain that responded to two independent images of a bar on a screen fired *asynchronously* when the bars were moving in different directions but fired synchronously when the same bars moved together. It appeared that the monkeys registered each bar as a single pattern of neuronal firing but their *awareness* that the bars represent two aspects of the same object, was encoded by synchrony of firing. In another experiment that examined interocular rivalry, it was discovered that neurons that responded to the attended image fired in synchrony, whereas the same neurons fired randomly when awareness was lost [18]. In each of these experiments, awareness correlated, not with a pattern of neuronal firing, but with synchrony of firing. Singer, Eckhorn and others have suggested that these 40–80 Hz synchronous oscil-

lations link distant neurons involved in registering different aspects (color, shape, movement, etc.) of the same visual perceptions and thereby *bind* together features of a sensory stimulus [12, 41, 42]. However, if synchronicity is involved in perceptual binding, it is unclear how the brain uses or even detects synchrony.

Clue 7: *Consciousness and awareness are associated not with neural firing per se but with neurons that fire in synchrony.*

12.2 Field Theories of Consciousness

The idea that our conscious minds are some kind of field goes back at least as far as the gestalt psychologists of the early twentieth century. Gestalt psychology emerged in opposition to the contemporary atomist movement, which claimed that perceptual experience is merely the sum of simple sensory inputs. The gestalt psychologists instead emphasized the holistic nature of perception that they claimed was more akin to fields, rather than particles. In this they were influenced by the ideas coming out of the newly emerging science of quantum mechanics (indeed, Wolfgang Köhler, one of the gestalt pioneers, studied with Max Planck, the founder of quantum mechanics). Fields share the holistic qualities of perceptual fields described by the gestalt psychologists but the Gestalt psychologists went on to propose that physical fields exist in the brain that are *isomorphic* to the objects they represented, in the sense that they had the same shape as the represented object. Palmer [36] generalizes this notion by distinguishing between intrinsic and extrinsic representation and claims that representation is intrinsic “whenever a representing relation has the same inherent constraints as its represented relation... [whereas] representation ... is extrinsic whenever the inherent structure of a representing relation is totally arbitrary and that of its represented relation is not.” A model motorcar is thereby an intrinsic representation of an actual motorcar, whereas the word “motorcar” is an extrinsic representation of the same object.

It was the proposal that the brain contains real physical fields that correspond to perceived objects (as Kohler described it, that the brain acts as a “physical Gestalt”) that led to the virtual abandonment of Gestalt psychology in the late 1950s. Modern neurobiology defined the neuron as the fundamental computational unit in the brain and there didn’t appear to be any way of forming isomorphic gestalt fields out of static neurons. But although much of what the brain does can be understood in terms of standard neuronal theory, the peculiar features of consciousness led many to retain the concept of a field in order to account for these properties. Karl Popper [39] proposed that consciousness was a manifestation of some kind of overarching *force field* in the brain that could integrate the diverse information held in

distributed neurons. The idea was further developed and extended by Lindahl and Århem [30] and by Libet [28, 29]. However, these authors considered that the conscious mind could not be a manifestation of any known form of a physical field and its nature remained mysterious.

Yet it has been known for more than a century that the brain generates its own electromagnetic (em) field, a fact that is widely utilized in brain scanning techniques such as EEG. In two papers published in 2002 I described the conscious electromagnetic field theory [35, 34], which was an extension of the CEMI field theory outlined in my book “Quantum Evolution” [33]. The theory has much in common with the electromagnetic field theory of consciousness proposed by Dr. Susan Pickett in her book “The Nature of Consciousness: A Hypothesis” [38]. The neurophysiologist E. Roy John has also recently published a theory of consciousness involving electromagnetic fields [26]. The key insight of these theories is the realization that, as well as generating chemical signals that are communicated via conventional synapses, neural firing also generates perturbations to the brain’s electromagnetic field.

12.3 The Brain’s Electromagnetic Field

At rest, the neuronal membrane forms a dipole in which the inside of the membrane is negatively (about -65 mV) charged in relation to the outside of the membrane. This charge difference is maintained by the action of ion pumps that pump cations (principally sodium and calcium) out of the neuron. Brain neurons are densely packed, with about 10^4 neurons/ mm^2 so the fields of adjacent neurons will not be discrete but form a complex overlapping field made up of the superposition of the fields of millions of neurons in the vicinity. The electrical field at any point in the brain will be a superposition of the induced fields from all of the neurons in the vicinity and will depend on the geometry and the dielectric properties of neurons and tissue. The combined activity of all the neurons in the brain generates a complex electromagnetic field whose strength can be estimated from theoretical principles and measured during EEG or MEG, and is about $20\text{--}250\text{ V/m}$ [34].

When any neuron receives a signal from upstream neurons, synaptic transmitters stimulate ion pumps that cause the membrane to become more or less negatively polarized, depending on the type of signal received. If the membrane charge falls below about -40 mV then the neuron “fires” and a chain of depolarizations is triggered that travels along the neuron and stimulates release of neurotransmitters. Conventional neurobiology has focused on the chemical signal that is transmitted from one neuron to another. There is absolutely no doubt at all that most of the information processing performed by the brain is due to this type of signaling. However, the massive membrane depolarization will also generate an electromagnetic field perturbation that,

traveling at the speed of light, will influence the probability of firing of adjacent neurons. Vigmond [44] modeled the electrical activity of pyramidal cells and demonstrated that neuron firing induced a peak of intracellular potential in receiver cells that ranged from a few microvolts to 0.8 mV, decaying with approximately the inverse of distance between the cells. For neurons that are arranged randomly, their induced fields will tend to sum to zero; but the laminar organization of structures such as the neocortex and hippocampus, with parallel arrays of neurons, will tend to amplify local fields. Using the model, a peak *intracellular voltage* of 2600 V/m (and thereby above the thermal noise level in the membrane) will be induced in receiving cells if they are located within a radius of 73–77 μm from the source cell [34]. Considering only those cells in the plane of the source cell embedded in the human cerebral cortex (about 10^4 neurons/mm²), then approximately 200 neighboring cells will be within that field volume. The firing of a single neuron will thereby be capable of modulating the firing pattern of many neighboring neurons through field effects.

12.4 The Influence of the Brain's Electromagnetic Field on Neural Firing

The field across a neuronal membrane will inevitably be the product of the field generated by membrane dynamics (the ion pumps) but also the fields generated by the resting states and firing of all the other neurons in the vicinity. Mostly, the influence of the endogenous fields will be quite weak – maybe up to a millivolt of induced voltage across the neuronal membrane [34] – and so will only be capable of influencing the probability of firing if the neural membrane is already close to the critical firing potential. However, in a busy brain it is very likely that many neurons will be in that state, so the electromagnetic field that the brain's activity generates will inevitably influence neural dynamics. This will create a self-referring feedback loop that, I propose, is the physical substrate of consciousness.

Unfortunately investigating the role of the brain's endogenous electromagnetic field on information processing in the brain presents huge experimental challenges, as it is not possible to turn the electromagnetic influence off and on (nerve firing always generates electromagnetic field perturbations). But indirect evidence for the proposal that the brain's endogenous field plays a role may be gained from studies of the effect of external fields on neural activity. In humans, the strongest evidence for the sensitivity of the brain to relatively weak electromagnetic fields comes from the therapeutic use of transcranial magnetic stimulation (TMS). In TMS, a current passing through a coil placed on the scalp of subjects is used to generate a time-varying magnetic field that penetrates the skull and induces an electrical field in neuronal

tissue. The precise mechanism by which TMS modulates brain activity is currently unclear but is generally assumed to be through electrical induction of local currents in brain tissue that modulate nerve firing patterns. TMS has been shown to generate a range of cognitive disturbances in subjects including: modification of reaction time, induction of phosphenes, suppression of visual perception, speech arrest, disturbances of eye movements and mood changes [21]. The field induced in cortical tissue by TMS cannot be measured directly but may be estimated from modeling studies. The evoked field depends critically on the instrumentation, particularly the coil geometry and strength and frequency of the stimulating magnetic field. In one study where stimulation utilized a set of four coils, the induced electrical field was estimated to be in the range of 20–150 V/m [16]. TMS voltages are thereby in the range of tens of volts per meter, values that are typical for the strength of the brain's endogenous electromagnetic field. Since TMS induces modulations of the brain's electromagnetic field that affect brain function and behavior, it follows that the brain's endogenous field must similarly influence neuronal computation.

There is also very solid *in vitro* evidence for very weak em fields modulating neuronal function. Fields as weak as 10–20 V/m have been shown to modulate neuron-firing patterns of Purkinje and stellate cells in the isolated turtle cerebellum *in vitro* [9] or the guinea-pig hippocampus [25]. A molluscan neuron has even been shown to be capable of responding to earth-strength (about 45 µT) magnetic fields [31], associated with induced electrical fields of just 2.6×10^{-4} V/m.

12.5 The CEMI Field Theory

It is clear that very weak electromagnetic field fluctuations are capable of modulating neuron-firing patterns. These exogenous fields are weaker than the perturbations in the brain's endogenous electromagnetic field that are induced during normal neuronal activity. The conclusion is inescapable: the brain's endogenous electromagnetic field must influence neuronal information processing in the brain.

Information in neurons is therefore pooled, integrated and reflected back into neurons through the brain's electromagnetic field and its influence on neuron-firing patterns. This self-referral loop has physical and dynamic properties that precisely map with consciousness and are most parsimoniously accounted for if the brain's electromagnetic field is the physical substrate of consciousness. Conscious volition results from the influence of the brain's electromagnetic field on neurons that initiate motor actions. The conscious electromagnetic information (CEMI) field theory thereby proposes:

Digital information within neurons is pooled and integrated to form an electromagnetic information field. Consciousness is that component of the

brain's electromagnetic information field that is downloaded to motor neurons and is thereby capable of communicating its state to the outside world.

The CEMI field theory [34, 35] suggests that processing information through the wave-mechanical dynamics of the CEMI field provided a significant advantage to our ancestors that was captured by natural selection to endow our minds with the capability to process information through fields. MacLennan [32] has proposed that the brain is capable of field computing (which has many of the attributes of quantum computing) that may perform some operations with greater efficiency, or with fewer resources, than can be achieved in a digital system. In a similar way, optical holograms can perform convolution, deconvolution and Fourier transforms, at the speed of light, acting on massively parallel data sets. Sending information through the electromagnetic field may similarly confer novel information processing capabilities on the human brain that have been captured by our conscious mind.

12.6 Why don't External Fields Influence our Minds?

The high conductivity of the cerebral fluid creates an effective “Faraday cage” that insulates the brain from most natural exogenous electric fields. A constant external electric field will thereby induce almost no field at all in the brain [2]. Alternating currents from technological devices (power lines, mobile phones, etc.) will generate an alternating induced field, but its magnitude will be very weak. For example, a 60 Hz electrical field of 1000 V/m (typical of a powerline) will generate a tissue field of only $4 \times 10^{-5} \text{ V/m}$ inside the head [2], clearly much weaker than either the endogenous electromagnetic field or the field due to thermal noise in cell membranes. Magnetic fields do penetrate tissue much more readily than electric fields but most naturally encountered magnetic fields, and also those experienced during nuclear magnetic resonance (NMR) scanning, are static (changing only the direction of moving charges) and are thereby unlikely to have physiological effects. Changing magnetic fields will, however, penetrate the skull and induce electric currents in the brain. However, there is abundant evidence (from, e.g., TMS studies as outlined above) that these do modify brain activity. Indeed, repetitive TMS is subject to strict safety guidelines to prevent inducing seizures in normal subjects through field effects. High-frequency electric fields generated by cellular (mobile) phones would be expected to penetrate the head more effectively (limited by the electromagnetic skin depth – the distance in which the field is attenuated by a factor of e^{-1} – which for the head is about one centimeter) but their high frequencies (in the MHz or GHz range) make them unlikely to interact with low-frequency brain waves.

Note, however, that although external fields are seldom able to influence nerve dynamics, this will not be true for endogenous fields. Indeed, the fact

that EEG signals can be detected on the scalp indicates that endogenous electromagnetic fields do penetrate brain tissue. The reason for this is that the major source of EEG signals (and more generally, the brain's electromagnetic field) is not the firing of single neurons but assemblies of neurons firing synchronously (as discussed in my earlier paper). By firing in synchrony, neurons distribute and amplify field effects.

12.7 Does the CEMI Field Theory Account for the Seven Clues to the Nature of Consciousness?

Clue 1: *Consciousness generates phenomena in the world. It is a cause of effects.*

A distinctive feature of the CEMI field theory is the proposal that consciousness corresponds to only that component of the brain's electromagnetic field that impacts on motor activity. This does not imply that the brain's electromagnetic field acts directly on motor neurons (which may of course be located outside the brain) but only that electromagnetic field information is communicated to the outside world via motor neurons [35]. The site of action of the brain's electromagnetic field is most likely to be neurons in the cerebral cortex involved in initiating motor actions, such as the areas that control speech, or the areas involved in laying down memories that may later be reported via motor actions (such as speech). Indeed, there is a good deal of evidence [1, 37] that all verbal thought is accompanied by subvocalizations (i.e. motor cortex activity accompanied by appropriate but normally undetectable vocal tract activity). This informational download via the brain's electromagnetic field avoids the pitfalls of most other field theories of consciousness that either suffer the classic "mind–matter problem" (a nonphysical consciousness whose interaction with the matter of the brain is left unresolved) or leave consciousness as a *ghost in the machine* (somehow generated by the brain but with no impact on its workings).

We experience the influence of the CEMI field as *free-will*. This is why our willed actions feel so different from automatic actions: they are the effects of the CEMI field as cause. Therefore, although like modern cognitive theory the CEMI theory views conscious will as a deterministic influence on our actions, in contrast to most cognitive theories it does at least provide a physically active role for "will" in driving our conscious actions. In the CEMI field theory, we are not simply automatons that happen to be aware of our actions. Our awareness (the global CEMI field) plays a causal role in determining our conscious actions.

Clue 2: *Consciousness is a property of living (human) brains. As far as we know, it is not a property of any other structure.*

The only place in the known universe where electromagnetic fields occur that are capable of communicating self-generated irreducibly complex concepts like “self” (and thereby persuading an observer that they are indeed conscious) is in the human brain. Artificially generated electromagnetic fields, such as the electromagnetic fields that communicate radio and TV signals, are only capable of communicating the information encoded and transmitted within their fields. They have *nothing else to say*. To question whether they are either aware or conscious is meaningless.

Clue 3: *Brain activity may be conscious or unconscious.*

Neurons in a complex brain display a range of excitability and in the busy brain of our ancestral animals there would have been many neurons poised close to their threshold potential with voltage-gated ion channels sensitive to small changes in the surrounding electromagnetic field. No less than electrochemical interactions, those field interactions would have been subject to natural selection. Wherever field effects provided a selective advantage to the host, natural selection would have acted to enhance neuron sensitivity (e.g. by maintaining neurons close to firing potential, increasing myelination or orientating neurons in the field). Conversely, wherever field influences were detrimental to the host (e.g. providing an electromagnetic field “feedback” that interfered with informational processing), natural selection would have acted to decrease that sensitivity (e.g. by maintaining neurons at membrane voltages close to resting). Therefore, with just the information that the brain’s electromagnetic field influences informational processing (as I have shown it must) and thereby affects host survival, the theory of natural selection predicts that over millions of years a complex brain will evolve into an electromagnetic field-sensitive system and a parallel electromagnetic field-insensitive system. These systems correspond to our conscious and unconscious minds, respectively.

Clue 4: *The unconscious mind can perform parallel computations but consciousness can only do one thing at a time.*

Neuronal computation, like any neural network, is ideally suited to parallel computations. So our unconscious mind is capable of performing many tasks in parallel. However, if conscious actions involve the influence of an electromagnetic field – the CEMI field – on neural pathways, then this interference is entirely explicable. Unlike digital (neural) addition, summation of two fields is not a simple addition but generates a linear superposition that depends on the phase relationships between the individual waves involved. Interference is therefore inevitable for conscious multiple tasks that require the influence of the CEMI field. The field can only do one thing at a time.

Clue 5: *Learning and memory require consciousness but recall may be unconscious.*

The job of the brain is straightforward: to decide what the body should do next. Mostly in humans, and probably all the time for most animals, these decisions are made automatically by standard neural networks without influence of the CEMI field. However, occasionally the automatic pilot routines may come unstuck. You may be presented with a new or unfamiliar situation. It is at these times that your brain will be more likely to have lots of neurons whose membranes are poised close to the firing threshold: the undecided brain. These undecided neurons will be sensitive to the (relatively weak) influence of the brain's electromagnetic field. Your conscious mind will be required to make a decision and the undecided neurons can plug into the vast quantity of information stored in the CEMI field. This proposed role for the CEMI field in brain activity in modulating neural activity is similar to what William James envisaged more than a century ago (as quoted in [40]) "if consciousness can load the dice, can exert a constant pressure in the right direction, can feel what nerve processes are leading to the goal, can reinforce and strengthen these and at the same time inhibit those that threaten to lead astray, why, consciousness will be of invaluable service".

So the CEMI field – our conscious mind – will be pushing and pulling on neurons to shift the brain towards some desired activity; like learning to play the piano. The CEMI field will initially be required to provide that fine control of motor activity necessary to perform the novel actions. But, if the target neurons for electromagnetic augmentation are connected by Hebbian synapses then the influence of the brain's electromagnetic field will tend to become hard-wired into either increased (long-term potentiation, LTP) or decreased (long-term depression) neural connectivity. After repeated augmentation by the brain's electromagnetic field, conscious motor actions will become increasingly independent of electromagnetic field influences. The motor activity will be "learned" and may thereafter be performed unconsciously, without the electromagnetic influence on the neural networks involved. We will then be able to play without conscious input. Similarly, in the absence of any motor output, the CEMI field may be involved in strengthening synapses to "hard-wire" neurons and thereby lay down long-term memories.

Clue 6: *Information that is encoded by widely distributed neurons in our brain is somehow bound together to form unified conscious percepts.*

Information in the conscious brain is encoded in the firing rates of billions of neurons scattered across the entire surface of the cerebral cortex. However, that information will be reflected into the electromagnetic field that permeates the cortex. In contrast to the discrete and distributed information encoded in the neurons, the field-based information is always unified.

Fields unify information. That is what we mean by a field. The brain's electromagnetic field has the same level of unity as a single photon. From the reference frame of an outside observer, a field is a continuum of values (information) extended in space and time. However, from the reference frame of the field, there is no space nor time between any part of the field or any bit of its information. This can be appreciated by following Einstein in imagining hitching a ride on the back of a photon. Because photons travel at the speed of light and time slows down to stop at this speed, it takes no time at all for the photon to travel from its point of creation to its point of annihilation – it is everywhere at once. So all of the information contained in the field is everywhere at once, bound into a single dimensionless point. The CEMI field theory proposes that consciousness resides in that dimensionless point.

Clue 7: *Consciousness and awareness are associated not with neural firing per se but with neurons that fire in synchrony.*

The superposition principle states that the em field at any point is a superposition of the component fields in the vicinity of that point. Like all wave phenomena, field modulations due to nerve firing will demonstrate constructive or destructive interference depending on the relative phase of the component fields. Temporally random nerve firing will generally generate incoherent field modulations leading to destructive interference and zero net field. In contrast, synchronous nerve firing will phase-lock the field modulations to generate a coherent field of magnitude that is the vector sum (the geometric sum – taking into account the direction of the field) of its components. The CEMI field – our conscious mind – will thereby be dominated by neurons that fire in synchrony. Synchronous firing will be a correlate of consciousness.

So the CEMI field theory accounts perfectly for each of the features of consciousness highlighted in the above seven clues. A challenge to any other theorist would be to do the same for their favorite theory of consciousness.

12.8 A Last Word, Concerning Quantum Theories of Consciousness

The em fields are not of course the only kind of field. Any quantum system may be described by a field and there is a great deal of interest in the possibility of quantum matter fields in the brain. However, whereas there is no doubt that electromagnetic fields exist in the brain there is no evidence for large-scale quantum coherence of matter in the brain on the scale that is necessary for quantum consciousness. There are also very real theoretical problems with understanding how quantum coherence in microtubules could be maintained for biological time scales [43]. The difficulty in maintaining

quantum coherence in order to perform quantum computing with just a few atoms maintained at a temperature close to absolute zero [17] is evidence for the implausibility of maintaining quantum coherence for physiologically relevant periods of time in a warm wet brain.

There are also many theoretical problems with quantum consciousness. Information in consciousness is undoubtedly complex and must be encoded by a physical informational substrate capable of encoding a complex message. Quantum consciousness theorists who propose that the physical substrate of consciousness is some kind of quantum state of matter, such as a Bose-Einstein condensate (BEC), often ignore this requirement. Even if it were physically feasible to maintain a BEC in a hot wet brain (which it isn't), such a state would be an unlikely substrate for consciousness because all the atoms in a BEC are in the same quantum state and thereby encode the same information. Quantum states are nearly always small and simple because as they get larger and more complex, it becomes harder to maintain all the information in a coherent state: the system decoheres. This is why quantum computation is so difficult (and why only very simple calculations have so far been performed with qubits).

A related problem is the fact that consciousness is continuous but temporally dynamic; so the contents of consciousness change on a time scale of milliseconds or less. The substrate of consciousness must therefore be similarly dynamic. However, dynamic quantum states of matter (such as the putative gigahertz oscillations of microtubule protein) decohere in nanoseconds or less. Quantum states of matter could therefore not remain coherent for long enough to encode the continuity of thought.

A further difficulty arises because consciousness exchanges information with the world. Whether this informational exchange is one way or in both directions depends on whether consciousness has a causal influence on the world. But this property is incompatible with large-scale coherence of matter as the substrate of consciousness, since information exchange of a quantum state with its environment is precisely what causes decoherence. It is simply not physically possible to maintain coherence within a large-scale quantum system if it is freely exchanging information with its environment.

Lastly, there is solid experimental evidence that appears to rule out large-scale quantum coherence mediated through microtubules, at least in the brain of mice. For quantum mechanics to account for binding, the microtubules must be entangled not only within single neurons but across the many millions of scattered neurons that encode conscious information. This is proposed to take place through “microtubule quantum states [that] link to those in other neurons and glia by tunneling through gap junctions (or quantum coherent photons traversing membranes)” [22]. However, a knock-out (KO) mouse has recently been generated that lacks the connexin-36 (Cx36) subunit of the principle gap junctions thought to be mediating neuronal electrotonic coupling mammalian brains [7, 20]. As expected, the connexin-36 KO mouse

lacks gap junctions and therefore lacks many (if not all) of the proposed sites for the putative inter-neuron quantum tunneling. Yet, the KO mice “showed no obvious behavioral abnormalities” [20]. The findings indicate that, if gap junctions are the site for tunneling of microtubule quantum states, then the process appears to play no obvious neurophysiological role, at least in mice. And although the question of whether mice are conscious is obviously a matter of conjecture, it would seem unlikely that a neurophysiological role for microtubules in man (information processing) could be completely absent in mouse. The lack of an obvious behavioral phenotype of the Cx36 mice undermines a central claim of the microtubule quantum consciousness theory.

Interestingly, the Cx36 KO mice provide evidence that supports the CEMI field theory proposal that electromagnetic fields are the substrate for conscious binding. As already discussed, synchronous neuronal firing is a correlate of attention and awareness and fast transmission of signals through gap junctions has previously been proposed to mediate synchrony. However, high-frequency synchronous neuronal oscillations are still observed in the Cx36 KO mice [24], indicating that other mechanisms (such as electromagnetic fields) may be involved in maintaining synchrony and thereby potentially providing a substrate for conscious binding.

Although quantum theories of consciousness based on microtubule coherence are highly tenuous, the CEMI field theory does not exclude the possibility of direct quantum effects in the brain. In my book “Quantum Evolution” [33], I proposed that the most likely source of quantum effects in the brain would not be microtubules (which have no established role in information processing) but interactions between the brain’s electromagnetic field and voltage-gated ion channels (with a clearly established role in information processing in the brain) in the neuronal membrane. Near to the neuronal cell body (where the decision to fire is made) the membrane potential is very close to threshold such that the opening or closing of just a few ion channels may be sufficient to trigger or inhibit firing. Opening of just a single ion channel *in vitro* has been shown to be capable of initiating an action potential [3]. The precise number of quanta of electromagnetic energy that must be absorbed from the surrounding field to open a single voltage-gated ion channel is currently unknown. The field has to push 7–12 charges of the channel molecule’s sensor towards the open position, but it is likely that when the membrane potential is already close to the firing threshold, very little additional energy need be absorbed from the field. Absorption of a single photon is sufficient to initiate proton pumping by the bacteriorhodopsin proton pump. It is therefore likely that nerve firing may in some circumstances be triggered (or inhibited) by just a few quanta of energy and thereby be subject to quantum dynamics. It is interesting to speculate on whether such uncaused events play a role in human spontaneity or creativity. Neils Bohr, the founding father of quantum mechanics, considered (according to Bohm) that it is likely that “thought involves such small amounts of

energy that quantum-theoretical limitations play an essential role in determining its character” [6]. It may be that to fully explain consciousness, we will have to bring quantum mechanics into our thinking. But what is needed is a quantum field theory for the brain’s electromagnetic fields, rather than yet more fruitless speculations on quantum coherence within microtubules.

12.9 Conclusions and the Way Forward

The CEMI field theory provides an elegant solution to many of the most intractable problems of consciousness and places consciousness within a secure physical framework that is amenable to experimental testing. The proposed interaction between the CEMI field and neuronal pathways restores to the mind a measure of dualism, but it is a dualism rooted in the real physical distinction between matter and energy, rather than the metaphysical (Cartesian) distinction between matter and soul. Although in the CEMI field theory, free-will is deterministic, it does at least retain a crucial role for our conscious minds in directing purposeful actions. Consciousness is not a steam whistle. As a wave-mechanical driver of free-will, it may be the key evolutionary capability that was acquired by the human mind.

There is no such thing as a theory that cannot be tested. In my first CEMI field paper, I highlighted eight predictions that were consequent on the theory [34]. In my follow-up paper [35], I discussed the implications of the theory for artificial intelligence (AI) and the possibility of engineering consciousness into an artificial system. Crucial areas that need to be tackled are the development of a mathematical model to examine the interaction between neurons and the brain’s electromagnetic field; analysis of the interaction between ion channels and the brain’s em field at a quantum-field level; exploration of the role of fields in information processing performed by biological neurons; and exploration of the potential role of electromagnetic fields in AI. With appropriate support, these issues could all be tackled within the coming years. Hopefully we will soon discover whether our minds are really electric.

References

1. Aarons, L. (1971). *Percept Mot Skills* **33**:271–306.
2. Adair, R.K. (1991). *Physical Review A* **43**:1039–1048.
3. Arhem, P. and Johansson, S. (1996). *Int J Neural Syst* **7**:369–376.
4. Baars, B.J. (1993). In *Experimental and Theoretical Studies of Consciousness*, (Chichester: Wiley): 282–303.

5. Blackmore, S.J., Brelstaff, G., Nelson, K., and Troćianko, T. (1995). *Perception* **24**:1075–1081.
6. Bohm, D. (1951). *Quantum Theory*. (Englewood Cliffs, NJ: Prentice Hall, Inc.).
7. Buhl, D.L., Harris, K.D., Hormuzdi, S.G., Monyer, H., and Buzsaki, G. (2003). *J Neurosci* **23**:1013–1018.
8. Buzsaki, G. and Draguhn, A. (2004). *Science* **304**:1926–1929.
9. Chan, C.Y. and Nicholson, C. (1986). *J Physiol (Lond)* **371**:89–114.
10. Dennett, D.C. (1991). *Consciousness Explained*. Boston: Little-Brown.
11. Eckhorn, R. (1994). *Prog Brain Res* **102**:405–426.
12. Eckhorn, R., Bauer, R., Jordan, W., Brosch, M., Kruse, W., Munk, M., and Reitboeck, H.J. (1988). *Biol Cybern* **60**:121–130.
13. Eckhorn, R., Frien, A., Bauer, R., Woelbern, T., and Kehr, H. (1993). *Neuroreport* **4**:243–246.
14. Engel, A.K., Kreiter, A.K., König, P., and Singer, W. (1991a). *Proc Natl Acad Sci USA* **88**:6048–6052.
15. Engel, A.K., König, P., Kreiter, A.K., and Singer, W. (1991b). *Science* **252**:1177–1179.
16. Epstein, C.M., Schwartzberg, D.G., Davey, K.R., and Sudderth, D.B. (1990). *Neurology* **40**:666–670.
17. Fisher, A.J. (2003). *Philos. Transact. Ser. A Math. Phys. Eng. Sci.* **361**:1441–1450.
18. Fries, P., Roelfsema, P.R., Engel, A.K., König, P., and Singer, W. (1997). *Proc Natl Acad Sci USA* **94**:12699–12704.
19. Gray, C.M., König, P., Engel, A.K., and Singer, W. (1989). *Nature* **338**:334–337.
20. Guldenagel, M., Ammermüller, J., Feigenspan, A., Teubner, B., Degen, J., Sohl, G., Willecke, K., and Weiler, R. (2001). *J Neurosci* **21**:6036–6044.
21. Hallett, M. (2000). *Nature* **406**:147–150.
22. Hameroff, S. (2001). *Ann. N Y Acad Sci* **929**:74–104.
23. Hardcastle, V.G. (1994). *Journal of Consciousness Studies* **1**:66–90.
24. Hormuzdi, S.G., Pais, I., LeBeau, F.E., Towers, S.K., Rozov, A., Buhl, E.H., Whittington, M.A., and Monyer, H. (2001). *Neuron* **31**:487–495.
25. Jefferys, J.G. (1981). *J Physiol (Lond)* **319**:143–152.
26. John, E.R. (2002). *Brain Res Brain Res Rev* **39**:1–28.
27. Kreiter, A.K. and Singer, W. (1996). *J Neurosci* **16**:2381–2396.
28. Libet, B. (1994). *Journal of Consciousness Studies* **1**:119–126.
29. Libet, B. (1996). *J Theor Biol* **178**:223–226.
30. Lindahl, B.I. and Arhem, P. (1994). *J Theor Biol* **171**:111–122.
31. Lohmann, K.J., Willows, A.O., and Pinter, R.B. (1991). *J Exp Biol* **161**:1–24.
32. MacLennan, B.J. (1999). *Information Sciences* **119**:73–89.
33. McFadden, J.J. (2001). *Quantum Evolution*. (New York: WW Norton).
34. McFadden, J.J. (2002a). *Journal of Consciousness Studies* **9**:23–50.
35. McFadden, J.J. (2002b). *Journal of Consciousness Studies* **9**:45–60.
36. Palmer, S.E. (1978). In *Cognition and Categorisation*, Rosch, E. and Lyoyd, B. (eds.). Hillsdale NJ: Lawrence Erlbaum.
37. Paulesu, E., Frith, C.D., and Frackowiak, R.S. (1993). *Nature* **362**:342–345.

38. Pockett, S. (2000). *The Nature of Consciousness: A Hypothesis*. (Lincoln, NE: Writers Club Press).
39. Popper, K.R., Lindahl, B.I., and Arhem, P. (1993). *Theor Med* **14**:167–180.
40. Richards, R.J. (1987). *Darwin and the Emergence of Evolutionary Theories of Mind and Behaviour*. (Chicago: The University of Chicago Press).
41. Singer, W. (1999). *Neuron* **24**:49–25.
42. Singer, W. (1998). *Philos Trans R Soc Lond B Biol Sci* **353**:1829–1840.
43. Tegmark, M. (2000). *Phys Rev E Stat Phys Plasmas Fluids Relat Interdiscip Topics* **61**:4194–4206.
44. Vigmond, E.J., Perez, V., Valiante, T.A., Bardakjian, B.L., and Carlen, P.L. (1997). *J Neurophysiol* **78**:3107–3116.
45. Interview with WIRED magazine, August 2003, available at:
<http://www.wired.com/wired/archive/11.08/view.html?pg=3>

13 Quantum Cosmology and the Hard Problem of the Conscious Brain

Chris King

Summary. The conscious brain poses the most serious unsolved problem for science at the beginning of the third millennium. Not only is the whole basis of subjective conscious experience lacking adequate physical explanation, but the relationship between causality and intentionally willed action remains equally obscure. We explore a model resolving major features of the so-called “hard problem in consciousness research” through cosmic subject–object complementarity. The model combines transactional quantum theory, with chaotic and fractal dynamics as a basis for a direct relationship between phase coherence in global brain states and anticipatory boundary conditions in quantum systems, complementing these with key features of conscious perception, and intentional will. The aim is to discover unusual physical properties of excitable cells that may form a basis for the evolutionary selection of subjective consciousness, because the physics involved in its emergence permits anticipatory choices that strongly favor survival.

13.1 Subject–Object Complementarity and the Hard Problem

In “The Puzzle of Conscious Experience” David Chalmers [21] summarizes some of the main points of his definition of the now renowned “hard problem in consciousness research”. He contrasts with the hard problem what he calls the “easy” problems such as: “How can a human subject discriminate sensory stimuli and react to them appropriately?” “How does the brain integrate information from many different sources and use this information to control behaviour?” “How is it that subjects can verbalize their internal states?” Each of these deal broadly with problems of consciousness, but in ways that could in principle be resolved by straightforward functional explanations.

The “hard problem”, by contrast, is the question of how physical processes in the brain give rise to subjective experience. This puzzle involves the inner aspects of thought and perception and the way things feel for the subject – all of them subjective experiences known only to the participant. This is much harder to resolve because trying to compare brain states, which are in principle objective and replicable, with subjective experiences, which, however rich for the experiencer, are unavailable to an external observer, pose a severe problem of qualitative difference, which seems almost unbridgeable.

Chalmers rejects any simple resort to neuroscience explanations about brain states in solving the hard problem. He notes for example that the 40-Hz oscillations made famous by Crick and Koch [27] and others, which might provide an explanation for the coherent binding together of different brain regions, for example visual and auditory into one attended perception, may explain how the brain integrates different processing tasks (an easy problem) but don't explain how any of these modes evoke the subjective conscious experiences of vision and sound. Likewise he rejects philosophical explanations such as Daniel Dennett's [28] "multiple-drafts" theory of consciousness as an explanation of "how we produce verbal reports on our internal states" (an easy problem) that tells us very little about why there should be a subjective experience behind these reports.

Even when we proceed to theories that attempt to use new types of physics to bridge this chasm, Chalmers remains skeptical:

"Some have suggested that to solve the hard problem, we need to bring in new tools of physical explanation: nonlinear dynamics, say, or new discoveries in neuroscience, or quantum mechanics. But these ideas suffer from exactly the same difficulty. Consider a proposal from Stuart R. Hameroff of the University of Arizona and Roger Penrose of the University of Oxford. They hold that consciousness arises from quantum-physical processes taking place in microtubules, which are protein structures inside neurons. It is possible (if not likely) that such a hypothesis will lead to an explanation of how the brain makes decisions or even how it proves mathematical theorems, as Hameroff and Penrose suggest. But even if it does, the theory is silent about how these processes might give rise to conscious experience. Indeed, the same problem arises with any theory of consciousness based only on physical processing."

Following on to examine the trend in cosmology and unified field theories, Chalmers speculates that conscious experience may be a fundamental feature cosmologically:

"If the existence of consciousness cannot be derived from physical laws, a theory of physics is not a true theory of everything. So a final theory must contain an additional fundamental component. Toward this end, I propose that conscious experience be considered a fundamental feature, irreducible to anything more basic."

This perception of the central nature of consciousness to the cosmological description is more acute than an academic or philosophical matter. Although the scientific description is based exclusively on the objective physical universe, our contact with reality is entirely *sine que non* through our subjective conscious experience. From birth to death, we experience only a stream of consciousness through which all our experience of the physical world is gained.

All scientific experiments performed on the physical world ultimately become validated by the subjective conscious experience of the experimenters, and the subsequent witnesses to the phenomena and conclusions.

Because its subjective nature makes it unavailable to objective investigation, reductionist descriptions identify subjective consciousness with functional attributes of the brain, inferring computational machines might also possess consciousness. At best in such views, the subjectively conscious mind remains an enigma considered to be merely a passive “epiphenomenon”. However, it is the physical world that is secondary to our personal experience, a consensus of stable subjective representations we assemble into our real world view. It thus remains unclear whether a physical universe without conscious observers could exist in any more than a purely conceptual or theoretical sense. Subjective consciousness may be necessary for the actualization of physical reality, and thus fundamental to physical existence in a cosmological sense, as expressed in the “anthropic cosmological principle” that “observers” are significant and possibly necessary boundary conditions for the existence of the universe [10].

Of course this somewhat “idealistic” view of subjectivity as a cosmic complement to the physical universe has a variety of critiques. Our conscious experience, while it remains mysterious, appears to be an inner manifestation of a functioning brain. Knock us out and consciousness is interrupted. The brain is a notoriously sensitive and easily damaged organ. Moreover, it is a recent development in a universe where brains are by no means a forgone conclusion, the product of an idiosyncratic process of biological evolution, which at the surface appears to have little to do with the vast energies and forces shaping the cosmology of the universe as a whole. Nevertheless, an argument based on nonlinear interactions arising from cosmic symmetry breaking and evolutionary universality can make the claim that the brain is accessing universal properties of a quantum nature, which may be the basis of its capacity for conscious subjectivity.

The conscious mind can also be described functionally as an internal model of reality. While such an explanation does not address the basis of subjectivity, it does help explain some of the more bizarre states of consciousness and is supported by many actively constructive aspects of sensory processing and the modular architecture of the cerebral cortex. Such an internal model can be described functionally in terms of dynamical brain processes that undergo unstable transitions to and from chaos [84]. Dynamical resonance and phase coherence also provide direct means to solve the “binding problem”, how the unitary nature of mind emerges from distributed parallel processing of many brain states.

A second critical property of subjective consciousness comes into play as we move from perception into volition. To quote Sir John Eccles: “It is a psychological fact that we believe we have the ability to control and modify our actions by the exercise of “will”, and in practical life all sane men will assume they have this ability” [46]. However, this premise, which is basic to all

human action, contradicts physical determinism, because any action of mind on brain contradicts the brain functioning as a deterministic computational machine, in its own right, in the physical world.

A confluence between quantum physics and the science of mind may resolve this apparent paradox. Firstly, physics has difficulty determining when collapse of the wave function from a set of probabilities into an actual choice takes place, leading to some interpretations in which the conscious observer collapses the wave function. Secondly, quantum uncertainty and nonlocality provide exactly the types of explanation that could enable the subjective experience of free-will to be consistent with a nondeterministic model of brain function. The unpredictability of chaos [85, 83] due to its amplification of arbitrarily small fluctuations in what is known as “sensitive dependence on initial conditions”, could provide a means to link quantum indeterminacy to global brain states.

13.2 Wave–Particle Complementarity, Uncertainty and Quantum Prediction

Associated with the nature of quanta themselves are unreconciled problems, which share an intriguing logical homology with the problem of conscious intent. To explore these we will first summarize some of the core ideas of quantum reality.

If we have to find the frequency of a wave using the beats we can produce by comparing it with another similar wave, without being able to measure the exact amplitude of the wave at a given time (the actual situation in root quantum interactions), we then have let a considerable time elapse, to gain enough beats for an accurate measurement so we don’t know exactly when the frequency was at this value. The relationship between the frequencies and the beats is: $\Delta v \Delta t \geq 1$, a smeared-out 2-D “interval” of time and frequency combined.

Einstein’s law is a fundamental equation of quantum mechanics that connects to every energetic particle a frequency $E = h\nu$. Measuring one is necessarily measuring the other. If we apply the above together, we immediately get the Heisenberg uncertainty relation:

$$\Delta E \Delta t = h \Delta \omega \Delta t \geq h . \quad (13.1)$$

Each quantum can be conceived as a particle or as a wave, but not both at the same time. Depending on how we are interacting with it or describing it, it may appear as either. We can visualize the interchange between particle and wave natures by generating photons and allowing them to flow through a pair of closely spaced slits. When many photons pass through, their waves interfere as shown and the photographic plate gets dark and light interference bands where the waves from the two slits cancel or reinforce, because the

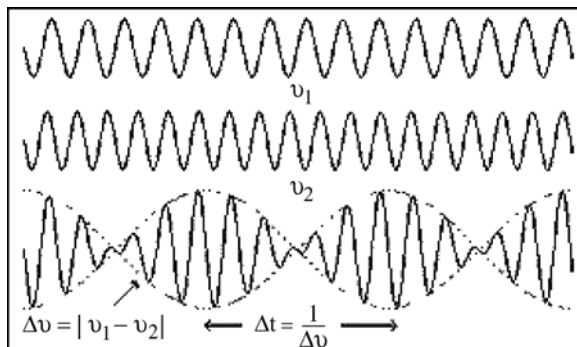


Fig. 13.1. Measuring a wave frequency with beats has intrinsic uncertainty as to the time

photons are more likely to end up where their superimposed wave amplitude is large. The experiment confirms the wave nature of light, since the size of the bands is determined by the distance between the slits in relation to the wavelength where c is the velocity of light: $\lambda = v/c$. We know each photon passes through both slits, because we can slow the experiment down so much that only one photon is released at a time and we still eventually get the interference pattern. Each photon released from the light bulb is emitted as a particle from a single hot atom, whose excited electron is jumping down from a higher energy orbit to a lower one. It is thus released locally and as a single “particle” created by a single transition between two stable electron orbitals, but it spreads and passes through both slits as a wave. After this the two sets of waves interfere as shown in Fig. 13.2 to make bands on the photographic plate.

The evolution of the wave is described by an equation involving rates of change of be a wave function ϕ with respect to space and time. For example,

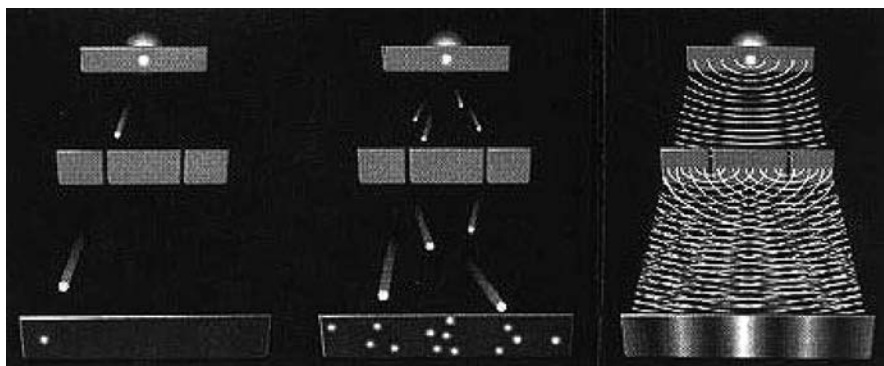


Fig. 13.2. Two-slit interference experiment (Sci. Am. Jul 92)

for a massive particle in one dimension we have a differential equation called the Klein–Gordon equation:

$$\left(\frac{\partial^2}{\partial t^2} - \frac{\partial^2}{\partial x^2} + m^2 \right) \varphi = 0. \quad (13.2)$$

For the bands to appear, each single photon has to travel through both slits as a wave. If you try to put any form of transparent detector in the slits to tell if it went through one or both, you will always find only one particle, but now the interference pattern will be destroyed. This happens even if you use the gentlest forms of detection possible, such as an empty resonant maser chamber (a maser is a microwave laser). Any measurement sensitive enough to detect a particle alters its momentum enough to smear the interference pattern into the same picture you would get if the particle just went through one slit. Knowing one aspect destroys the other.

At the other end of the process, the photon has to be absorbed again as a particle by an atom on the photographic plate, or somewhere else if it doesn't career forever through empty space, something we shall deal with shortly. Where exactly does it go? The rules of quantum mechanics are only statistical. They tell us only that the particle is more likely to end up where the amplitude of the wave is large, not where it will actually go on any one occasion. The probability is precisely the complex square of the wave's amplitude at any point:

$$P = \varphi^* \varphi. \quad (13.3)$$

Hence the probability is spread throughout the extent of the wave function, potentially extending throughout the entire universe at very low probabilities. Quantum theory thus describes all future (and past) states as probabilities. Unlike classical probabilities, we cannot find out more about the situation and reduce the probability to a certainty by deeper investigation, because of the limits imposed by quantum uncertainty. The photon could end up anywhere the wave is nonzero. Nobody can tell exactly where, for a single photon. However, each individual photon really does seem to end up getting absorbed as a particle somewhere, because we get a scattered pattern of individual dark crystals on the film at very low light intensities, which slowly build up to make the bands again. This is the mysterious phenomenon known as reduction of the wave packet. Effectively, the photon was in a superposition of states represented by all the possible locations within the wave, but suddenly became one of those possible states, now absorbed into a single localized atom, where we can see its evidence as a silver crystal on the film. Only when there are many photons does the behavior average out to the wave distribution. Thus each photon seems to make its own mind up about where it is going to end up, with the proviso that on average many do this according to the wave amplitude's probability distribution. So is this quantum “free-will”?

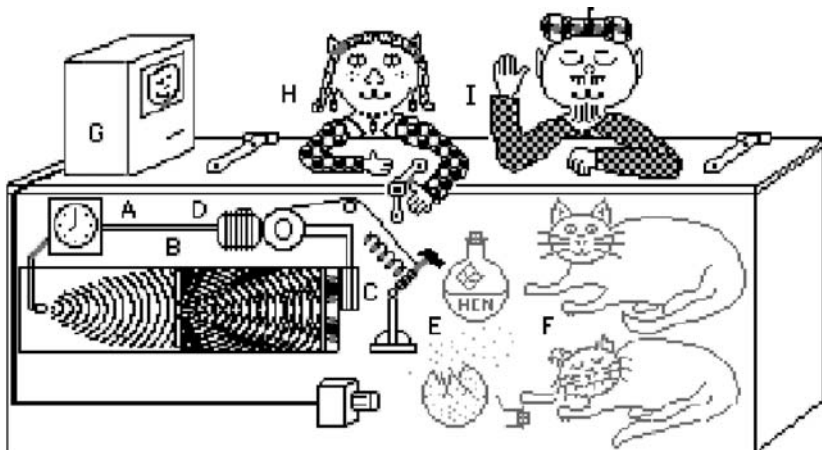


Fig. 13.3. Varieties of forms of the “Cat Paradox” experiment

This situation is the subject of a famous thought experiment by Schrödinger, who invented the wave equation, called the “cat paradox”. In the cat paradox, we use an interference experiment with about one photon a second and we detect whether the photon hits one of the bright bands to the left. If it does then a cat is killed by smashing a cyanide flask. Now when the experimenter opens the box, they find the cat is either alive or dead, but quantum theory simply tells us that the cat is both alive and dead, each with differing probabilities – superimposed alive and dead states. This is very counterintuitive, but fundamental to quantum reality. In the cat paradox experiment, Fig. 13.3, the wave function remains uncollapsed, at least until the experimenter I opens the box. Heisenberg suggested representing the collapse as occurring when the system enters the domain of thermodynamic irreversibility, i. e. at C. Schrödinger suggested the formation of a permanent record, e. g. classical physical events D, E, or computer data G. However, even these classical outcomes could be superpositions, at least until a conscious observer experiences them, as the many-worlds theory below suggests. Wigner’s friend is a version of the cat paradox in which an assistant G reports on the result, establishing that unless the first conscious observer collapses the wave function, there will be a conscious observer in a multiplicity of alternative states, which is an omnipresent drawback of the many-worlds view. In a macabre version the conscious assistant is of course the cat. According to the Copenhagen interpretation, it is not the system that collapses, but only our knowledge of its behavior. The superimposed state within the wave function is then not regarded as a real physical entity at all, but only a means of describing our knowledge of the quantum system, and calculating probabilities.

This clash between subjective experience and quantum theory has led to much soul-searching. The Copenhagen interpretation says quantum theory

just describes our state of knowledge of the system and is essentially incomplete. This effectively passes the problem back from physics to the observer. Some physicists think the wave function never “collapses” – all the possibilities happen and there is a probability universe for each case. This is the many-worlds interpretation of Hugh Everett III. The universe then becomes a superabundant superimposed set of all possible probability futures, and indeed all pasts as well, in a smeared out “holographic” multiverse in which everything happens. It suffers from a key difficulty. All the experience we have suggests just one possibility is chosen in each situation – the one we actually experience. Some scientists thus think collapse depends on a conscious observer. Many-worlds defenders claim an observer wouldn’t see the probability branching because they too would be split but this leaves us either with infinite split consciousness, or we lose all forms of decision-making process, all forms of historicity in which there is a distinct line of history, in which watershed events do actually occur, and the role of memory in representing it.

Zurek [92] describes decoherence as an inevitable result of interactions with other particles, however, his theory forces the effect as an artificial parameter. Penrose in OOR, or “orchestrated objective reduction” [44], singles out gravity as the key unifying force because of its relationship with space-time, and suggests that interaction with gravitons splits the wave function [74, 75], causing reduction. Others try to discover hidden laws that might provide the subquantum process, for example a particle piloted within a wave as suggested by David Bohm [16]. This has difficulties defining positions when new particles, with new quantum degrees of freedom, are created. Another approach we will explore is the transactional interpretation, which has features of all these ideas and seeks to explain this process in terms of a hand-shaking relationship between the past and the future, in which space-time itself becomes sexual in a quantum match-making. Key here is the fact that reduction is not like any other physical process. One cannot tell when or where it happens, again suggesting it is part of the “spooky” interface between quantum and consciousness.

In many situations, people try to pass the intrinsic problems of uncertainty away on the basis that in the large real processes we witness, individual quantum uncertainties cancel in the law of averages of large numbers of particles. They will suggest, for example, that neurons are huge in terms of quantum phenomena and that the “law of mass action” engulfs quantum effects. However, brain processes are, by necessity, notoriously sensitive. Moreover, history itself is a unique process out of many such “unstable” possibilities arise at each stage of the process. Critical decisions we make become watersheds. History and evolution are both processes littered with unique idiosyncratic acts in a counterpoint to the major forces shaping the environment and landscape. Chaotic processes are potentially able to inflate arbitrarily small fluctuations, so molecular chaos may “inflate” the fluctuations associated with quantum uncertainty.

13.3 The Two-Timing Nature of Special Relativity

We also live in a paradoxical relationship with space and time. While space is to all purposes symmetric and multidimensional, and not polarized in any particular direction, time is singular in the present and polarized between past and future. We talk about the arrow of time as a mystery related to the increasing disorder or entropy of the universe. We imagine space-time as a four-dimensional manifold, but we live out a strange sequential reality, in which the present is evanescent. In the words of the song “time keeps slipping, slipping, slipping . . . into the future”. There is also a polarized gulf between a past we can remember, the living present, and a shadowy future of nascent potentialities and foreboding uncertainty. In a sense, space and time are complementary dimensionalities, which behave rather like real and imaginary complex variables, as we shall see below.

A second fundamentally important discovery in twentieth-century physics, complementing quantum theory, which transformed our notions of time and space, was the special theory of relativity. In Maxwell’s classical equations for transmission for light, light always has the same velocity, c regardless of the movement of the observer, or the source. Einstein realized that Maxwell’s equations and the properties of physics could be preserved under all inertial systems – the principle of special relativity – only if the properties of space and time changed according to the Lorenz transformations as a particle approaches the velocity of light c :

$$x' = \frac{x - vt}{\sqrt{1 - v^2/c^2}}, y' = y, x' = x, t' = \frac{t - (v/c^2)x}{\sqrt{1 - v^2/c^2}}. \quad (13.4)$$

Space becomes shortened along the line of movement and time becomes dilated. Effectively space and time are each being rotated towards one-another like a pair of closing scissors. Consequently the mass and energy of any particle with nonzero rest mass tend to infinity at the velocity of light: $m = \frac{m_0}{\sqrt{1-v^2/c^2}}$. By integrating this equation, Einstein was able to deduce that the rest mass must also correspond to a huge energy $E_0 = m_0c^2$ that could be released for example in a nuclear explosion, as the mass of the radioactive products is less than the mass of the uranium that produces them, thus becoming the doom equation of the atom bomb. General relativity goes beyond this to associate gravity with the curvature of space-time caused by mass-energy.

In special relativity, space and time become related entities, which form a composite four-dimensional space-time, in which points are related by light cones – signals traveling at the speed of light from a given origin. In space-time, time behaves differently from space. When time is squared it has a negative sign just like the imaginary complex number $i = \sqrt{-1}$ does.

Hence the negative sign in the formula for space-time distance $\Delta S^2 = x^2 + y^2 + z^2 - c^2 t^2$ and the scissor-like reversed rotations of time and space

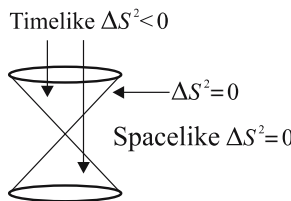


Fig. 13.4. Space-time light cone permits linkage of “time-like” points connected by slower-than-light communication. In the “space-like” region, temporal order of events and causality depends on the observer

into one another expressed in the Lorenz transformations. Stephen Hawking has noted that if we treat time as an imaginary variable, the space-time universe could become a closed “manifold” rather like a 4-D sphere, in which the cosmic origin is rather like the north pole of Earth, because imaginary time will reverse the above negative sign and give us the usual Pythagorean distance formula in four dimensions.

A significant feature of special relativity is the fact that the relativistic energy-momentum equation $E^2 = \mathbf{p}^2 + m^2$ has dual energy solutions: $E = \pm(\sqrt{\mathbf{p}^2 + m^2})$.

The negative-energy solution has reversed temporal direction. Effectively, a negative-energy antiparticle traveling backwards in time is exactly the same as a positive energy particle traveling forwards in time in the usual manner. The solution that travels in the normal direction (subsequent points are reached later) is called the *retarded* solution. The one that travels backwards in time is called the *advanced* solution. A photon is its own antiparticle so in this case we just have an advanced or retarded photon.

13.4 Reality and Virtuality: Quantum Fields and Seething Uncertainty

The theories describing force fields such as electromagnetism through the interaction of wave-particles are the most succinct theories ever invented by the human mind. Richard Feynman and others discovered the field is generated by uncertainty itself through particles propagated by a rule based on wave spreading. These particles are called *virtual* because they have no net positive energy and appear and disappear entirely within the window of quantum uncertainty, so we never see them except as expressed in the force itself. This seething tumult of virtual particles exactly produces the familiar effects of the electromagnetic field and other fields as well. We can find the force between two electrons by integrating the effects of every virtual photon that could be exchanged within the limits of uncertainty and of every other possible virtual particle system, including pairs of electrons and positrons coming

into a fleeting existence. However, we can't eliminate the wave description because the amplitudes with which the particles are propagated from point to point are wave amplitudes. Uncertainty not only can create indefiniteness but it can actively create every conceivable particle out of the vacuum, and does so. Each more complex interaction involving one more particle vertex is smaller by a factor $\frac{e^2}{\hbar c} = \frac{1}{137}$ where e is the electron charge and \hbar and c are as above, called the "fine structure constant". This allows the contribution of all the diagrams to sum to a finite interaction unlike many unified theories, which are plagued by infinities. The electromagnetic force is generated by virtual photons exchanged between charged particles existing only for a time and energy permitted by the uncertainty relation. The closer the two electrons, the larger the energy fluctuation possible over the shorter time taken to travel between them, and hence the greater the force upon them. Even in the vacuum, where we think there is nothing at all, there is actually a sea of all possible particles being created and destroyed by the rules of uncertainty.

The virtual particles of a force field and the *real* particles we experience as radiation such as light are one and the same. If we pump energy into the field, for example by oscillating it in a radio transmitter, the virtual photons composing the electromagnetic field become the real positive energy photons in radio waves entering the receiver as a coherent stream of real photons, encoding the music we hear.

Relativistic quantum field theories always have both advanced and retarded solutions, one with positive and the other with negative energy, because of the two square roots of special relativity. They are often described by Feynman space-time diagrams. When the Feynman diagram for electron scattering becomes time reversed, it then becomes precisely the diagram for creation and annihilation of the electron's antiparticle, the positron, as shown above. This hints at a fundamental role for the exotic time-reversed advanced solutions.

The weak and strong nuclear forces can be explained by similar field theories related to electromagnetism through symmetry breaking, but gravity holds out further serious catch-22s. Gravity is associated with the curvature of space-time, but this introduces fundamental contradictions with quantum field theory. To date, there remains no fully consistent way to reconcile quantum field theory and gravitation although higher-dimensional string and membrane theories show promise [45].

13.5 The Spooky Nature of Quantum Entanglement

We have already seen how the photon wave passing through two slits ends up being absorbed by a single atom. But how does the wave avoid two particles accidentally being absorbed in far flung parts of its wave function out of direct communication? Just how large such waves can become can be appreciated if we glance out at a distant galaxy, whose light has had to traverse the universe

to reach us. The ultimate size of the wave of such a photon is almost as big as the universe. Only one photon is ever absorbed for each such wave, so once we detect it, the probability of finding the photon anywhere else, and hence the amplitude of the wave, must immediately become zero everywhere. How can this happen, if information cannot travel faster than the speed of light? The same thing happens when I shine my torch against the window. The amplitude of each photon is both reflected, so I can see it, and transmitted, so that it could also escape into the night sky. Although the wave may spread far and wide, if the particle is absorbed anywhere, the probability across vast tracks of space has to suddenly become zero.

Moreover, collapse may involve the situation at the end of the path influencing the earlier history, as in the Wheeler delayed-choice experiment illustrated in Fig. 13.5. In this experiment we can determine whether a photon went both ways round a lensing galaxy, focusing the light from a very distant quasar long after the light has passed across the universe, by either measuring the interference between the paths as in the double-slit experiment or by detecting light from one direction or another.

Because we can't sample two different points of a single-particle wave, it is impossible to devise an experiment that can test how a wave might collapse.

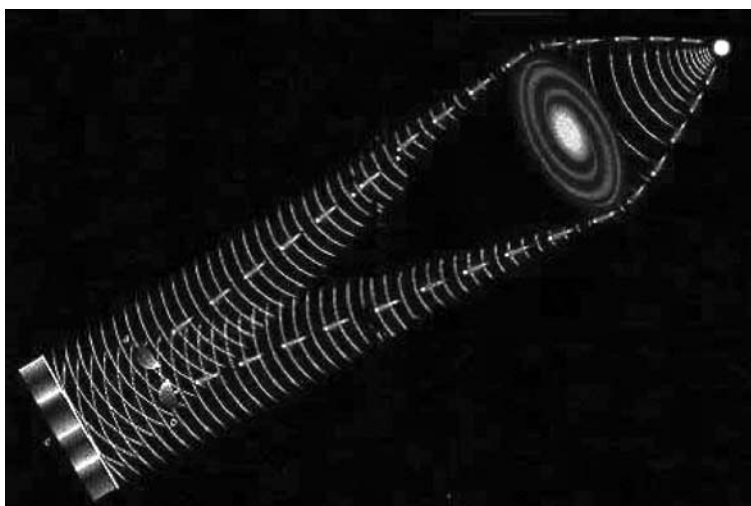


Fig. 13.5. Wheeler delayed-choice experiment (Scientific American): A very distant quasar is gravitationally lensed by an intervening galaxy. We can sample photons either by an interference pattern, verifying they went around both sides of the galaxy, or place separate directional detectors that will detect they went one way around only as particles (which will destroy the interference pattern). Moreover, we can decide which to perform after the photon has passed the galaxy, at the end of its path. Thus the configuration of the latter parts of the wave appear to be able to alter the earlier history

One way to learn more about this situation is to try to find situations in which two or more correlated particles will be released coherently in a single wave. This happens with many particles in a laser and in the holograms made by coherent laser light and in Bose-Einstein condensates. It also happens in other situations where two particles of opposite spin or complementary polarization become created together. Many years ago Einstein, Rosen and Podolsky suggested we might be able to break through the veil of quantum uncertainty this way, indirectly finding out more about a single particle than it is usually prepared to let on.

For example, a calcium atom's electron excited into a higher orbital sometimes cannot fall back to its original orbital in one step because a photon always turns out to have spin 1 and the spins don't match. For example, you can't go between two orbits of equal spin and radiate a spin-1 photon or the spins don't tally. The atom, however, can radiate two photons thereby canceling one another's spins, to transit to its ground state, via an intermediate spin-1 orbit. This releases a blue and a yellow photon, each of which travel off in opposite directions, with complementary polarizations.

When we perform the experiment, it turns out that the polarization of neither photon is defined until we measure one of them. When we measure the polarization of one photon, the other immediately – instantaneously – has complementary polarization. The nature of the angular correlations between the detectors is inconsistent with any locally causal theory – that is no theory based on information exchanged between the detectors by particles at the speed of light can do the trick, as proved in a famous result by John Bell [13] and subsequent experiments [25]. The correlation persists even if the detectors' configurations are changed so fast that there is no time for information to be exchanged between them at the speed of light, as demonstrated by Alain Aspect et al. [5]. This phenomenon has been called quantum nonlocality and in its various forms quantum "entanglement", a name itself very suggestive of the throes of a sexual "affair".

The situation is subtly different from any kind of classical causality we can imagine. The information at either detector looks random until we compare the two. When we do, we find the two seemingly random lists are precisely correlated in a way that implies instantaneous correlatedness, but there is no way we can use the situation to send classically precise information faster than the speed of light by this means. We can see, however, in the correlations just how the ordinary one-particle wave function can be instantaneously auto-correlated and hence not slip up in its accounting during collapse.

Since this result in the 1980s there have been a veritable conjurer's collection of experiments, including quantum teleportation, erasure computing and encryption, all of which verify the predictions of quantum mechanics in every case and confirm all the general principles of the pair-splitting experiment. Even if we clone photons to form quartets of correlated particles, any attempt to gain information about one of such a multiple collection collapses the correlations between the related twins.

Some of the more challenging aspects of quantum entanglement arise when we consider quantum computation. Classical computation has a problem, which is the potentially unlimited time it takes to check out every one of a collection of possibilities. For example, to crack a code we need to check all the combinations, whose numbers can increase more than exponentially with the size of the code numbers and possibly taking as long as the history of the universe to compute. For example, factorizing a large number composed of two primes is known to be computationally intractable enough to provide the basis for public key encryption by which banks records and passwords are kept safe. Although the brain ingeniously uses massively parallel computation, there is as yet no systematic way to bootstrap an arbitrary number of parallel computations together in a coherent manner. Quantum reality is a superposition of all the possible states in a single wave function, so if we can arrange a wave function to represent all the possibilities in such a computation, superposition might give us the answer by a form of parallel quantum computation. A large number could in principle be factorized in a few superimposed steps, which would otherwise require vast time-consuming classical computer power to check all the possible factors one by one.

13.6 Quantum Match-Making: Transactional Supercausality and Reality

For reasons that immediately become apparent, the collapse in the pair-splitting experiment has to not only be immediate, but also to reconcile information looking backwards in time. The two photons we are trying to detect are linked through the common calcium atom. Their absorptions are thus actually connected via a path traveling back in space-time from one detector to the calcium atom and forward again to the other detector. Trying to connect the detectors directly, for example by hypothetical faster-than-light tachyons, leads to contradictions. Tachyons transform by the rules of special relativity, so a tachyon that appears to be traveling at an infinite speed according to one observer, is traveling only at a little more than the speed of light according to another. One traveling in one direction to one observer may be traveling in the opposite direction to another. They also cause weird causality violations. There is thus no consistent way of knitting together all parts of a wave using tachyons. Even in a single-particle wave, regions the wave has already traversed also have to collapse retrospectively so that no inconsistencies can occur in which a particle is created in two locations in space-time from the same wave function, as the Wheeler delayed choice experiment makes clear.

In the *transactional interpretation* [26], such an advanced “backward traveling” wave in time gives a neat explanation, not only for the above effect, but also for the probability aspect of the quantum in every quantum experiment. Instead of one photon traveling between the emitter and absorber,

there are two shadow waves, which superimposed make up the complete photon. The emitter transmits an *offer* wave both forwards and backwards in time, declaring its capacity to emit a photon. The potential absorbers of this photon transmit a corresponding *confirmation* wave. These, traveling backwards in time, send a hand-shaking signal back to the emitter, Fig. 13.6a. The offer and confirmation waves superimpose constructively to form a real photon only on the space-time path connecting the emitter to the absorber.

In the extension of the transactional approach to supercausality [50, 56], a nonlinearity reduces the set of contingent possibilities to one offer and confirmation wave, Fig. 13.6c,d. Thus at the beginning, we have two sets of contingent emitters and absorbers as in Fig. 13.6c and at the end each emitter is now exchanging with a specific absorber. Before collapse of the wave function, we have many potential emitters interacting with many potential absorbers. After all the collapses have taken place, each emitter is paired with an absorber in a kind of marriage dance. One emitter cannot connect with two absorbers without violating the quantum rules, so there is a frustration between the possibilities that can only be fully resolved if emitters and absorbers can be linked in pairs. The number of contingent emitters and absorbers are not necessarily equal, but the number of matched pairs is equal to the number of real particles exchanged, Fig. 13.6d. The transition is not difficult to model as a sequence of nonlinear bifurcations, in which one emitter-absorber pair becomes committed, but notice that the time parameter we are dealing with lies outside space-time, as it is transforming one space-time diagram into another, yet it is happening experientially in real time. This is because collapse of the wave function is a space-time process. Causality with its symmetry-broken sequential time and supercausality with

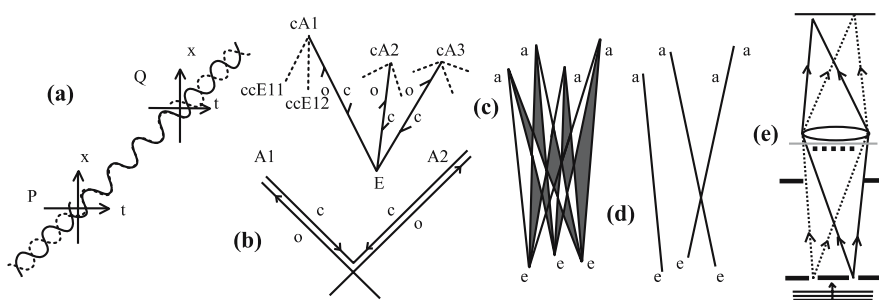


Fig. 13.6. (a) In the transactional interpretation, a single photon exchanged between emitter and absorber is formed by constructive interference between a retarded offer wave (solid) and an advanced confirmation wave (dotted). (b) The transactional interpretation of pair-splitting. Confirmation waves intersect at the emission point. (c) Contingent absorbers of an emitter in a single passage of a photon. (d) Collapse of contingent emitters and absorbers in a transactional matchmaking (King). (e) Experiment by Shahri Afshar (see Chown [24])

its time-symmetric hand-shaking form complementary domains, which is why the model is also called dual-time supercausality [52]. Directed and symmetric time thus coexist in the model. Notice also that the past contains causal records as well as superpositions, but the future is purely extrapolation plus superpositions. It is at this point that the influence of the conscious observer and the hard problem become pivotal. This transactional time symmetry is paralleled in the time reversibility of a quantum computation so long as it remains in the original superposition of states contrasted with the time-directed nature of classical computation, and with it the definitive results of any quantum computation arising from collapse.

The transactional process connects an emitter at an earlier time to an absorber at a later time because a real positive energy photon is a retarded particle that travels in the usual direction in time. If you wish, you can think of a negative-energy photon traveling backwards in time as the antiparticle of the positive one and it will have just the same effect. The two are thus identifiable in the transaction, just as in quantum electrodynamics above, where time-reversed electron scattering is the same as positron creation and annihilation. One can also explain the arrow of time if the cosmic origin is a reflecting boundary that causes all the positive-energy real particles in our universe to move in the retarded direction we all experience in the arrow of time. This in turn gives the sign for increasing disorder or entropy as it is called and the direction for the second law of thermodynamics to work in terms of positive energy. In the pair-splitting experiment, Fig. 13.6b, one can also see that the calcium atom emits in response to the advanced confirmation waves reaching it from both the detectors simultaneously right at the time it is emitting the photon pair. Thus the faster-than-light linkage is neatly explained by the combined retarded and advanced aspects of the photon having a net forwards and backwards connection that is instantaneous at the detectors.

The equivalence of real and virtual particles raises the possibility that all particles have an emitter and absorber and arose, like virtual particles, through mutual interaction when the universe first emerged. However, even if dark-energy, “quintessence” causes an increasing expansion, or fractal inflation leads to an open-universe model in which some photons may never find an absorber, the excitations of brain oscillations, because they are both emitted and absorbed by past and future brain states could still be universally subject to transactional supercausal coupling.

The hand-shaking space-time relation implied by the transactional interpretation makes it possible that the apparent randomness of quantum events masks a vast interconnectivity at the subquantum level, reflecting Bohm’s [17] *implicate order*. Although one can readily envisage a nonlinear interaction where a sequence of bifurcations result from the mutual frustration between the emitters and absorbers, because this connects past and future in a time-symmetric way, it cannot be reduced to predictive determinism, because the

initial conditions are insufficient to describe the transaction, which also includes quantum “information” coming from the future. However, this future is also unformed in real terms at the early point in time emission takes place. My eye didn’t even exist, when the quasar emitted its photon, except as a profoundly unlikely branch of the combined probability “waves” of all the events throughout the history of the universe between the ancient time the quasar released its photon, my eye developing, and me being in the right place at the right time to see it. Transactional supercausality thus involves a huge catch-22 about space, time and prediction, uncertainty and destiny. It doesn’t suggest the future is determined, but that the contingent futures do superimpose to create a space-time paradox in collapsing the wave function.

The transactional interpretation may combine with quantum computation to produce a space-time anticipating quantum entangled system, which may be pivotal in how the conscious brain does its computation (see Sect. 13.13). The brain is not a marvelous computer in any classical sense. We can barely repeat seven digits. But it is a phenomenally sensitive anticipator of environmental and behavioral change. Subjective consciousness has its survival value in enabling us to jump out of the way when the tiger is about to strike, not so much in computing which path the tiger might be on, because this is an intractable problem and the tiger can also take it into account in avoiding the places we would expect it to most likely be, but by intuitive conscious anticipation.

13.7 Exploring the “Three Pound Universe”

The human brain has been described as the “three-pound universe” [46] because, along with some other mammalian brains, it is the single most complex system so far discovered in the entire cosmological realm. It is also the most mysterious. Although we have developed supercomputers, their architecture remains that of a simplistic deterministic automaton by comparison with the brain. Despite the vast increases of speed and memory capacity of modern computers, they remain trivial by comparison. Few have more than a few processing units and the communication protocols for parallel processing, outside simple matrix calculations, remain simple procedural farming out. The notion that a computer may some day also become subjectively conscious is at this point a science fiction fantasy.

Theoretical models of neural nets likewise remain trivial by comparison with brain structures. Neurons are frequently modeled as simple additive modules summing their inputs and making synaptic adjustments to their connections in response to stimulus. Continuous nets such as the Hopfield net have only transient dynamics seeking a simple energy minimum as an equilibrium condition, perhaps with some thermodynamic annealing to avoid getting stuck in the “rut” of a suboptimal local minimum. Biological neurons by contrast are dynamically active, adaptive single-celled “organisms”, having

up to 10^4 synaptic connections each and possessing a variety of excitatory and inhibitory neurotransmitters, as well as both dynamical and pulse-coded means of activation. They display both chaos and self-organized criticality and threshold tuning.

The brain is par excellence a distributed parallel processing system in which there are only perhaps four to ten serial links between sensory input and motor output, modulated by connections involving up to 10^{11} cells and 10^{15} synapses. Its protocols are thus “lateral” rather than “serial”. The mammalian brain is dominated by the cerebral cortex. We are now beginning to gain some idea of how it processes sensory information through a combination of electrical probing and various types of scans.

The cortex has a dynamic modular organization, in which aspects of sensory “information” are processed in parallel in distinct areas, including the regions specialized for primary vision and hearing and for somatosensory perception and motor functions. Many of these modular regions can be divided further, for example into specific areas to do with language, such as Wernicke’s and Broca’s areas for semantic meaning and linguistic articulation. Using active scanning by multichannel electroencephalograms, positron emission tomography, or functional magnetic resonance imaging, it is possible to follow conscious activity and compare it with modular activation of the cortex, Fig. 13.7. Visual processing can be divided into a significant number of distinct modular areas (see Fig. 13.8), complementing the primary visual area, with distinct processing for color, movement and moving form. These areas can be investigated, both in scans and through people who display sometimes bizarre perceptual anomalies caused by local damage to these areas, such as colorless visual perception, or fragmented motion.

The cerebral cortex is divided between front and rear into broadly motor and broadly perception by the Sylvian fissure, dividing frontal regions and the motor cortex from the somatosensory (touch) and other sensory areas, including vision and hearing. The broadly sensory “input” and associated areas of the parietal and temporal cortices are complemented by frontal and prefrontal areas that deal with “output” in the form of action rather than perception and with forming anticipatory models of our strategic and living futures. These active roles of decision making and “working memory” [39], which interact from pre frontal cortical areas complement the largely sensory processing of the temporal, parietal and occipital lobes with a space-time representation of our “sense of future” and of our will or intent.

However, these areas are not rigidly hard-wired genetically. Neurogenesis and neurophysiology are dynamic. The allocation of a given region is a dynamical consequence of a series of interactive processes. These begin in embryogenesis, where neurons migrate up the glial cellular scaffold to make specific types of global connection. Neurogenesis is accompanied by growth and migration and also sacrifice in programmed cell death, and removal as well as establishment of synapses. The overall organization is not static, but derived from the dynamics itself. In visual development, the retina and then

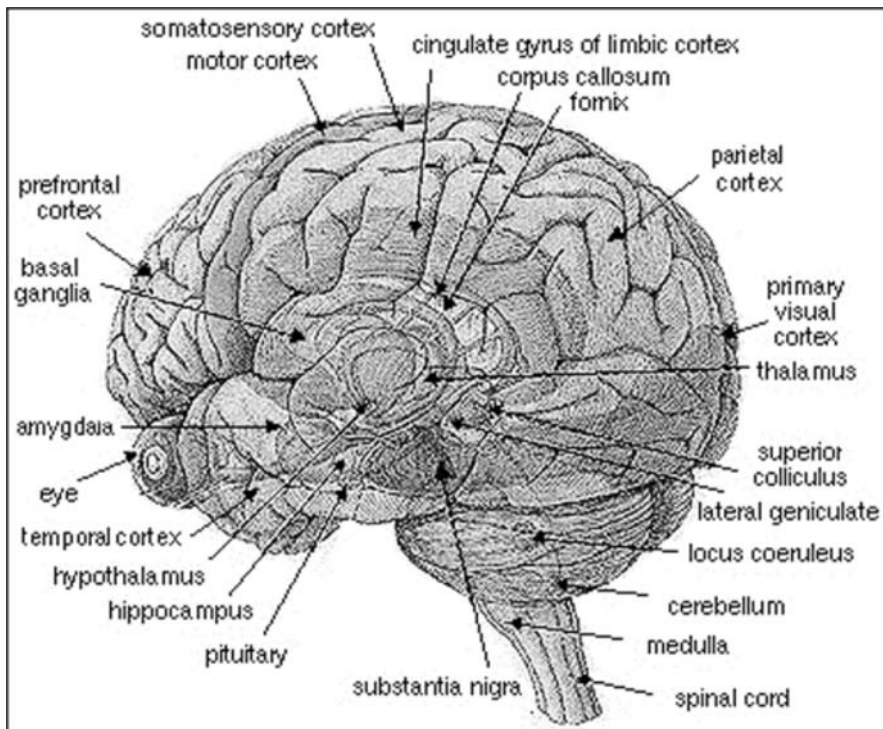


Fig. 13.7. Human brain showing key underlying structures (Sci. Am. Sep 92) indicate a massively parallel organization with feedback loops linking major cortical and limbic areas and interfacing them with midbrain centers in the thalamus, and basal brain. The limbic structures of the hippocampus and amygdala are indicated. There are only about ten serial connections between sensory input and motor output

the geniculate and finally the cortex become organized, each deriving organizing stimulus from the chaotic excitations established at the previous level. This cortical dynamic plasticity is preserved into later life, where injury, compensation, or a major new learned skill can result in development of new functional areas or significant rearrangement of existing areas. A person studied on live PET before and after becoming a real-time translator at the UN, for example, showed the development of a whole new language area.

The cortex itself is relatively inert in electrodynamical terms and may actually form a complex boundary constraint on the activity of more active underlying areas such as the thalamus, which contains a number of centers with ordered projections to and from corresponding areas of the cortex. This suggests in turn that the thalamic centers are the driving force of cortical activity and that conscious activity may result from the flux of thalamocortical loops spanning the entire cortex, giving the cortex a role similar to

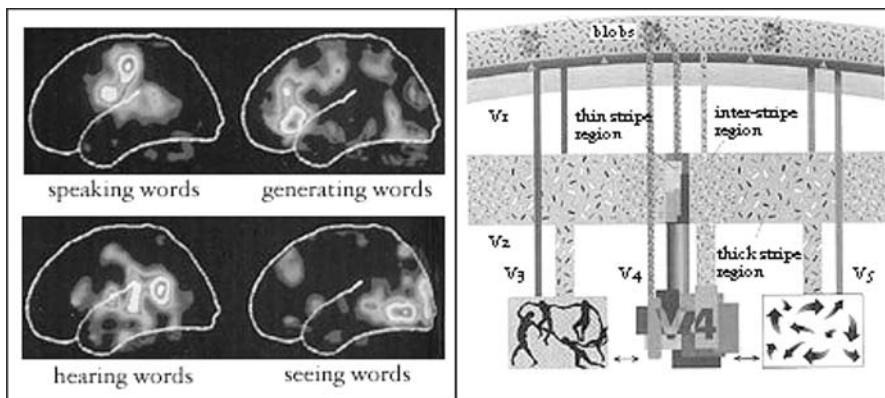


Fig. 13.8. Despite the development of sophisticated techniques for visualizing brain activity such as those for speech (*left*), and ingenious work tracing connectivity of activity between neurons in the cortex such as that establishing distinct parallel processing regions for color and movement in vision (*right*, [91]), no objective brain state is equivalent to a subjective conscious experience. The difficulty of bridging this abyss is called the hard problem in consciousness research [21]

a meta-sensory organ of the thalamus, collectively forming the internal model of reality.

Finally, we have the so-called limbic system, Fig. 13.7, around the edges of the cortex, involving the hippocampus, amygdala, hypothalamus and areas of the cingulate cortex in a large feedback loop that becomes associated with emotional mood, flight and fight, cross-sensory integration and the fixation of long-term sequential memory. These structures fall very centrally into our concept of the psyche because they mediate the central emotional orientations that govern our survival and our social interaction with others, including the capacity for love, hate, jealousy, compassion and nongenetic altruism.

The varying modes of alert consciousness, dreaming and deep sleep are generated from deeper brain stem centers that have ascending neural pathways that fan out widely across the cortex into specific cortical layers, thus providing long-term modulation of mood and conscious attention, Fig. 13.10. Two pathways lead from the Raphe Nuclei and the Locus Coeruleus to diverse cortical areas and involve the modulating neurotransmitters, serotonin and nor-epinephrine. The onset of dreaming sleep is heralded by activity of cells in the Pons and silencing of cells in the Raphe Nuclei and Locus Coeruleus. Similar dopamine paths spread out from the Substantia Nigra selectively into the frontal lobes and motor centers. The ascending pathways have been implicated in mental illness, addiction and motor syndromes such as Parkinson's disease. Dopamine is sometimes associated with pleasure and nor-adrenaline with anxiety. The hallucinogens psilocin and mescaline are serotonin and catecholamine analogs, although both appear to interact primarily

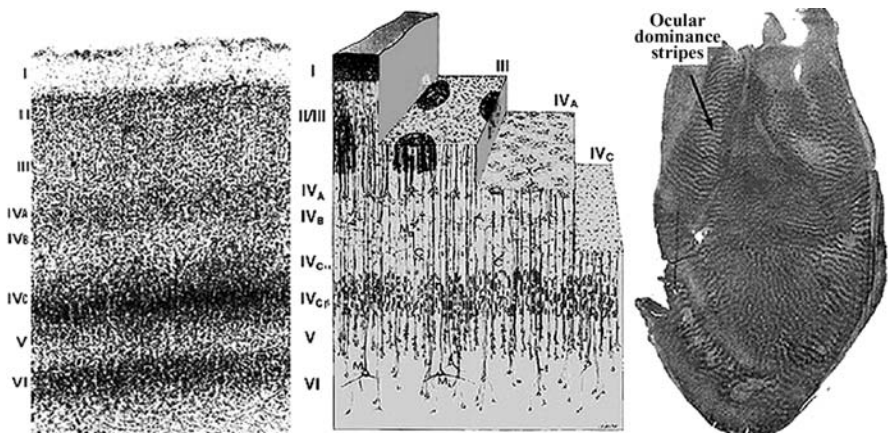


Fig. 13.9. Typical cortical structures (*center*) are a combination of five layers of neurons each composed into columnar modules on a scale of about 1mm on the cortical surface. Such modules are sensitive to particular stimuli such as a line of a given orientation. Blob centers in layer II are also shown (see Fig. 13.8). Although specific sensory areas have functional and anatomical specializations neural plasticity can enable changes of functional assignment indicating common principles throughout the cortex. *Left:* anatomical view of the five layers. *Right:* Ocular dominance columns illustrate functional columnar architecture

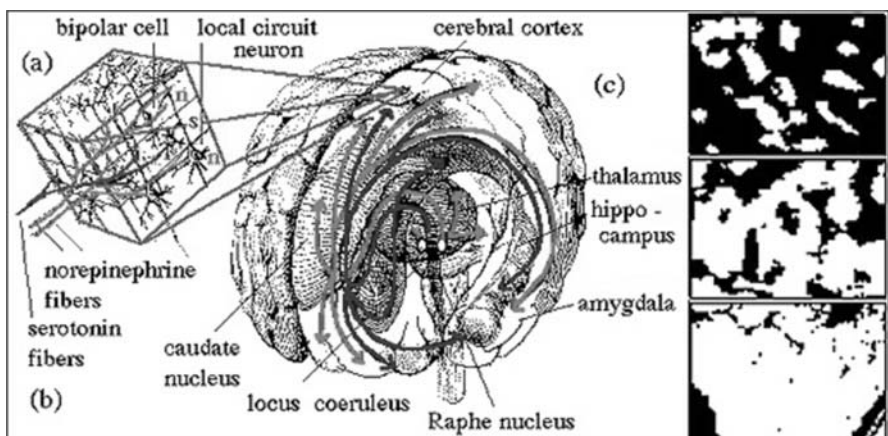


Fig. 13.10. *Left:* Ascending serotonin and norepinephrine pathways are evidence for a parallel-distributed cortex based on dynamical activation of conscious modes. Serotonin receptors are notably involved in psychedelic effects. *Right:* Neural plasticity of local cortical function, in changes in regions of optical dominance in the visual cortex after the dominant eye is shade support dynamical rather than hard-wired cortical organization. Such plasticity extends across the senses, enabling the assignment of new functions under the demands of new experiential situations such as learning a new language

with serotonin receptors. These pathways clearly have much to do with modulating conscious states of the cortex as a whole and an understanding of their exact mechanism of action would give a very productive insight into the brain mechanisms supporting consciousness.

Dreaming or REM (rapid eye movement) sleep in which cortical activation alternates with phases of deep sleep is both one of the most singular phases of conscious activity in which experiential feedback appears to be accentuated at the expense of external input, generating episodic subjective realities or “worlds within”. The nature and function of dreaming consciousness and its wealth of detail remain obscure although the experiences themselves are intense, sometimes in full sumptuous color vision as evidenced in lucid dreaming [61]. There is some indication that these two phases are complementary and involve reciprocal communication between the hippocampus and the cortex in consolidating long-term sequential memories ([90, 86, 73]), but the subjective consequences, and the need for them to occur subjectively as well, as functionally remain enigmatic. Accounts of precognitive dreaming [30] challenge our very notions of causality.

13.8 Chaos and Fractal Dynamics as a Source of Sensitivity, Unpredictability and Uncertainty

Walter Freeman’s model of chaos in sensory perception [84, 37] gives a good feeling for how transitions in and out of chaos – a so-called “edge-of-chaos” complexity phenomenon [80], could play a key role in sensory recognition. The olfactory cortex undergoes high-energy chaotic excitation in time to form a spatially correlated wave across the cortex, as a rabbit sniffs, causing the cortical dynamics to travel through its phase space of possibilities without becoming stuck in any mode. As the sniff ends, the energy parameter reduces, carrying the dynamic down towards basins in the potential energy landscape. If the smell is recognized, the dynamic ends in an existing basin, but if it is new, a bifurcation occurs to form a new basin (a new symbol is created) constituting the learning process, as illustrated below. The same logic can be applied to cognitive problem solving in which the unresolved aspects of the problem undergo chaotic evolution until a bifurcation from chaos to order arrives at the “eureka” of the solution.

A fundamental reason for any dynamical nervous system to enter chaos is that chaotic systems are arbitrarily sensitive on their initial or external conditions, so a system entering chaos is capable of being acutely responsive to its environment over time, while any stable process heads inexorably towards its equilibrium states or periodicities, entrapped by its very stability. While artificial neural nets invoke thermodynamic “randomness” in *annealing* to ensure the system doesn’t get caught in a suboptimal local minimum, biological systems appear to exploit chaos to free up their dynamics to explore the

“phase space” of possibilities available, without becoming locked in a local energy valley that keeps it far from a global optimum.

Several indicators of the use of chaos in neurodynamics come from measurements of the fractal dimension of a variety of brain states, from pathology through sleep to restful wakefulness [6–8, 79]. Recordings from single neurons, and from other cells such as the insulin-releasing cells of the pancreas indicate their capacity for chaotic excitation. The organizers of neural systems are also frequently nonpulse-coded “silent” cells capable of continuous nonlinear dynamics. Despite the classical result of quasilinearity of the axonal discharge rate with depolarization, virtually all aspects of synaptic transmission and excitation have nonlinear characteristics capable of chaos and bifurcation. For example, the acetyl-choline ion channel has quadratic concentration dynamics, requiring two molecules to activate. Many cells have sigmoidal responses providing nonlinear sensitivity and are tuned to threshold. Nonlinear feedback between excitatory and inhibitory neurotransmitters in cortical layers is believed to be a source of the electroencephalogram [37]. The activity of single neurons has been found to include both cells with activity indistinguishable from noise and also neurons displaying low-dimensional chaos [2]. The electroencephalogram itself, although nominally described as having brain rhythms such as alpha, beta, gamma and theta actually consists of broadband frequencies, rather than harmonic resonances, consistent with a ground-swell of chaotic excitation [52–54]. Broadly speaking neurodynamics is “edge of chaos” in the time domain and parallel distributed in a coherent “holographic” manner [77] spatially. Phase coherence (e.g. in the 40-Hz band) is also associated with perception, providing a mathematical parallel with quantum wave coherence.

Into this picture of global and cellular chaos [23] comes a second complementary aspect, the fractal nature of neuronal architecture and brain processes and their capacity for self-organized criticality at a microscopic level. The many-to-many connectivity of synaptic connection, the tuning of responsiveness to a sigmoidal threshold, and the fractal architecture of individual neurons combine with the sensitive dependence of chaotic dynamics and self-organized criticality of global dynamics to provide a rich conduit for instabilities at the level of the synaptic vesicle or ion channel to become amplified into a global change. The above description of chaotic transitions in perception and cognition leads naturally to critical states in a situation of choice between conflicting outcomes and this is exactly where the global dynamic would become critically poised and thus sensitive to microscopic or even quantum instabilities.

Because of the intrinsic nonlinearity of charge interactions, (see Sect. 13.10), this fractal process runs all the way from the global brain state to molecular quantum chaos [41]. From the synaptic vesicle we converge to the ion channel that in the case of the K^+ voltage channel is determined to have a fractal kinetics [63–65], and further to the structure and dynam-

ics of proteins and their conformational dynamics [4], both of which operate on nonlinear fractal protocols. The brain is thus an organ capable of supersensitivity to the instabilities of the quantum milieu. The phenomenon of stochastic resonance has been demonstrated to enable a single ion channel to excite a hippocampal neuron and for a single hippocampal neuron to elicit global excitation changes, demonstrating such sensitivity (Liljenström 2005 conference lecture).

13.9 Classical and Quantum Computation, Anticipation and Survival

A computational process is intractable if the number of computational steps required grows superexponentially with the complexity. The traveling salesman problem [14], finding the shortest route round n cities illustrates this, growing with $(n - 1)!/2$. A proposition may also be formally undecidable in the sense of Gödel's incompleteness theorem that says that any logical system containing finite arithmetic contains undecidable propositions. Many adaption–survival problems in the open environment are intractable problems, because the number of options rapidly exponentiates. This would leave a gazelle stranded at the crossroads unable to decide which path to take eaten in a “catatonic” state due to Turing’s “halting” problem – the undecidability of whether a computational process will actually complete. An active organism must complete any processing task within 0.1–1 sec if it is going to have survival utility, regardless of its complexity. Such arguments make it clear why dynamic parallel processing is an integral feature of vertebrate nervous systems.

Recent models of the quantum mind attempt to solve this problem by suggesting the brain is capable of a form of quantum computing that may be also associated with conscious awareness. For example, Hameroff and Penrose [44] have suggested that microtubules may permit a form of molecular quantum computing through two-state qubits formed from tubulin monomers that exist in two quantum states. They suggest the tubulin monomers form a type of cellular automaton. While these ideas are exciting, they also introduce new problems. Microtubules are involved in neuronal activity and their pathologies do affect learning and memory, but it remains unclear if their changes operate on the rapid time scale of electrodynamical changes and consciousness. The quantum-computing model proposes individual cellular quantum computation through quantum isolation of the microtubules within the neuron to prevent decoherence, preventing the quantum computations from being integrable with many-cell resonances and hence the global brain states we naturally associate with conscious awareness.

However, we may be able to harness the superposition of all the possible states in a single wave function. If we can arrange a wave function to represent all the possibilities in such a computation, superposition might give us

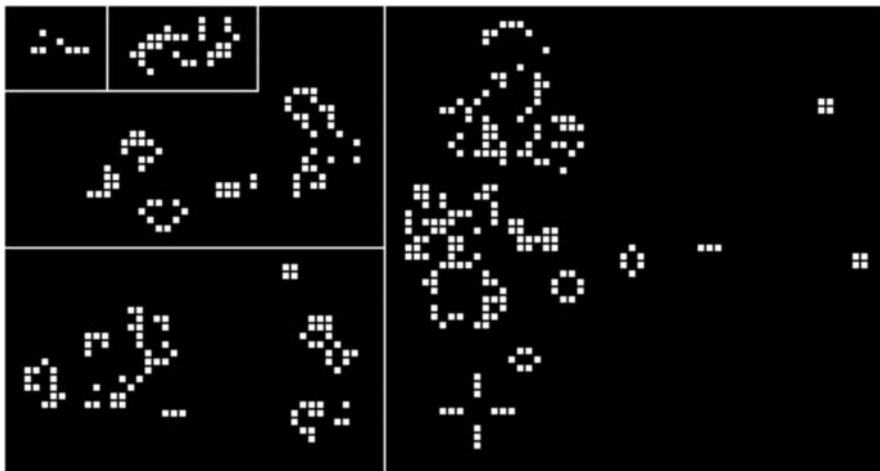


Fig. 13.11. Conway's game of life is a two-dimensional cellular automaton with simple rules. Any cell with 2 or 3 of its 8 possible neighbors alive "survives" and one with just 3 is "born". The rest die. The system, which is a digital version of edge of chaos complexity dynamics, is capable of universal computation

the answer by a form of parallel quantum computation. A large number could in principle be factorized in a few superimposed steps, which would otherwise require vast time-consuming classical computer power to check all the possible factors one by one. Suppose we know an atom is excited by a certain quantum of energy, but only provide it a part of the energy required. The atom then enters a superposition of the ground state and the excited state, suspended between the two like Schrödinger's cat. If we then collapse the wave function, squaring it to its probability, as in $P = \varphi^* \varphi$, it will be found to be in either the ground state or excited state with equal probability. This superimposed state is sometimes called the "square root of not" when it is used to partially excite a system that flips between 0 and 1 corresponding to a logical negation.

Suppose we want to factorize a large number. We devise a single quantum system in two parts. The left part is excited to a superposition. Suppose we have a collection of such atoms, which effectively form the 0s and 1s of a binary number – 0 in the ground state and 1 in the excited state. If we then partially excite them all they represent a superposition of all the binary numbers – e.g. 00, 01, 10 and 11. The right half is designed to give the factorization remainder of a test number taken to the power of each of the possible numbers in the left. These turn out to be periodic, so if we measure the right we get one of the values. This in turn collapses the left side into a superposition of only those numbers with this particular value in the right. We can then recombine the reduced state on the left to find its frequency spectrum and decode the answer. As a simple example, you are trying to

factorize 15. Take the test number $x = 2$. The powers of 2 give you 2, 4, 8, 16, 32, 64, 128, 256 ... Now divide by 15, and if the number won't go, keep the remainder. That produces a repeating sequence 2, 4, 8, 1, 2, 4, 8, 1 ... with period $n = 4$ we can use this periodicity as an "interference pattern" to figure $x^{n/2} - 1 = 2^{4/2} - 1 = 3$ is a factor of 15. Quantum parallelism solves all the computations simultaneously.

The essential principles of this calculation may pass over into a general problem-solving paradigm. Key is the idea that measurement of part of an entangled system may enable the whole system to collectively solve a problem connecting its entangled parts.

Nevertheless, although it may be able to solve some intractable problems by parallel superposition, [29, 20], quantum computing alone may not solve the deeper problems of the open environment. Many critical decisions a living animal has to make to survive are not simply a matter of computation because many problems of survival are intrinsically unstable. Each strategy tends to be matched by a competing strategy in another organism, so that a predator may choose a less likely path for the very reason that the prey may be more likely to take it knowing it is safer in computational terms. These many options may not be able to be decided on by optimizing computationally on past histories, as illustrated by neural net "over fit" errors, when circumstances change. Survival depends more on intuitive anticipation and paranoia taken to a hair-trigger, when the tiger is about to strike, rather than brute-force computation. This is where the evolutionary value of subjective consciousness begins to become apparent. It is thus insufficient to replace a computational model of brain function, as exemplified by "artificial intelligence", with a form of quantum consciousness that is simply a reflection of quantum computation through nonlocal molecular automata or other mechanisms. Although quantum computation might act more quickly, avoiding the gazelle becoming stranded catatonically at the crossroads because of computational intractability, it still doesn't go any way to solving the questions of free-will and creative choice, nor does it compensate for the perfidy of the predator. Raw conscious anticipation is the key. Attentiveness and hunch in the shadow of paranoia is the best survival strategy.

Intentional generation of novelty and unpredictability for its own sake is also key to survival in many species, and strongly manifest in *Homo sapiens*. A pivotal aspect of novelty in our own context is that, in all species, decisions are not just made for survival but to express reproductive fitness. Geoffrey Miller [71] in "The Mating Mind" has suggested that the development of human culture is an indicator of reproductive fitness in which both sexes are "running while standing still" in a genetic race generated through novelty, music art, story telling as well as resourcefulness and protection. This theme is further developed in "Sexual Paradox" [34]. All of these features also need explaining and involve diversity and complexity generation that no computational model, quantum or otherwise, focusing on a fixed "solution" can generate.

Quantum computing on its own does not solve the problem of “will” involved in decision making when many choices are available, several of which may be successful to varying degrees. The capacity to make a decision, given many options is pivotal. To explain free choice, it is also necessary to explain all the manifestations of noncomputational complexity, such as the creativity that enables a new musical theme, or an art form, or other innovation to be created. None of this complexifying behavior is explained by any form of computation that seeks a single optimal outcome or even a specific heuristic array of options. Creative variety is the essence of human diversity and our success as a species. Neither does quantum computing alone indicate why we experience a subjective impression of free-choice central to the exercise of subjective consciousness. In the Hameroff–Penrose OOR model, *reduction* of the wave function is regarded as *orchestrated* and *objective* and is thus independent of the conscious will of the experiencer. If intentional consciousness is only a retrospective reflection of an orchestrated objective collapse, it still has no evolutionary role in terms of selective advantage.

We thus need to explain not just how computation might be accelerated in quantum consciousness, but the origin of will in the subjective affecting and in effecting physical outcomes. We need to deal with dynamics in which many choices are available, not one computational solution, quantum or otherwise, and to explain how “free-will” can achieve real physical choices, and the endless variety of novelty that we associate with living systems and particularly with human culture. We need to consider not only computation but creativity – how the symphony emerges from the composer.

13.10 The Cosmic Primality of Membrane Excitation

Rather than a molecular accident, the emergence of life can be modeled as a tree of critical cosmological quantum bifurcations, or splittings, interactively between quantum features emerging from the interaction of the atomic and molecular structures that arise in turn as complex asymmetric hierarchical structures from cosmic symmetry breaking itself, Fig. 13.12. The nonlinear nature of charge interactions results in a succession of bonding effects, from strong covalent and ionic bonds, through H-bonds, polar and hydrophobic interactions, to van der Waal’s effects. Cooperative weak bonding results in globally interactive enzyme structures, Fig. 13.12e and in fractally increasing scales, molecular complexes, organelles, cells, tissues and organisms. The central bifurcation tree, Fig. 13.12d is an interaction of the 1s orbital of H with the $2sp^3$ hybrid orbitals of C, N, and O as most strongly covalent multi-bonding elements. Secondary bifurcation of polarity between C, N, and O in order of increasing electronegativity in relation to H generates the polar nonpolar bifurcation in which the phase division leading to the lipid bilayer membrane and ion-based excitation arises. H_2O becomes the optimal formative substrate in terms of its diversity of quantum modes (reflected in its

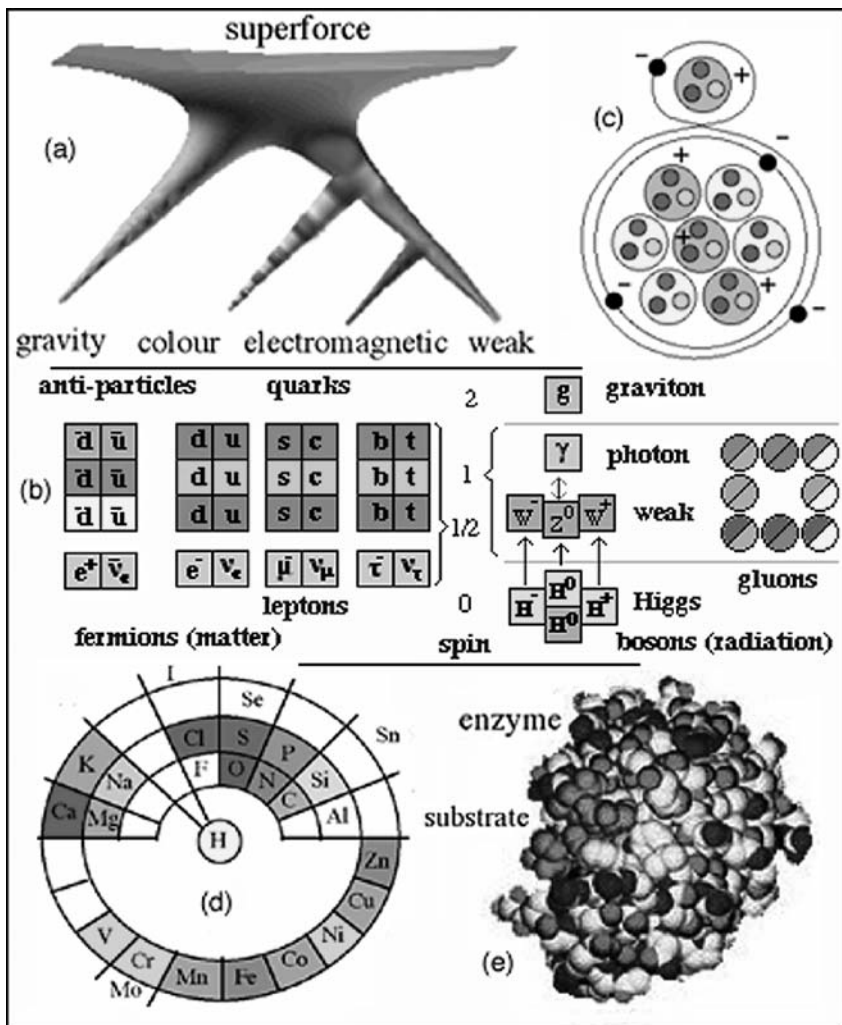


Fig. 13.12. (a) Cosmic symmetry breaking as a fractal generator of life [57, 58, 59]. The four forces of nature emerge from a single unified field theory, probably a 10- to 12-dimensional superstring or membrane theory based on supersymmetry – a pairing between the bosons and fermions, which cancels the infinities that would otherwise result in the theory. (b) The standard model showing the key fermions making up matter and bosons making force and radiation. Added to the 4 dimensions of space-time, the dimensions of the internal symmetries of color, charge-flavor and the Higgs particle give a strong hint of the grand unification. (c) Because the resulting fermions are highly charge asymmetric they associate to form the hierarchical structures of atomic and molecular matter. The nonlinear charge interactions result in a cascade of chemical-bonding effects, generating higher molecular fractal structures, leading to organelles, cells and tissues. The bioelements form a key symmetry-breaking interaction among the principal orbital types

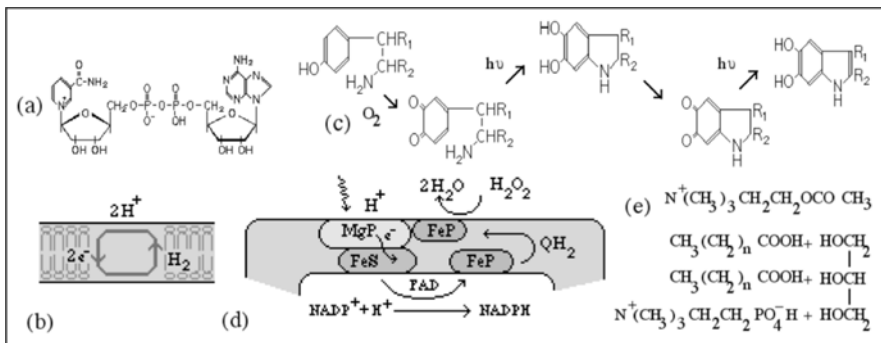


Fig. 13.13. (a) NAD structure permits linkage of other energies to a redox bifurcation. (b) H^+ and e^- transport linked by H_2 in membrane due to insolubility of e^- and solubility of H^+ . (c) Prebiotic link between catecholamines and indole via quinone-type photoreduction. (d) Hypothetical form of primitive electron transport as a nonequilibrium limit cycle. (e) Acetyl-choline and phosphatidyl choline compared. Phosphatidyl choline lipid stacks tail to tail as shown in the clothes pegs (b)

high specific heat), and diverse ionic and polar structures, giving rise to the interactive properties that make the polar-hydrophobic phase bifurcation of protein enzymes, Fig. 13.12e, nucleic acid base stacking and lipid membranes, Fig. 13.13b, and hence excitable cells possible.

Subsequent orbital bifurcations divide alkali and alkaline earth metal ions according to ionic radius, secondary involvement of second row elements in S-S weak covalency, PO_4^{3-} dehydration energy and Cl^- ions. Subsequently the d-orbital catalysis of the transition elements completes the orbital symmetry-breaking interaction. This bifurcation pathway leads directly to polypeptides, nucleotides and membranous lipid structures as complexity polymers, with RNA and monomers such as ATP having a central formative replicative role.

All life as we know it is dependent on maintaining a distinct internal microenvironment as an open far-from-equilibrium thermodynamic system [38, 1, 33], through the topological closure of the cell. Viruses for example all depend on cellular life. The structure of the bilayer membrane is a direct consequence of the polarity bifurcation. The formation of amphophilic lipid-like molecules, joining a linear nonpolar hydrocarbon section to an ionic or H-bonding polar terminal, leaves 2 degrees of freedom for layer formation. Backing of the nonpolar moieties to one another, Fig. 13.13b, completes the bilayer. Cell structure can then arise directly from budding of the bilayer, as illustrated in budding in several types of prebiotic reaction medium. Micro-cellular structures are abundant in many origin-of-life syntheses, Fig. 13.14. The use of cytosine diphosphate CDP associated with choline, inositol and lipids in membrane construction is consistent with membrane formation in the RNA era along with the ubiquitous energy molecule the nucleotide ade-

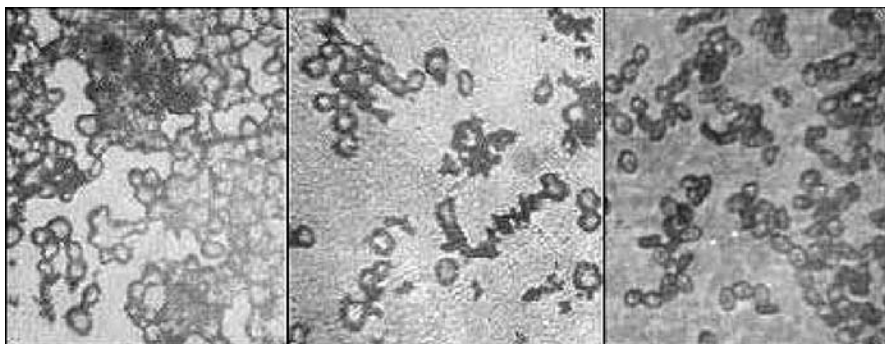


Fig. 13.14. *Left and center:* Microcellular formations generated by the author from HCN and HCHO (King). *Right:* Spores of a psilocybe species at the same magnification for size comparison

nine triphosphate ATP. The structure of typical biological lipids such as phosphatidyl choline display a modular structure consisting of fatty acid, glycerol, and substituted amine, linked by dehydration and involving phosphate, Fig. 13.13e.

The existence of the membrane as a nonpolar structure leads to segregation into ionic and nonpolar reaction phases. Ion transport is essential in maintaining the concentration gradients that distinguish the cytoplasm from the external environment and thus must develop in the earliest cellular systems [69]. Ion transport is a source of significant electronic effects, because the membrane under polarization is piezoelectric and is capable of excitation in the presence of suitable ions. Model systems using the simple 19-unit oligopeptide Na^+ ionopore alamethicin and artificial membranes display action potentials [72]. Similar results have been reported for microcells produced by prebiotic techniques containing light-irradiated chromophores [78], demonstrating that such effects are fundamental to the quantum architecture of lipid membranes [51]. Four groups of nonpolypeptide neurotransmitters: acetyl-choline, catecholamines (epinephrine and dopamine), serotonin and histamine are all amines, the latter three being derived from amino acids tyrosine, tryptophan and histidine by decarboxylation. Two others are amino acids and thus also contain amine groups. This may represent a fundamental chemical bifurcation between basic amines and the acidic phosphate groups in the lipid membrane. Alamethicin also has glutamine amides located in the core of the pore [35]. The catecholamines are linked to indoles such as serotonin by a prebiotic pathway, Fig. 13.13c.

Ion transport, the membrane and excitability appear to have a common progenitor in the phase transition to ordered water gels [76] with negatively charged proteins, under ion gradients that reject Na^+ and attract K^+ , the latter leading to a compact ordered water-phase transition leading to a stable gel-phase cytoplasm without the need to impose a structurally unstable mem-

brane and ion transport mechanism at the birth of the first cell to maintain a far-from-equilibrium thermodynamic limit cycle.

The proton is soluble in water to form the hydrogen ion H^+ , but the electron is not, unless attached to another group such as a protein. This causes a physical linkage between the polarity bifurcation and the charge bifurcations associated with electron and proton transfer, Fig. 13.13b mediated by H transport through quinone reduction, (c). Despite the complexity of modern electron transport in photosynthesis and respiration, there is considerable evidence that membrane electrochemistry could have arisen before translation produced coded enzymes. There is a consistent basis for the existence of many of the components of electron transport during the RNA era. The nucleotide coenzymes provide evidence for this system emerging in the RNA era. Nicotine and flavin adenine dinucleotide NAD, FAD, a nucleotide-bound Mg/Fe-porphyrin ring similar to B_{12} , a cysteine-bound FeS group [43], possibly based on glutathione (g-glutamyl-cysteinyl-glycine) and quinones would provide all the key components of electron transport in an RNA-dependent but protein-free form, Fig. 13.13d [51]. The Fe–S center has also been cited as a basis for prebiotic metabolism. Both porphyrins and quinones have obvious prebiotic syntheses and the primal role of nucleotide coenzymes has already been discussed. Secondly, membrane structure and the solubility differences between the electron and proton guarantee a link between electron and hydrogen ion transport fundamental to quantum symmetry breaking. Electron transfer does not in principle require the complex coded active sites required to catalyze specific molecular transformations. Model systems using Fe-porphyrins and imidazole can couple oxidative electron transport to phosphorylation [18] and photoactivated Mg-porphyrin to phosphate [40, 68]. These would initially have used H_2S as a substrate rather than the higher splitting energy of H_2O .

These primal features give a basis for the occurrence of excitable membranes associated with cells as an interactive manifestation of cosmic symmetry breaking. While this doesn't solve the hard problem, it does go some way towards a description in which the cellular excitability we do associate with consciousness does have a possible cosmological status in physical terms, rather than being an idiosyncratic result of biological evolution alone. We thus next look at the ways evolution may have selected for subjective consciousness.

13.11 Chaotic Excitability and Quantum Sensitivity as a Founding Eucaryote Characteristic

The evidence of the preceding section suggests that chaotic excitability may be one of the founding features of eukaryote cells dating from the purely replicative RNA era, before coded protein translation [49, 51]. The piezoelectric nature and high voltage gradient of the excitable membrane provides an

excitable single cell with a generalized quantum sense organ. Chaotic-sensitive dependence would enable such a cell to gain feedback about its external environment, rather than becoming locked in a particular oscillatory mode. Excitation would be perturbed by a variety of modes – chemically through molecular interaction, electromagnetically through photon absorption and the perturbations of the fluctuating fields generated by the excitations themselves, and mechanically through acoustic interaction. Such excitability in the single cell would predate the computational function of neural nets, making chaos fundamental to the evolution of neuronal computing rather than vice versa. Key chemical modifiers may have been precursors of the amine-based neurotransmitters that span acetyl-choline, serotonin, catecholamines and the amino acids such as glutamate and GABA, several of which have a primal status chemically. The use of positive amines may have chemically complemented the negatively charged phosphate-based lipids in modulating membrane excitability in primitive cells without requiring complex proteins. It is possible that chaotic excitation dates from as early a period as the genetic code itself and that the first RNA-based cells may have been excitable via direct electrochemical transfer from light energy, before enzyme-based metabolic pathways based on protein translation had developed.

The sense modes we experience are not simply biological as such but more fundamentally the qualitative modes of quantum interaction between molecular matter and the physical universe. They thus have plausible cosmological status. Vision deals with interaction between orbitals and photons, hearing with the harmonic excitations of molecules and membrane solitons or piezoelectric excitons, as evidenced in the action potential. Smell is the avenue of orbital–orbital interaction, as is taste. Touch is a hybrid sense involving a mixture of these. The limits to the sensitivity of nervous systems are constrained only by the physics of quanta, rather than biological limits. This is exemplified by the capacity of retinal rod cells to record single quanta, and by the fact that membranes of cochlear cells oscillate by only about one H atom radius at the threshold of hearing, well below the scale of individual thermodynamic fluctuations and vastly below the bilayer membrane thickness. Moth pheromones are similarly effective at concentrations consistent with one molecule being active, as are the sensitivities of some olfactory mammals.

The very distinct qualitative differences between vision, hearing, touch and smell do not appear to be paralleled in the very similar patterns of electrical excitation evoked in their cortical areas. If all these excitations can occur simultaneously in the excitable cell, its quantum-chaotic excitation could represent a form of cellular multisensory *synaesthesia*, which is later specialized in the brain in representing each individual sense mode. Thus, in the evolution of the cortical senses from the most diffuse, olfaction, the mammalian brain may be using an ultimate universality, returning to the original quantum modes of physics in a way that can readily be expressed in

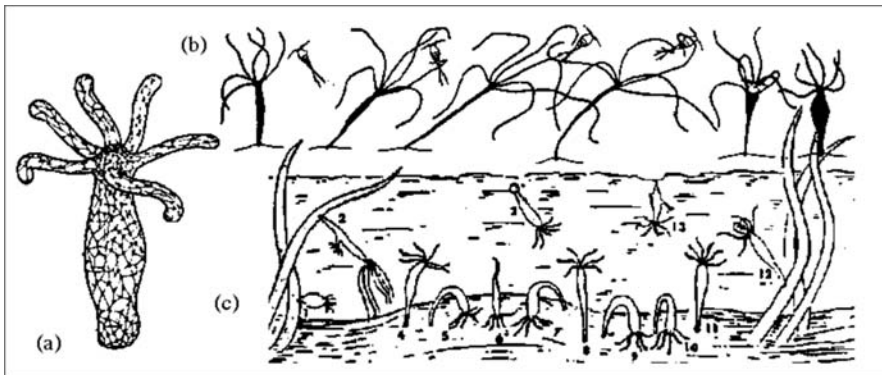


Fig. 13.15. Hydra poses a dilemma for theories of cognitive development based on neural net organization rather than the complex adaptability of individual neurons. Hydra can reassemble ectoderm and endoderm if turned inside out and has a disseminated neural net (a) with no global structure, except for a slight focus around the mouth. Nevertheless, it can coordinate eating in a similar manner to an octopus (b) and possesses more diverse types of locomotion than animals such as molluscs and arthropods that have structured ganglia. These include snail-like sliding, tumbling, inch-worm motion and use of bubbles and surface films

differential organization of the visual, auditory, and somatosensory cortices according to a single common theme of quantum excitability. This is consistent with cortical plasticity that enables a blind person to use their visual areas for other sensory modes.

It is thus natural to postulate that, far from being an epiphenomenon, consciousness is a feature that has been elaborated and conserved by nervous systems because it has had unique survival value for the organism. We are thus led to an examination of how chaotic excitation may have evolved from single-celled animals through the early stages represented by Hydra, Fig. 13.15, with its diffuse neural net, to the complex nervous systems of metazoa. We have seen how chaotic excitation provides for exploration of phase space and sensitivity to internal and external fluctuations. However, the conservation of consciousness may also involve features expressed only by chaotic systems that are fractal to the quantum level.

It is a logical conclusion that the conscious brain has been selected by evolution because its biophysical properties provide access to an additional principle of predictivity not possessed by formal computational systems. One of the key strategies of survival implicated in brain dynamics is anticipation and prediction of events [49, 52, 12, 66, 70]. Computational systems achieve this by a combination of deductive logic and heuristic calculation of contingent probabilities. However, quantum nonlocality may also provide another avenue for anticipation that might be effective even across the membrane of a single cell, if wave reductions are correlated in a nonlocal manner in space-time.

13.12 Models of the Global-Molecular-Quantum Interface

The question of free-will in a quantum uncertain universe led several of the early researchers of quantum physics to propose that the brain may be in some way utilizing the uncertainty of individual quanta that appears to violate causality at the foundation of physics [67], to give rise to a quantum uncertain brain state consistent with free-will. Eddington [32], for example, noted that the uncertainty of position of a synaptic vesicle was large enough to be comparable with the width of the membrane, making synaptic release potentially subject to quantum uncertainty. Walker [87] noted quantum tunneling in synaptic transmission and Eccles [31] noted the relation between mental events, neural events and quantum probability fields.

To mount an effective solution to the hard problem requires making a connection between subjective consciousness and the physical world, which has mutual explanatory power. The functionally closest phenomena to subjective consciousness we know of are global electrochemical brain processes that appear to be “holographically” distributed, chaotic, and potentially relate to the binding problem of the central theater of conscious attention through phase coherence. The most promising avenue, given what we have discovered about the quantum world is to look for a bridge between global phase coherences and those we associate with quantum entanglement and transactions. This raises the enticing possibility of linking the paradox of conscious will with the paradox of reduction of the superposition of quantum states to a physical history, thus providing a complementary view of the mystery the hard problem presents both from physical unpredictability and from subjective intentional decision making.

The fractal dynamics model proposes that the conscious state corresponds to phase-coherent, temporally edge-of-chaos, excitations of coupled regions of the cortex and thalamus, capable of entering a critically poised unstable state if faced with conflicting stimuli that cannot be resolved from learned experience. This would in turn enable quantum fluctuations at the molecular level to become an unstable “watershed” that tips the global state towards a resolution. The fractal model uses the molecular processes of synaptic vesicles and ion channels currently believed to be pivotal in supporting active conscious states. Such a model enables instability at the quantum level to become amplified when the global brain state is critically poised, in a way that could be possible even though the corresponding excitations are distributed across the cortex. The situation could in principle enable global excitations to be considered as “inflated” quanta – either simple harmonic excitations or solitons, and phase coherence of global brain states to thus be interpreted as coherent quantum states.

The model of Hameroff and Penrose seeks a more specific mechanism in the microtubules of the neuron. In particular, they have noted that tubulin exists in two forms and could thus enter a quantum superposition of

states. They thus envisage tubulin acting as a quantum cellular automation, interleaving between classical and quantum computational states. However, microtubules are extensively involved in transport of essential molecules and whole organelles, as well as cytoskeletal architecture and synaptic growth and it is unclear whether they have a direct role in the fast forms of excitation of the electrochemical states we associate with conscious awareness. Generally, when a single cellular system serves two critical, yet differing functions, evolution by gene duplication is likely to occur, so that both characteristics can be selected for independently. It is hard to see how the microtubules can be both involved in active transport and at the same time performing quantum calculations essential to the organism without potential conflicts of interest. These considerations do not apply to membrane excitation and synaptic transduction, which are already directly connected to excitability.

In the OOR model, consciousness is a passive result of a quantum computation that occurs in the pre-conscious state and is resolved objectively by a self-energy splitting of the gravitational centers of mass of the superimposed states in “objective reduction” and conscious awareness emerges only subsequently, based on the outcome. Effective quantum computation of even simple problems, such as Shor’s algorithm [19] for factoring a number, involve complex boundary constraints, including the capacity to Fourier transform one part of a quantum “register” to represent periodicities in the superimposed states of the other part (see p. 431). It is unclear whether the microtubular automation can be configured to do this at the same time as serving the active transport of molecules and organelles. The Penrose and Hameroff model suggests the neuron can very rapidly alternate quantum computing with normal function by temporarily isolating the microtubules from the membrane through disassociating the linking MAP proteins (to avoid quantum decoherence effects). This means the quantum computation is isolated from the global brain state during the quantum computation cycle. The quantum computation phase would thus be fragmented at the cellular level and could not correspond to the subjectively conscious state.

Quantum computing is subject to decoherence because any quantum interaction with the outside world except the measurement itself disrupts the superposition of states by interacting with it. By contrast, transactional supercausality incorporates contingent interaction foci, in developing the complexity of the subquantum system, and would thus be robust to decoherence.

The fractal model envisages chaotic and unstable processes penetrating the quantum level in a way that minimizes decoherence because of the self-coupling of the brain state to a restricted class of global excitations. A variety of closed quantum systems that correspond to classical chaos, including nuclear dynamics, the quantum stadium and magnetically perturbed high-energy orbitals display inhibition of quantum chaos in phenomena such as scarring of the wave function, in which periodic repelling orbits “reclaim” the probability distribution. However, quantum-kinetic interactions in an

open molecular system [41] do appear to retain the attributes of chaotic instability. Unlike the OOR model the transactional model we investigate next envisages subjectively conscious decision making associated with a global dynamical criticality as capable of participating in “anticipatory” collapse of the wave function and thus actively changing subsequent brain dynamics.

13.13 Quantum Mind and Transactional Supercausality

Recapitulating on our ideas of transactions we note the following points:

1. Since the first ideas linking quantum uncertainty and free-will were proposed, the nonlocal space-time spanning manifestations of uncertainty have become more apparent and given rise to the concepts of quantum nonlocality and entanglement. A key example of this is the pair-splitting experiment, Fig. 13.16, in which a single quantum event releases two particles in the same wave function. If the state of either is measured, the particles’ complementary spins or polarizations then become immediately correlated in such a way that an exchange of local information limited by the speed of light cannot achieve.
2. The space-time properties of quantum phenomena also have a peculiar hand-shaking potentiality, in which future can affect past as well as past affect future. In Fig. 13.5 is an illustration of the Wheeler delayed-choice experiment on a cosmic scale in which the route taken by a photon around

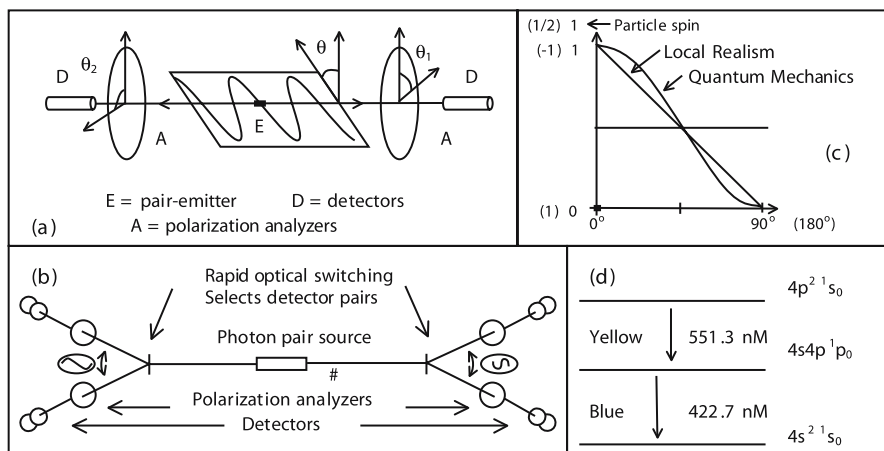


Fig. 13.16. (a) Pair-splitting experiment for photons. (b) Time-varying analyzers are added driven by an optical switch too fast for light to cross the apparatus. (c) The results are consistent with quantum mechanics but inconsistent with Bell’s inequalities for a locally causal system. (d) The calcium transition [5]

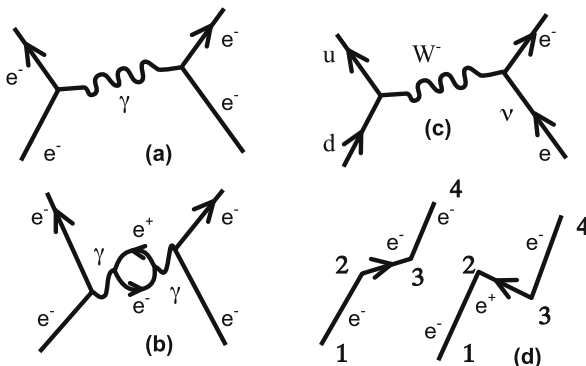


Fig. 13.17. Quantum electrodynamics: (a,b) Two Feynman diagrams in the repulsion of two electrons. In the first a single virtual photon is exchanged between two electrons, in the second the photon becomes a virtual electron–positron pair during its transit. All such diagrams are integrated together to calculate the strength of the electromagnetic force. (c) A similar diagram shows how neutron decay occurs via the W^- -particle of the weak nuclear force, which itself is a heavy charged photon. (d) A time-reversed electron scattering is the same as positron creation and annihilation

a gravitational lens can be determined after it has already passed, by rearranging the detection apparatus at the end of its path, reinforcing the notion of future–past hand-shaking. The concept is also fully consistent with quantum field theory formulations as exemplified by Feynman diagrams, Fig. 13.17, which themselves can be time reversed, resulting for example in interconversion between positrons and electrons.

3. These paradoxes are resolved by the transactional interpretation, Fig. 13.6. In this description each contingent emitter of a quantum sends out an offer wave and each contingent absorber sends out a confirmation wave. In reduction of the wave function the interrelationship of all these together throughout space-time collapses (possibly sequentially) into a match-making pairing of real interactions between paired emitters and absorbers as in Fig. 13.6a. The decision-making process results in collapse of the wave function of many possibilities to the actual unique real quantum event. This becomes an interference between one emitter and one absorber superimposing to form the real particle traveling between. In the transactional interpretation, Sect. 13.5, the absorber, such as my eye looking at a distant star is thus as essential to the transaction as the star that long ago emitted the light. In this view of quantum mechanics there is then a sense in which any quantum emitter is implicitly aware of the future existence of the absorber by the very act of engaging the transaction.
4. The force field is explained through virtual particles (such as the photon) appearing and disappearing through uncertainty. Such particles must

necessarily link an emitter and an absorber. The theory of virtual and real particles demonstrates that real and virtual particles are, in principle, indistinguishable. If we oscillate the electromagnetic field we elicit a radio broadcast. Virtual photons generating the electromagnetic field have become real ones telling us the news. If the universe emerged from a single wave function all real particles may also be entangled. Even if the universe expands forever and some quanta, such as photons, are disseminated into space, causing a permanent disparity between emitters and absorbers, the kinds of excitons we naturally associate with phase correlations in global brain dynamics are all transient excitations, both emitted and absorbed by the brain and its neurons as boundary conditions as an integral part of dynamical systems feedback.

We have discussed the idea that chaotic excitation was a primal phenomenon that occurred in the first cells, even as the metabolic pathways were becoming established. Chaotic excitation leads to a multiquantum-mode sense organ responding to external perturbations of the environment by sensitive dependence. The idea is that this sense organ then found that through the exchange of transactional hand-shaking with its own emission and absorption states, a form of quantum anticipation of its own immediate future resulted. This anticipation then proved to have significant selective advantage for the organism and thus became fixed in evolution as the sentient conscious brain, complementing computational capacity with transactional anticipation through the chaotically fractal central nervous system.

An evolutionary explanation for the role of subjective consciousness intervening in the states of the brain emerges if the brain uses unstable processes and nervous systems can access the laws of quantum nonlocality to enable a form of temporal anticipation of pivotal survival value, which would hence be strongly selected as a trait. This could affect global brain states if they are critically poised or have chaotic sensitive dependence. The hard problem then exerts a complementarity between entangled quantum states along with their corresponding contingent transactions, and subjective states, in which conscious choice becomes physical action partly through collapse of the wave function – the component that corresponds to the “free” component of will not determined by initial conditions or computational constraints. Even if the universe expands forever and some quanta such as photons are disseminated into space, the kinds of excitons we naturally associate with phase correlations in global brain dynamics are all transient excitations both emitted and absorbed by the brain and its neurons as boundary conditions.

The transactional process closely parallels known techniques of quantum computation [19] using a superposition of states as boundary condition rather than the finite number of real particles exchanged in transactions. The use by the brain of complex excitons may make it sensitive to an envelope of states spanning immediate past, present and future [62] – the anticipatory “quantum of the conscious present”. We can model the evolving brain dynamic

as a complementation between two processes, an ordered process of computation based on the “initial” conditions forming a skeleton defining the ordered context and a chaotic, uncertain complement. It is thus possible for the brain to utilize all the prevailing contexts in coming to a decision and yet involve some free choice in the outcome. Such excitons might have restricted interactions that would isolate them from quantum decoherence effects [92] as illustrated by quantum coherence imaging [82, 88] and would also serve to ensure transactional hand-shaking occurred. The ordered aspect of the dynamic would be a function of initial conditions but the complementary chaotic, uncertain regime would involve inflated future states through transactional hand-shaking. The uncertainty in the transition from chaos to order representing, perception, or cognitive “eureka”, corresponds to an inflated reduction of the wave function. The physical model of historicity and the subjective experience of conscious intentionality will thus coincide.

The “binding problem” – how sensory experiences being processed in parallel in different parts of the cortex are bound together to give the conscious expression we associate with our integrated perception of the world – has no direct solution in terms of being hard-wired to some collection point – the ultimate seat of consciousness. Every indication is that consciousness is distributed and bound together by nonlinear resonances in the brain, which is exactly what we would expect in a situation self-resonances were being used as part of a transactionally supercausal solution to the perception–cognition dilemma.

The problem of consciousness is consummated by the question of free-will. What is the function of subjective consciousness if it is only brain states and not the subjective aspect that effect our future physical states? Put in reverse, if subjective consciousness has any evolutionary advantage then it can manifest itself only by perturbing in some way the physical causality of brain processes. This is the problem of intent. Everyone who sets foot into the world invests in the principal of personal autonomy, that we have subjective control over our physical circumstances. All questions of legal responsibility hinge on it. Yet this implies mind affecting matter, something that mechanistic science struggles to deny. In the transactional model of perception, intention, and will, subjective consciousness enters into the picture as the inner complement of the quantum nonlocal hand-shaking process that violates the causality of initial or former states determining future states, which we associate with the Newtonian universe and temporal determinism. This occurs as a consequence of special relativity and the fact that the boundary conditions of collapse include future contingent absorbing states.

Since the quantum transaction is a fundamental interpretation of all quanta, it is general to all quantum interaction. Its manifestation in resolving the fundamental questions of interaction with the physical world thus adopts a cosmological dimension, in which the sentient conscious brain becomes a central avenue for the expression of subjectivity through quantum nonlocality in space-time.

At the same time, the brain has been evolving towards a type of universality expressed in flexible algorithms for multisense processing and modeling, which experiencers of synesthesia can witness are capable of coexisting in one multisense perception mode. A huge cosmological question is now raised. Is evolution simply adventitious accident, or is it part of the way the quantum universe explores its own phase space of possibilities in reaching towards a universal expression of the quantum entangled physical universe? In a quantum universe we have the dilemma of the many-universes problem. How does reduction of the wave packet result in one history or another occurring?

Transactional supercausality explains the cat paradox, Fig. 13.3, by interlacing contingent emitters and absorbers across space-time in a hand-shaking, to form a complex subquantum system whose outcomes are naturally distributed according to the wave amplitude because they are the result of bifurcations of offer and confirmation waves dependent on their relative amplitudes. Reduction of the wave function corresponds to a particular matching of emitter and absorber for one exchanged wave-particle. Determining which part of the wave function a particle appears in is converted into the combinatorial one of which emitter and absorber pair are matched up. One can model the transition from many-to-many to one-on-one in terms of a nonlinearity in which pairs become “mated” in sequence. However, this process cannot be resolved causally, based on initial conditions because of the hand-shaking, leaving a loophole that only the “anticipatory” mind and not computation per se can resolve. The many probability multiverses thus become resolved from superimposed multiverse superabundance by hand-shaking across space-time sequentially, reducing the packet of all possible emitter-absorber connections to a sequence of “happy marriages” as illustrated in Fig. 13.6a.

The transactional principle also teaches us that modeling the interior domain of the quantum entanglement, even if it can be understood as an interactive sequence of emitter-absorber reductions, will only give indeterminate predictions if only past boundary conditions are defined. It also shows us how symmetric hand-shaking time occurring in reduction fits with the sequential arrow of time defined by real, retarded, positive energy particles. The universe, thus becomes experientially historical through the uncertainty of free choice and perception itself in distinguishing the perceived from the uncertain background. Napoleon does not win the Battle of Waterloo, but Britain wins Trafalgar, despite the feigned uncertainty of Nelson’s blind eye. The same goes for all the hopeful monsters of evolution that never came to be. Quantum nonlocality thus appears to have a method through space-time hand-shaking of determining which one of the multiverses hovering in the virtual continuum will actually manifest itself. The role of consciousness as a cosmological process appears to mediate effectively between the world of the cosmic subjective, represented in physics as quantum nonlocality, with the uniqueness of historicity, which never fully converges to the statistical interpretation of the cosmic wave function, because each change leads to another, throughout cosmic epochs.

This leads to a deep question shared by all human cultural traditions from the dawning of shamanism, through Vedanta to the Tao and even in the Judeo-Christian prophetic tradition, that mental states of awareness and subsequent physical happenings are interrelated by an anticipatory principle. If historicity is interactive with both the quantum realm and the existential condition, what are the consequences for science, society and cosmology itself? The description of reality here suggests that the physical universe has a complement – the subjectively conscious existential condition. Such a view both of the cosmological role of evolution to sentience and the brain as an interface between the cosmic subjective and the physical universe puts us right back into the center of the cosmic cyclone in a way that Copernicus, Galileo, Descartes, Leonardo and Albert Einstein would have all appreciated.

Consciousness is then not just a globally modulated functional monitor of attention subject helplessly to the physical states of the brain, but a complementary aspect to physical reality, interacting with space-time through uncertainty and quantum entanglement in a manner anticipated by Taoist [89] and Jungian ideas of synchronicity [47]. The same considerations apply to the use of chance oracles such as the I Ching, and the Hebrew Urim and Thummim, both of which use chaotic processes to divine an uncertain outcome. It is also possible to model hunches or premonitions as perceptions of partially collapsed contingent transactional ensembles, making certain perceived outcomes more likely than they would have been had no perception occurred. The anthropic cosmological principle [10] declares that possible universes are constrained by the existence of observers. In the weakest terms the anthropic principle ensures laws of nature compatible with the complexity of life. In stronger forms the existential nature of the universe is partially dependent on the existence of conscious observers. In transactional super-causal forms, conscious perception is resulting in the collapse of multiverses to the historical physical universe we experience. These observations illustrate anthropic aspects of the subject-object complementary hard problem model.

Although subjective consciousness, by necessity, reflects the constructive model of reality the brain adopts in its sensory processing and associative areas, this does not fully explain the subjective aspect of conscious experience. Conscious experience is our only direct avenue to existence. It underlies and is a necessary foundation for all our access to the physical world. Without the consensuality of our collective subjective conscious experiences as observers, it remains uncertain that the physical world would have an actual existence. It is only through stabilities of subjective conscious experience that we come to infer the objective physical world model of science as an indirect consequence. For this reason, subjective consciousness may be too fundamental a property to be explained, except in terms of fundamental physical principles, as a complementary manifestation to quantum nonlocality, which directly manifests the principle of choice in free-will in generating history.

13.14 Complementarity and the Sexuality of Quantum Entanglement

This cosmology is intrinsically sexual and gives rise to cosmological prisoners' dilemma paradoxes similar to those of sexually antagonistic coevolution in which any attempt to mount a description based on only one aspect results in impasse [34]. This sexuality is manifest in wave–particle complementarity and successive complementarities in physics from advanced and retarded solutions, through boson–fermion complementarity. It is also manifest in subject–object complementarity.

Subject–object complementarity is different from either panpsychism or Cartesian duality. The subjective distinction is described as complimentary to the physical “loophole” of quantum uncertainty and entanglement, just as the wave and particle aspects of the quantum universe are complementary. Subjective and objective are interdependent upon one another with neither fully described in terms of the other. Furthermore, the transactional interpretation is intrinsically sexual in the sense that all exchanges are mediated through entangled relationship between an emitter and an absorber in which reduction of the wave function is a match-making sequence of marriages. This sexual paradigm is not simply an analogy, but is a deep expression of the mutual complementarity and intrinsic relationship manifest in the existential realm, physically and subjectively and between.

Extrapolating, the theory suggests the evolution of gendered recombinational sexuality, as is found in biology in the metaphyta, is not simply an analogy with quantum complementarity, but is an emergent expression of the same complementarity principle. The single ovum, by necessity, is driven to seek fertilization through a solitonic wave of excitation that extends across the membrane. The multiple sperm, by contrast, are particulate packets of molecular DNA, without a cellular cytoplasmic contribution. Thus biological sexuality is utilizing quantum complementarity in the symmetry breaking of gender.

In Tantra, the subject–object relation is an intimate sexual union, which, in its retreat from complete intimacy, spawns all the complexity of the existential realm. In the Taoist view the same two dyadic principles are the creative and receptive forces that in their mutual transformation give rise to all the dynamic states of existence. In Taoist thought, the cosmological principle is manifest in three phenomena, chance, life and consciousness, the very phenomena appearing in physical terms in quantum physics, evolution and brain dynamics. The transactional principle clearly establishes the marital dance of emitter and absorber as the foundation of historicity – the collapse of the infinite shadow worlds of multiverses into the one line of history we experience in life, evolution, consciousness and social and natural history.

Randomness remains a scientific mystery, explained ultimately in cosmological terms by quantum entanglement. The source of the scientific concept of randomness lies in theories, such as probability theory, statistical mechanics,

and the Copenhagen interpretation of quantum mechanics, which draw generalities from an incomplete knowledge of the system. However, the source of supposedly random events in the real world lies either in highly unstable systems, which themselves may draw their uncertainty from the quantum level, or directly from the phenomena of reduction of the wave function under the probability interpretation. The transactional approach seeks to explain the substratum of entanglement in a deeper interaction. This complex system could provide an ultimate explanation for the origin of randomness.

13.15 The Hard Problem: Subjective Experience, Intentional Will and Quantum Mind Theories

This chapter proposes that the existential realm is a complementarity between subjective consciousness and the objective physical universe, of a founding cosmological nature. It advances a basis for natural selection of subjective awareness through a quantum entangled form of anticipation independent from computation as such. This presents a unique solution to the hard problem, not by attempting to explain subjective consciousness through objective brains states (the “classical” error), but by elaborating a theory based on the complementarity between subjective consciousness and physical brain states, in which these features are complementary views of existential reality as are wave and particle in the physical realm. These are manifest in the subjective aspect in conscious perception and intentional will and in the objective aspect in physical indeterminacy accompanied by reduction of the wave packet and the consequent historicity of the universe collapsing the quantum superabundance of multiverses to the physically historical world we experience.

In this view, subjective awareness is not identifiable with quantum entanglement but is complementary to it. Through chaotic instability and its fractal interaction with quantum uncertainty, a loophole is created in the physical description that allows subjective consciousness to have anticipatory selective advantage. This advantage is in turn given expression in the physical world through the capacity to intend, or “will”. Neither is willing performed exclusively by the subject, for if a person’s mind is already made up either by prejudice or by the logic of the circumstances, we are not discussing the “free” aspect of will, but rather when they are making a genuine choice in spite of all the prevailing circumstances, even by hunch or intuition. Here, intentional will is not any kind of specific drive possessed or directed by the organism, but the very capacity for subjective experience to, in turn, affect the physical universe and the future potentialities it may perceive, by an act of free-will. Subjective consciousness transforms incoming sensory and other forms of perception into the outgoing expression of creative consequences in intentional action. The freedom of will also means it is not entirely under ordered conscious control. We depend on a founding sense of personal autonomy to be able to act as sane individuals, without

which we might all become catatonic or robotic automata. Intentional will is a mystery, both from the objective physical description, and from subjective existence. Just as uncertainty and unpredictability open the loophole making free-will possible in the quantum universe, so the subjective aspect of will remains potentially as free of internal conditioning by drive or ego as it is potentially free of becoming completely conditioned by the circumstances of the physical world. In so far as we, as sentient conscious individuals, treat love and will as mysteries in their own right, so they become the subjective complement of an integrated expression of quantum nonlocality and an entanglement that permeates the entire universe. In applying our free-will, we each contribute collectively to the collapse of the infinite possibilities of the multiverses before us into a beneficent or sterile outcome. Just as the choice is ours at all points to enhance or diminish the diversity and abundance of life, so our world history becomes one of abundance or poverty.

We also have to consider how sensory information, which may be preconscious, achieves a level of consensual arousal, e.g. through “phase coherence” sufficient to draw attention to itself and become a fully fledged conscious experience. As [62] has noted, this may involve backward time referral of a conscious experience to its first preconscious manifestation.

The transactional perspective stands unique among quantum theories in providing an explanation for anticipatory consciousness that can affect the future of the physical universe through will. The Copenhagen interpretation, being essentially a theory of our knowledge, rather than the universe itself, can say nothing on this question of interactivity between subjective and objective aspects. Many-worlds interpretations, having no process of collapse provide no mechanism whatever for consciousness to interact to influence the physical future. The Bohm pilot wave theory being a semiquantum theory with a classical underpinning in the quantum potential likewise remains a purely objective description, which also has specific problems dealing with situations that can generate new quantum degrees of freedom such as a high-energy photon creating a particle–antiparticle pair. Penrose and Hameroff’s [44] OOR model likewise provides an objective reduction process driven in the limit by gravitational decoherence (the gravitational self-energy between the differing mass distributions of the outcomes), which permits subjective consciousness (or the transition from the preconscious state) only to reflect the objective reduction, and thus cannot explain how intentional consciousness can affect the physical universe.

Hameroff and Penrose concentrate on the microtubule as a possible basis for quantum computation using two states of the tubulin monomer, in the form of a quantum cellular automation, because it displays convenient automata-like structure. Certainly this is an interesting hypothesis and the possible involvement of microtubules in conscious states is a significant area of research, however, the hypothetical process requires the isolation of microtubules to avoid decoherence, possibly through delinking of MAP protein

connections with the excitable membrane. This effectively reduces any form of quantum consciousness to collections of isolated cell interiors, preventing a direct feedback between the electrodynamical global brain resonances we identify with active conscious states (e.g. in the 40-Hz region) and quantum nonlocality. Microtubules possess many interesting properties, including possible solitonic interactions. It has also been suggested microtubular proteins might possess topological quantum computing properties [36] of noncommutative anyons [60], which would be robust to quantum decoherence [92]. However, their primary functions are transport of essential chemicals and components such as vesicle and maintaining structural integrity of graduated processes such as synaptic adaption and long-term potentiation.

What is really needed is a quantum mind theory capable of linking the fast electrodynamical resonances we associate with active conscious states directly to an anticipatory form of quantum nonlocality. The supercausal version of transactional quantum theory, which allows for mutual collapse of an entangled transaction to specific real connections between emitters and their future absorbers, is unique in providing such a possibility. The use of chaos and fractal dynamics provides mechanisms to inflate quantum uncertainties and the use of wave coherence in global brain states forms a direct basis for exciton exchange between emitters and absorbers consisting of immediate past and future brain states, thus linking them into a hand-shaking resonant system.

13.16 Consciousness and Neurocosmology

The diversity of wave-particles resulting from symmetry breaking of the four fundamental forces, the weak and color nuclear forces, electromagnetism, and gravitation, finds its final interactional complexity, in which all forces have a common asymmetric mode of expression, in complex molecular systems. It is thus natural that fundamental principles of this quantum interaction may be ultimately realized in the most delicate, complex and globally interconnected molecular systems known – those of the conscious brain. The brain may be one of the few places where the supercausal aspects of wave-packet reduction can be clearly manifest, as a result of its unique capacity to utilize entanglement in its dynamics. Although other unstable systems, from the weather to axionic dark-matter condensates [81] may also display, or amplify, features of nonlocality, it is difficult to conceive of a physical system that could in any way match the brain as a potential detector of correlations and interrelationships within the domain of quantum mechanics. Cosmology is not simply a matter of vast energies, but also quantum rules. In these rules of engagement, more fundamental even than symmetry breaking, the stage appears to be set for the emergence of sentient organism as the culminating manifestation in complexity of quantum interaction. In this sense the conscious brain may be the ultimate inheritor and interactive culmination of the

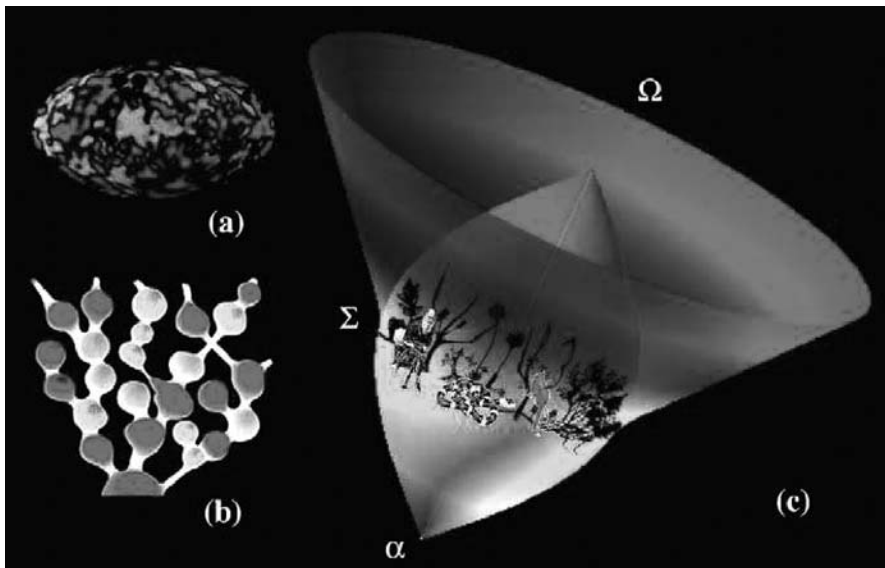


Fig. 13.18. (a): The cosmic background – a red-shifted primal fireball. This radiation separated from matter, as charged plasma condensed to atoms. The fluctuations are smoothed in a manner consistent with subsequent inflation. (b) Fractal inflation model leaves behind mature universes while inflation continues. (c) Darwin in Eden: “Paradise on the cosmic equator” – life is an interactive complexity catastrophe resulting from force differentiation representing the Σ of interactive complexity rather than the α cosmic origin or the Ω of final culmination

quantum process at the foundation of the universe itself. This is the consumption of cosmology, not in the alpha of the Big Bang, nor in the omega of finality but in the sigma of its interactive complexity, Fig. 13.18c.

The deepest question that can be posed about cosmology is precisely that of the hard problem: What is the relationship between the existential observer and the universe at large? What is the relation between conscious subjectivity and the objective physical world? This is a question that has plagued philosophers and scientists from the early Greeks through Bishop Berkeley and Descartes to David Chalmers’ [21, 22] description of the “hard problem in consciousness research” as a fundamental philosophical chasm that can only be crossed through a greater description of reality.

Despite the advances of modern scanning techniques such as PET (positron emission tomography) and fMRI (functional magnetic resonance imaging) and electro- and magnetoencephalographic studies, a chasm still remains between the brain states under a researcher’s probe and the subjective experiences of reality we depend on for our awareness of the physical world. This comes on top of a fundamental complementarity upon which we depend for our existence. Although we live as biological organisms, raise families,

navigate our lives and perform our science on the assumption of the existence of the physical world, we access physical reality only through our subjective sensory experiences. Without the direct veridical access we have to subjective experience, there would be no conscious “observers”. It remains unclear under these circumstances that one could establish that the physical universe would exist in any objective “sense”.

Ironically, a purely objective physical world description considers only brain states, leaving subjective consciousness to the perilously ephemeral status of an epiphenomenon, or not existent at all. However, the physical world is really a consensual stability property of our conscious experiences, despite the fact that we are physical organisms whose consciousness appears to depend on our remaining alive. We can both consciously agree that the table is made of wood, or that we will bleed if cut, so the subjective aspect is capable of representing the objective. The objective is capable in turn of “incorporating” the subjective in terms of uncertainty in the physical. A fully cosmological theory thus has to encompass both realms.

This access to the subjective is profoundly augmented by a variety of subjective states, some of which have no direct correlate in the physical world, yet can be commandingly real to the observer. Firstly, consciousness is constructive, and fills in details to generate a subjective description of reality that can often lead to peculiar results as illustrated by visual illusions, Fig. 13.19. More significantly, we have states of meditative trance, psychedelic hallucination and the intense phases of dreaming. Although various tests can be made by the astute subject to distinguish dreaming from waking reality, the very fact

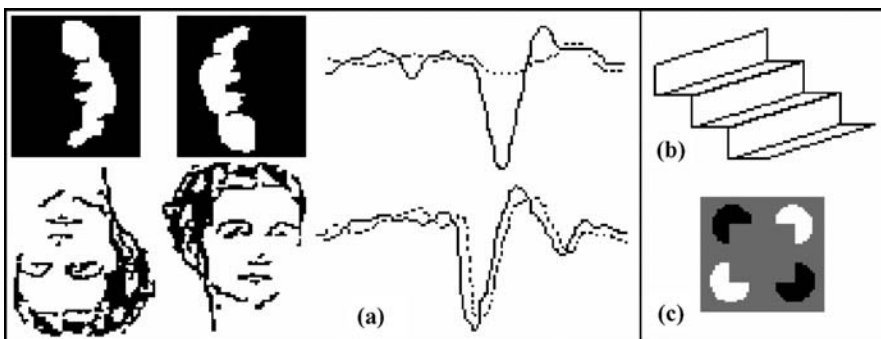


Fig. 13.19. (a) Correspondence between brain states and subjectively perceived differences, is illustrated by the differing evoked potentials (averages of many recordings triggered by the same stimulus) when an inverted face is easily recognized as below, from the ambiguous image above. However the differing electrical potentials are qualitatively quite distinct from the differing subjective experiences in the two cases. Conscious experience cannot thus be reduced to brain states. Right: Visual illusions stimulate neurons that code explicitly for illusory contours (c), and mutually interfering 3D perspectives (b)

of dreaming as an alternative veridical reality raises a deep question about the nature of the everyday world we perceive. Is it nothing but an internal dream state anchored by additional stability constraints provided by sensory input? If we are actually witnessing exclusively and only our internal model of reality, what then is the manifest nature of the physical world?

References

1. Agladze, K., Kinsky, V., Pertsov, A. (1984). *Nature* **308**:834–5.
2. Albano, A.M., Abraham, N., de Guzman, G., Tarroja, M., Bandy, D., Gioggia, R., Rapp, P.E., Zimmerman, I., Greenbaum, N., Bashore, T. (1986a). In *Dimensions & Entropies in Chaotic Systems* (ed.) Mayer-Kress, G. Springer-Verlag, Berlin:231–240.
3. Albano, A.M., Mees, A., de Guzman, G., Rapp, P.E. (1986b). In *Chaos in Biological Systems* (eds.) Degn, H., Holden, A.V., Olsen, L.F., Plenum Press, New York:207–220.
4. Ansari, A., Berendzen, J., Bowne, S., Frauenfelder, H., Iben, I., Sauke, T., Shyamsunder, E., Young, R. (1985). *Proc. Nat. Acad. Sci.* **82**:5000–4.
5. Aspect, A., Dalibard, J., Roger, G. (1982). *Phys. Rev. Lett.* **49**:1804.
6. Babloyantz, A. (1989). In *Brain Dynamics*, Basar, E., Bullock, T.H. (eds.) Springer-Verlag, Heidelberg:122–130.
7. Babloyantz, A. and Salazar, J.M. (1985). *Phys. Lett.* **111A**:152–156.
8. Babloyantz, A. and Destexhe, A. (1986). *Proc. Nat. Acad. Sci.* **83**:3513–3517.
9. Ball, P. (2003). *Nature* **5** Sept.
10. Barrow, J., Tipler, F. (1988). *The Anthropic Cosmological Principle*, Oxford Univ. Press, Oxford.
11. Basar, E. (1990). In *Chaos in Brain Function*:1–30, Basar, E. (ed.). Heidelberg: Springer-Verlag.
12. Basar, E., Basar-Eroglu, J., Röschke, J., and Schütt, A. (1989). In *Brain Dynamics*:43–71, Basar, E., Bullock, T.H. (eds.). Heidelberg: Springer-Verlag.
13. Bell, J.S. (1966). *Rev. Mod. Phys.* **38/3**:447.
14. Bern, M. and Graham, R. (1989). *Sci. Am.* **Jan**:66–71.
15. Blakemore, C. (1991). *Sir Douglas Robb Lectures*, Auckland, N.Z.
16. Bohm, D. (1952). *Phys. Rev.* **85**:166–93.
17. Bohm, D. (1980). *Wholeness and the Implicate Order*. London, Boston and Henley, U.K. Routledge and Kegan Paul.
18. Brinigar, W., Knaff, D., Wang, J. (1966). *Biochemistry*:36–42.
19. Brown, J. (1994). *New Scientist* **Sept 24**.
20. Calude, C., Pavlov, B. (2002). *New Scientist* **6 Apr.**
21. Chalmers, D.J. (1995). *Scientific American* **Dec.**:62–69
22. Chalmers, D.J. (1996). *The Conscious Mind*. Oxford University Press, Oxford.
23. Chay, T.R., Rinzel, J. (1985). *Biophys. J.* **47**:357–366.
24. Chown, Marcus (2004). *New Scientist*, **183**:2457 24th July 30.
25. Clauser, J.F., Shimony, A. (1978). *Reports in the Progress of Physics*, **41**:1881–1927.
26. Cramer, J.G. (1986). *Rev. Mod. Phys.* **58**:647–687.
27. Crick, F., Koch, C. (1992). *Sci. Am.* **Sep**:110–117.

28. Dennett, D.C. (1991). *Consciousness Explained*. Little Brown and Co., Boston.
29. Deutsch, D. (1985). *Proc. Roy. Soc. Lond. A* **400**:97–117.
30. Dunne, J.W. (c 1935). *An Experiment With Time*. Faber, (c1935 1st edn.). London.
31. Eccles, J.C. (1986). *Proc. R. Soc. Lond. B* **227**:411–428.
32. Eddington, A.S. (1935). *New Pathways in Science*. Cambridge University Press, Cambridge.
33. Epstein, I., Kustin, K., DeKepper, P., Orbán, M. (1983). *Sci. Am.* **Mar**:112–123.
34. Fielder, Ch., King, Ch. (2004). *Sexual Paradox*. <http://www.dhushara.com/>
35. Fox, R.O., Richards, F. (1982). *Nature* **300**:325–330.
36. Freedman, M., Kitaev, A., Larsen, M., Wang, Z. (2002). *Topological Quantum Computing ArXiv*.
37. Freeman, W. (1991). *Sci. Am.* **264**, Feb:35–41.
38. Glansdorff, P., Prigogine, I. (1971). *Thermodynamic Theory of Structure, Stability and Fluctuations*. Wiley-Interscience, London.
39. Goldman-Rakic, P. (1992). *Scientific American* **Sep**:73–79.
40. Goncharova, N., Goldfelt, M. (1990). *Origins of Life* **20**:309–319.
41. Gutzwiller, M.C. (1992). *Sci. Am.* **266**:78–84.
42. Hackermüller, L. et al. (2003). *Physical Review Letters* **91**:090408.
43. Hall, D., Cammack, R., Rao, K. (1974). *Origins of Life* **5**:363–386.
44. Hameroff, S., Penrose, R. (2003). *NeuroQuantology*, **1**:10–35
45. Hawking, S. (2001). *The Universe in a Nutshell*. Bantam Press, N.Y.
46. Hooper, J. and Teresi, D. (1986). *The Three-Pound Universe*, MacMillan, New York.
47. Jung, Carl (1952). *Synchronicity an Acausal Connecting Principle*, in *The Structure and Dynamics of the Psyche*, Routledge and Kegan Paul, London.
48. Kandel, E., Schwartz, J., Jessel, T. (2000). *Principles of Neural Science* 5th edn. McGraw-Hill, NY.
49. King, C.C. (1978). *Univ. Auck. Math. Rept. Ser.* **134**.
50. King, C.C. (1989). *Phys. Essays* **2**:128–151.
51. King, C.C. (1990). *Origins of Life Evol. Biosph.* **20**:15.
52. King, C.C. (1991). *Prog. Neurobiol.* **36**:279–308.
53. King, C.C. (1996). *Fractal Neurodynamics and Quantum Chaos*, in *Fractals of Brain Fractals of Mind Advances in Consciousness Research 7* (eds.) MacCormac, E., Stamenov, M.:179–233.
54. King, C.C. (1997). *J. Mind and Behavior* **18**:155–170.
55. King, C.C. (2001). *WED Monographs* **1**:1–775 <http://www.dhushara.com>
56. King, C.C. (2003). *NeuroQuantology* **1**:129–148.
57. King, C.C. (2002). *WED Reviewed Monographs* <http://www.dhushara.com> **2/1**:1–20
58. King, C.C. (2002). *WED Reviewed Monographs* <http://www.dhushara.com> **2/2**:21–30.
59. King, C.C. (2004). *Neuroquantology* **3**:149–18.
60. Kitaev Alexei (2003). *Annals of Physics* **303**:2–30.

61. LaBerge, S. (1990). *Exploring the World of Lucid Dreaming*. Ballantine Books, Random House, New York.
62. Libet, B. (1989). *Behavioral Brain Sciences* **12**:183–5.
63. Liebovitch, L.S., Fischbarg, J., Konairek, J.P., Todorova, I., Wang Mei (1987a). *Biochim. Biophys. Acta* **896**:173–180.
64. Liebovitch, L.S., Sullivan, J.M. (1987b). *Biophys. J.* **52**:979–988.
65. Liebovitch, L.S., T. Toth (1991). *J. Theor. Biol.* **148**:243–267.
66. Llinás, R., (1987). In *Mindwaves*, Blakemore, C., Greenfield, S. (eds.) Basil Blackwell, Oxford.
67. Lockwood, M. (1989). *Mind, Brain and the Quantum*, Basil Blackwell, Oxford.
68. Lozovaya, G., Masinovsky, Z., Sivash, A. (1990). *Origins of Life* **20**:321–330.
69. MacElroy, R., Morowitz, H., Pohorille, A. *Orig. of Life* **19**:295–296.
70. MacLean, P. (1991). In *Cognitive Microgenesis: A New Psychological Perspective*, Hanlon, R. (ed.):3–33 New York: Springer-Verlag.
71. Miller, G. (2000). *The Mating Mind*. Doubleday, NY.
72. Mueller, R. (1968). *Nature* **217**:713–719.
73. *New Scientist*, 28 Jun 2003:29.
74. Penrose, R. (1989). *The Emperor's New Mind*, Oxford University Press. Oxford
75. Penrose, R. (1994). *Shadows of the Mind*. Oxford University Press, Oxford.
76. Pollack, G. (2001). *Cells, Gels and the Engines of Life*. Ebner and Sons, Seattle, WA 98105, USA
77. Pribram, K.H. ed. (1993). *Rethinking Neural Networks: Quantum Fields and Biological Data*. Erlbaum, Hillsdale, N.J.
78. Przybylski, A., Fox, S.W. (1986). *Origins of Life* **16**:395–396.
79. Rapp, P.E., Bashore, T., Martinerie, J., Albano, A., Zimmerman, I., Mees, A. (1989). *Brain Topography* **2**:99–118.
80. Ruthen, R. (1993). *Scientific American*, **268**:110–117.
81. Ryquist, R. (2003). Quantum Mind 2003 Poster Session.
82. Samuel, E. (2001). *New Scientist* **24 Mar**:42–45.
83. Schuster, H.J. (1986). *Deterministic Chaos*. Berlin: Springer-Verlag.
84. Skarda, C.J., Freeman, W.J. (1987). *Behavioral and Brain Sciences* **10**:161–195.
85. Stewart, I. (1989). *Does God Play Dice?* Basil Blackwell, Oxford.
86. Stickgold, R. (1998). *Trends in Cognitive Sciences* **2**:484
87. Walker, E.H. (1977). *T. Jour. Quant. Chem.* **11**:103–127.
88. Warren, W. (1998). *Science* **281**:247.
89. Wilhelm, R. (1951). *The I Ching*, Routledge and Kegan Paul, N.Y.
90. Winson, J. (1990). *Scientific American* **Nov**:42–48.
91. Zeki, S. (1992). *Sci. Am. Sep* :43–50.
92. Zurek, W. (1991). *Physics Today Oct.*

14 Consciousness and Logic in a Quantum-Computing Universe

Paola Zizzi

Summary. The early inflationary universe can be described in terms of quantum information. More specifically, the inflationary universe can be viewed as a superposed state of quantum registers. Actually, during inflation, one can speak of a quantum superposition of universes. At the end of inflation, only one universe is selected, by a mechanism called self-reduction, which is consistent with Penrose's objective reduction (OR) model. The quantum gravity threshold of (OR) is reached at the end of inflation, and corresponds to a superposed state of 10^9 quantum registers. This is also the number of superposed tubulins – qubits in our brain, which undergo the Penrose–Hameroff orchestrated objective reduction, (Orch OR), leading to a conscious event. Then, an analogy naturally arises between the very early quantum-computing universe, and our mind. In fact, we argue that at the end of inflation, the universe underwent a cosmic conscious event, the so-called “Big Wow”, which acted as an imprinting for the future minds to come, with future modes of computation, consciousness and logic. The postinflationary universe organized itself as a cellular automaton (CA) with two computational modes: quantum and classical, like the two conformations assumed by the cellular automaton of tubulins in our brain, as in Hameroff's model. In the quantum configuration, the universe quantum-evaluates recursive functions, which are the laws of physics in their most abstract form. To do so in a very efficient way, the universe uses, as subroutines, black holes – quantum computers and quantum minds, which operate in parallel. The outcomes of the overall quantum computation are the universals, the attributes of things in themselves. These universals are partially obtained also by the quantum minds, and are endowed with subjective meaning. The units of the subjective universals are qualia, which are strictly related to the (virtual) existence of Planckian black holes. Further, we consider two aspects of the quantum mind, which are not algorithmic in the usual sense: the self, and mathematical intuition. The self is due to a reversible self-measurement of a quantum state of superposed tubulins. Mathematical intuition is due to the paraconsistent logic of the internal observer in a quantum-computing universe.

14.1 Introduction

*Consciousness... is the phenomenon
Whereby the universe's very existence is made known*

Roger Penrose
The Emperor's New Mind

What is consciousness? Everybody knows about his/her own consciousness, but it is nearly impossible to communicate our subjective knowledge of it to others. Moreover, a complete scientific definition of consciousness is still missing. However, quite recently, it has been realized that the study of consciousness should not be restricted to the fields of cognitive science, philosophy and biology, but enlarged to physics, more precisely, to quantum physics.

The most popular (and conventional) description of consciousness is based on the classical computing activities in the brain's neural networks, correlated with mental states. In this case, mind and brain are the same, and are compared to a classical computer. This approach (see, for example, [10, 11]) is called in various ways: physicalism, reductionism, materialism, functionalism, computationalism.

However, although the brain can actually support classical computation, there is an element of consciousness that is noncomputable (in the classical sense), as was shown by Penrose [36, 37]. Moreover, the seminal paper by Stapp [43, 44] clarified why classical mechanics cannot accommodate consciousness, but quantum mechanics can.

Finally, reductionism cannot explain the “hard problem” of consciousness, which deals with our “inner life”, as illustrated by Chalmers [8].

A quite different line of thought about consciousness is the one that comprises panpsychism, pan-experientialism, idealism, and fundamentalism. Pan-experientialism states that consciousness (or better protoconsciousness) is intrinsically unfolded in the universe, and that our mind can grasp those proto-conscious experiences. This line of thought goes back to Democritus, Spinoza [42], Leibniz [29], until Whitehead [49] who reinterpreted Leibniz's “monads” as “occasions of experience”. Shimony [41] compared Whitehead's occasions of experience to quantum jumps.

More recently, Penrose interpreted the occasions of experience as the quantum-state reductions occurring at the Planck scale, where spin networks [38, 39] encode protoconsciousness. This is a pan-experiential approach to consciousness that is consistent with quantum gravity, and is called “objective reduction” (OR) [36, 37]. A further development is the Penrose–Hameroff “orchestrated objective reduction” (Orch OR) [22, 23, 24], which deals with the self-collapse of superposed states of the tubulins in the brain. Superposed tubulin states are qubits, and perform quantum computation, until they reach the quantum gravity threshold, then they collapse to classical bits, giving rise to a conscious event.

Finally, Chalmers [8] claimed that physical systems that share the same organization will lead to the same kind of conscious experience (principle of organizational invariance). As physical systems that have the same organization (no matter what they are made of) encompass the same information, it follows, from the above principle, that information is the source of consciousness. The present chapter is consistent with Chalmers' conclusions. This is of course valid also for an immaterial system, like the vacuum-dominated early inflationary universe that, as was shown in [53], is a superposed quantum state of qubits.

At this point, a conjecture arises very naturally: the early universe had a cosmic conscious experience at the end of inflation [54], when the superposed quantum state of $n = 10^9$ quantum gravity registers underwent objective reduction. The striking point is that this value of n equals the number of superposed tubulins – qubits in our brain, which undergo orchestrated objective reduction, leading to a conscious event. Then, we conjecture that the early universe and our mind share the same organization, encompass the same quantum information, and undergo similar conscious experiences. In other words, consciousness might have a cosmic origin, with roots in the preconsciousness ingrained directly from the Planck time. In this context, we revisit the concept of qualia, and we interpret them as units of the universals, which are global properties of quantum-evaluated recursive functions at the Planck scale (the laws of physics in their most primordial form). In this way, the universals and qualia in particular, provide a bridge between our minds and the physical world.

The mathematical world is also committed with our consciousness: it deals with the most profound part of it, the self. Self-awareness and mathematical intuition are the outcomes of nonalgorithmic processes, which are due to self-measurements without decoherence, and to the sequent calculus of a paraconsistent, symmetric logic.

14.2 The “Big Wow”

*Had I been present at the creation,
I would have given some useful hints
for the better ordering of the universe.*

Alphonso the Wise
King of Castile & Leon
(1221–1284)

The hot Big Bang theory of the formation of the universe raises some problems that are (partially) solved by the inflationary theory [21]. The early inflationary universe is proposed to have had an accelerated expansion, the

duration of which depends on the particular inflationary model. In any case, inflation is believed to have lasted an extremely short time: in the range of $10^{-33} - 10^{-35}$ s. In particular, in the chaotic inflationary model [32], inflation starts at the Planck time, $t_P \approx 10^{-44}$ s. (In this chapter, we also consider inflation starting at the Planck time, and the end of inflation occurring at time $t \sim 10^{-34}$ s.)

During inflation, the universe behaves like a de Sitter space-time, which is empty (no matter, no radiation – it is a vacuum-dominated universe), expands exponentially, and has an event horizon.

In previous work, [52] we considered quantum de Sitter horizons and, by means of the holographic principle [26, 27, 46] and spin networks [38, 39], the early inflationary universe was described in terms of quantum information. How does it work? In this model, time is discrete, and is quantized in Planck time units: $t_n = (n+1)t_P$ with $n = 0, 1, 2, 3, \dots$. At each time step, there is a de Sitter horizon with the quantized area of $A_n = Nl_P^2$ (where $N = (n+1)^2$ and $l_P \approx 10^{-33}$ cm is the Planck length). The holographic principle states that all the information enclosed in a region of space with volume V , is encoded on the surface S bounding V . More precisely, each pixel of area (a pixel is one unit of the Planck area) of S encodes one bit of information. In a more sophisticated (quantum) version of the holographic principle [53] the encoded information is quantum, and each pixel encodes one quantum bit (or “qubit”) of information, which is a quantum superposition of the two classical bits, 0 and 1. By the holographic principle, then, it turns out that each de Sitter horizon’s quantized area A_n encodes N qubits. At this point, every quantized horizon can be viewed as a quantum register (a quantum register is the memory of a quantum computer, built with qubits).

Through considerations of the actual entropy of our universe, (and of the maximal possible one), we found [54] that the amount of quantum information processed during inflation was $N \sim 10^{18}$ qubits, corresponding to the “selection” of the n -th $\sim 10^9$ quantum register. But what stopped the N -qubit quantum state from “decohering” if there was no environment surrounding it (the universe was empty)?

The n quantum registers $Q_1, Q_2, Q_3, \dots, Q_n$ built, respectively, with 1, 4, 9, ..., 10^{18} qubits can be thought to be in a superposed state like the “many-universes” interpretation of quantum mechanics [17]. In [54], a single “universe” is selected, the n -th $\sim 10^9$ quantum register, by a mechanism (self-decoherence), which is very similar to the objective reduction model (OR) of Penrose [36, 37] related to instability in the superposition/separation of the fundamental structure of the universe at the Planck scale.

In our case, the quantum gravity threshold of OR is reached at the end of inflation, with gravitational self-energy $E \sim 10^{10}$ GeV and preconscious time $T \sim 10^{-34}$, (corresponding to a superposed state of $n \sim 10^9$ quantum registers for a total of $N \sim 10^{18}$ qubits). According to the Penrose–Hameroff consciousness model of “orchestrated objective reduction” (Orch OR) [22,

23, 24], as calculated by the uncertainty principle, $\sim 10^9$ is the number of superposed tubulins proteins qubits in our brain that undergo Orch OR for conscious events of cognitive relevance, i. e. several hundred milliseconds, and that $\sim 10^{18}$ is the total number of tubulins protein qubits in our brain. Then, we suggested that at the end of inflation, the universe had a cosmic conscious experience (the “Big Wow”, so renamed by Hameroff) and, according to Chalmers’ principle of organizational invariance [8] an analogy naturally arises between the very early quantum-computing universe, and our conscious minds.

14.3 How the “Big Wow” Drove Human Minds

*There is a coherent plan to the universe
Though I don’t know what’s a plan for*

Fred Hoyle

Quantum gravity registers do perform quantum computation, but in a rather particular way, showing up some features of self-organizing systems. We recall that self-organization is a process of evolution taking place basically inside the system, with minimal or even null effect due to the environment.

In fact, the dynamical behavior of quantum gravity registers follows some cybernetic principles:

i) Autocatalytic growth

At each computational time step, the presence of a Planckian black hole (which acts as a creation operator), makes the quantum gravity register grow autocatalytically. As N qubits represent here a de Sitter horizon with an area of N pixels, the autocatalytic growth, in this case, is exponential expansion, i. e. inflation.

ii) Autopoiesis (or self-production)

The quantum gravity register produces itself. The components of the quantum gravity register generate recursively the same network of processes that produced them.

In this case recursion is defining the program in such a way that it may call itself. This is along the same line of thought as Kauffman’s “Fourth Law” [28]: “... The hypothesis that the universe as a whole might be a self-constructing coevolving community of autonomous agents that maximizes the sustainable growth...”.

For Kauffman, the autonomous agents are knotted structures created of spin networks that act on one another and become collectively autocatalytic. Our picture and Kauffman’s picture, are equivalent, because spin networks pierce the de Sitter horizons’ surfaces [53, 52].

iii) Self-similarity

This model of the early inflationary universe is based on the holographic principle [26, 27, 46], in particular, on the quantum holographic principle [53]. But each part of a hologram carries information about the whole hologram. So, there is a physical correspondence between the parts and the whole.

iv) Self-reproduction

Can a quantum gravity register, as a unit, produce another unit with a similar organization? This possibility, which could be taken into account because the quantum gravity register is an autopoietic system, (and only autopoietic systems can self-reproduce), is in fact forbidden by the no-cloning theorem [50] (quantum information cannot be copied).

However, there is a way out. When the selected quantum gravity register collapses to classical bits, it is not just an ordinary quantum register that collapses, but an autopoietic one. The outcomes (classical bits) carry along the autopoiesis. The resulting classical automaton is then autopoietic and, in principle, can self-reproduce.

Moreover, Chalmers' principle of organizational invariance would assign to the (produced) unit with similar organization, the same amount of information, and the same conscious experience as the original one.

From the cybernetic principles, the organizational invariance principle and from the no-cloning theorem, we get *the principle of alternating computational modes*: “A unit produced by an autopoietic classical computing system built up from the outcomes of a decohered quantum autopoietic system, shares the same organization, the same amount of information, and the same conscious experience as the producing unit. Moreover, in order to share the same conscious experience as the decohered quantum system, the produced unit must alternate quantum and classical computational modes at least once”.

The above arguments are summarized in the following scheme:

- Autopoietic quantum register**
- **no-cloning theorem**
- **no self-reproduction**
- **decoherence**
- **autopoietic classical cellular automaton**
- **self-reproduction**
- **produced unit with the same organization**
- **principle of organizational invariance**
- **the produced unit shares the same information content, and the same conscious experience**

- the produced unit gets both quantum and classical computational modes, the former from the autopoietic quantum register, the latter from the autopoietic classical cellular automaton
- the modes alternate with respect to each other.

Then, we are led to make the conjecture that the final outcome of a quantum gravity register might be a brain. In fact, tubulins in the brain alternate classical and quantum computational modes [22, 23, 24].

A related paper on the issue of a cybernetic approach to consciousness can be found in [19].

14.3.1 Entanglement with the Environment

This superposed state will collapse to classical bits by getting entangled with the emergent environment (radiation-dominated universe). This entanglement process with the environment can be interpreted as the action of an XOR (or controlled NOT) gate, as was illustrated in [53], which gives the output of the quantum computation in terms of classical bits: the source of classical information in the postinflationary universe.

14.3.2 Holography and Cellular Automata

Cellular automata (CA) were originally conceived by von Neumann [47], to provide a mathematical framework for the study of complex systems. A cellular automaton is a regular spatial lattice where cells can have any of a finite number of states. The state of a cell at time t_n depends only on its own state and on the states of its nearby neighbours at time t_{n-1} (with $n \in \mathbb{Z}$). All the cells are identically programmed. The program is the set of rules defining how the state of a cell changes with respect of its current state, and that of its neighbors.

It holds that the classical picture of holography (given in terms of classical bits) can be described by a classical CA. The rules do force patterns to emerge (self-organization). By taking into account the “classical” holographic principle, we are led to believe that at the end of inflation, the universe starts to behave as a CA that self-organizes and evolves complexity and structure.

It should be noted that this CA is made out of the bits that are the outcomes of the collapse of the qubits of the quantum gravity register that is an autopoietic quantum system. Then, this CA is an autopoietic classical system.

There are two important consequences that follow.

i) The CA, being autopoietic, undergoes autocatalytic growth, and the classical universe is still expanding. However, as classical computation is slower than quantum computation, the expansion is no longer exponential (postinflationary universe).

ii) The CA, being a classical autopoietic system, can self-reproduce. According to the “principle of alternating computational modes” discussed in Sect. 14.3, the produced units will be able to perform both quantum and classical computation. We conclude by saying that in our model, the postinflationary, classically holographic universe, follows the laws of classical complex adaptive systems (systems at the edge of chaos).

14.4 Consciousness and Tubulins/Qubits

*The state of least excitation
Of consciousness is the field
Of all possibilities*

Maharishi Mahesh Yogi

So far, consciousness was studied in the context of neuroscience, and was described as an emergent feature of classical computing in the brain’s neural networks. But neuroscience fails to explain some features of consciousness as, for example, subjective experience (Chalmers’ “hard problem” [8]). A new, different approach to the study of consciousness is due to Hameroff and Penrose [22, 23, 24] and it is based on quantum effects occurring in tubulins. In a brain’s neuron there is the cytoskeleton, which is made of protein networks. The most important components of the cytoskeleton are microtubules. Microtubules are hollow cylindrical polymers of proteins called tubulins. Tubulins have electrical dipoles and they can be in (at least) two different states (or conformations). Tubulins have been studied in classical computing. In fact simulations suggest that tubulins behave as a classical CA. But tubulins can also be in a superposition of two (or more) conformation states. In this case they represent qubits, and they behave as a biological quantum cellular automaton. Indeed, tubulins can perform both classical and quantum computing. In a classical computing mode, patterns of tubulins move, evolve, interact and lead to new patterns. Quantum coherence emerges from resonance in classical patterns. When the quantum gravity threshold is reached, self-collapse occurs and then tubulins evolve as a classical CA. In the orchestrated objective reduction (Orch OR) model of Penrose and Hameroff [22, 23, 24], the number of tubulins/cell involved in the threshold is $n = 10^9$, with a coherence time $T = 500$ ms. As tubulins are qubits, we can indulge in speculating about the brain-universe, with $n = 10^9$ quantum gravity registers, and a coherence time $T = 10^{-34}$, which might have a conscious experience. Since the inflationary universe performed quantum computation, and was able to achieve consciousness, we might ask if this will be the case with any quantum computer? For the moment, the only possible answer is no, for three reasons:

1. Because quantum computers are very difficult to build in practice, as the technology is not yet so advanced to maintain coherence for a sufficiently long time.

2. Because quantum computers (at least the first generations) will not have enough mass.
3. For a quantum system to be able to get a conscious experience, it is a necessary but not sufficient condition that it performs quantum-computation. The extra requirement is that the quantum-computing system must be quantum-autopoietic. However, we cannot really foresee anything definitive yet: In the long run quantum computers might have conscious experiences.

14.5 Consciousness Arises in the “Bits Era”

In our model, during the “qubit era” there are no events in the usual sense, (occasions of experience, in the philosophical language of Whitehead [49]). So, if we, Boolean-minded beings, conceive consciousness in terms of occasions of experience (events in the Boolean sense), we can argue that in the qubits era there was no consciousness at all in the universe (perhaps, there was just preconsciousness).

Consciousness appeared in the classical “bits era”: it was the projection in the past of future internal observers who had to be programmed by the self-organizing CA, in order to observe the emergent events.

14.5.1 The Boolean Observer

*The mind is like a parachute
It works only when it is open*

Unknown

To observe the events in the postinflationary universe, the observers should be Boolean. This means that the qubits – tubulins of the observers’ brain should collapse to classical bits at a rather high frequency. Of course, being the Boolean observers, they will not be able to grasp the unfolding quantum computing structure of space-time at the fundamental level (the Planck scale).

The problem is that a Boolean observer is endowed with the concept of time, which is a mere artifact of his/her own perception, and moreover, he/she tends to extend this concept to regions of reality where it is meaningless. A Boolean observer, is a classical logician, like Aristotle. He/she is not capable of putting himself/herself in relation with a quantum system without the mediacy of an external quantum observer. Even worse, he/she will never be able to recognize the quantum universe as a whole, as an internal observer [3]. This would lead him/her into a contradiction with himself/herself. Eventually, he/she will be replaced by a double logic-minded observer in Sect. 14.6.

14.5.2 The Analogy

Inflation (the qubit era) is for the universe what preconsciousness (superposed tubulins) is for our mind/brain. The end of inflation (beginning of the “bits era”) is for the universe what consciousness (Orch OR of superposed states of tubulins) is for our mind.

The analogy goes like this:

For tubulins in the brain:

- CLASSICAL CA
- EMERGENCE OF QUANTUM COHERENCE
(PRECONSCIOUSNESS)
- QUANTUM CA
- SELF-COLLAPSE BY ORCHESTRATED OBJECTIVE REDUCTION
- CONSCIOUS EXPERIENCE
- CLASSICAL CA.

For qubits in the early universe:

- CLASSICAL BIT (THE VACUUM)
- HADAMARD QUANTUM LOGIC GATE
- QUBIT
- BEGINNING OF INFLATION (THE UNIVERSE IS A SUPERPOSED STATE OF QUANTUM REGISTERS)
- SELF-REDUCTION BY OBJECTIVE REDUCTION (END OF INFLATION)
- COLLAPSE OF QUBITS TO BITS (THE XOR GATE)
- CONSCIOUS EXPERIENCE
- CLASSICAL CA.

Of course, the analogy between our mind and the universe is very speculative at this stage, but the emergent picture is quite exciting: it seems that our mind/brain owes its structure and organization to the very early universe. This is in agreement with the Penrose–Hameroff belief that consciousness is a fundamental property of reality, and has its roots in the space-time structure at the Planck scale. Then, although we can be just classical as observers, we can be also quantum as thinkers. In fact, for example, we can conceive quantum computation. This fact must be the result of a kind of *imprinting* we received from the quantum-computing early universe. If we did not have both quantum and classical computational modes available in our brain, in other words, if we were always conscious and Boolean, we would not be able to think in a quantum mode.

14.6 The Double Logic of the Observer Inside a Quantum Universe

*Logic is just the premise
Of wisdom,
Not the conclusion*

Mr. Spock
Star Trek Enterprise

In a recent paper, [3] we inquired about the internal logic of a quantum computer, in the simplest case of one qubit. Standard quantum logic [4] in fact fails when it tries to describe a closed quantum system, like a quantum computer during the computational process. Then, standard quantum logic is confined to describe the projective measurement performed by an external observer, not the whole quantum computation, which appears as a black box to the external observer.

The alternatives to standard quantum logic are, for example paraconsistent logic, [12] linear logic [18] and basic logic [40]. In our approach, we illustrated, in logical terms, a reversible quantum measurement, with no hidden quantum information, performed by a hypothetical “insider observer” [56]. In our case, the reversible measurement was a purely theoretical tool to investigate the internal computational state. And the “insider observer” was a fictitious being inside the quantum computer, used to illustrate the quantum measurement scheme in a quantum-space background. The resulting logic of the insider observer is paraconsistent and symmetric, like basic logic.

In a paraconsistent logic, the well-known laws of noncontradiction and excluded middle do not hold. In our case, then, we admit a superposition of the opposite truth values 0 and 1, that is, true and false.

It was quite natural to wonder what would happen if the whole universe were a quantum computer, and the previously fictitious insider observer were instead a true human being. In this case, the observer would be internal with respect to the universe as a whole, and thus endowed with a paraconsistent logic, and external with respect to any other quantum subsystem, and thus endowed with standard quantum logic. We argue that in the former case, the mental states of the observer are superposed, while in the latter they are not. The corresponding “hardware” would be a quantum configuration of superposed tubulins, and a classical configuration, respectively, as in Penrose–Hameroff model.

The double-minded observer, apart from accommodating the Orch OR model of consciousness, has some other intriguing features, like a modification [55] of Goedel’s first incompleteness theorem [20].

14.7 IT from Qubit: The Whole Universe as a Quantum Computer

*I've made such a terrible
Mess of things... and all I wanted
To do was to rule the universe*

Unknown

We believe that the offspring of the universal cellular automaton (CA) discussed in Sect. 14.3.2, are quantum minds in the sense of Hameroff–Penrose [22, 23, 24], and black holes – quantum computers on a noncommutative geometry background [57]. The event horizon of such quantum black holes is the surface of a fuzzy sphere [33]. If the black hole – quantum computer is processing N qubits, its event horizon is a fuzzy sphere with $n = 2^N$ elementary cells. Each cell encodes a string of N bits. For example, a black hole – quantum computer with two qubits has an event horizon that is a fuzzy sphere with four elementary cells, each cell encoding one of the four states: $|00\rangle, |01\rangle, |10\rangle, |11\rangle$.

At first glance, one might visualize this as a classical CA, each cell encoding a string of bits. It should be noticed, however, that due to the non-commutative structure of the background geometry, these basis states can be superposed and entangled! At the end of computation, the black hole emits one string of N bits (for example $|00\rangle$, for $N = 2$) and the corresponding cell evaporates. The end of a quantum computation corresponds to decoherence of the quantum computer. If we suppose that these quantum black holes undergo OR, we are surprised to find very long decoherence times, as we show in what follows.

The area of a fuzzy quantum black hole is given by [30]: $A = N A_P$ where N is the number of qubits and A_P is the Planck area: $A_P = l_P^2$, where $l_P \approx 10^{-33}$ cm is the Planck length. For a black hole, the following relation holds between its mass and the surface area of its event horizon: $M = \sqrt{A}$. In the case of fuzzy black holes, one has then: $M = \sqrt{N} l_P$. The OR decoherence time T is given by: $T = \frac{\hbar}{E}$, where E is the mass energy $E = mc^2$. In our case we have: $T = \frac{1}{\sqrt{N} t_P}$ (with $\hbar = c = 1$), where $t_P \approx 10^{-43}$ is the Planck time.

One can easily calculate that for a black-hole encoding, for example, the same number of qubits as the average number of superposed tubulins in our brain, that is, 10^9 , the decoherence time is about $T = 10^{31}$ s, which is a very long time, even compared to the age of our universe, that is $H^{-1} \approx 10^{17}$ s, where H is the Hubble constant. Of course, the bigger the number of qubits encoded by a black hole, the shorter will be its decoherence time.

Let us suppose that the whole universe alternates between two configurations, the first like a classical CA, the second like a fuzzy black hole – quantum computer, performing classical and quantum computational tasks, respectively. This behavior is similar to that of the CA of tubulins in our

brain, that can undergo both quantum and classical configurations. In the quantum configuration, the universe decoheres by OR, and emits one classical string as its output, with the evaporation of the associated cell. However, the cell is instantaneously replaced, because of the universe's expansion. The age of the universe is, as we said above, 10^{17} s. Since the Big Bang, the universe encoded, in its cosmological horizon, 10^{120} qubits [58]. The area of the cosmological horizon is then: $A = 10^{120} A_P$. If the whole universe can be described at present as a giant fuzzy black hole –quantum computer, its decoherence time is: $T_U = \frac{1}{10^{60} t_P} \approx 10^{-26}$ s.

As we see, the quantum universe has an extremely short decoherence time, and suddenly recomposes as a classical CA, because of its own expansion, and then reorganizes as a fuzzy quantum computer, and so on. One might argue that, due to the fact that the decoherence time of the universe is much smaller than its “dynamical” time: $T_U \ll H^{-1}$, the universe should not be considered a quantum system. However, its quantum-computational efficiency is enormous, as in that very short lapse of time, the universe can perform a huge computational task at the Planck scale. In fact, at the Planck scale, space-time can quantum evaluate a composite function of depth $d = 10^{120}$ [58].

Moreover, it should be noticed that the decoherence time of the quantum state of superposed quantum universes at the end of inflation, was not calculated in this way, as that quantum system was not a fuzzy black hole – quantum computer.

14.8 Quantum Minds and Black – Hole Quantum Computers in a Quantum Game

Calculemus

G.W. Leibniz

Fuzzy quantum black holes and quantum human minds can be viewed as subroutines of the whole quantum-computing universe discussed in Sect. 14.7.

This cosmic network exploits quantum communication complexity, and, thanks to entanglement, allows its parts to accomplish a distributed task without the need of any kind of communication. This is possible because all its parts share a common quantum space-time background, which is nonlocal as it is pointless (in a fuzzy sphere, points are replaced by elementary cells). In this picture, the fuzzy black holes –quantum computers and the quantum minds who share prior entanglement, are the players of a quantum game, and do not necessitate to communicate among them (*pseudotelepathy* [6]).

The literary analog of this game played by minds and black holes might be the cosmic game (as far as minds are concerned, at least) considered in “The Glass Bead Game” [25], by Hermann Hesse. An interesting scientific/philosophical interpretation of that novel can be found in Zimmermann’s

paper [51]. In our case, all the players are quantum-evaluating recursive functions that are the laws of physics in their discrete and most primordial form [58]. More precisely, some elements of the net are quantum memory registers, others are scratch registers needed to store intermediate results. However, according to the history of the patterns of the original CA, the role of a register may change with time.

The global properties of the quantum-evaluated functions can be interpreted as the universals (*universalia*). More specifically, we will call the results obtained by black holes *universalia in re* (universals in the thing), the universal features of singular things, inherent in the things themselves. A human mind has a much shorter decoherence time than that of a fuzzy black hole –quantum computer. Then the results obtained by a human mind will be partial, with respect to black holes' results.

Then, after objective reduction, the quantum mind can start again the computational process in parallel with black holes, but the resulting knowledge of the physical laws will be partial, discontinuous, and random. Of course, the fact that the knowledge of the physical world can be acquired by us only partially, might disturb physicists who believe in a TOE (theory of everything). However, the process discussed above, allows humans to have at least a summary understanding of the physical world, which would be impossible otherwise. As Einstein noted: “The most incomprehensible thing about the world is that it is comprehensible”.

The quantum mind outputs are to be considered as *universalia post rem* (universals after the thing), the concepts of the human mind regarded as posterior to the things represented by these concepts. So, *universalia post rem* are algorithmic in nature, and have a counterpart in the physical world. They belong to the set of computational aspects of consciousness. The bridge between our consciousness and the physical world is given by the common language of our minds and the universe. In fact, the outputs of all quantum-evaluated functions form a set of finite strings of bits that is a language based on the alphabet {0, 1}. Of course, this bridge is possible because our consciousness is, in some of its aspects, algorithmic.

As we will see in what follows, qualia are, in a sense, units of *universalia post rem*. There are, however, two aspects of consciousness, namely, mathematical intuition, and the self, which are not algorithmic.

14.9 Qualia and Quantum Space-Time

*You have to ask children and birds
How cherries and strawberries taste*
Goethe

What is the relation between the “occasions of experience” of Whitehead and the subjective aspects of conscious experience known as “qualia” (subjective

conscious experiences), a term coined by Lewis [31]? In fact, what is the wider, basic field of protoconsciousness Whitehead talked about? The old question is: is there any explanatory bridge between brain functions and qualia? As was pointed out by Levine [30], there is an “explanatory gap”: and it does not matter how well we can know the brain functions, this knowledge will not explain how a conscious experience is generated.

Chalmers [8] states that reductionism cannot explain the “hard problem” of consciousness, which deals with our “inner life”: how can a conscious experience (a quale) emerge from a physical function of the brain? His way out to the explanatory gap is to consider the conscious experience as a fundamental entity. A theory of consciousness can then be built on fundamental entities, as in physics.

There are other authors who simply deny the existence of qualia, like Dennet [13], or say that the hard problem will never be solved, like McGinn [34], who claims that our mind is too limited to afford the problem. (Or: Why we cannot observe our inner-selves? Because there is not an observer inside the system: we are the system itself.) Why others cannot observe (test) our conscious experience from outside as well? Why the knowledge of consciousness cannot be objective? If we make the analogy between our inner life and the universe, then we get the answer, as we know that there is no definition of an external observer outside the universe. This does not mean, however, that the problem of consciousness is not a scientific one. It is a bit like the problems of quantum gravity (no possibility to test it directly) and quantum cosmology (no external observer). Quantum gravity is the theory that should reconcile quantum mechanics and general relativity. Even if one day we would be able to build the theory of quantum gravity, it will be a very peculiar theory: based mostly on mathematical consistency, but not directly testable, as it deals with space-time at the Planck scale.

It should be noted that the Planck scale couldn't be tested not only because at present we don't have at our disposal such a huge energy like the Planck energy, but also for impossibility a priori. In fact, at the Planck scale, space-time starts to lose its well-known smooth structure, and becomes a *marasmus* of virtual black holes and wormholes: the “quantum foam” [48]. Any attempt at probing space-time at this scale would then lead to outcomes belonging to another universe [59]. General relativity and quantum mechanics can be considered to be the two distinct offspring of quantum gravity at scales far above the Planck scale. They can both be tested directly (and separately), but their origin, quantum gravity, cannot. Following McGinn and Chalmers together, we would say then that consciousness exists, is fundamental, but its origin cannot be probed, just like Planck-scale physics. The quale and the Planck scale event might then be identified with the Kantian noumenon: the thing in itself. This should not be too surprising, in fact, protoconsciousness is rooted at the Planck scale which is not testable itself. But, why is protoconsciousness rooted at the Planck scale? Here we give an explanation

slightly different from that of Penrose, although the two interpretations are closely related.

In quantum gravity, more precisely in loop quantum gravity, it is believed that quantum space-time is made of spin networks. This is the mathematical structure introduced by Penrose and developed by Smolin and Rovelli [38, 39] in the context of loop quantum gravity. However, it is also determined that quantum space-time is a quantum foam of virtual black holes and wormholes: this is Wheeler's description [48] of the quantum foam. Can the two views go along together? We believe so, because of the following arguments.

Consider a macroscopic black hole. The edges of spin networks pierce the black-hole horizon and excite curvature degrees of freedom on the surface [1]. These excitations (microstates) account for the black-hole entropy that turns out to be a quarter of the area of the horizon, (in units of Planck area), in accordance with the holographic principle [26, 27, 46]. Moreover, the states that dominate the counting correspond to punctures of spin $j = 1/2$ and one can in fact visualize each microstate as a bit of information. The obvious generalization of this result is to consider open spin networks with edges labeled by the spin $-1/2$ representation of $SU(2)$ in a superposed state of spin "up" and spin "down". The microstate corresponding to such a puncture will be a unit of area that is "on" and "off" at the same time, and it will encode a qubit of information [53].

Now, let us go back to the virtual black-holes in the quantum foam. Spin networks' edges pierce each virtual black-hole horizon in one point (puncture). The surface area of a virtual (Planckian) black hole is one pixel, (one unit of Planck area) and by the (quantum) holographic principle, it encodes one qubit of information. So, while in Penrose's view qualia can be identified with spin networks, in our view, qualia are the result of the action of spin networks on the quantum foam, that is, quantum information (qubits). We really think it is just a matter of interpretation, saying that qualia are spin networks or qubits encoded in virtual black holes' horizons pierced by spin network's edges.

McGinn [34] suggests that consciousness was present before the Big Bang, because the Big Bang is the beginning of space, and consciousness is nonspatial in nature. Although we also think that consciousness was indeed present in the early universe (as protoconsciousness), we wish to clarify that the problem of the nonspatial nature of consciousness is ill-posed. Consciousness itself distorts our understanding of space-time. Humans perceive space-time as a four-dimensional continuum, a smooth manifold. But space-time has a discrete structure, which becomes apparent at the Planck scale. At that scale, the familiar notion of an event like a point in a four-dimensional manifold loses its meaning. "Points" at the Planck scale are extended objects [57]. So, it is protoconsciousness that holds the right place in (quantum) space-time. Consciousness, the classical one we human beings deal with, appears to be nonspatial because (classical) space-time, as we understand it, is not the

real thing. Qualia correspond to the computational outputs of fuzzy Planck-scale black hole –quantum computers, encoding one qubit of information. Planck-scale black holes are virtual objects, they are the constituents of the quantum foam [48]. Notice, however, that although being a virtual object, a Planckian black hole can be considered “eternal” as a quantum superposition: (its decoherence time is 10^{34} s, equal to the squared age of the universe). In a sense, a fuzzy Planckian black hole is the very quantum object. Qualia can be considered to be the “units” of universalia post rem, and are not physically detectable because of their virtual nature.

14.10 Mathematical Intuition and the Logic of the Internal Observer

*It is by logic that we prove, but
by intuition that we discover*

Henri Poincaré

As we have seen, quantum space-time is a quantum computer that quantum-evaluates recursive functions that are the laws of physics in their most primordial and symbolic form. In agreement with Deutsch [15], we believe that the laws of physics determine which functions can be computed by a universal computer. Further, we claim that the laws of physics *are* the recursive functions that are quantum evaluated by space-time at the Planck scale [58].

The global properties of the recursive functions that are quantum evaluated by quantum space-time (fuzzy black holes-quantum computers, and the universe as a whole) are to be considered as the “universals in the thing”. The same quantum computation performed by the brain microtubules, are to be considered as the “universals after the thing”. This is why our minds are compatible with computable functions (and thus with the laws of physics). In fact, Deutsch says that, since any computational task that is repeatable or checkable may be regarded as the simulation of one physical process by another, all computer programs may be regarded as symbolic representations of some of the laws of physics. But it might be that not all the computational tasks performed by our brains are repeatable and checkable, in fact Penrose believes that most probably our thought is not algorithmic [36, 37]. Penrose might be right in saying that (some aspects of) consciousness are noncomputable, although some further considerations should be added to his statement, as follows.

If our mind is a quantum computer, we know that a quantum computer has the same computational power as a classical computer, (and this means that a quantum computer can compute only Turing-computable functions) although it is much more efficient. However, there are indeed some aspects of our consciousness that are not algorithmic in the usual sense. In a recent

study [3], we considered the internal logic of a quantum computer, and found out that it is not the standard quantum logic endowed by an external observer, instead it is a paraconsistent, symmetric logic like basic logic [40]. In fact, we argue that the logic underlying quantum computation at the Planck scale is not just standard quantum logic, (as in the case of ordinary quantum computers), but it is basic logic.

In the internal logic of a quantum computer, there are two very strong axioms, the reverse of both the noncontradiction and the excluded middle principles, which are obtained as reversible measurements. These two strong axioms, which are the manifestation of a great amount of quantum information, as the superposed state is maintained, are associated with a very weak calculus (the conclusions are almost similar to the axioms, but the axioms are very strong). The weakness of the sequent calculus indicates that there is almost no algorithm, but the conclusions are not trivial, as the premises are very strong. This might describe the immediacy of mathematical intuition, once the mind is regarded as an internal observer of the whole quantum universe, as in this case the logic it is using is paraconsistent.

It is generally assumed that there is a fundamental difference between the “axiomatic reasoning” and the informal mathematical reasoning. Instead, we believe that there are no proofs in mathematics that can be obtained without following the usual path from premises to conclusions, the only difference, in the case of intuition, is that the path is much shorter than usual. Moreover, since the information stored in the axioms cannot be provided twice as the source cannot be duplicated because of the no-cloning theorem [50], intuition is given only once. In this sense we meet Penrose, as repeatability is of course an intrinsic feature of algorithms. The absence of repeatability is a property of basic logic, due to the absence of the contraction rule, by which an operation cannot be repeated once the context within a particular sequent has been exhausted.

As we have seen, it is the attitude of a mind to place itself as an internal observer with respect to the quantum universe as a whole that allows it to acquire mathematical intuition. In other words, mathematical intuition is an interactive task between the mind and the universe, in some sense different from the understanding of physical laws, which includes all minds and black holes. Mathematical intuition is a private communication between one single mind and the whole universe. This sounds much like Platonism, but in our case the Platonic world of ideas is replaced by the physical universe. Goedel’s first incompleteness theorem [20], which somehow stresses the imperfectness of the Platonic world, in this context actually reveals the incompleteness of any possible unified physical theory. Intuitionistic logic, for which the law of excluded middle is invalid, replaces Platonism by a constructive approach to mathematics. Surprisingly enough, we see that paraconsistent logic, for which both the laws of noncontradiction and of excluded middle are invalidated, still leaves room for Platonism to a certain degree.

14.11 The Self

Know yourself

Socrates

14.11.1 The Self and the Mirror Measurement

In two recent papers [3, 56], we considered a new kind of quantum measurement, performed by a (fictitious) internal observer placed inside a quantum computer on a quantum-space background. This measurement is reversible because it is achieved by means of a unitary operator instead of a projector operator. Thus, the superposition can be recovered, and there is no loss of quantum information. Let us consider, for example the superposed state of one qubit: $|q\rangle = a|0\rangle + b|1\rangle$, where a and b are complex numbers, called the probability amplitudes, and the probabilities sum up to one: $|a|^2 + |b|^2 = 1$. Among all unitary 2×2 matrices acting on the qubit state as reversible measurements, there is one set of diagonal matrices, that we called “mirror” measurement:

$$M = e^{i\phi} \begin{pmatrix} \alpha & 0 \\ 0 & \alpha^* \end{pmatrix},$$

which has the property of leaving the probabilities unchanged, although modifying the probability amplitudes. The logical consequences of the mirror measurement, is that the internal observer gets rid of the noncontradiction principle. By symmetry, he also gets rid of the excluded middle principle. The internal observer is then endowed with a paraconsistent and symmetric logic, as we already said in the previous section.

There are two very strong axioms, in this logic, the mirror measurement leading to the one that states that: A and not A is true, which is the converse of the noncontradiction principle. The philosophical meaning of this axiom is that the superposed state $|q\rangle$ reflects in a slightly deformed mirror, that is, the diagonal unitary operator M, which just changes the probability amplitudes, but leaves unchanged the truth values (the identity operator being the perfect mirror). This analogy would suggest that the qubit has undergone a reversible self-measurement (without decoherence). The act of “looking at itself in the mirror” confirms the objective existence of the qubit. This is along the same line of thought as that of Mermin [35], who looks for an interpretation of quantum mechanics where objective reality should be separated from external observers and their knowledge.

We believe that the sense of “self” in human minds arises when a superposed state of tubulins undergoes a mirror measurement, without OR. This might sound like the antithesis of consciousness, as any conscious event originates from OR, which is subsequent to a quantum superposition. And in fact, self-awareness should be the purest form of consciousness! The sense of “self”, however, seems to baffle our beliefs. This is due to the fact that in

a mirror measurement, there is the maximal conservation of quantum information. And this maximal information is somehow stored and reused several times, without being ever dispersed in the environment. The sense of “self” in fact must be the most inner, persistent, indestructible feature of our mind.

14.11.2 Nonself

This is not mine, this I am not, this is not my Self
Buddha Gautama (563 B. C.)

One might wonder what happens when, instead of undergoing a mirror measurement, a quantum state of superposed tubulins is processed by a Liar measurement [3, 2]:

$$L = e^{i\phi} \begin{pmatrix} 0 & \beta \\ -\beta^* & 0 \end{pmatrix},$$

which is an off-diagonal unitary matrix, or by a general unitary quantum logic gate [3, 56]:

$$U = e^{i\phi} \begin{pmatrix} \alpha & \beta \\ -\beta^* & \alpha^* \end{pmatrix}.$$

In the first case, the probabilities (and the truth values) are interchanged, in the second case, they are mixed up, although the state is still superposed, until it decoheres by OR.

The mirrored self is a very peculiar case, most of the times our self is reversed, or distorted, and then, annihilated. A conscious experience arises after OR. We give up our self every time we become conscious about something else. Then the process restarts again, and again.

We recover our self, and then we lose it once more.

In summary, a conscious experience coincides with the minimum quantum information about itself of a quantum system, while the self corresponds to the maximum quantum information.

14.11.3 The Universal Self: The Universe and the Mirror

The objective world simply is; it does not happen.
Herman Weyl

The universe, as a whole, can undergo, as any other quantum system, a mirror measurement. However, the consequences of this cosmic mirroring are by far the most intriguing. In fact, the universe is the ensemble of all existing things, and its mirroring is the mirroring of everything that exists at the same time. The objective existence of existence itself is recognized. All things then acquire a collective sense of self, as if they were a Bose–Einstein condensate [5].

14.11.4 The Universal Self: The Mathematical Truth

*Why are you a physicist?
Why aren't you a mathematician?*

Paul Erdos

I agree with Deutsch [14], who recognizes the dependence of our mathematical knowledge on physics. Mathematics is in fact the language by which we express our knowledge of the physical world. The effectiveness of this language is due to the fact that the laws of physics are Turing-computable functions. However, like Deutsch, I also believe that our knowledge of the mathematical truth (or mathematical intuition) does not depend on physics.

As a physicist, I feel a kind of reverence for mathematics. Most probably, this leads me to idealize it too much, and all my considerations about mathematics sound quite platonic. “This is not fine”, a colleague of mine told me, who is a logician: “The world of ideas does not exist, we are the ones who construct Math”. Although respecting intuitionist philosophy, I suggested the following compromise.

When the quantum universe, mirrors itself in a mirror quantum logic gate, its superposed state gets slightly changed, but maintains the truth values at the “right place”. This, as we have seen, is the universal self. Is not that a kind of universal (although slightly imperfect) mathematical truth? Actually Brouwer, the founder of intuitionism, considered the self closely related to the “immanent truth” [7].

Also, for Brouwer, “The ego (self), at the onset of mathematical activity, is simply given; introspection is its natural form of knowing... the ego is... consciousness transformed to mind. The primordial intuition..is direct insight, introspection by and in the individual mind...” [45].

Similarly, we would argue, the universal self might be related to a “universal immanent truth”, which is recognized, by the observer, as the universal mathematical truth. In other words, when the human mind places itself as an internal observer of the universe as a whole, (the master program), it behaves as a fixed point, and is able to grasp the code (the mathematical truth).

14.12 Conclusion

*The theory of Knowledge
is a Product of Doubt*

Bertrand Russel

In this chapter, we described the early inflationary universe as an ensemble of quantum gravity registers in parallel. At the end of inflation, the superposed state self-reduces by reaching the quantum gravity threshold as in Penrose’s

objective reduction model. This self-reduction can be interpreted as a primordial conscious experience. Actually, the number of quantum gravity registers involved in the OR equals the number of superposed tubulins in our brain, which are involved in the Orch OR, leading to a conscious experience. It should be noticed that, in this model, the quantum gravity registers in parallel are parallel universes. This interpretation is very much along the same line with Deutsch' idea relating quantum computers to parallel universes (the "multiverse") [16].

However, at the end of inflation, only one universe is selected, the one that is endowed with that particular amount of entropy that makes it our world. Further, the qubits of the selected quantum gravity register get entangled with the emergent environment (radiation-dominated universe) and collapse to classical bits.

We make the conjecture that the postinflationary universe starts to organize itself, very likely as a cellular automaton, and necessarily produces self-similar computing systems. Actually, the CA-universe can undergo two different configurations, a classical one, performing classical computation, and a quantum one, performing quantum computation. The same can be done by tubulins in our brain. The universe, as a quantum computer, has subroutines that are black holes quantum computers with fuzzy spheres as event horizons. These black holes, and the universe itself as a whole, quantum evaluate the laws of physics in their primordial form. The outputs are the universals. Due to quantum entanglement, our minds operate in parallel with black holes in the computation of the physical laws, but the outputs are interpreted in a subjective way. The results of these computational tasks, are our concepts on the universals and this is an aspect of our mind that, although being quantum, is certainly algorithmic. It is in fact the algorithmic nature of such aspects of our consciousness that allows us to comprehend the physical world. Qualia might be considered units of the universals.

However, there are two aspects of our consciousness that are not algorithmic in the usual sense. They are mathematical intuition, and the self. The first corresponds to the attitude of one single mind to place itself as an internal observer, endowed with paraconsistent logic, with respect to the quantum universe as a whole. The second corresponds to the reversible self-measurement of the mind by means of the mirror-quantum logic gate. The self-measurement of the whole quantum universe in the mirror-gate corresponds to the universal self, which we interpret as the primordial origin of any form of self-awareness in terms of mathematical truth.

To conclude, we would like to stress the fact that, in this work, our study of consciousness required the use of some theoretical physics, some mathematics and also some philosophy. We think, in fact that consciousness is a highly interdisciplinary issue, and deserves the best of combined efforts from different disciplines. In this field, the "expert" does not exist yet. However, as Niels Bohr said once, "An expert is a man who has made all the mistakes, which can be made, in a very narrow field".

Acknowledgement. I am grateful to my colleague Giulia Battilotti, logician, for some useful comments and discussions. I also wish to acknowledge informal conversations on the subject with my cousin Dolores Fidelibus, chemist, and my sister Patrizia Zizzi, painter. I am indebted to Stuart Hameroff for enlightening discussions, which, although they took place a few years ago, still have influenced my present work. Finally, I wish to thank Giovanni Sambin, Head of the Logic Group, and Advisor of my research project in logic, for moral support, and encouragement. Work supported by the research project “Logical Tools for Quantum Information Theory”, Department of Pure and Applied Mathematics, University of Padova.

References

1. Ashtekar, A., Baez, J., Corichi, A., Krasnov, K. (1998). *Phys. Rev. Lett.* **80**:904
2. Battilotti, G. To be published in *International Journal of Quantum Information*.
3. Battilotti, G., and Zizzi, P. “Logical Interpretation of a Reversible Measurement in Quantum Computing”.
4. Birkhoff, G., von Neumann, J. (1936). *Annals of Mathematics* **37**:823–843.
5. Bose, S.N. (1924). *Z. Phys.* **26**: 178; A. Einstein (1924). *Sitz. Ber. Preuss. Akad. Wiss* (Berlin) **22**:261.
6. Brassard, G., Broadbent, A., Tapp, A. (2005). *Foundations of Physics* **35**:1877
7. Brouwer, L.E.J. (1905). In: *Collected works* **Vol. 1**:1. (ed.) Heyting and Freudenthal.
8. Chalmers, D. (1995). *Journal of Consciousness Studies*, and in: *Toward a Science of Consciousness – The First Tucson Discussions and debates*, (eds.) S. Hameroff, A. Kaszniak, A. Scott, MIT Press, Cambridge, MA:5–28, also available online, at: <http://www.Starlab.org/>
9. Chalmers, D. (1996). *The Conscious Mind – In Search of a Fundamental Theory*, Oxford University Press, New York.
10. Churchland, P.S. (1986). *Neurophilosophy: Toward a Unified Science of the Mind-Brain*, Cambridge, MA, MIT Press.
11. Churchland, P.S. (1998). In: *Toward a Science of Consciousness II – The Second Tucson Discussions and Debates*, (eds.) S. Hameroff, A. Kaszniak, A. Scott, MIT Press. Cambridge, MA: MIT Press, (1996)
12. Dalla Chiara, M.L., Giuntini, R., Leporini, R. *Quantum Computational Logics. A survey*. <http://arXiv.org/abs/quant-ph/0305029>
13. Dennett, D.C. (1988). In: *Consciousness in Contemporary Science*. Oxford: Oxford University Press.
14. Deutsch, D., Ekert, A., Lupacchini, R.. *Machines, Logic and quantum Physics..* <http://arXiv:math.HO/9911150v1>
15. Deutsch, D. (2003). *Proc. Sixth Int. Conf. on Quantum Communication, Measurement and Computing*, Rinton Press, Princeton, NJ.
16. Deutsch, D. (2002). *Proc. Royal Soc. A***458**:2911–23.
17. Everett, III,H. (1957). *Rev. of Modern Phys.* Vol. **29**:454–462.
18. Girard, J-Y. (1987). *Theor. Computer Sc.* **50**:1–102.
19. Globus, G. (1995). *Psyche*, **2** (12), August.

20. Goedel, K. (1931). *Monatshefte für Mathematik und Physik*, **38**:173–198. Translated in van Heijenoort, (1971). *From Frege to Gödel*. Harvard University Press.
21. Guth, A. (1998). *The Inflationary Universe: The Quest for a New Theory of Cosmic Origins*, Perseus Publishing.
22. Hameroff, S. (1997). In: *Geometry and the foundations of Science: Contributions from an Oxford Conference Honouring Roger Penrose*. Oxford University Press.
23. Hameroff, S., and Penrose, R. (1996). In: *Toward a Science of Consciousness – The First Tucson Discussions and Debates*, (eds.) S. Hameroff, A. Kaszniak, and A. Scott. MIT Press, Cambridge, MA.
24. Hameroff, S., and Penrose, R. (1996). *Journal of Consciousness Studies* **3**: 1:36–53.
25. Hesse, H. (1943). *Des Glasperlenspiel*, Fretz&Wasmuth, Zurich.
26. 't Hooft, G. *Dimensional reduction in quantum gravity*. In *Salamfestschrift: a collection of talks*, World Scientific Series in 20th Century Physics, vol. 4, ed. A. Ali, J. Ellis and S. Randjbar-Daemi (World Scientific, 1993), THU-93/26, gr-qc/9310026.
27. 't Hooft, G. *The Holographic Principle*, Opening Lecture, in *Basics and Highlights in Fundamental Physics*, The Subnuclear series, Vol. 37, World Scientific, 2001 (Erice, August 1999), A. Zichichi, ed., pp. 72-100, SPIN-2000/06, hep-th/0003004.
28. Kauffman, S. Available online at: <http://www.santafe.edu/sfi/People/kauffman/lecture-7.html>
29. Leibniz, G.W. (1768), *Opera Omnia*, 6 volumes, Louis Dutens, (ed.) Geneva.
30. Levine, J. (1983). *Pacific Philosophical Quarterly* **64**:354–361.
31. Lewis, C.I. (1929). *Mind and the World Order*. New York: C. Scribner's & Sons.
32. Linde, A. (1983). *Phys. Lett.* **129B**:177.
33. Madore, J. (1992). *Classical and Quantum Gravity* **9**:69–87.
34. McGinn, C. (1995). *Journal of Consciousness Studies* **2**:220–230.
35. Mermin, N.D. (1998). *Pramana* **51**:549–565.
36. Penrose, R. (1989). *The Emperor's New Mind*, Oxford University Press, Oxford, UK.
37. Penrose, R. (1994). *Shadows of the Mind*, Oxford University Press, Oxford, UK.
38. Penrose, R. (1971). In: *Quantum Theory and Beyond*, (ed.) T. Bastin, Cambridge University Press:875.
39. Rovelli, C. and Smolin, L. (1995). *Phys. Rev.* **D52**:5743.
40. Sambin, G., Battilotti, G., and Faggian, C. (2000). *The Journal of Symbolic Logic* **65**:979–1013.
41. Shimony, A. (1993). *Search for a Naturalistic World View*-Volume II. Natural Science and Metaphysics. Cambridge University Press, Cambridge, UK.
42. Spinoza, B. (1677). *Ethica in Opera quotque reperta sunt*. 3rd edn, (eds.) J. van Vloten and J.P.N. Land, Netherlands: Den Haag.
43. Stapp, H.P. (1995). *Psyche* **2**:5.
44. Stapp, H.P. (1993). *Mind, Matter, and Quantum Mechanics*, Springer- Verlag, Berlin.

45. van Stigt, W.P. (1990). *Brouwer's Intuitionism*, Amsterdam: North-Holland.
46. Susskind, L. (1995). *J.Math.Phys.* **36**:6377–6396
47. von Neumann, J. (1996). *Theory of Self-Reproducing Automata*, University of Illinois Press, Illinois.
48. Wheeler, J.A. (1962). *Geometrodynamics*, Academic Press, New York.
49. Whitehead, A.N. (1929). *Process and Reality*, Macmillan, New York.
50. Wootters, W.K. and Zurek, W.H. (1982). *Nature* **299**:802–819.
51. Zimmermann, R. (2003). *Conference Human Approaches to the Universe. An Interdisciplinary perspective.*, Helsinki.
52. Zizzi, P.A. (1999). *International Journal of Transport Phenomena* **Vol. 38, N 9**:2333–2348.
53. Zizzi, P.A.(2000). *Entropy* **(2)**:39–69.
54. Zizzi, P.A.(2003). *NeuroQuantology* **3**:285–301.
55. Zizzi, P.A. (2004). “Computability at the Planck scale”. Talk given at Foundations of quantum mechanics Cesena, Italy, 4–9 October, 2004. Forthcoming paper.
56. Zizzi, P.A. To appear in *International Journal of Quantum Information*.
57. Zizzi, P.A. (2005). *Mod.Phys.Lett A* **20**:645–653.
58. Zizzi, P.A. “Spacetime at the Planck Scale: The quantum Computer View”. <http://arXiv.org/gr-qc/0304032>
59. Zizzi, P.A. “Ultimate Internets”. <http://arXiv.org/gr-qc/0110122>

Index

- action potential 2, 11, 53, 77, 88, 115, 117, 194, 208, 209, 223, 225, 255, 267, 295, 299, 313, 317–320, 403, 436, 438
AMPA receptors 58–60, 67, 72, 76, 80, 217, 243
anesthesia 196, 199, 201, 206, 212, 225, 226
arrhythmia 269
axon 6, 9, 14, 21, 22, 51, 55, 57, 60, 68, 69, 77, 78, 82, 89, 121, 122, 134, 208–211, 213–219, 293–297, 301, 302, 313, 314, 316–318, 320
axonal 65, 87, 120–122, 135, 144, 194–196, 209, 211, 213–215, 223, 232, 233, 238, 293, 295, 296, 301, 320, 429

basilar membrane 273, 278, 279
Belousov–Zhabotinsky (BZ) 277
Belousov-Zhabotinsky (BZ) 277
binding site 70
binding problem 13, 23, 212, 391, 409, 440, 445
binding site 57, 58, 75, 118, 119, 124, 134, 233, 263, 306, 308
biological hierarchy 172, 174, 176, 180, 182, 184
butterfly effect 174, 175, 181

C-termini 15, 18, 57, 139, 235, 293, 302–305, 313–315
causality 114, 172, 174, 179–181, 183, 184, 188, 189, 204, 206, 407, 416, 419–423, 428, 440–442, 445, 446
cellular automata 100, 220, 221, 232
CEMI Field 398
CEMI field 16, 396

chaotic excitation 425, 428, 429, 438, 439, 444
classical
 information processing 106, 354
classical functionalism 194, 195
closed causal loop 175, 186, 187, 189, 190, 206
cognition 2, 4, 5, 8, 12, 14, 17, 20, 49, 55, 85, 88, 89, 95, 195, 198, 203, 212–215, 217, 223, 235–237, 241, 255–257, 278, 280–282, 286–288, 321, 335, 337, 351, 374, 376, 428, 429, 445
colchicine 101, 319
collapse 4–7, 11, 17, 27–31, 33, 34, 42, 46, 102, 110, 117, 196, 197, 226, 227, 229, 243, 410, 413, 414, 418–422, 431, 433, 442–445, 447, 448, 450, 451, 458, 462–465, 478
color phi effect 193, 198, 199, 202, 203, 238
complex conjugate 377, 378
confirmation wave 421, 422, 446
conformational changes 106, 119, 135, 220, 225, 262, 263, 273
conformations 17, 22, 99, 101, 105, 106, 218, 220, 221, 224, 233, 305, 338, 457, 464
connexin,- 36 54, 402
conscious states 287, 288, 376, 428, 440, 450, 451
consciousness 1–13, 16, 17, 22–27, 29, 48, 49, 77, 78, 83, 95, 96, 102, 159, 163, 190, 191, 193, 194, 196, 240, 241, 245–248, 250, 251, 253, 371, 372, 374, 375, 377, 383, 387, 388, 393, 394, 396, 398, 401, 404–406,

- 447, 451, 455, 457, 458, 464, 465, 472, 477, 479, 480
- contingent negative variation (CNV) 45
- de Sitter 460, 461
- decision making 414, 424, 433, 440, 442, 443
- decoherence 5, 8, 10, 13, 86, 103, 108, 110, 113–115, 161, 171, 173, 196, 227, 229, 233, 235, 236, 240, 241, 348, 352, 402, 414, 430, 441, 445, 450, 451, 459, 460, 462, 468–470, 473, 475
- dendrite 14, 18–22, 51, 52, 55–57, 59–61, 63–74, 79, 83, 84, 88, 121, 122, 181, 196, 208–213, 215–217, 219, 223, 226, 233, 234, 236, 241, 243, 293–295, 297–299, 301–303, 314–318
- dielectric spectroscopy 153, 154, 158, 164
- dipole 18, 21, 63, 97–100, 102, 104–106, 108–111, 116, 118, 119, 135–141, 145, 152, 153, 158, 161–164, 209, 219, 221, 224, 232, 236, 311, 353, 354, 360, 361, 374, 394, 464
- discretization points 357, 360, 364
- DNA 2, 7, 113, 114, 180, 181, 183, 184, 255, 262, 267, 269, 273, 292, 306, 309, 448
- downward causation 172, 184, 185, 188
- dreams 80, 81, 89, 204, 230, 231
- Drosophila 12, 13
- dynamic systems 14, 256, 259, 276, 289
- Einstein–Podolsky–Rosen 23, 160, 204, 205, 228, 239, 240, 243
- electric dipole 97, 100–102, 104–106, 109, 110, 137, 138, 160–163, 218, 374
- electroencephalogram (EEG) 13, 31, 33, 34, 36, 37, 41, 80, 95, 194–197, 206, 209, 212–215, 225, 394, 398
- emergence 10, 11, 13, 96, 115, 124, 172, 175, 184–190, 239, 259, 271, 276, 280, 283–285, 288, 289, 407, 433, 451
- energy barrier 263, 264, 266, 273, 305, 356
- entanglement 5, 7, 17, 21–23, 85–89, 95, 97, 102, 103, 114, 115, 117, 159, 161, 196, 204, 205, 226, 228, 230, 233, 235, 240, 258, 369, 419, 420, 440, 442, 446–451, 463, 469, 478
- enthalpy 263, 273
- entropy 262, 263, 284, 285, 287, 288, 373, 415, 422, 460, 472, 478
- environmental survival space 272
- enzyme catalysis 263, 265–268, 287–289
- evoked potential 32, 33, 160, 198, 200–204, 206, 209, 225, 318
- primary 11, 27, 33, 35, 38–40, 42–45, 200–202
- primary IV 33
- visual 23
- excitable medium 14, 255, 268, 271–277, 279, 284, 285, 288, 317
- feedback 46, 82, 83, 172, 175, 176, 182, 187–190, 273, 279, 318–320, 329, 330, 395, 425, 426, 428, 429, 438, 444, 451
- Feynman path integral 356
- fractal 16, 231, 260, 261, 373, 407, 422, 429, 430, 433, 434, 439–441, 444, 449, 451
- dynamics model 440
- free-will 5, 11, 238, 239, 404, 433, 445, 450
- gamma oscillation 212
- gap junction 2, 3, 7, 10, 54, 86, 195, 196, 209, 214–216, 226, 233, 234, 236, 243, 244, 402, 403
- gel phase 233, 234, 236
- gel-phase 436
- Gestalt psychology 393
- global workspace 207, 208
- gravitational self-energy 233, 450, 460
- harmonics 380, 381
- Heisenberg uncertainty relation 410
- Hopfield neural network 15, 354, 355

- hydrophobic pockets 100, 105, 111, 224–226, 232, 235
- hyper neuron 214
- hyperneuron 196, 214–216, 233, 238, 238, 241
- ICA algorithm 37, 38, 41
- identity theory 287
- induction 73, 131, 283, 300, 320, 396
- information processing 2, 8, 11, 13, 15, 55, 56, 65, 106, 118, 119, 163, 164, 193–196, 216, 217, 219, 220, 223, 226, 241, 243, 297, 317, 347, 348, 351, 352, 354, 364, 365, 388–390, 392, 395, 396, 403, 404
- information-processing 388
- ionic wave 9, 15, 293, 308, 312, 313, 313, 320
- kinesin 12, 15, 18, 19, 22, 57, 59, 60, 64, 69, 74–76, 80, 81, 83, 293, 302
- kinetic isotope effects (KIE) 264
- learning 3, 9, 12, 13, 20, 21, 37, 49, 51, 55, 65–68, 70, 71, 73, 74, 76, 81, 84, 85, 88, 96, 120–122, 126, 128, 129, 132–135, 183, 185, 198, 206, 208, 210, 219, 223, 283, 285, 295, 297, 298, 302, 329, 331, 333, 342, 348, 391, 400, 427, 428, 430
- liquid phase 233
- liquid-state machines (LSM) 317
- local field potential 213
- local minimum 352, 355, 361, 423, 428
- London forces 100, 218, 224–226, 232, 241
- long-term memory 77, 83, 298
- maya 382, 383
- medial lemniscus 202
- membrane potential 53, 63, 77, 88, 89, 209, 210, 297, 318, 403
- metastable state 303–305
- microfluidic 147
- microtubule 3, 4, 7–10, 12, 13, 15, 17–23, 49, 54–66, 68–70, 72–81, 83–89, 96–99, 104, 108, 111, 113, 114, 117, 120, 124, 125, 134, 135, 143, 158, 160, 161, 163, 164, 195, 196, 209–211, 215, 217, 219, 220, 226, 232, 236, 239, 240, 242, 243, 269, 293, 295, 296, 299–303, 313–315, 338, 351–354, 361, 373, 374, 401–404, 408, 430, 440, 441, 450, 464, 473
- associated proteins 70
- associated proteins 9, 10, 12, 13, 15, 18, 19, 49, 55–65, 68–76, 79–81, 86, 88, 89, 96, 97, 101, 117, 119, 121–123, 210, 217, 219, 233, 299, 301–304, 306–308, 314–317, 340, 341, 352, 441, 450
- polymerization 49, 58, 61, 62, 65, 68, 72, 88, 300
- stability 57, 69, 74, 135
- motor neurons 397, 398
- neurocognition 9, 10, 12
- neurocosmology 451
- neuromodulators 53, 54, 63
- neuron 1–3, 8–10, 12, 15, 19, 20, 22, 23, 50–55, 58, 59, 62, 64, 66–69, 72, 74, 76, 78–80, 84–89, 95, 102, 117, 120–124, 129–135, 164, 174, 176, 177, 181, 183, 185, 189, 195, 196, 206–217, 223, 226, 230, 232–234, 239, 241, 243, 278, 280, 281, 293–301, 313–317, 319, 320, 328, 330, 331, 334–336, 339, 340, 352, 354, 355, 359, 361, 373, 388, 389, 392–396, 398–404, 408, 414, 423, 424, 426, 427, 429, 430, 439–441, 444, 453, 464
- neuronal 2, 3, 6–8, 11, 12, 15, 18, 21, 49, 53, 56, 59, 66, 69, 77, 84, 88, 89, 106, 120–122, 134, 135, 194–196, 199, 200, 202, 207, 208, 214–218, 232, 242, 243, 293–296, 299, 301, 313, 318–320, 328, 338–340, 373, 390–396, 402–404, 429, 430, 438
- neurotransmitters 49, 53, 54, 68, 78, 81, 89, 209, 394, 424, 426, 429, 436, 438
- nonlinear 14, 15, 21, 22, 172–176, 181, 183–190, 194, 238, 239, 256, 259, 265, 267–270, 273, 274, 279, 282, 285, 288, 289, 298, 313, 317, 318,

- 327–332, 338–341, 345, 347, 381, 408
- phenomena 173, 181, 182
- nonspecificity 262
- nontrivial zeros 379–381
- objective reduction 5, 195, 197, 227, 232, 352, 414, 441, 450, 470
- Orch 14
- ontology 30, 281–283, 285, 287–289
- parallel computation 399, 420
- partial collapse 44
- phase space 185, 187, 188, 317, 357, 358, 428, 429, 439, 446
- physical field 393
- physicalism 172, 178, 179, 190, 458
- Planck scale 228, 229, 236, 238, 240, 241, 458–460, 466, 469, 471, 472, 473, 481
- protein folding 14, 224, 255, 273
- prototype process 261
- pyramidal cells 52–56, 67, 88, 208, 209, 215, 395
- quanglement 204, 206
- quantum
 - brain dynamics 383
 - brain dynamics 16, 371, 373–378, 381, 382
 - computation 4, 7, 8, 15, 17, 120, 195, 224, 228–230, 232, 233, 237, 339, 351, 352, 420, 422, 431, 432, 441, 444, 450, 457, 458, 461, 463, 465–468, 473, 474, 478
 - computational 441, 463, 468, 469
 - computer 7, 8, 17, 114, 120, 164, 228, 229, 240, 351, 364, 457, 460, 464, 465, 467–470, 473–475, 478
 - computing 7, 8, 22, 23, 29, 196, 228, 229, 342, 348, 351, 397, 402, 430, 432, 433, 451, 461, 465, 466
 - gravity 227, 240, 457–464, 471, 472, 477, 478
 - loop 359, 364
 - quantum Hopfield network 15, 351, 355, 357–366
 - qubit 4, 7, 9, 15, 87, 97, 102, 114, 115, 120, 161, 196, 224, 228–230, 232, 233, 238, 240, 351, 352, 355–365, 367–369, 402, 457–461, 463–469, 472, 473, 475, 478
 - reaction times 197, 243
 - readiness potential 203
 - reductionism 172, 177–179, 186, 188–190, 458, 471
 - relativity 36, 227, 228, 415–417, 420, 445, 471
 - retrospective construction 199, 201–204, 238
 - Riemann hypothesis 377
 - scale-invariant process 260, 262
 - sensory systems 78, 275
 - sexual paradigm 448
 - sol phase 233
 - soliton 100, 103, 107, 108, 110, 111, 113, 114, 119, 174, 188, 235, 255, 265–274, 278–284, 286, 288, 289, 291, 309, 312, 313, 328, 329, 331, 335, 336, 340–342, 345, 347, 350, 374, 438, 440
 - soliton wave 220, 265, 266, 268, 271
 - solitonic 103, 107, 108, 110, 111, 118, 119, 266, 268, 273, 276, 278, 281, 283, 286, 312, 451
 - space-time geometry 197, 227, 230, 235, 240
 - stable state 351, 352, 354, 355, 359, 361
 - stimuli 6, 20, 21, 46, 65, 77, 78, 81, 82, 95, 126, 128, 200, 202, 204, 212, 273, 279–281, 285, 287, 407, 427, 440
 - subject-object complementarity 407
 - subjective awareness 449
 - subjective reduction 29–31, 33, 45
 - superconductivity 103, 112
 - superposition 4–7, 10, 27–29, 31, 32, 35, 95, 106, 115, 196, 197, 205, 218, 224, 226–230, 232–238, 240, 241, 243, 338, 339, 352, 358, 359, 364, 365, 372, 382, 394, 399, 401, 412, 413, 420, 422, 430–432, 440, 441, 444, 457, 460, 464, 467, 473, 475
 - surface plasmon resonance 102, 142, 145, 146, 164, 242

- surface plasmon resonance (SPR) 102, 117, 136, 142, 143, 145–147, 149, 150, 152, 161, 163
symmetrons 374
synaptic change 49, 66, 208
TAU accumulation 124, 125, 129, 130, 132–135
taxol 101, 300, 319
teleportation 96, 102, 103, 105, 115–118, 159, 228, 419
tennis 193, 198, 203, 238
theory of metabolism 256, 257
thermodynamics 204, 255, 259, 262, 263, 283, 287, 289, 422
thermofield dynamics 375–377
transactional perspective 450
transcranial magnetic stimulation (TMS) 87, 88, 395–397
transition state theory 264, 265
tubulin dimers 4, 8, 10, 18, 55, 69, 102, 104, 106, 109, 110, 114, 119, 141, 143, 150, 152, 158, 162, 219, 301–303, 352, 353, 360, 367
tunneling 113, 196, 233, 243, 264–266, 356–359, 361
unconsciousness 389
vacuum-field Rabi splitting 108, 109, 162
vibrational mode 265, 266
visual consciousness 95
visual cortex 9, 20, 53, 67, 81, 82, 198, 207, 212, 214, 278–280, 340, 392, 427